

**Ongoing Face Recognition  
Vendor Test (FRVT)**  
**Part 1: Verification**

Patrick Grother  
Mei Ngan  
Kayee Hanaoka  
Joyce C. Yang  
Austin Hom

*Information Access Division  
Information Technology Laboratory*

This publication is available free of charge from:  
<https://www.nist.gov/programs-projects/face-recognition-vendor-test-frvt-ongoing>

2022/05/06

## ACKNOWLEDGMENTS

The authors are grateful for the long-standing support and collaboration of the the Department of Homeland Security's Science & Technology Directorate (S&T) and the Office of Biometric Identity Management (OBIM).

Additionally, the authors are grateful to staff in the NIST Biometrics Research Laboratory for infrastructure supporting rapid evaluation of algorithms.

## DISCLAIMER

Specific hardware and software products identified in this report were used in order to perform the evaluations described in this document. In no case does identification of any commercial product, trade name, or vendor, imply recommendation or endorsement by the National Institute of Standards and Technology, nor does it imply that the products and equipment identified are necessarily the best available for the purpose.

## INSTITUTIONAL REVIEW BOARD

The National Institute of Standards and Technology's Research Protections Office reviewed the protocol for this project and determined it is not human subjects research as defined in Department of Commerce Regulations, 15 CFR 27, also known as the Common Rule for the Protection of Human Subjects (45 CFR 46, Subpart A).

## FRVT STATUS

**This report** is a draft NIST Interagency Report, and is open for comment. It is the thirty sixth edition of the report since the first was published in June 2017. Prior editions of this report are maintained on the FRVT [website](#), and may contain useful information about older algorithms and datasets no longer used in FRVT.

**FRVT remains open:** All [four tracks](#) of the FRVT are open to new algorithm submissions.

**2022-05-05** changes since 2022-03-18:

- ▷ We have added results for first algorithms from seven developers: Accurascan, DICIO, FacePhi, Pangiam, University of Surrey-CVSSP, and Veridium.
- ▷ We have added results for new algorithms from sixteen returning developers: ACI Software, Canon Inc, Cloudwalk - Moontime Smart Technology, Cybercore, Cyberextruder, Gemalto Cogent, HyperVerge Inc, KuKe3D Technology, Megvii/Face++, Mobbeel Solutions, Panasonic R+D Center Singapore, Qnap Security, Samsung-SDS, Vietnam Posts and Telecommunications Group, Viettel Group, and Vision Intelligence Center of Meituan.
- ▷ We have retired results for 12 algorithms per our policy to only list results for two algorithms per developer. Results for retired algorithms appear in prior versions of this report in the [archive](#).

**2022-03-18** changes since 2022-02-23:

- ▷ We have added support for the detection of multiple people in a single image (see Section 1.2). Specifically the API allows an algorithm to extract features from one or more faces it detects in an image. NIST scores such cases as a correct match when any detected face matches the reference photo, and as a false positive when either face matches a non-mated reference photo. The expected effect of doing this will be to improve reported false non-match rates, and to minimally elevate false match rates. This technique was only applied to images of type "border" and "kiosk".
- ▷ We have added results for first algorithms from four developers: IntelliVIX, Kasikorn Labs, Lebentech Biometrics, and Wicket.
- ▷ We have added results for new algorithms from 10 returning developers: Chunghwa Telecom, Cloudmatrix, Beijing DeepSense Technologies, FarBar Inc, Imagus Technology Pty, Intellivision, Maxvision Technology, NHN Corp, Seventh Sense Artificial Intelligence, and Verigram.
- ▷ We have retired results for 4 algorithms per our policy to only list results for two algorithms per developer. Results for retired algorithms appear in prior versions of this report in the [archive](#).

**2022-02-23** changes since 2022-01-24:

- ▷ We have added results for first algorithms from four developers: AFIS and Biometrics Consulting, Digidata, Graymatics, Hangzhuo Allu Network Information Technology, KnowUTech LLC, Sukshi Technology Innovation, T4iSB, and TuringTech.vip
- ▷ We have added results for new algorithms from 18 returning developers: Cognitec Systems GmbH, GeoVision Inc, Glory, Herta Security, Intel Research Group, InsightFace AI, Kakao Enterprise, N-Tech Lab, Omnidarde Ltd, Papilon Savunma, Paravision, Realnetworks Inc, Reveal Media Ltd, Shenzhen Inst Adv Integrated Tech CAS, Suprema AI Inc, Toshiba, Universidade de Coimbra, and Yuan High-Tech Development

- ▷ We have retired results for 14 algorithms per our policy to only list results for two algorithms per developer. Results for retired algorithms appear in prior versions of this report in the [archive](#).

**2022-01-24** changes since 2022-01-20:

- ▷ We have added results for new algorithms from one returning developer: Vocord.

**2022-01-20** changes since 2021-12-18:

- ▷ We have added results for first algorithms from four developers: Armatura, Beyne.AI, One More Security, and VinBigData
- ▷ We have added results for new algorithms from 19 returning developers: AuthenMetric, BOE Technology Group, Cybercore, Cyberlink, Dahua Technology, FaceTag Co, Innovatrics, Megvii, Mobbeel Solutions, Neurotechnology, Oz Forensics, Rank One Computing, Regula Forensics, Samsung S1, Securif AI, Sensetime Group, TigerIT Americas, Videmo Intelligent Videoanalyse, and YooniK.
- ▷ We have retired results for 14 algorithms per our policy to only list results for two algorithms per developer. Results for retired algorithms appear in prior versions of this report in the [archive](#).

: **2021-12-16** changes since 2021-11-22:

- ▷ We have added results for first algorithms from five developers: Alfabeta, Cloudmatrix, Euronovate SA, FaceOnLive Inc, and Mobiclip Technology.
- ▷ We have added results for new algorithms from ten returning developers: ACI Software, ITMO University, NEO Systems, Guangzhou Pixel Solutions, Panasonic R+D Center Singapore, Qnap Security, Scanovate, Tevian, Unissey, and Vietnam Posts and Telecommunications Group.
- ▷ We have retired results for eight algorithms per our policy to only list results for two algorithms per developer. Results for retired algorithms appear in prior versions of this report in the [archive](#).
- ▷ We have revamped Figure 21 showing performance on 20 pairs of open-source images. It now color-codes false negatives and positives against a default threshold value.

**2021-11-22** changes since 2021-10-28:

- ▷ We have added results to the [website](#) for kiosk-collected images where the design and geometry configuration mean that many images have considerable downward pitch angle. In some images, the face is partially cropped. Some images have other background faces.
- ▷ We have stopped using child exploitation images in FRVT, as we lost access to the imagery. All results for that set have been removed from the [website](#), and will be removed from future PDF reports.
- ▷ We have added results for first algorithms from seven new developers: CUDO Communication, Daon, KuKe3D Technology, Mantra Softtech India, Maxvision Technology, Multi-Modality Intelligence, and Samsung-SDS.
- ▷ We have added results for new algorithms from seven returning developers: Acer Incorporated, Cloudwalk-Moontime Smart Technology, Gorilla Technology, ID3 Technology, Incode Technologies, NSENSE Corp., and SQISoft.
- ▷ We have retired results for six algorithms per our policy to only list results for two algorithms per developer. Results for retired algorithms appear in prior versions of this report in the [archive](#).

**2021-10-28 changes since 2021-09-08:**

- ▷ We have substantially revised the algorithm-specific report cards that are linked from the [FRVT results page](#). (Example: [HTML](#)).
- ▷ We have added results for first algorithms from eight new developers: Beijing Mendaxia Technology, Beijing Hisign Technology, Biocube Matrics, Clearview AI, Reveal Media, Toppan ID Gate, Verigram, and Viettel High Technology.
- ▷ We have added results for new algorithms from thirty returning developers: 20Face, 3divi, Canon Inc Chunghwa Telecom, Corsight, Decatur Industries, Deepglint, Dermalog, FaceTag, Fiberhome Telecommunication Technologies, GeoVision, ICM Airport Technics, Imagus Technology, InsightFace AI, Kakao Enterprise, Kookmin University, Line Corporation, N-Tech Lab, NotionTag Technologies, Realnetworks, Suprema ID, Taiwan-Certificate Authority, Toshiba, Tripleize, Trueface.ai, Veridas Digital Authentication, Visidon, VisionLabs, YooniK, and Yuan High-Tech Development.
- ▷ We have retired results for twenty algorithms per our policy to only list results for two algorithms per developer. Results for retired algorithms appear in prior versions of this report in the [archive](#).

**2021-09-08 changes since 2021-08-02:**

- ▷ We have added results for first algorithms from seven new developers: Griaule, SQISoft, Qnap Security, Techsign, Smart Engines, Verihubs, and Wuhan Tianyu Information Industry.
- ▷ We have added results for new algorithms from sixteen returning developers: ADVANCE.AI, AuthenMetric, CloudSmart Consulting, Code Everest Pvt, Cognitec Systems, Thales Gemalto Cogent, Intel Research Group, Omnidarde, Oz Forensics, Rank One Computing, Samsung S1 Corp, Securif AI, Tevian, TigerIT Americas, Universidade de Coimbra, and Vigilant Solutions
- ▷ We have retired results for eleven algorithms per our policy to only list results for two algorithms per developer. Results for retired algorithms appear in prior versions of this report in the [archive](#).

**2021-08-02 changes since 2021-06-25:**

- ▷ We have added results for first algorithms from eight new developers: Bee the Data, Closeli Inc, Coretech Knowledge Inc, Deepsense (France), ioNetworks Inc, Kakao Pay Corp, Seventh Sense Artificial Intelligence, and SK Telecom.
- ▷ We have added results for new algorithms from fifteen returning developers: Alchera Inc, Adera Global PTE, Aware, Bresee Technology, Cyberlink Corp, Expasoft LLC, Fujitsu Research and Development Center, Gorilla Technology, Idemia, Neurotechnology, NEO Systems, NHN Corp, Paravision, Panasonic R+D Center Singapore, and Shenzhen University-Macau University of Science and Technology.
- ▷ We have retired results for twelve algorithms per our policy to only list results for two algorithms per developer. Results for retired algorithms appear in prior versions of this report in the [archive](#).

**2021-06-25 changes since 2021-05-21:**

- ▷ We have added results for first algorithms from six new developers: Alice Biometrics, BOE Technology Group, Fincore, Neosecu, Sodec App, and Yuntu Data and Technology.

- ▷ We have added results for new algorithms from seven returning developers: Incode Technologies, HyperVerge, Mobbeel Solutions, Guangzhou Pixel Solutions, Remark Holdings, Sensetime, and Vietnam Posts and Telecommunications Group.
- ▷ We have retired results for four algorithms per our policy to only list results for two algorithms per developer. Results for retired algorithms appear in prior versions of this report in the [archive](#).

**2021-05-21** changes since 2021-04-26:

- ▷ We have added results for first algorithms from five new developers: Ekin Smart City Technologies, Suprema ID, Tripleize, Taiwan-Certificate Authority, and Vision Intelligence Center of Meituan.
- ▷ We have added results for new algorithms from eight returning developers: ID3 Technology, Imagus Technology, Momentum Digital, N-Tech Lab, NSENSE, Shanghai Jiao Tong University, Vision-Box, and Yuan High-Tech Development
- ▷ We have retired results for seven algorithms per our policy to only list results for two algorithms per developer. Results for retired algorithms appear in prior versions of this report in the [archive](#).

**2021-04-26** changes since 2021-04-16:

- ▷ We have added results for first algorithms from three new developers: Quantasoft, Rendip, and NEO Systems.
- ▷ We have added results for new algorithms from four returning developers: 3Divi, Realnetworks, Veridas Digital Authentication Solutions, and Universidade de Coimbra.
- ▷ We have retired results for three algorithms per our policy to only list results for two algorithms per developer. Results for retired algorithms appear in prior versions of this report in the [archive](#).

**2021-04-16** changes since 2021-03-19:

- ▷ We have added results for first algorithms from six new developers: 20Face, Beijing DeepSense Technologies, BitCenter UK, Enface, FaceTag, InsightFace AI, Line Corporation, Lema Labs, Nanjing Kiwi Network Technology, Omnidarde, Regula Forensics, and Suprema.
- ▷ We have added results for new algorithms from ten returning developers: CloudSmart Consulting, Dermalog, GeoVision, Neurotechnology, Panasonic R+D Center Singapore, Samsung S1, Securif AI, Trueface.ai, Vigilant Solutions, and Visidon.
- ▷ We have retired results for ten algorithms per our policy to only list results for two algorithms per developer. Results for retired algorithms appear in prior versions of this report in the [archive](#).

**2021-03-19** changes since 2021-03-05:

- ▷ We have added results for first algorithms from six new developers: Ajou University, AuthenMetric, Code Everest, Corsight, Papilon Savunma, and NHN Corp
- ▷ We have added results for new algorithms from seven returning developers: Alchera, Deepglint, Fiber-home Telecommunication Technologies, Kakao Enterprise, Kookmin University, Megvii/Face++, and NotionTag Technologies.

- ▷ We have updated many of the hyperlinked HTML report-cards to include seven figures on demographic dependence. Figures of this kind first appeared, and are documented in, the December 2019 document, [NIST Interagency Report 8280](#) on demographic differentials in face recognition. The figures quantify false negative dependence on demographics using “visa-border” comparisons, and false positive dependence using comparisons of “application” photos that uniformly of quality and similar to visa photos.

**2021-03-05** changes since 2021-01-19:

- ▷ We have added results for first algorithms from three new developers: IVA Cognitive, Mobbeel, and MoreDian Technology.
- ▷ We have added results for new algorithms from returning developers: Ability Enterprise - Andro Video, ACI Software, Adera Global, AnyVision, BioID Technologies, China Electronics Import-Export, Cognitec Systems, Fujitsu Research and Development Center, Glory, Guangzhou Pixel Solutions, Hengrui AI Technology, Incode Technologies, Intel Research, iQIYI, Mobai, Oz Forensics, Paravision, VisionLabs, and Xforward AI Technology.
- ▷ We have added a new “resources” tab to the main [webpage](#). It includes sortable columns for data related to speed, model size, storage, and memory consumption.
- ▷ We have retired results for 13 algorithms per our policy to only list results for two algorithms per developer. Results for retired algorithms appear in prior versions of this report in the [archive](#).

**2021-01-19** changes since 2020-12-18:

- ▷ This report adds results for first algorithms from four developers: Herta Security, Irex AI, Shenzhen University-Macau University of Science and Technology, and Vietnam Posts and Telecommunications Group. See Table 6 for more information.
- ▷ The report also includes results for thirteen developers who have previously submitted algorithms: Bresee Technology, Canon (previously Canon Information Technology (Beijing)), Cyberlink, CSA IntelliCloud Technology, Dahua Technology, ID3 Technology, Imagus Technology (Vixvizon), Moontime Smart Technology, N-Tech Lab, Thales Cogent, Veridas Digital Authentication Solutions, Vocord, and Yuan High-Tech Development.
- ▷ We have retired results for ten algorithms per our policy to only list results for two algorithms per developer. Results for retired algorithms appear in prior versions of this report in the [archive](#).

**2020-12-18** changes since 2020-10-09:

- ▷ This report adds results for first algorithms from ten developers: BitCenter UK, CloudSmart Consulting, Cubox, Institute of Computing Technology, Naver Corp, Minivision, NSENSE Corp, Viettel Group, Visage Technologies, and Xiamen University. See Table 6 for more information.
- ▷ The report also includes results for eighteen developers who have previously submitted algorithms: ADVANCE.AI, Awidit Systems, Chosun University, Dermalog, GeoVision, ICM Airport Technics, Idemia, Institute of Information Technologies, Kakao Enterprise, Neurotechnology, Panasonic R+D Center Singapore, Rank One Computing, SenseTime Group, Shanghai Jiao Tong University, TigerIT Americas LLC, Vigilant Solutions, Winsense, and YooniK

- ▷ We have retired results for twelve algorithms per our policy to only list results for two algorithms per developer. Results for retired algorithms appear in prior versions of this report in the [archive](#).

#### **Changes since September 18, 2020:**

- ▷ This report adds results for first algorithms from five developers: Aigen, Cortica, Kookmin University, Securif AI and Vinai.
- ▷ The report also includes results for three developers who have previously submitted algorithms: Fujitsu Laboratories, Hengrui AI, and X-Forward AI.
- ▷ In the per-algorithm report-cards linked from tables and the main webpage, we have added a chart to showing reduction in error rates over the course of FRVT i.e. from 2017 onwards for all algorithms supplied by that developer. Similarly we have added a chart showing error rate reductions for our test of protective face mask verification.
- ▷ We plan to continue evaluating algorithms on various mask datasets. We hold that algorithms should be capable of detecting masks and verifying identity of all combinations of masked and unmasked faces. We have accordingly increased the amount of time allowed to extract those features from 1.0 to 1.5 seconds.

#### **Changes since August 25, 2020:**

- ▷ This report adds results for first algorithms from eight new developers. Akurat Satu Indonesia, Cybercore, Decatur Industries, Innef Labs, Satellite Innovation/Eocortex, Expasoft, and Mobai.
- ▷ The report includes results for seven developers who have previously submitted algorithms: 3Divi, BioID Technologies, Incode Technologies, Innovatrics, iSAP Solution, Synology, and Tevian.
- ▷ We have retired results for five algorithms per our policy to only list results for two algorithms per developer. Results for retired algorithms appear in prior versions of this report in the [archive](#).

#### **Changes since July 27, 2020:**

- ▷ We have introduced per-algorithm report sheets. These are HTML documents linked from the accuracy tables in this report (i.e. Table 26) and on the FRVT 1:1 [homepage](#). The sheets contain interactive graphics allowing, for example, mouseover exploration of FNMR(T) and FMR(T). Some of their content had previously appeared in this document.
- ▷ This report adds results for algorithms from six new developers. ACI Software, Bresee Technology, Fiberhome Telecommunication Technologies, Imageware Systems, Oz Forensics, and Pensees.
- ▷ The report includes results for thirteen developers who have previously submitted algorithms: Canon Information Technology (Beijing), Cyberlink, Dahua Technology, Gorilla Technology, ID3 Technology, Intel Research Group, iQIYI Inc, Momentum Digital, Netbridge Technology, Tech5 SA, Shenzhen AiMall Tech, Vigilant Solutions, and VisionLabs.
- ▷ We have retired results for nine algorithms per our policy to only list results for two algorithms per developer. Results for retired algorithms appear in prior versions of this report in the [archive](#).

#### **Changes since May 18, 2020:**

- ▷ The report is the first FRVT update since the pandemic closed it from March to June 2020.

- ▷ This report includes results for algorithms from nine new developers: GeoVision Inc, Su Zhou NaZhi-TianDi Intelligent Technology, YooniK, AYF Technology, PXL Vision AG, Yuan High-Tech Development, Beihang University-ERCACAT, ICM Airport Technics, and Staqu Technologies
- ▷ This report includes results for algorithms from 15 returning developers Acer Incorporated, Antheus Technologia, Chosun University, Chunghwa Telecom, Idemia, Moontime Smart Technology, Neurotechnology, Guangzhou Pixel Solutions, Panasonic R+D Center Singapore, Rank One Computing, Scanovate, Shanghai University - Shanghai Film Academy, Synesis, Trueface.ai, and Veridas Digital Authentication Solutions
- ▷ We have retired results for ten algorithms per our policy to only list results for two algorithms per developer. Results for retired algorithms appear in prior versions of this report in the [archive](#).
- ▷ We separated timing and other resource consumption from the main participation table. The new Table 16 includes template generation durations for four kinds of images, not just mugshots.
- ▷ We have published a separate report, [NIST Interagency Report 8311](#) on accuracy of pre-pandemic algorithms on subjects wearing face masks. We plan to track improvements in accuracy on masked images going forward. In particular, we invite submission of algorithms that can detect whether a person is wearing a mask, extract features from the full face or the exposed periocular region, and do appropriate comparison. We do not intend to evaluate algorithms that assume 100% of images will be of masked individuals.

#### **Changes since March 25, 2020:**

- ▷ The report is a maintenance release - it does not add any new algorithms, and FRVT has been closed to new algorithms since mid March 2020.
- ▷ We modified the primary accuracy summary, Table 26, as follows:
  - ▷▷ For visa images, the column for FNMR at FMR = 0.0001 has been removed. The visa images are so highly controlled that the error rates for the most accurate algorithms are dominated by false rejection of very young children and by the presence of a few noisy greyscale images. For now, two visa columns remain: FNMR at  $FMR = 10^{-6}$  and, for matched covariates, FNMR at  $FMR = 10^{-4}$ .
  - ▷▷ We have inserted a new column labelled "BORDER" giving accuracy for comparison of moderately poor webcam border-crossing photos that exhibit pose variations, poor compression, and low contrast due to strong background illumination. The accuracies are the worst from all cooperative image datasets used in FRVT.
- ▷ Accordingly, we updated the failure-to-template rates in Table 34.
- ▷ We withdrew a figure showing how false matches are concentrated in certain visa images used in cross-comparison, because it didn't attempt to include demographic information.

#### **Changes since February 27, 2020:**

- ▷ The report adds results algorithms from two new developers: Beijing Alleyes Technology, and the Chinese University of Hong Kong. Results for newly submitted algorithms from two other developers will appear in the next report.
- ▷ The report adds results for algorithms from thirteen returning developers: ASUSTek Computer, Aware, Cyberlink Corp, Gorilla Technology, Innovative Technology, Kakao Enterprise, Lomonosov Moscow State University, Panasonic R+D Center Singapore, Shenzhen AiMall Technology, Shenzhen Intellifusion Technologies, Synology, Tech5 SA, and Via Technologies.

- ▷ Per policy to only list results for two algorithms per developer, we have dropped results for algorithms from Aware, Cyberlink, Gorilla Technology, Kakao Enterprise, Lomonosov Moscow State University, Panasonic R+D Center Singapore, and Tech5 SA.

### **Changes since January 20, 2020:**

- ▷ The report adds results for five new developers: Ability Enterprise (Andro Video), Chosun University, Fujitsu Research and Development Center, University of Coimbra, and Xforward AI Technology.
- ▷ The report adds results for algorithms from six returning developers: AlphaSSTG, Incode Technologies, Kneron, Shanghai Jiao Tong University, Vocord, and X-Laboratory.
- ▷ We have corrected template comparison timing numbers for algorithms submitted September 2019 to January 2020. The values reported previously were slower due to a software bug.
- ▷ We have dropped results for algorithms from Vocord and Incode per policy to only list results for two algorithms per developer.
- ▷ The [FRVT 1:1 homepage](#) has been updated with latest accuracy results.
- ▷ The [FRVT 1:N homepage](#) now includes an update to the September 2019 NIST Interagency Report 8271. The new report adds results for one-to-many search algorithms submitted to NIST from June 2019 to January 2020.

### **Changes since January 6, 2020:**

- ▷ Section 2 has been updated to better describe the Visa and Border images. The caption for Table 26 has been updated to better relate the accuracy values to particular image comparisons.
- ▷ The report adds results for five new developers: Acer, Advance.AI, Expasoft, Netbridge Technology, and Videmo Intelligent Videoanalyse.
- ▷ The report adds results for algorithms from 7 returning developers: China Electronics Import-Export Corp, Intel Research Group, ITMO University, Neurotechnology, N-Tech Lab, Rokid, and VisionLabs.
- ▷ We have dropped results from this edition of the report per policy to only list results for two algorithms per developer: N-Tech Lab, Neurotechnology, ITMO, Visionlabs, and CEIEC.
- ▷ The [FRVT homepage](#) has been updated with latest accuracy results.

### **Changes since November 11, 2019:**

- ▷ Table 16 has been updated to include runtime memory usage. This is the first time such a quantity has been reported. The value is the peak size of the resident set size logged during enrollment of single images.
- ▷ We have migrated summary results table to a new platform that supports sortable tables:  
<https://pages.nist.gov/frvt/html/frvt11.html>
- ▷ The report adds results for four new developers: Antheus Technologia, BioID Technologies SA, Canon Information Tech. (Beijing), Samsung S1 (listed in the tables as S1), and Taiwan AI Labs.
- ▷ The report adds results for algorithms from 13 returning developers: Anke Investments, Chunghwa Telecom, Deepglint, Institute of Information Technologies, iQIYI, Kneron, Ping An Technology, Paravision, KanKan Ai, Rokid Corporation, Shanghai Universiy - Shanghai Film Academy, Veridas Digital Authentication Solutions, and Videonetics Technology.

- ▷ We have dropped results from this edition of the report per policy to only list results for two algorithms per developer: remarkai-000, veridas-001, sensetime-001, iit-000, anke-003, and everai-002. Results for these are available in prior editions of this report linked from the FRVT page.
- ▷ We issued [NIST Interagency Report 8280: FRVT Part 3: Demographics](#) on 2019-12-19. It includes results for many of the algorithms covered by this report.

#### **Changes since October 16, 2019:**

- ▷ The report adds results for ten new developers: Ai-Union Technology, ASUSTek Computer, DiDi ChuXing Technology, Innovative Technology, Luxand, MVision, Pyramid Cyber Security + Forensic, Scanovate, Shenzhen AiMall Tech, and TUPU Technology.
- ▷ The report adds results for 12 returning developers: CTBC Bank Glory Gorilla Technology Guangzhou Pixel Solutions Imagus Technology Incode Technologies Lomonosov Moscow State University Rank One Computing Samtech InfoNet Shanghai Ulucu Electronics Technology Synesis, and Winsense.
- ▷ We have dropped results from this edition of the report per policy to only list results for two algorithms per developer: glory-000, gorilla-002, incode-003, rankone-006, and synesis-004.
- ▷ Results for five recently submitted algorithms will appear in the next report.

#### **Changes since September 11, 2019:**

- ▷ The report adds results for five new participants: Awidit Systems (Awiros), Momenmtum Digital (Sertis), Trueface AI, Shanghai Jiao Tong University, and X-Laboratory.
- ▷ The reports adds results for five new algorithms from returning developers: Cyberlink, Hengrui AI Technology, Idemia, Panasonic R+D Singapore, and Tevian. This causes three algorithm, to be de-listed from the report per policy to list results for two algorithms per developer.

#### **Changes since July 31 2019:**

- ▷ The HTML table on the [FRVT 1:1 homepage](#) has been updated to include a column for cross-domain Visa-Border verification. Results for this new dataset appeared in the July 29 report under the name "CrossEV" - these are now renamed "Visa-Border".
- ▷ The [FRVT 1:1 homepage](#) lists algorithms according to lowest mean rank accuracy:
 
$$\begin{aligned} & \text{Rank(FNMR}_{\text{VISA}} \text{ at FMR = 0.000001}) + \\ & \text{Rank(FNMR}_{\text{VISA-BORDER}} \text{ at FMR = 0.000001}) + \\ & \text{Rank(FNMR}_{\text{MUGSHOT}} \text{ at FMR = 0.00001 after 14 years}) + \\ & \text{Rank(FNMR}_{\text{WILD}} \text{ at FMR = 0.00001}) \end{aligned}$$

This ordering rewards high accuracy across all datasets.
- ▷ The main results in Table 26 is now in landscape format to accomodate extra columns for the Visa-Border set, and mugshot comparisons after at least 12 years.
- ▷ The report adds results for nine new participants: Alpha SSTG, Intel Research, ULSee, Chungwa Telecon, iSAP Solution, Rokid, Shenzhen EI Networks, CSA Intellicloud, Shenzhen Intellifusion Technologies.
- ▷ The reports adds results for six new algorithms from returning developers: Innovatrics, Dahua Technology, Tech5 SA, Intellivision, Nodeflux and Imperial College, London. One algorithm, from Imperial has been retired, per policy to list results for two algorithms per developer.
- ▷ The cross-country false match rate heatmaps have been replotted to reveal more structure by listing countries by region instead of alphabetically.

- ▷ The next version of this report will be posted around October 18, 2019.

#### **Changes since July 3 2019:**

- ▷ The HTML table on the [FRVT 1:1 homepage](#) has been updated to list the 20 most accurate developers rather than algorithms, choosing the most accurate algorithm from each developer based on visa and mugshot results. Also, the algorithms are ordered in terms of lowest mean rank across mugshot, visa and wild datasets, rewarding broad accuracy over a good result on one particular dataset.
- ▷ This report includes results for a new dataset - see the column labelled "visa-border" in Table 5. It compares a new set of high quality visa-like portraits with a set webcam border-crossing photos that exhibit moderately poor pose variations and background illumination. The two new sets are described in sections [2.2](#) and [2.3](#). The comparisons are "cross-domain" in that the algorithm must compare "visa" and "wild" images. Results for other algorithms will be added in future reports as they become available.
- ▷ This report adds results for algorithms from 9 developers submitted in early July 2019. These are from 3DiVi, Camvi, EverAI-Paravision, Facesoft, Farbar (F8), Institute of Information Technologies, Shanghai U. Film Academy, Via Technologies, and Ulucu Electronics Tech. Six of these are new participants.
- ▷ Several other algorithms have been submitted and are being evaluated. Results will be released in the next report, scheduled for September 5. That report will include results for new datasets.
- ▷ Older algorithms from Everai, Camvi and 3DiVi, have been retired, per the policy to list only two algorithms per developer.

#### **Changes since June 20 2019:**

- ▷ This report adds results for algorithms from 18 developers submitted in early June 2019. These are from CTBC Bank, Deep Glint, Thales Cogent, Ever AI Paravision, Gorilla Technology, Imagus, Incode, Kneron, N-Tech Lab, Neurotechnology, Notiontag Technologies, Star Hybrid, Videonetics, Vigilant Solutions, Winsense, Anke Investments, CEIEC, and DSK. Nine of these are new participants.
- ▷ Several other algorithms have been submitted and are being evaluated. Results will be released in the next report, scheduled for August 1.
- ▷ Older algorithms from Everai, Thales Cogent, Gorilla Technology, Incode, Neurotechnology, N-Tech Lab and Vigilant Solutions have been retired, per the policy to list only two algorithms per developer.

#### **Changes since April 2019:**

- ▷ This report adds results for nine algorithms from nine developers submitted in early June 2019. These are from Tencent Deepsea, Hengrui, Kedacom, Moontime, Guangzhou Pixel, Rank One Computing, Synesis, Sensetime and Vocord.
- ▷ Another 23 algorithms have been submitted and are being evaluated. Results will be released in the next report, scheduled for July 3.
- ▷ Older algorithms for Rank One, Synesis, and Vocord have been retired, per the policy to list only two algorithms per developer.

#### **Changes since February 2019:**

- ▷ This report adds results for 49 algorithms from 42 developers submitted in early March 2019.
- ▷ This report omits results for algorithms that we retired. We retired for three reasons: 1. The developer submitted a new algorithm, and we only list two. 2. The algorithm needs a GPU, and we no longer allow GPU-based algorithms. 3. Inoperable algorithms.
- ▷ Previous results for retired algorithms are available in older editions of this report linked [here](#).
- ▷ The mugshot database used from February 2017 to January 2019 has been replaced with an extract of the mugshot database documented in NIST Interagency Report 8238, November 2018. The new mugshot set is described in section [2.4](#) and is adopted because:

- ▷▷ It has much better identity label integrity, so that false non-match rates are substantially lower than those reported in FRVT 1:1 reports to date - see Figure 84.
- ▷▷ It includes images collected over a 17 year period such that ageing can be much better characterized - - see Figure 303.
- ▷ Using the new mugshot database, Figure 303 shows accuracy for four demographic groups identified in the biographic metadata that accompanies the data: black females, black males, white females and white males.
- ▷ The report adds Figure 21 with results for the twenty human-difficult pairs used in the May 2018 paper *Face recognition accuracy of forensic examiners, superrecognition, and face recognition algorithms* by Phillips et al. [1].
- ▷ The report uses an update to the wild image database that corrects some ground truth labels.
- ▷ Some results for the child exploitation database are not complete. They are typically updated less frequently than for other image sets.

## Contents

<b>ACKNOWLEDGMENTS</b>	<b>1</b>
<b>DISCLAIMER</b>	<b>1</b>
<b>INSTITUTIONAL REVIEW BOARD</b>	<b>1</b>
<b>1 METRICS</b>	<b>49</b>
1.1 CORE ACCURACY . . . . .	49
1.2 MULTI-TEMPLATE SCORING METHODOLOGY . . . . .	49
<b>2 DATASETS</b>	<b>50</b>
2.1 VISA IMAGES . . . . .	50
2.2 APPLICATION IMAGES . . . . .	50
2.3 BORDER CROSSING IMAGES . . . . .	50
2.4 MUGSHOT IMAGES . . . . .	51
2.5 WILD IMAGES . . . . .	51
<b>3 RESULTS</b>	<b>51</b>
3.1 TEST GOALS . . . . .	51
3.2 TEST DESIGN . . . . .	52
3.3 FAILURE TO ENROLL . . . . .	55
3.4 RECOGNITION ACCURACY . . . . .	64
3.5 GENUINE DISTRIBUTION STABILITY . . . . .	304
3.5.1 EFFECT OF BIRTH PLACE ON THE GENUINE DISTRIBUTION . . . . .	304
3.5.2 EFFECT OF AGEING . . . . .	340
3.5.3 EFFECT OF AGE ON GENUINE SUBJECTS . . . . .	367
3.6 IMPOSTOR DISTRIBUTION STABILITY . . . . .	404
3.6.1 EFFECT OF BIRTH PLACE ON THE IMPOSTOR DISTRIBUTION . . . . .	404
3.6.2 EFFECT OF AGE ON IMPOSTORS . . . . .	408

## List of Tables

1 PARTICIPANT INFORMATION . . . . .	21
2 PARTICIPANT INFORMATION . . . . .	22
3 PARTICIPANT INFORMATION . . . . .	23
4 PARTICIPANT INFORMATION . . . . .	24
5 PARTICIPANT INFORMATION . . . . .	25
6 PARTICIPANT INFORMATION . . . . .	26
7 ALGORITHM SUMMARY . . . . .	27
8 ALGORITHM SUMMARY . . . . .	28
9 ALGORITHM SUMMARY . . . . .	29
10 ALGORITHM SUMMARY . . . . .	30
11 ALGORITHM SUMMARY . . . . .	31
12 ALGORITHM SUMMARY . . . . .	32
13 ALGORITHM SUMMARY . . . . .	33
14 ALGORITHM SUMMARY . . . . .	34
15 ALGORITHM SUMMARY . . . . .	35
16 ALGORITHM SUMMARY . . . . .	36
17 FALSE NON-MATCH RATE . . . . .	37
18 FALSE NON-MATCH RATE . . . . .	38
19 FALSE NON-MATCH RATE . . . . .	39
20 FALSE NON-MATCH RATE . . . . .	40

21	FALSE NON-MATCH RATE	41
22	FALSE NON-MATCH RATE	42
23	FALSE NON-MATCH RATE	43
24	FALSE NON-MATCH RATE	44
25	FALSE NON-MATCH RATE	45
26	FALSE NON-MATCH RATE	46
27	FAILURE TO ENROL RATES	56
28	FAILURE TO ENROL RATES	57
29	FAILURE TO ENROL RATES	58
30	FAILURE TO ENROL RATES	59
31	FAILURE TO ENROL RATES	60
32	FAILURE TO ENROL RATES	61
33	FAILURE TO ENROL RATES	62
34	FAILURE TO ENROL RATES	63

## List of Figures

1	PERFORMANCE SUMMARY: FNMR VS. TEMPLATE SIZE TRADEOFF	47
2	PERFORMANCE SUMMARY: FNMR VS. TEMPLATE TIME TRADEOFF	48
3	EXAMPLE IMAGES	52
(A)	Visa	52
(B)	MUGSHOT	52
(C)	WILD	52
(D)	BORDER	52
4	PERFORMANCE ON 20 HUMAN-DIFFICULT PAIRS	65
5	PERFORMANCE ON 20 HUMAN-DIFFICULT PAIRS	66
6	PERFORMANCE ON 20 HUMAN-DIFFICULT PAIRS	67
7	PERFORMANCE ON 20 HUMAN-DIFFICULT PAIRS	68
8	PERFORMANCE ON 20 HUMAN-DIFFICULT PAIRS	69
9	PERFORMANCE ON 20 HUMAN-DIFFICULT PAIRS	70
10	PERFORMANCE ON 20 HUMAN-DIFFICULT PAIRS	71
11	PERFORMANCE ON 20 HUMAN-DIFFICULT PAIRS	72
12	PERFORMANCE ON 20 HUMAN-DIFFICULT PAIRS	73
13	PERFORMANCE ON 20 HUMAN-DIFFICULT PAIRS	74
14	PERFORMANCE ON 20 HUMAN-DIFFICULT PAIRS	75
15	PERFORMANCE ON 20 HUMAN-DIFFICULT PAIRS	76
16	PERFORMANCE ON 20 HUMAN-DIFFICULT PAIRS	77
17	PERFORMANCE ON 20 HUMAN-DIFFICULT PAIRS	78
18	PERFORMANCE ON 20 HUMAN-DIFFICULT PAIRS	79
19	PERFORMANCE ON 20 HUMAN-DIFFICULT PAIRS	80
20	PERFORMANCE ON 20 HUMAN-DIFFICULT PAIRS	81
21	PERFORMANCE ON 20 HUMAN-DIFFICULT PAIRS	82
22	ERROR TRADEOFF CHARACTERISTIC: VISA IMAGES	83
23	ERROR TRADEOFF CHARACTERISTIC: VISA IMAGES	84
24	ERROR TRADEOFF CHARACTERISTIC: VISA IMAGES	85
25	ERROR TRADEOFF CHARACTERISTIC: VISA IMAGES	86
26	ERROR TRADEOFF CHARACTERISTIC: VISA IMAGES	87
27	ERROR TRADEOFF CHARACTERISTIC: VISA IMAGES	88
28	ERROR TRADEOFF CHARACTERISTIC: VISA IMAGES	89
29	ERROR TRADEOFF CHARACTERISTIC: VISA IMAGES	90
30	ERROR TRADEOFF CHARACTERISTIC: VISA IMAGES	91
31	ERROR TRADEOFF CHARACTERISTIC: VISA IMAGES	92
32	ERROR TRADEOFF CHARACTERISTIC: VISA IMAGES	93
33	ERROR TRADEOFF CHARACTERISTIC: VISA IMAGES	94
34	ERROR TRADEOFF CHARACTERISTIC: VISA IMAGES	95

35	ERROR TRADEOFF CHARACTERISTIC: VISA IMAGES	96
36	ERROR TRADEOFF CHARACTERISTIC: VISA IMAGES	97
37	ERROR TRADEOFF CHARACTERISTIC: VISA IMAGES	98
38	ERROR TRADEOFF CHARACTERISTIC: VISA IMAGES	99
39	ERROR TRADEOFF CHARACTERISTIC: VISA IMAGES	100
40	ERROR TRADEOFF CHARACTERISTIC: VISA IMAGES	101
41	ERROR TRADEOFF CHARACTERISTIC: VISA IMAGES	102
42	ERROR TRADEOFF CHARACTERISTIC: VISA IMAGES	103
43	ERROR TRADEOFF CHARACTERISTIC: VISA IMAGES	104
44	ERROR TRADEOFF CHARACTERISTIC: VISA IMAGES	105
45	ERROR TRADEOFF CHARACTERISTIC: VISA IMAGES	106
46	ERROR TRADEOFF CHARACTERISTIC: VISA IMAGES	107
47	ERROR TRADEOFF CHARACTERISTIC: VISA IMAGES	108
48	ERROR TRADEOFF CHARACTERISTIC: VISA IMAGES	109
49	ERROR TRADEOFF CHARACTERISTIC: VISA IMAGES	110
50	ERROR TRADEOFF CHARACTERISTIC: VISA IMAGES	111
51	ERROR TRADEOFF CHARACTERISTIC: VISA IMAGES	112
52	ERROR TRADEOFF CHARACTERISTIC: VISA IMAGES	113
53	ERROR TRADEOFF CHARACTERISTIC: VISA IMAGES	114
54	ERROR TRADEOFF CHARACTERISTIC: VISA IMAGES	115
55	ERROR TRADEOFF CHARACTERISTIC: VISA IMAGES	116
56	ERROR TRADEOFF CHARACTERISTIC: VISA IMAGES	117
57	ERROR TRADEOFF CHARACTERISTIC: VISA IMAGES	118
58	ERROR TRADEOFF CHARACTERISTIC: VISA IMAGES	119
59	ERROR TRADEOFF CHARACTERISTIC: VISA IMAGES	120
60	ERROR TRADEOFF CHARACTERISTIC: VISA IMAGES	121
61	ERROR TRADEOFF CHARACTERISTIC: VISA IMAGES	122
62	ERROR TRADEOFF CHARACTERISTIC: VISA IMAGES	123
63	ERROR TRADEOFF CHARACTERISTIC: VISA IMAGES	124
64	ERROR TRADEOFF CHARACTERISTIC: MUGSHOT IMAGES	125
65	ERROR TRADEOFF CHARACTERISTIC: MUGSHOT IMAGES	126
66	ERROR TRADEOFF CHARACTERISTIC: MUGSHOT IMAGES	127
67	ERROR TRADEOFF CHARACTERISTIC: MUGSHOT IMAGES	128
68	ERROR TRADEOFF CHARACTERISTIC: MUGSHOT IMAGES	129
69	ERROR TRADEOFF CHARACTERISTIC: MUGSHOT IMAGES	130
70	ERROR TRADEOFF CHARACTERISTIC: MUGSHOT IMAGES	131
71	ERROR TRADEOFF CHARACTERISTIC: MUGSHOT IMAGES	132
72	ERROR TRADEOFF CHARACTERISTIC: MUGSHOT IMAGES	133
73	ERROR TRADEOFF CHARACTERISTIC: MUGSHOT IMAGES	134
74	ERROR TRADEOFF CHARACTERISTIC: MUGSHOT IMAGES	135
75	ERROR TRADEOFF CHARACTERISTIC: MUGSHOT IMAGES	136
76	ERROR TRADEOFF CHARACTERISTIC: MUGSHOT IMAGES	137
77	ERROR TRADEOFF CHARACTERISTIC: MUGSHOT IMAGES	138
78	ERROR TRADEOFF CHARACTERISTIC: MUGSHOT IMAGES	139
79	ERROR TRADEOFF CHARACTERISTIC: MUGSHOT IMAGES	140
80	ERROR TRADEOFF CHARACTERISTIC: MUGSHOT IMAGES	141
81	ERROR TRADEOFF CHARACTERISTIC: MUGSHOT IMAGES	142
82	ERROR TRADEOFF CHARACTERISTIC: MUGSHOT IMAGES	143
83	ERROR TRADEOFF CHARACTERISTIC: MUGSHOT IMAGES	144
84	ERROR TRADEOFF CHARACTERISTIC: MUGSHOT IMAGES	145
85	ERROR TRADEOFF CHARACTERISTIC: WILD IMAGES	146
86	ERROR TRADEOFF CHARACTERISTIC: WILD IMAGES	147
87	ERROR TRADEOFF CHARACTERISTIC: WILD IMAGES	148
88	ERROR TRADEOFF CHARACTERISTIC: WILD IMAGES	149
89	ERROR TRADEOFF CHARACTERISTIC: WILD IMAGES	150
90	ERROR TRADEOFF CHARACTERISTIC: WILD IMAGES	151

91	ERROR TRADEOFF CHARACTERISTIC: WILD IMAGES	152
92	ERROR TRADEOFF CHARACTERISTIC: WILD IMAGES	153
93	ERROR TRADEOFF CHARACTERISTIC: WILD IMAGES	154
94	ERROR TRADEOFF CHARACTERISTIC: WILD IMAGES	155
95	ERROR TRADEOFF CHARACTERISTIC: WILD IMAGES	156
96	ERROR TRADEOFF CHARACTERISTIC: WILD IMAGES	157
97	ERROR TRADEOFF CHARACTERISTIC: WILD IMAGES	158
98	ERROR TRADEOFF CHARACTERISTIC: WILD IMAGES	159
99	ERROR TRADEOFF CHARACTERISTIC: WILD IMAGES	160
100	ERROR TRADEOFF CHARACTERISTIC: WILD IMAGES	161
101	ERROR TRADEOFF CHARACTERISTIC: WILD IMAGES	162
102	FALSE MATCH RATES WITHIN AND ACROSS DEMOGRAPHIC GROUPS	163
103	FALSE MATCH RATES WITHIN AND ACROSS DEMOGRAPHIC GROUPS	164
104	FALSE MATCH RATES WITHIN AND ACROSS DEMOGRAPHIC GROUPS	165
105	FALSE MATCH RATES WITHIN AND ACROSS DEMOGRAPHIC GROUPS	166
106	FALSE MATCH RATES WITHIN AND ACROSS DEMOGRAPHIC GROUPS	167
107	FALSE MATCH RATES WITHIN AND ACROSS DEMOGRAPHIC GROUPS	168
108	FALSE MATCH RATES WITHIN AND ACROSS DEMOGRAPHIC GROUPS	169
109	FALSE MATCH RATES WITHIN AND ACROSS DEMOGRAPHIC GROUPS	170
110	FALSE MATCH RATES WITHIN AND ACROSS DEMOGRAPHIC GROUPS	171
111	FALSE MATCH RATES WITHIN AND ACROSS DEMOGRAPHIC GROUPS	172
112	FALSE MATCH RATES WITHIN AND ACROSS DEMOGRAPHIC GROUPS	173
113	FALSE MATCH RATES WITHIN AND ACROSS DEMOGRAPHIC GROUPS	174
114	FALSE MATCH RATES WITHIN AND ACROSS DEMOGRAPHIC GROUPS	175
115	FALSE MATCH RATES WITHIN AND ACROSS DEMOGRAPHIC GROUPS	176
116	FALSE MATCH RATES WITHIN AND ACROSS DEMOGRAPHIC GROUPS	177
117	FALSE MATCH RATES WITHIN AND ACROSS DEMOGRAPHIC GROUPS	178
118	FALSE MATCH RATES WITHIN AND ACROSS DEMOGRAPHIC GROUPS	179
119	FALSE MATCH RATES WITHIN AND ACROSS DEMOGRAPHIC GROUPS	180
120	FALSE MATCH RATES WITHIN AND ACROSS DEMOGRAPHIC GROUPS	181
121	FALSE MATCH RATES WITHIN AND ACROSS DEMOGRAPHIC GROUPS	182
122	FALSE MATCH RATES WITHIN AND ACROSS DEMOGRAPHIC GROUPS	183
123	SEX AND RACE EFFECTS: MUGSHOT IMAGES	184
124	SEX AND RACE EFFECTS: MUGSHOT IMAGES	185
125	SEX AND RACE EFFECTS: MUGSHOT IMAGES	186
126	SEX AND RACE EFFECTS: MUGSHOT IMAGES	187
127	SEX AND RACE EFFECTS: MUGSHOT IMAGES	188
128	SEX AND RACE EFFECTS: MUGSHOT IMAGES	189
129	SEX AND RACE EFFECTS: MUGSHOT IMAGES	190
130	SEX AND RACE EFFECTS: MUGSHOT IMAGES	191
131	SEX AND RACE EFFECTS: MUGSHOT IMAGES	192
132	SEX AND RACE EFFECTS: MUGSHOT IMAGES	193
133	SEX AND RACE EFFECTS: MUGSHOT IMAGES	194
134	SEX AND RACE EFFECTS: MUGSHOT IMAGES	195
135	SEX AND RACE EFFECTS: MUGSHOT IMAGES	196
136	SEX AND RACE EFFECTS: MUGSHOT IMAGES	197
137	SEX AND RACE EFFECTS: MUGSHOT IMAGES	198
138	SEX AND RACE EFFECTS: MUGSHOT IMAGES	199
139	SEX AND RACE EFFECTS: MUGSHOT IMAGES	200
140	SEX AND RACE EFFECTS: MUGSHOT IMAGES	201
141	SEX AND RACE EFFECTS: MUGSHOT IMAGES	202
142	SEX AND RACE EFFECTS: MUGSHOT IMAGES	203
143	SEX AND RACE EFFECTS: MUGSHOT IMAGES	204
144	SEX EFFECTS: VISA IMAGES	205
145	SEX EFFECTS: VISA IMAGES	206
146	SEX EFFECTS: VISA IMAGES	207
147	SEX EFFECTS: VISA IMAGES	208

148 SEX EFFECTS: VISA IMAGES . . . . .	209
149 SEX EFFECTS: VISA IMAGES . . . . .	210
150 SEX EFFECTS: VISA IMAGES . . . . .	211
151 SEX EFFECTS: VISA IMAGES . . . . .	212
152 SEX EFFECTS: VISA IMAGES . . . . .	213
153 SEX EFFECTS: VISA IMAGES . . . . .	214
154 SEX EFFECTS: VISA IMAGES . . . . .	215
155 SEX EFFECTS: VISA IMAGES . . . . .	216
156 SEX EFFECTS: VISA IMAGES . . . . .	217
157 SEX EFFECTS: VISA IMAGES . . . . .	218
158 SEX EFFECTS: VISA IMAGES . . . . .	219
159 SEX EFFECTS: VISA IMAGES . . . . .	220
160 SEX EFFECTS: VISA IMAGES . . . . .	221
161 SEX EFFECTS: VISA IMAGES . . . . .	222
162 SEX EFFECTS: VISA IMAGES . . . . .	223
163 SEX EFFECTS: VISA IMAGES . . . . .	224
164 SEX EFFECTS: VISA IMAGES . . . . .	225
165 SEX EFFECTS: VISA IMAGES . . . . .	226
166 SEX EFFECTS: VISA IMAGES . . . . .	227
167 SEX EFFECTS: VISA IMAGES . . . . .	228
168 SEX EFFECTS: VISA IMAGES . . . . .	229
169 SEX EFFECTS: VISA IMAGES . . . . .	230
170 SEX EFFECTS: VISA IMAGES . . . . .	231
171 SEX EFFECTS: VISA IMAGES . . . . .	232
172 SEX EFFECTS: VISA IMAGES . . . . .	233
173 SEX EFFECTS: VISA IMAGES . . . . .	234
174 SEX EFFECTS: VISA IMAGES . . . . .	235
175 SEX EFFECTS: VISA IMAGES . . . . .	236
176 SEX EFFECTS: VISA IMAGES . . . . .	237
177 SEX EFFECTS: VISA IMAGES . . . . .	238
178 SEX EFFECTS: VISA IMAGES . . . . .	239
179 FALSE MATCH RATE CALIBRATION: MUGSHOT IMAGES . . . . .	240
180 FALSE MATCH RATE CALIBRATION: MUGSHOT IMAGES . . . . .	241
181 FALSE MATCH RATE CALIBRATION: MUGSHOT IMAGES . . . . .	242
182 FALSE MATCH RATE CALIBRATION: MUGSHOT IMAGES . . . . .	243
183 FALSE MATCH RATE CALIBRATION: MUGSHOT IMAGES . . . . .	244
184 FALSE MATCH RATE CALIBRATION: MUGSHOT IMAGES . . . . .	245
185 FALSE MATCH RATE CALIBRATION: MUGSHOT IMAGES . . . . .	246
186 FALSE MATCH RATE CALIBRATION: MUGSHOT IMAGES . . . . .	247
187 FALSE MATCH RATE CALIBRATION: MUGSHOT IMAGES . . . . .	248
188 FALSE MATCH RATE CALIBRATION: MUGSHOT IMAGES . . . . .	249
189 FALSE MATCH RATE CALIBRATION: MUGSHOT IMAGES . . . . .	250
190 FALSE MATCH RATE CALIBRATION: MUGSHOT IMAGES . . . . .	251
191 FALSE MATCH RATE CALIBRATION: MUGSHOT IMAGES . . . . .	252
192 FALSE MATCH RATE CALIBRATION: MUGSHOT IMAGES . . . . .	253
193 FALSE MATCH RATE CALIBRATION: MUGSHOT IMAGES . . . . .	254
194 FALSE MATCH RATE CALIBRATION: MUGSHOT IMAGES . . . . .	255
195 FALSE MATCH RATE CALIBRATION: MUGSHOT IMAGES . . . . .	256
196 FALSE MATCH RATE CALIBRATION: MUGSHOT IMAGES . . . . .	257
197 FALSE MATCH RATE CALIBRATION: MUGSHOT IMAGES . . . . .	258
198 FALSE MATCH RATE CALIBRATION: MUGSHOT IMAGES . . . . .	259
199 FALSE MATCH RATE CALIBRATION: MUGSHOT IMAGES . . . . .	260
200 FALSE MATCH RATE CALIBRATION: VISA IMAGES . . . . .	261
201 FALSE MATCH RATE CALIBRATION: VISA IMAGES . . . . .	262
202 FALSE MATCH RATE CALIBRATION: VISA IMAGES . . . . .	263
203 FALSE MATCH RATE CALIBRATION: VISA IMAGES . . . . .	264
204 FALSE MATCH RATE CALIBRATION: VISA IMAGES . . . . .	265

205	FALSE MATCH RATE CALIBRATION: VISA IMAGES	266
206	FALSE MATCH RATE CALIBRATION: VISA IMAGES	267
207	FALSE MATCH RATE CALIBRATION: VISA IMAGES	268
208	FALSE MATCH RATE CALIBRATION: VISA IMAGES	269
209	FALSE MATCH RATE CALIBRATION: VISA IMAGES	270
210	FALSE MATCH RATE CALIBRATION: VISA IMAGES	271
211	FALSE MATCH RATE CALIBRATION: VISA IMAGES	272
212	FALSE MATCH RATE CALIBRATION: VISA IMAGES	273
213	FALSE MATCH RATE CALIBRATION: VISA IMAGES	274
214	FALSE MATCH RATE CALIBRATION: VISA IMAGES	275
215	FALSE MATCH RATE CALIBRATION: VISA IMAGES	276
216	FALSE MATCH RATE CALIBRATION: VISA IMAGES	277
217	FALSE MATCH RATE CALIBRATION: VISA IMAGES	278
218	FALSE MATCH RATE CALIBRATION: VISA IMAGES	279
219	FALSE MATCH RATE CALIBRATION: VISA IMAGES	280
220	FALSE MATCH RATE CALIBRATION: VISA IMAGES	281
221	FALSE MATCH RATE CALIBRATION: VISA IMAGES	282
222	FALSE MATCH RATE CALIBRATION: VISA IMAGES	283
223	FALSE MATCH RATE CALIBRATION: VISA IMAGES	284
224	FALSE MATCH RATE CALIBRATION: VISA IMAGES	285
225	FALSE MATCH RATE CALIBRATION: VISA IMAGES	286
226	FALSE MATCH RATE CALIBRATION: VISA IMAGES	287
227	FALSE MATCH RATE CALIBRATION: VISA IMAGES	288
228	FALSE MATCH RATE CALIBRATION: VISA IMAGES	289
229	FALSE MATCH RATE CALIBRATION: VISA IMAGES	290
230	FALSE MATCH RATE CALIBRATION: VISA IMAGES	291
231	FALSE MATCH RATE CALIBRATION: VISA IMAGES	292
232	FALSE MATCH RATE CALIBRATION: VISA IMAGES	293
233	FALSE MATCH RATE CALIBRATION: VISA IMAGES	294
234	FALSE MATCH RATE CALIBRATION: VISA IMAGES	295
235	FALSE MATCH RATE CALIBRATION: VISA IMAGES	296
236	FALSE MATCH RATE CALIBRATION: VISA IMAGES	297
237	FALSE MATCH RATE CALIBRATION: VISA IMAGES	298
238	FALSE MATCH RATE CALIBRATION: VISA IMAGES	299
239	FALSE MATCH RATE CALIBRATION: VISA IMAGES	300
240	FALSE MATCH RATE CALIBRATION: VISA IMAGES	301
241	FALSE MATCH RATE CALIBRATION: VISA IMAGES	302
242	FALSE MATCH RATE CALIBRATION: VISA IMAGES	303
243	EFFECT OF COUNTRY OF BIRTH ON FNMR	305
244	EFFECT OF COUNTRY OF BIRTH ON FNMR	306
245	EFFECT OF COUNTRY OF BIRTH ON FNMR	307
246	EFFECT OF COUNTRY OF BIRTH ON FNMR	308
247	EFFECT OF COUNTRY OF BIRTH ON FNMR	309
248	EFFECT OF COUNTRY OF BIRTH ON FNMR	310
249	EFFECT OF COUNTRY OF BIRTH ON FNMR	311
250	EFFECT OF COUNTRY OF BIRTH ON FNMR	312
251	EFFECT OF COUNTRY OF BIRTH ON FNMR	313
252	EFFECT OF COUNTRY OF BIRTH ON FNMR	314
253	EFFECT OF COUNTRY OF BIRTH ON FNMR	315
254	EFFECT OF COUNTRY OF BIRTH ON FNMR	316
255	EFFECT OF COUNTRY OF BIRTH ON FNMR	317
256	EFFECT OF COUNTRY OF BIRTH ON FNMR	318
257	EFFECT OF COUNTRY OF BIRTH ON FNMR	319
258	EFFECT OF COUNTRY OF BIRTH ON FNMR	320
259	EFFECT OF COUNTRY OF BIRTH ON FNMR	321
260	EFFECT OF COUNTRY OF BIRTH ON FNMR	322
261	EFFECT OF COUNTRY OF BIRTH ON FNMR	323

262	EFFECT OF COUNTRY OF BIRTH ON FNMR . . . . .	324
263	EFFECT OF COUNTRY OF BIRTH ON FNMR . . . . .	325
264	EFFECT OF COUNTRY OF BIRTH ON FNMR . . . . .	326
265	EFFECT OF COUNTRY OF BIRTH ON FNMR . . . . .	327
266	EFFECT OF COUNTRY OF BIRTH ON FNMR . . . . .	328
267	EFFECT OF COUNTRY OF BIRTH ON FNMR . . . . .	329
268	EFFECT OF COUNTRY OF BIRTH ON FNMR . . . . .	330
269	EFFECT OF COUNTRY OF BIRTH ON FNMR . . . . .	331
270	EFFECT OF COUNTRY OF BIRTH ON FNMR . . . . .	332
271	EFFECT OF COUNTRY OF BIRTH ON FNMR . . . . .	333
272	EFFECT OF COUNTRY OF BIRTH ON FNMR . . . . .	334
273	EFFECT OF COUNTRY OF BIRTH ON FNMR . . . . .	335
274	EFFECT OF COUNTRY OF BIRTH ON FNMR . . . . .	336
275	EFFECT OF COUNTRY OF BIRTH ON FNMR . . . . .	337
276	EFFECT OF COUNTRY OF BIRTH ON FNMR . . . . .	338
277	EFFECT OF COUNTRY OF BIRTH ON FNMR . . . . .	339
278	ERROR TRADEOFF CHARACTERISTIC: MUGSHOT IMAGES . . . . .	341
279	ERROR TRADEOFF CHARACTERISTIC: MUGSHOT IMAGES . . . . .	342
280	ERROR TRADEOFF CHARACTERISTIC: MUGSHOT IMAGES . . . . .	343
281	ERROR TRADEOFF CHARACTERISTIC: MUGSHOT IMAGES . . . . .	344
282	ERROR TRADEOFF CHARACTERISTIC: MUGSHOT IMAGES . . . . .	345
283	ERROR TRADEOFF CHARACTERISTIC: MUGSHOT IMAGES . . . . .	346
284	ERROR TRADEOFF CHARACTERISTIC: MUGSHOT IMAGES . . . . .	347
285	ERROR TRADEOFF CHARACTERISTIC: MUGSHOT IMAGES . . . . .	348
286	ERROR TRADEOFF CHARACTERISTIC: MUGSHOT IMAGES . . . . .	349
287	ERROR TRADEOFF CHARACTERISTIC: MUGSHOT IMAGES . . . . .	350
288	ERROR TRADEOFF CHARACTERISTIC: MUGSHOT IMAGES . . . . .	351
289	ERROR TRADEOFF CHARACTERISTIC: MUGSHOT IMAGES . . . . .	352
290	ERROR TRADEOFF CHARACTERISTIC: MUGSHOT IMAGES . . . . .	353
291	ERROR TRADEOFF CHARACTERISTIC: MUGSHOT IMAGES . . . . .	354
292	ERROR TRADEOFF CHARACTERISTIC: MUGSHOT IMAGES . . . . .	355
293	ERROR TRADEOFF CHARACTERISTIC: MUGSHOT IMAGES . . . . .	356
294	ERROR TRADEOFF CHARACTERISTIC: MUGSHOT IMAGES . . . . .	357
295	ERROR TRADEOFF CHARACTERISTIC: MUGSHOT IMAGES . . . . .	358
296	ERROR TRADEOFF CHARACTERISTIC: MUGSHOT IMAGES . . . . .	359
297	ERROR TRADEOFF CHARACTERISTIC: MUGSHOT IMAGES . . . . .	360
298	ERROR TRADEOFF CHARACTERISTIC: MUGSHOT IMAGES . . . . .	361
299	ERROR TRADEOFF CHARACTERISTIC: MUGSHOT IMAGES . . . . .	362
300	ERROR TRADEOFF CHARACTERISTIC: MUGSHOT IMAGES . . . . .	363
301	ERROR TRADEOFF CHARACTERISTIC: MUGSHOT IMAGES . . . . .	364
302	ERROR TRADEOFF CHARACTERISTIC: MUGSHOT IMAGES . . . . .	365
303	ERROR TRADEOFF CHARACTERISTIC: MUGSHOT IMAGES . . . . .	366
304	EFFECT OF SUBJECT AGE ON FNMR . . . . .	368
305	EFFECT OF SUBJECT AGE ON FNMR . . . . .	369
306	EFFECT OF SUBJECT AGE ON FNMR . . . . .	370
307	EFFECT OF SUBJECT AGE ON FNMR . . . . .	371
308	EFFECT OF SUBJECT AGE ON FNMR . . . . .	372
309	EFFECT OF SUBJECT AGE ON FNMR . . . . .	373
310	EFFECT OF SUBJECT AGE ON FNMR . . . . .	374
311	EFFECT OF SUBJECT AGE ON FNMR . . . . .	375
312	EFFECT OF SUBJECT AGE ON FNMR . . . . .	376
313	EFFECT OF SUBJECT AGE ON FNMR . . . . .	377
314	EFFECT OF SUBJECT AGE ON FNMR . . . . .	378
315	EFFECT OF SUBJECT AGE ON FNMR . . . . .	379
316	EFFECT OF SUBJECT AGE ON FNMR . . . . .	380

317	EFFECT OF SUBJECT AGE ON FNMR	381
318	EFFECT OF SUBJECT AGE ON FNMR	382
319	EFFECT OF SUBJECT AGE ON FNMR	383
320	EFFECT OF SUBJECT AGE ON FNMR	384
321	EFFECT OF SUBJECT AGE ON FNMR	385
322	EFFECT OF SUBJECT AGE ON FNMR	386
323	EFFECT OF SUBJECT AGE ON FNMR	387
324	EFFECT OF SUBJECT AGE ON FNMR	388
325	EFFECT OF SUBJECT AGE ON FNMR	389
326	EFFECT OF SUBJECT AGE ON FNMR	390
327	EFFECT OF SUBJECT AGE ON FNMR	391
328	EFFECT OF SUBJECT AGE ON FNMR	392
329	EFFECT OF SUBJECT AGE ON FNMR	393
330	EFFECT OF SUBJECT AGE ON FNMR	394
331	EFFECT OF SUBJECT AGE ON FNMR	395
332	EFFECT OF SUBJECT AGE ON FNMR	396
333	EFFECT OF SUBJECT AGE ON FNMR	397
334	EFFECT OF SUBJECT AGE ON FNMR	398
335	EFFECT OF SUBJECT AGE ON FNMR	399
336	EFFECT OF SUBJECT AGE ON FNMR	400
337	EFFECT OF SUBJECT AGE ON FNMR	401
338	EFFECT OF SUBJECT AGE ON FNMR	402
339	WORST CASE REGIONAL EFFECT FNMR	405
340	IMPOSTOR DISTRIBUTION SHIFTS FOR SELECT COUNTRY PAIRS	407

	Location	Developer Name	Short Name	Seq. Num.	Validation Date
1	NL	20Face	20face-000	000	2021-04-12
2	NL	20Face	20face-001	001	2021-09-29
3	US	3Divi	3divi-006	006	2021-04-14
4	US	3Divi	3divi-007	007	2021-09-27
5	TH	ACI Software	acisw-007	007	2021-11-15
6	TH	ACI Software	acisw-008	008	2022-03-22
7	SG	ADVANCE.AI	advance-002	002	2019-12-19
8	SG	ADVANCE.AI	advance-003	003	2021-08-05
9	US	AFIS and Biometrics Consulting	afisbiometrics-000	000	2022-01-27
10	TW	ASUSTek Computer Inc	asusaics-000	000	2019-10-24
11	TW	ASUSTek Computer Inc	asusaics-001	001	2020-02-25
12	CN	AYF Technology	ayftech-001	001	2020-07-06
13	TW	Ability Enterprise - Andro Video	androvideo-000	000	2021-01-25
14	TW	Acer Incorporated	acer-001	001	2020-06-30
15	TW	Acer Incorporated	acer-002	002	2021-11-10
16	SG	Adera Global PTE	adera-002	002	2021-02-16
17	SG	Adera Global PTE	adera-003	003	2021-07-12
18	TH	Ai First	aifirst-001	001	2019-11-21
19	TW	AiUnion Technology	aiunionface-000	000	2019-10-22
20	TH	Aigen	aigen-001	001	2020-10-06
21	TH	Aigen	aigen-002	002	2021-03-15
22	KR	Ajou University	ajou-001	001	2021-03-08
23	ID	Akurat Satu Indonesia	ptakuratsatu-000	000	2020-09-11
24	KR	Alchera Inc	alchera-002	002	2021-03-05
25	KR	Alchera Inc	alchera-003	003	2021-07-13
26	ID	Alfabeta	alfabeta-001	001	2021-12-02
27	ES	Alice Biometrics	alice-000	000	2021-06-15
28	RU	Alivia / Innovation Sys	isystems-001	001	2018-06-12
29	RU	Alivia / Innovation Sys	isystems-002	002	2018-10-18
30	IN	AllGoVision	allgovision-000	000	2019-03-01
31	CN	AlphaSTG	alphaface-001	001	2019-09-03
32	CN	AlphaSTG	alphaface-002	002	2020-02-20
33	GB	Amplified Group	amplifiedgroup-001	001	2019-03-01
34	CN	Anke Investments	anke-004	004	2019-06-27
35	CN	Anke Investments	anke-005	005	2019-11-21
36	BR	Antheus Technologia	antheus-000	000	2019-12-05
37	BR	Antheus Technologia	antheus-001	001	2020-06-25
38	GB	AnyVision	anyvision-004	004	2018-06-15
39	GB	AnyVision	anyvision-005	005	2021-02-03
40	US	Armatura LLC	armatura-001	001	2022-01-04
41	CN	AuthenMetric	authenmetric-003	003	2021-08-09
42	CN	AuthenMetric	authenmetric-004	004	2022-01-03
43	US	Aware	aware-005	005	2020-02-27
44	US	Aware	aware-006	006	2021-07-03
45	IN	Awidit Systems	awiros-001	001	2019-09-23
46	IN	Awidit Systems	awiros-002	002	2020-10-28
47	JP	Ayonix	ayonix-000	000	2017-06-22
48	CN	BOE Technology Group	boetech-001	001	2021-06-22
49	CN	BOE Technology Group	boetech-002	002	2021-12-21
50	ES	Bee the Data	beethedata-000	000	2021-07-26
51	CN	Beihang University-ERCACAT	ercacat-001	001	2020-07-06
52	CN	Beijing Alleyes Technology	alleyes-000	000	2020-03-09
53	CN	Beijing DeepSense Technologies	deepsense-000	000	2021-03-19
54	CN	Beijing DeepSense Technologies	deepsense-001	001	2022-03-11
55	CN	Beijing Hisign Technology	hisign-001	001	2021-09-24
56	CN	Beijing Mendaxia Technology	mendaxiatech-000	000	2021-09-15
57	CN	Beijing Vion Technology Inc	vion-000	000	2018-10-19
58	KZ	Beyne.AI	beyneai-000	000	2022-01-03
59	CH	BioID Technologies SA	bioidechswiss-001	001	2020-08-28
60	CH	BioID Technologies SA	bioidechswiss-002	002	2021-02-17
61	IN	Biocube Matrics	biocube-001	001	2021-09-08
62	UK	BitCenter UK	farfaces-001	001	2021-04-09
63	CN	Bitmain	bm-001	001	2018-10-17
64	CN	Bresee Technology	bresee-001	001	2020-12-30
65	CN	Bresee Technology	bresee-002	002	2021-06-30
66	CN	CSA IntelliCloud Technology	intellicloudai-001	001	2019-08-13
67	CN	CSA IntelliCloud Technology	intellicloudai-002	002	2020-12-17
68	TW	CTBC Bank	ctbcbank-000	000	2019-06-28
69	TW	CTBC Bank	ctbcbank-001	001	2019-10-28
70	KR	CUDO Communication	cudocommunication-001	001	2021-10-20

Table 1: Summary of participant information included in this report.

	Location	Developer Name	Short Name	Seq. Num.	Validation Date
71	US	Camvi Technologies	camvi-002	002	2018-10-19
72	US	Camvi Technologies	camvi-004	004	2019-07-12
73	JP	Canon Inc	canon-003	003	2021-09-15
74	JP	Canon Inc	canon-004	004	2022-04-25
75	CN	China Electronics Import-Export Corp	ceiec-003	003	2020-01-06
76	CN	China Electronics Import-Export Corp	ceiec-004	004	2021-01-18
77	CN	China University of Petroleum	upc-001	001	2019-06-05
78	CN	Chinese University of Hong Kong	cuhkee-001	001	2020-03-18
79	KR	Chosun University	chosun-001	001	2020-07-01
80	KR	Chosun University	chosun-002	002	2020-11-25
81	TW	Chunghwa Telecom	chtface-004	004	2021-10-08
82	TW	Chunghwa Telecom	chtface-005	005	2022-03-09
83	US	Clearview AI Inc	clearviewai-000	000	2021-09-22
84	CN	Closeli Inc	closeli-001	001	2021-07-15
85	US	CloudSmart Consulting LLC	csc-002	002	2021-03-24
86	US	CloudSmart Consulting LLC	csc-003	003	2021-08-26
87	TW	Cloudmatrix	cloudmatrix-000	000	2021-10-22
88	TW	Cloudmatrix	cloudmatrix-001	001	2022-02-16
89	CN	Cloudwalk - Hengrui AI Technology	cloudwalk-hr-003	003	2020-09-25
90	CN	Cloudwalk - Hengrui AI Technology	cloudwalk-hr-004	004	2021-02-10
91	CN	Cloudwalk - Moontime Smart Technology	cloudwalk-mt-004	004	2021-11-09
92	CN	Cloudwalk - Moontime Smart Technology	cloudwalk-mt-005	005	2022-03-29
93	IN	Code Everest Pvt	facex-001	001	2021-03-08
94	IN	Code Everest Pvt	facex-002	002	2021-08-24
95	DE	Cognitec Systems GmbH	cognitec-003	003	2021-07-30
96	DE	Cognitec Systems GmbH	cognitec-004	004	2022-02-10
97	TW	Coretech Knowledge Inc	coretech-000	000	2021-07-12
98	IL	Corsight	corsight-001	001	2021-03-11
99	IL	Corsight	corsight-002	002	2021-09-01
100	IL	Cortica	cor-001	001	2020-09-24
101	KR	Cubox	cubox-001	001	2020-12-07
102	KR	Cubox	cubox-002	002	2021-08-24
103	JP	Cybercore	cybercore-001	001	2021-12-15
104	JP	Cybercore	cybercore-002	002	2022-04-25
105	US	Cyberextruder	cyberextruder-002	002	2018-01-30
106	US	Cyberextruder	cyberextruder-003	003	2022-03-16
107	TW	Cyberlink Corp	cyberlink-007	007	2021-07-16
108	TW	Cyberlink Corp	cyberlink-008	008	2022-01-07
109	MX	DICIO	dicio-001	001	2022-03-22
110	CN	DSK	dsk-000	000	2019-06-28
111	CN	Dahua Technology	dahua-006	006	2020-12-30
112	CN	Dahua Technology	dahua-007	007	2021-12-20
113	IE	Daon	daon-000	000	2021-11-03
114	US	Decatur Industries Inc	decatur-000	000	2020-08-18
115	US	Decatur Industries Inc	decatur-001	001	2021-09-27
116	CN	Deepglint	deepglint-003	003	2021-03-03
117	CN	Deepglint	deepglint-004	004	2021-09-17
118	FR	Deepsense	dps-000	000	2021-07-16
119	DE	Dermalog	dermalog-008	008	2021-03-25
120	DE	Dermalog	dermalog-009	009	2021-10-06
121	CN	DiDi ChuXing Technology	didiglobalface-001	001	2019-10-23
122	IN	Digidata	digidata-000	000	2022-01-27
123	GB	Digital Barriers	digitalbarriers-002	002	2019-03-01
124	TR	Ekin Smart City Technologies	ekin-002	002	2021-05-04
125	RU	Enface	enface-000	000	2021-04-09
126	RU	Enface	enface-001	001	2021-12-17
127	CH	Euronovate SA	euronovate-001	001	2021-11-15
128	RU	Expasoft LLC	expasoft-001	001	2020-09-03
129	RU	Expasoft LLC	expasoft-002	002	2021-07-26
130	DE	FaceOnLive Inc	faceonlive-001	001	2021-11-23
131	ES	FacePhi	facephi-000	000	2022-04-06
132	GB	FaceSoft	facesoft-000	000	2019-07-10
133	KR	FaceTag Co	facetag-000	000	2021-03-22
134	KR	FaceTag Co	facetag-002	002	2022-01-06
135	TW	FarBar Inc	f8-001	001	2019-07-11
136	TW	FarBar Inc	f8-002	002	2022-03-02
137	CN	Fiberhome Telecommunication Technologies	fiberhome-nanjing-003	003	2021-03-12
138	CN	Fiberhome Telecommunication Technologies	fiberhome-nanjing-004	004	2021-09-14
139	UK	Fincore Ltd	fincore-000	000	2021-06-07
140	CN	Fujitsu Research and Development Center	fujitsulab-002	002	2021-02-24

Table 2: Summary of participant information included in this report.

	Location	Developer Name	Short Name	Seq. Num.	Validation Date
141	CN	Fujitsu Research and Development Center	fujitsulab-003	003	2021-07-12
142	US	Gemalto Cogent	cogent-006	006	2021-07-28
143	US	Gemalto Cogent	cogent-007	007	2022-04-11
144	TW	GeoVision Inc	geo-002	002	2021-04-01
145	TW	GeoVision Inc	geo-004	004	2022-02-10
146	JP	Glory	glory-003	003	2021-01-15
147	JP	Glory	glory-004	004	2022-02-08
148	TW	Gorilla Technology	gorilla-007	007	2021-06-28
149	TW	Gorilla Technology	gorilla-008	008	2021-11-08
150	US	Graymatics	graymatics-001	001	2022-01-13
151	US	Griaule	griaule-000	000	2021-08-20
152	CN	Guangzhou Pixel Solutions	pixelall-006	006	2021-06-17
153	CN	Guangzhou Pixel Solutions	pixelall-007	007	2021-12-01
154	CN	Hangzhou Allu Network Information Technology	hzaillu-001	001	2022-01-27
155	ES	Herta Security	hertasecurity-000	000	2021-01-05
156	ES	Herta Security	hertasecurity-001	001	2022-01-18
157	CN	Hikvision Research Institute	hik-001	001	2019-03-01
158	IN	HyperVerge Inc	hyperverge-002	002	2021-05-27
159	IN	HyperVerge Inc	hyperverge-003	003	2022-04-11
160	AU	ICM Airport Technics	icm-002	002	2020-11-13
161	AU	ICM Airport Technics	icm-003	003	2021-09-06
162	FR	ID3 Technology	id3-006	006	2020-12-17
163	FR	ID3 Technology	id3-008	008	2021-11-10
164	RU	ITMO University	itmo-007	007	2020-01-06
165	RU	ITMO University	itmo-008	008	2021-11-19
166	RU	IVA Cognitive	ivacognitive-001	001	2021-01-29
167	FR	Idemia	idemia-007	007	2020-12-04
168	FR	Idemia	idemia-008	008	2021-07-07
169	US	Imageware Systems	iws-000	000	2020-08-12
170	AU	Imagus Technology Pty	imagus-004	004	2021-09-20
171	AU	Imagus Technology Pty	imagus-005	005	2022-03-03
172	GB	Imperial College London	imperial-000	000	2019-03-01
173	GB	Imperial College London	imperial-002	002	2019-08-28
174	US	Incode Technologies Inc	incode-009	009	2021-06-22
175	US	Incode Technologies Inc	incode-010	010	2021-10-22
176	IN	Innef Labs	inneflabs-000	000	2020-09-04
177	GB	Innovative Technology	innovativetechnologyltd-001	001	2019-10-22
178	GB	Innovative Technology	innovativetechnologyltd-002	002	2020-02-26
179	SK	Innovatrics	innovatrics-007	007	2020-08-19
180	SK	Innovatrics	innovatrics-008	008	2021-12-15
181	CN	InsightFace AI	insightface-001	001	2021-09-27
182	CN	InsightFace AI	insightface-002	002	2022-01-31
183	CN	Institute of Computing Technology	icthtc-000	000	2020-11-29
184	RU	Institute of Information Technologies	iit-002	002	2019-12-04
185	RU	Institute of Information Technologies	iit-003	003	2020-12-01
186	IS	Intel Research Group	intelresearch-004	004	2021-08-24
187	IS	Intel Research Group	intelresearch-005	005	2022-02-13
188	KR	IntellivIX	intellivix-001	001	2022-02-25
189	US	Intellivision	intellivision-002	002	2019-08-23
190	US	Intellivision	intellivision-003	003	2022-03-07
191	US	IrexAI	irex-000	000	2020-12-17
192	IL	Is It You	isityou-000	000	2017-06-26
193	KR	Kakao Enterprise	kakao-005	005	2021-03-09
194	KR	Kakao Enterprise	kakao-007	007	2022-01-12
195	KR	Kakao Pay Corp	kakaopay-001	001	2021-07-06
196	TH	Kasikorn Labs	kasikornlabs-000	000	2022-03-02
197	SG	Kedacom International Pte	kedacom-000	000	2019-06-03
198	US	Kneron Inc	kneron-003	003	2019-07-01
199	US	Kneron Inc	kneron-005	005	2020-02-21
200	US	KnowUTech LLC	knowutech-000	000	2022-02-13
201	KR	Kookmin University	kookmin-002	002	2021-03-05
202	CN	KuKe3D Technology	kuke3d-001	001	2021-10-28
203	CN	KuKe3D Technology	kuke3d-002	002	2022-04-14
204	MX	Lebentech Biometrics	lebentech-000	000	2022-02-16
205	IN	Lema Labs	lemalabs-001	001	2021-04-13
206	JP	Line Corporation	line-000	000	2021-03-31
207	JP	Line Corporation	line-001	001	2021-09-26
208	RU	Lomonosov Moscow State University	intsy whole-001	001	2019-10-22
209	RU	Lomonosov Moscow State University	intsy whole-002	002	2020-03-12
210	IN	Lookman Electroplast Industries	lookman-002	002	2018-06-13

Table 3: Summary of participant information included in this report.

	Location	Developer Name	Short Name	Seq. Num.	Validation Date
211	IN	Lookman Electroplast Industries	lookman-004	004	2019-06-03
212	US	Luxand Inc	luxand-000	000	2019-11-07
213	RU	MVision	mvision-001	001	2019-11-12
214	IN	Mantra Softech India	mantra-000	000	2021-10-28
215	CN	Maxvision Technology	maxvision-000	000	2021-10-27
216	CN	Maxvision Technology	maxvision-001	001	2022-03-03
217	CN	Megvii/Face++	megvii-004	004	2021-11-19
218	CN	Megvii/Face++	megvii-005	005	2022-03-28
219	GB	MicroFocus	microfocus-001	001	2018-06-13
220	GB	MicroFocus	microfocus-002	002	2018-10-17
221	CN	Minivision	minivision-000	000	2020-10-28
222	NO	Mobai	mobai-000	000	2020-08-26
223	NO	Mobai	mobai-001	001	2021-02-17
224	ES	Mobbeel Solutions	mobbl-001	001	2021-06-16
225	ES	Mobbeel Solutions	mobbl-003	003	2022-04-19
226	KR	Mobipin Technology	mobipintech-000	000	2021-11-23
227	TH	Momentum Digital	sertis-000	000	2019-10-07
228	TH	Momentum Digital	sertis-002	002	2021-05-13
229	CN	MoreDian Technology	moreedian-000	000	2021-02-24
230	US	Mukh Technologies	mukh-001	001	2022-03-22
231	CN	Multi-Modality Intelligence	multimodality-000	000	2021-10-19
232	RU	N-Tech Lab	ntechlab-011	011	2021-09-13
233	RU	N-Tech Lab	ntechlab-012	012	2022-01-20
234	CA	NEO Systems	neosystems-002	002	2021-07-03
235	CA	NEO Systems	neosystems-003	003	2021-11-11
236	KR	NHN Corp	nhn-002	002	2021-07-15
237	KR	NHN Corp	nhn-003	003	2022-02-22
238	KR	NSENSE Corp	nsensecorp-002	002	2021-05-06
239	KR	NSENSE Corp	nsensecorp-003	003	2021-10-29
240	CN	Nanjing Kiwi Network Technology	kiwitech-000	000	2021-03-19
241	KR	Naver Corp	clova-000	000	2020-10-21
242	KR	Neosecu Co	openface-001	001	2021-06-15
243	TW	Netbridge Technology Incoporation	netbridgetech-001	001	2020-01-08
244	TW	Netbridge Technology Incoporation	netbridgetech-002	002	2020-08-11
245	LT	Neurotechnology	neurotechnology-012	012	2021-07-26
246	LT	Neurotechnology	neurotechnology-013	013	2022-01-07
247	ID	Nodeflux	nodeflux-002	002	2019-08-13
248	IN	NotionTag Technologies Private Limited	notiontag-001	001	2021-03-04
249	IN	NotionTag Technologies Private Limited	notiontag-002	002	2021-09-17
250	US	Omnigarde Ltd	omnigarde-001	001	2021-08-23
251	US	Omnigarde Ltd	omnigarde-002	002	2022-01-19
252	KR	One More Security	omsecurity-000	000	2021-12-15
253	RU	Oz Forensics LLC	oz-003	003	2021-08-09
254	RU	Oz Forensics LLC	oz-004	004	2021-12-13
255	CH	PXL Vision AG	pxl-001	001	2020-06-30
256	SG	Panasonic R+D Center Singapore	psl-009	009	2021-12-08
257	SG	Panasonic R+D Center Singapore	psl-010	010	2022-04-19
258	US	Pangiam	pangiam-000	000	2022-04-04
259	TR	Papilon Savunma	papsav1923-001	001	2021-03-10
260	TR	Papilon Savunma	papsav1923-002	002	2022-01-20
261	US	Paravision	paravision-008	008	2021-06-30
262	US	Paravision (EverAI)	paravision-010	010	2022-02-02
263	SG	Pensees Pte	pensees-001	001	2020-08-17
264	IN	Pyramid Cyber Security + Forensic (P)	pyramid-000	000	2019-11-04
265	TW	Qnap Security	qnap-001	001	2021-12-09
266	TW	Qnap Security	qnap-002	002	2022-04-15
267	CZ	Quantasoft	quantasoft-003	003	2021-04-19
268	US	Rank One Computing	rankone-011	011	2021-08-27
269	US	Rank One Computing	rankone-012	012	2021-12-27
270	US	Realnetworks Inc	realnetworks-005	005	2021-09-27
271	US	Realnetworks Inc	realnetworks-006	006	2022-02-09
272	US	Regula Forensics	regula-000	000	2021-04-13
273	US	Regula Forensics	regula-001	001	2021-12-14
274	CN	Remark Holdings	remarkai-001	001	2019-03-01
275	CN	Remark Holdings	remarkai-003	003	2021-06-22
276	SG	Rendip	rendip-000	000	2021-04-19
277	UK	Reveal Media Ltd	revealmedia-005	005	2021-09-24
278	UK	Reveal Media Ltd	revealmedia-006	006	2022-01-26
279	CN	Rokid Corporation	rokid-000	000	2019-08-01
280	CN	Rokid Corporation	rokid-001	001	2019-12-13

Table 4: Summary of participant information included in this report.

	Location	Developer Name	Short Name	Seq. Num.	Validation Date
281	KR	SK Telecom	sktelecom-000	000	2021-07-09
282	KR	SQIsoft	sqisoft-001	001	2021-07-27
283	KR	SQIsoft	sqisoft-002	002	2021-11-03
284	DE	Saffe	saffe-001	001	2018-10-19
285	DE	Saffe	saffe-002	002	2019-03-01
286	KR	Samsung S1 Corp	s1-003	003	2021-08-24
287	KR	Samsung S1 Corp	s1-004	004	2022-01-04
288	KR	Samsung-SDS	samsungsds-000	000	2021-10-28
289	KR	Samsung-SDS	samsungsds-001	001	2022-04-18
290	IN	Samtech InfoNet Limited	samtech-001	001	2019-10-15
291	RU	Satellite Innovation/Eocortex	eocortex-000	000	2020-08-26
292	IL	Scanovate	scanovate-002	002	2020-06-26
293	IL	Scanovate	scanovate-003	003	2021-11-15
294	RO	Securif AI	securifai-003	003	2021-08-03
295	RO	Securif AI	securifai-004	004	2021-12-21
296	CN	Sensetime Group	sensetime-005	005	2021-05-24
297	CN	Sensetime Group	sensetime-006	006	2021-12-28
298	SG	Seventh Sense Artificial Intelligence	seventhsense-000	000	2021-06-29
299	SG	Seventh Sense Artificial Intelligence	seventhsense-001	001	2022-03-04
300	US	Shaman Software	shaman-000	000	2017-12-05
301	US	Shaman Software	shaman-001	001	2018-01-13
302	CN	Shanghai Jiao Tong University	sjtu-003	003	2020-11-02
303	CN	Shanghai Jiao Tong University	sjtu-004	004	2021-05-13
304	CN	Shanghai Ulucus Electronics Technology	uluface-002	002	2019-07-10
305	CN	Shanghai Ulucus Electronics Technology	uluface-003	003	2019-11-12
306	CN	Shanghai University - Shanghai Film Academy	shu-002	002	2019-12-10
307	CN	Shanghai University - Shanghai Film Academy	shu-003	003	2020-06-24
308	CN	Shanghai Yitu Technology	yitu-003	003	2019-03-01
309	CN	Shenzhen AiMall Tech	aimall-002	002	2020-03-12
310	CN	Shenzhen AiMall Tech	aimall-003	003	2020-08-12
311	CN	Shenzhen EI Networks	einetworks-000	000	2019-08-13
312	CN	Shenzhen Inst Adv Integrated Tech CAS	siat-002	002	2018-06-13
313	CN	Shenzhen Inst Adv Integrated Tech CAS	siat-005	005	2022-02-08
314	CN	Shenzhen Intellifusion Technologies	intellifusion-001	001	2019-08-22
315	CN	Shenzhen Intellifusion Technologies	intellifusion-002	002	2020-03-18
316	CN	Shenzhen University-Macau University of Science and Technology	sztu-000	000	2020-12-17
317	CN	Shenzhen University-Macau University of Science and Technology	sztu-001	001	2021-07-13
318	RU	Smart Engines	smartengines-000	000	2021-08-25
319	DE	Smilart	smilart-002	002	2018-02-06
320	DE	Smilart	smilart-003	003	2019-03-01
321	TR	Sodec App Inc	sodec-000	000	2021-06-02
322	IN	Staqu Technologies	st aqu-000	000	2020-07-15
323	CN	Star Hybrid Limited	starhybrid-001	001	2019-06-19
324	CN	Su Zhou NaZhiTianDi intelligent technology	nazhai-000	000	2020-06-25
325	IN	Sukshi Technology Innovation	sukshi-000	000	2022-02-13
326	KR	Suprema AI Inc	suprema-001	001	2021-09-23
327	KR	Suprema AI Inc	suprema-002	002	2022-02-11
328	KR	Suprema ID Inc	supremaid-001	001	2021-05-04
329	RU	Synesis	synesis-006	006	2019-10-10
330	RU	Synesis	synesis-007	007	2020-06-24
331	TW	Synology Inc	synology-000	000	2019-10-23
332	TW	Synology Inc	synology-002	002	2020-08-20
333	BR	T4iSB	t4isb-000	000	2022-01-28
334	CN	TUPU Technology	tuputech-000	000	2019-10-11
335	TW	Taiwan AI Labs	ailabs-001	001	2019-12-18
336	TW	Taiwan-Certificate Authority Incorporation	twface-000	000	2021-05-14
337	TW	Taiwan-Certificate Authority Incorporation	twface-001	001	2021-09-14
338	CH	Tech5 SA	tech5-004	004	2020-03-09
339	CH	Tech5 SA	tech5-005	005	2020-07-24
340	TR	Techsign	techsign-000	000	2021-08-25
341	CN	Tencent Deepsea Lab	deepsea-001	001	2019-06-03
342	RU	Tevian	tevian-007	007	2021-08-06
343	RU	Tevian	tevian-008	008	2021-12-06
344	US	TigerIT Americas LLC	tiger-005	005	2021-07-29
345	US	TigerIT Americas LLC	tiger-006	006	2021-12-13
346	RU	Tinkoff Bank	tinkoff-001	001	2021-05-13
347	CN	TongYi Transportation Technology	tongyi-005	005	2019-06-12
348	TW	Toppan ID Gate	toppanidgate-000	000	2021-09-28
349	JP	Toshiba	toshiba-004	004	2021-09-27
350	JP	Toshiba	toshiba-005	005	2022-02-09

Table 5: Summary of participant information included in this report.

	Location	Developer Name	Short Name	Seq. Num.	Validation Date
351	JP	Tripleize	aize-001	001	2021-04-23
352	JP	Tripleize	aize-002	002	2021-10-08
353	US	Trueface.ai	trueface-002	002	2021-03-29
354	US	Trueface.ai	trueface-003	003	2021-09-30
355	CN	TuringTech.vip	turingtechvip-001	001	2022-02-03
356	CN	ULSee Inc	ulsee-001	001	2019-07-31
357	FR	Unissey	unissey-001	001	2021-11-29
358	PT	Universidade de Coimbra	visteam-002	002	2021-08-20
359	PT	Universidade de Coimbra	visteam-003	003	2022-01-31
360	UK	University of Surrey-CVSSP	surrey-cvssp-000	000	2022-03-25
361	US	VCognition	vcog-002	002	2017-06-12
362	ES	Veridas Digital Authentication Solutions S.L.	veridas-006	006	2021-04-15
363	ES	Veridas Digital Authentication Solutions S.L.	veridas-007	007	2021-09-02
364	UK	Veridium	veridium-000	000	2022-03-28
365	KZ	Verigram	verigram-000	000	2021-09-06
366	KZ	Verigram	verigram-001	001	2022-03-09
367	ID	Verihubs	verihubs-inteligensia-000	000	2021-07-27
368	TW	Via Technologies Inc	via-000	000	2019-07-08
369	TW	Via Technologies Inc	via-001	001	2020-01-08
370	DE	Videmo Intelligent Videoanalyse	videmo-000	000	2019-12-19
371	DE	Videmo Intelligent Videoanalyse	videmo-001	001	2021-12-22
372	IN	Videonetech Technology Pvt	videonetechs-001	001	2019-06-19
373	IN	Videonetech Technology Pvt	videonetechs-002	002	2019-11-21
374	VN	Vietnam Posts and Telecommunications Group	vnpt-003	003	2021-12-01
375	VN	Vietnam Posts and Telecommunications Group	vnpt-004	004	2022-04-15
376	VN	Viettel Group	vts-000	000	2020-11-04
377	VN	Viettel Group	vts-001	001	2022-04-20
378	VN	Viettel High Technology	viettelhightech-000	000	2021-08-04
379	US	Vigilant Solutions	vigilantsolutions-010	010	2021-04-07
380	US	Vigilant Solutions	vigilantsolutions-011	011	2021-08-07
381	VN	VinAI Research VietNam	vinai-000	000	2020-09-24
382	VN	VinBigData	vinbigdata-001	001	2022-01-06
383	SE	Visage Technologies	visage-000	000	2020-12-09
384	FI	Visidon	vd-002	002	2021-04-12
385	FI	Visidon	vd-003	003	2021-10-12
386	CN	Vision Intelligence Center of Meituan	meituan-000	000	2021-05-14
387	CN	Vision Intelligence Center of Meituan	meituan-001	001	2022-03-25
388	PT	Vision-Box	visionbox-001	001	2019-03-01
389	PT	Vision-Box	visionbox-002	002	2021-04-29
390	RU	VisionLabs	visionlabs-010	010	2021-01-25
391	RU	VisionLabs	visionlabs-011	011	2021-10-13
392	RU	Vocord	vocord-009	009	2020-12-28
393	RU	Vocord	vocord-010	010	2021-12-20
394	US	Wicket	wicket-000	000	2022-02-14
395	CN	Winsense	winsense-001	001	2019-10-16
396	CN	Winsense	winsense-002	002	2020-11-20
397	CN	Wuhan Tianyu Information Industry	wuhantianyu-001	001	2021-08-05
398	CN	X-Laboratory	x-laboratory-000	000	2019-09-03
399	CN	X-Laboratory	x-laboratory-001	001	2020-01-21
400	CN	Xforward AI Technology	xforwardai-001	001	2020-09-25
401	CN	Xforward AI Technology	xforwardai-002	002	2021-02-10
402	CN	Xiamen Meiya Pico Information	meiya-001	001	2019-03-01
403	CN	Xiamen University	xm-000	000	2020-10-19
404	PT	YooniK	yoonik-002	002	2021-09-06
405	PT	YooniK	yoonik-003	003	2022-01-06
406	TW	Yuan High-Tech Development	yuan-003	003	2021-09-17
407	TW	Yuan High-Tech Development	yuan-004	004	2022-01-14
408	CN	Yuntu Data and Technology	ytu-000	000	2021-06-16
409	CN	Zhuhai Yisheng Electronics Technology	yisheng-004	004	2018-06-12
410	CN	iQIYI Inc	iqface-000	000	2019-06-04
411	CN	iQIYI Inc	iqface-003	003	2021-02-23
412	TW	iSAP Solution Corporation	isap-001	001	2019-08-07
413	TW	iSAP Solution Corporation	isap-002	002	2020-09-01
414	TW	ioNetworks Inc	ionetworks-000	000	2021-07-20

Table 6: Summary of participant information included in this report.

	ALGORITHM	CONFIG	LIBRARY	TEMPLATE								COMPARISON <sup>4</sup>									
				NAME	DATA		MEMORY	SIZE	GENERATION TIME (ms) <sup>4</sup>				TIME (ns) <sup>5</sup>								
					(KB) <sup>1</sup>	(KB) <sup>2</sup>			(B)	MUGSHOT	480x720	960x1440	1600x2400	3000x4500	GENUINE	IMPOSTOR					
1	20face-000	117155	324083	195	905	179	2048 ± 0	35	232 ± 1	25	223 ± 1	20	226 ± 4	18	222 ± 1	13	224 ± 1	385	44880 ± 134	384	44462 ± 163
2	20face-001	226824	324119	326	1940	365	4096 ± 0	45	279 ± 2	29	266 ± 1	22	266 ± 1	21	267 ± 1	16	267 ± 0	306	5553 ± 54	304	5541 ± 65
3	3divi-006	273866	52656	77	472	157	2048 ± 0	197	654 ± 1	162	651 ± 0	143	660 ± 1	128	678 ± 2	127	759 ± 13	102	775 ± 19	101	770 ± 22
4	3divi-007	483115	24723	258	1285	243	2048 ± 0	179	615 ± 1	151	616 ± 1	129	623 ± 1	116	644 ± 1	117	727 ± 5	87	707 ± 31	91	712 ± 25
5	acer-001	36650	66086	62	417	21	512 ± 0	32	199 ± 0	26	237 ± 28	21	229 ± 26	20	242 ± 37	15	259 ± 21	231	2453 ± 44	233	2461 ± 62
6	acer-002	43922	624858	32	187	229	2048 ± 0	28	184 ± 0	19	184 ± 0	14	185 ± 0	11	185 ± 0	11	186 ± 0	269	3370 ± 47	269	3350 ± 54
7	acisw-007	267619	36111	45	286	278	2048 ± 0	50	283 ± 0	39	293 ± 3	53	414 ± 0	42	404 ± 0	47	484 ± 1	156	1316 ± 22	156	1297 ± 23
8	acisw-008	171703	39359	233	1101	167	2048 ± 0	82	400 ± 1	56	362 ± 28	40	369 ± 9	24	300 ± 2	20	336 ± 5	157	1327 ± 19	159	1337 ± 32
9	ader-a-002	0	749797	200	921	401	5120 ± 0	398	1394 ± 11	351	1381 ± 1	349	1393 ± 1	329	1403 ± 1	281	1464 ± 2	222	2163 ± 32	224	2158 ± 28
10	ader-a-003	0	749778	198	917	400	5120 ± 0	393	1381 ± 12	353	1385 ± 1	350	1394 ± 1	326	1401 ± 1	282	1469 ± 1	221	2148 ± 34	221	2130 ± 32
11	advance-002	257173	20434	48	295	197	2048 ± 0	249	811 ± 2	203	803 ± 2	157	696 ± 2	132	699 ± 4	113	718 ± 1	120	987 ± 10	118	988 ± 45
12	advance-003	258867	78699	93	518	164	2048 ± 0	163	586 ± 0	136	584 ± 0	113	583 ± 0	94	588 ± 0	76	591 ± 1	201	1813 ± 17	197	1788 ± 26
13	afisbiometrics-000	545886	32882	231	1088	33	512 ± 0	360	1219 ± 1	299	1135 ± 1	285	1137 ± 2	253	1137 ± 1	211	1147 ± 1	163	1400 ± 29	160	1357 ± 32
14	aifirst-001	224157	808777	80	485	252	2048 ± 0	163	587 ± 2	130	568 ± 2	114	584 ± 3	101	601 ± 6	125	755 ± 5	136	1099 ± 14	138	1087 ± 45
15	aigen-001	256958	595227	240	1136	149	2048 ± 0	408	1448 ± 9	365	1451 ± 8	370	1759 ± 6	368	2594 ± 4	355	5691 ± 44	284	3772 ± 57	283	3736 ± 56
16	aigen-002	205300	1316138	190	874	273	2048 ± 0	162	586 ± 24	135	582 ± 4	223	920 ± 4	351	1758 ± 5	354	5427 ± 17	280	3678 ± 44	278	3646 ± 48
17	ailabs-001	1054663	338989	252	1252	230	2048 ± 0	203	664 ± 4	197	774 ± 50	288	1145 ± 12	357	1972 ± 74	351	5205 ± 272	406	104034 ± 661	406	103415 ± 7722
18	aimall-002	370156	25210	293	1576	263	2048 ± 0	238	776 ± 4	252	927 ± 27	231	940 ± 21	211	955 ± 34	183	1003 ± 75	403	72811 ± 7399	402	7216 ± 6286
19	aimall-003	504324	171935	322	1913	62	1024 ± 0	200	662 ± 1	187	740 ± 51	173	752 ± 62	149	741 ± 46	137	807 ± 47	379	34565 ± 93	380	34598 ± 118
20	aiunionface-000	241642	840295	59	402	212	2048 ± 0	189	637 ± 13	192	754 ± 41	259	1025 ± 28	265	1179 ± 29	301	1639 ± 47	131	1072 ± 19	136	1080 ± 47
21	aize-001	268456	168970	281	1436	241	2048 ± 0	101	437 ± 10	81	440 ± 8	99	542 ± 17	152	756 ± 27	298	1583 ± 53	211	1937 ± 22	207	1919 ± 23
22	aize-002	257106	182517	112	586	101	2048 ± 0	113	467 ± 1	93	479 ± 1	175	756 ± 1	339	1477 ± 1	349	4617 ± 41	55	597 ± 16	60	598 ± 14
23	ajou-001	363257	31734	69	442	161	2048 ± 0	136	530 ± 0	113	536 ± 0	97	535 ± 0	87	549 ± 0	71	577 ± 0	56	597 ± 19	59	596 ± 13
24	alchera-002	405409	22275	250	1233	147	2048 ± 0	310	968 ± 1	262	976 ± 2	249	979 ± 1	219	988 ± 1	188	1025 ± 2	275	3488 ± 63	273	3430 ± 63
25	alchera-003	487718	24613	269	1376	185	2048 ± 0	270	854 ± 3	224	862 ± 2	202	870 ± 1	185	882 ± 2	162	918 ± 1	272	3426 ± 57	270	3383 ± 53
26	alfabeta-001	128232	21780	6	73	20	512 ± 0	40	271 ± 0	34	276 ± 0	68	459 ± 2	186	886 ± 2	332	2547 ± 9	40	470 ± 25	42	458 ± 20
27	alice-000	1741293	19355	309	1732	353	4096 ± 0	304	950 ± 2	254	933 ± 1	236	949 ± 1	227	1011 ± 3	237	1264 ± 8	352	14975 ± 201	352	14890 ± 229
28	alleys-000	507636	997090	187	857	223	2048 ± 0	241	784 ± 1	261	970 ± 61	243	974 ± 62	207	943 ± 69	196	1057 ± 23	155	1298 ± 34	157	1303 ± 51
29	allgovision-000	172509	155862	105	561	115	2048 ± 0	80	384 ± 8	64	395 ± 17	52	413 ± 14	63	471 ± 14	109	710 ± 21	375	29903 ± 406	376	29735 ± 194
30	alphaface-001	259849	81636	95	527	265	2048 ± 0	173	612 ± 1	146	613 ± 3	125	612 ± 1	106	619 ± 1	93	640 ± 2	124	1008 ± 10	124	1002 ± 19
31	alphaface-002	768995	70692	280	1434	95	2048 ± 0	185	628 ± 2	189	746 ± 19	172	751 ± 18	157	779 ± 22	142	828 ± 40	115	945 ± 25	116	935 ± 17
32	amplifiedgroup-001	0	47053	10	81	57	866 ± 2	10	93 ± 0	-	-	-	-	-	-	396	57803 ± 4210	394	56365 ± 1196		
33	androvideo-000	174847	585063	60	403	174	2048 ± 0	44	277 ± 0	37	285 ± 0	28	314 ± 0	33	372 ± 1	83	620 ± 0	249	2847 ± 22		
34	anke-004	349388	410776	145	706	319	2056 ± 0	182	625 ± 1	153	627 ± 2	138	635 ± 3	120	653 ± 2	178	982 ± 8	72	633 ± 22	74	632 ± 34
35	anke-005	328553	429160	238	1134	329	2056 ± 0	166	590 ± 2	141	594 ± 5	121	601 ± 3	115	638 ± 4	141	821 ± 24	83	685 ± 19	87	687 ± 26
36	antheus-000	119453	41994	19	116	47	520 ± 0	14	109 ± 1	21	187 ± 1	17	189 ± 1	13	195 ± 1	14	236 ± 2	321	6901 ± 268	321	6936 ± 103
37	antheus-001	119453	41962	20	118	45	520 ± 0	17	120 ± 1	28	265 ± 13	74	468 ± 22	279	1223 ± 27	333	2660 ± 87	317	6218 ± 47	316	6216 ± 45
38	anyvision-004	401001	630797	234	1102	70	1024 ± 0	66	355 ± 1	-	-	-	-	-	-	207	1891 ± 51	201	1829 ± 85		
39	anyvision-005	190979	116595	208	963	61	1024 ± 0	313	985 ± 1	266	997 ± 1	255	1004 ± 1	220	995 ± 1	180	995 ± 1	95	733 ± 14	96	733 ± 16
40	armatura-001	0	374608	241	1151	153	2048 ± 0	213	688 ± 1	173	689 ± 1	155	693 ± 1	137	708 ± 3	126	756 ± 13	16	270 ± 17	19	268 ± 11
41	asusaics-000	257418	245320	120	605	114	2048 ± 0	121	484 ± 13	109	506 ± 21	198	850 ± 26	352	1789 ± 61	357	6305 ± 188	304	5455 ± 78	303	5422 ± 112
42	asusaics-001	257418	245330	117	595	373	4096 ± 0	267	842 ± 17	270	1008 ± 20	343	1377 ± 28	367	2423 ± 90	362	7284 ± 277	332	8618 ± 42	332	8638 ± 136
43	authenmetric-003	293599	39492	212	982	193	2048 ± 0	316	992 ± 1	269	1006 ± 1	254	1003 ± 2	224	1002 ± 1	190	1036 ± 1	190	1757 ± 19	190	1755 ± 19
44	authenmetric-004	381165	39492	245	1214	186	2048 ± 0	289	910 ± 1	246	909 ± 1	219	915 ± 1	199	921 ± 2	170	950 ± 1	185	1724 ± 14	182	1691 ± 29

## Notes

- 1 The configuration size does not capture static data included in libraries.
- 2 The library size is the combined total of all files provided in the submission lib folder. These libraries e.g. OpenCV may or may not be installed on any end user's platform natively and would not need to be installed with the algorithm. Some developers put neural network models in their libraries.
- 3 The memory usage is the peak resident set size reported by the ps system call during template generation.
- 4 The median template creation times are measured on Intel®Xeon®CPU E5-2630 v4 @ 2.20GHz processors.
- 5 The comparison durations, in nanoseconds, are estimated using std::chrono::high\_resolution\_clock which on the machine in (2) counts 1ns clock ticks. Precision is somewhat worse than that however. The ± value is the median absolute deviation times 1.48 for Normal consistency.

Table 7: Summary of algorithms and properties included in this report. The red superscripts give ranking for the quantity in that column.

	ALGORITHM	CONFIG	LIBRARY	TEMPLATE								COMPARISON <sup>4</sup>							
				NAME	DATA	DATA	MEMORY	SIZE	GENERATION TIME (ms) <sup>4</sup>				TIME (ns) <sup>5</sup>						
									(KB) <sup>1</sup>	(KB) <sup>2</sup>	(MB) <sup>3</sup>	(B)	MUGSHOT	480x720	960x1440	1600x2400	3000x4500	GENUINE	IMPOSTOR
45	aware-005	300017	26320	<sup>254</sup> 1265	<sup>91</sup> 1572 ± 0	<sup>286</sup> 886 ± 23	<sup>281</sup> 1038 ± 21	<sup>280</sup> 1121 ± 22	<sup>305</sup> 1337 ± 58	<sup>316</sup> 2195 ± 144	<sup>170</sup> 1475 ± 63	<sup>166</sup> 1427 ± 115							
46	aware-006	298543	14124	<sup>206</sup> 943	<sup>13</sup> 352 ± 0	<sup>349</sup> 1148 ± 3	<sup>305</sup> 1146 ± 2	<sup>301</sup> 1190 ± 2	<sup>296</sup> 1306 ± 20	<sup>309</sup> 1754 ± 84	<sup>239</sup> 2598 ± 42	<sup>239</sup> 2559 ± 60							
47	awiros-001	15499	87480	<sup>13</sup> 88	<sup>31</sup> 512 ± 0	<sup>11</sup> 97 ± 6	<sup>8</sup> 98 ± 4	<sup>10</sup> 138 ± 6	<sup>19</sup> 225 ± 7	<sup>68</sup> 556 ± 8	<sup>133</sup> 1079 ± 44	<sup>132</sup> 1050 ± 45							
48	awiros-002	289016	203723	<sup>106</sup> 562	<sup>222</sup> 2048 ± 0	<sup>117</sup> 479 ± 0	<sup>106</sup> 500 ± 0	<sup>96</sup> 534 ± 0	<sup>105</sup> 618 ± 0	<sup>167</sup> 946 ± 1	<sup>212</sup> 1966 ± 31	<sup>212</sup> 1957 ± 25							
49	ayftech-001	195423	43580	<sup>155</sup> 731	<sup>16</sup> 512 ± 0	<sup>90</sup> 408 ± 23	<sup>92</sup> 476 ± 52	<sup>186</sup> 814 ± 108	<sup>354</sup> 1827 ± 384	<sup>353</sup> 5412 ± 1029	<sup>65</sup> 615 ± 16	<sup>113</sup> 885 ± 44							
50	ayonix-000	58505	5252	<sup>5</sup> 69	<sup>76</sup> 1036 ± 0	<sup>2</sup> 18 ± 2	-	-	-	-	-	<sup>68</sup> 621 ± 23	<sup>70</sup> 620 ± 26						
51	beethedata-000	227849	1087592	<sup>104</sup> 555	<sup>264</sup> 2048 ± 0	<sup>111</sup> 465 ± 0	<sup>91</sup> 467 ± 0	<sup>73</sup> 468 ± 0	<sup>61</sup> 467 ± 0	<sup>43</sup> 467 ± 0	<sup>219</sup> 2121 ± 34	<sup>220</sup> 2110 ± 38							
52	beynai-000	256958	591433	<sup>236</sup> 1124	<sup>136</sup> 2048 ± 0	<sup>105</sup> 451 ± 8	<sup>84</sup> 449 ± 1	<sup>177</sup> 767 ± 7	<sup>347</sup> 1603 ± 25	<sup>350</sup> 4669 ± 124	<sup>282</sup> 3730 ± 57	<sup>280</sup> 3668 ± 54							
53	biocube-001	25030	6192987	<sup>73</sup> 458	<sup>356</sup> 4096 ± 0	<sup>49</sup> 282 ± 22	<sup>38</sup> 292 ± 24	<sup>94</sup> 521 ± 57	<sup>126</sup> 684 ± 59	<sup>240</sup> 1282 ± 68	<sup>365</sup> 21787 ± 96	<sup>365</sup> 21812 ± 109							
54	bioidechswiss-001	1178769	120811	<sup>283</sup> 1455	<sup>32</sup> 512 ± 0	<sup>309</sup> 966 ± 4	<sup>331</sup> 1270 ± 270	<sup>323</sup> 1294 ± 96	<sup>330</sup> 1409 ± 157	<sup>311</sup> 1793 ± 79	<sup>240</sup> 2610 ± 25	<sup>240</sup> 2624 ± 32							
55	bioidechswiss-002	744786	114842	<sup>216</sup> 993	<sup>28</sup> 512 ± 0	<sup>292</sup> 917 ± 2	<sup>253</sup> 930 ± 2	<sup>237</sup> 952 ± 2	<sup>209</sup> 947 ± 3	<sup>197</sup> 1058 ± 11	<sup>223</sup> 2177 ± 29	<sup>225</sup> 2170 ± 31							
56	bm-001	287734	38076	<sup>26</sup> 148	<sup>1</sup> 64 ± 0	<sup>103</sup> 444 ± 88	-	-	-	-	-	<sup>206</sup> 1887 ± 31	<sup>205</sup> 1877 ± 26						
57	boetech-001	261376	88710	<sup>272</sup> 1384	<sup>148</sup> 2048 ± 0	<sup>41</sup> 271 ± 1	<sup>30</sup> 268 ± 1	<sup>23</sup> 273 ± 0	<sup>23</sup> 286 ± 1	<sup>18</sup> 318 ± 1	<sup>400</sup> 68519 ± 1921	<sup>400</sup> 67648 ± 822							
58	boetech-002	294347	88710	<sup>287</sup> 1489	<sup>239</sup> 2048 ± 0	<sup>56</sup> 305 ± 4	<sup>41</sup> 296 ± 1	<sup>26</sup> 302 ± 1	<sup>25</sup> 313 ± 1	<sup>23</sup> 348 ± 2	<sup>401</sup> 68921 ± 2137	<sup>401</sup> 69473 ± 2104							
59	bresee-001	287880	23227	<sup>246</sup> 1214	<sup>248</sup> 2048 ± 0	<sup>361</sup> 1223 ± 3	<sup>318</sup> 1216 ± 1	<sup>334</sup> 1331 ± 1	<sup>282</sup> 1227 ± 1	<sup>256</sup> 1360 ± 1	<sup>380</sup> 37240 ± 655	<sup>381</sup> 37167 ± 584							
60	bresee-002	313627	30902	<sup>328</sup> 1956	<sup>231</sup> 2048 ± 0	<sup>228</sup> 743 ± 4	<sup>302</sup> 1143 ± 2	<sup>289</sup> 1146 ± 2	<sup>256</sup> 1148 ± 2	<sup>222</sup> 1176 ± 2	<sup>193</sup> 1778 ± 22	<sup>193</sup> 1775 ± 23							
61	camvi-002	236278	225285	<sup>156</sup> 737	<sup>65</sup> 1024 ± 0	<sup>208</sup> 677 ± 7	<sup>185</sup> 726 ± 36	<sup>201</sup> 869 ± 28	<sup>249</sup> 1129 ± 43	<sup>338</sup> 2785 ± 113	<sup>64</sup> 612 ± 26	<sup>64</sup> 603 ± 20							
62	camvi-004	280733	615819	<sup>199</sup> 919	<sup>146</sup> 2048 ± 0	<sup>232</sup> 759 ± 10	<sup>223</sup> 861 ± 17	<sup>249</sup> 986 ± 34	<sup>292</sup> 1279 ± 51	<sup>340</sup> 2891 ± 158	<sup>116</sup> 948 ± 40	<sup>117</sup> 963 ± 31							
63	canon-003	2550850	101378	<sup>399</sup> 5472	<sup>404</sup> 6180 ± 0	<sup>371</sup> 1263 ± 3	<sup>329</sup> 1263 ± 1	<sup>319</sup> 1283 ± 1	<sup>303</sup> 1320 ± 1	<sup>280</sup> 1482 ± 2	<sup>296</sup> 4783 ± 17	<sup>293</sup> 4780 ± 19							
64	canon-004	2399160	114188	<sup>400</sup> 5956	<sup>405</sup> 6200 ± 0	<sup>302</sup> 948 ± 4	-	-	-	-	-	<sup>328</sup> 7172 ± 63	<sup>327</sup> 7169 ± 51						
65	ceiec-003	260371	88707	<sup>66</sup> 430	<sup>234</sup> 2048 ± 0	<sup>254</sup> 817 ± 4	<sup>236</sup> 883 ± 57	<sup>210</sup> 897 ± 60	<sup>192</sup> 899 ± 72	<sup>166</sup> 944 ± 72	<sup>227</sup> 2256 ± 38	<sup>227</sup> 2241 ± 54							
66	ceiec-004	2634746	67011	<sup>61</sup> 408	<sup>172</sup> 2048 ± 0	<sup>321</sup> 1024 ± 1	<sup>275</sup> 1027 ± 1	<sup>261</sup> 1027 ± 1	<sup>229</sup> 1030 ± 1	<sup>194</sup> 1055 ± 1	<sup>203</sup> 1844 ± 26	<sup>202</sup> 1836 ± 20							
67	chosun-001	765615	707	<sup>84</sup> 491	<sup>259</sup> 2048 ± 0	<sup>240</sup> 783 ± 2	<sup>211</sup> 826 ± 4	<sup>369</sup> 1662 ± 13	<sup>373</sup> 3679 ± 67	<sup>370</sup> 11694 ± 243	<sup>121</sup> 998 ± 25	<sup>130</sup> 1035 ± 11							
68	chosun-002	234001	31875	<sup>70</sup> 450	<sup>94</sup> 2048 ± 0	<sup>36</sup> 248 ± 3	<sup>32</sup> 273 ± 3	<sup>365</sup> 1495 ± 14	<sup>374</sup> 7920 ± 90	<sup>371</sup> 80302 ± 1349	<sup>69</sup> 623 ± 17	<sup>77</sup> 634 ± 13							
69	chtface-004	409656	311027	<sup>286</sup> 1487	<sup>270</sup> 2048 ± 0	<sup>60</sup> 332 ± 0	<sup>44</sup> 323 ± 1	<sup>32</sup> 329 ± 1	<sup>28</sup> 335 ± 1	<sup>26</sup> 377 ± 1	<sup>186</sup> 1727 ± 17	<sup>185</sup> 1720 ± 16							
70	chtface-005	408364	311100	<sup>276</sup> 1412	<sup>283</sup> 2048 ± 0	<sup>58</sup> 322 ± 0	<sup>42</sup> 316 ± 1	<sup>30</sup> 325 ± 2	<sup>26</sup> 324 ± 1	<sup>34</sup> 411 ± 2	<sup>208</sup> 1907 ± 19	<sup>206</sup> 1898 ± 23							
71	clearviewai-000	342491	211852	<sup>361</sup> 2750	<sup>194</sup> 2048 ± 0	<sup>402</sup> 1402 ± 1	<sup>360</sup> 1403 ± 1	<sup>354</sup> 1412 ± 1	<sup>332</sup> 1420 ± 1	<sup>273</sup> 1418 ± 1	<sup>175</sup> 1592 ± 37	<sup>173</sup> 1561 ± 37							
72	closeli-001	420342	9851	<sup>162</sup> 773	<sup>378</sup> 4096 ± 0	<sup>266</sup> 839 ± 1	<sup>218</sup> 843 ± 1	<sup>196</sup> 841 ± 1	<sup>175</sup> 845 ± 1	<sup>154</sup> 865 ± 1	<sup>303</sup> 5404 ± 17	<sup>302</sup> 5400 ± 25							
73	cloudmatrix-000	309939	542141	<sup>151</sup> 727	<sup>162</sup> 2048 ± 0	<sup>231</sup> 754 ± 10	<sup>190</sup> 750 ± 2	<sup>174</sup> 754 ± 4	<sup>156</sup> 764 ± 1	<sup>133</sup> 793 ± 2	<sup>389</sup> 49192 ± 206	<sup>389</sup> 49275 ± 176							
74	cloudmatrix-001	10390	542121	<sup>39</sup> 249	<sup>97</sup> 2048 ± 0	<sup>16</sup> 114 ± 1	<sup>11</sup> 117 ± 0	<sup>9</sup> 118 ± 0	<sup>8</sup> 123 ± 1	<sup>10</sup> 169 ± 1	<sup>390</sup> 50263 ± 212	<sup>390</sup> 50243 ± 237							
75	cloudwalk-hr-003	383739	144263	<sup>214</sup> 984	<sup>331</sup> 2057 ± 0	<sup>172</sup> 606 ± 0	<sup>138</sup> 588 ± 0	<sup>117</sup> 594 ± 0	<sup>104</sup> 612 ± 1	-	<sup>324</sup> 6982 ± 80	<sup>323</sup> 6972 ± 84							
76	cloudwalk-hr-004	502916	520169	<sup>274</sup> 1394	<sup>288</sup> 2049 ± 0	<sup>279</sup> 873 ± 1	<sup>232</sup> 877 ± 1	<sup>206</sup> 876 ± 1	<sup>184</sup> 879 ± 1	<sup>159</sup> 902 ± 3	<sup>341</sup> 11652 ± 127	<sup>341</sup> 11608 ± 123							
77	cloudwalk-mt-004	1384602	512628	<sup>397</sup> 5426	<sup>211</sup> 2048 ± 0	<sup>294</sup> 923 ± 2	<sup>248</sup> 919 ± 1	<sup>221</sup> 918 ± 0	<sup>198</sup> 919 ± 0	<sup>163</sup> 927 ± 1	<sup>342</sup> 11744 ± 170	<sup>342</sup> 11631 ± 126							
78	cloudwalk-mt-005	846026	573253	<sup>370</sup> 2928	<sup>111</sup> 2048 ± 0	<sup>352</sup> 1179 ± 3	<sup>315</sup> 1200 ± 3	<sup>305</sup> 1209 ± 3	<sup>281</sup> 1226 ± 5	<sup>232</sup> 1229 ± 3	<sup>347</sup> 12525 ± 225	<sup>346</sup> 12394 ± 152							
79	clova-000	198420	6824	<sup>75</sup> 464	<sup>155</sup> 2048 ± 0	<sup>102</sup> 437 ± 0	<sup>77</sup> 431 ± 0	<sup>61</sup> 435 ± 0	<sup>55</sup> 452 ± 2	<sup>51</sup> 508 ± 7	<sup>194</sup> 1794 ± 16	<sup>198</sup> 1795 ± 19							
80	cogent-006	1078167	58108	<sup>291</sup> 1547	<sup>79</sup> 1062 ± 0	<sup>236</sup> 768 ± 0	<sup>200</sup> 789 ± 1	<sup>191</sup> 831 ± 2	<sup>201</sup> 930 ± 1	<sup>176</sup> 971 ± 1	<sup>197</sup> 1802 ± 17	<sup>199</sup> 1797 ± 23							
81	cogent-007	621565	72316	<sup>321</sup> 1884	<sup>54</sup> 550 ± 0	<sup>387</sup> 1329 ± 2	<sup>344</sup> 1333 ± 5	<sup>336</sup> 1337 ± 4	<sup>309</sup> 1353 ± 5	<sup>266</sup> 1390 ± 4	<sup>30</sup> 355 ± 8	<sup>32</sup> 367 ± 14							
82	cognitec-003	471458	62502	<sup>176</sup> 817	<sup>291</sup> 2052 ± 0	<sup>73</sup> 366 ± 9	<sup>68</sup> 403 ± 9	<sup>50</sup> 408 ± 9	<sup>48</sup> 424 ± 9	<sup>52</sup> 509 ± 13	<sup>271</sup> 3417 ± 51	<sup>274</sup> 3433 ± 53							
83	cognitec-004	705645	62678	<sup>111</sup> 585	<sup>304</sup> 2052 ± 0	<sup>109</sup> 463 ± 9	<sup>103</sup> 497 ± 9	<sup>85</sup> 504 ± 10	<sup>77</sup> 521 ± 10	<sup>84</sup> 631 ± 12	<sup>257</sup> 3028 ± 197	<sup>258</sup> 3059 ± 238							
84	cor-001	1194948	11240	<sup>251</sup> 1249	<sup>333</sup> 2060 ± 0	<sup>220</sup> 699 ± 3	<sup>226</sup> 863 ± 76	<sup>199</sup> 865 ± 80	<sup>181</sup> 872 ± 89	<sup>173</sup> 952 ± 39	<sup>410</sup> 270145 ± 2259	<sup>410</sup> 282686 ± 11788							
85	coretech-000	186423	43964	<sup>58</sup> 393	<sup>38</sup> 512 ± 0	<sup>171</sup> 602 ± 15	<sup>163</sup> 659 ± 12	<sup>286</sup> 1139 ± 24	<sup>258</sup> 1149 ± 25	<sup>218</sup> 1165 ± 23	<sup>25</sup> 333 ± 14	<sup>25</sup> 321 ± 13							
86	corsight-001	1437763	31525	<sup>334</sup> 2040	<sup>335</sup> 2064 ± 0	<sup>377</sup> 1291 ± 3	<sup>333</sup> 1285 ± 1	<sup>322</sup> 1293 ± 1	<sup>295</sup> 1303 ± 2	<sup>259</sup> 1379 ± 3	<sup>409</sup> 249340 ± 1713	<sup>409</sup> 248929 ± 1909							
87	corsight-002	1474921</td																	

	ALGORITHM	CONFIG	LIBRARY	TEMPLATE								COMPARISON <sup>4</sup>											
				NAME		DATA		MEMORY		SIZE		GENERATION TIME (ms) <sup>4</sup>				TIME (ns) <sup>5</sup>							
				(KB) <sup>1</sup>	(KB) <sup>2</sup>	(MB) <sup>3</sup>	(B)	MUGSHOT	480x720	960x1440	1600x2400	3000x4500	GENUINE	IMPOSTOR									
89	csc-003	0	400435	300	1609	51	544 ± 0	127	499 ± 0	105	500 ± 1	84	502 ± 0	73	508 ± 1	60	535 ± 4	35	393 ± 8	36	397 ± 7		
90	ctcbcbank-000	257208	599238	109	570	128	2048 ± 0	155	568 ± 43	144	606 ± 38	154	690 ± 53	139	711 ± 50	144	831 ± 51	276	3551 ± 87	295	4805 ± 209		
91	ctcbcbank-001	275511	599238	118	603	125	2048 ± 0	194	652 ± 35	199	781 ± 30	205	875 ± 43	191	898 ± 51	189	1030 ± 47	285	3926 ± 45	284	3924 ± 56		
92	cubox-001	369627	75427	126	649	152	2048 ± 0	287	907 ± 1	244	902 ± 1	214	903 ± 0	197	917 ± 0	164	931 ± 0	159	1379 ± 37	165	1417 ± 38		
93	cubox-002	542254	90975	329	1964	165	2048 ± 0	293	921 ± 1	249	921 ± 1	225	922 ± 1	203	933 ± 1	182	1003 ± 1	214	2008 ± 72	214	1969 ± 57		
94	cudocommunication-001	385258	341277	227	1077	189	2048 ± 0	296	925 ± 1	250	923 ± 1	230	928 ± 1	202	932 ± 0	173	964 ± 1	233	2534 ± 20	237	2537 ± 20		
95	cuuhkee-001	787853	74917	349	2515	293	2052 ± 0	311	977 ± 31	-	-	-	-	-	-	242	2719 ± 60	246	2783 ± 56				
96	cybercore-001	166096	7791	352	2574	106	2048 ± 0	123	487 ± 0	97	486 ± 0	80	488 ± 0	67	487 ± 0	50	502 ± 0	393	52119 ± 111	393	52127 ± 111		
97	cybercore-002	166096	7374	351	2564	163	2048 ± 0	124	489 ± 1	-	-	-	-	-	-	345	12389 ± 123	345	12352 ± 112				
98	cyberextruder-002	168909	13924	36	194	117	2048 ± 0	139	532 ± 6	-	-	-	-	-	-	198	1803 ± 14	194	1779 ± 22				
99	cyberextruder-003	253300	12354	67	437	20	512 ± 0	81	390 ± 1	62	388 ± 1	46	393 ± 1	39	399 ± 1	37	435 ± 1	8	198 ± 4	9	189 ± 8		
100	cyberlink-007	380046	102446	310	1743	406	6212 ± 0	223	725 ± 1	186	732 ± 1	169	734 ± 1	147	736 ± 1	131	767 ± 1	22	304 ± 19	23	304 ± 16		
101	cyberlink-008	380047	102470	311	1748	407	6212 ± 0	224	729 ± 1	183	725 ± 0	166	727 ± 0	145	732 ± 0	128	760 ± 0	15	263 ± 17	18	255 ± 13		
102	dahua-006	831641	119261	393	5068	199	2048 ± 0	400	1398 ± 2	359	1397 ± 1	352	1404 ± 1	328	1402 ± 1	269	1402 ± 1	14	249 ± 13	17	250 ± 11		
103	dahua-007	1578737	119418	406	7237	367	4096 ± 0	397	1393 ± 2	350	1373 ± 1	345	1378 ± 1	318	1378 ± 1	260	1379 ± 2	32	367 ± 102	37	434 ± 108		
104	daon-000	280726	2307	333	2013	336	2065 ± 0	150	562 ± 3	133	581 ± 5	180	791 ± 9	171	838 ± 15	195	1055 ± 32	354	16052 ± 88	354	16041 ± 85		
105	decatur-000	350495	171271	196	907	384	4100 ± 0	323	1024 ± 2	-	-	-	-	-	-	340	11439 ± 80	340	11418 ± 112				
106	decatur-001	342866	253734	288	1507	294	2052 ± 0	335	1103 ± 2	285	1064 ± 2	271	1063 ± 2	238	1067 ± 2	201	1084 ± 2	63	610 ± 19	63	602 ± 8		
107	deepglint-003	838065	262081	345	2374	403	6144 ± 0	350	1159 ± 1	303	1145 ± 1	290	1148 ± 1	257	1148 ± 1	217	1163 ± 1	356	17227 ± 41	356	17210 ± 51		
108	deepglint-004	1073382	261571	372	3084	269	2048 ± 0	411	1470 ± 1	370	1474 ± 1	364	1485 ± 1	338	1474 ± 1	287	1492 ± 2	312	5961 ± 34	313	5955 ± 29		
109	deepsea-001	147497	336250	55	358	66	1024 ± 0	186	630 ± 7	191	752 ± 37	171	746 ± 30	143	727 ± 32	140	820 ± 32	164	1401 ± 37	167	1467 ± 50		
110	deeepsense-000	357113	936618	407	7618	256	2048 ± 0	201	664 ± 3	161	645 ± 1	142	660 ± 2	128	687 ± 2	138	808 ± 3	41	480 ± 22	43	459 ± 34		
111	deeepsense-001	73173	1288355	394	5314	36	512 ± 0	345	1142 ± 2	307	1164 ± 3	300	1183 ± 3	276	1201 ± 3	250	1323 ± 2	230	2356 ± 35	230	2354 ± 42		
112	dermalog-008	0	937895	392	4989	30	512 ± 0	85	404 ± 2	69	410 ± 3	58	424 ± 5	50	430 ± 5	46	477 ± 5	38	468 ± 31	27	328 ± 13		
113	dermalog-009	0	319363	129	664	23	512 ± 0	65	349 ± 0	50	351 ± 0	30	352 ± 0	32	357 ± 0	29	389 ± 0	43	487 ± 34	35	385 ± 29		
114	dicio-001	61751	119517	977	44	520 ± 0	142	538 ± 0	128	563 ± 10	218	915 ± 3	353	1800 ± 7	352	5286 ± 30	246	2818 ± 20	247	2807 ± 31			
115	didiglobalface-001	259849	70680	94	527	225	2048 ± 0	174	612 ± 1	157	633 ± 3	136	634 ± 3	118	650 ± 15	99	666 ± 4	118	973 ± 20	119	988 ± 20		
116	digidata-000	133370	30249	41	257	250	2048 ± 0	72	361 ± 0	54	360 ± 0	38	361 ± 0	33	363 ± 0	27	380 ± 0	218	2084 ± 37	216	2039 ± 42		
117	digitalbarriers-002	83002	598577	324	1930	326	2056 ± 0	33	209 ± 11	27	250 ± 19	51	411 ± 37	162	808 ± 72	318	2236 ± 123	348	13409 ± 228	349	13267 ± 206		
118	dps-000	0	2211812	222	1058	357	4096 ± 0	272	868 ± 2	241	893 ± 6	358	1445 ± 9	370	2910 ± 38	365	9345 ± 17	169	1473 ± 37	169	1479 ± 37		
119	dsk-000	11967	782905	40	252	26	512 ± 0	54	304 ± 47	43	317 ± 33	253	1001 ± 96	369	2660 ± 170	368	10451 ± 832	327	7152 ± 115	325	7134 ± 111		
120	einetworks-000	372608	219883	192	880	330	2056 ± 0	192	645 ± 3	-	-	-	-	-	-	298	4876 ± 66	299	5156 ± 77				
121	ekin-002	51434	278	23	139	344	3072 ± 0	357	1186 ± 13	312	1180 ± 12	297	1181 ± 11	273	1191 ± 11	227	1207 ± 8	290	4294 ± 80	306	5569 ± 112		
122	enface-000	369598	153781	128	662	60	1024 ± 0	149	555 ± 4	127	558 ± 4	146	669 ± 6	218	987 ± 15	323	2349 ± 54	325	7059 ± 62	324	6980 ± 65		
123	enface-001	370710	173609	132	670	67	1024 ± 0	147	550 ± 4	125	555 ± 3	145	668 ± 7	215	981 ± 15	327	2416 ± 59	319	6734 ± 68	319	6766 ± 69		
124	eocortex-000	255937	59432	38	224	216	2048 ± 0	55	305 ± 22	48	341 ± 25	65	440 ± 47	59	464 ± 45	54	513 ± 44	114	923 ± 11	115	918 ± 11		
125	ercacat-001	811623	58012	363	2816	303	2052 ± 0	330	1052 ± 3	-	-	-	-	-	-	237	2551 ± 62	234	2501 ± 81				
126	euronovate-001	0	1774966	263	1308	82	1177 ± 0	326	1034 ± 2	308	1165 ± 3	293	1160 ± 3	264	1177 ± 3	221	1172 ± 2	405	81294 ± 591	405	81631 ± 931		
127	expasoft-001	39057	983064	24	142	169	2048 ± 0	70	70 ± 0	574	70 ± 0	57	77 ± 0	473	70 ± 0	474	74 ± 0	179	1660 ± 35	180	1676 ± 48		
128	expasoft-002	38760	59825	29	168	116	2048 ± 0	5	34 ± 0	3	34 ± 0	3	34 ± 0	2	34 ± 0	234	70 ± 0	333	8870 ± 78	333	8838 ± 77		
129	f8-001	272977	19668	255	1276	274	2048 ± 0	260	822 ± 39	-	-	-	-	-	-	353	15262 ± 139	353	15277 ± 212				
130	f8-002	28278	215616	12	83	103	2048 ± 0	6	39 ± 0	4	41 ± 0	4	75 ± 0	15	197 ± 1	107	702 ± 1	351	14765 ± 131	351	14790 ± 133		
131	faceonlive-001	0	71529	50	302	317	2056 ± 0	25	179 ± 0	16	179 ± 0	18	190 ± 0	16	217 ± 0	21	343 ± 1	130	1064 ± 37	129	1033 ± 35		
132	facephi-000	148904	5219	409	11481	238	2048 ± 0	275	871 ± 2	234	881 ± 3	208	880 ± 4	189	888 ± 4	169	949 ± 12	288	4067 ± 53	287	4047 ± 53		

Notes  
 1 The configuration size does not capture static data included in libraries.  
 2 The library size is the combined total of all files provided in the submission lib folder. These libraries e.g. OpenCV may or may not be installed on any end user's platform natively and would not need to be installed with the algorithm. Some developers put neural network models in their libraries.  
 3 The memory usage is the peak resident set size reported by the ps system call during template generation.  
 4 The median template creation times are measured on Intel®Xeon®CPU E5-2630 v4 @ 2.20GHz processors.  
 5 The comparison durations, in nanoseconds, are estimated using std::chrono::high\_resolution\_clock which on the machine in (2) counts 1ns clock ticks. Precision is somewhat worse than that however. The ± value is the median absolute deviation times 1.48 for Normal consistency.

	ALGORITHM	CONFIG	LIBRARY	TEMPLATE								COMPARISON <sup>4</sup>					
				NAME		DATA		MEMORY		SIZE		GENERATION TIME (ms) <sup>4</sup>				TIME (ns) <sup>5</sup>	
				(KB) <sup>1</sup>	(KB) <sup>2</sup>	(MB) <sup>3</sup>	(B)	MUGSHOT	480x720	960x1440	1600x2400	3000x4500	GENUINE	IMPOSTOR			
133	facesoft-000	370120	10612	<sup>166</sup> 796	<sup>190</sup> 2048	<sup>± 0</sup>	<sup>206</sup> 675 ± 18	<sup>166</sup> 669 ± 3	<sup>152</sup> 686 ± 3	<sup>123</sup> 675 ± 5	<sup>103</sup> 687 ± 2	<sup>226</sup> 2239 ± 28	<sup>228</sup> 2277 ± 96				
134	facetag-000	1232331	4022	<sup>210</sup> 965	<sup>56</sup> 684 ± 0	<sup>67</sup> 355 ± 17	<sup>57</sup> 369 ± 8	<sup>251</sup> 989 ± 33	<sup>366</sup> 2408 ± 91	<sup>363</sup> 7930 ± 316	<sup>402</sup> 72003 ± 625	<sup>403</sup> 71912 ± 612					
135	facetag-002	819806	4021	<sup>150</sup> 726	<sup>246</sup> 2048 ± 0	<sup>143</sup> 544 ± 1	<sup>119</sup> 544 ± 0	<sup>100</sup> 542 ± 0	<sup>83</sup> 545 ± 0	<sup>66</sup> 554 ± 0	<sup>187</sup> 1730 ± 25	<sup>187</sup> 1733 ± 25					
136	facex-001	305074	930372	<sup>371</sup> 2931	<sup>150</sup> 2048 ± 0	<sup>94</sup> 422 ± 4	<sup>79</sup> 434 ± 4	<sup>93</sup> 520 ± 7	<sup>148</sup> 737 ± 13	<sup>303</sup> 1670 ± 27	<sup>204</sup> 1871 ± 23	<sup>203</sup> 1846 ± 29					
137	facex-002	305074	928334	<sup>373</sup> 3095	<sup>98</sup> 2048 ± 0	<sup>95</sup> 426 ± 5	<sup>76</sup> 429 ± 4	<sup>91</sup> 516 ± 8	<sup>144</sup> 730 ± 12	<sup>308</sup> 1738 ± 36	<sup>77</sup> 631 ± 25	<sup>68</sup> 614 ± 19					
138	farfaces-001	346494	44581	<sup>42</sup> 261	<sup>15</sup> 512 ± 0	<sup>353</sup> 1179 ± 1	<sup>313</sup> 1180 ± 1	<sup>296</sup> 1180 ± 0	<sup>268</sup> 1185 ± 1	<sup>228</sup> 1209 ± 2	<sup>111</sup> 855 ± 25	<sup>110</sup> 860 ± 31					
139	fiberhome-nanjing-003	352895	1482309	<sup>184</sup> 845	<sup>245</sup> 2048 ± 0	<sup>341</sup> 1136 ± 7	<sup>298</sup> 1134 ± 4	<sup>284</sup> 1132 ± 3	<sup>254</sup> 1139 ± 3	<sup>212</sup> 1154 ± 5	<sup>135</sup> 1097 ± 38	<sup>137</sup> 1083 ± 42					
140	fiberhome-nanjing-004	443779	1482313	<sup>219</sup> 1048	<sup>381</sup> 4096 ± 0	<sup>385</sup> 1321 ± 5	<sup>337</sup> 1304 ± 3	<sup>327</sup> 1307 ± 2	<sup>300</sup> 1308 ± 3	<sup>252</sup> 1326 ± 5	<sup>154</sup> 1276 ± 40	<sup>154</sup> 1265 ± 38					
141	fincore-000	256615	19409	<sup>98</sup> 535	<sup>134</sup> 2048 ± 0	<sup>132</sup> 508 ± 3	<sup>108</sup> 505 ± 0	<sup>87</sup> 508 ± 1	<sup>75</sup> 513 ± 2	<sup>59</sup> 535 ± 1	<sup>191</sup> 1765 ± 31	<sup>191</sup> 1763 ± 22					
142	fujitsulab-002	0	1088887	<sup>301</sup> 1613	<sup>391</sup> 4104 ± 0	<sup>364</sup> 1237 ± 2	<sup>320</sup> 1222 ± 2	<sup>307</sup> 1236 ± 1	<sup>284</sup> 1251 ± 2	<sup>253</sup> 1327 ± 2	<sup>247</sup> 2836 ± 25	<sup>248</sup> 2809 ± 44					
143	fujitsulab-003	662263	318209	<sup>405</sup> 6907	<sup>390</sup> 4104 ± 0	<sup>305</sup> 951 ± 20	<sup>256</sup> 941 ± 19	<sup>239</sup> 952 ± 19	<sup>214</sup> 971 ± 20	<sup>192</sup> 1045 ± 21	<sup>248</sup> 2855 ± 16	<sup>250</sup> 2849 ± 19					
144	geo-002	369903	98667	<sup>217</sup> 1018	<sup>244</sup> 2048 ± 0	<sup>244</sup> 791 ± 1	<sup>201</sup> 793 ± 0	<sup>181</sup> 794 ± 0	<sup>159</sup> 795 ± 1	<sup>135</sup> 803 ± 1	<sup>270</sup> 3407 ± 45	<sup>272</sup> 3422 ± 65					
145	geo-004	168980	107714	<sup>257</sup> 1280	<sup>119</sup> 2048 ± 0	<sup>372</sup> 1268 ± 1	<sup>332</sup> 1279 ± 1	<sup>317</sup> 1274 ± 0	<sup>287</sup> 1259 ± 1	<sup>244</sup> 1296 ± 1	<sup>127</sup> 1023 ± 20	<sup>128</sup> 1028 ± 22					
146	glory-003	0	536910	<sup>275</sup> 1400	<sup>396</sup> 4234 ± 0	<sup>125</sup> 489 ± 0	<sup>129</sup> 565 ± 0	<sup>168</sup> 732 ± 0	<sup>356</sup> 1876 ± 2	<sup>364</sup> 8941 ± 20	<sup>314</sup> 6020 ± 90	<sup>315</sup> 6003 ± 72					
147	glory-004	0	999639	<sup>341</sup> 2181	<sup>395</sup> 4182 ± 0	<sup>214</sup> 688 ± 0	<sup>194</sup> 759 ± 1	<sup>234</sup> 941 ± 1	<sup>360</sup> 2134 ± 4	<sup>366</sup> 4982 ± 47	<sup>300</sup> 4982 ± 66	<sup>298</sup> 4990 ± 63					
148	gorilla-007	441058	708166	<sup>303</sup> 1691	<sup>408</sup> 6288 ± 0	<sup>168</sup> 592 ± 1	<sup>140</sup> 592 ± 1	<sup>122</sup> 603 ± 1	<sup>111</sup> 625 ± 2	<sup>116</sup> 722 ± 9	<sup>281</sup> 3686 ± 37	<sup>282</sup> 3709 ± 36					
149	gorilla-008	450175	707000	<sup>314</sup> 1789	<sup>410</sup> 8338 ± 0	<sup>170</sup> 595 ± 1	<sup>139</sup> 590 ± 0	<sup>120</sup> 600 ± 1	<sup>109</sup> 621 ± 2	<sup>114</sup> 720 ± 9	<sup>293</sup> 4530 ± 44	<sup>291</sup> 4524 ± 38					
150	graymatics-001	13095	70406	<sup>21</sup> 127	<sup>354</sup> 4096 ± 0	<sup>30</sup> 191 ± 1	<sup>22</sup> 203 ± 1	<sup>116</sup> 592 ± 5	<sup>349</sup> 1698 ± 9	<sup>361</sup> 7150 ± 34	<sup>382</sup> 39874 ± 309	<sup>382</sup> 39762 ± 295					
151	griaule-000	0	598214	<sup>221</sup> 1054	<sup>309</sup> 2052 ± 0	<sup>92</sup> 416 ± 6	<sup>74</sup> 425 ± 7	<sup>178</sup> 770 ± 14	<sup>350</sup> 1749 ± 43	<sup>359</sup> 6406 ± 189	<sup>286</sup> 3987 ± 42	<sup>285</sup> 3938 ± 38					
152	hertasecurity-000	0	780014	<sup>92</sup> 516	<sup>2</sup> 256 ± 0	<sup>12</sup> 99 ± 0	<sup>9</sup> 98 ± 0	<sup>8</sup> 100 ± 0	<sup>7</sup> 107 ± 0	<sup>7</sup> 139 ± 0	<sup>89</sup> 710 ± 31	<sup>83</sup> 667 ± 28					
153	hertasecurity-001	0	944427	<sup>243</sup> 1183	<sup>37</sup> 512 ± 0	<sup>64</sup> 346 ± 0	<sup>49</sup> 345 ± 0	<sup>34</sup> 349 ± 0	<sup>30</sup> 354 ± 0	<sup>28</sup> 388 ± 0	<sup>192</sup> 1770 ± 45	<sup>186</sup> 1726 ± 48					
154	hik-001	667866	9290	<sup>403</sup> 6597	<sup>86</sup> 1408 ± 0	<sup>193</sup> 651 ± 0	<sup>165</sup> 667 ± 8	<sup>149</sup> 677 ± 16	<sup>127</sup> 686 ± 13	<sup>120</sup> 737 ± 12	<sup>44</sup> 488 ± 19	<sup>44</sup> 477 ± 22					
155	hisign-001	732412	167488	<sup>292</sup> 1553	<sup>338</sup> 2080 ± 0	<sup>380</sup> 1306 ± 1	<sup>341</sup> 1320 ± 1	<sup>329</sup> 1315 ± 1	<sup>302</sup> 1312 ± 1	<sup>251</sup> 1325 ± 1	<sup>10</sup> 201 ± 10	<sup>7</sup> 185 ± 13					
156	hyperverge-002	2951900	198832	<sup>330</sup> 1975	<sup>69</sup> 1024 ± 0	<sup>298</sup> 938 ± 1	<sup>255</sup> 939 ± 1	<sup>232</sup> 941 ± 1	<sup>208</sup> 945 ± 1	<sup>177</sup> 975 ± 1	<sup>315</sup> 6023 ± 37	<sup>314</sup> 5966 ± 40					
157	hyperverge-003	1167779	282156	<sup>360</sup> 2748	<sup>63</sup> 1024 ± 0	<sup>413</sup> 1477 ± 2	<sup>371</sup> 1503 ± 3	<sup>366</sup> 1520 ± 3	<sup>341</sup> 1525 ± 4	<sup>296</sup> 1565 ± 3	<sup>51</sup> 566 ± 11	<sup>52</sup> 561 ± 8					
158	hzailu-001	0	372018	<sup>107</sup> 563	<sup>325</sup> 2056 ± 0	<sup>339</sup> 1126 ± 1	<sup>297</sup> 1128 ± 1	<sup>283</sup> 1130 ± 1	<sup>251</sup> 1132 ± 1	<sup>216</sup> 1159 ± 1	<sup>113</sup> 894 ± 19	<sup>114</sup> 899 ± 22					
159	icm-002	621586	903	<sup>79</sup> 484	<sup>151</sup> 2048 ± 0	<sup>325</sup> 1031 ± 7	-	-	-	-	<sup>369</sup> 24052 ± 118	<sup>368</sup> 24049 ± 124					
160	icm-003	1513988	940	<sup>86</sup> 500	<sup>108</sup> 2048 ± 0	<sup>209</sup> 681 ± 6	<sup>167</sup> 672 ± 4	<sup>163</sup> 714 ± 11	<sup>170</sup> 837 ± 41	<sup>261</sup> 1381 ± 131	<sup>370</sup> 24351 ± 161	<sup>369</sup> 24227 ± 146					
161	ichthtc-000	172459	1471004	<sup>316</sup> 1805	<sup>133</sup> 2048 ± 0	<sup>63</sup> 338 ± 11	<sup>47</sup> 338 ± 9	<sup>62</sup> 437 ± 16	<sup>135</sup> 705 ± 24	<sup>307</sup> 1719 ± 44	<sup>302</sup> 5284 ± 63	<sup>301</sup> 5290 ± 54					
162	id3-006	210116	7706	<sup>213</sup> 982	<sup>46</sup> 520 ± 0	<sup>210</sup> 683 ± 0	<sup>288</sup> 1088 ± 1	<sup>302</sup> 1192 ± 1	<sup>278</sup> 1209 ± 1	<sup>305</sup> 5547 ± 34	<sup>305</sup> 5563 ± 34						
163	id3-008	242416	8151	<sup>225</sup> 1068	<sup>8</sup> 264 ± 0	<sup>255</sup> 819 ± 0	<sup>317</sup> 1209 ± 2	<sup>325</sup> 1297 ± 2	<sup>304</sup> 1329 ± 1	<sup>277</sup> 1433 ± 1	<sup>308</sup> 5658 ± 44	<sup>308</sup> 5624 ± 40					
164	idemia-007	353242	67485	<sup>220</sup> 1051	<sup>14</sup> 468 ± 0	<sup>79</sup> 384 ± 0	<sup>63</sup> 389 ± 0	<sup>47</sup> 393 ± 1	<sup>43</sup> 405 ± 2	<sup>38</sup> 441 ± 8	<sup>265</sup> 3243 ± 63	<sup>265</sup> 3202 ± 63					
165	idemia-008	374017	69922	<sup>244</sup> 1194	<sup>12</sup> 348 ± 0	<sup>107</sup> 457 ± 1	<sup>89</sup> 461 ± 0	<sup>71</sup> 466 ± 1	<sup>64</sup> 476 ± 2	<sup>53</sup> 513 ± 10	<sup>260</sup> 3080 ± 41	<sup>260</sup> 3046 ± 56					
166	iit-002	259579	52070	<sup>153</sup> 731	<sup>140</sup> 2048 ± 0	<sup>138</sup> 514 ± 1	<sup>111</sup> 531 ± 2	<sup>104</sup> 547 ± 1	<sup>91</sup> 583 ± 1	<sup>118</sup> 733 ± 2	<sup>126</sup> 1023 ± 7	<sup>125</sup> 1011 ± 66					
167	iit-003	261288	53791	<sup>175</sup> 817	<sup>221</sup> 2048 ± 0	<sup>119</sup> 482 ± 0	<sup>100</sup> 493 ± 0	<sup>88</sup> 509 ± 0	<sup>83</sup> 541 ± 0	<sup>97</sup> 661 ± 0	<sup>24</sup> 324 ± 17	<sup>26</sup> 326 ± 8					
168	imagus-004	254405	380049	<sup>141</sup> 697	<sup>127</sup> 2048 ± 0	<sup>181</sup> 624 ± 1	<sup>137</sup> 587 ± 10	<sup>130</sup> 626 ± 3	<sup>99</sup> 592 ± 3	<sup>112</sup> 717 ± 6	<sup>99</sup> 760 ± 22	<sup>90</sup> 703 ± 28					
169	imagus-005	38886	534579	<sup>154</sup> 731	<sup>105</sup> 2048 ± 0	<sup>99</sup> 433 ± 4	<sup>60</sup> 381 ± 3	<sup>43</sup> 383 ± 3	<sup>36</sup> 373 ± 1	<sup>32</sup> 411 ± 1	<sup>94</sup> 731 ± 63	<sup>73</sup> 632 ± 32					
170	imperial-000	370120	10623	<sup>167</sup> 796	<sup>137</sup> 2048 ± 0	<sup>205</sup> 669 ± 1	<sup>169</sup> 675 ± 3	<sup>150</sup> 683 ± 17	<sup>124</sup> 676 ± 2	<sup>104</sup> 689 ± 2	<sup>220</sup> 2130 ± 32	<sup>215</sup> 2052 ± 100					
171	imperial-002	472327	16134	<sup>317</sup> 1826	<sup>144</sup> 2048 ± 0	<sup>156</sup> 569 ± 1	<sup>134</sup> 581 ± 15	<sup>111</sup> 575 ± 5	<sup>89</sup> 576 ± 2	<sup>74</sup> 588 ± 3	<sup>228</sup> 2278 ± 90	<sup>222</sup> 2131 ± 44					
172	incode-009	266103	21014	<sup>204</sup> 939	<sup>205</sup> 2048 ± 0	<sup>128</sup> 503 ± 0	<sup>99</sup> 490 ± 1	<sup>83</sup> 498 ± 0	<sup>72</sup> 505 ± 0	<sup>61</sup> 537 ± 0	<sup>138</sup> 1102 ± 28	<sup>141</sup> 1113 ± 29					
173	incode-010	627808	21014	<sup>354</sup> 2628	<sup>170</sup> 2048 ± 0	<sup>355</sup> 1180 ± 2	<sup>310</sup> 1178 ± 1	<sup>298</sup> 1182 ± 1	<sup>267</sup> 1184 ± 1	<sup>229</sup> 1221 ± 1	<sup>144</sup> 1164 ± 32	<sup>145</sup> 1144 ± 32					
174	innefulabs-000	370588	162172	<sup>68</sup> 439	<sup>139</sup> 2048 ± 0	<sup>319</sup> 1006 ± 3	<sup>273</sup> 1025 ± 3	<sup>262</sup> 1030 ± 4	<sup>233</sup> 1041 ± 2	<sup>209</sup> 1135 ± 3	<sup>309</sup> 5782 ± 41	<sup>311</sup> 5741 ± 45					
175	innovativetechnologyltd-001	177232	335757	<sup>52</sup> 341	<sup>217</sup> 2048 ± 0	<sup>98</sup> 433 ± 7	<sup>83</sup> 446 ± 8	<sup>63</sup> 439 ± 4	<sup>48</sup> 485 ± 7	<sup>205</sup> 1877 ± 42	<sup>208</sup> 1924 ± 97						
176	innovativetechnologyltd-002	173939	372324	<sup>197</sup> 912	<sup>275</sup> 2048 ± 0	<sup>198</sup> 661 ± 2	<sup>184</sup> 726 ± 4	<sup>246</sup> 981 ± 27	<sup>221</sup> 997 ± 40	<sup>130</sup> 766 ± 3	<sup>202</sup> 1841 ± 50	<sup>204</sup> 1857 ± 59					

Notes  
 1 The configuration size does not capture static data included in libraries.  
 2 The library size is the combined total of all files provided in the submission lib folder. These libraries e.g. OpenCV may or may not be installed on any end user's platform natively and would not need to be installed with the algorithm. Some developers put neural network models in their libraries.  
 3 The memory usage is the peak resident set size reported by the ps system call during template generation.  
 4 The median template creation times are measured on Intel®Xeon®CPU E5-2630 v4 @ 2.20GHz processors.  
 5 The comparison durations, in nanoseconds, are estimated using std::chrono::high\_resolution\_clock which on the machine in (2) counts 1ns clock ticks. Precision is somewhat worse than that however. The ± value is the median absolute deviation times 1.48 for Normal consistency.

	ALGORITHM	CONFIG	LIBRARY	TEMPLATE								COMPARISON <sup>4</sup>									
				NAME	DATA	DATA	MEMORY	SIZE	GENERATION TIME (ms) <sup>4</sup>				TIME (ns) <sup>5</sup>								
									(KB) <sup>1</sup>	(KB) <sup>2</sup>	(MB) <sup>3</sup>	(B)	MUGSHOT	480x720	960x1440	1600x2400	3000x4500	GENUINE	IMPOSTOR		
177	innovatrics-007	0	493269	325	1937	80	1064 ± 0	414	1485 ± 7	373	1785 ± 184	372	2078 ± 24	359	2123 ± 15	317	2210 ± 42	313	5978 ± 88	310	5690 ± 102
178	innovatrics-008	307323	59842	278	1424	49	538 ± 0	239	778 ± 6	195	767 ± 3	179	770 ± 3	161	803 ± 3	150	853 ± 10	256	3021 ± 66	242	2673 ± 88
179	insightface-001	776777	16606	381	3852	192	2048 ± 0	390	1366 ± 2	347	1368 ± 3	341	1372 ± 3	317	1375 ± 5	263	1386 ± 4	140	1119 ± 29	139	1108 ± 34
180	insightface-002	800572	16606	380	3819	122	2048 ± 0	399	1396 ± 2	355	1389 ± 4	351	1403 ± 3	327	1402 ± 2	272	1413 ± 3	145	1169 ± 40	142	1118 ± 38
181	intellicloudai-001	220831	868246	127	655	262	2048 ± 0	114	468 ± 2	86	456 ± 1	70	466 ± 3	71	492 ± 1	85	632 ± 2	129	1056 ± 4	133	1051 ± 72
182	intellicloudai-002	259047	58559	377	3584	388	4100 ± 0	268	847 ± 1	219	847 ± 2	197	849 ± 1	178	853 ± 1	155	878 ± 4	108	822 ± 28	107	818 ± 23
183	intellifusion-001	271872	289387	160	762	142	2048 ± 0	233	764 ± 38	198	774 ± 39	182	797 ± 42	160	803 ± 34	136	805 ± 33	139	1112 ± 28	143	1128 ± 41
184	intellifusion-002	762731	385841	205	941	360	4096 ± 0	303	950 ± 2	292	1096 ± 42	275	1088 ± 33	262	1168 ± 31	219	1171 ± 10	183	1713 ± 57	179	1665 ± 87
185	intellivision-002	43692	14505	11	81	322	2056 ± 0	59	322 ± 1	51	355 ± 2	41	372 ± 1	47	422 ± 2	78	600 ± 1	349	13525 ± 134	348	12782 ± 278
186	intellivision-003	64023	133748	168	799	314	2056 ± 0	89	407 ± 3	68	398 ± 2	54	418 ± 2	54	450 ± 1	75	591 ± 4	339	11069 ± 56	339	11066 ± 75
187	intellivix-001	256654	111858	182	842	251	2048 ± 0	75	378 ± 1	58	379 ± 1	43	381 ± 1	38	384 ± 1	35	421 ± 3	137	1100 ± 16	140	1109 ± 22
188	intelresearch-004	646918	85290	320	1856	183	2048 ± 0	384	1319 ± 2	342	1322 ± 3	333	1330 ± 3	307	1345 ± 3	271	1411 ± 5	294	4696 ± 63	292	4692 ± 66
189	intelresearch-005	398137	85290	242	1158	184	2048 ± 0	386	1328 ± 1	345	1334 ± 2	337	1344 ± 2	310	1356 ± 2	274	1423 ± 4	292	4524 ± 87	290	4461 ± 74
190	intsysmsu-001	384409	172480	165	789	145	2048 ± 0	177	614 ± 2	150	615 ± 2	140	642 ± 2	150	750 ± 3	214	1159 ± 4	67	621 ± 8	66	611 ± 31
191	intsysmsu-002	765921	172298	164	786	58	1024 ± 0	169	593 ± 1	202	793 ± 2	189	827 ± 1	182	875 ± 104	243	1293 ± 3	48	549 ± 25	50	548 ± 29
192	ionetworks-000	287609	51236	54	351	166	2048 ± 0	97	430 ± 0	80	435 ± 0	60	433 ± 0	51	432 ± 0	40	444 ± 0	322	6913 ± 102	326	7150 ± 160
193	iqface-000	268819	596337	144	704	398	4750 ± 32	141	538 ± 26	102	494 ± 2	102	543 ± 3	140	734 ± 4	267	1393 ± 4	413	636433 ± 38446	413	632654 ± 85615
194	iqface-003	370803	963398	175	817	399	4763 ± 37	135	529 ± 1	112	532 ± 2	119	599 ± 8	176	850 ± 2	304	1694 ± 2	412	575924 ± 2601	412	576653 ± 2051
195	irex-000	741899	47419	337	2086	346	3080 ± 0	269	852 ± 2	221	850 ± 1	204	874 ± 2	205	939 ± 1	234	1249 ± 5	11	201 ± 11	11	208 ± 8
196	isap-001	99049	204201	1	18	362	4096 ± 0	1	0 ± 0	-	-	-	-	-	-	-	37	459 ± 17	41	456 ± 11	
197	isap-002	256765	49931	47	288	279	2048 ± 0	237	769 ± 3	274	1027 ± 2	207	877 ± 2	155	761 ± 1	160	912 ± 2	258	3045 ± 94	253	2973 ± 66
198	isityou-000	48010	36621	16	110	411	19200 ± 0	15	113 ± 5	-	-	-	-	-	-	408	237517 ± 1318	408	237374 ± 1279		
199	isystems-001	274621	639268	232	1091	237	2048 ± 0	51	291 ± 9	-	-	-	-	-	-	50	557 ± 16	53	564 ± 22		
200	isystems-002	358984	803389	298	1595	260	2048 ± 0	239	822 ± 8	-	-	-	-	-	-	90	749 ± 31	75	632 ± 28		
201	itmo-007	415979	245376	343	2199	200	2048 ± 0	227	741 ± 2	-	-	-	-	-	-	236	2551 ± 50	236	2529 ± 80		
202	itmo-008	726866	318238	271	1377	372	4096 ± 0	331	1060 ± 1	283	1058 ± 1	270	1059 ± 1	240	1072 ± 4	204	1104 ± 1	277	3578 ± 25	277	3580 ± 28
203	ivacognitive-001	256958	62791	207	947	220	2048 ± 0	378	1292 ± 3	335	1289 ± 4	321	1292 ± 4	294	1292 ± 3	249	1321 ± 4	289	4228 ± 41	288	4226 ± 41
204	iws-000	30875	3063	8	77	24	512 ± 0	43	277 ± 5	36	283 ± 1	81	494 ± 3	217	984 ± 3	341	2987 ± 39	122	999 ± 40	121	992 ± 22
205	kakao-005	414316	152216	294	1581	300	2052 ± 0	332	1068 ± 1	287	1073 ± 1	273	1079 ± 0	241	1077 ± 1	203	1089 ± 1	217	2067 ± 26	217	2043 ± 34
206	kakao-007	526993	129545	387	3953	129	2048 ± 0	306	952 ± 1	259	961 ± 1	240	958 ± 1	213	962 ± 1	175	968 ± 1	128	1056 ± 16	131	1047 ± 28
207	kakaoipay-001	397864	179869	134	684	369	4096 ± 0	104	448 ± 0	118	542 ± 0	101	542 ± 0	84	542 ± 0	65	553 ± 0	73	633 ± 22	72	630 ± 22
208	kasikornlabs-000	256471	61000	138	693	182	2048 ± 0	288	908 ± 36	233	878 ± 22	241	969 ± 39	266	1184 ± 54	325	2382 ± 145	376	31669 ± 188	377	31714 ± 182
209	kedacom-000	245292	37401	413	23574	10	292 ± 0	130	506 ± 3	122	547 ± 10	127	614 ± 9	96	588 ± 10	98	665 ± 24	81	684 ± 14	85	682 ± 16
210	kiwitech-000	369711	21375	171	808	120	2048 ± 0	167	591 ± 0	142	594 ± 0	118	595 ± 1	100	596 ± 0	80	609 ± 0	189	1755 ± 20	188	1734 ± 16
211	kneron-003	58366	1747	33	188	112	2048 ± 0	46	281 ± 3	35	280 ± 1	29	315 ± 13	34	365 ± 7	231	1224 ± 30	301	5237 ± 63	300	5274 ± 99
212	kneron-005	375374	13633	72	457	209	2048 ± 0	518 ± 2	110	522 ± 4	107	556 ± 5	153	757 ± 19	310	1760 ± 25	209	1922 ± 11	209	1926 ± 20	
213	knowutech-000	808045	32886	262	1303	88	1536 ± 0	406	1419 ± 2	349	1372 ± 1	344	1377 ± 1	319	1382 ± 2	264	1386 ± 2	283	3743 ± 31	281	3693 ± 38
214	kookmin-002	371771	30734	180	827	138	2048 ± 0	328	1038 ± 2	282	1047 ± 1	267	1045 ± 1	237	1061 ± 1	205	1116 ± 1	75	638 ± 19	78	636 ± 20
215	kuke3d-001	403462	68786	96	530	349	4096 ± 0	251	814 ± 2	205	811 ± 2	187	814 ± 2	163	814 ± 1	147	834 ± 1	318	6412 ± 57	318	6413 ± 51
216	kuke3d-002	270544	1227855	172	809	281	2048 ± 0	129	504 ± 3	107	504 ± 1	89	511 ± 1	79	523 ± 2	73	585 ± 1	252	2943 ± 22	252	2966 ± 38
217	lebentech-000	0	10360	17	110	27	512 ± 0	3	22 ± 0	122	22 ± 0	122	23 ± 0	123	23 ± 0	106	801 ± 42	108	825 ± 51	108	825 ± 51
218	lemalabs-001	748400	198794	359	2738	173	2048 ± 0	248	810 ± 0	206	812 ± 0	184	813 ± 0	165	819 ± 0	149	844 ± 1	344	11930 ± 35	344	11913 ± 37
219	line-000	264443	407003	114	590	126	2048 ± 0	164	586 ± 0	147	612 ± 0	124	609 ± 1	103	611 ± 0	82	618 ± 1	245	2753 ± 19	245	2745 ± 23
220	line-001	944355	407058	344	2373	271	2048 ± 0	264	833 ± 10	214	830 ± 3	190	828 ± 4	172	838 ± 8	146	833 ± 4	241	2696 ± 23	243	2677 ± 35

## Notes

- 1 The configuration size does not capture static data included in libraries.
- 2 The library size is the combined total of all files provided in the submission lib folder. These libraries e.g. OpenCV may or may not be installed on any end user's platform natively and would not need to be installed with the algorithm. Some developers put neural network models in their libraries.
- 3 The memory usage is the peak resident set size reported by the ps system call during template generation.
- 4 The median template creation times are measured on Intel®Xeon®CPU E5-2630 v4 @ 2.20GHz processors.
- 5 The comparison durations, in nanoseconds, are estimated using std::chrono::high\_resolution\_clock which on the machine in (2) counts 1ns clock ticks. Precision is somewhat worse than that however. The ± value is the median absolute deviation times 1.48 for Normal consistency.

Table 11: Summary of algorithms and properties included in this report. The red superscripts give ranking for the quantity in that column.

	ALGORITHM	CONFIG	LIBRARY	TEMPLATE								COMPARISON <sup>4</sup>									
				NAME	DATA	DATA	MEMORY	SIZE	GENERATION TIME (ms) <sup>4</sup>				TIME (ns) <sup>5</sup>								
									(KB) <sup>1</sup>	(KB) <sup>2</sup>	(MB) <sup>3</sup>	(B)	MUGSHOT	480x720	960x1440	1600x2400	3000x4500	GENUINE	IMPOSTOR		
221	lookman-002	138200	25410	411	16518	52	548 ± 0	23	173 ± 1	-	-	-	-	-	62	610 ± 19	67	612 ± 22			
222	lookman-004	244775	37401	412	23548	53	548 ± 0	131	507 ± 5	120	545 ± 12	126	613 ± 12	98	590 ± 11	94	656 ± 16	112	871 ± 29	112	878 ± 29
223	luxand-000	0	57908	268	1366	77	1040 ± 0	87	407 ± 23	78	433 ± 11	66	444 ± 14	60	464 ± 14	69	562 ± 25	109	828 ± 28	109	828 ± 32
224	mantra-000	471458	62566	158	749	296	2052 ± 0	91	413 ± 18	98	487 ± 19	82	494 ± 18	75	511 ± 18	77	598 ± 19	262	3151 ± 51	261	3127 ± 63
225	maxvision-000	133114	56426	315	1791	17	512 ± 0	70	359 ± 0	53	356 ± 0	37	359 ± 0	31	356 ± 0	25	370 ± 1	232	2461 ± 20	231	2452 ± 17
226	maxvision-001	256146	61793	367	2880	253	2048 ± 0	42	275 ± 3	33	274 ± 2	24	277 ± 4	22	280 ± 4	19	325 ± 3	90	714 ± 13	93	717 ± 13
227	megvii-004	3962505	44019	391	4436	382	4097 ± 0	375	1287 ± 1	348	1369 ± 2	328	1310 ± 2	321	1384 ± 3	278	1436 ± 5	387	46801 ± 204	387	46832 ± 207
228	megvii-005	1378009	44038	389	4036	289	2049 ± 0	383	1319 ± 5	324	1247 ± 6	308	1240 ± 2	283	1245 ± 2	245	1298 ± 3	378	32025 ± 121	379	32008 ± 114
229	meituuan-000	259514	333178	102	554	104	2048 ± 0	100	436 ± 4	82	441 ± 1	131	626 ± 5	244	1098 ± 15	343	3126 ± 53	76	638 ± 17	76	633 ± 16
230	meituuan-001	615387	333249	235	1106	201	2048 ± 0	320	1017 ± 4	271	1008 ± 3	257	1010 ± 2	226	1010 ± 3	184	1011 ± 4	78	654 ± 10	81	658 ± 14
231	meiya-001	280055	264913	88	507	287	2049 ± 0	180	622 ± 12	-	-	-	-	-	-	331	8356 ± 615	331	8134 ± 97		
232	mendaxiatech-000	1941475	45484	375	3195	383	4097 ± 0	366	1243 ± 2	326	1255 ± 1	342	1373 ± 2	346	1598 ± 3	334	2689 ± 8	388	46906 ± 275	388	46872 ± 217
233	microfocus-001	104524	27242	34	190	4	256 ± 0	39	264 ± 18	-	-	-	-	-	-	13	215 ± 8	13	217 ± 10		
234	microfocus-002	96288	27362	31	176	5	256 ± 0	37	259 ± 18	-	-	-	-	-	-	26	337 ± 34	15	230 ± 25		
235	minivision-000	836697	16597	388	4013	368	4096 ± 0	327	1035 ± 1	278	1033 ± 2	265	1035 ± 1	232	1037 ± 1	198	1059 ± 2	233	2466 ± 26	232	2460 ± 25
236	mobai-000	365451	80573	163	786	402	6144 ± 0	235	766 ± 8	228	869 ± 6	304	1205 ± 31	355	1867 ± 45	347	3549 ± 190	355	16458 ± 333	355	16423 ± 1473
237	mobai-001	265297	60164	97	534	215	2048 ± 0	175	612 ± 3	148	614 ± 3	153	687 ± 9	188	886 ± 31	306	1707 ± 103	160	1386 ± 25	161	1377 ± 26
238	mobbl-001	231160	58706	37	223	132	2048 ± 0	27	183 ± 32	20	184 ± 25	36	354 ± 76	168	823 ± 396	337	2781 ± 1166	343	11832 ± 109	343	11851 ± 88
239	mobbl-003	172248	60960	44	270	202	2048 ± 0	204	664 ± 6	-	-	-	-	-	-	346	12506 ± 111	347	12509 ± 100		
240	mobilpintech-000	370514	303291	237	1130	208	2048 ± 0	367	1245 ± 1	321	1234 ± 1	314	1264 ± 1	314	1360 ± 1	305	1707 ± 1	350	14506 ± 214	350	14433 ± 197
241	moreedian-000	525259	21374	202	932	171	2048 ± 0	217	694 ± 0	175	698 ± 0	159	699 ± 0	133	700 ± 0	111	713 ± 1	199	1803 ± 11	195	1779 ± 23
242	mukhh-001	866223	451194	302	1637	64	1024 ± 0	392	1375 ± 17	356	1390 ± 12	353	1406 ± 8	324	1394 ± 10	255	1360 ± 11	36	433 ± 14	38	435 ± 14
243	multimodality-000	0	503924	277	1417	175	2048 ± 0	93	416 ± 0	73	420 ± 0	57	423 ± 0	49	427 ± 0	42	463 ± 0	110	848 ± 25	105	800 ± 28
244	mvision-001	227502	149531	149	723	34	512 ± 0	215	691 ± 21	177	702 ± 19	158	697 ± 24	138	708 ± 29	110	710 ± 27	141	1123 ± 40	147	1154 ± 38
245	nazhiai-000	547484	16141	356	2716	235	2048 ± 0	211	683 ± 3	172	687 ± 2	193	835 ± 27	174	840 ± 31	148	834 ± 34	225	2230 ± 34	223	2133 ± 81
246	neosystems-002	599441	349942	249	1222	176	2048 ± 0	340	1135 ± 2	378	1855 ± 3	373	2258 ± 5	362	2238 ± 3	319	2247 ± 3	358	18752 ± 167	359	18610 ± 213
247	neosystems-003	599442	349942	247	1215	210	2048 ± 0	346	1143 ± 2	374	1836 ± 7	374	2260 ± 3	365	2273 ± 6	320	2273 ± 3	361	19167 ± 186		
248	netbridgegetch-001	133108	205875	89	508	370	4096 ± 0	9	85 ± 1	83	80 ± 0	84	80 ± 0	6	92 ± 0	6	113 ± 4	334	9280 ± 74	334	9446 ± 512
249	netbridgegetch-002	257687	49931	49	299	218	2048 ± 0	265	838 ± 6	217	838 ± 2	194	839 ± 1	173	839 ± 3	151	859 ± 3	250	2893 ± 65	257	3050 ± 123
250	neurotechnology-012	147830	51395	174	814	3	256 ± 0	78	384 ± 0	61	387 ± 0	49	404 ± 1	53	435 ± 1	72	583 ± 7	4	119 ± 7	4	116 ± 7
251	neurotechnology-013	474749	85552	369	2894	42	514 ± 0	317	1000 ± 1	268	1006 ± 2	258	1022 ± 2	236	1053 ± 2	223	1195 ± 8	2	109 ± 4	1	110 ± 4
252	nhn-002	363471	817674	131	667	371	4096 ± 0	344	1141 ± 3	300	1138 ± 2	287	1141 ± 2	259	1151 ± 6	226	1203 ± 2	394	56608 ± 579	395	56549 ± 606
253	nhn-003	933665	432730	284	1464	358	4096 ± 0	362	1229 ± 2	328	1261 ± 1	313	1263 ± 3	293	1279 ± 2	258	1375 ± 3	391	50560 ± 105	391	50592 ± 142
254	nodeflux-002	774668	690213	76	466	228	2048 ± 0	222	708 ± 4	179	709 ± 4	164	716 ± 5	142	716 ± 7	119	736 ± 3	274	3475 ± 62	271	3408 ± 143
255	notiontag-001	92753	427967	108	566	55	584 ± 0	297	929 ± 35	289	1092 ± 39	375	3709 ± 81	375	10233 ± 180	-	383	43636 ± 286	383	43724 ± 330	
256	notiontag-002	271987	967207	364	2840	341	2120 ± 0	106	453 ± 2	85	453 ± 3	67	453 ± 3	57	458 ± 2	44	471 ± 3	364	20278 ± 194	364	20195 ± 186
257	nsensecorp-002	187421	122407	103	554	113	2048 ± 0	62	333 ± 0	46	333 ± 0	33	337 ± 0	29	338 ± 0	24	351 ± 0	386	45965 ± 213	386	45988 ± 158
258	nsensecorp-003	199895	117041	147	710	219	2048 ± 0	199	661 ± 0	164	664 ± 0	144	662 ± 1	121	659 ± 1	95	659 ± 0	384	44658 ± 51	385	44654 ± 72
259	ntechlab-011	786933	209458	404	6867	83	1280 ± 0	348	1148 ± 2	301	1142 ± 1	292	1159 ± 1	269	1185 ± 1	242	1290 ± 3	5	179 ± 11	6	173 ± 11
260	ntechlab-012	570796	212350	398	5451	342	2560 ± 0	381	1309 ± 1	343	1323 ± 1	335	1331 ± 1	313	1360 ± 1	280	1460 ± 3	12	211 ± 8	12	211 ± 7
261	omnigarde-001	200523	32882	74	464	19	512 ± 0	299	941 ± 0	237	883 ± 1	209	886 ± 1	190	891 ± 1	156	898 ± 0	165	1405 ± 31	162	1379 ± 26
262	omnigarde-002	368860	32882	159	757	71	1024 ± 0	379	1303 ± 1	323	1246 ± 1	310	1249 ± 1	285	1253 ± 1	236	1261 ± 1	244	2727 ± 34	244	2686 ± 32
263	omsecurity-000	45945	844976	27	150	59	1024 ± 0	29	185 ± 1	24	206 ± 2	19	203 ± 1	12	195 ± 1	12	193 ± 1	42	481 ± 42	40	456 ± 20
264	openface-001	0	40111	15	100	131	2048 ± 0	20	148 ± 1	14	154 ± 0	39	365 ± 3	45	409 ± 9	81	616 ± 31	61	608 ± 14	65	604 ± 13

## Notes

- 1 The configuration size does not capture static data included in libraries.
- 2 The library size is the combined total of all files provided in the submission lib folder. These libraries e.g. OpenCV may or may not be installed on any end user's platform natively and would not need to be installed with the algorithm. Some developers put neural network models in their libraries.
- 3 The memory usage is the peak resident set size reported by the ps system call during template generation.
- 4 The median template creation times are measured on Intel®Xeon®CPU E5-2630 v4 @ 2.20GHz processors.
- 5 The comparison durations, in nanoseconds, are estimated using std::chrono::high\_resolution\_clock which on the machine in (2) counts 1ns clock ticks. Precision is somewhat worse than that however. The ± value is the median absolute deviation times 1.48 for Normal consistency.

Table 12: Summary of algorithms and properties included in this report. The red superscripts give ranking for the quantity in that column.

	ALGORITHM	CONFIG	LIBRARY	TEMPLATE								COMPARISON <sup>4</sup>									
				NAME	DATA	DATA	MEMORY	SIZE	GENERATION TIME (ms) <sup>4</sup>				TIME (ns) <sup>5</sup>								
									(KB) <sup>1</sup>	(KB) <sup>2</sup>	(MB) <sup>3</sup>	(B)	MUGSHOT	480x720	960x1440	1600x2400	3000x4500	GENUINE	IMPOSTOR		
265	oz-003	484147	519652	410	11949	311	2053 ± 0	391	1375 ± 12	354	1388 ± 3	371	1773 ± 16	358	2039 ± 6	345	3209 ± 5	404	73905 ± 456	404	73892 ± 444
266	oz-004	373982	1075452	408	8071	310	2053 ± 0	263	832 ± 7	229	871 ± 6	212	899 ± 10	242	1078 ± 12	299	1608 ± 10	398	61654 ± 418	397	61749 ± 450
267	pangiam-000	464252	24512	386	3919	159	2048 ± 0	184	627 ± 5	152	618 ± 4	128	615 ± 3	107	620 ± 3	91	639 ± 3	3	118 ± 7	3	113 ± 7
268	papsav1923-001	279210	52652	78	473	178	2048 ± 0	183	626 ± 1	154	628 ± 1	133	630 ± 1	117	648 ± 2	123	744 ± 3	92	725 ± 25	95	731 ± 28
269	papsav1923-002	491185	24727	239	1136	301	2052 ± 0	245	792 ± 1	263	978 ± 1	266	1042 ± 1	260	1158 ± 1	302	1641 ± 19	147	1209 ± 29	150	1206 ± 38
270	paravision-008	542190	204400	282	1448	379	4096 ± 0	219	699 ± 0	176	700 ± 0	160	701 ± 0	134	702 ± 1	108	702 ± 0	27	337 ± 17	29	330 ± 13
271	paravision-010	688291	205854	339	2150	387	4100 ± 0	188	634 ± 0	159	635 ± 0	137	635 ± 0	89	635 ± 1	174	1577 ± 35	174	1571 ± 32		
272	pensees-001	1619431	408932	323	1922	409	8200 ± 0	337	1108 ± 3	364	1448 ± 17	355	1439 ± 10	337	1464 ± 5	295	1546 ± 9	263	3151 ± 34	262	3143 ± 25
273	pixelall-006	0	746305	203	934	343	2560 ± 0	322	1024 ± 3	276	1028 ± 2	263	1033 ± 1	230	1032 ± 1	193	1054 ± 2	97	754 ± 14	94	722 ± 10
274	pixelall-007	0	444912	266	1349	284	2048 ± 0	324	1026 ± 4	279	1038 ± 2	276	1089 ± 2	243	1087 ± 2	206	1124 ± 2	88	708 ± 14	89	701 ± 19
275	psl-009	411027	411504	396	5369	393	4168 ± 0	394	1382 ± 2	352	1381 ± 1	346	1383 ± 1	320	1383 ± 2	262	1385 ± 1	23	316 ± 14	22	289 ± 14
276	psl-010	411027	591157	395	5361	394	4168 ± 0	403	1403 ± 9	-	-	-	-	-	-	29	354 ± 53	28	329 ± 29		
277	ptakuratsatu-000	0	585434	265	1347	48	538 ± 0	280	875 ± 3	225	863 ± 48	229	928 ± 9	212	958 ± 17	200	1066 ± 26	311	5900 ± 103	309	5687 ± 167
278	pxl-001	110116	78231	28	168	25	512 ± 0	13	101 ± 5	10	104 ± 5	16	189 ± 12	44	408 ± 27	283	1470 ± 144	307	5598 ± 45	307	5590 ± 68
279	pyramid-000	372608	219883	169	804	315	2056 ± 0	159	583 ± 2	-	-	-	-	-	-	326	7147 ± 59	329	7586 ± 425		
280	qnap-001	196210	13399	46	286	258	2048 ± 0	176	614 ± 1	149	615 ± 1	132	627 ± 1	110	623 ± 1	88	634 ± 2	77	649 ± 11	79	648 ± 14
281	qnap-002	346963	33284	142	700	240	2048 ± 0	257	821 ± 1	210	824 ± 1	188	824 ± 1	169	826 ± 1	145	832 ± 1	19	293 ± 13	20	287 ± 17
282	quantasoft-003	370518	211354	223	1058	100	2048 ± 0	187	632 ± 2	158	634 ± 0	135	632 ± 0	112	631 ± 1	86	634 ± 0	9	201 ± 7	10	203 ± 8
283	rankone-011	0	179209	25	146	7	261 ± 0	152	567 ± 1	126	557 ± 1	109	567 ± 1	93	586 ± 1	101	682 ± 3	18	283 ± 14	14	220 ± 19
284	rankone-012	0	264182	22	134	6	261 ± 0	151	564 ± 3	124	554 ± 1	108	564 ± 1	92	586 ± 1	105	695 ± 1	17	273 ± 17	16	231 ± 14
285	realnetworks-005	172253	56755	140	697	313	2056 ± 0	34	211 ± 4	23	205 ± 3	25	290 ± 6	76	515 ± 17	246	1312 ± 78	148	1213 ± 17	151	1207 ± 16
286	realnetworks-006	466225	56771	296	1588	328	2056 ± 0	190	638 ± 4	155	630 ± 3	147	672 ± 5	136	706 ± 5	132	774 ± 5	39	469 ± 19	45	478 ± 25
287	regula-000	262444	29384	121	610	118	2048 ± 0	358	1187 ± 1	296	1126 ± 1	282	1129 ± 0	250	1132 ± 1	215	1159 ± 1	46	491 ± 16	47	500 ± 22
288	regula-001	256075	25980	211	976	141	2048 ± 0	374	1284 ± 1	319	1220 ± 1	306	1222 ± 1	280	1226 ± 1	235	1255 ± 1	31	361 ± 10	30	342 ± 25
289	remarkai-001	241857	868314	152	730	308	2052 ± 0	262	831 ± 6	220	849 ± 18	269	1055 ± 25	274	1198 ± 34	291	1519 ± 38	152	1229 ± 20	106	805 ± 56
290	remarkai-003	280516	58559	384	3896	386	4100 ± 0	314	986 ± 1	265	993 ± 1	252	992 ± 1	222	999 ± 3	186	1019 ± 2	104	787 ± 20	103	793 ± 22
291	rendip-000	0	437653	133	682	158	2048 ± 0	110	464 ± 2	87	458 ± 0	75	473 ± 0	65	483 ± 1	67	556 ± 4	52	576 ± 13	54	573 ± 11
292	revealmedia-005	293933	202465	161	763	385	4100 ± 0	96	428 ± 0	75	428 ± 0	59	430 ± 0	52	433 ± 0	39	442 ± 0	215	2023 ± 38	215	2009 ± 26
293	revealmedia-006	293933	200912	157	741	305	2052 ± 0	77	381 ± 0	59	381 ± 0	44	382 ± 0	37	384 ± 0	31	394 ± 0	70	626 ± 35	62	600 ± 2
294	rokid-000	258612	396624	248	1218	323	2056 ± 0	144	546 ± 3	117	542 ± 2	103	545 ± 1	78	522 ± 3	70	563 ± 4	273	3457 ± 62	275	3463 ± 77
295	rokid-001	641223	413733	226	1071	334	2060 ± 0	290	911 ± 2	243	901 ± 5	211	899 ± 2	193	900 ± 3	158	901 ± 3	268	3345 ± 50	268	3346 ± 149
296	s1-003	145509	95446	177	817	352	4096 ± 0	301	947 ± 0	258	959 ± 0	238	952 ± 0	210	952 ± 1	172	955 ± 1	279	3657 ± 19	279	3652 ± 16
297	s1-004	246514	202623	143	700	160	2048 ± 0	252	815 ± 0	207	818 ± 1	187	818 ± 1	166	820 ± 1	143	828 ± 1	266	3245 ± 100	263	3161 ± 88
298	saffe-001	85973	62488	30	168	84	1280 ± 0	47	281 ± 1	-	-	-	-	-	-	153	1274 ± 19	155	1277 ± 26		
299	saffe-002	260622	28285	186	855	224	2048 ± 0	253	817 ± 11	204	805 ± 15	183	809 ± 19	164	815 ± 29	139	813 ± 23	91	717 ± 7	92	714 ± 29
300	samsungsds-000	0	307431	229	1083	257	2048 ± 0	57	316 ± 0	45	326 ± 5	31	328 ± 4	27	327 ± 1	22	343 ± 0	367	23722 ± 295	367	23874 ± 305
301	samsungsds-001	1189592	147444	383	3893	361	4096 ± 0	342	1140 ± 3	304	1145 ± 4	338	1344 ± 5	316	1366 ± 5	289	1514 ± 7	392	51559 ± 773	392	51721 ± 1003
302	samtech-001	288082	219883	119	605	316	2056 ± 0	53	294 ± 3	-	-	-	-	-	-	330	7694 ± 59	330	7678 ± 91		
303	scanovate-002	256986	457227	185	850	102	2048 ± 0	218	696 ± 32	180	713 ± 33	170	738 ± 28	158	779 ± 32	220	1172 ± 53	255	3021 ± 38	260	3120 ± 163
304	scanovate-003	135585	89469	170	808	143	2048 ± 0	160	585 ± 1	147	613 ± 12	115	591 ± 1	102	610 ± 2	251	2926 ± 22	251	2925 ± 20		
305	securifai-003	303794	13512	366	2868	389	4104 ± 0	146	549 ± 7	123	550 ± 7	105	549 ± 7	86	546 ± 6	62	546 ± 6	184	1714 ± 26	184	1713 ± 37
306	securifai-004	282177	12027	125	636	285	2048 ± 0	273	869 ± 1	227	867 ± 1	200	867 ± 1	180	867 ± 1	153	865 ± 1	182	1711 ± 19	183	1705 ± 29
307	sensetime-005	765353	37673	402	6133	73	1028 ± 0	389	1361 ± 27	338	1304 ± 1	331	1319 ± 1	315	1360 ± 1	290	1514 ± 1	151	1223 ± 28	149	1184 ± 29
308	sensetime-006	765353	37673	401	5994	72	1028 ± 0	388	1352 ± 17	339	1311 ± 1	332	1323 ± 1	311	1357 ± 1	292	1523 ± 2	146	1179 ± 28	148	1157 ± 29

## Notes

- 1 The configuration size does not capture static data included in libraries.
- 2 The library size is the combined total of all files provided in the submission lib folder. These libraries e.g. OpenCV may or may not be installed on any end user's platform natively and would not need to be installed with the algorithm. Some developers put neural network models in their libraries.
- 3 The memory usage is the peak resident set size reported by the ps system call during template generation.
- 4 The median template creation times are measured on Intel®Xeon®CPU E5-2630 v4 @ 2.20GHz processors.
- 5 The comparison durations, in nanoseconds, are estimated using std::chrono::high\_resolution\_clock which on the machine in (2) counts 1ns clock ticks. Precision is somewhat worse than that however. The ± value is the median absolute deviation times 1.48 for Normal consistency.

Table 13: Summary of algorithms and properties included in this report. The red superscripts give ranking for the quantity in that column.

	ALGORITHM	CONFIG	LIBRARY	TEMPLATE							COMPARISON <sup>4</sup>										
				NAME	DATA	DATA	MEMORY	SIZE	GENERATION TIME (ms) <sup>4</sup>				TIME (ns) <sup>5</sup>								
									(KB) <sup>1</sup>	(KB) <sup>2</sup>	(MB) <sup>3</sup>	(B)	MUGSHOT	480x720	960x1440	1600x2400	3000x4500	GENUINE	IMPOSTOR		
309	sertis-000	265572	68770	64	427	249	2048 ± 0	230	754 ± 0	193	759 ± 0	176	764 ± 0	154	760 ± 0	129	763 ± 0	171	1497 ± 29	175	1582 ± 38
310	sertis-002	460790	68929	273	1391	242	2048 ± 0	356	1181 ± 1	309	1178 ± 0	299	1183 ± 0	272	1187 ± 0	230	1221 ± 0	134	1086 ± 32	134	1076 ± 31
311	seventhsense-000	369850	1561668	179	824	292	2052 ± 0	369	1250 ± 3	327	1257 ± 1	312	1261 ± 1	288	1259 ± 1	239	1272 ± 2	196	1800 ± 35	196	1787 ± 32
312	seventhsense-001	369850	3183365	173	811	290	2052 ± 0	370	1255 ± 2	336	1294 ± 15	318	1277 ± 3	291	1275 ± 2	241	1288 ± 3	210	1936 ± 26	211	1943 ± 34
313	shaman-000	0	120033	87	507	375	4096 ± 0	193	653 ± 16	-	-	-	-	-	-	-	-	34	380 ± 25	34	379 ± 31
314	shaman-001	0	174446	91	511	363	4096 ± 0	52	294 ± 2	-	-	-	-	-	-	-	74	635 ± 19	39	441 ± 25	
315	shu-002	731250	148309	193	890	364	4096 ± 0	229	751 ± 2	196	769 ± 4	224	922 ± 4	333	1431 ± 9	340	3489 ± 47	414	2930763 ± 47355	414	2929759 ± 39149
316	shu-003	428774	146940	90	511	130	2048 ± 0	256	820 ± 6	213	828 ± 3	233	941 ± 9	299	1308 ± 15	342	3045 ± 44	234	2506 ± 26	235	2512 ± 38
317	siat-002	486842	7738	346	2434	298	2052 ± 0	157	579 ± 0	-	-	-	-	-	-	-	-	101	769 ± 13	99	750 ± 13
318	siat-005	380936	16935	261	1298	206	2048 ± 0	84	403 ± 0	67	400 ± 0	48	401 ± 0	41	403 ± 1	36	422 ± 7	53	577 ± 13	55	580 ± 17
319	sjtu-003	480795	148243	99	538	188	2048 ± 0	258	821 ± 2	208	820 ± 2	220	923 ± 3	275	1201 ± 3	324	2373 ± 9	173	1560 ± 20	172	1560 ± 14
320	sjtu-004	1953267	241108	357	2727	397	4608 ± 0	363	1236 ± 2	316	1209 ± 2	324	1294 ± 4	344	1554 ± 5	336	2738 ± 8	259	3057 ± 14	259	3070 ± 20
321	sktelecom-000	527132	298496	264	1311	87	1536 ± 0	338	1110 ± 1	293	1113 ± 1	279	1114 ± 1	246	1120 ± 1	213	1155 ± 1	374	26583 ± 128	373	26508 ± 126
322	smartengines-000	1711	3025	350	9	288 ± 0	22	168 ± 7	17	180 ± 1	15	188 ± 3	17	217 ± 3	17	275 ± 1	7	197 ± 5	5	167 ± 11	
323	smilart-002	111826	87805	43	263	68	1024 ± 0	24	176 ± 16	-	-	-	-	-	-	-	-	359	18784 ± 136	360	18795 ± 151
324	smilart-003	67339	91670	35	192	22	512 ± 0	26	180 ± 12	18	181 ± 10	27	313 ± 22	122	665 ± 49	321	2299 ± 196	161	1395 ± 74	127	1027 ± 66
325	sodec-000	836592	13142	374	3186	376	4096 ± 0	329	1041 ± 2	277	1032 ± 1	264	1035 ± 1	231	1037 ± 2	199	1061 ± 2	195	1794 ± 37	192	1775 ± 23
326	sqisoft-001	278968	386291	136	688	321	2056 ± 0	116	477 ± 5	346	1348 ± 18	339	1353 ± 26	306	1340 ± 14	268	1393 ± 28	105	797 ± 22	102	788 ± 22
327	sqisoft-002	278039	386291	130	666	320	2056 ± 0	112	466 ± 8	90	466 ± 2	72	468 ± 11	58	461 ± 6	45	472 ± 4	98	758 ± 11	100	760 ± 23
328	stاقو-000	879661	624676	224	1064	377	4096 ± 0	250	813 ± 25	-	-	-	-	-	-	-	-	253	2979 ± 31	255	3007 ± 75
329	starhybrid-001	100509	289356	183	845	191	2048 ± 0	69	358 ± 82	52	355 ± 49	42	379 ± 58	40	401 ± 79	30	393 ± 67	132	1075 ± 51	135	1078 ± 53
330	sukshi-000	94035	688738	56	372	413	32768 ± 0	86	407 ± 11	70	413 ± 8	86	504 ± 8	129	689 ± 11	297	1574 ± 28	338	9817 ± 50	337	9787 ± 62
331	suprema-001	373423	41460	308	1731	213	2048 ± 0	243	788 ± 1	212	826 ± 2	217	914 ± 2	255	1146 ± 7	329	2443 ± 4	264	3212 ± 16	266	3220 ± 22
332	suprema-002	373808	41473	307	1731	195	2048 ± 0	242	787 ± 3	216	833 ± 3	227	924 ± 4	270	1185 ± 6	331	2479 ± 3	267	3255 ± 17	267	3235 ± 14
333	supremaid-001	258193	23479	100	541	177	2048 ± 0	118	479 ± 1	95	481 ± 0	77	481 ± 0	68	490 ± 0	58	522 ± 0	86	704 ± 19	80	652 ± 19
334	surrey-cvssp-000	158030	70795	191	879	286	2048 ± 0	343	1141 ± 3	306	1157 ± 3	291	1158 ± 4	261	1163 ± 3	233	1245 ± 3	336	9557 ± 143	335	9602 ± 186
335	synesis-006	731941	21817	285	1472	392	4104 ± 0	145	549 ± 1	121	546 ± 1	106	552 ± 1	88	558 ± 2	92	639 ± 28	85	697 ± 32	88	688 ± 31
336	synesis-007	1442961	24145	347	2443	347	3080 ± 0	359	1215 ± 5	330	1268 ± 30	326	1306 ± 67	301	1311 ± 58	275	1423 ± 52	82	684 ± 32	86	686 ± 25
337	synology-000	221021	25809	71	453	207	2048 ± 0	88	407 ± 14	71	415 ± 14	156	694 ± 31	325	1396 ± 58	348	4568 ± 211	363	19720 ± 203	362	19767 ± 379
338	synology-002	256713	25943	82	488	266	2048 ± 0	285	886 ± 4	239	892 ± 3	222	920 ± 2	223	1000 ± 5	247	1317 ± 12	168	1466 ± 32	170	1496 ± 45
339	sztu-000	338637	15871	259	1298	180	2048 ± 0	138	531 ± 0	113	532 ± 0	95	533 ± 0	81	537 ± 0	63	548 ± 0	54	585 ± 11	57	592 ± 13
340	sztu-001	338650	15871	260	1298	181	2048 ± 0	140	535 ± 0	116	537 ± 0	98	538 ± 0	82	540 ± 0	64	553 ± 0	58	599 ± 10	61	598 ± 10
341	t4isb-000	234227	115237	53	343	156	2048 ± 0	318	1006 ± 5	267	1001 ± 1	256	1006 ± 1	225	1009 ± 1	187	1022 ± 2	278	3586 ± 34	276	3534 ± 34
342	tech5-004	2410272	118858	358	2733	11	321 ± 0	276	872 ± 2	294	1117 ± 164	278	1114 ± 182	252	1134 ± 179	181	999 ± 44	57	597 ± 13	58	592 ± 16
343	tech5-005	1178769	120517	279	1426	35	512 ± 0	373	1272 ± 109	280	1038 ± 63	268	1046 ± 39	247	1124 ± 38	254	1351 ± 44	238	2573 ± 37	238	2545 ± 32
344	techsign-000	0	1101622	327	1955	135	2048 ± 0	74	366 ± 1	66	398 ± 1	294	1172 ± 3	372	3065 ± 18	369	10460 ± 65	295	4758 ± 112	294	4789 ± 93
345	tevian-007	779934	19523	306	1714	74	1032 ± 0	158	583 ± 1	132	579 ± 0	112	580 ± 0	95	588 ± 1	90	636 ± 0	299	4894 ± 65	297	4841 ± 83
346	tevian-008	847177	19519	370	3490	75	1032 ± 0	284	884 ± 2	245	903 ± 1	213	903 ± 1	195	911 ± 1	168	946 ± 1	297	4828 ± 40	296	4811 ± 41
347	tiger-005	342866	253734	290	1531	307	2052 ± 0	333	1097 ± 2	286	1065 ± 2	272	1066 ± 2	239	1067 ± 3	202	1088 ± 3	66	620 ± 19	69	615 ± 16
348	tiger-006	421186	394688	146	707	297	2052 ± 0	396	1392 ± 16	361	1411 ± 10	357	1444 ± 10	342	1531 ± 11	312	1848 ± 10	200	1810 ± 20	200	1801 ± 13
349	tinkoff-001	274660	389272	116	592	227	2048 ± 0	351	1176 ± 3	311	1179 ± 3	295	1178 ± 3	263	1169 ± 2	224	1203 ± 3	291	4361 ± 74	289	4364 ± 75
350	tongyi-005	1140701	138919	338	2121	340	2089 ± 0	21	165 ± 1	-	-	-	-	-	-	-	360	18924 ± 65	363	20158 ± 103	
351	toppanidgate-000	671181	711850	313	1786	351	4096 ± 0	291	915 ± 1	247	916 ± 1	220	916 ± 1	196	917 ± 1	161	917 ± 1	372	25262 ± 84	371	25264 ± 97
352	toshiba-004	599297	27880	299	1595	312	2056 ± 0	407	1447 ± 3	366	1453 ± 2	361	1457 ± 9	335	1457 ± 3	285	1479 ± 4	125	1020 ± 25	122	998 ± 32

Table 14: Summary of algorithms and properties included in this report. The red superscripts give ranking for the quantity in that column.

Notes  
 1 The configuration size does not capture static data included in libraries.  
 2 The library size is the combined total of all files provided in the submission lib folder. These libraries e.g. OpenCV may or may not be installed on any end user's platform natively and would not need to be installed with the algorithm. Some developers put neural network models in their libraries.  
 3 The memory usage is the peak resident set size reported by the ps system call during template generation.  
 4 The median template creation times are measured on Intel®Xeon®CPU E5-2630 v4 @ 2.20GHz processors.  
 5 The comparison durations, in nanoseconds, are estimated using std::chrono::high\_resolution\_clock which on the machine in (2) counts 1ns clock ticks. Precision is somewhat worse than that however. The ± value is the median absolute deviation times 1.48 for Normal consistency.

	ALGORITHM	CONFIG	LIBRARY	TEMPLATE								COMPARISON <sup>4</sup>										
				NAME	DATA	DATA	MEMORY	SIZE	GENERATION TIME (ms) <sup>4</sup>				TIME (ns) <sup>5</sup>									
									(KB) <sup>1</sup>	(KB) <sup>2</sup>	(MB) <sup>3</sup>	(B)	MUGSHOT	480x720	960x1440	1600x2400	3000x4500	GENUINE	IMPOSTOR			
353	toshiba-005		599298	61113	297	1593	318	2056 ± 0	409	1456 ± 4	367	1454 ± 2	362	1461 ± 2	334	1455 ± 2	279	1459 ± 2	176	1613 ± 34	176	1607 ± 28
354	trueface-002		253947	123116	81	486	93	2000 ± 0	71	360 ± 0	55	361 ± 0	56	423 ± 0	97	590 ± 1	-	6	192 ± 14	8	186 ± 19	
355	trueface-003		346530	24308	385	3915	96	2048 ± 0	336	1107 ± 22	170	677 ± 3	167	732 ± 7	194	905 ± 5	-	1	103 ± 11	2	112 ± 29	
356	tuputech-000		11476	17185	23	33	154	2048 ± 0	18	122 ± 4	12	120 ± 1	11	142 ± 2	14	196 ± 5	33	411 ± 14	368	23893 ± 406	372	25279 ± 406
357	turingtechvip-001		399874	54535	123	617	255	2048 ± 0	395	1384 ± 4	357	1391 ± 1	348	1393 ± 1	331	1411 ± 1	284	1476 ± 2	188	1733 ± 19	189	1734 ± 20
358	twiface-000		661735	11782	353	2610	277	2048 ± 0	274	871 ± 1	230	873 ± 1	203	873 ± 2	183	876 ± 2	157	898 ± 1	172	1504 ± 29	171	1510 ± 34
359	twiface-001		671511	11782	365	2855	168	2048 ± 0	295	923 ± 1	251	925 ± 2	228	926 ± 1	200	929 ± 2	165	940 ± 2	162	1400 ± 32	163	1402 ± 37
360	ulsee-001		370519	57261	-	-	280	2048 ± 0	196	654 ± 2	-	-	-	-	-	-	-	316	6065 ± 94	317	6228 ± 77	
361	uluface-002	0	480761	230	1088	272	2048 ± 0	278	873 ± 42	222	855 ± 9	244	978 ± 24	289	1271 ± 40	322	2333 ± 68	362	19207 ± 1114	358	18501 ± 274	
362	uluface-003	97357	529422	253	1264	345	3072 ± 0	308	965 ± 11	260	968 ± 10	274	1087 ± 20	322	1387 ± 36	330	2469 ± 86	373	26057 ± 195	375	26865 ± 566	
363	unissey-001	0	1956593	295	1584	366	4096 ± 0	282	880 ± 3	240	892 ± 3	360	1452 ± 8	371	3048 ± 12	367	10017 ± 387	167	1463 ± 35	168	1471 ± 34	
364	upc-001	0	89914	228	1077	78	1052 ± 0	148	551 ± 15	178	703 ± 56	165	724 ± 51	151	751 ± 49	152	863 ± 33	261	3114 ± 44	264	3165 ± 97	
365	vcog-002	3229434	118946	378	3666	414	61504 ± 5	68	357 ± 25	-	-	-	-	-	-	-	411	296154 ± 3077	411	296436 ± 4183		
366	vd-002	254498	34389	137	688	43	516 ± 0	212	684 ± 5	171	679 ± 4	148	676 ± 5	131	693 ± 5	124	754 ± 5	21	300 ± 14	24	319 ± 32	
367	vd-003	254505	44051	139	696	299	2052 ± 0	216	691 ± 5	174	690 ± 5	151	683 ± 4	130	691 ± 5	115	722 ± 5	123	1003 ± 11	123	1001 ± 7	
368	veridas-006	355669	896424	332	1990	109	2048 ± 0	283	880 ± 8	238	885 ± 8	316	1271 ± 18	364	2242 ± 38	360	6414 ± 156	395	56940 ± 149	399	66077 ± 194	
369	veridas-007	355105	891492	350	2527	261	2048 ± 0	277	872 ± 9	231	875 ± 8	311	1261 ± 18	363	2238 ± 38	358	6374 ± 147	79	655 ± 16	82	660 ± 19	
370	veridium-000	0	47198	1498	412	29399	2045	879 ± 0	80	80 ± 0	789	80 ± 0	590	80 ± 0	511	80 ± 0	399	64880 ± 171	398	64697 ± 247		
371	verigram-000	256209	7798	318	1842	267	2048 ± 0	246	807 ± 1	209	821 ± 1	242	972 ± 2	312	1358 ± 3	339	2848 ± 13	150	1222 ± 17	152	1219 ± 17	
372	verigram-001	282155	11773	355	2638	232	2048 ± 0	202	664 ± 2	168	675 ± 2	192	833 ± 4	277	1202 ± 7	335	2733 ± 32	180	1664 ± 60	178	1648 ± 56	
373	verihubs-inteligensia-000	209562	51877	65	427	226	2048 ± 0	153	567 ± 0	372	1558 ± 8	368	1560 ± 8	345	1568 ± 8	300	1621 ± 8	366	22351 ± 91	366	22371 ± 81	
374	via-000	124422	11151	209	964	99	2048 ± 0	221	707 ± 8	188	740 ± 5	215	906 ± 41	206	941 ± 40	191	1040 ± 5	117	966 ± 28	126	1021 ± 44	
375	via-001	370255	11151	304	1697	187	2048 ± 0	307	964 ± 3	272	1011 ± 3	260	1026 ± 4	234	1045 ± 3	210	1137 ± 28	119	983 ± 31	120	989 ± 40	
376	videmo-000	139643	39470	57	390	123	2048 ± 0	19	142 ± 5	13	150 ± 4	12	150 ± 6	9	151 ± 4	8	155 ± 8	47	513 ± 16	48	523 ± 38	
377	videmo-001	212051	95063	51	304	254	2048 ± 0	31	199 ± 0	15	164 ± 0	13	164 ± 0	10	164 ± 0	9	165 ± 0	20	296 ± 17	21	288 ± 16	
378	videonetics-001	30875	5963	4	61	39	512 ± 0	38	262 ± 3	31	273 ± 1	64	439 ± 3	167	820 ± 3	326	2393 ± 43	142	1153 ± 38	144	1142 ± 65	
379	videonetics-002	121981	6289	18	115	295	2052 ± 0	48	282 ± 5	40	295 ± 1	90	513 ± 4	228	1029 ± 3	344	3151 ± 46	149	1219 ± 57	153	1262 ± 56	
380	viettelhightech-000	259471	215557	63	419	276	2048 ± 0	108	461 ± 1	88	461 ± 2	69	461 ± 1	62	467 ± 2	49	494 ± 0	59	599 ± 11	56	591 ± 13	
381	vigilantsolutions-010	348798	49973	181	840	90	1548 ± 0	178	615 ± 0	156	631 ± 0	134	632 ± 0	114	636 ± 0	96	659 ± 0	45	490 ± 13	46	488 ± 11	
382	vigilantsolutions-011	256661	49973	115	591	89	1548 ± 0	83	402 ± 0	72	418 ± 0	55	418 ± 0	46	422 ± 0	41	445 ± 0	28	339 ± 20	31	366 ± 37	
383	vinal-000	402391	866522	218	1032	204	2048 ± 0	334	1099 ± 1	291	1095 ± 1	277	1093 ± 1	245	1099 ± 1	207	1126 ± 1	254	2996 ± 20	254	2993 ± 26	
384	vinbigdata-001	271405	44746	113	589	124	2048 ± 0	401	1400 ± 5	358	1393 ± 2	347	1391 ± 2	323	1393 ± 1	270	1404 ± 1	158	1351 ± 50	158	1310 ± 38	
385	vion-000	228219	7533	85	498	306	2052 ± 0	61	333 ± 1	-	-	-	-	-	-	-	381	39839 ± 3561	374	26830 ± 2241		
386	visage-000	49218	70150	7	73	18	512 ± 0	4	27 ± 0	2	27 ± 0	2	31 ± 0	3	38 ± 0	3	63 ± 0	224	2220 ± 14	226	2218 ± 14	
387	visionbox-001	256869	190645	110	579	203	2048 ± 0	312	983 ± 7	290	1093 ± 46	340	1360 ± 68	361	2181 ± 105	356	5955 ± 281	143	1161 ± 22	140	1154 ± 20	
388	visionbox-002	259063	135281	122	612	332	2059 ± 0	120	482 ± 1	96	482 ± 0	79	484 ± 1	70	492 ± 1	56	517 ± 3	213	1969 ± 44	210	1931 ± 42	
389	visionlabs-010	1067280	19357	194	902	41	513 ± 0	225	730 ± 0	181	717 ± 1	161	709 ± 0	140	713 ± 1	121	739 ± 0	60	600 ± 41	71	626 ± 35	
390	visionlabs-011	1067280	19353	188	862	40	513 ± 0	226	731 ± 1	182	717 ± 1	162	710 ± 1	141	714 ± 1	122	741 ± 1	49	556 ± 26	51	559 ± 25	
391	visteam-002	186440	30888	101	547	380	4096 ± 0	261	829 ± 5	215	832 ± 6	195	839 ± 7	177	853 ± 6	185	1013 ± 14	323	6952 ± 118	322	6970 ± 120	
392	visteam-003	215359	33730	83	489	355	4096 ± 0	368	1249 ± 4	325	1251 ± 4	315	1266 ± 5	290	1272 ± 5	257	1370 ± 9	320	6816 ± 111	320	6816 ± 105	
393	vnpt-003	369956	297799	148	714	350	4096 ± 0	382	1315 ± 4	340	1315 ± 4	330	1318 ± 2	308	1350 ± 3	276	1428 ± 3	329	7397 ± 31	328	7384 ± 29	
394	vnpt-004	370110	240841	215	988	110	2048 ± 0	365	1238 ± 1	322	1241 ± 1	309	1242 ± 2	298	1307 ± 2	288	1505 ± 2	287	4047 ± 48	286	4008 ± 108	
395	vocord-009	1380132	201560	390	4162	92	1920 ± 0	412	1472 ± 2	369	1472 ± 1	367	1549 ± 1	348	1667 ± 2	315	2064 ± 2	216	2052 ± 50	219	2056 ± 39	
396	vocord-010	902552	206873	382	3858	81	1088 ± 0	410	1459 ± 2	368	1459 ± 1	363	1463 ± 2	340	1484 ± 1	293	1535 ± 3	243	2724 ± 31	241	2653 ± 45	

Notes

1 The configuration size does not capture static data included in libraries.

2 The library size is the combined total of all files provided in the submission lib folder. These libraries e.g. OpenCV may or may not be installed on any end user's platform natively and would not need to be installed with the algorithm. Some developers put neural network models in their libraries.

3 The memory usage is the peak resident set size reported by the ps system call during template generation.

4 The median template creation times are measured on Intel®Xeon®CPU E5-2630 v4 @ 2.20GHz processors.

5 The comparison durations, in nanoseconds, are estimated using std::chrono::high\_resolution\_clock which on the machine in (2) counts 1ns clock ticks. Precision is somewhat worse than that however. The ± value is the median absolute deviation times 1.48 for Normal consistency.

Table 15: Summary of algorithms and properties included in this report. The red superscripts give ranking for the quantity in that column.

ALGORITHM			CONFIG	LIBRARY	TEMPLATE						COMPARISON <sup>4</sup>										
NAME		DATA	DATA	MEMORY	SIZE	GENERATION TIME (ms) <sup>4</sup>				TIME (ns) <sup>5</sup>											
		(KB) <sup>1</sup>	(KB) <sup>2</sup>	(MB) <sup>3</sup>	(B)	MUGSHOT	480x720	960x1440	1600x2400	3000x4500	GENUINE	IMPOSTOR									
397	vts-000	256589	169760	305	1704	247	2048 ± 0	122	486 ± 1	94	481 ± 0	78	484 ± 0	66	485 ± 1	57	517 ± 0	407	124209 ± 352	407	123652 ± 358
398	vts-001	293000	475743	124	618	268	2048 ± 0	207	676 ± 1	-	-	-	-	-	-	337	9620 ± 44	336	9618 ± 54		
399	wicket-000	826392	641802	336	2071	233	2048 ± 0	409	1419 ± 2	363	1429 ± 3	356	1444 ± 4	336	1460 ± 3	294	1537 ± 6	397	60976 ± 232	396	61096 ± 323
400	winsense-001	264428	32035	201	922	85	1280 ± 0	234	766 ± 7	284	1058 ± 47	247	983 ± 97	235	1053 ± 119	248	1320 ± 84	177	1631 ± 28	213	1964 ± 171
401	winsense-002	281379	25780	312	1781	107	2048 ± 0	126	494 ± 2	104	498 ± 1	92	519 ± 1	80	537 ± 1	87	634 ± 1	181	1683 ± 8	181	1685 ± 7
402	wuhantianyu-001	465118	66457	189	866	196	2048 ± 0	191	642 ± 1	160	642 ± 1	141	644 ± 0	119	652 ± 0	106	697 ± 0	335	9502 ± 151	338	9920 ± 253
403	x-laboratory-000	520020	197310	289	1524	324	2056 ± 0	247	808 ± 7	242	897 ± 113	216	907 ± 103	187	886 ± 103	100	673 ± 39	93	725 ± 19	98	749 ± 34
404	x-laboratory-001	625140	398792	319	1844	327	2056 ± 0	161	586 ± 2	143	596 ± 5	123	603 ± 6	108	620 ± 7	134	793 ± 14	107	813 ± 28	111	872 ± 32
405	xforwardai-001	340100	51163	340	2173	214	2048 ± 0	354	1180 ± 2	314	1182 ± 1	303	1194 ± 1	271	1186 ± 2	225	1203 ± 1	103	779 ± 17	104	797 ± 13
406	xforwardai-002	707715	51163	331	1989	374	4096 ± 0	300	944 ± 1	257	942 ± 1	235	943 ± 4	204	935 ± 1	174	967 ± 1	166	1406 ± 8	164	1405 ± 13
407	xm-000	578041	148920	135	688	302	2052 ± 0	281	878 ± 2	235	882 ± 1	250	988 ± 2	286	1258 ± 3	328	2434 ± 7	178	1634 ± 17	177	1632 ± 20
408	yisheng-004	486351	38653	256	1279	348	3704 ± 0	76	378 ± 12	-	-	-	-	-	-	84	693 ± 137	49	526 ± 34		
409	yitu-003	1525719	138919	379	3737	339	2082 ± 0	271	860 ± 0	-	-	-	-	-	-	357	18305 ± 71	357	18286 ± 62		
410	yoonik-002	453720	265415	362	2755	236	2048 ± 0	347	1145 ± 4	295	1123 ± 2	281	1124 ± 2	248	1125 ± 2	208	1126 ± 3	100	761 ± 32	97	736 ± 32
411	yoonik-003	346691	265415	342	2196	121	2048 ± 0	315	991 ± 3	264	980 ± 1	248	984 ± 4	216	982 ± 1	179	983 ± 1	80	684 ± 45	84	678 ± 41
412	ytu-000	1477360	44032	348	2484	198	2048 ± 0	137	530 ± 0	114	533 ± 0	139	640 ± 0	179	861 ± 2	314	1949 ± 8	377	31797 ± 131	378	31794 ± 133
413	yuan-003	370419	147783	368	2885	282	2048 ± 0	404	1405 ± 2	362	1413 ± 3	359	1446 ± 3	343	1547 ± 5	313	1878 ± 5	229	2320 ± 32	229	2287 ± 34
414	yuan-004	428665	50011	267	1353	359	4096 ± 0	154	567 ± 0	131	569 ± 0	110	573 ± 0	90	579 ± 0	79	607 ± 0	310	5816 ± 35	312	5800 ± 31

Notes

- The configuration size does not capture static data included in libraries.
- The library size is the combined total of all files provided in the submission lib folder. These libraries e.g. OpenCV may or may not be installed on any end user's platform natively and would not need to be installed with the algorithm. Some developers put neural network models in their libraries.
- The memory usage is the peak resident set size reported by the ps system call during template generation.
- The median template creation times are measured on Intel®Xeon®CPU E5-2630 v4 @ 2.20GHz processors.
- The comparison durations, in nanoseconds, are estimated using std::chrono::high\_resolution\_clock which on the machine in (2) counts 1ns clock ticks. Precision is somewhat worse than that however. The ± value is the median absolute deviation times 1.48 for Normal consistency.

Table 16: Summary of algorithms and properties included in this report. The red superscripts give ranking for the quantity in that column.

	Algorithm	FALSE NON-MATCH RATE (FNMR)										LESS CONSTRAINED, NON-COOP.					
		CONSTRAINED, COOPERATIVE								WILD							
		Name	VISAMC	VISA	MUGSHOT	MUGSHOT12+YRS	VISABORDER	BORDER	BORDER								
	FMR	0.0001	1E-06	1E-05	1E-05	1E-06	1E-06	1E-06	1E-05	0.0001							
1	20face-000	0.1268	359	0.1828	352	0.1748	361	0.2768	361	0.1765	350	0.1864	288	0.0927	315	0.0405	249
2	20face-001	0.0521	337	0.0732	335	0.1414	357	0.2549	359	0.0769	330	0.1354	283	0.0419	278	0.0295	150
3	3divi-006	0.0064	160	0.0094	157	0.0047	139	0.0066	144	0.0091	147	0.0191	149	0.0113	138	0.0289	130
4	3divi-007	0.0024	42	0.0038	42	0.0028	45	0.0034	41	0.0046	60	0.0101	68	0.0082	82	0.0300	163
5	acer-001	0.0294	317	0.0504	320	0.0240	314	0.0463	316	0.0436	310	0.0622	251	0.0360	272	0.0307	175
6	acer-002	0.0169	287	0.0262	287	0.0103	246	0.0167	257	0.0182	247	0.0281	193	0.0159	194	0.0297	156
7	acisw-007	0.4276	388	0.5493	388	0.8425	400	0.9185	400	0.8424	388	0.9976	380	0.9930	394	0.4963	383
8	acisw-008	0.0100	227	0.0147	219	0.0094	240	0.0126	213	0.1740	349	0.6651	333	0.4545	359	0.0925	316
9	ader-a-002	0.0052	123	0.0071	118	0.0047	136	0.0064	139	0.0087	139	0.0159	124	0.0136	166	0.0990	319
10	ader-a-003	0.0043	101	0.0059	99	0.0036	93	0.0043	77	0.0076	118	0.0151	112	0.0128	159	0.0989	318
11	advance-002	0.0089	205	0.0137	207	0.0073	203	0.0115	206	0.0400	303	0.0722	258	0.0593	298	0.0498	274
12	advance-003	0.0060	155	0.0087	145	0.0052	154	0.0067	145	0.0389	302	0.4914	318	0.1291	321	0.0508	276
13	afisbiometrics-000	0.0051	122	0.0073	123	0.0030	59	0.0050	98	0.0044	53	0.0077	32	0.0057	25	0.0282	82
14	aifirst-001	0.0119	246	0.0170	240	0.0084	223	0.0127	219	0.0131	206	0.0212	161	0.0138	169	0.0432	258
15	aigen-001	0.0124	254	0.0219	264	0.0143	284	0.0217	280	0.0236	272	0.8960	355	0.3255	346	0.0681	299
16	aigen-002	0.0192	299	0.0343	302	0.0256	315	0.0402	310	0.0389	301	0.9196	358	0.3876	353	0.1096	326
17	ailabs-001	0.0158	280	0.0276	292	0.0192	301	0.0317	302	0.0352	295	0.0608	248	0.0434	282	0.0338	214
18	aimall-002	0.0119	248	0.0167	237	0.0224	309	0.0411	312	0.0233	269	0.0373	223	0.0235	245	0.0327	203
19	aimall-003	0.0033	64	0.0041	52	0.0033	82	0.0035	47	0.0056	86	0.0109	76	0.0087	95	0.0312	185
20	aiunionface-000	0.0104	230	0.0154	226	0.0082	221	0.0122	209	0.0141	213	0.0243	176	0.0169	202	0.0306	172
21	aize-001	0.0223	307	0.0344	303	0.0199	302	0.0313	301	0.0367	297	0.0522	241	0.0359	271	0.0446	264
22	aize-002	0.0210	305	0.0327	298	0.0280	318	0.0489	319	0.0504	315	0.0692	255	0.0434	281	0.0854	312
23	ajou-001	0.0093	214	0.0147	217	0.0071	200	0.0126	214	0.0173	245	0.0274	188	0.0186	218	0.0348	221
24	alchera-002	0.0107	233	0.0157	228	0.0104	250	0.0229	283	0.0144	218	0.0246	177	0.0198	229	0.0328	205
25	alchera-003	0.0044	103	0.0055	89	0.0031	63	0.0039	64	0.0042	48	0.0077	34	0.0065	38	0.0339	216
26	alfabeta-001	0.4867	396	0.5831	392	0.6855	388	0.8156	392	0.8253	387	0.7765	346	0.6416	372	0.3427	370
27	alice-000	0.0119	249	0.0192	253	0.0106	254	0.0170	258	0.0167	237	0.0265	184	0.0150	186	0.0288	120
28	alleyes-000	0.0058	145	0.0090	152	0.0055	163	0.0087	182	0.0068	110	0.0105	74	0.0076	69	0.0282	80
29	allgovision-000	0.0346	327	0.0527	323	0.0232	311	0.0339	303	0.0372	300	0.0620	250	0.0443	285	0.0607	291
30	alphaface-001	0.0065	162	0.0097	165	0.0039	109	0.0063	138	0.0083	132	-	-	-	0.0280	65	
31	alphaface-002	0.0052	125	0.0075	129	0.0030	54	0.0044	80	0.0000	406	0.0115	86	0.0084	88	0.0279	54
32	amplifiedgroup-001	0.5034	398	0.5848	393	0.6973	392	0.8316	393	0.7807	382	0.7724	344	0.6354	369	0.4250	377
33	androvideo-000	0.0243	309	0.0438	316	0.0239	313	0.0365	307	0.0483	314	0.1870	289	0.0635	301	0.1163	329
34	anke-004	0.0080	194	0.0154	227	0.0073	202	0.0112	203	0.0102	173	0.0178	142	0.0118	145	0.0288	122
35	anke-005	0.0070	170	0.0109	184	0.0059	175	0.0094	188	0.0105	176	0.0142	102	0.0102	118	0.0289	127
36	antheus-000	0.2564	371	0.3776	374	0.7240	394	0.8699	397	0.8899	394	0.9872	370	0.9483	388	0.7668	391
37	antheus-001	0.1311	360	0.2306	360	0.5113	379	0.6797	381	0.8748	393	0.9908	374	0.9649	391	0.7586	390
38	anyvision-004	0.0267	314	0.0385	310	0.0258	316	0.0487	318	0.0234	271	0.0301	199	0.0191	222	0.0470	268
39	anyvision-005	0.0023	38	0.0037	41	0.0027	43	0.0035	46	0.0049	67	0.0084	44	0.0069	52	0.0285	99
40	armatura-001	0.0033	67	0.0042	57	0.0031	62	0.0037	54	0.0056	85	0.0110	77	0.0092	104	0.0815	310
41	asusaics-000	0.0125	257	0.0209	259	0.0085	224	0.0134	226	0.0143	216	0.7189	338	0.0285	259	0.0295	149
42	asusaics-001	0.0125	258	0.0210	260	0.0085	226	0.0134	227	0.0143	217	0.7437	341	0.0289	260	0.0295	148
43	authenmetric-003	0.0036	82	0.0053	86	0.0039	113	0.0051	101	0.0095	160	0.9930	375	0.5932	366	0.0290	132
44	authenmetric-004	0.0027	49	0.0042	58	0.0033	78	0.0036	51	0.0083	135	0.9879	372	0.4058	355	0.0290	136

Table 17: FNMR is the proportion of mated comparisons below a threshold set to achieve the FMR given in the header on the fourth row. FMR is the proportion of impostor comparisons at or above that threshold. The light grey values give rank over all algorithms in that column. The pink columns use only same-sex impostors; others are selected regardless of demographics. The exception, in the green column, uses “matched-covariates” i.e. impostors of the same sex, age group, and country of birth. The second pink column includes effects of extended ageing. Missing entries for border, visa, mugshot and wild images generally mean the algorithm did not run to completion. The VISA columns compare images described in section 2.1. The MUGSHOT columns compare images described in section 2.4. The VISA-BORDER column compare images described in section 2.2 with those of section 2.3. The BORDER column compares images described in section 2.3. The WILD columns compare images described in section 2.5.

	Algorithm	FALSE NON-MATCH RATE (FNMR)										LESS CONSTRAINED, NON-COOP.					
		CONSTRAINED, COOPERATIVE								WILD							
		Name	VISAMC	VISA	MUGSHOT	MUGSHOT12+YRS	VISABORDER	BORDER	BORDER	1E-06	1E-05						
	FMR	0.0001	1E-06	1E-05	1E-05	1E-06	1E-06	1E-06	1E-05	0.0001							
45	aware-005	0.0457	334	0.0643	330	0.0603	341	0.1094	343	0.0613	321	0.1075	276	0.0491	287	0.0314	189
46	aware-006	0.0487	335	0.0819	339	0.0529	336	0.1090	342	0.1011	341	0.1058	272	0.0502	290	0.0317	193
47	awiros-001	0.4044	385	0.4622	381	0.5530	381	0.6518	378	0.2008	353	0.1994	292	0.1386	325	0.5584	386
48	awiros-002	0.1990	365	0.2561	362	0.3319	370	0.4411	370	0.3821	366	0.9938	376	0.2634	340	0.0997	320
49	ayftech-001	0.0946	352	0.1941	354	0.2438	366	0.3625	366	0.1558	346	0.1589	285	0.0936	316	0.0785	306
50	ayonix-000	0.4351	391	0.4872	382	0.6150	386	0.7510	386	0.6557	376	0.6361	329	0.4981	360	0.3635	372
51	beethedata-000	0.0127	259	0.0195	254	0.0092	236	0.0157	248	0.0171	242	0.0306	201	0.0204	230	0.0285	101
52	beyneai-000	0.0071	177	0.0107	181	0.0104	251	0.0131	224	0.0170	241	0.9837	369	0.6171	368	0.0597	290
53	biocube-001	0.5596	403	0.6834	400	0.7700	399	0.8712	398	0.8446	389	0.9661	366	0.7922	380	0.2377	356
54	bioidtechswiss-001	0.0054	134	0.0072	119	0.0069	194	0.0124	212	0.0060	94	0.0094	57	0.0065	42	0.0313	187
55	bioidtechswiss-002	0.0049	114	0.0067	112	0.0064	183	0.0116	207	0.0067	108	0.0117	88	0.0086	93	0.0279	47
56	bm-001	0.7431	409	0.9494	409	0.9586	404	0.9843	403	0.9049	395	0.9021	357	0.8395	384	0.9935	400
57	boetech-001	0.0662	344	0.0802	338	0.0493	333	0.0791	333	0.0682	326	0.1074	275	0.0758	309	0.1719	342
58	boetech-002	0.0535	339	0.0565	327	0.0114	269	0.0136	229	0.0403	304	0.0650	252	0.0606	299	0.1697	341
59	bresee-001	0.0085	201	0.0143	214	0.0086	230	0.0153	246	0.0108	181	0.0168	133	0.0115	142	0.0355	234
60	bresee-002	0.0079	193	0.0101	172	0.0065	187	0.0079	166	0.0129	201	0.0263	183	0.0224	241	0.0327	204
61	camvi-002	0.0125	256	0.0221	265	0.0089	234	0.0145	239	0.0142	214	0.2650	303	0.0166	201	0.0288	118
62	camvi-004	0.0171	291	0.0316	297	0.0042	124	0.0049	96	0.0097	165	0.6636	332	0.0141	173	0.0284	91
63	canon-003	0.0041	98	0.0059	100	0.0030	53	0.0040	67	0.0040	41	0.0073	26	0.0059	28	0.0274	20
64	canon-004	0.0052	127	0.0091	154	0.0033	80	0.0058	122	0.0037	34	0.0770	260	0.0494	288	-	
65	ceiec-003	0.0071	175	0.0107	179	0.0061	178	0.0079	168	0.0160	228	0.0316	204	0.0260	253	0.0308	181
66	ceiec-004	0.0038	88	0.0051	80	0.0045	134	0.0053	105	0.0062	101	0.3939	312	0.0104	125	0.0325	200
67	chosun-001	0.0525	338	0.0936	341	0.0742	346	0.1263	348	0.0978	340	1.0000	399	0.9354	387	0.4446	379
68	chosun-002	0.0390	329	0.0646	331	0.0339	326	0.0576	326	0.0455	313	0.6904	335	0.1746	333	0.0696	301
69	chtface-004	0.0046	107	0.0062	105	0.0052	153	0.0080	169	0.0088	144	0.0152	113	0.0106	128	0.0306	174
70	chtface-005	0.0033	69	0.0049	74	0.0029	50	0.0041	69	0.0044	52	0.0317	205	0.0066	45	0.0306	173
71	clearviewai-000	0.0010	5	0.0019	11	0.0024	10	0.0028	22	0.0030	15	0.0058	10	0.0050	9	0.0271	5
72	closeli-001	0.0136	262	0.0163	231	0.0039	110	0.0054	108	0.0072	114	1.0000	393	0.0094	108	0.0318	194
73	cloudmatrix-000	0.0192	300	0.0340	301	0.0133	279	0.0220	281	0.9837	400	1.0000	395	0.0281	258	0.0668	296
74	cloudmatrix-001	0.0668	345	0.1141	344	0.0539	337	0.0905	336	0.3509	363	0.9819	368	0.9010	386	0.0636	293
75	cloudwalk-hr-003	0.0026	47	0.0041	51	0.0040	117	0.0058	121	0.0060	99	0.9992	383	0.0094	106	0.7206	389
76	cloudwalk-hr-004	0.0009	2	0.0018	7	0.0034	84	0.0028	26	0.0052	74	0.9992	384	0.0093	105	0.1625	340
77	cloudwalk-mt-004	0.0009	4	0.0013	2	0.0024	12	0.0021	2	0.0028	12	0.0054	6	0.0050	10	0.0285	104
78	cloudwalk-mt-005	0.0006	1	0.0009	1	0.0025	21	0.0022	5	0.0017	1	0.9286	361	0.5956	367	0.0287	115
79	clova-000	0.0099	223	0.0150	221	0.0094	241	0.0147	242	0.0136	208	0.0213	163	0.0152	189	0.0307	176
80	cogent-006	0.0046	108	0.0059	101	0.0036	89	0.0047	86	0.0058	91	0.0113	83	0.0091	101	0.0343	218
81	cogent-007	0.0022	37	0.0038	43	0.0028	47	0.0031	35	0.0040	42	0.0082	40	0.0067	46	0.0438	261
82	cognitec-003	0.0038	86	0.0052	81	0.0054	162	0.0057	118	0.0225	266	0.0416	229	0.0388	275	0.0348	222
83	cognitec-004	0.0036	77	0.0053	84	0.0053	155	0.0056	113	0.0098	166	0.0202	159	0.0154	190	0.0352	232
84	cor-001	0.0075	185	0.0113	190	0.0055	166	0.0084	175	0.0091	149	0.0148	108	0.0092	103	0.0277	37
85	coretech-000	0.7699	411	1.0000	416	1.0000	410	-	1.0000	413	1.0000	410	1.0000	412	1.0000	404	
86	corsight-001	0.0040	95	0.0057	95	0.0033	81	0.0047	85	0.0045	56	0.0095	60	0.0063	36	0.0276	28
87	corsight-002	0.0053	130	0.0068	115	0.0030	57	0.0041	70	0.0039	39	0.0079	36	0.0054	22	0.0276	33
88	csc-002	0.0099	224	0.0132	203	0.0077	209	0.0142	236	0.0126	199	0.0195	152	0.0146	180	0.1779	344

Table 18: FNMR is the proportion of mated comparisons below a threshold set to achieve the FMR given in the header on the fourth row. FMR is the proportion of impostor comparisons at or above that threshold. The light grey values give rank over all algorithms in that column. The pink columns use only same-sex impostors; others are selected regardless of demographics. The exception, in the green column, uses “matched-covariates” i.e. impostors of the same sex, age group, and country of birth. The second pink column includes effects of extended ageing. Missing entries for border, visa, mugshot and wild images generally mean the algorithm did not run to completion. The VISA columns compare images described in section 2.1. The MUGSHOT columns compare images described in section 2.4. The VISA-BORDER column compare images described in section 2.2 with those of section 2.3. The BORDER column compares images described in section 2.3. The WILD columns compare images described in section 2.5.

Algorithm	FALSE NON-MATCH RATE (FNMR)																
	CONSTRAINED, COOPERATIVE								LESS CONSTRAINED, NON-COOP.								
	Name	VISAMC	VISA	MUGSHOT	MUGSHOT12+YRS	VISABORDER	BORDER	BORDER	WILD								
	FMR	0.0001	1E-06	1E-05	1E-05	1E-06	1E-06	1E-05	0.0001	0.0001	0.0001						
89	csc-003	0.0053	129	0.0065	109	0.0037	97	0.0047	88	0.0074	116	0.0124	95	0.0112	137	0.1773	343
90	ctbcbank-000	0.0168	285	0.0250	280	0.0146	287	0.0224	282	0.0211	263	0.8964	356	0.3779	352	1.0000	405
91	ctbcbank-001	0.0155	278	0.0235	273	0.0148	292	0.0243	288	0.0207	260	0.9279	360	0.3469	348	1.0000	410
92	cubox-001	0.0064	159	0.0080	138	0.0037	96	0.0055	110	0.0060	95	0.0111	79	0.0077	70	0.0300	161
93	cubox-002	0.0034	75	0.0041	50	0.0025	18	0.0025	13	0.0033	23	0.0064	15	0.0058	27	0.0480	271
94	cudocommunication-001	0.4777	394	1.0000	415	0.4373	375	0.5360	373	1.0000	410	1.0000	415	1.0000	409	1.0000	408
95	cuhkee-001	0.0036	83	0.0045	65	0.0031	68	0.0046	83	0.0051	73	0.0095	61	0.0079	73	0.1492	335
96	cybercore-001	0.3759	383	0.5677	390	0.6928	391	0.7926	388	0.8118	385	0.9291	364	0.7080	376	0.3811	373
97	cybercore-002	0.0092	212	0.0119	192	0.0049	144	0.0072	151	0.9105	397	1.0000	398	1.0000	402	-	
98	cyberextruder-002	0.0811	350	0.1336	346	0.1465	358	0.2266	356	0.2086	356	1.0000	407	1.0000	413	0.1000	321
99	cyberextruder-003	0.0109	236	0.0169	239	0.0071	199	0.0112	204	0.0165	235	0.0410	228	0.0272	257	0.0302	168
100	cyberlink-007	0.0032	63	0.0053	83	0.0041	120	0.0043	75	0.0052	77	0.0243	175	0.0084	89	0.0280	63
101	cyberlink-008	0.0042	100	0.0056	94	0.0038	106	0.0048	90	0.0053	78	0.0099	65	0.0074	64	0.0274	17
102	dahua-006	0.0027	48	0.0039	46	0.0031	66	0.0039	65	0.0039	38	0.0067	20	0.0058	26	0.0280	57
103	dahua-007	0.0017	23	0.0023	14	0.0026	30	0.0032	39	0.0033	21	0.0060	11	0.0054	21	0.0278	41
104	daon-000	0.0095	217	0.0117	191	0.0068	190	0.0077	163	0.0092	153	0.0174	138	0.0137	168	0.0331	208
105	decatur-000	0.0714	346	0.1115	343	0.0608	342	0.1106	344	0.0866	334	1.0000	396	0.0714	306	0.0658	295
106	decatur-001	0.0424	331	0.0711	333	0.0237	312	0.0458	315	0.0447	311	1.0000	391	0.9969	397	0.0280	60
107	deepglint-003	0.0027	50	0.0038	44	0.0030	56	0.0032	38	0.0043	50	0.0082	41	0.0076	68	0.0279	48
108	deepglint-004	0.0025	44	0.0034	37	0.0039	111	0.0061	134	0.0050	70	0.0091	52	0.0082	81	0.0285	106
109	deepsea-001	0.0136	264	0.0215	262	0.0142	283	0.0214	279	0.0163	232	0.0250	179	0.0192	223	0.0347	220
110	deepsense-000	0.0145	271	0.0265	288	0.0113	267	0.0196	272	0.0151	222	0.0215	165	0.0129	160	0.0290	133
111	deepsense-001	0.0013	13	0.0019	8	0.0024	16	0.0025	12	0.0027	10	0.0115	87	0.0053	17	0.0285	100
112	dermalog-008	0.0096	220	0.0166	236	0.0086	227	0.0133	225	0.0165	234	0.0586	245	0.0226	242	0.0277	36
113	dermalog-009	0.0067	166	0.0094	158	0.0051	152	0.0069	147	0.0116	191	0.0312	202	0.0177	209	0.0270	4
114	dicio-001	0.5486	402	0.6442	395	0.7516	396	0.8607	395	0.8678	392	0.8268	352	0.7034	375	0.3605	371
115	didiglobalface-001	0.0055	137	0.0092	155	0.0030	55	0.0045	81	0.0088	142	0.0119	92	0.0085	91	0.0282	78
116	digidata-000	0.0967	353	0.1410	348	0.2596	367	0.3462	365	0.0293	288	0.0363	219	0.0212	235	0.0310	182
117	digitalbarriers-002	0.3360	380	0.3690	372	0.0877	349	0.1557	349	0.0971	339	0.0951	268	0.0497	289	0.0436	260
118	dps-000	0.0115	241	0.0176	244	0.0149	294	0.0185	267	0.0173	244	0.0275	190	0.0180	212	0.1067	324
119	dsk-000	0.1526	361	0.2169	359	0.3787	372	0.5426	375	0.3115	359	0.3089	307	0.1994	334	0.2201	352
120	einetworks-000	0.0099	225	0.0180	246	0.0088	233	0.0140	234	0.0130	203	0.0225	171	0.0147	182	0.0293	143
121	ekin-002	0.1168	356	0.2042	356	0.1530	359	0.2524	358	0.1777	352	0.2773	304	0.1347	323	0.4801	382
122	enface-000	0.0028	53	0.0049	75	0.0043	126	0.0072	150	0.0058	92	0.0150	110	0.0090	100	0.0290	138
123	enface-001	0.0072	180	0.0107	180	0.0071	196	0.0138	231	0.0068	111	0.0151	239	0.0094	109	0.0284	96
124	eocortexx-000	0.3485	381	0.6943	401	0.1122	351	0.1574	350	0.2155	358	0.2257	299	0.1606	332	0.2546	362
125	ercacat-001	0.0036	79	0.0044	63	0.0033	77	0.0047	89	0.0106	178	0.0202	158	0.0184	216	0.0258	1
126	euronovate-001	0.2786	374	0.3608	371	0.4489	377	0.6105	377	0.5010	371	0.5392	323	0.3769	351	0.4333	378
127	expasoft-001	0.0328	324	0.0488	318	0.0211	306	0.0342	305	0.0629	324	0.6483	330	0.2816	343	0.0552	285
128	expasoft-002	0.0170	289	0.0274	290	0.0787	348	0.0768	332	0.1629	347	0.9996	387	0.9631	390	0.0337	212
129	f8-001	0.0249	310	0.0336	299	0.0178	299	0.0232	284	0.0303	291	0.0615	249	0.0408	277	0.0475	270
130	f8-002	0.0340	326	0.0591	329	0.0213	308	0.0374	308	0.0452	312	0.0760	259	0.0502	291	0.1601	339
131	faceonlive-001	0.0269	315	0.0359	306	0.0387	329	0.0721	331	0.0246	280	0.0349	216	0.0220	238	0.0548	283
132	facephi-000	0.0044	104	0.0059	98	0.0047	137	0.0057	119	0.0088	143	1.0000	402	1.0000	403	0.0308	178

Table 19: FNMR is the proportion of mated comparisons below a threshold set to achieve the FMR given in the header on the fourth row. FMR is the proportion of impostor comparisons at or above that threshold. The light grey values give rank over all algorithms in that column. The pink columns use only same-sex impostors; others are selected regardless of demographics. The exception, in the green column, uses “matched-covariates” i.e. impostors of the same sex, age group, and country of birth. The second pink column includes effects of extended ageing. Missing entries for border, visa, mugshot and wild images generally mean the algorithm did not run to completion. The VISA columns compare images described in section 2.1. The MUGSHOT columns compare images described in section 2.4. The VISA-BORDER column compare images described in section 2.2 with those of section 2.3. The BORDER column compares images described in section 2.3. The WILD columns compare images described in section 2.5.

Algorithm	FALSE NON-MATCH RATE (FNMR)										LESS CONSTRAINED, NON-COOP.						
	CONSTRAINED, COOPERATIVE								WILD								
	Name	VISAMC	VISA	MUGSHOT	MUGSHOT12+YRS	VISABORDER	BORDER	BORDER	1E-06	1E-05							
FMR	0.0001	1E-06	1E-05	1E-05	1E-06	1E-06	1E-06	1E-05	0.0001	0.0001							
133	facesoft-000	0.0085	202	0.0112	188	0.0064	185	0.0107	200	0.0091	148	0.0171	135	0.0107	129	0.0275	22
134	facetag-000	0.2836	375	0.4081	378	0.2933	369	0.4303	369	0.3448	361	0.6312	328	0.3530	349	0.2087	351
135	facetag-002	0.0098	222	0.0147	218	0.0064	186	0.0110	201	0.0116	190	0.0190	148	0.0119	149	0.0675	298
136	facex-001	1.0000	416	1.0000	413	1.0000	409	-	1.0000	414	1.0000	404	1.0000	406	1.0000	402	
137	facex-002	0.0803	348	0.1404	347	0.1283	353	0.1979	354	0.1440	345	0.1952	291	0.1299	322	0.2377	355
138	farfaces-001	0.4890	397	0.5860	394	0.5650	382	0.7268	384	0.8015	384	0.7511	342	0.5892	365	0.1976	349
139	fiberhome-nanjing-003	0.0090	206	0.0139	211	0.0082	220	0.0144	237	0.0110	183	0.0174	136	0.0107	130	0.0272	11
140	fiberhome-nanjing-004	0.0037	85	0.0056	93	0.0031	64	0.0043	76	0.0043	51	0.0083	42	0.0061	33	0.0272	9
141	fincore-000	0.0309	322	0.0502	319	0.0281	319	0.0510	321	0.0521	317	0.0815	262	0.0522	292	0.0681	300
142	fujitsulab-002	0.0091	209	0.0124	197	0.0105	252	0.0156	247	0.0169	240	0.0345	215	0.0146	181	0.0282	75
143	fujitsulab-003	0.0045	106	0.0065	110	0.0057	171	0.0083	173	0.0080	125	0.0154	118	0.0101	115	0.0280	56
144	geo-002	0.0171	292	0.0187	250	0.0035	88	0.0051	103	0.0064	103	0.0117	89	0.0083	86	0.0302	167
145	geo-004	0.0030	54	0.0041	49	0.0025	24	0.0030	30	0.0035	29	0.0065	17	0.0053	19	0.0286	109
146	glory-003	0.0076	186	0.0125	200	0.0077	211	0.0103	197	0.0130	202	0.0205	160	0.0143	177	0.0763	304
147	glory-004	0.0077	189	0.0123	194	0.0074	206	0.0098	194	0.0122	196	0.0193	150	0.0134	164	0.0743	303
148	gorilla-007	0.0074	183	0.0111	187	0.0065	188	0.0126	215	0.0100	171	0.0151	111	0.0102	117	0.0278	38
149	gorilla-008	0.0058	147	0.0091	153	0.0049	143	0.0079	167	0.0079	124	0.0126	97	0.0091	102	0.0278	45
150	graymatics-001	0.1039	355	0.1620	350	0.1344	355	0.1917	352	0.1648	348	0.5160	321	0.2689	341	0.3057	368
151	griaule-000	0.0071	174	0.0099	168	0.0050	147	0.0072	149	0.0160	226	0.0304	200	0.0267	255	0.0338	213
152	hertasecurity-000	0.0630	343	0.0780	337	0.0503	335	0.0898	335	0.0738	327	0.0693	257	0.0420	279	0.0575	288
153	hertasecurity-001	0.0249	311	0.0309	296	0.0105	253	0.0161	250	0.0245	278	0.0447	232	0.0359	270	0.0486	273
154	hik-001	0.0096	219	0.0125	199	0.0093	239	0.0164	255	0.0108	182	0.0937	265	0.0127	157	0.0271	6
155	hisign-001	0.0036	81	0.0050	78	0.0034	83	0.0046	82	0.0079	123	0.0153	117	0.0133	162	0.0286	112
156	hyperverge-002	0.0050	115	0.0066	111	0.0035	87	0.0051	100	0.0062	100	0.0107	75	0.0074	65	0.0276	31
157	hyperverge-003	0.0019	30	0.0030	29	0.0025	19	0.0029	29	0.0027	8	0.0049	3	0.0042	4	0.0280	64
158	hzailu-001	0.0122	250	0.0164	233	0.0095	243	0.0196	271	0.0079	121	0.0118	90	0.0090	99	0.0392	245
159	icm-002	0.0143	268	0.0249	279	0.0144	285	0.0256	289	0.0236	274	0.0386	225	0.0263	254	0.0339	215
160	icm-003	0.0138	265	0.0222	266	0.0149	293	0.0282	296	0.0227	267	0.0384	224	0.0257	251	0.0333	210
161	icthtc-000	0.0260	313	0.0396	311	0.0207	305	0.0339	304	0.0291	287	0.0474	235	0.0346	267	0.0459	267
162	id3-006	0.0072	181	0.0103	174	0.0049	145	0.0074	157	0.0095	159	0.0165	132	0.0119	148	0.9938	401
163	id3-008	0.0039	89	0.0055	90	0.0032	73	0.0042	72	0.0081	129	0.0155	119	0.0134	163	0.8856	395
164	idemia-007	0.0024	41	0.0039	47	0.0032	75	0.0038	61	0.0046	59	0.0092	54	0.0070	56	0.0288	125
165	idemia-008	0.0023	39	0.0032	31	0.0023	7	0.0028	21	0.0034	26	0.0067	19	0.0056	23	0.0290	135
166	iit-002	0.0111	238	0.0177	245	0.0085	225	0.0140	233	0.0193	256	0.0332	210	0.0260	252	0.1373	332
167	iit-003	0.0082	200	0.0151	224	0.0053	157	0.0084	176	0.0122	195	0.0199	156	0.0137	167	0.0407	250
168	imagus-004	0.0063	157	0.0094	159	0.0055	165	0.0081	171	0.0098	167	0.0157	122	0.0111	134	0.0283	88
169	imagus-005	0.0276	316	0.0420	313	0.0302	323	0.0629	327	0.0288	286	0.0447	231	0.0235	246	0.0265	2
170	imperial-000	0.0067	165	0.0108	183	0.0080	217	0.0134	228	0.0087	140	0.0581	243	0.0102	119	0.0281	69
171	imperial-002	0.0058	148	0.0081	142	0.0055	164	0.0085	178	0.0083	133	0.0157	120	0.0103	120	0.0273	15
172	incode-009	0.0044	105	0.0067	114	0.0034	86	0.0051	99	0.0049	68	0.0091	51	0.0067	47	0.0296	154
173	incode-010	0.0041	97	0.0063	106	0.0028	48	0.0043	74	0.0047	64	0.0077	33	0.0061	32	0.0296	155
174	innefulabs-000	0.0122	252	0.0199	255	0.0112	266	0.0197	273	0.0222	265	0.0372	222	0.0271	256	0.0348	223
175	innovativetechnologyltd-001	0.0578	341	0.0938	342	0.0501	334	0.0981	337	0.0592	320	0.0779	261	0.0422	280	0.0449	266
176	innovativetechnologyltd-002	0.0451	333	0.0716	334	0.0541	338	0.1009	340	0.0506	316	0.0682	253	0.0371	273	0.0804	309

Table 20: FNMR is the proportion of mated comparisons below a threshold set to achieve the FMR given in the header on the fourth row. FMR is the proportion of impostor comparisons at or above that threshold. The light grey values give rank over all algorithms in that column. The pink columns use only same-sex impostors; others are selected regardless of demographics. The exception, in the green column, uses “matched-covariates” i.e. impostors of the same sex, age group, and country of birth. The second pink column includes effects of extended ageing. Missing entries for border, visa, mugshot and wild images generally mean the algorithm did not run to completion. The VISA columns compare images described in section 2.1. The MUGSHOT columns compare images described in section 2.4. The VISA-BORDER column compare images described in section 2.2 with those of section 2.3. The BORDER column compares images described in section 2.3. The WILD columns compare images described in section 2.5.

	Algorithm	FALSE NON-MATCH RATE (FNMR)															
		CONSTRAINED, COOPERATIVE								LESS CONSTRAINED, NON-COOP.							
		Name	VISAMC	VISA	MUGSHOT	MUGSHOT12+YRS	VISABORDER	BORDER	BORDER	WILD							
	FMR	0.0001	1E-06	1E-05	1E-05	1E-05	1E-06	1E-06	1E-05	0.0001							
177	innovetrics-007	0.0040	96	0.0054	87	0.0057	170	0.0078	164	0.0079	122	0.0123	93	0.0088	96	0.0282	81
178	innovetrics-008	0.0047	111	0.0064	108	0.0038	105	0.0052	104	0.0053	79	0.0088	49	0.0069	53	0.0287	113
179	insightface-001	0.0009	3	0.0014	3	0.0027	35	0.0024	7	0.0035	28	0.0070	23	0.0065	40	0.0279	51
180	insightface-002	0.0011	7	0.0019	9	0.0027	40	0.0026	15	0.0036	33	0.0069	22	0.0065	39	0.0280	55
181	intellicloudai-001	0.0142	267	0.0234	271	0.0092	238	0.0145	238	0.0162	230	0.0371	221	0.0171	204	0.0409	251
182	intellicloudai-002	0.0059	151	0.0085	144	0.0060	177	0.0069	148	0.0108	180	0.2477	302	0.0171	203	0.0303	169
183	intellifusion-001	0.0072	178	0.0094	160	0.0056	169	0.0085	179	0.0111	186	0.0212	162	0.0143	176	0.0289	126
184	intellifusion-002	0.0059	150	0.0077	130	0.0040	116	0.0074	156	0.0085	138	0.5352	322	0.0104	126	0.0305	171
185	intellivision-002	0.1000	354	0.1775	351	0.0610	343	0.1009	339	0.0805	332	0.1074	274	0.0682	302	0.0768	305
186	intellivision-003	0.1177	357	0.2006	355	0.0760	347	0.1244	347	0.1069	342	0.1431	284	0.0839	312	0.0829	311
187	intellivix-001	0.0064	161	0.0087	148	0.0046	135	0.0063	137	0.0072	113	0.9233	359	0.7856	379	0.0340	217
188	intelresearch-004	0.0025	46	0.0035	38	0.0032	71	0.0038	59	0.0049	69	0.0094	56	0.0072	58	0.0290	137
189	intelresearch-005	0.0016	19	0.0023	16	0.0028	44	0.0034	43	0.0042	49	0.0084	43	0.0066	44	0.0290	134
190	intsysmsu-001	0.9543	414	0.9888	411	0.9923	405	-	0.9977	401	0.9955	377	0.9892	393	0.7871	392	
191	intsysmsu-002	0.0130	260	0.0254	282	0.0137	281	0.0267	294	0.0160	227	0.0267	186	0.0145	179	0.0289	129
192	ionetworks-000	0.0060	154	0.0087	146	0.0044	127	0.0058	124	0.0080	128	0.0144	106	0.0112	135	0.0319	195
193	iqface-000	0.0091	211	0.0143	212	0.0075	207	0.0110	202	0.0171	243	0.2234	297	0.0359	269	0.0381	241
194	iqface-003	0.0058	144	0.0079	137	0.0051	151	0.0058	125	0.0104	175	0.0200	157	0.0193	224	0.0402	247
195	irex-000	0.0052	124	0.0099	167	0.0056	168	0.0083	174	0.0137	211	0.0163	130	0.0078	71	0.0285	102
196	isap-001	0.5092	399	0.6588	397	0.6899	390	0.7978	389	0.7200	378	0.7253	339	0.5373	362	0.1931	348
197	isap-002	0.0114	240	0.0186	249	0.0087	231	0.0151	245	0.0156	225	0.5134	320	0.0333	263	0.0354	233
198	isityou-000	0.5682	404	0.7033	403	1.0000	412	-	1.0000	409	1.0000	416	1.0000	410	1.0000	409	
199	isystems-001	0.0149	275	0.0245	277	0.0138	282	0.0210	277	0.0209	262	0.0332	209	0.0223	240	0.0524	280
200	isystems-002	0.0118	244	0.0182	247	0.0111	263	0.0162	253	0.0166	236	0.0284	195	0.0195	226	0.0516	277
201	itmo-007	0.0080	195	0.0125	198	0.0107	255	0.0185	265	0.0167	238	0.0222	169	0.0144	178	0.0300	162
202	itmo-008	0.0090	207	0.0150	222	0.0058	173	0.0059	129	0.0187	252	0.0355	217	0.0339	264	0.1498	336
203	ivacognitive-001	0.0189	297	0.0351	304	0.0123	274	0.0235	285	0.0198	258	0.0274	189	0.0155	191	0.0296	152
204	iws-000	0.4824	395	0.5801	391	0.6859	389	0.8155	391	0.8251	386	0.7756	345	0.6400	371	0.3251	369
205	kakao-005	0.0040	91	0.0059	97	0.0036	95	0.0057	117	0.0085	137	0.0239	174	0.0125	155	0.0280	62
206	kakao-007	0.0019	29	0.0028	26	0.0024	9	0.0026	16	0.0033	22	0.0061	12	0.0053	18	0.0427	256
207	kakaopay-001	0.0152	277	0.0252	281	0.0145	286	0.0270	295	0.0232	268	0.0344	214	0.0194	225	0.0416	254
208	kasikornlabs-000	0.0112	239	0.0184	248	0.0086	228	0.0137	230	0.0130	204	0.0225	170	0.0148	184	0.0674	297
209	kedacom-000	0.0055	136	0.0081	141	0.0111	265	0.0120	208	0.0415	306	0.0966	270	0.0686	303	0.2511	360
210	kiwitech-000	0.0076	187	0.0105	176	0.0081	219	0.0128	221	0.0096	161	0.0163	129	0.0101	116	0.0279	53
211	kneron-003	0.0542	340	0.0902	340	0.0346	327	0.0562	324	0.0919	336	0.1251	280	0.0973	317	0.3053	367
212	kneron-005	0.0157	279	0.0259	284	0.0126	277	0.0212	278	0.0406	305	0.0693	256	0.0542	295	0.0471	269
213	knowutech-000	0.0039	90	0.0055	91	0.0028	49	0.0042	71	0.0042	46	0.0077	31	0.0059	29	0.0271	7
214	kookmin-002	0.0054	135	0.0077	131	0.0043	125	0.0065	141	0.0123	197	0.7591	343	0.0198	228	0.0285	103
215	kuke3d-001	0.0058	140	0.0104	175	0.0083	222	0.0093	187	0.0270	283	0.9901	373	0.8341	383	0.0404	248
216	kuke3d-002	0.0077	188	0.0135	206	0.0069	193	0.0098	193	0.0111	185	1.0000	401	1.0000	405	0.0316	191
217	lebentech-000	0.5940	405	0.7032	402	0.8854	402	0.9511	401	0.9089	396	0.9970	379	0.9861	392	0.6250	387
218	lemalabs-001	0.0111	237	0.0175	242	0.0088	232	0.0142	235	0.0143	215	0.0228	172	0.0140	171	0.0281	66
219	line-000	0.0172	293	0.0236	274	0.0109	259	0.0194	270	0.0183	248	0.0291	196	0.0204	231	0.0298	157
220	line-001	0.0025	45	0.0040	48	0.0026	34	0.0034	45	0.0045	57	0.4127	314	0.0080	77	0.0283	87

Table 21: FNMR is the proportion of mated comparisons below a threshold set to achieve the FMR given in the header on the fourth row. FMR is the proportion of impostor comparisons at or above that threshold. The light grey values give rank over all algorithms in that column. The pink columns use only same-sex impostors; others are selected regardless of demographics. The exception, in the green column, uses “matched-covariates” i.e. impostors of the same sex, age group, and country of birth. The second pink column includes effects of extended ageing. Missing entries for border, visa, mugshot and wild images generally mean the algorithm did not run to completion. The VISA columns compare images described in section 2.1. The MUGSHOT columns compare images described in section 2.4. The VISA-BORDER column compare images described in section 2.2 with those of section 2.3. The BORDER column compares images described in section 2.3. The WILD columns compare images described in section 2.5.

	Algorithm	FALSE NON-MATCH RATE (FNMR)										LESS CONSTRAINED, NON-COOP.					
		CONSTRAINED, COOPERATIVE								WILD							
		Name	VISAMC	VISA	MUGSHOT	MUGSHOT12+YRS	VISABORDER	BORDER	BORDER								
	FMR	0.0001	1E-06	1E-05	1E-05	1E-05	1E-06	1E-06	1E-05		0.0001						
221	lookman-002	0.0297	319	0.0547	326	0.0339	325	0.0562	323	0.0614	322	0.0960	269	0.0790	310	0.2640	364
222	lookman-004	0.0074	184	0.0099	169	0.0124	276	0.0149	243	0.0430	309	0.0866	263	0.0694	304	0.2516	361
223	luxand-000	0.2056	366	0.2814	365	0.4053	374	0.5365	374	0.3497	362	0.3743	310	0.2605	338	0.2222	354
224	mantra-000	0.0037	84	0.0052	82	0.0054	160	0.0056	115	0.0097	164	0.0181	144	0.0151	187	0.0350	227
225	maxvision-000	0.0078	192	0.0106	178	0.0110	261	0.0147	241	0.0368	299	1.0000	405	0.1545	328	0.0445	263
226	maxvision-001	0.0305	321	0.0528	324	0.1028	350	0.1921	353	0.0650	325	0.3001	306	0.1553	330	0.0539	281
227	megvii-004	0.0020	31	0.0033	34	0.0028	46	0.0035	48	0.0037	36	0.0074	28	0.0068	51	0.0283	89
228	megvii-005	0.0010	6	0.0015	4	0.0026	29	0.0031	37	0.0019	2	0.0500	237	0.0057	24	0.0292	141
229	meituan-000	0.0197	301	0.0424	315	0.0078	212	0.0074	155	0.0103	174	0.0193	151	0.0164	198	0.1063	323
230	meituan-001	0.0164	284	0.1886	353	0.0025	20	0.0026	14	0.0030	17	0.0074	27	0.0051	12	0.1157	328
231	meiya-001	0.0171	290	0.0275	291	0.0159	296	0.0261	293	0.0311	292	0.2250	298	0.0245	249	0.0363	238
232	mendaxiatech-000	0.0027	51	0.0036	39	0.0029	51	0.0036	52	0.0031	19	0.0057	9	0.0051	13	0.0275	24
233	microfocus-001	0.4482	392	0.5524	389	0.7256	395	0.8416	394	0.7301	379	0.6926	336	0.5180	361	0.2567	363
234	microfocus-002	0.3605	382	0.5057	384	0.5783	384	0.7223	383	0.5909	372	0.5963	327	0.4160	356	0.1582	338
235	minivision-000	0.0033	66	0.0048	73	0.0038	103	0.0049	93	0.0055	83	0.0094	59	0.0079	75	0.0273	12
236	mobai-000	0.0360	328	0.0439	317	0.0372	328	0.0700	329	0.0367	298	0.0939	266	0.0795	311	0.2640	365
237	mobai-001	0.0199	304	0.0219	263	0.0047	138	0.0061	131	0.0093	157	0.0174	137	0.0138	170	0.1045	322
238	mobbl-001	0.3208	377	0.4375	379	0.5680	383	0.7193	382	0.6282	374	0.5783	326	0.3984	354	0.1866	346
239	mobbl-003	0.0087	203	0.0134	205	0.0062	179	0.0087	181	0.0099	168	0.0197	153	0.0122	152	-	-
240	mobilpintech-000	0.0090	208	0.0149	220	0.0039	115	0.0057	116	0.0115	189	0.0465	234	0.0182	214	0.0315	190
241	moreedian-000	0.3874	384	0.4912	383	0.9988	407	-	-	0.9990	403	0.9999	389	0.9998	400	0.4788	381
242	mukh-001	0.0170	288	0.0285	293	0.0225	310	0.0405	311	0.0272	284	0.0950	267	0.0291	262	0.0301	164
243	multimodality-000	0.0034	74	0.0047	68	0.0036	94	0.0044	79	0.0077	119	0.9976	381	0.4456	358	0.0287	114
244	mvision-001	0.0191	298	0.0233	269	0.0204	304	0.0356	306	0.0198	259	0.0337	212	0.0242	248	0.0431	257
245	nazhiai-000	0.0040	92	0.0059	102	0.0036	90	0.0048	92	0.0057	88	0.0125	96	0.0083	85	0.0275	25
246	neosystems-002	0.2905	376	0.4077	377	0.2028	364	0.3252	363	0.4088	368	0.5519	324	0.3331	347	0.4500	380
247	neosystems-003	0.2429	368	0.3349	368	0.1844	362	0.2999	362	0.5942	373	0.3936	311	0.2292	335	0.1404	333
248	netbridgegetech-001	0.4749	393	0.6599	398	0.4438	376	0.5676	376	0.4491	369	1.0000	392	0.9541	389	0.1098	327
249	netbridgegetech-002	0.0101	228	0.0166	235	0.0077	210	0.0127	218	0.0133	207	0.8215	350	0.0523	293	0.0351	229
250	neurotechnology-012	0.0051	121	0.0070	117	0.0038	100	0.0056	114	0.0066	107	0.0112	82	0.0075	66	0.0279	52
251	neurotechnology-013	0.0032	60	0.0045	66	0.0026	33	0.0036	49	0.0037	35	0.0068	21	0.0052	16	0.0278	42
252	nhn-002	0.0068	168	0.0096	164	0.0057	172	0.0087	183	0.0136	210	0.0253	181	0.0186	220	0.0302	166
253	nhn-003	0.0033	68	0.0048	71	0.0027	38	0.0038	58	0.0036	31	0.0198	154	0.0071	57	0.0285	108
254	nodeflux-002	0.0186	296	0.0340	300	0.0261	317	0.0451	314	0.0548	318	1.0000	397	1.0000	404	0.0299	159
255	notiontag-001	0.6846	407	0.8006	406	0.3955	373	0.5247	372	0.8669	391	0.8313	353	0.6362	370	0.2221	353
256	notiontag-002	0.0066	163	0.0089	150	0.0045	133	0.0061	132	0.0077	120	0.0137	100	0.0104	123	0.0299	158
257	nsensemcorp-002	0.4277	389	0.5375	387	0.6734	387	0.7924	387	0.7194	377	0.6937	337	0.5617	363	0.5530	385
258	nsensemcorp-003	0.0251	312	0.0295	295	0.0212	307	0.0305	299	0.0131	205	0.2139	296	0.0141	174	0.0872	314
259	ntechlab-011	0.0012	10	0.0019	10	0.0024	14	0.0028	27	0.0029	14	0.0055	7	0.0047	7	0.0288	121
260	ntechlab-012	0.0011	8	0.0016	5	0.0023	8	0.0030	31	0.0026	7	0.0050	4	0.0043	5	0.0280	61
261	omnigarde-001	0.0168	286	0.0260	285	0.0203	303	0.0402	309	0.0243	276	0.0327	207	0.0177	207	0.0288	119
262	omnigarde-002	0.0033	70	0.0046	67	0.0027	42	0.0039	62	0.0041	44	0.0076	30	0.0059	31	0.0278	44
263	omsecurity-000	0.2573	372	0.3835	375	0.3590	371	0.4903	371	0.3956	367	0.5003	319	0.2595	337	0.2400	357
264	openface-001	0.1804	363	0.2921	366	0.2878	368	0.3906	368	0.2054	355	0.2338	301	0.1549	329	0.2445	358

Table 22: FNMR is the proportion of mated comparisons below a threshold set to achieve the FMR given in the header on the fourth row. FMR is the proportion of impostor comparisons at or above that threshold. The light grey values give rank over all algorithms in that column. The pink columns use only same-sex impostors; others are selected regardless of demographics. The exception, in the green column, uses “matched-covariates” i.e. impostors of the same sex, age group, and country of birth. The second pink column includes effects of extended ageing. Missing entries for border, visa, mugshot and wild images generally mean the algorithm did not run to completion. The VISA columns compare images described in section 2.1. The MUGSHOT columns compare images described in section 2.4. The VISA-BORDER column compare images described in section 2.2 with those of section 2.3. The BORDER column compares images described in section 2.3. The WILD columns compare images described in section 2.5.

	Algorithm	FALSE NON-MATCH RATE (FNMR)										LESS CONSTRAINED, NON-COOP.					
		CONSTRAINED, COOPERATIVE								WILD							
		Name	VISAMC	VISA	MUGSHOT	MUGSHOT12+YRS	VISABORDER	BORDER	BORDER								
	FMR	0.0001	1E-06	1E-05	1E-05	1E-05	1E-06	1E-06	1E-05		0.0001						
265	oz-003	0.0095	218	0.0143	213	0.0054	161	0.0077	162	0.0096	162	0.0175	140	0.0118	146	0.0288	123
266	oz-004	0.0033	71	0.0049	76	0.0038	107	0.0055	109	0.0081	130	0.0163	131	0.0142	175	0.0329	206
267	pangiam-000	0.0031	58	0.0043	61	0.0026	26	0.0030	34	0.0038	37	0.0071	25	0.0061	35	0.0424	255
268	papsav1923-001	0.0078	191	0.0130	202	0.0068	191	0.0105	199	0.0119	192	0.0221	168	0.0136	165	0.0293	142
269	papsav1923-002	0.0021	35	0.0034	35	0.0026	27	0.0030	33	0.0048	65	0.0093	55	0.0086	92	0.0312	186
270	paravision-008	0.0018	25	0.0025	20	0.0024	11	0.0025	11	0.0036	30	0.0070	24	0.0063	37	0.0279	50
271	paravision-010	0.0012	9	0.0021	12	0.0022	3	0.0021	4	0.0027	9	0.0055	8	0.0050	11	0.0288	124
272	pensees-001	0.0087	204	0.0133	204	0.0071	198	0.0122	211	0.0145	219	0.0252	180	0.0195	227	0.0283	85
273	pixelall-006	0.0032	61	0.0042	55	0.0032	70	0.0039	63	0.0063	102	0.9960	378	0.0723	307	0.0283	84
274	pixelall-007	0.0036	80	0.0049	77	0.0039	108	0.0044	78	0.0068	109	0.9873	371	0.0217	237	0.0285	107
275	psl-009	0.0161	282	0.0294	294	0.0023	5	0.0025	9	0.0036	32	0.0065	18	0.0048	8	0.0482	272
276	psl-010	0.0017	24	-	0.0023	4	0.0025	8	0.0035	27	0.0104	70	0.0052	15	-	-	-
277	ptakuratsatu-000	0.0060	153	0.0089	151	0.0070	195	0.0104	198	0.0096	163	0.0152	115	0.0100	113	0.0284	93
278	pxl-001	0.0488	336	0.0752	336	0.0586	340	0.1087	341	0.0946	337	0.1065	273	0.0625	300	0.1088	325
279	pyramid-000	0.0136	263	0.0233	270	0.0117	272	0.0192	269	0.0185	251	0.0322	206	0.0206	233	0.0304	170
280	qnap-001	0.0148	272	0.0215	261	0.0103	247	0.0162	252	0.0183	250	0.0301	198	0.0186	219	0.0360	237
281	qnap-002	0.0122	251	0.0191	251	0.0075	208	0.0095	191	0.0146	220	0.0281	194	0.0184	215	0.0352	231
282	quantasoft-003	0.0081	198	0.0113	189	0.0056	167	0.0076	160	0.0091	150	0.0161	126	0.0107	131	0.0414	253
283	rankone-011	0.0049	112	0.0075	128	0.0038	99	0.0048	91	0.0060	98	0.0143	105	0.0080	78	0.0359	236
284	rankone-012	0.0043	102	0.0058	96	0.0031	69	0.0038	57	0.0047	62	0.0081	38	0.0065	41	0.0358	235
285	realnetworks-005	0.0070	169	0.0093	156	0.0063	182	0.0089	185	0.0092	152	0.0161	127	0.0104	124	0.0289	128
286	realnetworks-006	0.0040	94	0.0056	92	0.8657	401	-	-	0.0059	93	0.0112	80	0.0085	90	0.1790	345
287	regula-000	0.0184	295	0.0376	309	0.0103	248	0.0185	264	0.0120	193	0.9983	382	0.0231	243	0.0273	14
288	regula-001	0.0072	179	0.0107	182	0.0102	245	0.0179	262	0.0123	198	0.0333	211	0.0174	205	0.0295	146
289	remarkai-001	0.0144	269	0.0256	283	0.0102	244	0.0159	249	0.0162	231	0.0582	244	0.0185	217	0.0308	180
290	remarkai-003	0.0047	110	0.0063	107	0.0033	79	0.0049	94	0.0054	80	0.0100	67	0.0072	59	0.0275	27
291	rendip-000	0.0055	138	0.0077	132	0.0048	141	0.0060	130	0.0080	126	0.0142	104	0.0110	133	0.0433	259
292	revealmedia-005	0.0050	118	0.0074	127	0.0050	148	0.0068	146	0.0075	117	0.0124	94	0.0104	127	0.3960	375
293	revealmedia-006	0.0040	93	0.0067	113	0.0041	122	0.0056	112	0.0056	84	0.0085	46	0.0068	49	0.0278	43
294	rokid-000	0.0093	215	0.0145	215	0.0073	204	0.0102	196	0.0164	233	0.0280	192	0.0214	236	0.0857	313
295	rokid-001	0.0105	232	0.0162	230	0.0094	242	0.0163	254	0.0181	246	0.0276	191	0.0165	200	0.0325	201
296	s1-003	0.0051	120	0.0073	122	0.0044	129	0.0063	136	0.0052	76	0.0096	63	0.0070	54	0.1321	331
297	s1-004	0.0053	128	0.0080	139	0.0038	101	0.0059	128	0.0057	87	0.0103	69	0.0073	62	0.0281	68
298	saffe-001	0.4339	390	0.5261	385	0.7539	398	0.8736	399	0.7977	383	0.9810	367	0.7435	378	0.3887	374
299	saffe-002	0.0119	247	0.0206	256	0.0107	258	0.0177	260	0.0244	277	0.9998	388	0.2785	342	0.0308	179
300	samsungsds-000	0.0046	109	0.0069	116	0.0132	278	0.0081	170	0.0099	169	0.0179	143	0.0162	196	0.1874	347
301	samsungsds-001	0.0015	17	0.0026	22	0.0023	6	0.0023	6	0.0024	5	0.1660	286	0.0536	294	0.0282	73
302	samtech-001	0.0197	302	0.0365	307	0.0146	290	0.0241	287	0.0238	275	0.0394	226	0.0251	250	0.0337	211
303	scanovate-002	0.0175	294	0.0355	305	0.0146	288	0.0286	297	0.0269	282	0.0301	197	0.0178	210	0.0301	165
304	scanovate-003	0.0054	132	0.0080	140	0.0054	158	0.0072	153	0.0312	293	0.0599	246	0.0568	296	0.0283	83
305	securifai-003	0.4086	386	0.7577	405	0.7233	393	0.8070	390	0.7787	381	1.0000	400	0.9988	399	0.8326	394
306	securifai-004	0.0136	261	0.0192	252	0.0064	184	0.0099	195	0.0115	188	0.0272	187	0.0127	158	0.0347	219
307	sensetime-005	0.0019	27	0.0029	27	0.0022	2	0.0021	3	0.0023	4	0.0044	2	0.0039	2	0.0273	13
308	sensetime-006	0.0014	15	0.0024	18	0.0021	1	0.0020	1	0.0021	3	0.0040	1	0.0036	1	0.0272	10

Table 23: FNMR is the proportion of mated comparisons below a threshold set to achieve the FMR given in the header on the fourth row. FMR is the proportion of impostor comparisons at or above that threshold. The light grey values give rank over all algorithms in that column. The pink columns use only same-sex impostors; others are selected regardless of demographics. The exception, in the green column, uses “matched-covariates” i.e. impostors of the same sex, age group, and country of birth. The second pink column includes effects of extended ageing. Missing entries for border, visa, mugshot and wild images generally mean the algorithm did not run to completion. The VISA columns compare images described in section 2.1. The MUGSHOT columns compare images described in section 2.4. The VISA-BORDER column compare images described in section 2.2 with those of section 2.3. The BORDER column compares images described in section 2.3. The WILD columns compare images described in section 2.5.

Algorithm	FALSE NON-MATCH RATE (FNMR)															
	CONSTRAINED, COOPERATIVE											LESS CONSTRAINED, NON-COOP.				
	Name	VISAMC	VISA	MUGSHOT	MUGSHOT12+YRS	VISABORDER	BORDER	BORDER	WILD							
	FMR	0.0001	1E-06	1E-05	1E-05	1E-06	1E-06	1E-05	0.0001							
309 <i>sertis-000</i>	0.0118	245	0.0208	258	0.0080	215	0.0127	217	0.0110	184	0.0176	141	0.0114	140	0.0285	105
310 <i>sertis-002</i>	0.0049	113	0.0061	103	0.0039	114	0.0061	135	0.0055	82	0.0099	66	0.0070	55	0.0281	67
311 <i>seventhsense-000</i>	0.0067	167	0.0099	171	0.0045	131	0.0065	142	0.0093	154	0.0169	134	0.0124	154	0.0275	26
312 <i>seventhsense-001</i>	0.0034	76	0.0047	70	0.0025	25	0.0031	36	0.0029	13	0.0338	213	0.0109	132	0.0279	46
313 <i>shaman-000</i>	0.9297	413	0.9774	410	0.9990	408	-	-	0.9999	404	1.0000	394	0.9999	401	0.9575	398
314 <i>shaman-001</i>	0.3346	379	0.4616	380	0.2368	365	0.3723	367	0.3574	364	0.3527	309	0.2304	336	0.1498	337
315 <i>shu-002</i>	-	-	0.0079	136	0.0146	289	0.0308	300	1.0000	405	0.0183	145	0.0115	141	0.0284	94
316 <i>shu-003</i>	0.0028	52	0.0041	53	0.0050	146	0.0088	184	0.0081	131	0.0133	99	0.0094	107	0.0283	90
317 <i>siat-002</i>	0.0091	210	0.0126	201	0.0109	260	0.0190	268	0.0276	285	0.0516	240	0.0464	286	0.0520	279
318 <i>siat-005</i>	0.0021	33	0.0038	45	0.0059	174	0.0049	95	0.0742	328	0.9623	365	0.6801	373	0.0279	49
319 <i>sjtu-003</i>	0.0017	21	0.0033	33	0.0030	58	0.0037	55	0.0058	89	0.0104	71	0.0081	80	0.0284	98
320 <i>sjtu-004</i>	0.0014	14	0.0025	19	0.0027	36	0.0028	28	0.0046	58	0.0086	48	0.0073	61	0.0272	8
321 <i>sktelecom-000</i>	0.0038	87	0.0054	88	0.0031	60	0.0051	102	0.0042	45	0.3418	308	0.0061	34	0.0293	144
322 <i>smartengines-000</i>	0.6240	406	0.7562	404	0.9552	403	0.9784	402	0.9515	399	0.9288	363	0.8200	382	0.8037	393
323 <i>smilart-002</i>	0.2440	369	0.3532	370	-	-	-	-	0.3785	365	0.4145	315	0.2611	339	-	-
324 <i>smilart-003</i>	0.6944	408	0.8836	407	0.0695	345	0.1193	345	0.0894	335	0.1221	279	0.0737	308	0.1190	330
325 <i>sodec-000</i>	0.0033	72	0.0044	64	0.0040	118	0.0053	107	0.0054	81	0.0096	62	0.0080	76	0.0274	18
326 <i>sqisoft-001</i>	0.1220	358	0.2088	357	0.1978	363	0.3386	364	0.2111	357	0.2798	305	0.1474	327	0.0519	278
327 <i>sqisoft-002</i>	0.0082	199	0.0124	196	0.0051	150	0.0086	180	0.0102	172	0.0183	146	0.0122	151	0.0287	116
328 <i>stagu-000</i>	0.0139	266	0.0208	257	0.0104	249	0.0145	240	0.0156	224	0.8063	348	0.1408	326	0.0332	209
329 <i>starhybrid-001</i>	0.0108	234	0.0138	208	0.0081	218	0.0113	205	0.0152	223	0.0265	185	0.0189	221	0.0350	228
330 <i>sukshi-000</i>	0.5409	400	0.6612	399	0.4556	378	0.6567	379	0.9296	398	0.8898	354	0.7384	377	0.6892	388
331 <i>suprema-001</i>	0.0041	99	0.0053	85	0.0038	104	0.0047	87	0.0060	97	0.0111	78	0.0095	110	0.0382	242
332 <i>suprema-002</i>	0.0030	56	0.0041	54	0.0034	85	0.0040	66	0.0045	54	0.0085	45	0.0072	60	0.0295	147
333 <i>supremaid-001</i>	0.0053	131	0.0073	125	0.0045	132	0.0066	143	0.0099	170	0.0186	147	0.0148	183	0.0352	230
334 <i>surrey-cvssp-000</i>	0.9084	412	0.9909	412	0.9923	406	0.9950	404	0.9981	402	0.9994	385	0.9979	398	0.9389	396
335 <i>synesis-006</i>	0.0070	173	0.0096	163	0.0107	256	0.0166	256	-	0.0128	98	0.0089	97	0.0292	140	
336 <i>synesis-007</i>	0.0050	116	0.0073	126	0.0062	181	0.0076	159	-	0.0105	72	0.0080	79	0.0288	117	
337 <i>synology-000</i>	0.0149	274	0.0238	275	0.0148	291	0.0261	291	0.0221	264	0.0331	208	0.0209	234	0.0330	207
338 <i>synology-002</i>	0.0104	231	0.0153	225	0.0107	257	0.0184	263	0.0189	254	0.2032	293	0.0180	211	0.0312	184
339 <i>sztu-000</i>	0.0092	213	0.0139	210	0.0091	235	0.0201	275	0.0136	209	0.0685	254	0.0118	147	0.0270	3
340 <i>sztu-001</i>	0.0031	57	0.0043	60	0.0025	22	0.0028	25	0.0051	71	0.0113	84	0.0089	98	0.0275	21
341 <i>t4isb-000</i>	0.0058	141	0.0087	149	0.0041	123	0.0064	140	0.0083	134	0.0157	121	0.0103	121	0.0282	76
342 <i>tech5-004</i>	0.0123	253	0.0234	272	0.0086	229	0.0162	251	0.0065	106	0.0112	81	0.0082	83	0.0281	72
343 <i>tech5-005</i>	0.0054	133	0.0072	120	0.0069	192	0.0122	210	0.0060	96	0.0094	58	0.0066	43	0.0349	225
344 <i>techsign-000</i>	0.0325	323	0.0511	321	0.0435	331	0.0710	330	0.0746	329	0.1104	277	0.0841	313	0.0639	294
345 <i>tevian-007</i>	0.0019	28	0.0027	24	0.0032	74	0.0041	68	0.0045	55	0.0086	47	0.0078	72	0.0310	183
346 <i>tevian-008</i>	0.0012	11	0.0017	6	0.0033	76	0.0042	73	0.0042	47	0.0081	37	0.0068	50	0.0290	131
347 <i>tiger-005</i>	0.0624	342	0.2450	361	0.0292	322	0.0556	322	0.0430	308	1.0000	390	0.9964	396	0.0278	40
348 <i>tiger-006</i>	0.0066	164	0.0101	173	0.0050	149	0.0075	158	0.0089	146	0.0158	123	0.0117	144	0.0290	139
349 <i>tinkoff-001</i>	0.0145	270	0.0244	276	0.0318	324	0.0636	328	0.0236	273	1.0000	413	0.0339	265	0.0563	287
350 <i>tongyi-005</i>	0.0073	182	0.0146	216	0.0187	300	0.0421	313	0.0161	229	0.0215	164	0.0149	185	0.0399	246
351 <i>toppanidgate-000</i>	0.0021	34	0.0033	32	0.0026	28	0.0028	23	0.0039	40	0.0075	29	0.0068	48	0.0376	240
352 <i>toshiba-004</i>	0.0030	55	0.0042	56	0.0025	23	0.0027	20	0.0034	25	0.0063	14	0.0053	20	0.0278	39

Table 24: FNMR is the proportion of mated comparisons below a threshold set to achieve the FMR given in the header on the fourth row. FMR is the proportion of impostor comparisons at or above that threshold. The light grey values give rank over all algorithms in that column. The pink columns use only same-sex impostors; others are selected regardless of demographics. The exception, in the green column, uses “matched-covariates” i.e. impostors of the same sex, age group, and country of birth. The second pink column includes effects of extended ageing. Missing entries for border, visa, mugshot and wild images generally mean the algorithm did not run to completion. The VISA columns compare images described in section 2.1. The MUGSHOT columns compare images described in section 2.4. The VISA-BORDER column compare images described in section 2.2 with those of section 2.3. The BORDER column compares images described in section 2.3. The WILD columns compare images described in section 2.5.

Algorithm	Name	FALSE NON-MATCH RATE (FNMR)										LESS CONSTRAINED, NON-COOP.					
		CONSTRAINED, COOPERATIVE								WILD							
		VISAMC	VISA	MUGSHOT	MUGSHOT12+YRS	VISA BORDER	BORDER	BORDER	1E-06	1E-05	0.0001						
FMR	FMR	0.0001	1E-06	1E-05	1E-05	1E-06	1E-06	1E-05	0.0001	0.0001	0.0001						
353	toshiba-005	0.0023	40	0.0037	40	0.0024	13	0.0026	17	0.0072	115	0.0141	101	0.0130	161	0.0281	70
354	trueface-002	0.0060	152	0.0096	162	0.0048	140	0.0061	133	0.0112	187	0.0198	155	0.0155	192	0.0793	308
355	trueface-003	0.0070	171	0.0094	161	0.0053	156	0.0081	172	0.0122	194	0.0217	167	0.0159	195	0.0785	307
356	tuputech-000	0.3218	378	0.3696	373	-	-	-	0.3237	360	0.4304	316	0.2973	345	0.9415	397	
357	turingtechvip-001	0.0330	325	0.0540	325	0.0458	332	0.1007	338	0.4715	370	0.9286	362	0.8448	385	0.4035	376
358	twface-000	0.0051	119	0.0072	121	0.0041	121	0.0058	120	0.0071	112	0.0153	116	0.0100	112	0.0276	30
359	twface-001	0.0036	78	0.0051	79	0.0031	67	0.0038	56	0.0049	66	0.0091	53	0.0075	67	0.0277	34
360	ulsee-001	0.0151	276	0.0246	278	0.0113	268	0.0185	266	0.0187	253	0.6766	334	0.0181	213	0.0316	192
361	ultinous-000	0.2343	367	0.3484	369	-	-	-	-	-	-	-	-	-	-	-	
362	ultinous-001	0.2485	370	0.4003	376	-	-	-	-	-	-	-	-	-	-	-	
363	uluface-002	0.0081	196	0.0123	193	0.0071	197	0.0095	192	0.0107	179	1.0000	411	0.0140	172	0.0444	262
364	uluface-003	0.0100	226	0.0150	223	0.0079	213	0.0128	220	-	-	-	-	-	-	0.0635	292
365	unissey-001	0.0095	216	0.0160	229	0.0134	280	0.0150	244	0.0147	221	0.0253	182	0.0163	197	0.0946	317
366	upc-001	0.0234	308	0.0519	322	0.0291	321	0.0490	320	0.0294	289	0.2316	300	0.0389	276	0.0314	188
367	vcog-002	0.7522	410	0.9033	408	-	-	-	-	-	-	-	-	-	-	-	
368	vd-002	0.0429	332	0.0704	332	0.0569	339	0.0844	334	0.0801	331	0.0937	264	0.0577	297	0.0556	286
369	vd-003	0.0199	303	0.0222	267	0.0115	271	0.0130	223	0.0138	212	0.0239	173	0.0177	208	0.0389	243
370	veridas-006	0.0098	221	0.0167	238	0.0079	214	0.0127	216	0.0127	200	0.0217	166	0.0151	188	0.0286	111
371	veridas-007	0.0063	158	0.0083	143	0.0044	128	0.0058	123	0.0080	127	0.0152	114	0.0120	150	0.0284	95
372	veridium-000	0.0726	347	0.1248	345	0.5226	380	0.6652	380	0.6425	375	0.8150	349	0.7989	381	0.4988	384
373	verigram-000	0.0032	59	0.0043	59	0.0031	61	0.0034	42	0.0093	156	0.0175	139	0.0164	199	0.0276	29
374	verigram-001	0.0032	62	0.0044	62	0.0027	37	0.0032	40	0.0030	16	0.9995	386	0.9953	395	0.0276	32
375	verihubs-inteligensia-000	0.0070	172	0.0098	166	0.0048	142	0.0076	161	0.0092	151	0.0160	125	0.0117	143	0.0283	86
376	via-000	0.0216	306	0.0365	308	0.0177	298	0.0287	298	0.0296	290	0.0572	242	0.0290	261	0.0349	224
377	via-001	0.0149	273	0.0229	268	0.0114	270	0.0177	261	0.0183	249	0.4056	313	0.0176	206	0.0373	239
378	videmo-000	0.0298	320	0.0423	314	0.0155	295	0.0260	290	0.0246	279	0.0397	227	0.0239	247	0.0541	282
379	videmo-001	0.0295	318	0.0417	312	0.0164	297	0.0261	292	0.0355	296	0.0603	247	0.0442	284	0.1473	334
380	videonetics-001	0.5483	401	0.6446	396	0.7517	397	0.8607	396	0.8664	390	0.8255	351	0.6956	374	0.2986	366
381	videonetics-002	0.4274	387	0.5329	386	0.6081	385	0.7438	385	0.7775	380	0.7297	340	0.5756	364	0.1976	350
382	viettelhightech-000	0.0117	243	0.0166	234	0.0110	262	0.0198	274	0.0167	239	0.0249	178	0.0158	193	0.0409	252
383	vigilantsolutions-010	0.0109	235	0.0164	232	0.0074	205	0.0095	190	0.0209	261	0.0365	220	0.0233	244	0.0277	35
384	vigilantsolutions-011	0.0124	255	0.0176	243	0.0073	201	0.0095	189	0.0196	257	0.0360	218	0.0221	239	0.0274	16
385	vinai-000	0.0081	197	0.0124	195	0.0045	130	0.0072	152	0.0089	145	0.1814	287	0.0112	136	0.0274	19
386	vinbigdata-001	0.2576	373	0.2763	363	0.1404	356	0.1988	355	0.1407	344	0.1150	278	0.0703	305	0.9767	399
387	vion-000	0.0419	330	0.0590	328	0.0422	330	0.0478	317	0.0581	319	0.0968	271	0.0847	314	0.2479	359
388	visage-000	0.0933	351	0.1441	349	0.1316	354	0.2416	357	0.1395	343	0.1920	290	0.1001	318	0.0500	275
389	visionbox-001	0.0159	281	0.0270	289	0.0111	264	0.0173	259	0.0190	255	0.0315	203	0.0205	232	0.0389	244
390	visionbox-002	0.0058	142	0.0079	135	0.0060	176	0.0074	154	0.0084	136	0.0149	109	0.0113	139	0.0447	265
391	visionlabs-010	0.0017	22	0.0024	17	0.0026	31	0.0030	32	0.0033	24	0.0061	13	0.0052	14	0.0282	79
392	visionlabs-011	0.0012	12	0.0022	13	0.0024	17	0.0026	18	0.0028	11	0.0053	5	0.0046	6	0.0280	59
393	visteam-002	0.1564	362	0.2789	364	0.1581	360	0.2567	360	0.1776	351	0.2090	295	0.1021	319	0.0349	226
394	visteam-003	0.0804	349	0.2166	358	0.0613	344	0.1204	346	0.0963	338	0.1269	281	0.0441	283	0.0296	153
395	vnpt-003	0.0117	242	0.0138	209	0.0040	119	0.0058	126	0.0087	141	0.0161	128	0.0126	156	0.0284	92
396	vnpt-004	0.0058	146	0.0078	134	0.0037	98	0.0053	106	0.0051	72	0.4640	317	0.1384	324	0.0275	23

Table 25: FNMR is the proportion of mated comparisons below a threshold set to achieve the FMR given in the header on the fourth row. FMR is the proportion of impostor comparisons at or above that threshold. The light grey values give rank over all algorithms in that column. The pink columns use only same-sex impostors; others are selected regardless of demographics. The exception, in the green column, uses “matched-covariates” i.e. impostors of the same sex, age group, and country of birth. The second pink column includes effects of extended ageing. Missing entries for border, visa, mugshot and wild images generally mean the algorithm did not run to completion. The VISA columns compare images described in section 2.1. The MUGSHOT columns compare images described in section 2.4. The VISA-BORDER column compare images described in section 2.2 with those of section 2.3. The BORDER column compares images described in section 2.3. The WILD columns compare images described in section 2.5.

	Algorithm	FALSE NON-MATCH RATE (FNMR)										LESS CONSTRAINED, NON-COOP.					
		CONSTRAINED, COOPERATIVE								WILD							
		Name	VISAMC	VISA	MUGSHOT	MUGSHOT12+YRS	VISABORDER	BORDER	BORDER								
	FMR	0.0001	1E-06	1E-05	1E-05	1E-05	1E-06	1E-06	1E-05		0.0001						
397	vocord-009	0.0022	36	0.0029	28	0.0036	91	0.0046	84	0.0052	75	0.0098	64	0.0086	94	0.0284	97
398	vocord-010	0.0024	43	0.0031	30	0.0036	92	0.0049	97	0.0025	6	0.0065	16	0.0040	3	0.0280	58
399	vts-000	0.0103	229	0.0174	241	0.0080	216	0.0129	222	0.0250	281	0.0450	233	0.0372	274	0.0596	289
400	vts-001	0.0033	65	0.0048	72	0.0027	39	0.0036	50	0.0032	20	0.6519	331	0.3563	350	-	
401	wicket-000	0.0018	26	0.0028	25	0.0024	15	0.0027	19	0.0031	18	0.7968	347	0.4340	357	0.0323	198
402	winsense-001	0.0062	156	0.0099	170	0.0092	237	0.0210	276	0.0093	155	0.0144	107	0.0098	111	0.0320	196
403	winsense-002	0.0050	117	0.0073	124	0.0038	102	0.0059	127	0.0064	104	0.0118	91	0.0084	87	0.0307	177
404	wuhantianyu-001	0.0163	283	0.0262	286	0.0281	320	0.0569	325	0.0316	294	0.0486	236	0.0344	266	0.0324	199
405	x-laboratory-000	0.0071	176	0.0106	177	0.0123	275	0.0138	232	0.0419	307	0.5629	325	0.2852	344	0.0295	151
406	x-laboratory-001	0.0059	149	0.0110	185	0.0054	159	0.0078	165	0.0094	158	0.0142	103	0.0100	114	0.0294	145
407	xforwardai-001	0.0021	32	0.0034	36	0.0027	41	0.0028	24	0.0046	61	0.0088	50	0.0079	74	0.0281	71
408	xforwardai-002	0.0016	20	0.0023	15	0.0026	32	0.0025	10	0.0040	43	0.0081	39	0.0074	63	0.0282	74
409	xm-000	0.0015	16	0.0026	23	0.0031	65	0.0038	60	0.0058	90	0.0105	73	0.0082	84	0.0282	77
410	yisheng-004	0.1988	364	0.3329	367	0.1147	352	0.1849	351	0.2044	354	-	-	-	-	0.0908	315
411	yitu-003	0.0015	18	0.0026	21	0.0066	189	0.0085	177	0.0064	105	0.0114	85	0.0103	122	0.0325	202
412	yoonik-002	0.0052	126	0.0062	104	0.0029	52	0.0034	44	0.0615	323	0.1279	282	0.1166	320	0.0549	284
413	yoonik-003	0.0034	73	0.0047	69	0.0032	72	0.0037	53	0.0816	333	0.2033	294	0.1601	331	0.0699	302
414	ytu-000	0.0057	139	0.0087	147	0.0121	273	0.0238	286	0.0047	63	0.0078	35	0.0059	30	0.0286	110
415	yuan-003	0.0078	190	0.0111	186	0.0062	180	0.0091	186	0.0106	177	0.0511	238	0.0123	153	0.0320	197
416	yuan-004	0.0058	143	0.0078	133	0.0039	112	0.0055	111	0.0234	270	0.0442	230	0.0353	268	0.0299	160

Table 26: FNMR is the proportion of mated comparisons below a threshold set to achieve the FMR given in the header on the fourth row. FMR is the proportion of impostor comparisons at or above that threshold. The light grey values give rank over all algorithms in that column. The pink columns use only same-sex impostors; others are selected regardless of demographics. The exception, in the green column, uses “matched-covariates” i.e. impostors of the same sex, age group, and country of birth. The second pink column includes effects of extended ageing. Missing entries for border, visa, mugshot and wild images generally mean the algorithm did not run to completion. The VISA columns compare images described in section 2.1. The MUGSHOT columns compare images described in section 2.4. The VISA-BORDER column compare images described in section 2.2 with those of section 2.3. The BORDER column compares images described in section 2.3. The WILD columns compare images described in section 2.5.

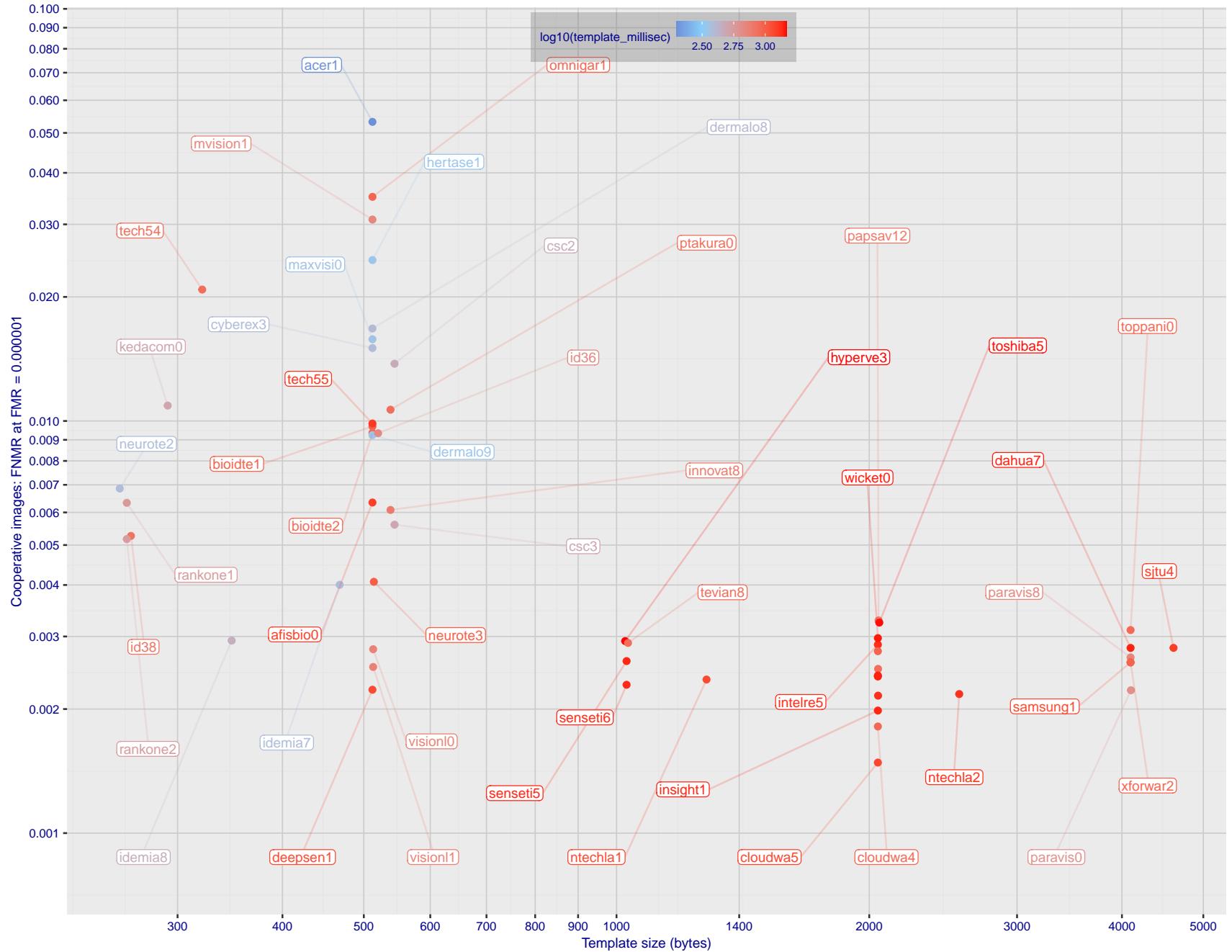


Figure 1: The points show false non-match rates (FNMR) versus the size of the encoded template. FNMR is the geometric mean of FNMR values for visa and mugshot images (from Figs. 63 and 84) at the false match rate (FMR) given in the y-axis label. The color of the points encodes template generation time - which spans at least one order of magnitude. Durations are measured on a single core of a c. 2016 Intel Xeon CPU E5-2630 v4 running at 2.20GHz. Algorithms with poor FNMR are omitted.

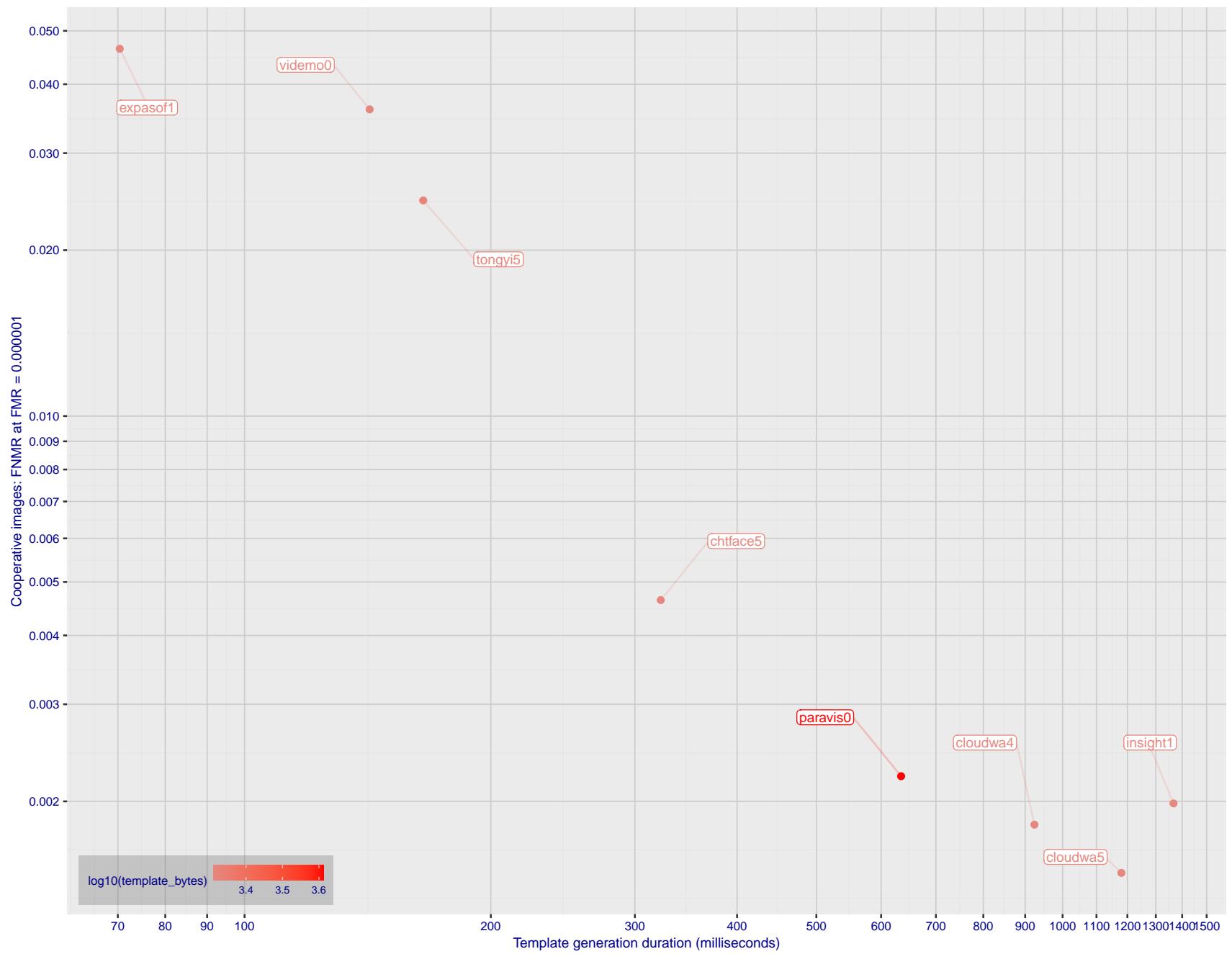


Figure 2: The points show false non-match rates (FNMR) versus the duration of the template generation operation. FNMR is the geometric mean of FNMR values for visa and mugshot images (from Figs. 63 and 84) at a false match rate (FMR) given in the y-axis label. Template generation time is a median estimated over 640 x 480 pixel portraits. It is measured on a single core of a c. 2016 Intel Xeon CPU E5-2630 v4 running at 2.20GHz. The color of the points encodes template size - which span two orders of magnitude. Algorithms with poor FNMR are omitted.

# 1 Metrics

## 1.1 Core accuracy

Given a vector of N genuine scores,  $u$ , the false non-match rate (FNMR) is computed as the proportion below some threshold, T:

$$\text{FNMR}(T) = 1 - \frac{1}{N} \sum_{i=1}^N H(u_i - T) \quad (1)$$

where  $H(x)$  is the unit step function, and  $H(0)$  taken to be 1.

Similarly, given a vector of N impostor scores,  $v$ , the false match rate (FMR) is computed as the proportion above T:

$$\text{FMR}(T) = \frac{1}{N} \sum_{i=1}^N H(v_i - T) \quad (2)$$

The threshold, T, can take on any value. We typically generate a set of thresholds from quantiles of the observed impostor scores,  $v$ , as follows. Given some interesting false match rate range,  $[\text{FMR}_L, \text{FMR}_U]$ , we form a vector of K thresholds corresponding to FMR measurements evenly spaced on a logarithmic scale

$$T_k = Q_v(1 - \text{FMR}_k) \quad (3)$$

where  $Q$  is the quantile function, and  $\text{FMR}_k$  comes from

$$\log_{10} \text{FMR}_k = \log_{10} \text{FMR}_L + \frac{k}{K} [\log_{10} \text{FMR}_U - \log_{10} \text{FMR}_L] \quad (4)$$

Error tradeoff characteristics are plots of FNMR(T) vs. FMR(T). These are plotted with  $\text{FMR}_U \rightarrow 1$  and  $\text{FMR}_L$  as low as is sustained by the number of impostor comparisons, N. This is somewhat higher than the “rule of three” limit  $3/N$  because samples are not independent, due to re-use of images.

## 1.2 Multi-template scoring methodology

There are some scenarios when one or more people exist and are detected in an image, and some of the proposed test images include  $K > 1$  persons for some images and situations where the subject of interest may or may not be the foreground face (largest face in the image). The NIST FRVT 1:1 API supports this by allowing generation of multiple templates representing each person detected in an image. When this occurs, NIST will match all templates generated from the enrollment image with all templates generated from the verification image and use the **maximum** similarity score across all template comparisons. This scoring approach will be used in our calculation of FMR and FNMR (this applies to both genuine and imposter comparisons).

## 2 Datasets

### 2.1 Visa images

- ▷ The number of images is on the order of  $10^5$ .
- ▷ The number of subjects is on the order of  $10^5$ .
- ▷ The number of subjects with two images is on the order of  $10^4$ .
- ▷ The images have geometry in reasonable conformance with the ISO/IEC 19794-5 Full Frontal image type. Pose is generally excellent.
- ▷ The images are of size 252x300 pixels. The mean interocular distance (IOD) is 69 pixels.
- ▷ The images are of subjects from greater than 100 countries, with significant imbalance due to visa issuance patterns.
- ▷ The images are of subjects of all ages, including children, again with imbalance due to visa issuance demand.
- ▷ Many of the images are live capture. A substantial number of the images are photographs of paper photographs.
- ▷ When these images are input to the algorithm, they are labelled as being of type "ISO" - see Table 4 of the FRVT API.

### 2.2 Application images

- ▷ The number of images is on the order of  $10^6$ .
- ▷ The number of subjects is on the order of  $10^6$ .
- ▷ The number of subjects with two images is on the order of  $10^6$ .
- ▷ The images have geometry in good conformance with the ISO/IEC 19794-5 Full Frontal image type. Pose is generally excellent.
- ▷ The images are of size 300x300 pixels. The mean interocular distance (IOD) is 61 pixels.
- ▷ The images are of subjects from greater than 100 countries, with significant imbalance due to population and immigration patterns.
- ▷ The images are of subjects of adults with imbalance due to population and immigration patterns and demand.
- ▷ All of the images are live capture.
- ▷ When these images are input to the algorithm, they are labelled as being of type "ISO" - see Table 4 of the FRVT API.

### 2.3 Border crossing images

- ▷ The number of images is on the order of  $10^6$ .
- ▷ The number of subjects is on the order of  $10^6$ .
- ▷ The number of subjects with two images is on the order of  $10^6$ .
- ▷ The images are taken with a camera oriented by an attendant toward a cooperating subject. This is done under time constraints so there are roll, pitch and yaw angle variations. Also background illumination is sometimes strong, so the face is under-exposed. There is some perspective distortion due to close range images. Some faces are partially cropped.
- ▷ The images are of subjects from greater than 100 countries, with significant imbalance due to population and immigration patterns.
- ▷ The images are of subjects of adults with imbalance due to population and immigration patterns and demand.

- ▷ The images have mean IOD of 38 pixels.
- ▷ The images are all live capture.
- ▷ When these images are input to the algorithm, they are labelled as being of type "WILD" - see Table 4 of the FRVT API.

## 2.4 Mugshot images

- ▷ The number of images is on the order of  $10^6$ .
- ▷ The number of subjects is on the order of  $10^6$ .
- ▷ The number of subjects with two images is on the order of  $10^6$ .
- ▷ The images have geometry in reasonable conformance with the ISO/IEC 19794-5 Full Frontal image type.
- ▷ The images are of variable sizes. The median IOD is 105 pixels. The mean IOD is 113 pixels. The 1-st, 5-th, 10-th, 25-th, 75-th, 90-th and 99-th percentiles are 34, 58, 70, 87, 121, 161 and 297 pixels.
- ▷ The images are of subjects from the United States.
- ▷ The images are of adults.
- ▷ The images are all live capture.
- ▷ When these images are input to the algorithm, they are labelled as being of type "mugshot" - see Table 4 of the FRVT API.

## 2.5 Wild images

- ▷ The number of images is on the order of  $10^5$ .
- ▷ The number of subjects is on the order of  $10^3$ .
- ▷ The number of subjects with two images on the order of  $10^3$ .
- ▷ The images include many photojournalism-style images. Images are given to the algorithm using a variable but generally tight crop of the head. Resolution varies very widely. The images are very unconstrained, with wide yaw and pitch pose variation. Faces can be occluded, including hair and hands.
- ▷ The images are of adults.
- ▷ All of the images are live capture, none are scanned.
- ▷ When these images are input to the algorithm, they are labelled as being of type "WILD" - see Table 4 of the FRVT API.

## 3 Results

### 3.1 Test goals

- ▷ To state absolute accuracy for different kinds of images, including those with and without subject cooperation.
- ▷ To state comparative accuracy, across algorithms.

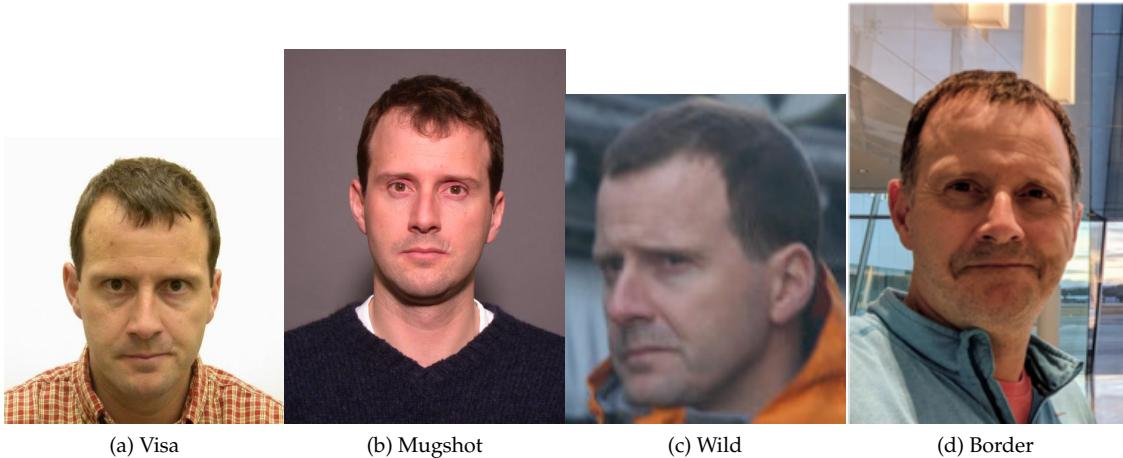


Figure 3: The figure gives simulated samples of image types used in this report.

### 3.2 Test design

**Method:** For visa images:

- ▷ The comparisons are of visa photos against visa photos.
  - ▷ The number of genuine comparisons is on the order of  $10^4$ .
  - ▷ The number of impostor comparisons is on the order of  $10^{10}$ .
  - ▷ The comparisons are fully zero-effort, meaning impostors are paired without attention to sex, age or other covariates. However, later analysis is conducted on subsets.
  - ▷ The number of persons is on the order of  $10^5$ .
  - ▷ The number of images used to make 1 template is 1.
  - ▷ The number of templates used to make each comparison score is two corresponding to simple one-to-one verification.

**Method:** For mugshot images:

- ▷ The comparisons are of mugshot photos against mugshot photos.
  - ▷ The number of genuine comparisons is on the order of  $10^6$ .
  - ▷ The number of impostor comparisons is on the order of  $10^8$ .
  - ▷ The impostors are paired by sex, but not by age or other covariates.
  - ▷ The number of persons is on the order of  $10^6$ .
  - ▷ The number of images used to make 1 template is 1.
  - ▷ The number of templates used to make each comparison score is two corresponding to simple one-to-one verification.

**Method:** For visa-border comparisons:

- ▷ The comparisons are of visa-like frontals against border crossing webcam photos.
  - ▷ The number of genuine comparisons is on the order of  $10^6$ .
  - ▷ The number of impostor comparisons is on the order of  $10^8$ .

- ▷ The impostors are paired by sex, but not by age or other covariates.
- ▷ The number of persons is on the order of  $10^6$ .
- ▷ The number of images used to make 1 template is 1.
- ▷ The number of templates used to make each comparison score is two corresponding to simple one-to-one verification.

**Method:** For border-border comparisons:

- ▷ The comparisons are of border crossing webcam photos.
- ▷ The number of genuine comparisons is on the order of  $10^6$ .
- ▷ The number of impostor comparisons is on the order of  $10^8$ .
- ▷ The impostors are paired by sex, but not by age or other covariates.
- ▷ The number of persons is on the order of  $10^6$ .
- ▷ The number of images used to make 1 template is 1.
- ▷ The number of templates used to make each comparison score is two corresponding to simple one-to-one verification.

**Method:** For wild images:

- ▷ The comparisons are of wild photos against wild photos.
- ▷ The number of genuine comparisons is on the order of  $10^6$ .
- ▷ The number of impostor comparisons is on the order of  $10^7$ .
- ▷ The comparisons are fully zero-effort, meaning impostors are paired without attention to sex, age or other covariates.
- ▷ The number of persons is on the order of  $10^4$ .
- ▷ The number of images used to make 1 template is 1.
- ▷ The number of templates used to make each comparison score is two corresponding to simple one-to-one verification.

**Method:** For child exploitation images:

- ▷ The comparisons are of unconstrained child exploitation photos against others of the same type.
- ▷ The number of genuine comparisons is on the order of  $10^4$ .
- ▷ The number of impostor comparisons is on the order of  $10^7$ .
- ▷ The comparisons are fully zero-effort, meaning impostors are paired without attention to sex, age or other covariates.
- ▷ The number of persons is on the order of  $10^3$ .
- ▷ The number of images used to make 1 template is 1.
- ▷ The number of templates used to make each comparison score is two corresponding to simple one-to-one verification.
- ▷ We produce two performance statements. First, is a DET as used for visa and mugshot images. The second is a cumulative match characteristic (CMC) summarizing a simulated one-to-many search process. This is done as follows.
  - We regard  $M$  enrollment templates as items in a gallery.

- These  $M$  templates come from  $M > N$  individuals, because multiple images of a subject are present in the gallery under separate identifiers.
- We regard the verification templates as search templates.
- For each search we compute the rank of the highest scoring mate.
- This process should properly be conducted with a 1:N algorithm, such as those tested in NIST IR 8009. We use the 1:1 algorithms in a simulated 1:N mode here to a) better reflect what a child exploitation analyst does, and b) to show algorithm efficacy is better than that revealed in the verification DETs.

### 3.3 Failure to enroll

	Algorithm	Failure to Enrol Rate <sup>1</sup>							
		Name	APPLICATION	BORDER	CHILD-EXPLOIT	MUGSHOT	VISA	WILD	
	Name	SEC. 2.2	SEC. 2.3	SEC. ??	SEC. 2.4	SEC. 2.1	SEC. 2.5		
1	20face-000	0.0000	252	0.0008	218	-	175	0.0000	126
2	20face-001	0.0000	229	0.0008	217	-	370	0.0000	127
3	3divi-006	0.0000	209	0.0007	190	-	354	0.0001	223
4	3divi-007	0.0000	259	0.0007	191	-	151	0.0001	220
5	acer-001	0.0000	238	0.0011	266	-	53	0.0001	199
6	acer-002	0.0000	343	0.0008	212	-	367	0.0003	296
7	acisw-007	0.0000	111	0.0000	91	-	49	0.0000	5
8	acisw-008	0.0000	234	0.0009	236	-	59	0.0004	323
9	adera-002	0.0000	323	0.0034	342	-	211	0.0003	304
10	adera-003	0.0000	322	0.0034	341	-	279	0.0003	305
11	advance-002	0.0000	244	0.0013	287	-	131	0.0000	180
12	advance-003	0.0000	309	0.0012	276	-	243	0.0001	241
13	afisbiometrics-000	0.0000	241	0.0008	205	-	134	0.0000	122
14	aifirst-001	0.0000	115	0.0000	95	0.0000	1	0.0000	8
15	aigen-001	0.0000	45	0.0000	9	-	351	0.0000	82
16	aigen-002	0.0000	60	0.0000	19	-	412	0.0000	100
17	ailabs-001	0.0000	185	0.0090	379	-	252	0.0007	357
18	aimall-002	0.0000	328	0.0043	356	-	394	0.0012	372
19	aimall-003	0.0000	306	0.0012	281	-	228	0.0004	318
20	aiunionface-000	0.0000	11	0.0000	42	-	242	0.0000	62
21	aize-001	0.0001	371	0.0040	351	-	69	0.0026	390
22	aize-002	0.0000	159	0.0014	291	-	227	0.0005	343
23	ajou-001	0.0000	223	0.0020	309	-	397	0.0001	226
24	alchera-002	0.0000	267	0.0008	223	-	205	0.0001	248
25	alchera-003	0.0001	382	0.0013	285	-	413	0.0002	278
26	alfabeto-001	0.0005	391	0.0650	409	-	124	0.0024	385
27	alice-000	0.0000	148	0.0006	166	-	153	0.0000	138
28	alleyes-000	0.0000	245	0.0010	249	-	116	0.0002	258
29	allgovision-000	0.0007	395	0.0062	373	-	88	0.0026	389
30	alphaface-001	0.0000	233	0.0012	272	-	84	0.0000	182
31	alphaface-002	0.0000	253	0.0012	271	-	176	0.0000	184
32	amplifiedgroup-001	0.0114	409	0.1023	411	-	322	0.0189	410
33	androvideo-000	0.0000	51	0.0000	12	-	335	0.0000	91
34	anke-004	0.0000	182	0.0011	263	0.0944	28	0.0001	232
35	anke-005	0.0000	263	0.0012	273	0.1228	30	0.0001	244
36	antheus-000	0.0000	79	0.0000	32	0.0000	19	0.0000	106
37	antheus-001	0.0000	131	0.0000	102	-	106	0.0000	32
38	anyvision-004	0.0000	310	0.0017	302	0.1660	33	0.0001	245
39	anyvision-005	0.0000	194	0.0013	282	-	311	0.0000	155
40	armatura-001	0.0000	332	0.0021	314	-	406	0.0005	338
41	asusaics-000	0.0000	106	0.0000	89	-	56	0.0000	10
42	asusaics-001	0.0000	98	0.0000	83	-	72	0.0000	15
43	authenmetric-003	0.0000	25	0.0000	49	-	292	0.0000	64
44	authenmetric-004	0.0000	47	0.0000	6	-	349	0.0000	81
45	aware-005	0.0000	291	0.0020	308	-	127	0.0001	257
46	aware-006	0.0000	258	0.0009	232	-	155	0.0000	159
47	awiros-001	0.0039	399	0.0369	402	-	150	0.0386	411
48	awiros-002	0.0000	346	0.0038	349	-	170	0.0007	356
49	ayftech-001	0.0002	384	0.0046	361	-	353	0.0043	400
50	ayonix-000	0.0053	402	0.0341	399	0.0000	4	0.0113	408
51	beethedata-000	0.0005	389	0.0042	355	-	277	0.0002	269
52	beyneai-000	0.0000	166	0.0000	70	-	209	0.0000	40
53	biocube-001	0.0006	393	0.0391	403	-	396	0.0015	377
54	boidtechswiss-001	0.0000	216	0.0007	186	-	328	0.0000	147
55	boidtechswiss-002	0.0000	250	0.0007	189	-	181	0.0000	149
56	bm-001	0.0000	83	0.0000	38	0.0000	18	0.0000	116
57	boetech-001	0.0087	406	0.0272	393	-	254	0.0032	396
58	boetech-002	0.0087	407	0.0272	394	-	305	0.0032	397

Table 27: FTE is the proportion of failed template generation attempts. Failures can occur because the software throws an exception, or because the software electively refuses to process the input image. This would typically occur if a face is not detected. FTE is measured as the number of function calls that give EITHER a non-zero error code OR that give a “small” template. This is defined as one whose size is less than 0.3 times the median template size for that algorithm. This second rule is needed because some algorithms incorrectly fail to return a non-zero error code when template generation fails.

A hyphen “-” indicates the dataset was not produced.<sup>1</sup> The effects of FTE are included in the accuracy results of this report by regarding any template comparison involving a failed template to produce a low similarity score. Thus higher FTE results in higher FNMR and lower FMR.

	Algorithm	Failure to Enrol Rate <sup>1</sup>											
		APPLICATION	BORDER	CHILD-EXPLOIT	MUGSHOT	VISA	WILD	SEC. 2.2	SEC. 2.3	SEC. ??	SEC. 2.4	SEC. 2.1	SEC. 2.5
59	bressee-001	0.0000	261	0.0010	256	-	141	0.0002	267	0.0003	160	0.0003	130
60	bressee-002	0.0000	316	0.0020	312	-	321	0.0008	358	0.0004	223	0.0031	309
61	camvi-002	0.0000	44	0.0000	8	0.0000	15	0.0000	83	0.0000	13	0.0000	22
62	camvi-004	0.0000	121	0.0000	115	0.0000	6	0.0000	21	0.0000	109	0.0000	70
63	canon-003	0.0000	228	0.0008	204	-	377	0.0000	179	0.0004	250	0.0003	164
64	canon-004	0.0000	207	0.0008	203	-	360	0.0000	178	0.0004	248	0.0003	163
65	ceiec-003	0.0000	9	0.0013	288	-	246	0.0001	206	0.0004	266	0.0004	175
66	ceiec-004	0.0000	30	0.0008	216	-	290	0.0000	154	0.0004	203	0.0004	212
67	chosun-001	0.0000	156	0.0000	63	-	143	0.0000	37	0.0000	62	0.0000	75
68	chosun-002	0.0000	164	0.0000	66	-	212	0.0000	42	0.0000	79	0.0000	90
69	chiface-004	0.0000	113	0.0017	300	-	54	0.0000	165	0.0004	276	0.0020	301
70	chtface-005	0.0000	50	0.0017	299	-	334	0.0000	168	0.0004	272	0.0020	300
71	clearviewai-000	0.0000	249	0.0003	138	-	183	0.0000	170	0.0003	147	0.0003	131
72	closeli-001	0.0000	101	0.0000	88	-	67	0.0000	13	0.0000	81	0.0001	117
73	cloudmatrix-000	0.0000	287	0.0012	277	-	92	0.0001	200	0.0004	194	0.0004	201
74	cloudmatrix-001	0.0000	297	0.0028	324	-	218	0.0001	202	0.0004	192	0.0004	203
75	cloudwalk-hr-003	0.0000	213	0.0008	219	-	343	0.0001	210	0.0004	196	0.0113	342
76	cloudwalk-hr-004	0.0000	273	0.0011	269	-	190	0.0004	321	0.0003	175	0.0129	345
77	cloudwalk-mt-004	0.0000	264	0.0009	224	-	222	0.0002	280	0.0004	295	0.0004	197
78	cloudwalk-mt-005	0.0000	230	0.0005	157	-	91	0.0003	292	0.0004	283	0.0004	190
79	clova-000	0.0000	335	0.0022	316	-	291	0.0006	350	0.0005	312	0.0019	298
80	cogent-006	0.0000	61	0.0000	17	-	411	0.0000	98	0.0000	32	0.0000	43
81	cogent-007	0.0000	317	0.0000	112	-	329	0.0000	156	0.0000	116	0.0001	110
82	cognitec-003	0.0001	365	0.0194	389	-	337	0.0003	312	0.0005	319	0.0039	313
83	cognitec-004	0.0001	366	0.0037	348	-	203	0.0003	311	0.0005	323	0.0035	310
84	cor-001	0.0000	227	0.0006	171	-	374	0.0002	289	0.0004	236	0.0004	224
85	coretech-000	0.0000	31	0.0000	54	-	288	0.0000	74	0.0000	49	0.0000	8
86	corsight-001	0.0000	206	0.0006	176	-	268	0.0001	252	0.0004	224	0.0004	200
87	corsight-002	0.0000	237	0.0005	164	-	55	0.0001	233	0.0004	226	0.0003	165
88	csc-002	0.0015	398	0.0033	337	-	320	0.0006	352	0.0006	355	0.0968	397
89	csc-003	0.0015	397	0.0033	338	-	239	0.0006	351	0.0006	356	0.0968	396
90	ctbcbank-000	0.0001	368	0.0051	366	0.3285	40	0.0011	370	0.0019	392	0.0868	389
91	ctbcbank-001	0.0000	345	0.0036	347	-	96	0.0005	339	0.0010	364	0.0844	386
92	cubox-001	0.0000	119	0.0000	97	-	128	0.0000	23	0.0000	105	0.0000	73
93	cubox-002	0.0000	277	0.0006	174	-	283	0.0002	288	0.0005	338	0.0016	292
94	cudocommunication-001	0.0000	134	0.0000	104	-	104	0.0000	29	0.0000	98	0.0000	97
95	cuhkee-001	0.0000	247	0.0011	268	-	100	0.0000	124	0.0004	228	0.1278	404
96	cybercore-001	0.0000	324	0.0001	125	-	249	0.0002	261	0.0002	125	0.0018	297
97	cybercore-002	0.0000	327	0.0001	124	-	402	0.0002	262	0.0002	124	0.0018	296
98	cyberextruder-002	0.0013	396	0.0840	410	0.2672	39	0.0027	391	0.0028	402	0.0335	374
99	cyberextruder-003	0.0000	325	0.0077	377	-	281	0.0001	253	0.0006	352	0.0009	268
100	cyberlink-007	0.0000	110	0.0003	131	-	47	0.0000	118	0.0003	162	0.0001	103
101	cyberlink-008	0.0000	150	0.0004	152	-	149	0.0000	119	0.0003	161	0.0002	128
102	dahua-006	0.0000	169	0.0000	111	-	207	0.0000	174	0.0003	174	0.0000	84
103	dahua-007	0.0000	149	0.0000	109	-	142	0.0000	172	0.0003	173	0.0000	76
104	daon-000	0.0000	350	0.0028	327	-	318	0.0014	376	0.0015	387	0.0030	308
105	decatur-000	0.0000	281	0.0020	307	-	341	0.0004	328	0.0005	309	0.0236	362
106	decatur-001	0.0000	271	0.0009	239	-	189	0.0001	213	0.0004	219	0.0004	218
107	deepglint-003	0.0000	211	0.0004	151	-	357	0.0002	281	0.0004	209	0.0003	144
108	deepglint-004	0.0000	197	0.0005	156	-	303	0.0002	287	0.0004	204	0.0003	149
109	deepsea-001	0.0000	23	0.0000	48	0.0000	14	0.0000	69	0.0000	58	0.0000	10
110	deepsense-000	0.0000	95	0.0006	177	-	76	0.0000	135	0.0004	181	0.0003	152
111	deepsense-001	0.0000	2	0.0006	180	-	264	0.0000	139	0.0004	183	0.0003	161
112	dermalog-008	0.0000	340	0.0031	334	-	130	0.0006	345	0.0003	140	0.0002	119
113	dermalog-009	0.0000	337	0.0031	333	-	417	0.0006	347	0.0003	137	0.0002	118
114	dicio-001	0.0005	392	0.0649	407	-	133	0.0024	383	0.0012	377	0.0935	392
115	didiglobalface-001	0.0000	219	0.0012	270	0.2175	35	0.0000	185	0.0004	273	0.0004	182
116	digidata-000	0.0000	232	0.0023	317	-	86	0.0004	331	0.0006	350	0.0006	244

Table 28: FTE is the proportion of failed template generation attempts. Failures can occur because the software throws an exception, or because the software electively refuses to process the input image. This would typically occur if a face is not detected. FTE is measured as the number of function calls that give EITHER a non-zero error code OR that give a “small” template. This is defined as one whose size is less than 0.3 times the median template size for that algorithm. This second rule is needed because some algorithms incorrectly fail to return a non-zero error code when template generation fails.

A hyphen “-” indicates the dataset was not produced.<sup>1</sup> The effects of FTE are included in the accuracy results of this report by regarding any template comparison involving a failed template to produce a low similarity score. Thus higher FTE results in higher FNMR and lower FMR.

	Algorithm	Failure to Enrol Rate <sup>1</sup>											
		APPLICATION	BORDER	CHILD-EXPLOIT	MUGSHOT	VISA	WILD	SEC. 2.2	SEC. 2.3	SEC. ??	SEC. 2.4	SEC. 2.1	SEC. 2.5
117	digitalbarriers-002	0.0001	374	0.0045	358	-	274	0.0028	393	0.0027	399	0.0071	328
118	dps-000	0.0000	172	0.0000	75	-	200	0.0000	51	0.0000	67	0.0000	87
119	dsk-000	0.0000	18	0.0000	46	0.0000	12	0.0000	58	0.0000	42	0.0000	2
120	einetworks-000	0.0000	344	0.0017	301	-	346	0.0002	276	0.0005	333	0.0008	265
121	ekin-002	0.0000	52	0.0000	113	-	333	0.0000	121	0.0000	114	0.0019	299
122	enface-000	0.0000	177	0.0012	280	-	195	0.0000	163	0.0004	232	0.0004	205
123	enface-001	0.0000	92	0.0012	279	-	83	0.0000	143	0.0004	227	0.0004	189
124	eocortex-000	0.0095	408	0.0602	406	-	359	0.0094	407	0.0059	407	0.1405	407
125	ercacat-001	0.0000	55	0.0005	158	-	319	0.0000	164	0.0003	163	0.0002	122
126	euronovate-001	0.0255	413	0.0102	381	-	179	0.0021	380	0.0004	303	0.2451	409
127	expasoft-001	0.0000	64	0.0000	23	-	408	0.0000	97	0.0000	28	0.0000	47
128	expasoft-002	0.0000	73	0.0000	30	-	392	0.0000	111	0.0000	18	0.0000	36
129	f8-001	0.0003	385	0.0059	372	0.2026	34	0.0035	398	0.0030	405	0.0087	335
130	f8-002	0.0000	362	0.0150	387	-	77	0.0005	334	0.0013	385	0.0883	390
131	faceonlive-001	0.0000	356	0.0029	330	-	118	0.0013	374	0.0011	372	0.0160	352
132	facephi-000	0.0000	179	0.0004	142	-	185	0.0001	235	0.0004	191	0.0003	154
133	facesoft-000	0.0000	27	0.0000	51	0.0000	13	0.0000	66	0.0000	56	0.0000	12
134	facetag-000	0.0000	57	0.0000	16	-	315	0.0000	88	0.0000	4	0.0000	17
135	facetag-002	0.0000	167	0.0000	71	-	210	0.0000	41	0.0000	77	0.0000	92
136	facex-001	0.0001	380	0.0360	401	-	81	0.0047	402	0.0027	401	0.1109	400
137	facex-002	0.0001	381	0.0360	400	-	172	0.0047	403	0.0027	400	0.1109	399
138	farfaces-001	0.0000	342	0.0007	188	-	244	0.0003	308	0.0003	155	0.0006	252
139	fiberhome-nanjing-003	0.0000	118	0.0004	149	-	139	0.0000	25	0.0003	143	0.0001	106
140	fiberhome-nanjing-004	0.0000	103	0.0004	148	-	66	0.0000	14	0.0003	141	0.0001	105
141	fincore-000	0.0000	246	0.0008	221	-	115	0.0001	192	0.0004	271	0.0006	245
142	fujitsulab-002	0.0000	93	0.0009	230	-	80	0.0001	240	0.0003	142	0.0003	136
143	fujitsulab-003	0.0000	123	0.0008	210	-	121	0.0001	230	0.0001	121	0.0003	132
144	geo-002	0.0000	212	0.0015	292	-	344	0.0001	190	0.0004	290	0.0017	295
145	geo-004	0.0000	187	0.0005	163	-	253	0.0001	222	0.0004	211	0.0009	270
146	glory-003	0.0000	308	0.0027	323	-	204	0.0004	320	0.0005	316	0.0244	365
147	glory-004	0.0000	285	0.0020	311	-	388	0.0001	238	0.0004	287	0.0167	353
148	gorilla-007	0.0000	224	0.0009	243	-	387	0.0001	214	0.0004	259	0.0004	193
149	gorilla-008	0.0000	256	0.0009	244	-	160	0.0001	212	0.0004	267	0.0004	192
150	graymatics-001	0.0000	90	0.0010	245	-	89	0.0001	251	0.0004	221	0.0006	246
151	griaule-000	0.0000	352	0.0026	321	-	339	0.0004	332	0.0010	365	0.0023	302
152	hertasecurity-000	0.0133	410	0.0077	378	-	184	0.0025	388	0.0243	414	0.0171	355
153	hertasecurity-001	0.0000	178	0.0000	116	-	186	0.0000	129	0.0001	117	0.0002	129
154	hik-001	0.0000	20	0.0000	118	-	306	0.0000	70	0.0000	52	0.0000	16
155	hisign-001	0.0000	108	0.0000	90	-	61	0.0000	11	0.0000	93	0.0000	49
156	hyperverge-002	0.0000	15	0.0008	209	-	233	0.0002	291	0.0004	215	0.0004	214
157	hyperverge-003	0.0000	147	0.0008	208	-	156	0.0002	290	0.0004	217	0.0004	217
158	hzailu-001	0.0000	333	0.0016	295	-	78	0.0003	313	0.0005	336	0.0075	330
159	icm-002	0.0000	22	0.0001	122	-	300	0.0000	68	0.0000	113	0.0000	99
160	icm-003	0.0000	43	0.0001	121	-	345	0.0000	77	0.0000	112	0.0000	100
161	icthtc-000	0.0001	379	0.0047	364	-	400	0.0028	394	0.0029	403	0.0086	334
162	id3-006	0.0000	299	0.0009	242	-	229	0.0004	324	0.0005	331	0.0008	263
163	id3-008	0.0000	143	0.0006	175	-	159	0.0001	250	0.0004	184	0.0003	133
164	idemia-007	0.0000	36	0.0004	154	-	270	0.0000	131	0.0003	165	0.0003	143
165	idemia-008	0.0000	12	0.0004	153	-	241	0.0000	130	0.0003	164	0.0003	142
166	iit-002	0.0000	349	0.0021	313	-	304	0.0009	366	0.0005	342	0.0443	378
167	iit-003	0.0000	192	0.0008	220	-	310	0.0000	153	0.0004	190	0.0069	327
168	imagus-004	0.0000	85	0.0000	35	-	368	0.0000	104	0.0000	23	0.0000	30
169	imagus-005	0.0000	99	0.0000	86	-	79	0.0000	18	0.0000	86	0.0000	55
170	imperial-000	0.0000	72	0.0000	29	-	393	0.0000	110	0.0000	19	0.0000	35
171	imperial-002	0.0000	86	0.0000	37	0.0000	16	0.0000	102	0.0000	24	0.0000	31
172	incode-009	0.0000	280	0.0009	234	-	269	0.0002	272	0.0004	213	0.0007	259
173	incode-010	0.0000	282	0.0009	233	-	331	0.0002	273	0.0004	207	0.0007	260
174	innefulabs-000	0.0000	272	0.0024	318	-	187	0.0003	307	0.0005	328	0.0004	202

Table 29: FTE is the proportion of failed template generation attempts. Failures can occur because the software throws an exception, or because the software electively refuses to process the input image. This would typically occur if a face is not detected. FTE is measured as the number of function calls that give EITHER a non-zero error code OR that give a “small” template. This is defined as one whose size is less than 0.3 times the median template size for that algorithm. This second rule is needed because some algorithms incorrectly fail to return a non-zero error code when template generation fails.

A hyphen “-” indicates the dataset was not produced.<sup>1</sup> The effects of FTE are included in the accuracy results of this report by regarding any template comparison involving a failed template to produce a low similarity score. Thus higher FTE results in higher FNMR and lower FMR.

	Algorithm	Failure to Enrol Rate <sup>1</sup>											
		APPLICATION	BORDER	CHILD-EXPLOIT	MUGSHOT	VISA	WILD	SEC. 2.2	SEC. 2.3	SEC. ??	SEC. 2.4	SEC. 2.1	SEC. 2.5
175	innovativetechnologyltd-001	0.0001	378	0.0050	365	-	97	0.0024	386	0.0025	398	0.0055	320
176	innovativetechnologyltd-002	0.0000	304	0.0046	360	-	122	0.0057	406	0.0005	330	0.0247	367
177	innovatrics-007	0.0000	251	0.0007	199	-	180	0.0001	188	0.0003	156	0.0003	147
178	innovatrics-008	0.0000	201	0.0009	237	-	295	0.0000	160	0.0004	179	0.0003	169
179	insightface-001	0.0000	176	0.0000	77	-	198	0.0000	49	0.0000	72	0.0000	82
180	insightface-002	0.0000	135	0.0000	105	-	101	0.0000	27	0.0000	103	0.0000	64
181	intellicloudai-001	0.0000	53	0.0000	13	-	324	0.0000	89	0.0000	1	0.0001	111
182	intellicloudai-002	0.0000	180	0.0008	213	-	191	0.0000	152	0.0004	186	0.0012	283
183	intellifusion-001	0.0000	195	0.0005	160	0.0949	29	0.0001	209	0.0003	169	0.0005	234
184	intellifusion-002	0.0000	151	0.0000	114	-	148	0.0000	112	0.0000	61	0.0001	112
185	intellivision-002	0.0000	363	0.0046	359	-	405	0.0012	371	0.0005	346	0.0146	348
186	intellivision-003	0.0000	220	0.0012	275	-	409	0.0003	301	0.0004	305	0.0185	358
187	intellivix-001	0.0000	174	0.0000	76	-	201	0.0000	53	0.0000	70	0.0000	86
188	intelresearch-004	0.0000	189	0.0006	169	-	248	0.0000	140	0.0004	202	0.0003	151
189	intelresearch-005	0.0000	248	0.0006	170	-	99	0.0000	137	0.0004	206	0.0003	153
190	intsysmsu-001	0.0000	4	0.0010	253	-	258	0.0001	225	0.0004	240	0.0004	210
191	intsysmsu-002	0.0000	82	0.0010	252	-	364	0.0001	227	0.0004	235	0.0004	211
192	ionetworks-000	0.0000	100	0.0016	297	-	68	0.0004	316	0.0005	318	0.0004	215
193	iqface-000	0.0000	155	0.0000	62	0.0000	7	0.0000	36	0.0000	63	0.0000	74
194	iqface-003	0.0000	347	0.0076	376	-	192	0.0006	346	0.0005	345	0.0069	326
195	irex-000	0.0000	313	0.0009	241	-	95	0.0000	169	0.0005	311	0.0003	166
196	isap-001	0.0000	94	0.0000	82	-	85	0.0000	2	0.0000	97	0.0000	59
197	isap-002	0.0000	141	0.0000	58	-	166	0.0000	34	0.0000	65	0.0000	79
198	isityou-000	0.0068	405	0.0316	397	0.4714	43	0.0023	382	0.0010	368	0.0663	383
199	isystems-001	0.0000	355	0.0035	344	0.1421	32	0.0010	368	0.0007	357	0.0128	344
200	isystems-002	0.0000	354	0.0035	345	0.1421	31	0.0010	367	0.0007	358	0.0128	343
201	itmo-007	0.0000	116	0.0009	229	-	135	0.0003	314	0.0000	106	0.0004	191
202	itmo-008	0.0000	32	0.0135	385	-	278	0.0024	387	0.0000	47	0.0836	385
203	ivacognitive-001	0.0000	283	0.0011	265	-	327	0.0001	203	0.0004	289	0.0011	275
204	iws-000	0.0005	390	0.0650	408	-	301	0.0024	384	0.0012	378	0.0936	393
205	kakao-005	0.0000	158	0.0000	110	-	226	0.0000	47	0.0000	115	0.0000	94
206	kakao-007	0.0000	170	0.0007	181	-	206	0.0001	219	0.0004	205	0.0097	340
207	kakaopay-001	0.0000	295	0.0013	286	-	152	0.0001	204	0.0004	294	0.0078	332
208	kasikornlabs-000	0.0000	359	0.0035	343	-	363	0.0004	329	0.0012	381	0.0270	369
209	kedacom-000	0.0000	91	0.0000	81	0.0000	3	0.0000	1	0.0000	96	0.0000	60
210	kiwitech-000	0.0000	204	0.0009	226	-	272	0.0004	327	0.0005	315	0.0004	220
211	kneron-003	0.0239	411	0.0306	395	0.4883	45	0.0044	401	0.0016	390	0.1823	408
212	kneron-005	0.0000	357	0.0226	390	-	267	0.0006	344	0.0005	324	0.0097	339
213	knowutech-000	0.0000	269	0.0008	206	-	197	0.0000	157	0.0004	254	0.0003	173
214	kookmin-002	0.0000	68	0.0000	26	-	395	0.0000	92	0.0000	34	0.0000	42
215	kuke3d-001	0.0000	165	0.0000	69	-	216	0.0000	44	0.0000	80	0.0000	89
216	kuke3d-002	0.0000	175	0.0000	78	-	196	0.0000	48	0.0000	73	0.0000	83
217	lebentech-000	0.0042	400	0.0029	332	-	161	0.0051	405	0.0066	408	0.0154	350
218	lemalabs-001	0.0000	122	0.0005	162	-	120	0.0002	275	0.0004	195	0.0004	184
219	line-000	0.0000	160	0.0000	64	-	220	0.0000	45	0.0000	74	0.0000	101
220	line-001	0.0000	96	0.0000	84	-	73	0.0000	16	0.0000	83	0.0001	113
221	lookman-002	0.0000	10	0.0000	41	-	247	0.0000	63	0.0000	39	0.0000	4
222	lookman-004	0.0000	144	0.0000	60	0.0000	8	0.0000	38	0.0000	59	0.0000	78
223	luxand-000	0.0000	14	0.0000	43	-	234	0.0000	60	0.0000	43	0.0000	1
224	mantra-000	0.0001	367	0.0041	354	-	371	0.0003	306	0.0004	301	0.0037	312
225	maxvision-000	0.0000	19	0.0000	108	-	231	0.0000	59	0.0000	41	0.0000	3
226	maxvision-001	0.0000	65	0.0000	24	-	404	0.0000	94	0.0000	36	0.0000	40
227	megvii-004	0.0000	181	0.0010	251	-	265	0.0002	270	0.0004	253	0.0011	278
228	megvii-005	0.0000	202	0.0010	246	-	285	0.0002	284	0.0004	274	0.0011	276
229	meituuan-000	0.0000	102	0.0001	123	-	65	0.0000	128	0.0002	127	0.0001	114
230	meituuan-001	0.0000	183	0.0014	290	-	259	0.0001	228	0.0004	261	0.0013	288
231	meiya-001	0.0000	353	0.0028	328	-	169	0.0004	330	0.0010	369	0.0025	304
232	mendaxiatech-000	0.0000	239	0.0010	247	-	52	0.0002	285	0.0004	277	0.0011	279

Table 30: FTE is the proportion of failed template generation attempts. Failures can occur because the software throws an exception, or because the software electively refuses to process the input image. This would typically occur if a face is not detected. FTE is measured as the number of function calls that give EITHER a non-zero error code OR that give a “small” template. This is defined as one whose size is less than 0.3 times the median template size for that algorithm. This second rule is needed because some algorithms incorrectly fail to return a non-zero error code when template generation fails.

A hyphen “-” indicates the dataset was not produced.<sup>1</sup> The effects of FTE are included in the accuracy results of this report by regarding any template comparison involving a failed template to produce a low similarity score. Thus higher FTE results in higher FNMR and lower FMR.

	Algorithm	Failure to Enrol Rate <sup>1</sup>									
		APPLICATION		BORDER		CHILD-EXPLOIT		MUGSHOT		VISA	
Name	SEC. 2.2	SEC. 2.3	SEC. ??	SEC. 2.4	SEC. 2.1	SEC. 2.5					
233	microfocus-001	0.0001	377	0.0053	369	0.0791	27	0.0008	361	0.0016	389
234	microfocus-002	0.0001	376	0.0053	368	0.0791	26	0.0008	360	0.0016	388
235	minivision-000	0.0000	67	0.0000	25	-	407	0.0000	95	0.0000	37
236	mobai-000	0.0000	315	0.0114	383	-	338	0.0003	310	0.0012	380
237	mobai-001	0.0000	292	0.0040	350	-	126	0.0001	234	0.0012	379
238	mobbl-001	0.0000	348	0.0052	367	-	174	0.0002	264	0.0005	334
239	mobbl-003	0.0000	358	0.0029	331	-	375	0.0002	279	0.0009	363
240	mobipintech-000	0.0000	37	0.0000	1	-	361	0.0000	85	0.0000	7
241	moreedian-000	0.0000	184	0.0009	225	-	262	0.0004	325	0.0005	314
242	mukh-001	0.0000	133	0.0010	255	-	105	0.0001	231	0.0003	135
243	multimodality-000	0.0000	63	0.0000	21	-	410	0.0000	96	0.0000	29
244	mvision-001	0.0000	28	0.0000	53	-	284	0.0000	73	0.0000	48
245	nazhai-000	0.0000	88	0.0000	79	-	93	0.0000	4	0.0000	95
246	neosystems-002	0.0000	120	0.0000	98	-	123	0.0000	20	0.0000	110
247	neosystems-003	0.0000	136	0.0000	106	-	102	0.0000	28	0.0000	104
248	netbridgetech-001	0.0000	48	0.0000	10	-	340	0.0000	75	0.0000	9
249	netbridgetech-002	0.0000	105	0.0000	87	-	63	0.0000	12	0.0000	82
250	neurotechnology-012	0.0000	338	0.0010	262	-	366	0.0001	243	0.0004	234
251	neurotechnology-013	0.0000	142	0.0008	222	-	164	0.0000	125	0.0001	118
252	nhn-002	0.0000	128	0.0004	155	-	108	0.0000	148	0.0003	148
253	nhn-003	0.0000	307	0.0000	68	-	213	0.0001	256	0.0004	264
254	nodeflux-002	0.0000	214	0.0261	392	-	332	0.0008	359	0.0005	329
255	notiontag-001	0.0000	62	0.0000	20	-	416	0.0027	392	0.0000	33
256	notiontag-002	0.0000	1	0.0000	40	-	266	0.0000	56	0.0000	45
257	nsensecorp-002	0.0000	196	0.0009	228	-	307	0.0003	297	0.0011	370
258	nsensecorp-003	0.0000	33	0.0000	119	-	280	0.0000	142	0.0007	360
259	ntechlab-011	0.0000	78	0.0003	132	-	372	0.0000	177	0.0004	177
260	ntechlab-012	0.0000	132	0.0003	133	-	111	0.0000	171	0.0004	182
261	null-020	-	416	-	417	-	112	-	414	-	416
262	omnigarde-001	0.0000	190	0.0008	201	-	235	0.0000	145	0.0004	237
263	omnigarde-002	0.0000	200	0.0008	202	-	296	0.0000	146	0.0004	242
264	omsecurity-000	0.0000	17	0.0000	45	-	230	0.0000	57	0.0000	40
265	openface-001	0.0000	331	0.0104	382	-	188	0.0004	322	0.0006	354
266	oz-003	0.0000	7	0.0002	127	-	260	0.0000	120	0.0003	134
267	oz-004	0.0000	336	0.0003	135	-	132	0.0000	123	0.0002	123
268	pangiam-000	0.0000	146	0.0021	315	-	162	0.0001	189	0.0005	313
269	papsav1923-001	0.0000	266	0.0007	192	-	208	0.0001	221	0.0002	131
270	papsav1923-002	0.0000	236	0.0018	304	-	48	0.0000	162	0.0004	255
271	paravision-008	0.0000	127	0.0010	250	-	110	0.0001	215	0.0004	188
272	paravision-010	0.0000	152	0.0010	248	-	146	0.0001	216	0.0004	185
273	pensees-001	0.0000	255	0.0000	59	-	167	0.0000	33	0.0000	66
274	pixelall-006	0.0000	58	0.0000	15	-	314	0.0000	87	0.0000	5
275	pixelall-007	0.0000	162	0.0000	67	-	214	0.0000	43	0.0000	78
276	psl-009	0.0000	203	0.0004	147	-	287	0.0000	115	0.0004	178
277	psl-010	0.0000	226	0.0004	146	-	382	0.0000	117	0.0004	176
278	ptakuratsatu-000	0.0000	222	0.0007	198	-	398	0.0001	191	0.0003	154
279	pxl-001	0.0000	364	0.0044	357	-	71	0.0005	337	0.0022	396
280	pyramid-000	0.0001	373	0.0041	353	-	70	0.0005	336	0.0007	359
281	qnap-001	0.0000	208	0.0000	117	-	355	0.0000	167	0.0001	119
282	qnap-002	0.0000	351	0.0033	336	-	114	0.0004	319	0.0002	122
283	quantasoft-003	0.0000	319	0.0015	293	-	74	0.0005	335	0.0006	351
284	rankone-011	0.0000	137	0.0000	107	-	98	0.0000	26	0.0000	102
285	rankone-012	0.0000	89	0.0000	80	-	87	0.0000	3	0.0000	94
286	realnetworks-005	0.0000	257	0.0002	129	-	158	0.0000	113	0.0002	133
287	realnetworks-006	0.0000	198	0.0002	130	-	302	0.0000	114	0.0002	132
288	regula-000	0.0000	112	0.0000	92	-	50	0.0000	6	0.0000	88
289	regula-001	0.0000	130	0.0000	101	-	107	0.0000	30	0.0000	99
290	remarkai-001	0.0000	16	0.0000	44	-	237	0.0000	61	0.0000	44

Table 31: FTE is the proportion of failed template generation attempts. Failures can occur because the software throws an exception, or because the software electively refuses to process the input image. This would typically occur if a face is not detected. FTE is measured as the number of function calls that give EITHER a non-zero error code OR that give a “small” template. This is defined as one whose size is less than 0.3 times the median template size for that algorithm. This second rule is needed because some algorithms incorrectly fail to return a non-zero error code when template generation fails.

A hyphen “-” indicates the dataset was not produced.<sup>1</sup> The effects of FTE are included in the accuracy results of this report by regarding any template comparison involving a failed template to produce a low similarity score. Thus higher FTE results in higher FNMR and lower FMR.

	Algorithm	Failure to Enrol Rate <sup>1</sup>							
		Name	APPLICATION	BORDER	CHILD-EXPLOIT	MUGSHOT	VISA	WILD	
	Name	SEC. 2.2	SEC. 2.3	SEC. ??	SEC. 2.4	SEC. 2.1	SEC. 2.5		
291	remarkai-003	0.0000	191	0.0007	187	-	232	0.0000	166
292	rendip-000	0.0000	300	0.0016	296	-	312	0.0002	271
293	revealmedia-005	0.0000	314	0.0007	194	-	157	0.0009	365
294	revealmedia-006	0.0000	140	0.0009	238	-	173	0.0001	229
295	rokid-000	0.0000	126	0.0072	375	-	113	0.0001	218
296	rokid-001	0.0000	3	0.0013	284	-	263	0.0000	55
297	s1-003	0.0000	8	0.0002	128	-	255	0.0007	354
298	s1-004	0.0000	104	0.0000	120	-	64	0.0000	183
299	saffe-001	0.0000	69	0.0000	27	0.0000	20	0.0000	93
300	saffe-002	0.0000	125	0.0000	100	-	117	0.0000	19
301	samsungsds-000	0.0000	301	0.0055	371	-	293	0.0038	399
302	samsungsds-001	0.0000	39	0.0005	159	-	352	0.0001	217
303	samtech-001	0.0001	372	0.0032	335	-	308	0.0004	326
304	scanovate-002	0.0000	286	0.0018	303	-	379	0.0000	186
305	scanovate-003	0.0000	293	0.0233	391	-	109	0.0006	348
306	securifai-003	0.0000	54	0.0000	14	-	330	0.0000	90
307	securifai-004	0.0000	49	0.0000	11	-	342	0.0000	76
308	sensetime-005	0.0000	76	0.0004	144	-	376	0.0000	151
309	sensetime-006	0.0000	157	0.0004	145	-	223	0.0000	150
310	sertis-000	0.0000	107	0.0007	193	-	60	0.0000	187
311	sertis-002	0.0000	29	0.0007	184	-	282	0.0000	181
312	seventhsense-000	0.0000	270	0.0006	178	-	194	0.0001	195
313	seventhsense-001	0.0000	235	0.0006	179	-	57	0.0001	194
314	shaman-000	0.0000	129	0.0000	103	0.0000	5	0.0000	31
315	shaman-001	0.0000	87	0.0000	36	0.0000	17	0.0000	103
316	shu-002	0.0000	290	0.0010	257	-	62	0.0005	333
317	shu-003	0.0000	77	0.0007	183	-	373	0.0001	198
318	siat-002	0.0000	210	0.0012	278	0.0616	25	0.0000	161
319	siat-005	0.0000	40	0.0000	3	-	356	0.0000	84
320	sjtu-003	0.0000	6	0.0005	165	-	261	0.0000	175
321	sjtu-004	0.0000	75	0.0000	31	-	384	0.0000	108
322	sktelecom-000	0.0000	217	0.0008	215	-	325	0.0000	176
323	smartengines-000	0.0066	404	0.0150	386	-	182	0.0022	381
324	smilart-002	0.0000	360	0.0036	346	0.2422	38	-	417
325	smilart-003	0.0003	386	0.0100	380	-	380	0.0014	375
326	sodec-000	0.0000	109	0.0000	93	-	51	0.0000	7
327	sqisoft-001	0.0000	74	0.0003	140	-	385	0.0000	132
328	sqisoft-002	0.0000	13	0.0003	137	-	240	0.0000	134
329	stauq-000	0.0000	97	0.0000	85	-	75	0.0000	17
330	starhybrid-001	0.0001	375	0.0033	340	0.2340	37	0.0009	364
331	sukshi-000	0.0000	46	0.0000	7	-	350	0.0000	80
332	suprema-001	0.0000	298	0.0027	322	-	236	0.0003	299
333	suprema-002	0.0000	284	0.0010	260	-	403	0.0002	266
334	supremaid-001	0.0000	260	0.0020	310	-	154	0.0001	224
335	surrey-cvssp-000	0.0000	41	0.0000	4	-	348	0.0000	78
336	synesis-006	0.0000	153	0.0003	141	-	144	0.0000	173
337	synesis-007	0.0000	243	0.0013	283	-	129	0.0002	283
338	synology-000	0.0000	24	0.0000	50	-	294	0.0000	65
339	synology-002	0.0000	117	0.0000	96	-	140	0.0000	24
340	sztu-000	0.0000	70	0.0000	28	-	389	0.0000	109
341	sztu-001	0.0000	35	0.0000	56	-	271	0.0000	71
342	t4isb-000	0.0000	34	0.0000	55	-	275	0.0000	72
343	tech5-004	0.0000	193	0.0008	207	-	313	0.0003	300
344	tech5-005	0.0000	262	0.0007	200	-	225	0.0000	144
345	techsign-000	0.0007	394	0.0334	398	-	289	0.0020	379
346	tevian-007	0.0000	221	0.0015	294	-	399	0.0002	277
347	tevian-008	0.0000	205	0.0006	167	-	276	0.0000	141
348	tiger-005	0.0000	242	0.0009	240	-	138	0.0001	211

Table 32: FTE is the proportion of failed template generation attempts. Failures can occur because the software throws an exception, or because the software electively refuses to process the input image. This would typically occur if a face is not detected. FTE is measured as the number of function calls that give EITHER a non-zero error code OR that give a “small” template. This is defined as one whose size is less than 0.3 times the median template size for that algorithm. This second rule is needed because some algorithms incorrectly fail to return a non-zero error code when template generation fails.

A hyphen “-” indicates the dataset was not produced.<sup>1</sup> The effects of FTE are included in the accuracy results of this report by regarding any template comparison involving a failed template to produce a low similarity score. Thus higher FTE results in higher FNMR and lower FMR.

	Algorithm	Failure to Enrol Rate <sup>1</sup>						
		APPLICATION	BORDER	CHILD-EXPLOIT	MUGSHOT	VISA	WILD	
Name	SEC. 2.2	SEC. 2.3	SEC. ??	SEC. 2.4	SEC. 2.1	SEC. 2.5		
349	tiger-006	0.0000	279	0.0011	267	-	273	0.0001
350	tinkoff-001	0.0000	278	0.0008	214	-	286	0.0001
351	tongyi-005	0.0000	114	0.0000	94	0.0000	2	0.0000
352	toppanidgate-000	0.0000	186	0.0008	211	-	251	0.0004
353	toshiba-004	0.0000	59	0.0000	18	-	414	0.0000
354	toshiba-005	0.0000	199	0.0004	150	-	297	0.0001
355	trueface-002	0.0000	289	0.0046	363	-	58	0.0003
356	trueface-003	0.0000	274	0.0046	362	-	256	0.0003
357	tuputech-000	0.0003	387	0.0116	384	-	415	-
358	turingtechvip-001	0.0001	369	0.0007	196	-	165	0.0007
359	twface-000	0.0000	26	0.0000	52	-	298	0.0000
360	twface-001	0.0000	42	0.0000	5	-	347	0.0000
361	ulsee-001	0.0000	161	0.0000	65	-	221	0.0000
362	ultinous-000	-	414	-	414	0.0007	23	-
363	ultinous-001	-	415	-	415	0.0007	22	-
364	uluface-002	0.0000	168	0.0000	72	0.0000	11	0.0000
365	uluface-003	0.0000	66	0.0001	126	-	401	0.0002
366	unissey-001	0.0000	124	0.0000	99	-	125	0.0000
367	upc-001	0.0000	334	0.0003	136	0.0450	24	0.0003
368	vcog-002	-	417	-	413	0.2209	36	-
369	vd-002	0.0000	84	0.0000	39	-	369	0.0000
370	vd-003	0.0001	370	0.0041	352	-	391	0.0030
371	veridas-006	0.0000	330	0.0026	320	-	202	0.0001
372	veridas-007	0.0000	329	0.0026	319	-	178	0.0001
373	veridium-000	0.0061	403	0.5956	412	-	383	0.0050
374	verigram-000	0.0000	302	0.0068	374	-	358	0.0003
375	verigram-001	0.0000	294	0.0003	139	-	171	0.0002
376	verihubs-inteligensia-000	0.0000	265	0.0029	329	-	217	0.0001
377	via-000	0.0000	171	0.0000	73	0.0000	10	0.0000
378	via-001	0.0000	38	0.0000	2	-	362	0.0000
379	videmo-000	0.0000	296	0.0019	305	-	224	0.0003
380	videmo-001	0.0000	320	0.0170	388	-	147	0.0010
381	videonetics-001	0.0004	388	0.0309	396	0.4799	44	0.0015
382	videonetics-002	0.0000	305	0.0459	405	0.4598	42	0.0006
383	viettelhightech-000	0.0000	339	0.0019	306	-	82	0.0007
384	vigilantsolutions-010	0.0000	321	0.0028	326	-	219	0.0001
385	vigilantsolutions-011	0.0000	318	0.0028	325	-	390	0.0001
386	vinai-000	0.0000	81	0.0000	34	-	365	0.0000
387	vinbigdata-001	0.0000	173	0.0000	74	-	199	0.0000
388	vion-000	0.0050	401	0.0392	404	0.6388	46	0.0130
389	visage-000	0.0000	341	0.0054	370	-	103	0.0009
390	visionbox-001	0.0000	361	0.0033	339	-	119	0.0005
391	visionbox-002	0.0000	138	0.0017	298	-	177	0.0000
392	visionlabs-010	0.0000	312	0.0009	231	-	136	0.0001
393	visionlabs-011	0.0000	154	0.0006	173	-	145	0.0001
394	visteam-002	0.0000	311	0.0014	289	-	238	0.0002
395	visteam-003	0.0000	218	0.0010	258	-	316	0.0001
396	vnpt-003	0.0000	163	0.0004	143	-	215	0.0002
397	vnpt-004	0.0000	254	0.0006	168	-	168	0.0002
398	vocord-009	0.0000	231	0.0006	172	-	90	0.0001
399	vocord-010	0.0000	276	0.0005	161	-	309	0.0002
400	vts-000	0.0000	303	0.0011	264	-	326	0.0001
401	vts-001	0.0000	71	0.0003	134	-	386	0.0000
402	wicket-000	0.0000	268	0.0009	227	-	193	0.0000
403	winsense-001	0.0000	139	0.0000	57	0.0000	9	0.0000
404	winsense-002	0.0000	145	0.0000	61	-	163	0.0000
405	wuhantianyu-001	0.0000	5	0.0007	185	-	257	0.0001
406	x-laboratory-000	0.0247	412	0.0000	22	0.0000	21	0.0005
								348

Table 33: FTE is the proportion of failed template generation attempts. Failures can occur because the software throws an exception, or because the software electively refuses to process the input image. This would typically occur if a face is not detected. FTE is measured as the number of function calls that give EITHER a non-zero error code OR that give a “small” template. This is defined as one whose size is less than 0.3 times the median template size for that algorithm. This second rule is needed because some algorithms incorrectly fail to return a non-zero error code when template generation fails.

A hyphen “-” indicates the dataset was not produced.<sup>1</sup> The effects of FTE are included in the accuracy results of this report by regarding any template comparison involving a failed template to produce a low similarity score. Thus higher FTE results in higher FNMR and lower FMR.

	Algorithm	Failure to Enrol Rate <sup>1</sup>											
		Name	APPLICATION	BORDER	CHILD-EXPLOIT	MUGSHOT	VISA	WILD	SEC. 2.2	SEC. 2.3	SEC. ??	SEC. 2.4	SEC. 2.1
407	x-laboratory-001	0.0000	225	0.0012	274	-	381	0.0001	239	0.0004	286	0.0007	253
408	xforwardai-001	0.0000	240	0.0007	197	-	137	0.0003	302	0.0004	285	0.0004	178
409	xforwardai-002	0.0000	215	0.0007	195	-	323	0.0003	303	0.0004	280	0.0004	176
410	xm-000	0.0000	56	0.0007	182	-	317	0.0001	197	0.0003	149	0.0004	221
411	yisheng-004	0.0002	383	-	416	0.4279	41	0.0013	373	0.0006	353	0.0321	370
412	yitu-003	0.0000	21	0.0000	47	-	299	0.0009	363	0.0000	57	0.0000	11
413	yoonik-002	0.0000	288	0.0010	254	-	94	0.0003	293	0.0006	347	0.0005	233
414	yoonik-003	0.0000	275	0.0009	235	-	250	0.0002	263	0.0004	262	0.0008	261
415	ytu-000	0.0000	188	0.0010	261	-	245	0.0002	286	0.0004	281	0.0011	282
416	yuan-003	0.0000	326	0.0010	259	-	336	0.0005	340	0.0005	327	0.0005	237
417	yuan-004	0.0000	80	0.0000	33	-	378	0.0000	107	0.0000	26	0.0000	29

Table 34: FTE is the proportion of failed template generation attempts. Failures can occur because the software throws an exception, or because the software electively refuses to process the input image. This would typically occur if a face is not detected. FTE is measured as the number of function calls that give EITHER a non-zero error code OR that give a “small” template. This is defined as one whose size is less than 0.3 times the median template size for that algorithm. This second rule is needed because some algorithms incorrectly fail to return a non-zero error code when template generation fails.

A hyphen “-” indicates the dataset was not produced. <sup>1</sup>The effects of FTE are included in the accuracy results of this report by regarding any template comparison involving a failed template to produce a low similarity score. Thus higher FTE results in higher FNMR and lower FMR.

### 3.4 Recognition accuracy

Core algorithm accuracy is stated via:

▷ **Cooperative subjects**

- The summary table of Figure 26;
- The visa image DETs of Figure 63;
- The mugshot DETs of Figure 84;
- The mugshot ageing profiles of Figure 303;
- The human-difficult pairs of Figure 21

▷ **Non-cooperative subjects**

- The photojournalism DET of Figure 101

Figure 242 shows dependence of false match rate on algorithm score threshold. This allows a deployer to set a threshold to target a particular false match rate appropriate to the security objectives of the application.

Figure 199 likewise shows FMR(T) but for mugshots, and specially four subsets of the population.

Note that in both the mugshot and visa sets false match rates vary with the ethnicity, age, and sex, of the enrollee and impostor. For example figure 122 summarizes FMR for impostors paired from four groups black females, black males, white females, white males.

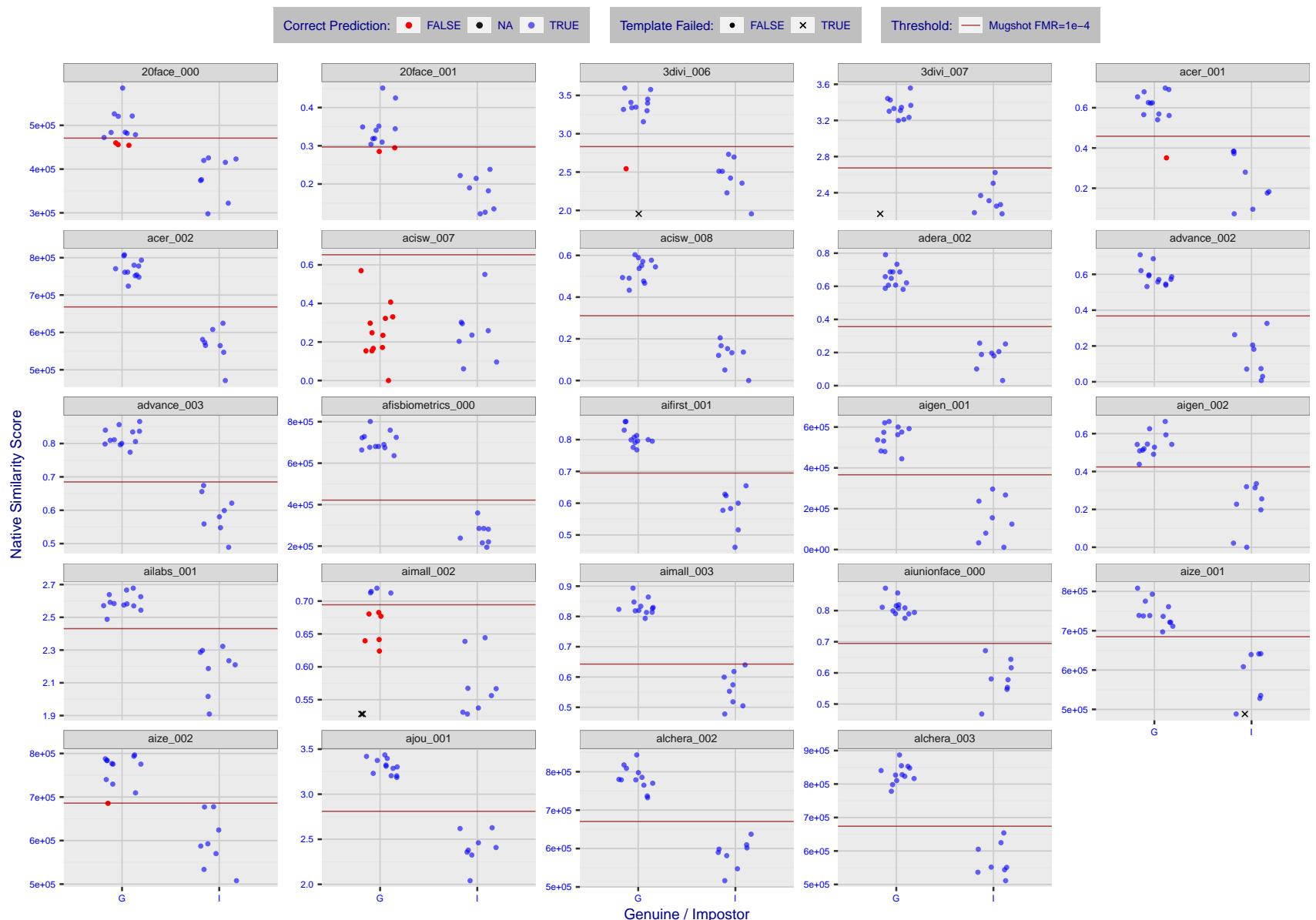


Figure 4: The figure shows algorithms' similarity scores for 12 genuine and 8 impostor image pairs used in the May 2018 paper Face recognition accuracy of forensic examiners, superrecognizers, and face recognition algorithms (Phillips et al. [1]). The threshold (red horizontal line) is a value calibrated to give  $FMR = 0.0001$  on mugshot images. Points above the threshold correspond to pairs predicted to be genuine, and points below the threshold correspond to pairs predicted to be impostors. The figure shows whether the predicted class (genuine or impostor) matches the real class. Blue denotes a correct prediction, and red denotes incorrect. An "X" represents face detection failure in either of the images in the pair. Note that the sample size ( $n=20$ ) is small, and the figure may change substantially if larger or different sets are used. The images can be downloaded from the [Supplemental Information](#) page provided with that publication.

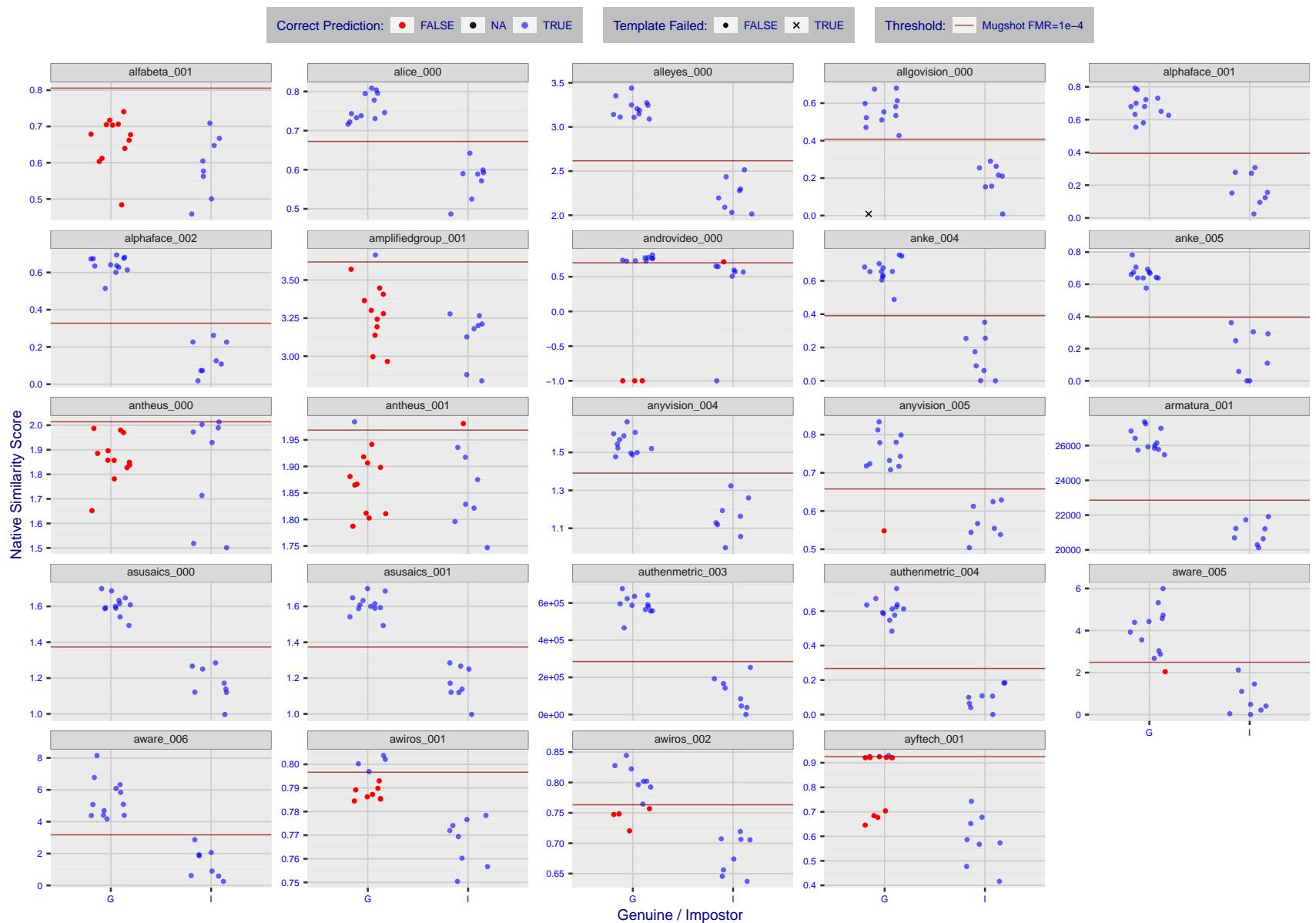


Figure 5: The figure shows algorithms' similarity scores for 12 genuine and 8 impostor image pairs used in the May 2018 paper Face recognition accuracy of forensic examiners, superrecognizers, and face recognition algorithms (Phillips et al. [1]). The threshold (red horizontal line) is a value calibrated to give  $FMR = 0.0001$  on mugshot images. Points above the threshold correspond to pairs predicted to be genuine, and points below the threshold correspond to pairs predicted to be impostors. The figure shows whether the predicted class (genuine or impostor) matches the real class. Blue denotes a correct prediction, and red denotes incorrect. An "X" represents face detection failure in either of the images in the pair. Note that the sample size ( $n=20$ ) is small, and the figure may change substantially if larger or different sets are used. The images can be downloaded from the [Supplemental Information](#) page provided with that publication.

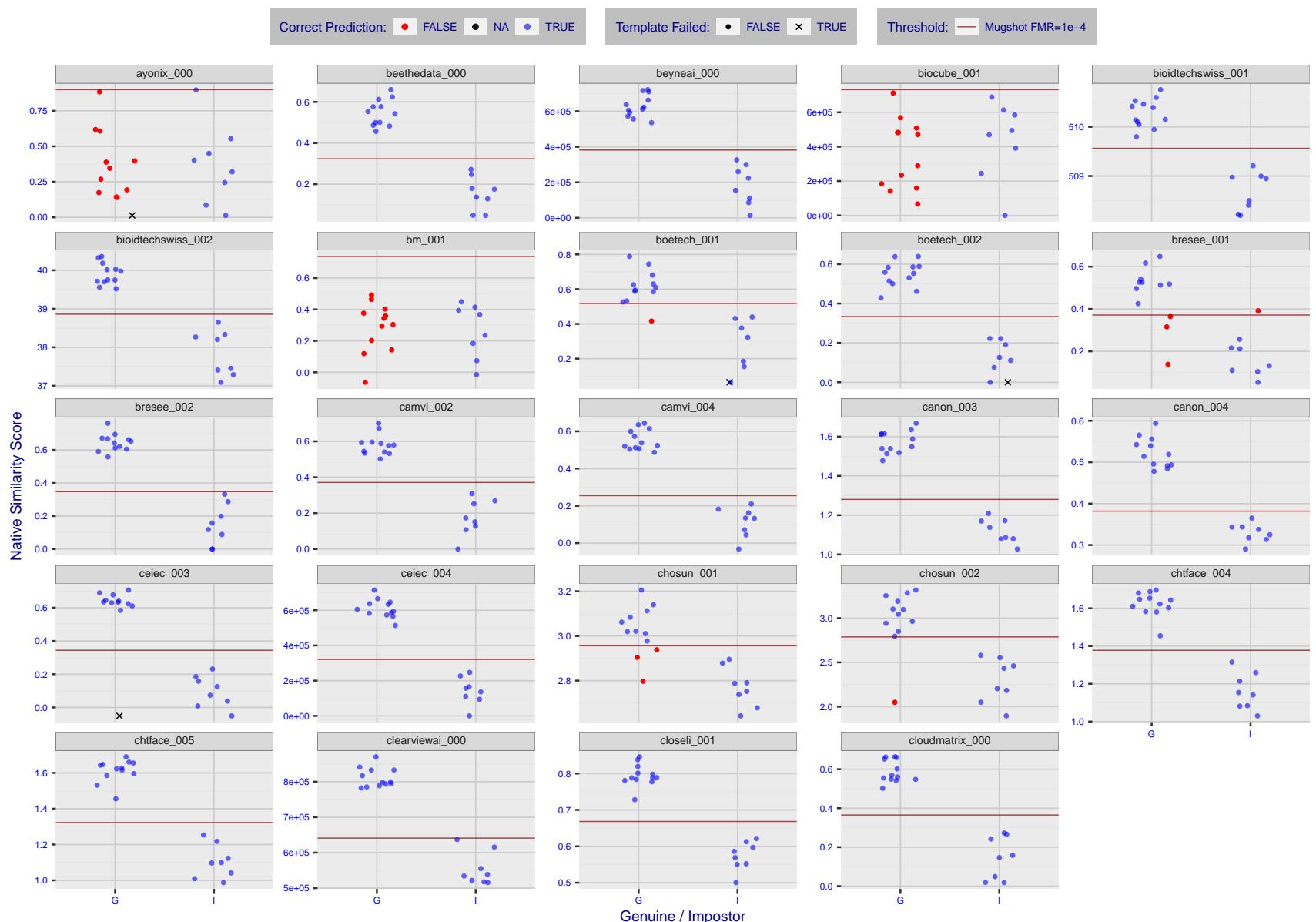


Figure 6: The figure shows algorithms' similarity scores for 12 genuine and 8 impostor image pairs used in the May 2018 paper Face recognition accuracy of forensic examiners, superrecognizers, and face recognition algorithms (Phillips et al. [1]). The threshold (red horizontal line) is a value calibrated to give  $FMR = 0.0001$  on mugshot images. Points above the threshold correspond to pairs predicted to be genuine, and points below the threshold correspond to pairs predicted to be impostors. The figure shows whether the predicted class (genuine or impostor) matches the real class. Blue denotes a correct prediction, and red denotes incorrect. An "X" represents face detection failure in either of the images in the pair. Note that the sample size ( $n=20$ ) is small, and the figure may change substantially if larger or different sets are used. The images can be downloaded from the [Supplemental Information](#) page provided with that publication.

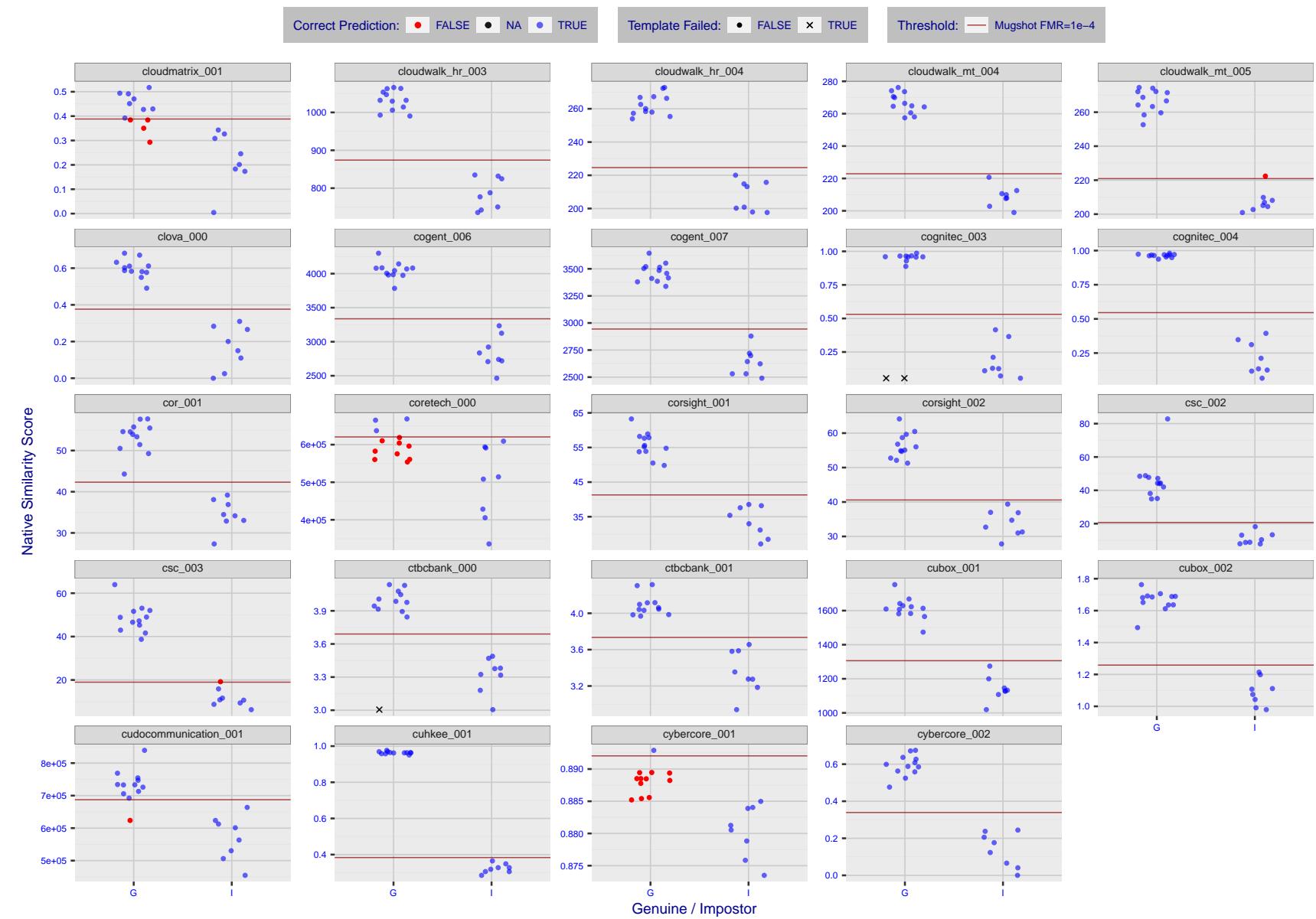


Figure 7: The figure shows algorithms' similarity scores for 12 genuine and 8 impostor image pairs used in the May 2018 paper Face recognition accuracy of forensic examiners, superrecognizers, and face recognition algorithms (Phillips et al. [1]). The threshold (red horizontal line) is a value calibrated to give  $FMR = 0.0001$  on mugshot images. Points above the threshold correspond to pairs predicted to be genuine, and points below the threshold correspond to pairs predicted to be impostors. The figure shows whether the predicted class (genuine or impostor) matches the real class. Blue denotes a correct prediction, and red denotes incorrect. An "X" represents face detection failure in either of the images in the pair. Note that the sample size ( $n=20$ ) is small, and the figure may change substantially if larger or different sets are used. The images can be downloaded from the [Supplemental Information](#) page provided with that publication.

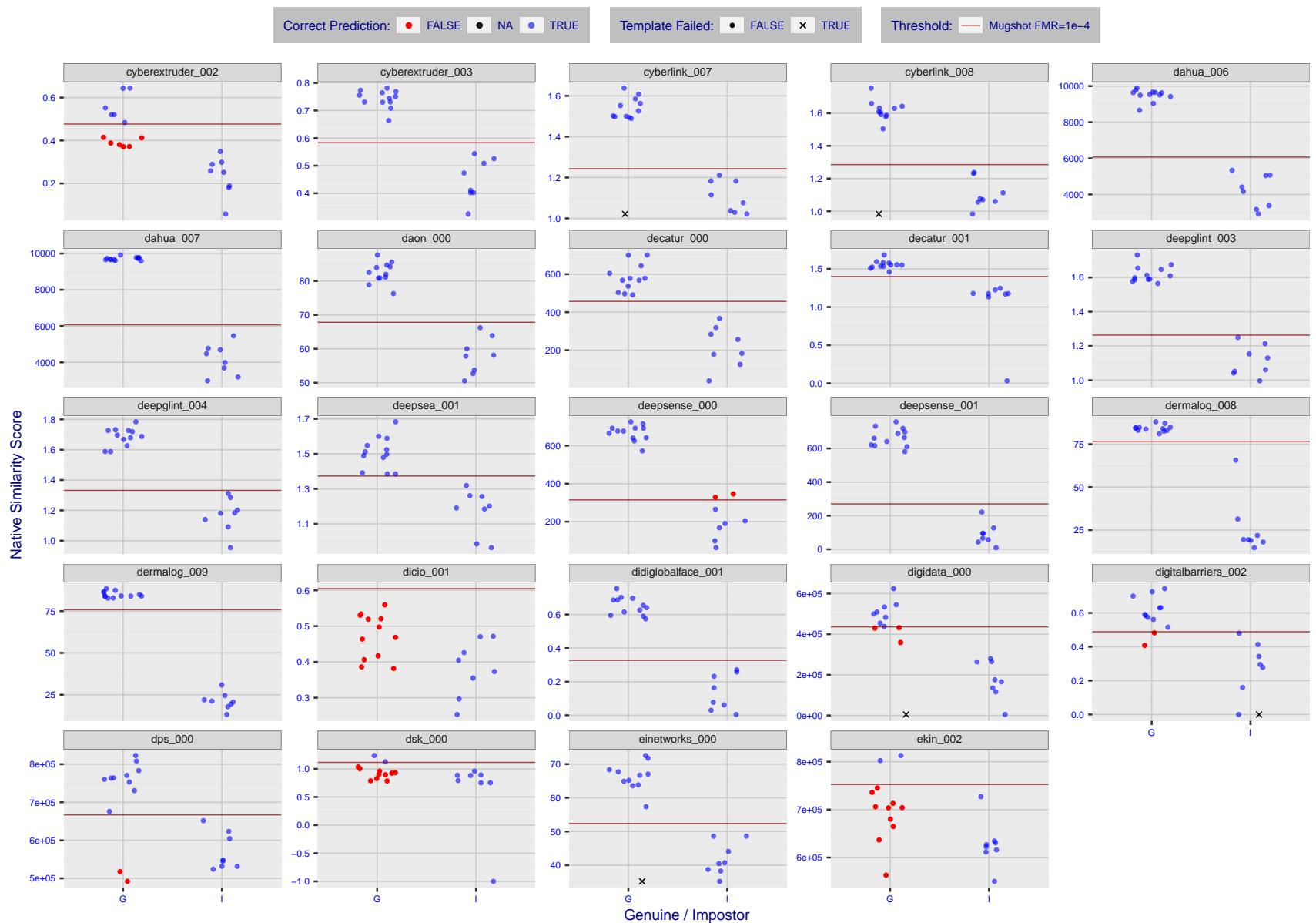


Figure 8: The figure shows algorithms' similarity scores for 12 genuine and 8 impostor image pairs used in the May 2018 paper Face recognition accuracy of forensic examiners, superrecognizers, and face recognition algorithms (Phillips et al. [1]). The threshold (red horizontal line) is a value calibrated to give  $FMR = 0.0001$  on mugshot images. Points above the threshold correspond to pairs predicted to be genuine, and points below the threshold correspond to pairs predicted to be impostors. The figure shows whether the predicted class (genuine or impostor) matches the real class. Blue denotes a correct prediction, and red denotes incorrect. An "X" represents face detection failure in either of the images in the pair. Note that the sample size ( $n=20$ ) is small, and the figure may change substantially if larger or different sets are used. The images can be downloaded from the [Supplemental Information](#) page provided with that publication.

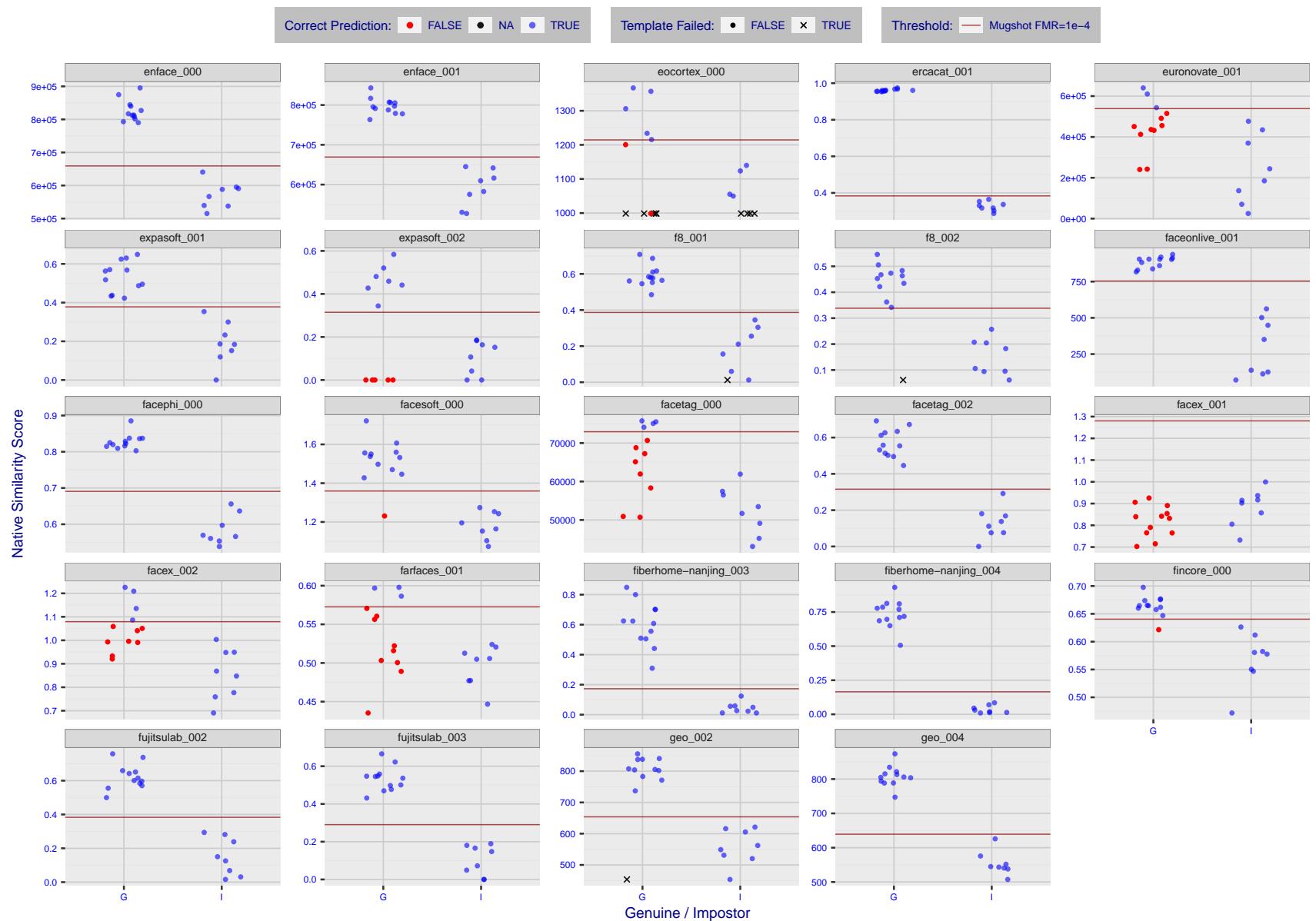


Figure 9: The figure shows algorithms' similarity scores for 12 genuine and 8 impostor image pairs used in the May 2018 paper Face recognition accuracy of forensic examiners, superrecognizers, and face recognition algorithms (Phillips et al. [1]). The threshold (red horizontal line) is a value calibrated to give  $FMR = 0.0001$  on mugshot images. Points above the threshold correspond to pairs predicted to be genuine, and points below the threshold correspond to pairs predicted to be impostors. The figure shows whether the predicted class (genuine or impostor) matches the real class. Blue denotes a correct prediction, and red denotes incorrect. An "X" represents face detection failure in either of the images in the pair. Note that the sample size ( $n=20$ ) is small, and the figure may change substantially if larger or different sets are used. The images can be downloaded from the [Supplemental Information](#) page provided with that publication.

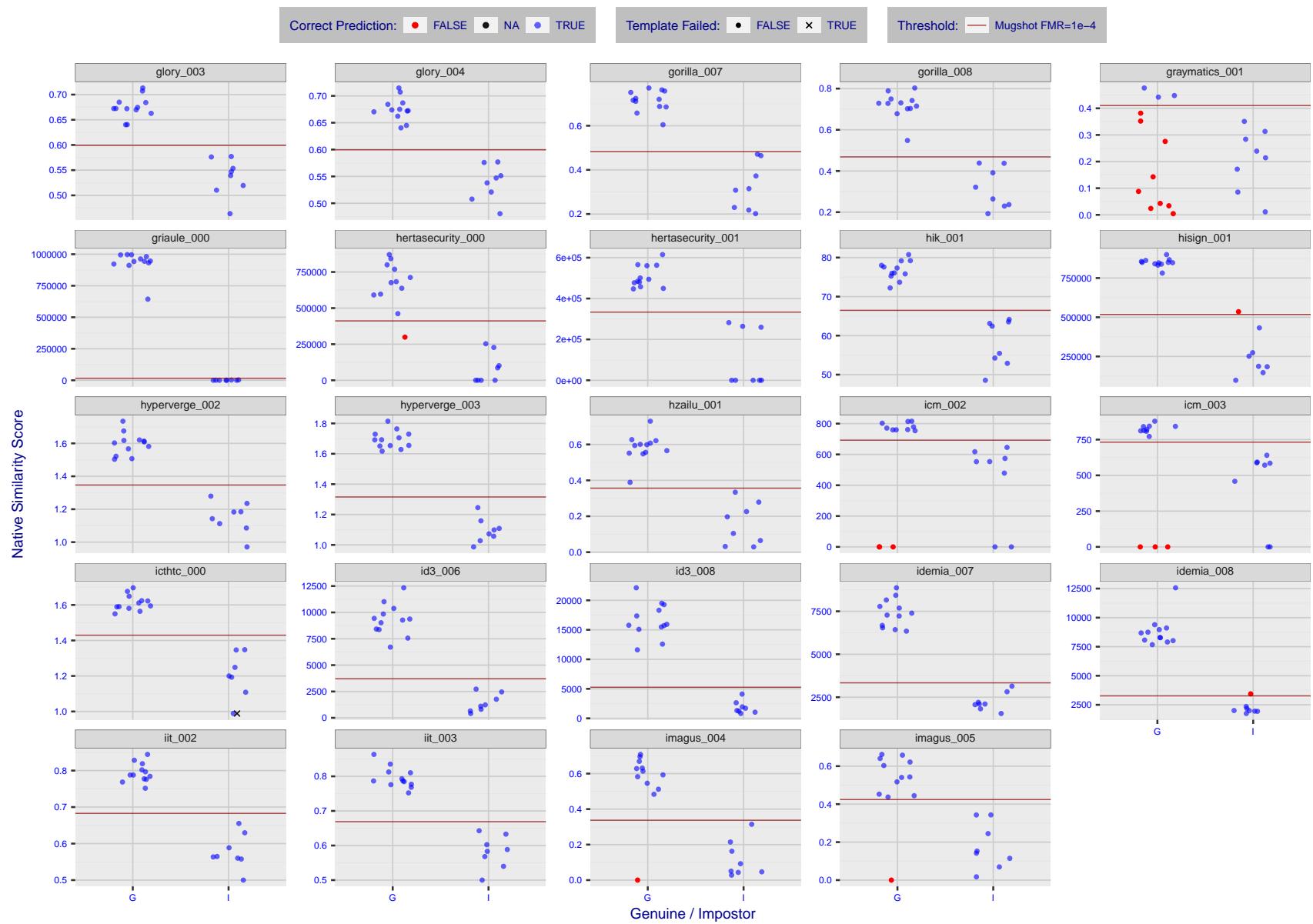


Figure 10: The figure shows algorithms' similarity scores for 12 genuine and 8 impostor image pairs used in the May 2018 paper Face recognition accuracy of forensic examiners, superrecognizers, and face recognition algorithms (Phillips et al. [1]). The threshold (red horizontal line) is a value calibrated to give  $FMR = 0.0001$  on mugshot images. Points above the threshold correspond to pairs predicted to be genuine, and points below the threshold correspond to pairs predicted to be impostors. The figure shows whether the predicted class (genuine or impostor) matches the real class. Blue denotes a correct prediction, and red denotes incorrect. An "X" represents face detection failure in either of the images in the pair. Note that the sample size ( $n=20$ ) is small, and the figure may change substantially if larger or different sets are used. The images can be downloaded from the [Supplemental Information](#) page provided with that publication.

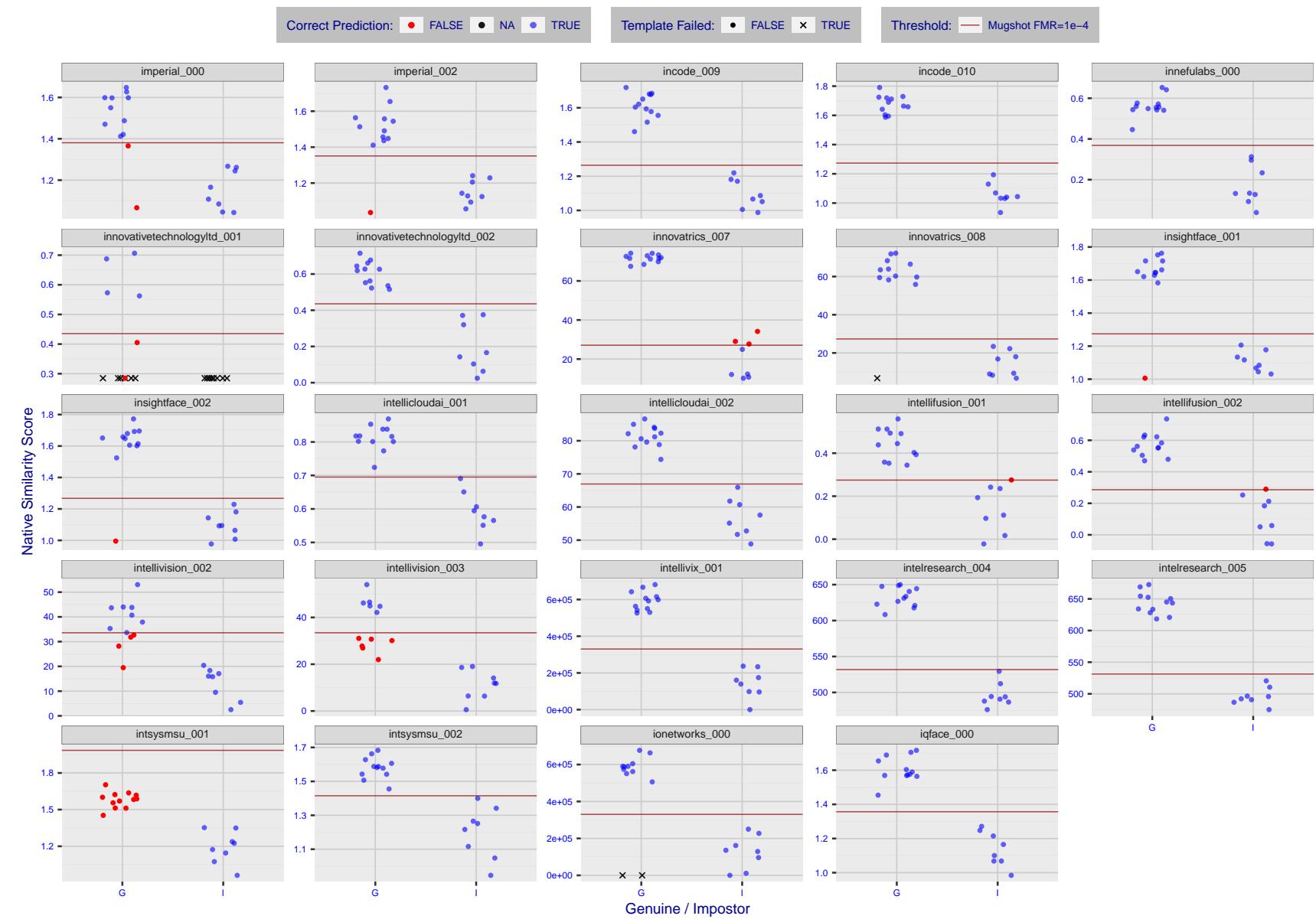


Figure 11: The figure shows algorithms' similarity scores for 12 genuine and 8 impostor image pairs used in the May 2018 paper Face recognition accuracy of forensic examiners, superrecognizers, and face recognition algorithms (Phillips et al. [1]). The threshold (red horizontal line) is a value calibrated to give  $FMR = 0.0001$  on mugshot images. Points above the threshold correspond to pairs predicted to be genuine, and points below the threshold correspond to pairs predicted to be impostors. The figure shows whether the predicted class (genuine or impostor) matches the real class. Blue denotes a correct prediction, and red denotes incorrect. An "X" represents face detection failure in either of the images in the pair. Note that the sample size ( $n=20$ ) is small, and the figure may change substantially if larger or different sets are used. The images can be downloaded from the [Supplemental Information](#) page provided with that publication.

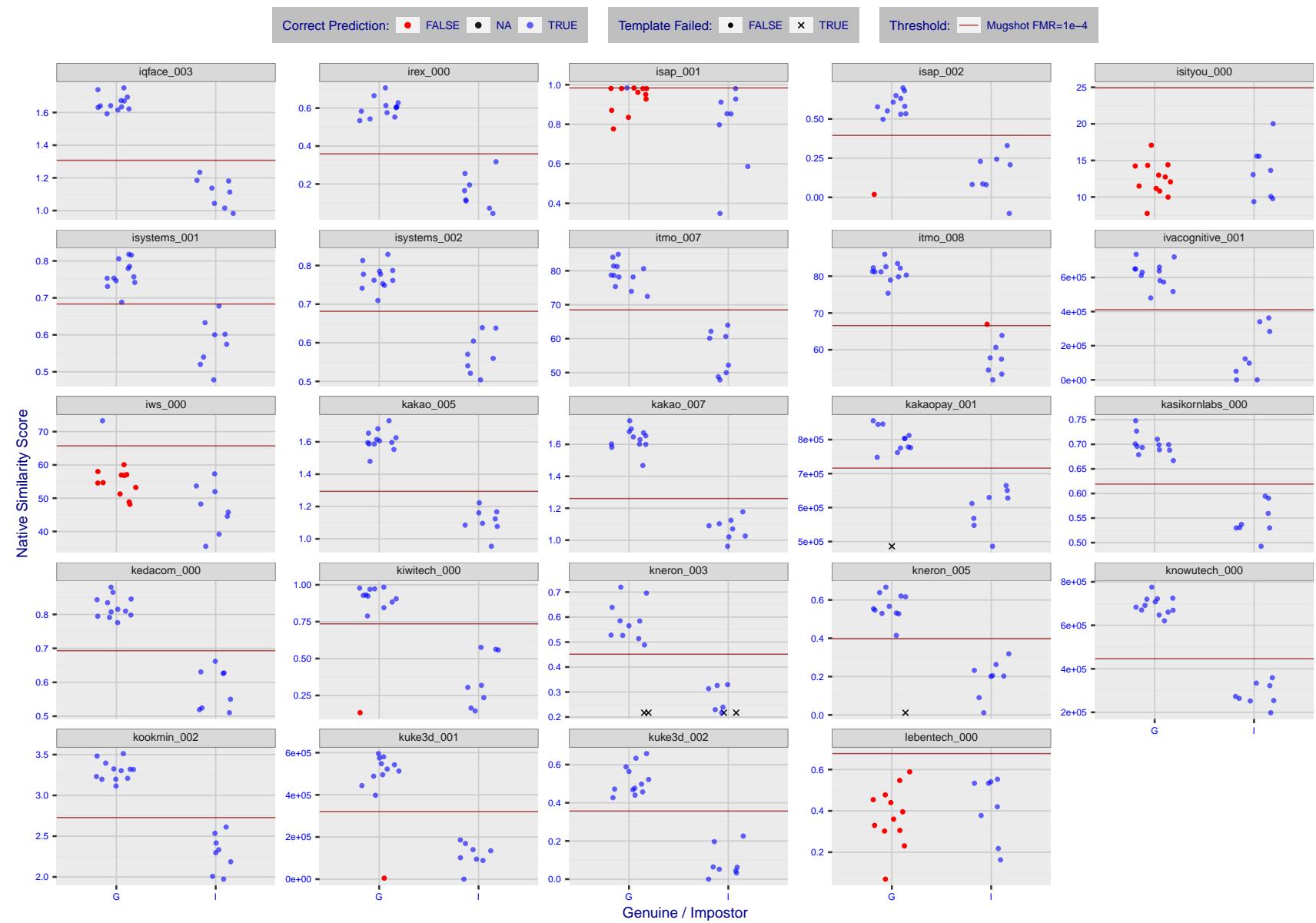


Figure 12: The figure shows algorithms' similarity scores for 12 genuine and 8 impostor image pairs used in the May 2018 paper Face recognition accuracy of forensic examiners, superrecognizers, and face recognition algorithms (Phillips et al. [1]). The threshold (red horizontal line) is a value calibrated to give  $FMR = 0.0001$  on mugshot images. Points above the threshold correspond to pairs predicted to be genuine, and points below the threshold correspond to pairs predicted to be impostors. The figure shows whether the predicted class (genuine or impostor) matches the real class. Blue denotes a correct prediction, and red denotes incorrect. An "X" represents face detection failure in either of the images in the pair. Note that the sample size ( $n=20$ ) is small, and the figure may change substantially if larger or different sets are used. The images can be downloaded from the [Supplemental Information](#) page provided with that publication.

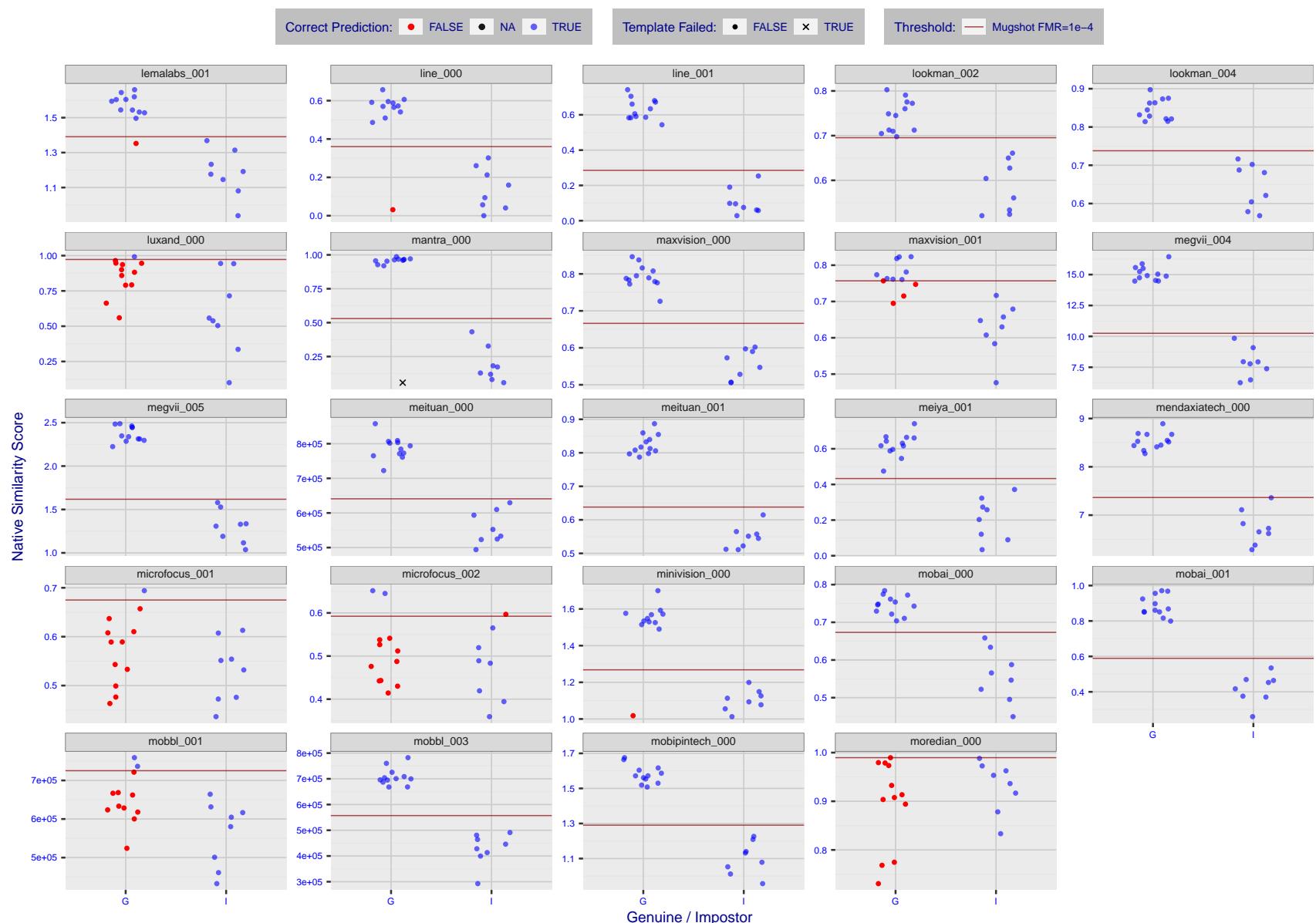


Figure 13: The figure shows algorithms' similarity scores for 12 genuine and 8 impostor image pairs used in the May 2018 paper Face recognition accuracy of forensic examiners, superrecognizers, and face recognition algorithms (Phillips et al. [1]). The threshold (red horizontal line) is a value calibrated to give  $FMR = 0.0001$  on mugshot images. Points above the threshold correspond to pairs predicted to be genuine, and points below the threshold correspond to pairs predicted to be impostors. The figure shows whether the predicted class (genuine or impostor) matches the real class. Blue denotes a correct prediction, and red denotes incorrect. An "X" represents face detection failure in either of the images in the pair. Note that the sample size ( $n=20$ ) is small, and the figure may change substantially if larger or different sets are used. The images can be downloaded from the [Supplemental Information](#) page provided with that publication.

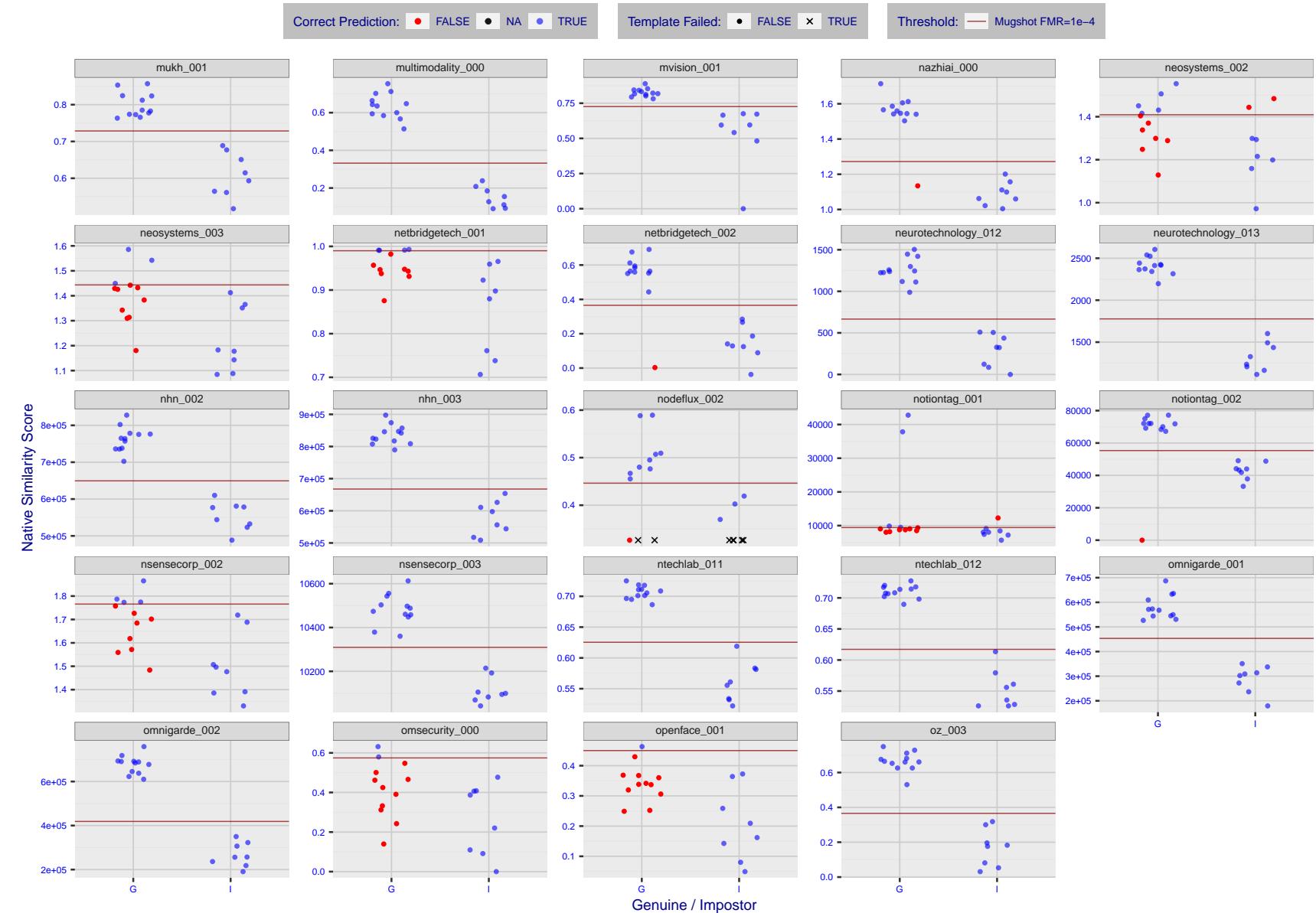


Figure 14: The figure shows algorithms' similarity scores for 12 genuine and 8 impostor image pairs used in the May 2018 paper Face recognition accuracy of forensic examiners, superrecognizers, and face recognition algorithms (Phillips et al. [1]). The threshold (red horizontal line) is a value calibrated to give  $FMR = 0.0001$  on mugshot images. Points above the threshold correspond to pairs predicted to be genuine, and points below the threshold correspond to pairs predicted to be impostors. The figure shows whether the predicted class (genuine or impostor) matches the real class. Blue denotes a correct prediction, and red denotes incorrect. An "X" represents face detection failure in either of the images in the pair. Note that the sample size ( $n=20$ ) is small, and the figure may change substantially if larger or different sets are used. The images can be downloaded from the [Supplemental Information](#) page provided with that publication.

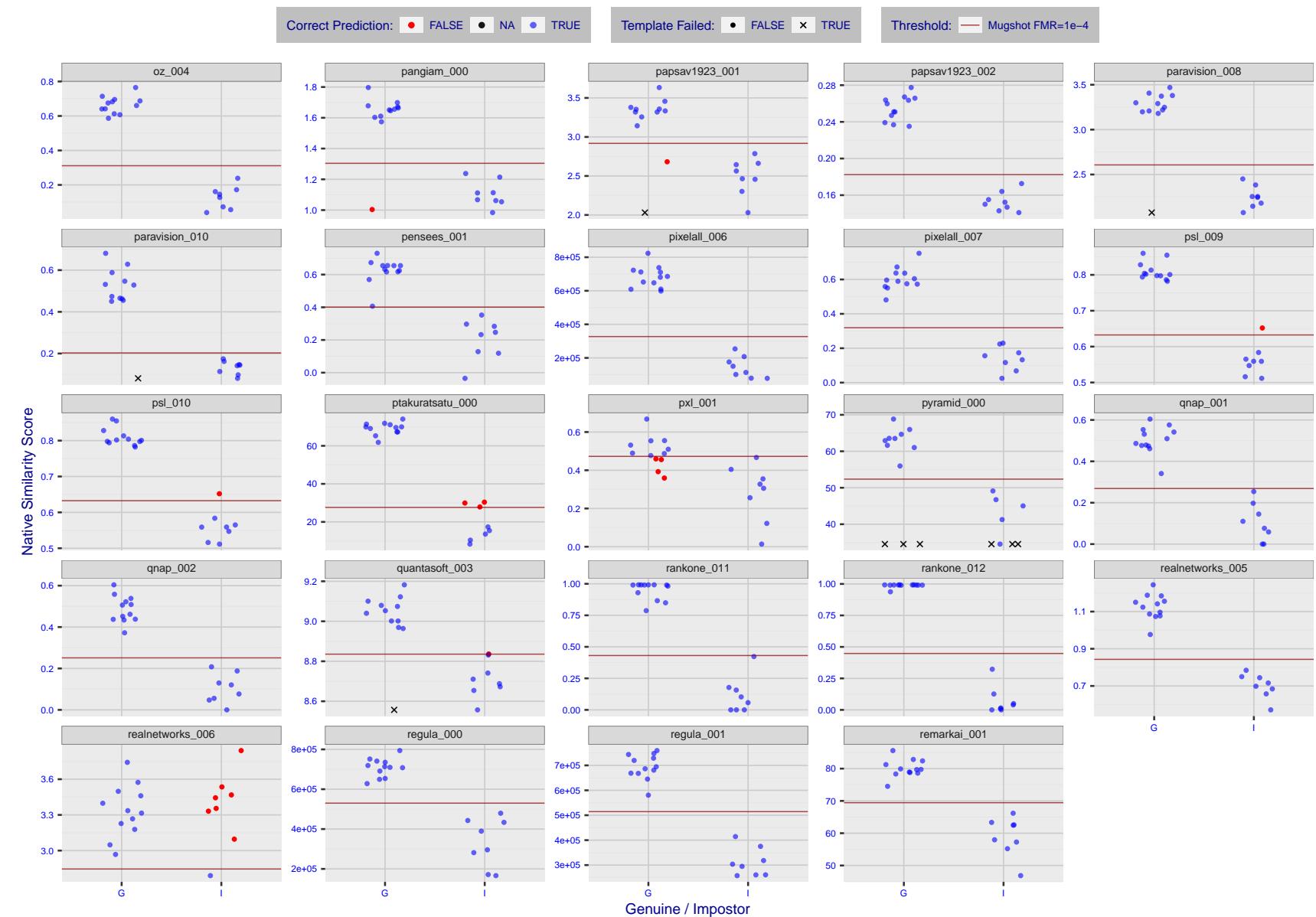


Figure 15: The figure shows algorithms' similarity scores for 12 genuine and 8 impostor image pairs used in the May 2018 paper Face recognition accuracy of forensic examiners, superrecognizers, and face recognition algorithms (Phillips et al. [1]). The threshold (red horizontal line) is a value calibrated to give  $FMR = 0.0001$  on mugshot images. Points above the threshold correspond to pairs predicted to be genuine, and points below the threshold correspond to pairs predicted to be impostors. The figure shows whether the predicted class (genuine or impostor) matches the real class. Blue denotes a correct prediction, and red denotes incorrect. An "X" represents face detection failure in either of the images in the pair. Note that the sample size ( $n=20$ ) is small, and the figure may change substantially if larger or different sets are used. The images can be downloaded from the [Supplemental Information](#) page provided with that publication.

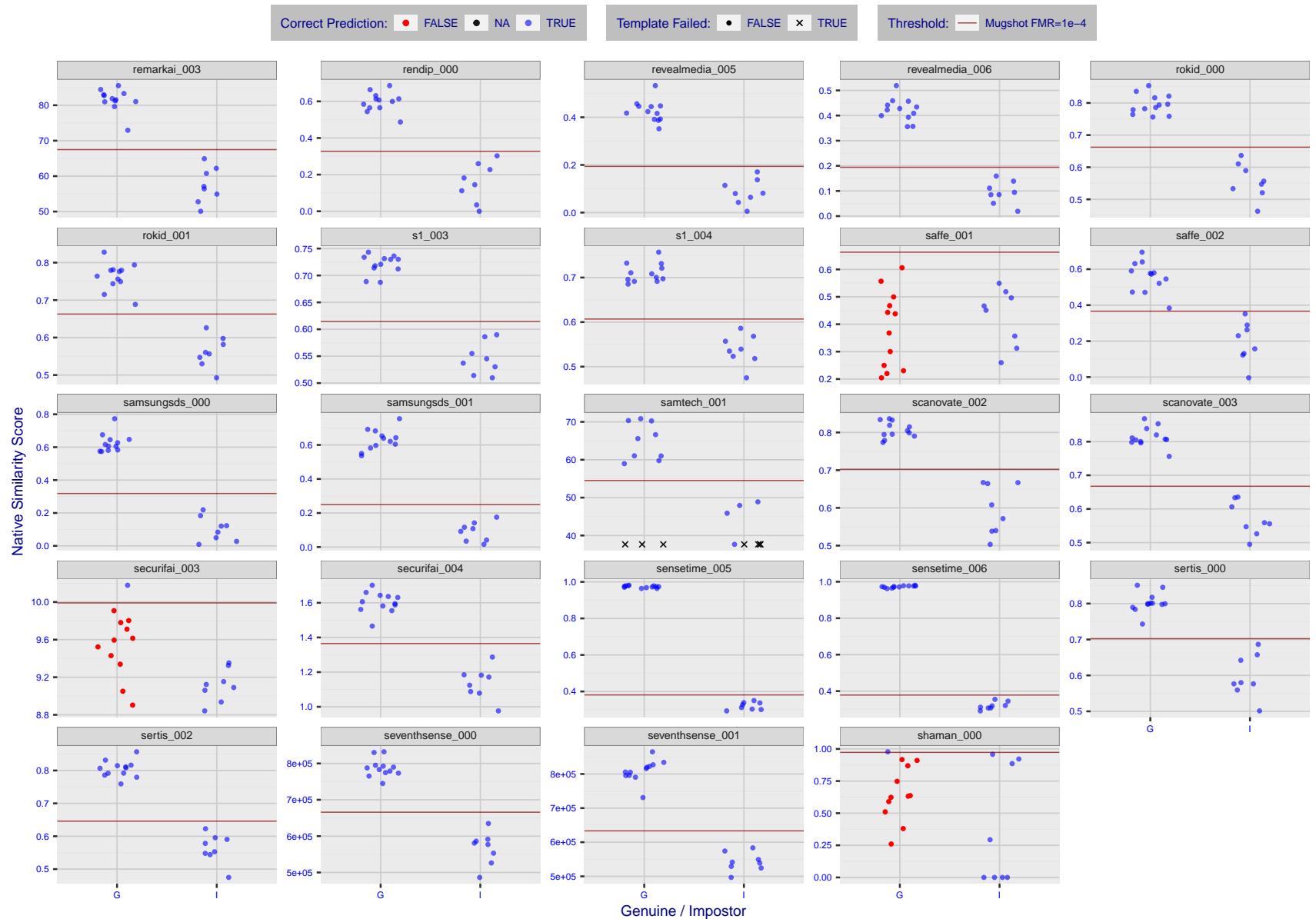


Figure 16: The figure shows algorithms' similarity scores for 12 genuine and 8 impostor image pairs used in the May 2018 paper Face recognition accuracy of forensic examiners, superrecognizers, and face recognition algorithms (Phillips et al. [1]). The threshold (red horizontal line) is a value calibrated to give  $FMR = 0.0001$  on mugshot images. Points above the threshold correspond to pairs predicted to be genuine, and points below the threshold correspond to pairs predicted to be impostors. The figure shows whether the predicted class (genuine or impostor) matches the real class. Blue denotes a correct prediction, and red denotes incorrect. An "X" represents face detection failure in either of the images in the pair. Note that the sample size ( $n=20$ ) is small, and the figure may change substantially if larger or different sets are used. The images can be downloaded from the [Supplemental Information](#) page provided with that publication.

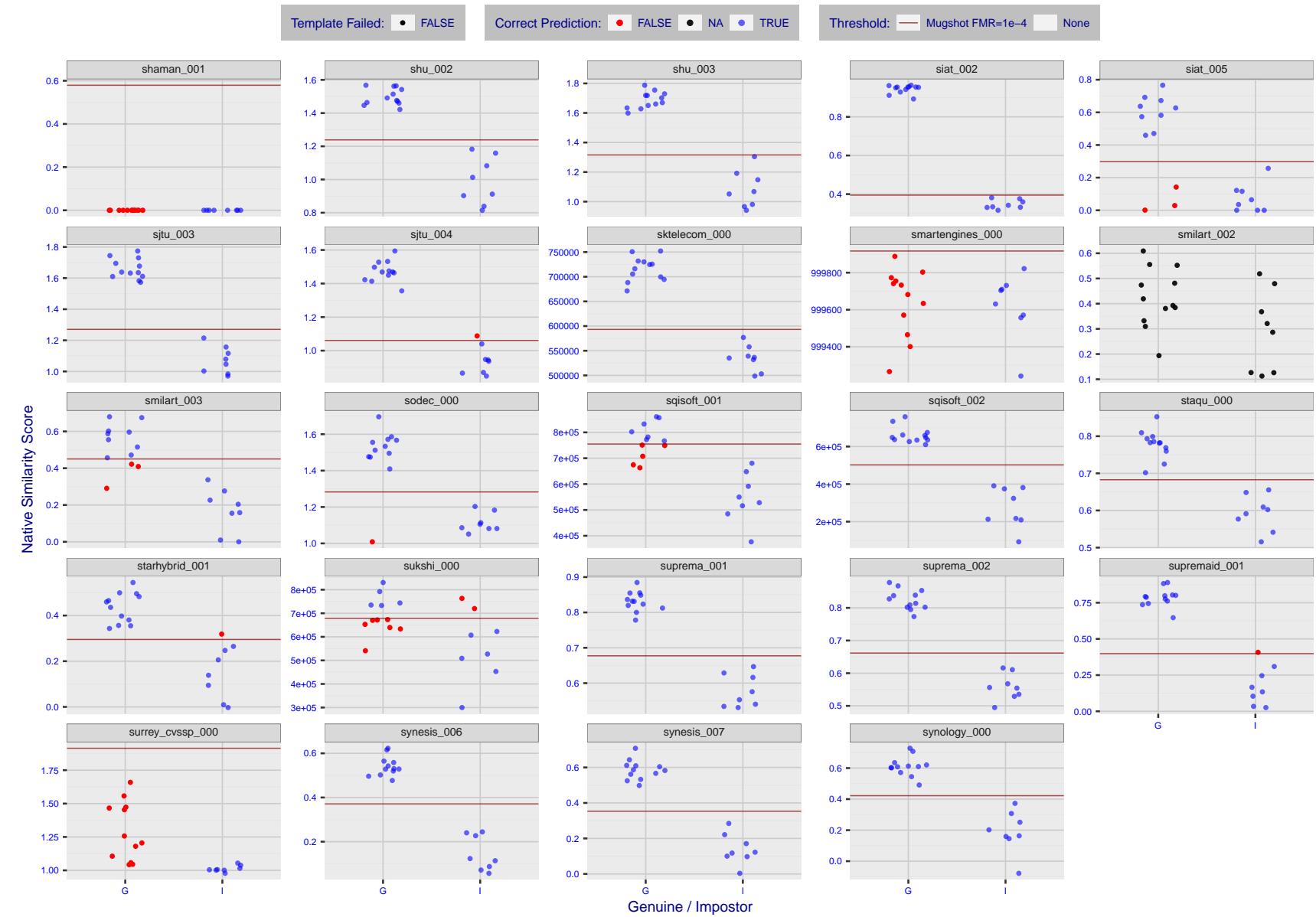


Figure 17: The figure shows algorithms' similarity scores for 12 genuine and 8 impostor image pairs used in the May 2018 paper Face recognition accuracy of forensic examiners, superrecognizers, and face recognition algorithms (Phillips et al. [1]). The threshold (red horizontal line) is a value calibrated to give  $FMR = 0.0001$  on mugshot images. Points above the threshold correspond to pairs predicted to be genuine, and points below the threshold correspond to pairs predicted to be impostors. The figure shows whether the predicted class (genuine or impostor) matches the real class. Blue denotes a correct prediction, and red denotes incorrect. An "X" represents face detection failure in either of the images in the pair. Note that the sample size ( $n=20$ ) is small, and the figure may change substantially if larger or different sets are used. The images can be downloaded from the [Supplemental Information](#) page provided with that publication.

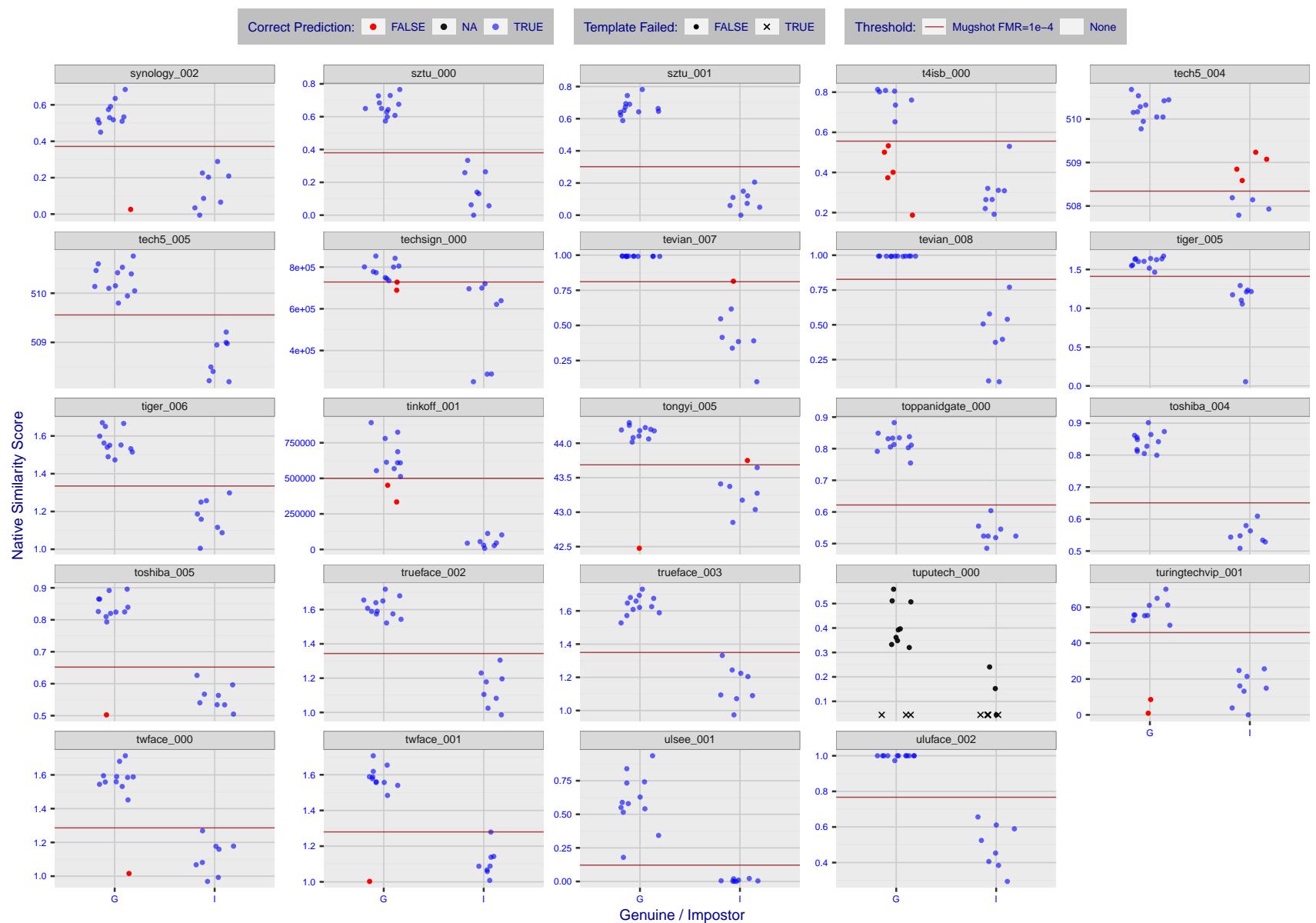


Figure 18: The figure shows algorithms' similarity scores for 12 genuine and 8 impostor image pairs used in the May 2018 paper Face recognition accuracy of forensic examiners, superrecognizers, and face recognition algorithms (Phillips et al. [1]). The threshold (red horizontal line) is a value calibrated to give  $FMR = 0.0001$  on mugshot images. Points above the threshold correspond to pairs predicted to be genuine, and points below the threshold correspond to pairs predicted to be impostors. The figure shows whether the predicted class (genuine or impostor) matches the real class. Blue denotes a correct prediction, and red denotes incorrect. An "X" represents face detection failure in either of the images in the pair. Note that the sample size ( $n=20$ ) is small, and the figure may change substantially if larger or different sets are used. The images can be downloaded from the [Supplemental Information](#) page provided with that publication.

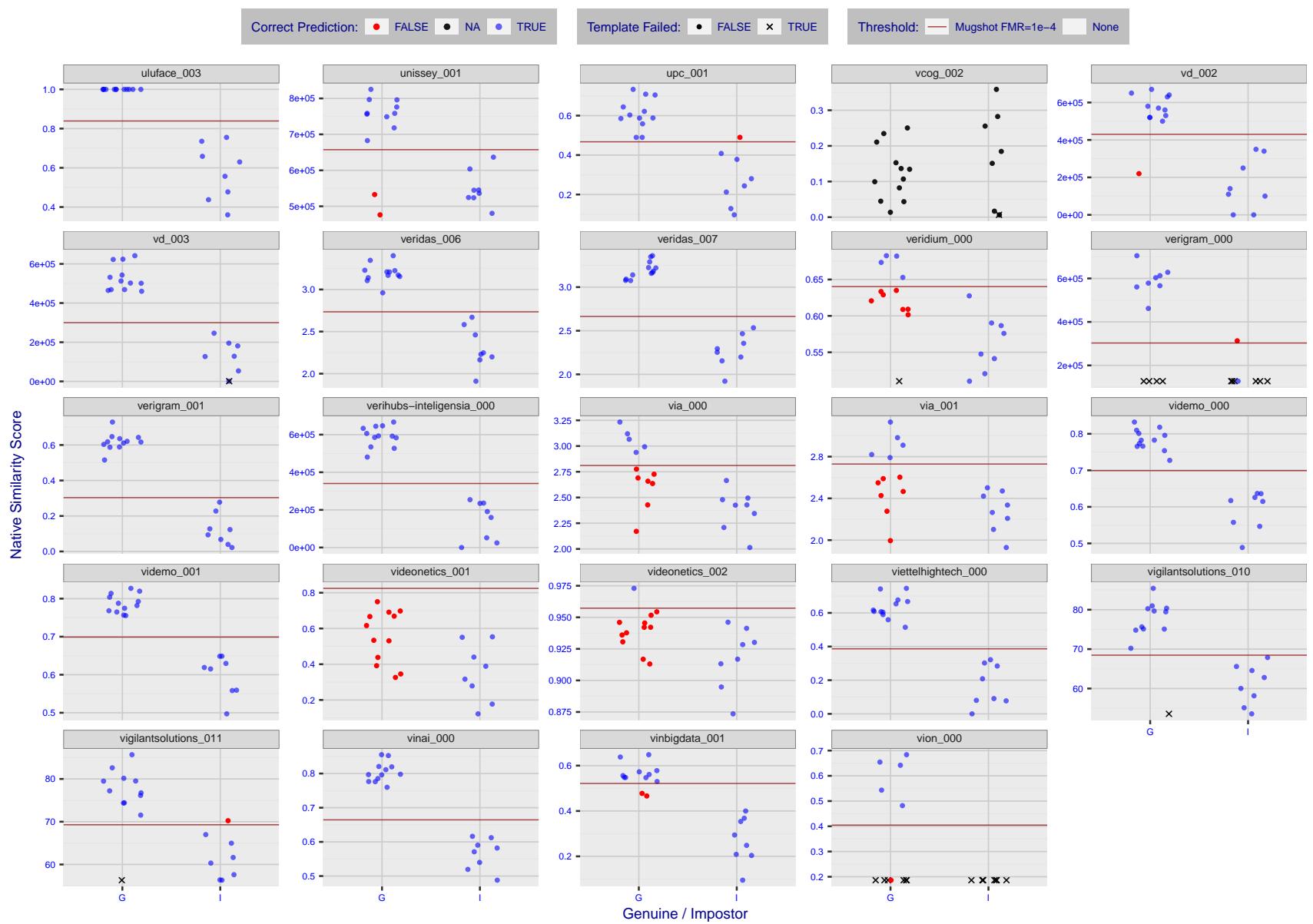


Figure 19: The figure shows algorithms' similarity scores for 12 genuine and 8 impostor image pairs used in the May 2018 paper Face recognition accuracy of forensic examiners, superrecognizers, and face recognition algorithms (Phillips et al. [1]). The threshold (red horizontal line) is a value calibrated to give  $FMR = 0.0001$  on mugshot images. Points above the threshold correspond to pairs predicted to be genuine, and points below the threshold correspond to pairs predicted to be impostors. The figure shows whether the predicted class (genuine or impostor) matches the real class. Blue denotes a correct prediction, and red denotes incorrect. An "X" represents face detection failure in either of the images in the pair. Note that the sample size ( $n=20$ ) is small, and the figure may change substantially if larger or different sets are used. The images can be downloaded from the [Supplemental Information](#) page provided with that publication.

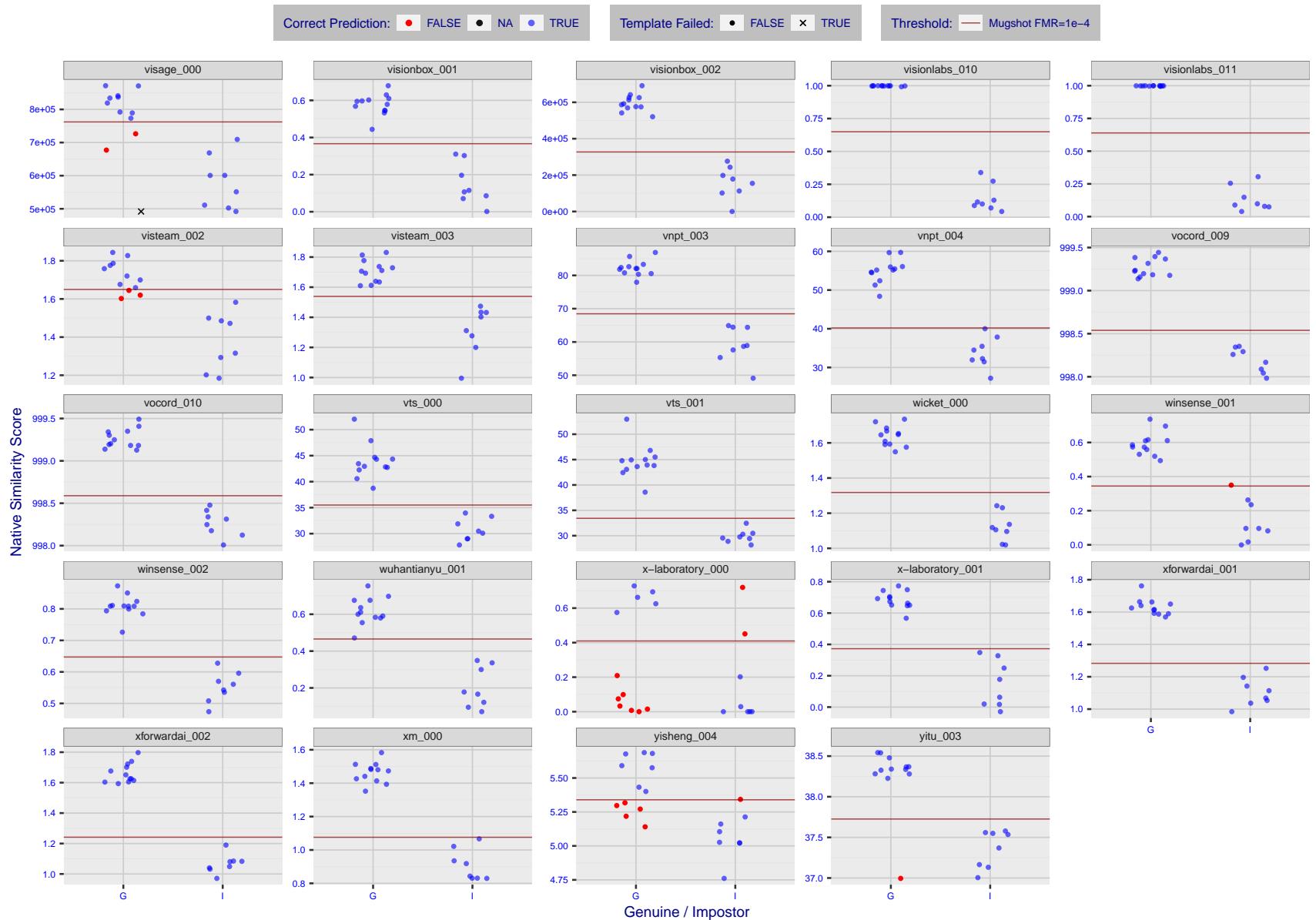


Figure 20: The figure shows algorithms' similarity scores for 12 genuine and 8 impostor image pairs used in the May 2018 paper Face recognition accuracy of forensic examiners, superrecognizers, and face recognition algorithms (Phillips et al. [1]). The threshold (red horizontal line) is a value calibrated to give  $FMR = 0.0001$  on mugshot images. Points above the threshold correspond to pairs predicted to be genuine, and points below the threshold correspond to pairs predicted to be impostors. The figure shows whether the predicted class (genuine or impostor) matches the real class. Blue denotes a correct prediction, and red denotes incorrect. An "X" represents face detection failure in either of the images in the pair. Note that the sample size ( $n=20$ ) is small, and the figure may change substantially if larger or different sets are used. The images can be downloaded from the [Supplemental Information](#) page provided with that publication.

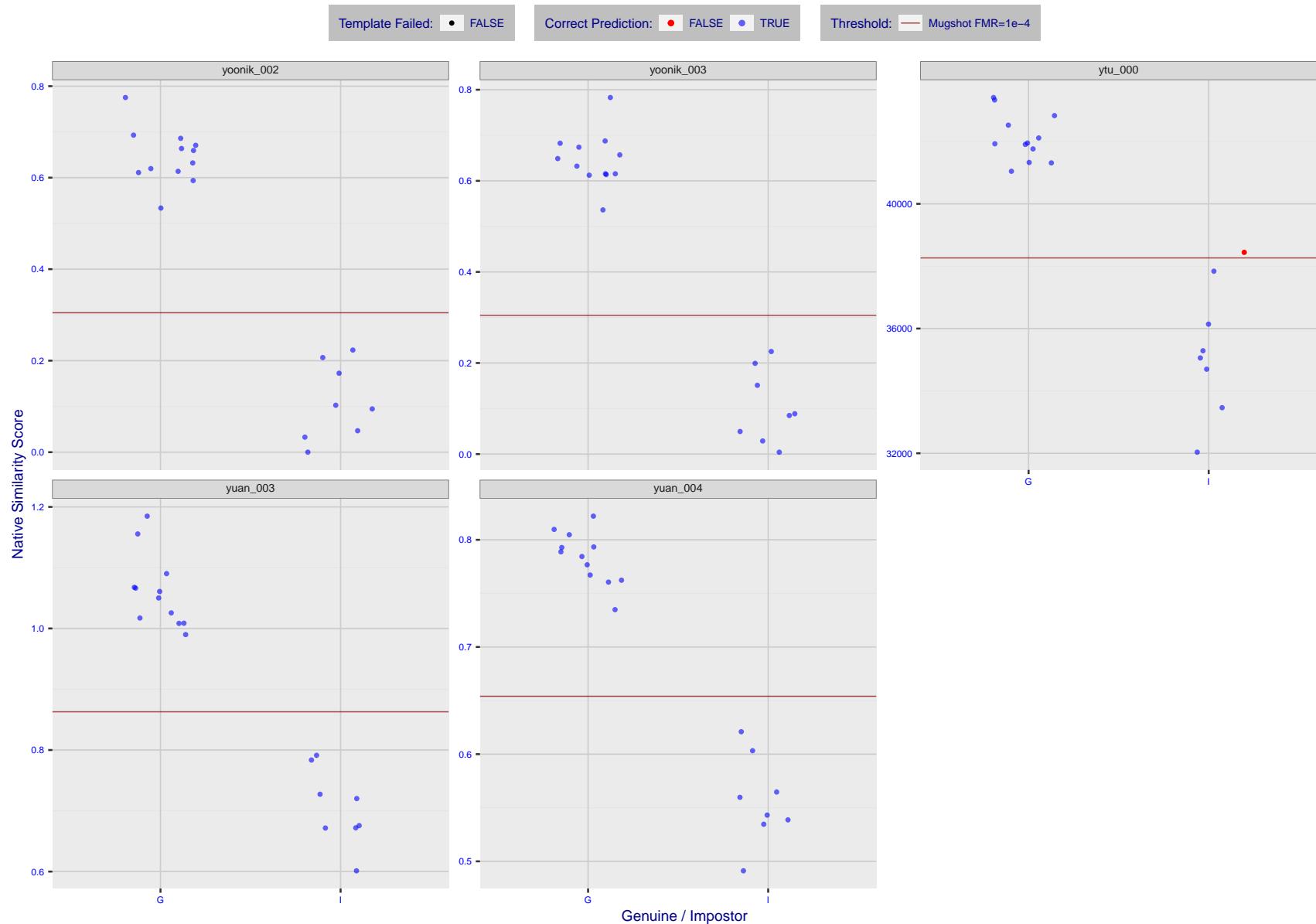


Figure 21: The figure shows algorithms' similarity scores for 12 genuine and 8 impostor image pairs used in the May 2018 paper [Face recognition accuracy of forensic examiners, superrecognizers, and face recognition algorithms](#) (Phillips et al. [1]). The threshold (red horizontal line) is a value calibrated to give  $FMR = 0.0001$  on mugshot images. Points above the threshold correspond to pairs predicted to be genuine, and points below the threshold correspond to pairs predicted to be impostors. The figure shows whether the predicted class (genuine or impostor) matches the real class. Blue denotes a correct prediction, and red denotes incorrect. An "X" represents face detection failure in either of the images in the pair. Note that the sample size ( $n=20$ ) is small, and the figure may change substantially if larger or different sets are used. The images can be downloaded from the [Supplemental Information](#) page provided with that publication.

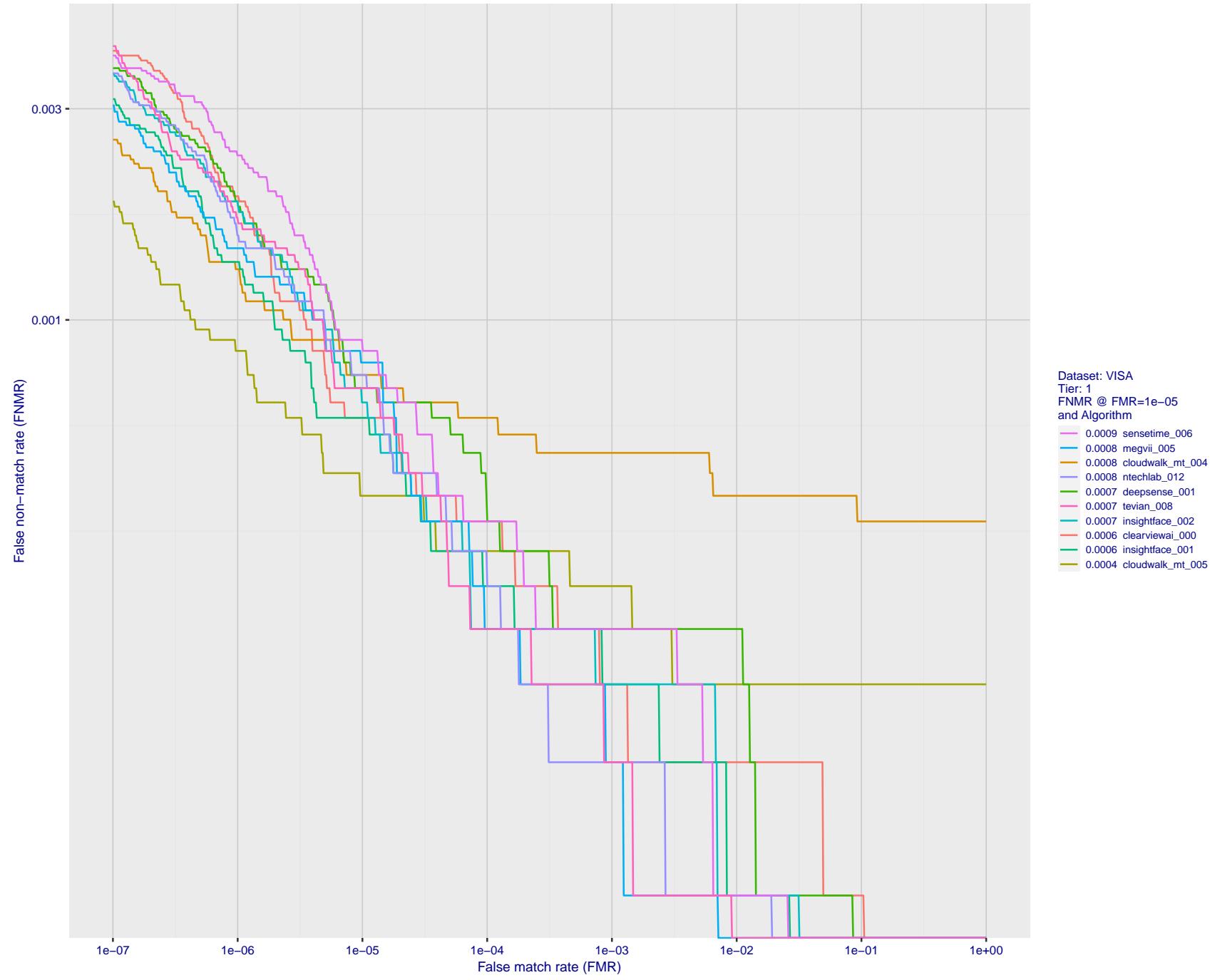


Figure 22: For the visa images, detection error tradeoff (DET) characteristics showing false non-match rate vs. false match rate plotted parametrically on threshold,  $T$ . The scales are logarithmic in order to show many decades of FMR.

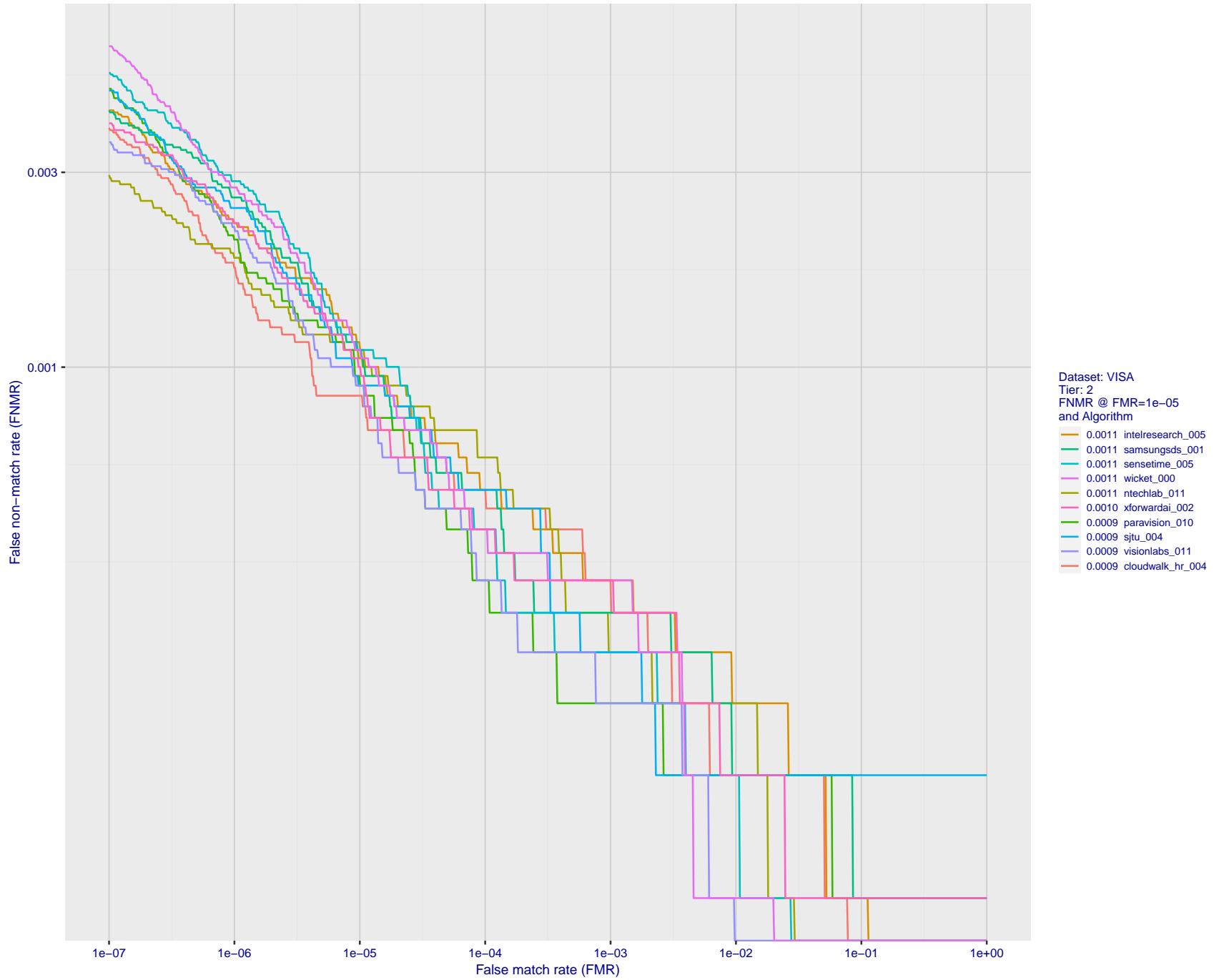


Figure 23: For the visa images, detection error tradeoff (DET) characteristics showing false non-match rate vs. false match rate plotted parametrically on threshold,  $T$ . The scales are logarithmic in order to show many decades of FMR.

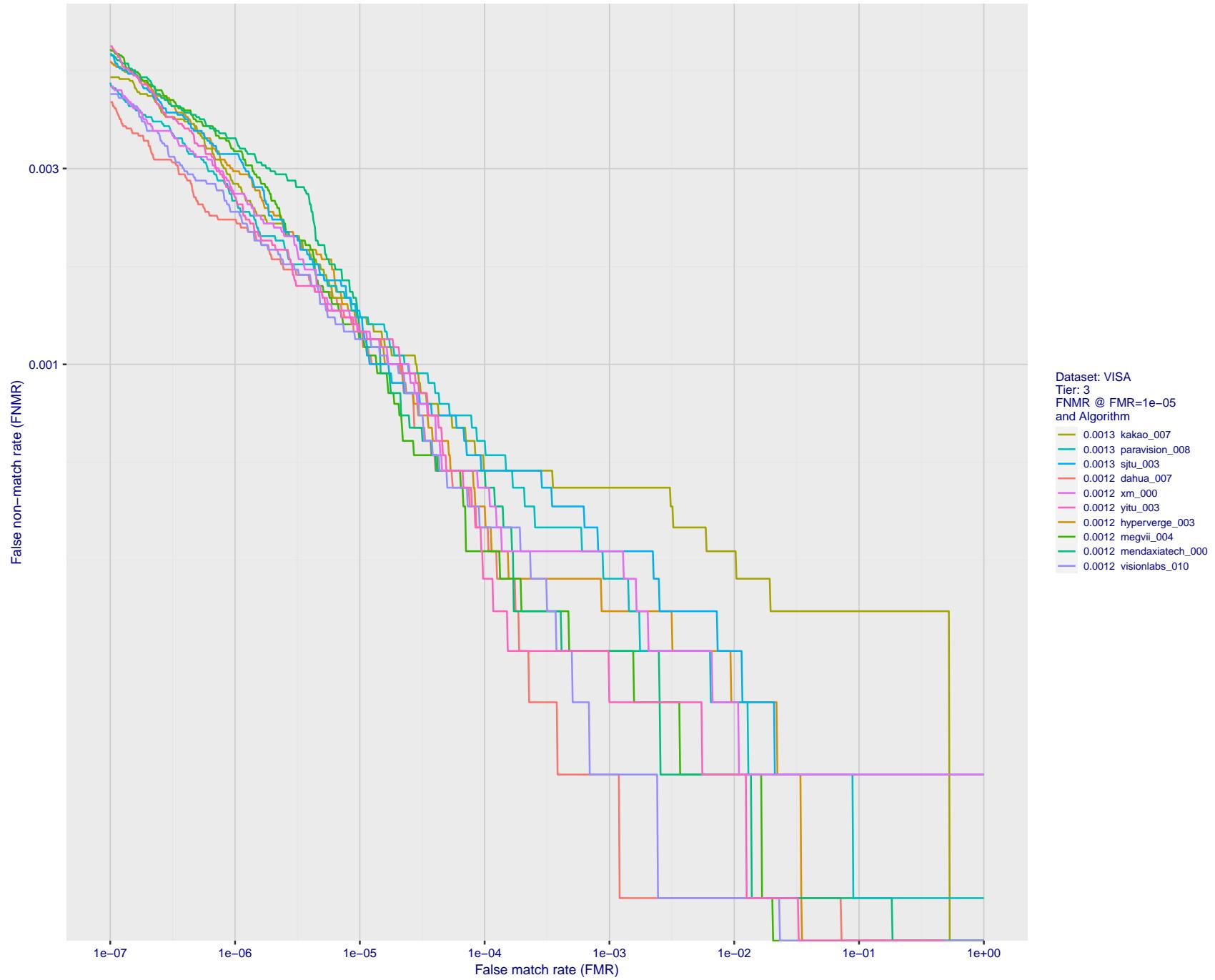


Figure 24: For the visa images, detection error tradeoff (DET) characteristics showing false non-match rate vs. false match rate plotted parametrically on threshold,  $T$ . The scales are logarithmic in order to show many decades of FMR.

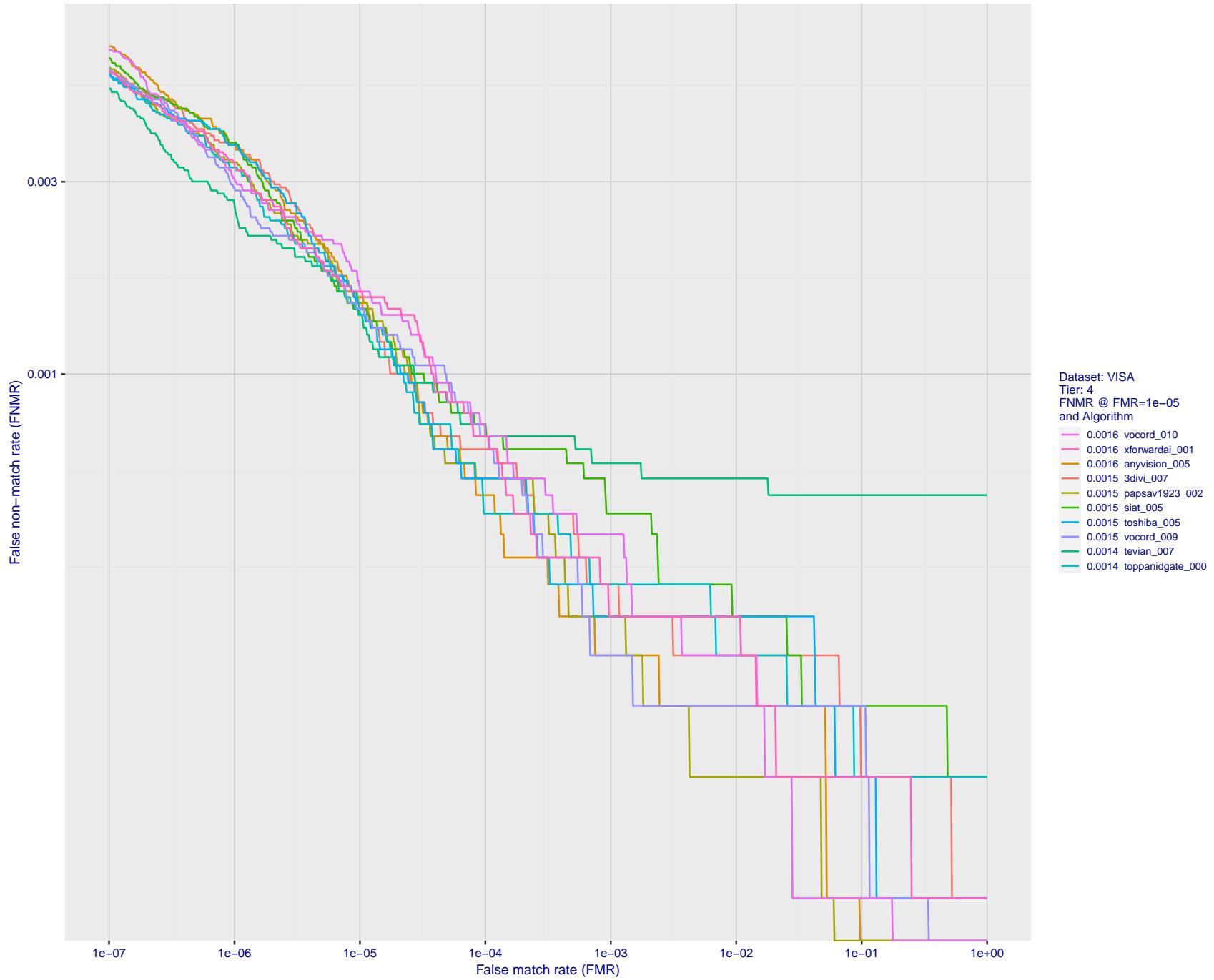


Figure 25: For the visa images, detection error tradeoff (DET) characteristics showing false non-match rate vs. false match rate plotted parametrically on threshold,  $T$ . The scales are logarithmic in order to show many decades of FMR.

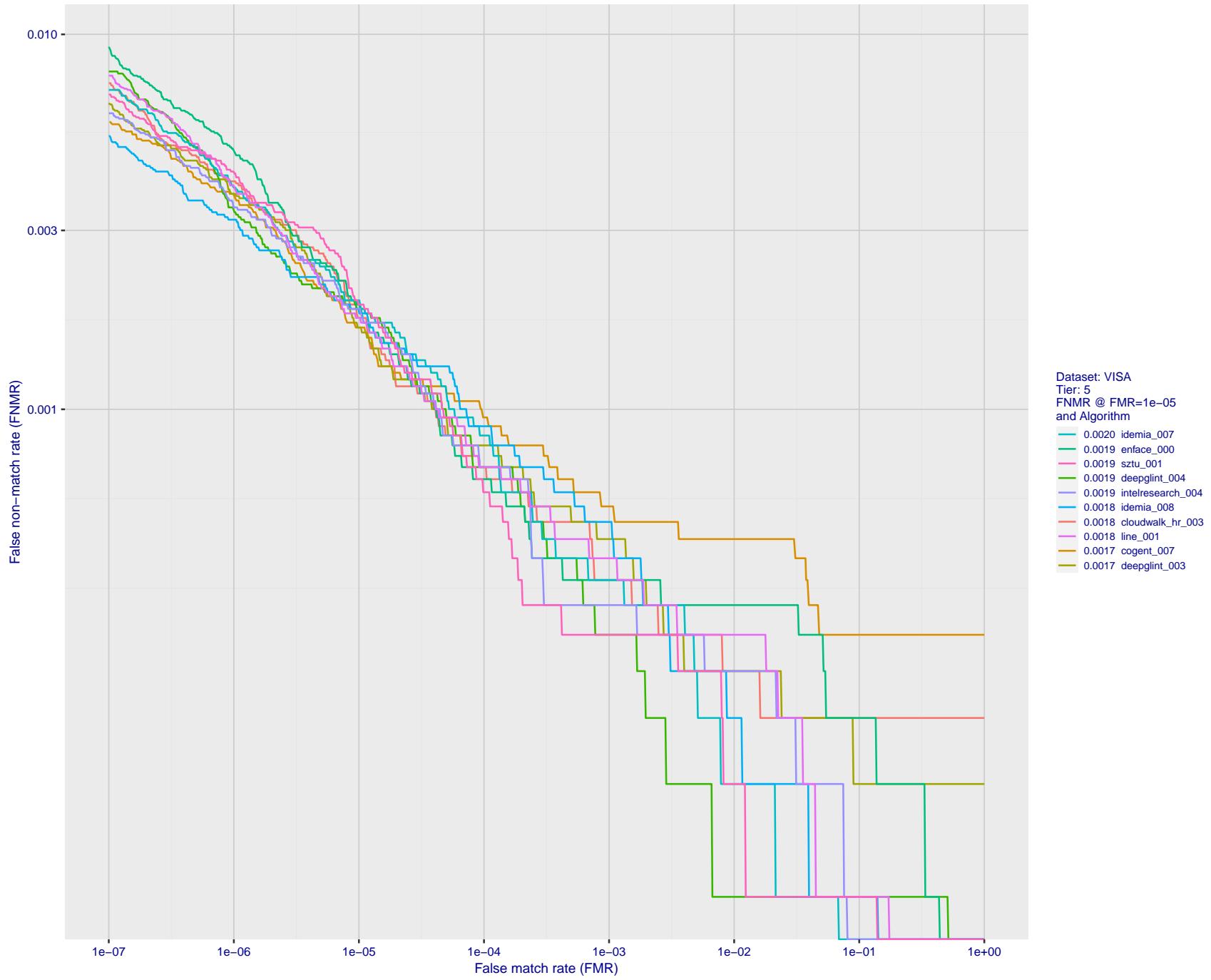


Figure 26: For the visa images, detection error tradeoff (DET) characteristics showing false non-match rate vs. false match rate plotted parametrically on threshold,  $T$ . The scales are logarithmic in order to show many decades of FMR.

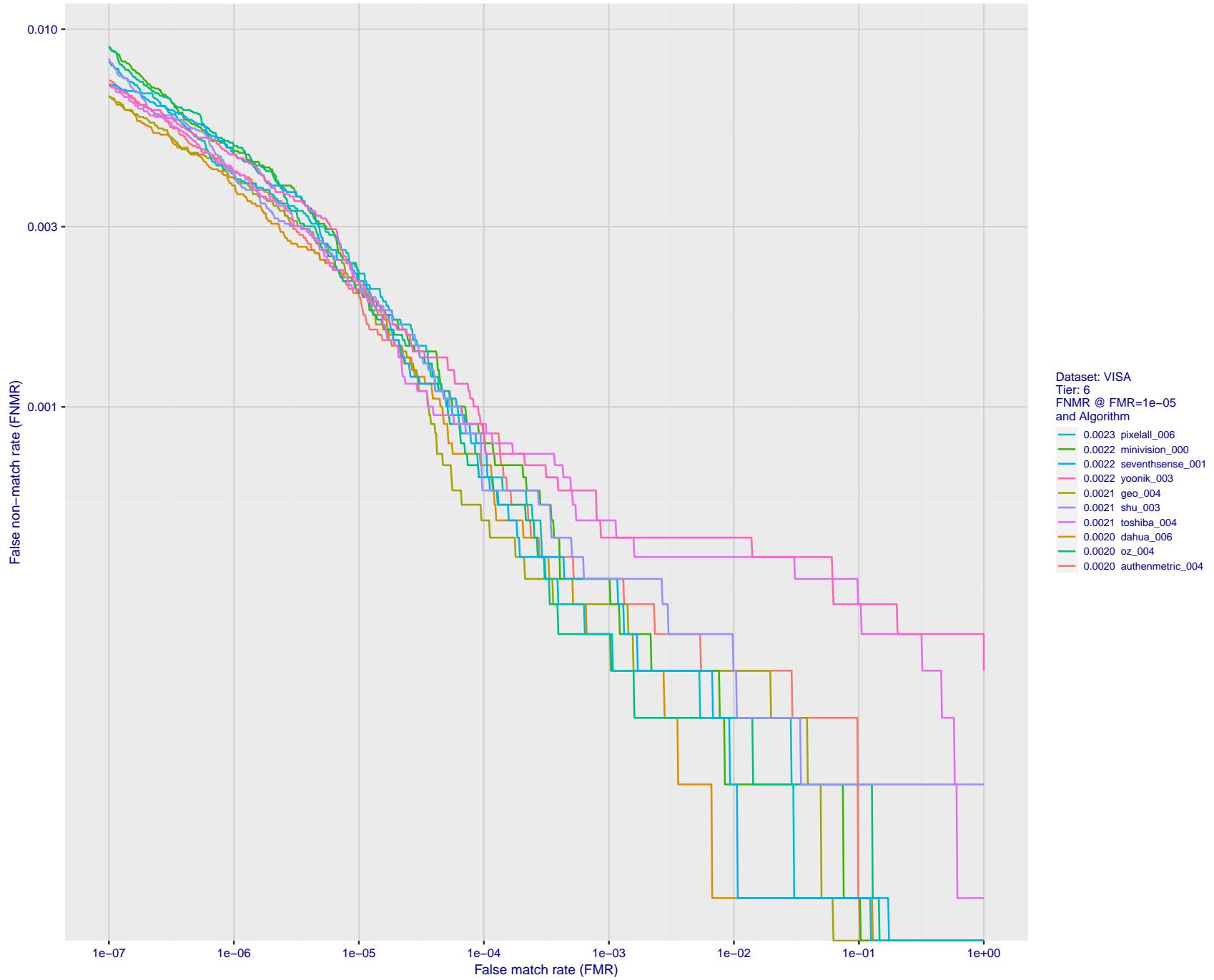


Figure 27: For the visa images, detection error tradeoff (DET) characteristics showing false non-match rate vs. false match rate plotted parametrically on threshold,  $T$ . The scales are logarithmic in order to show many decades of FMR.

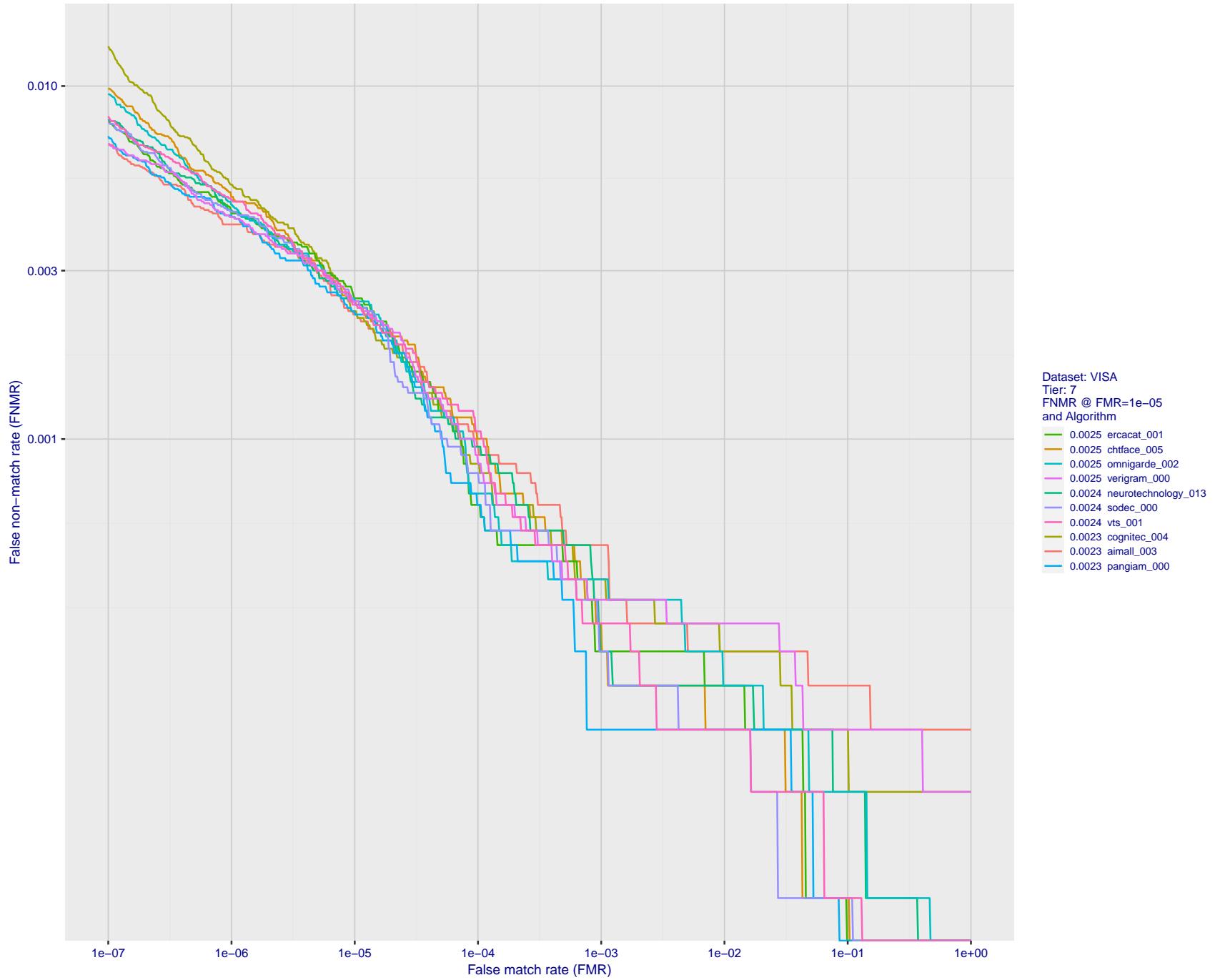


Figure 28: For the visa images, detection error tradeoff (DET) characteristics showing false non-match rate vs. false match rate plotted parametrically on threshold,  $T$ . The scales are logarithmic in order to show many decades of FMR.

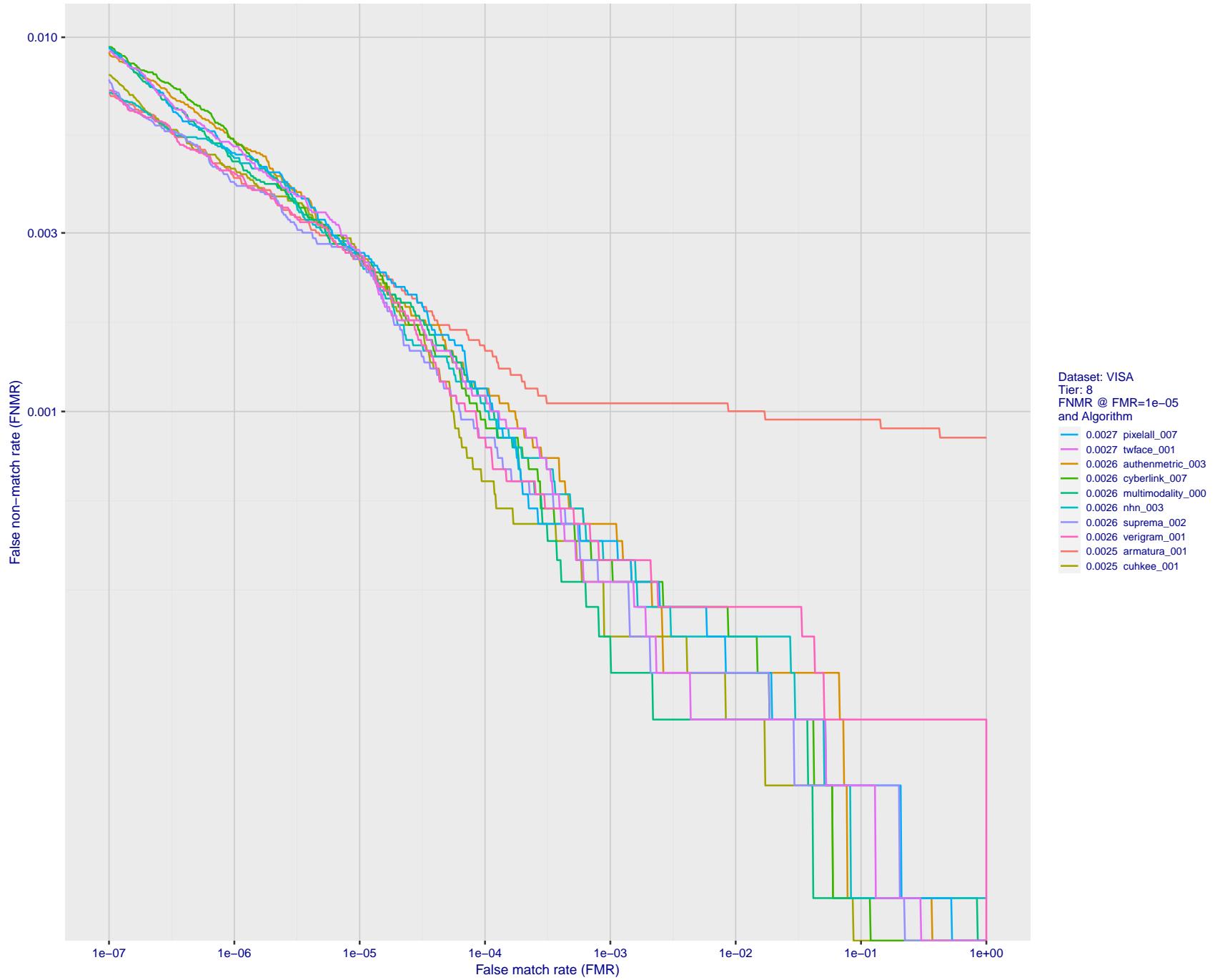


Figure 29: For the visa images, detection error tradeoff (DET) characteristics showing false non-match rate vs. false match rate plotted parametrically on threshold,  $T$ . The scales are logarithmic in order to show many decades of FMR.

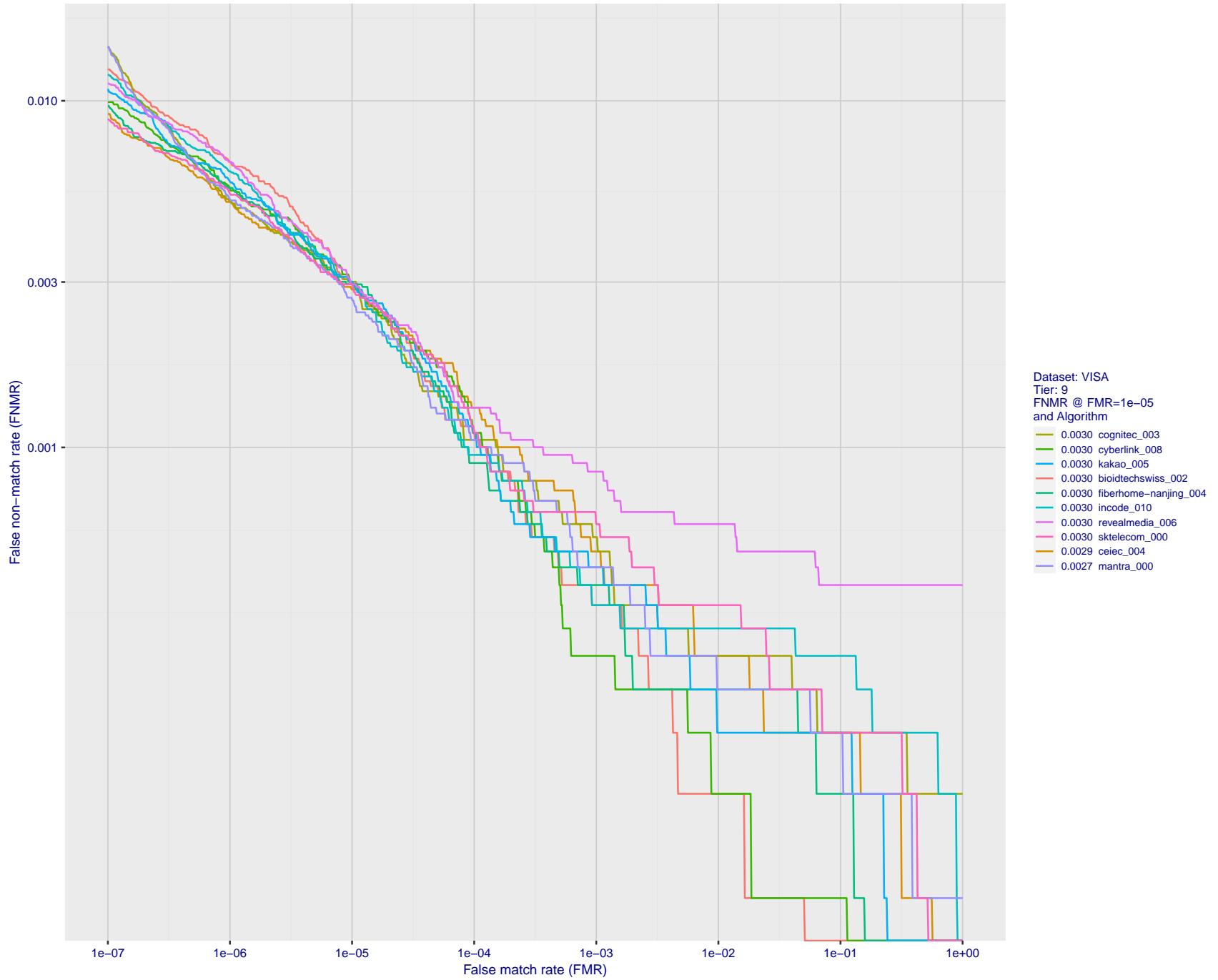


Figure 30: For the visa images, detection error tradeoff (DET) characteristics showing false non-match rate vs. false match rate plotted parametrically on threshold,  $T$ . The scales are logarithmic in order to show many decades of FMR.

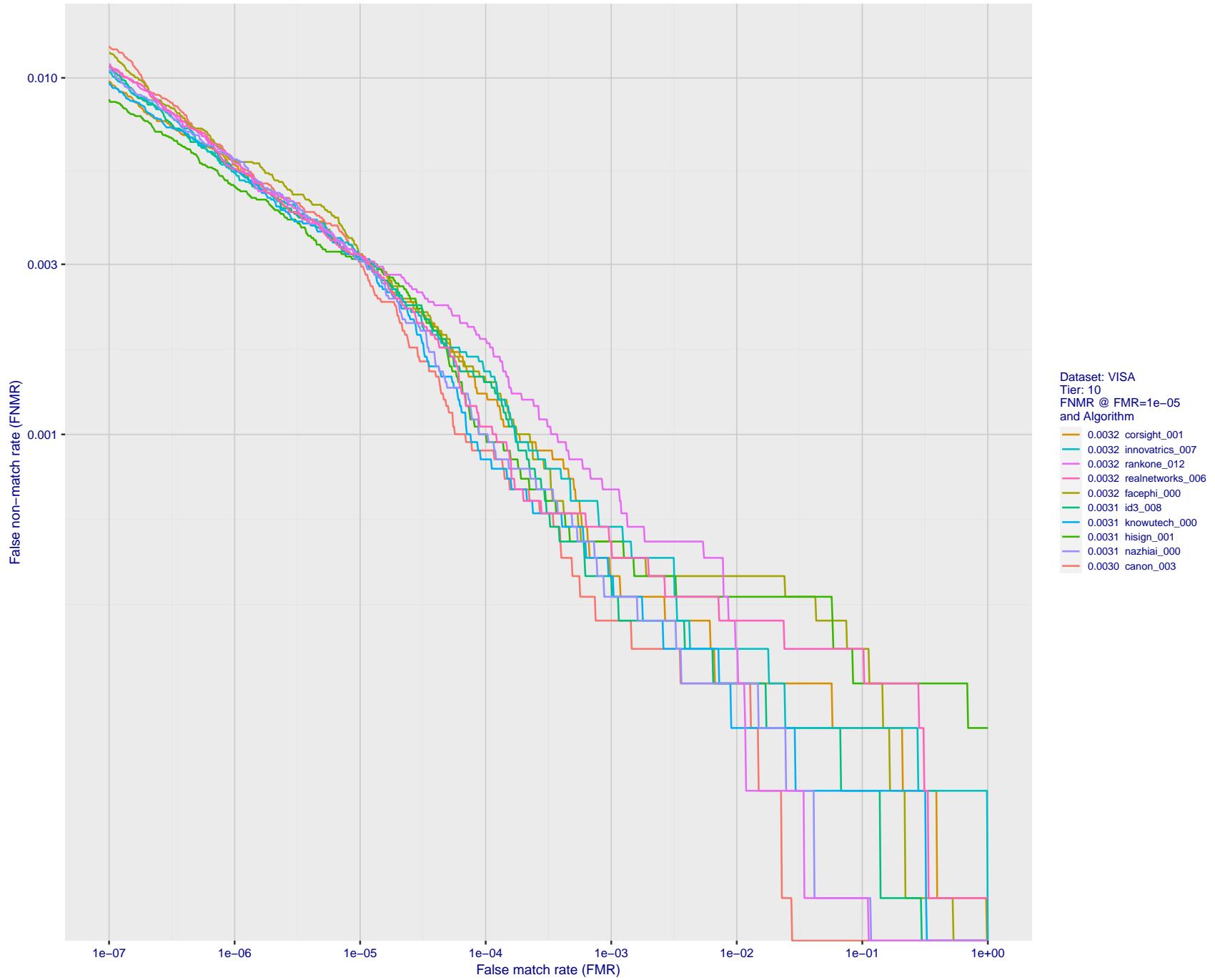


Figure 31: For the visa images, detection error tradeoff (DET) characteristics showing false non-match rate vs. false match rate plotted parametrically on threshold,  $T$ . The scales are logarithmic in order to show many decades of FMR.

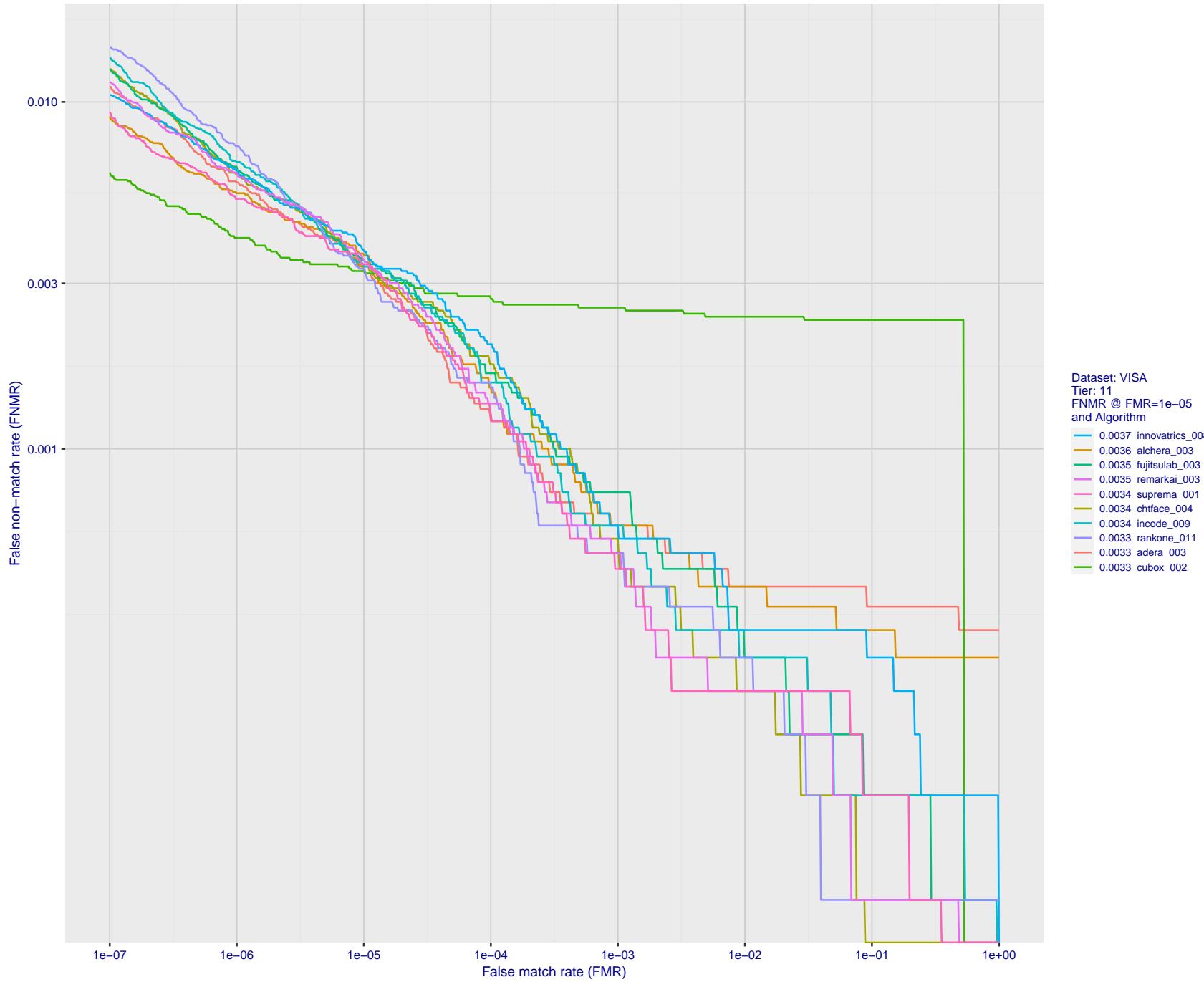


Figure 32: For the visa images, detection error tradeoff (DET) characteristics showing false non-match rate vs. false match rate plotted parametrically on threshold,  $T$ . The scales are logarithmic in order to show many decades of FMR.

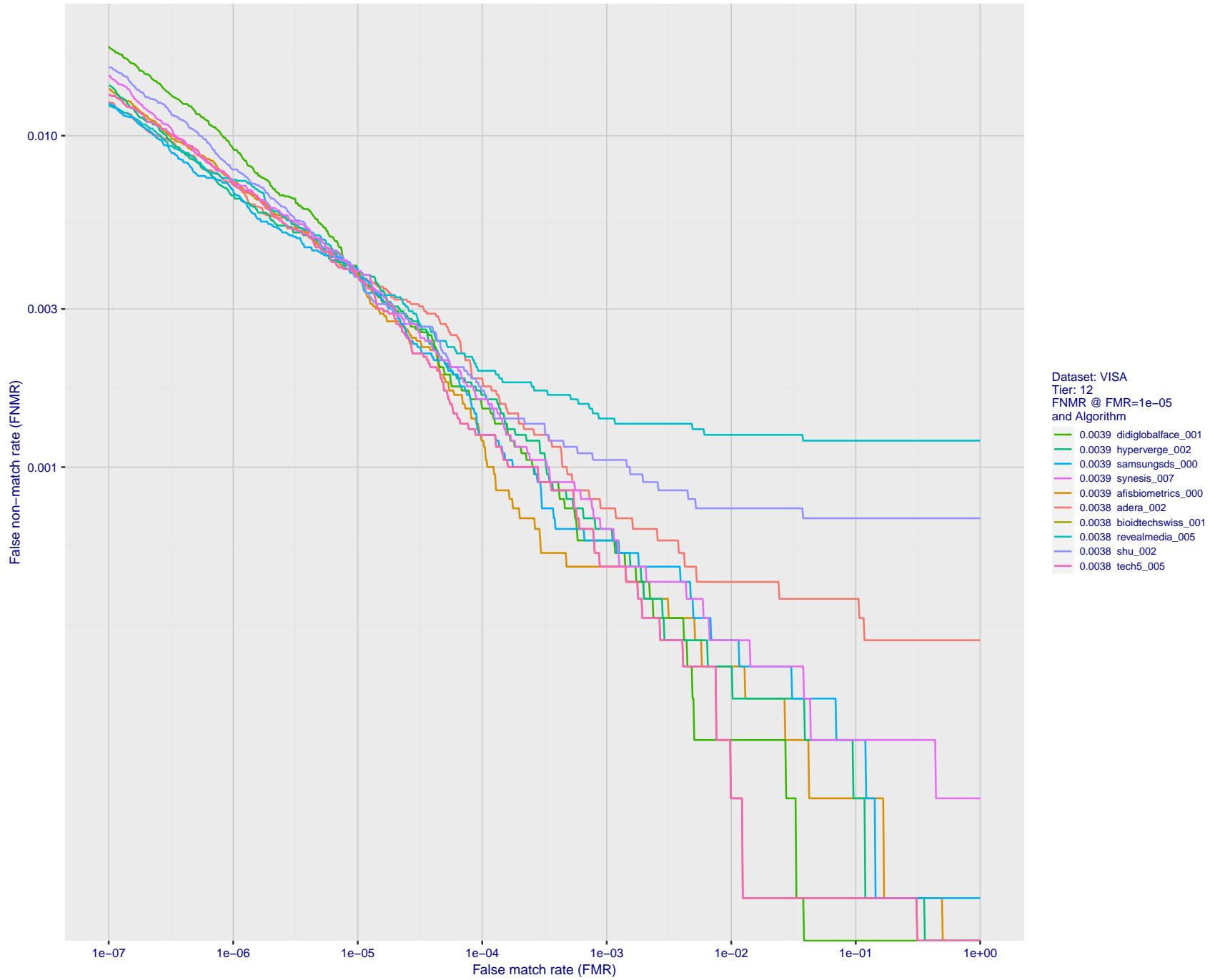


Figure 33: For the visa images, detection error tradeoff (DET) characteristics showing false non-match rate vs. false match rate plotted parametrically on threshold,  $T$ . The scales are logarithmic in order to show many decades of FMR.

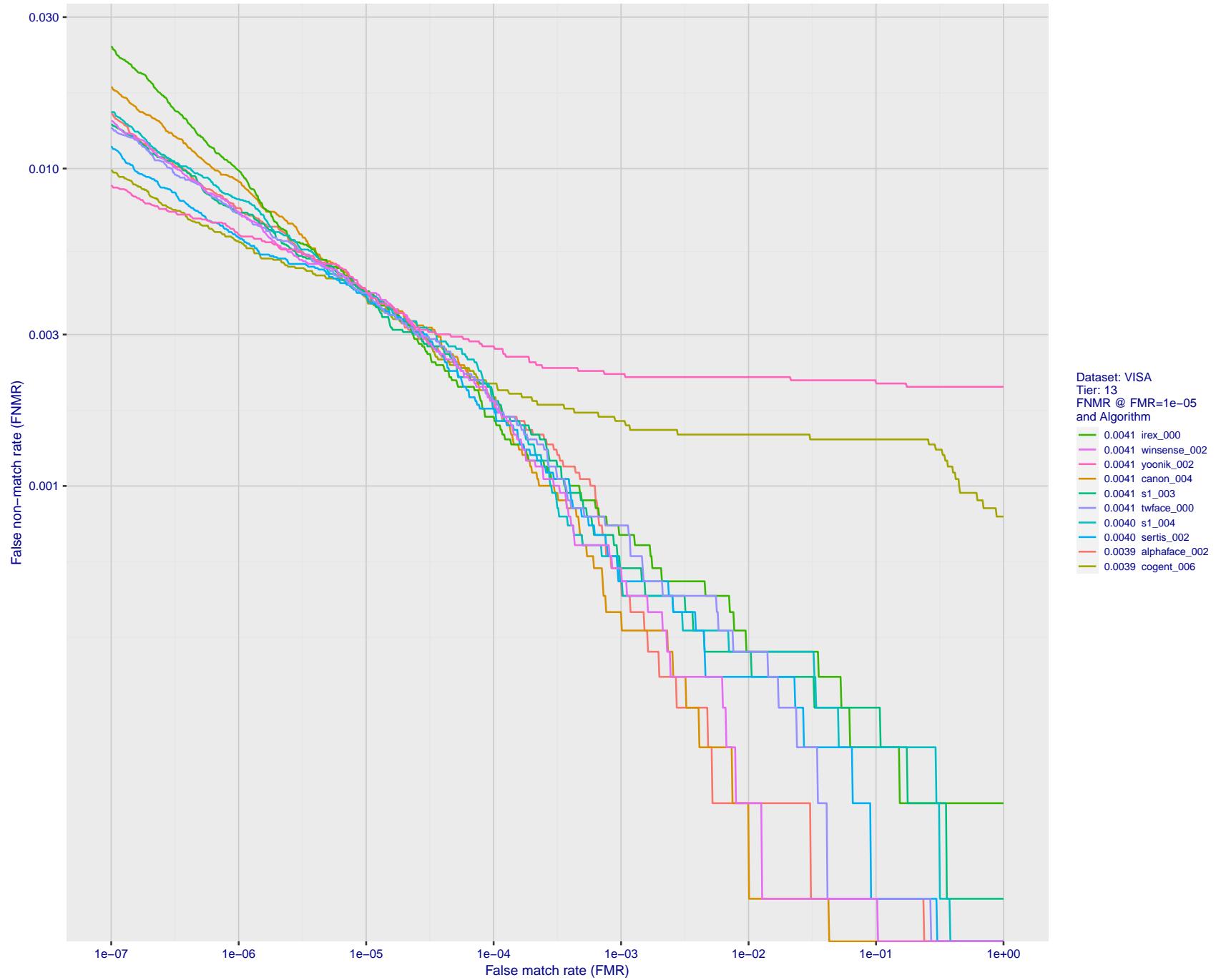


Figure 34: For the visa images, detection error tradeoff (DET) characteristics showing false non-match rate vs. false match rate plotted parametrically on threshold,  $T$ . The scales are logarithmic in order to show many decades of FMR.

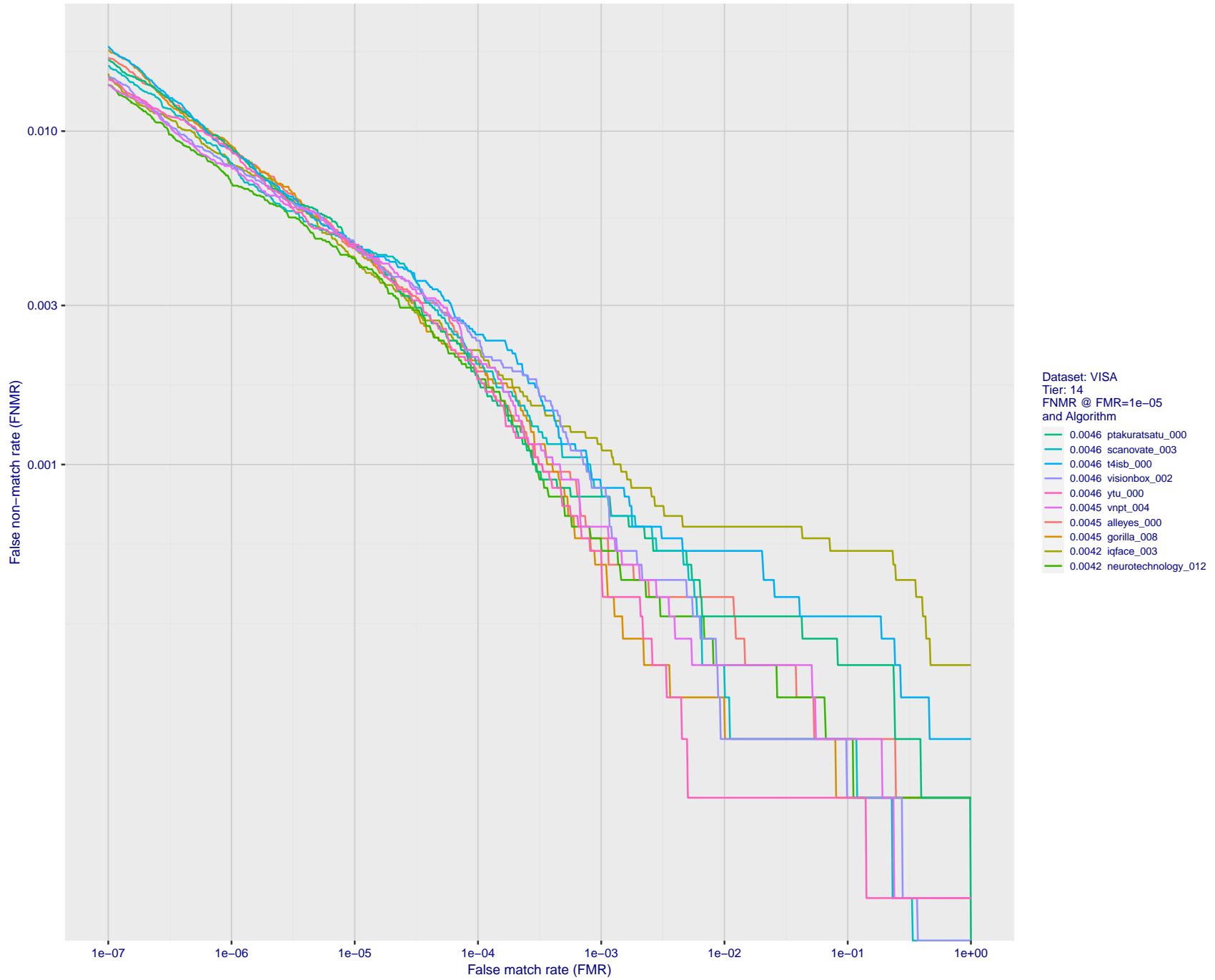


Figure 35: For the visa images, detection error tradeoff (DET) characteristics showing false non-match rate vs. false match rate plotted parametrically on threshold,  $T$ . The scales are logarithmic in order to show many decades of FMR.

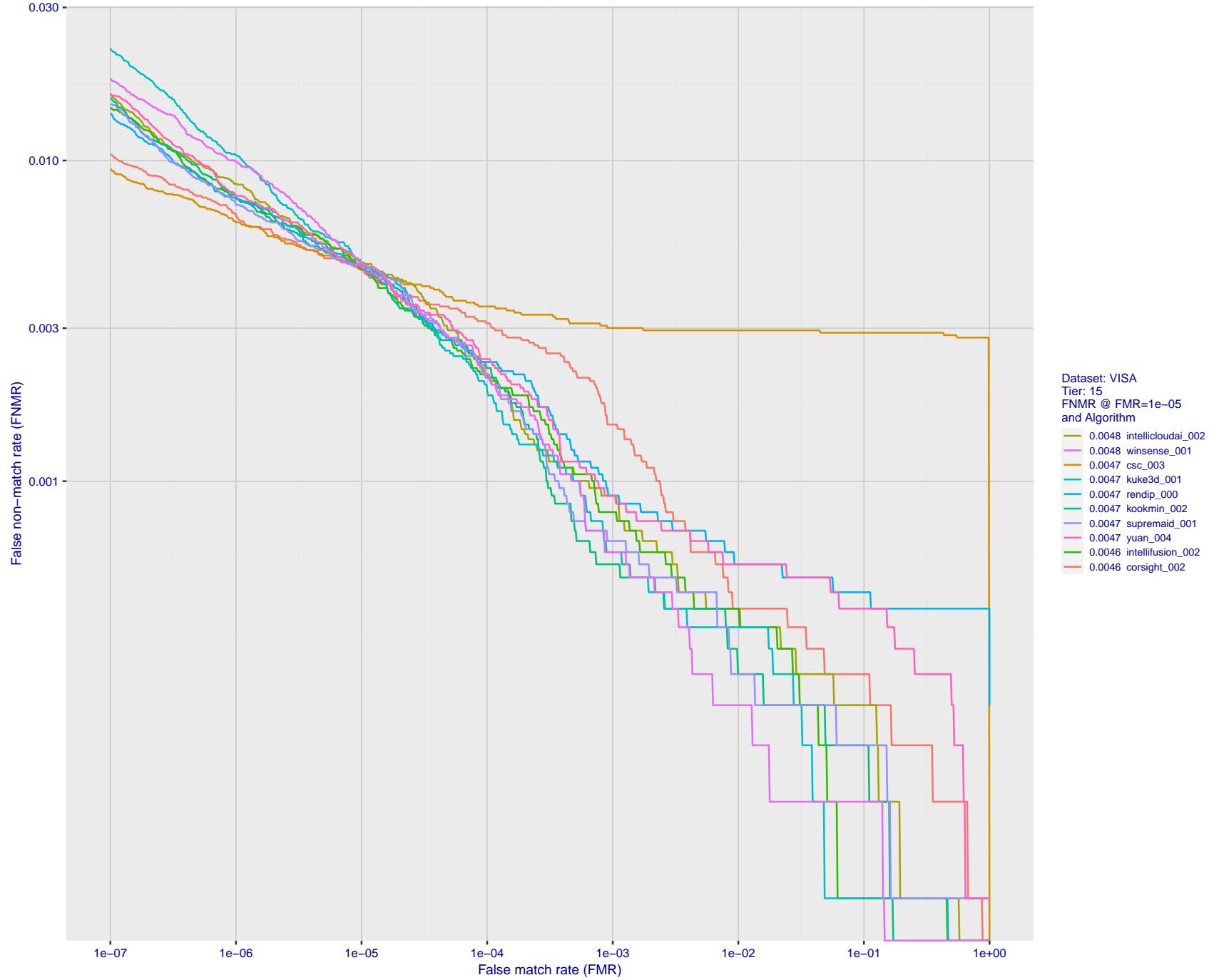


Figure 36: For the visa images, detection error tradeoff (DET) characteristics showing false non-match rate vs. false match rate plotted parametrically on threshold,  $T$ . The scales are logarithmic in order to show many decades of FMR.

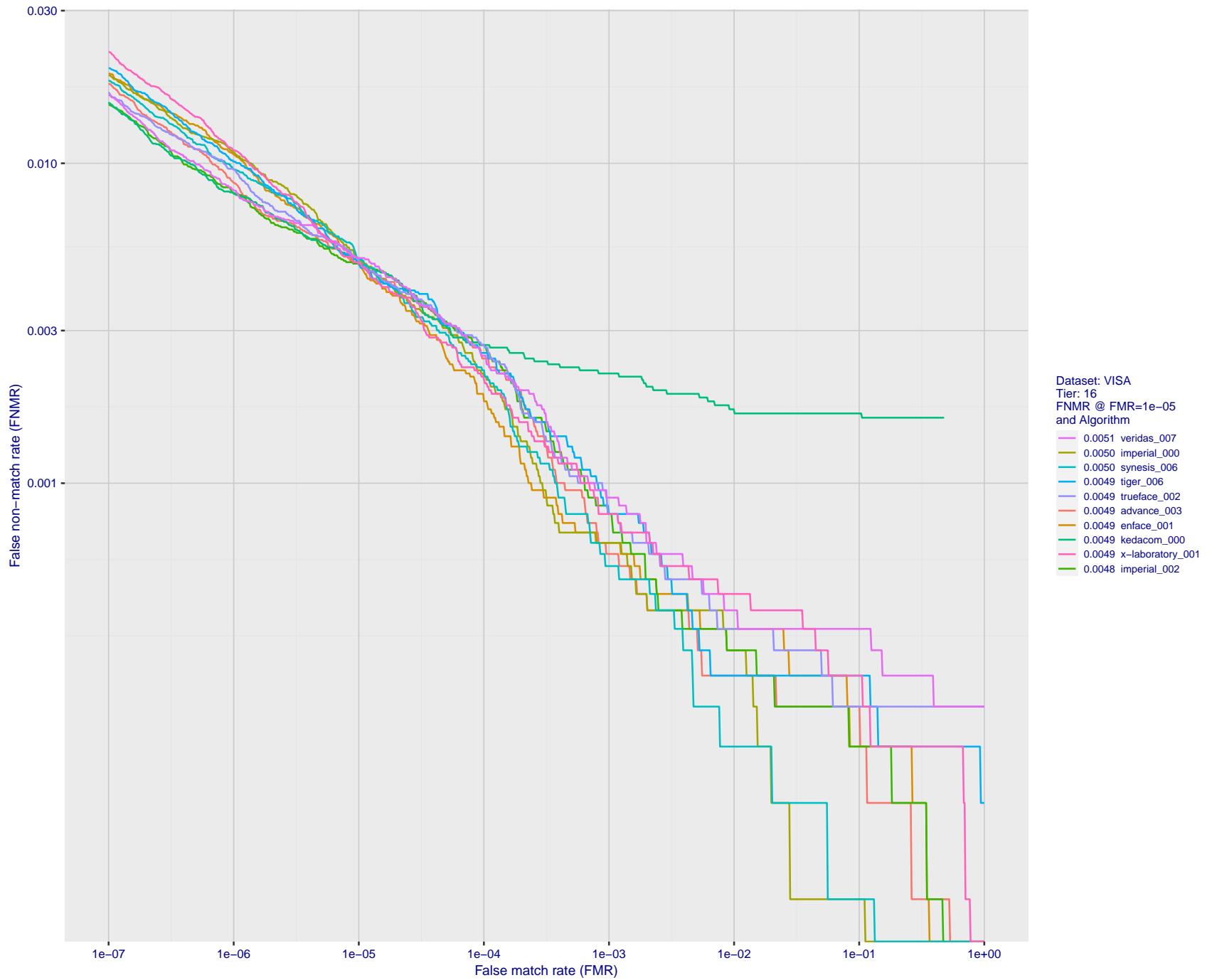


Figure 37: For the visa images, detection error tradeoff (DET) characteristics showing false non-match rate vs. false match rate plotted parametrically on threshold,  $T$ . The scales are logarithmic in order to show many decades of FMR.

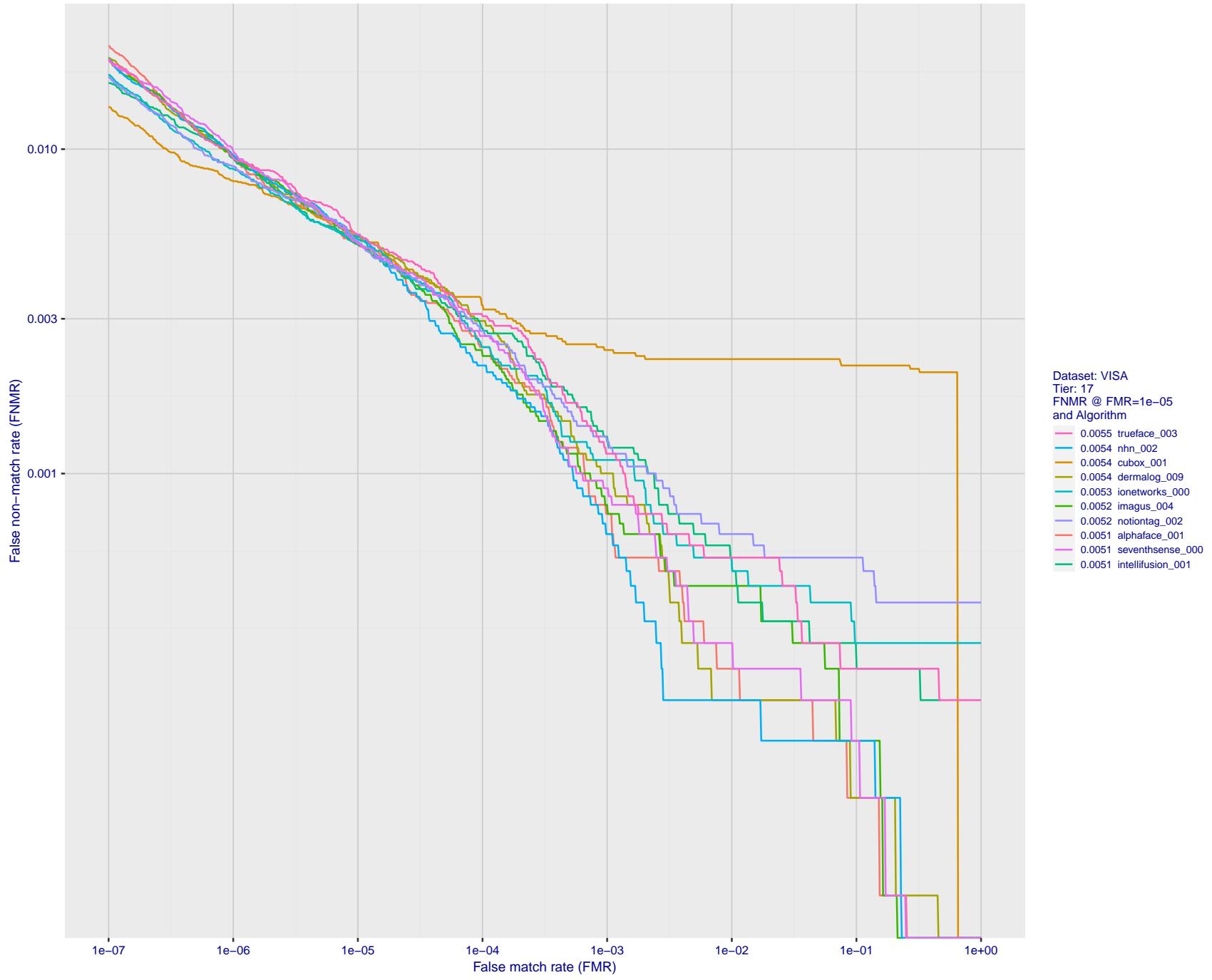


Figure 38: For the visa images, detection error tradeoff (DET) characteristics showing false non-match rate vs. false match rate plotted parametrically on threshold,  $T$ . The scales are logarithmic in order to show many decades of FMR.

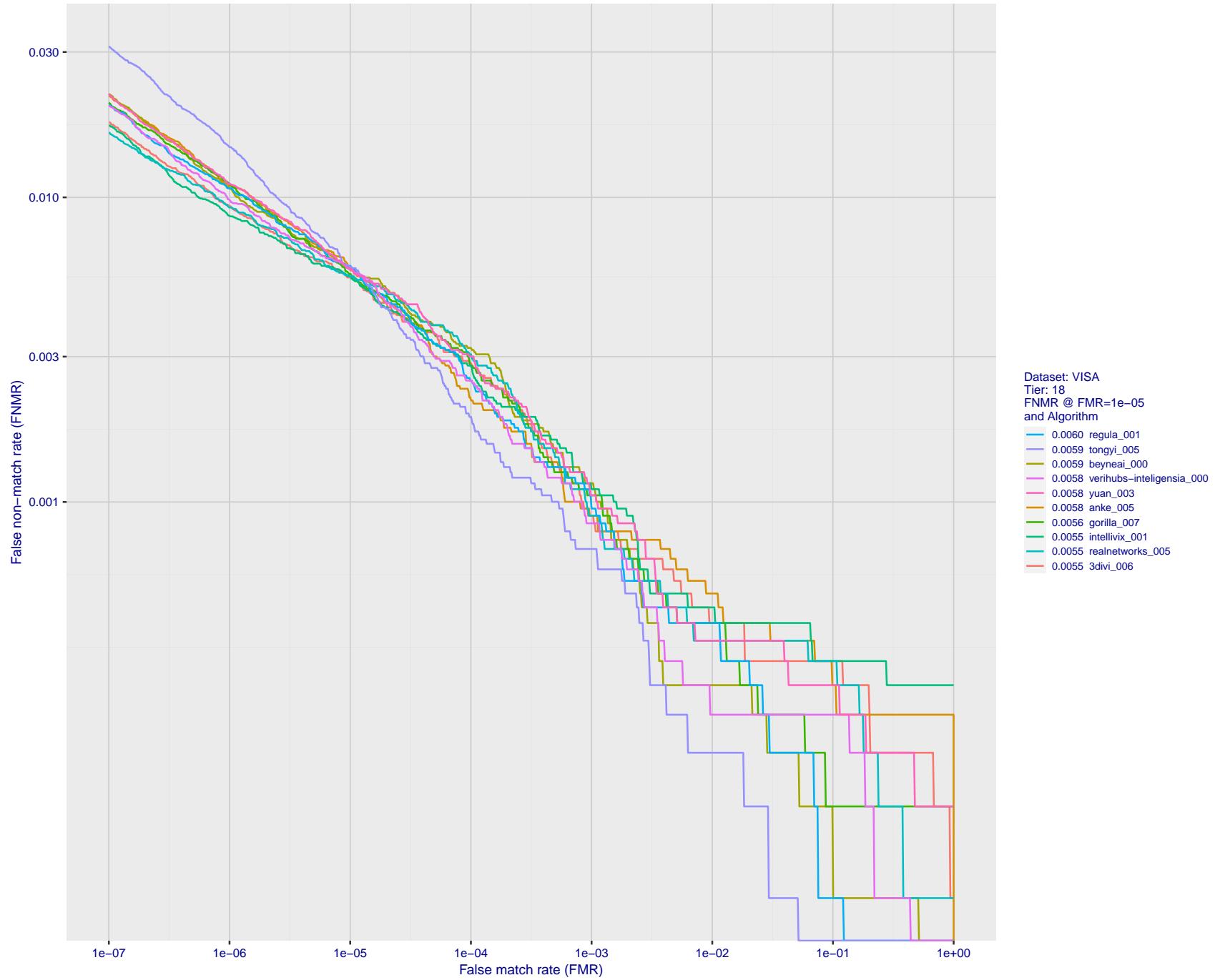


Figure 39: For the visa images, detection error tradeoff (DET) characteristics showing false non-match rate vs. false match rate plotted parametrically on threshold,  $T$ . The scales are logarithmic in order to show many decades of FMR.

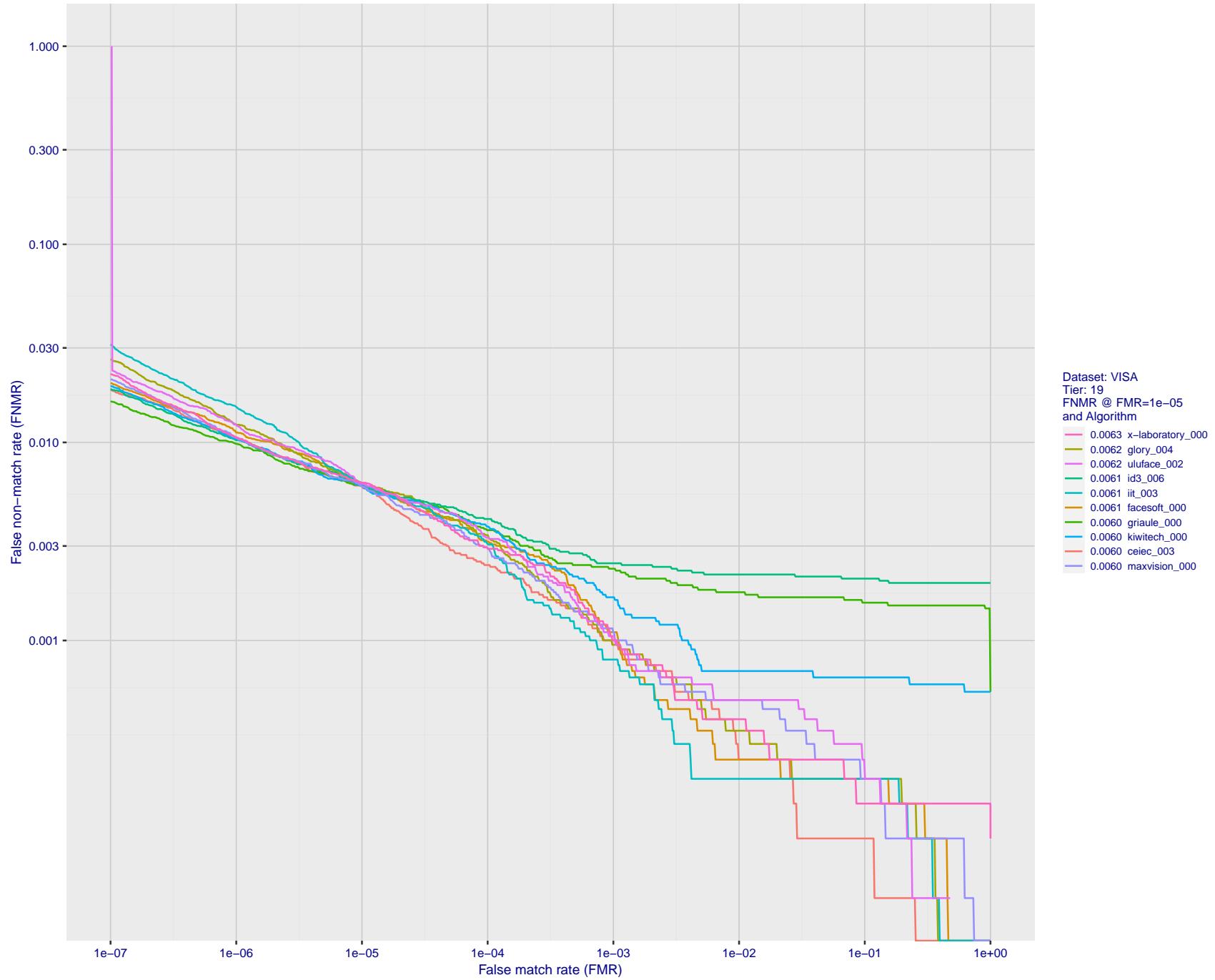


Figure 40: For the visa images, detection error tradeoff (DET) characteristics showing false non-match rate vs. false match rate plotted parametrically on threshold,  $T$ . The scales are logarithmic in order to show many decades of FMR.

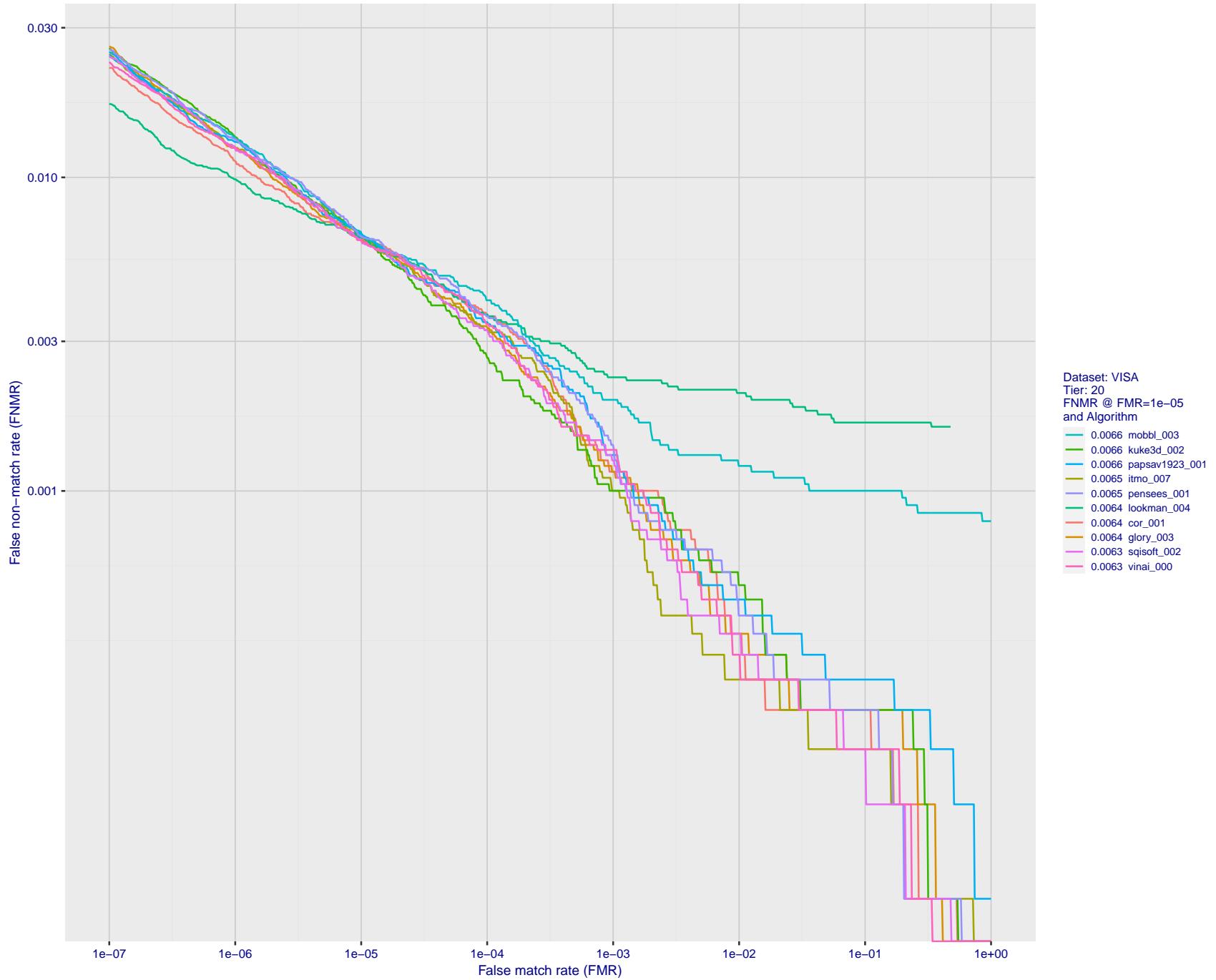


Figure 41: For the visa images, detection error tradeoff (DET) characteristics showing false non-match rate vs. false match rate plotted parametrically on threshold,  $T$ . The scales are logarithmic in order to show many decades of FMR.

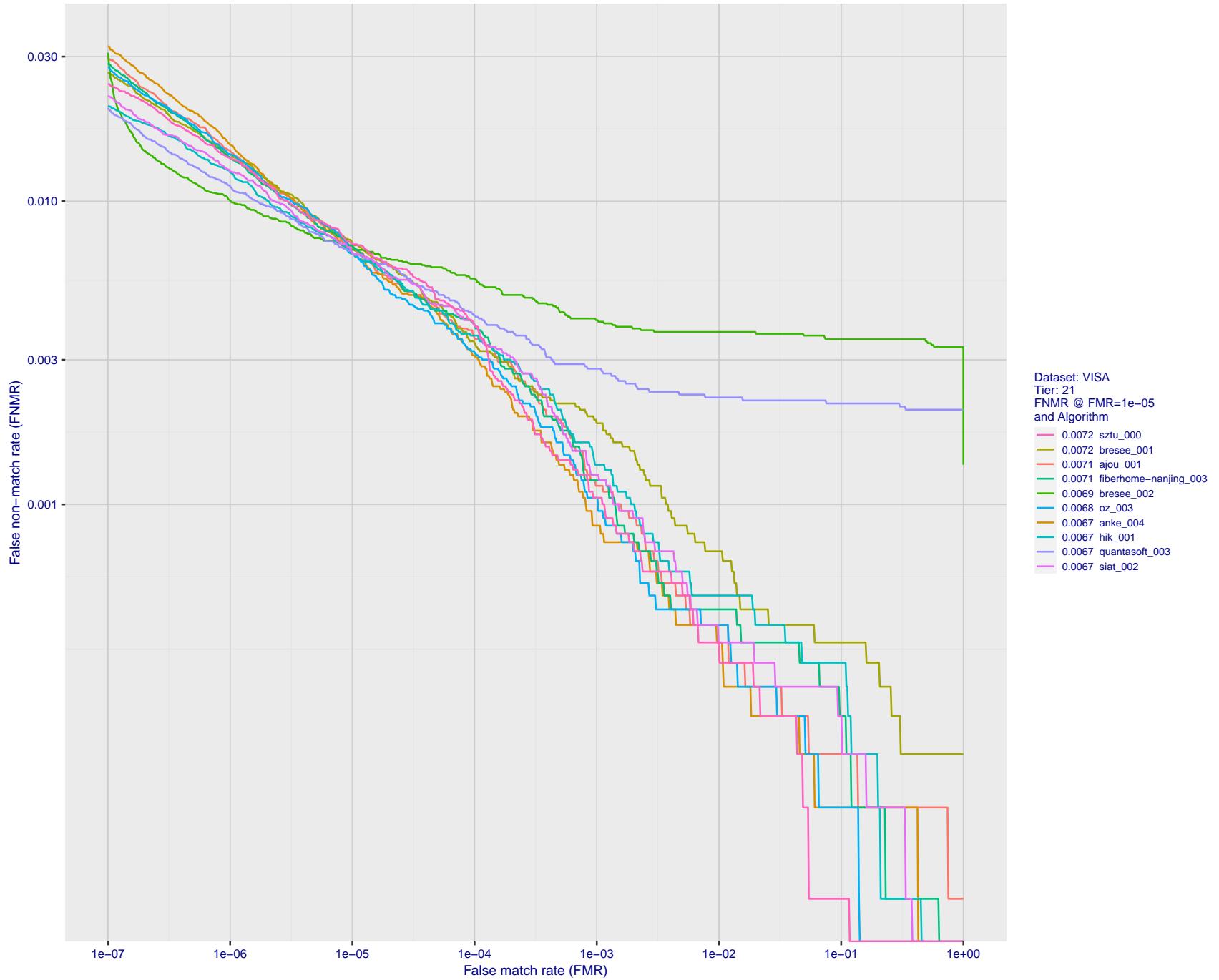


Figure 42: For the visa images, detection error tradeoff (DET) characteristics showing false non-match rate vs. false match rate plotted parametrically on threshold,  $T$ . The scales are logarithmic in order to show many decades of FMR.

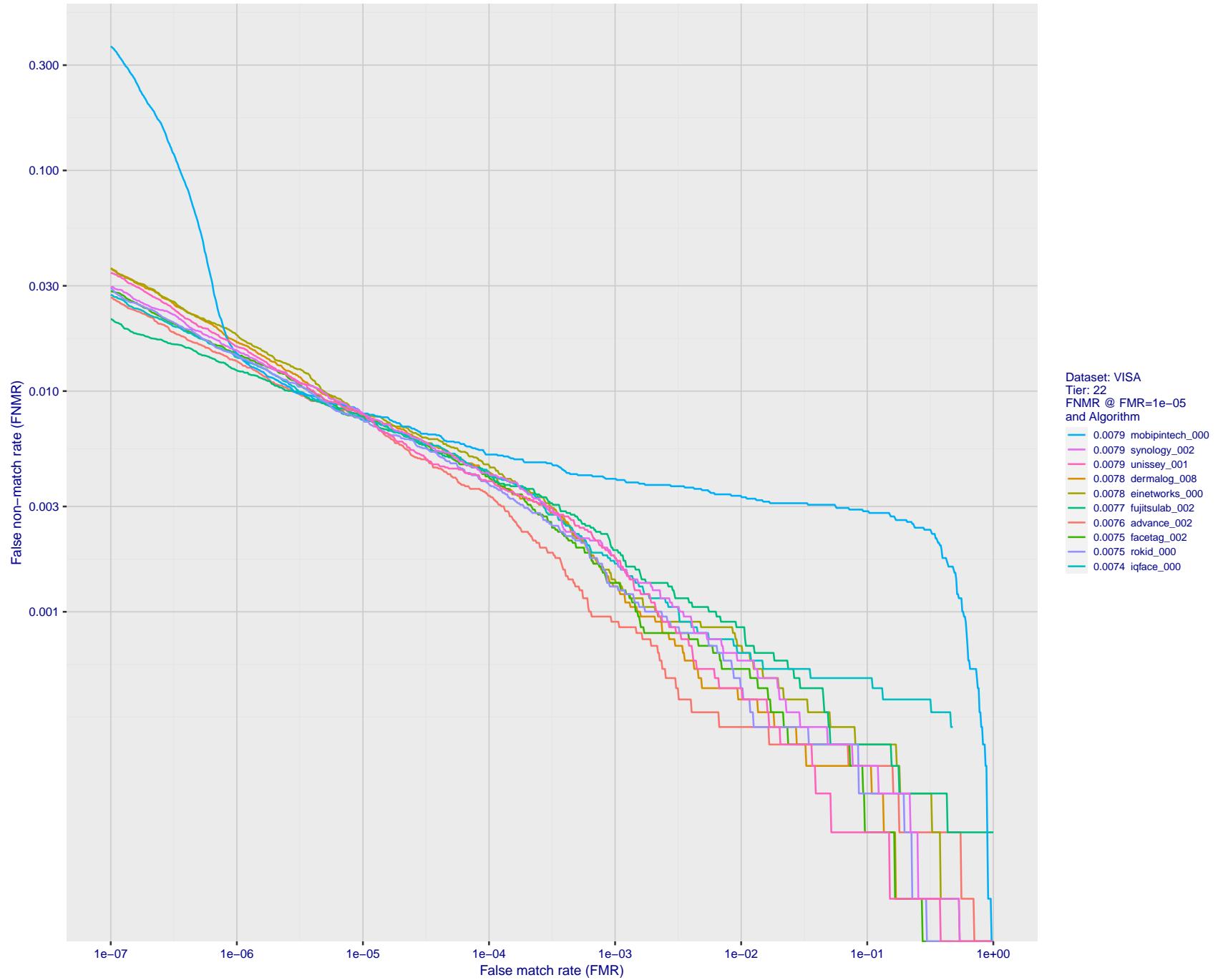


Figure 43: For the visa images, detection error tradeoff (DET) characteristics showing false non-match rate vs. false match rate plotted parametrically on threshold,  $T$ . The scales are logarithmic in order to show many decades of FMR.

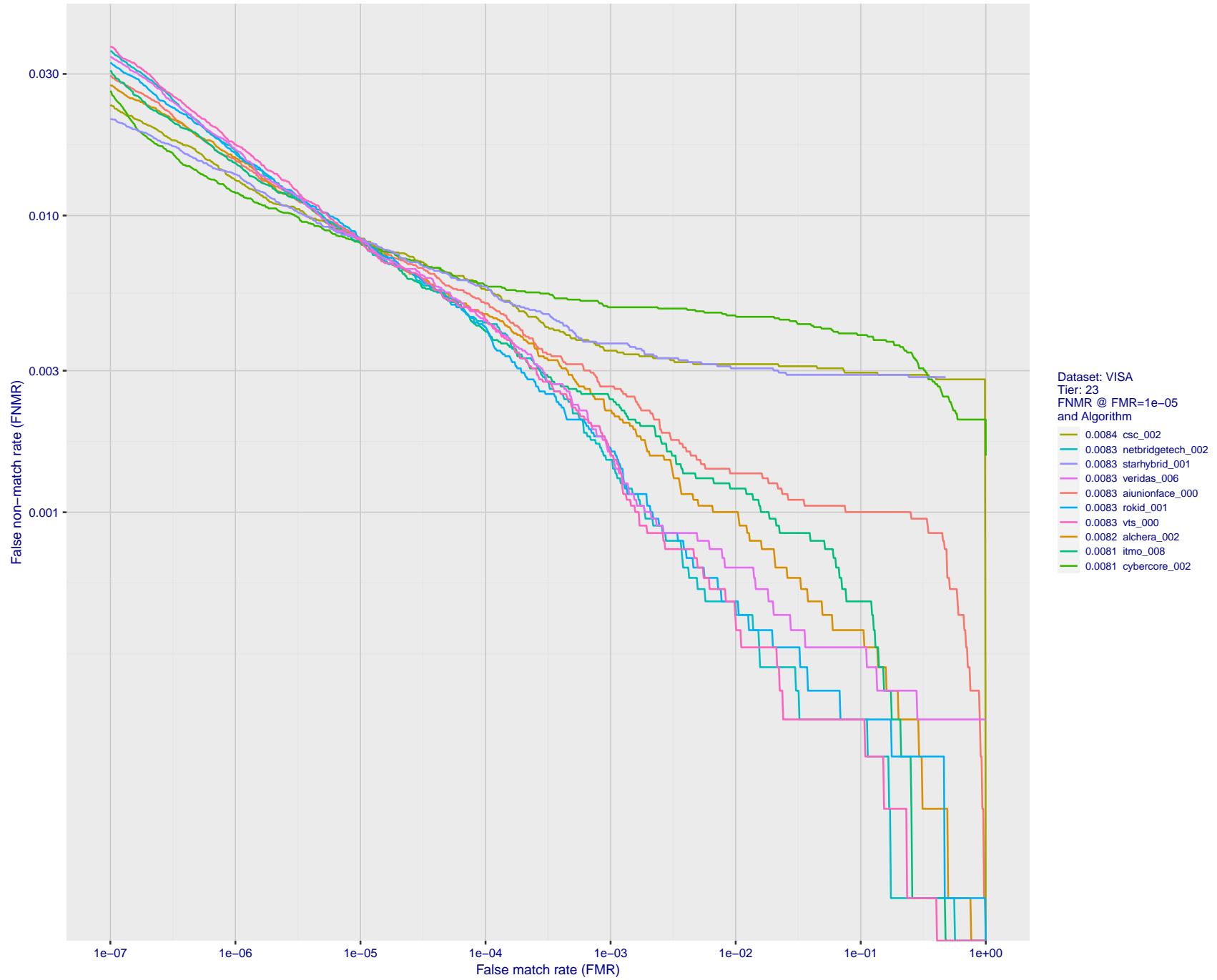


Figure 44: For the visa images, detection error tradeoff (DET) characteristics showing false non-match rate vs. false match rate plotted parametrically on threshold,  $T$ . The scales are logarithmic in order to show many decades of FMR.

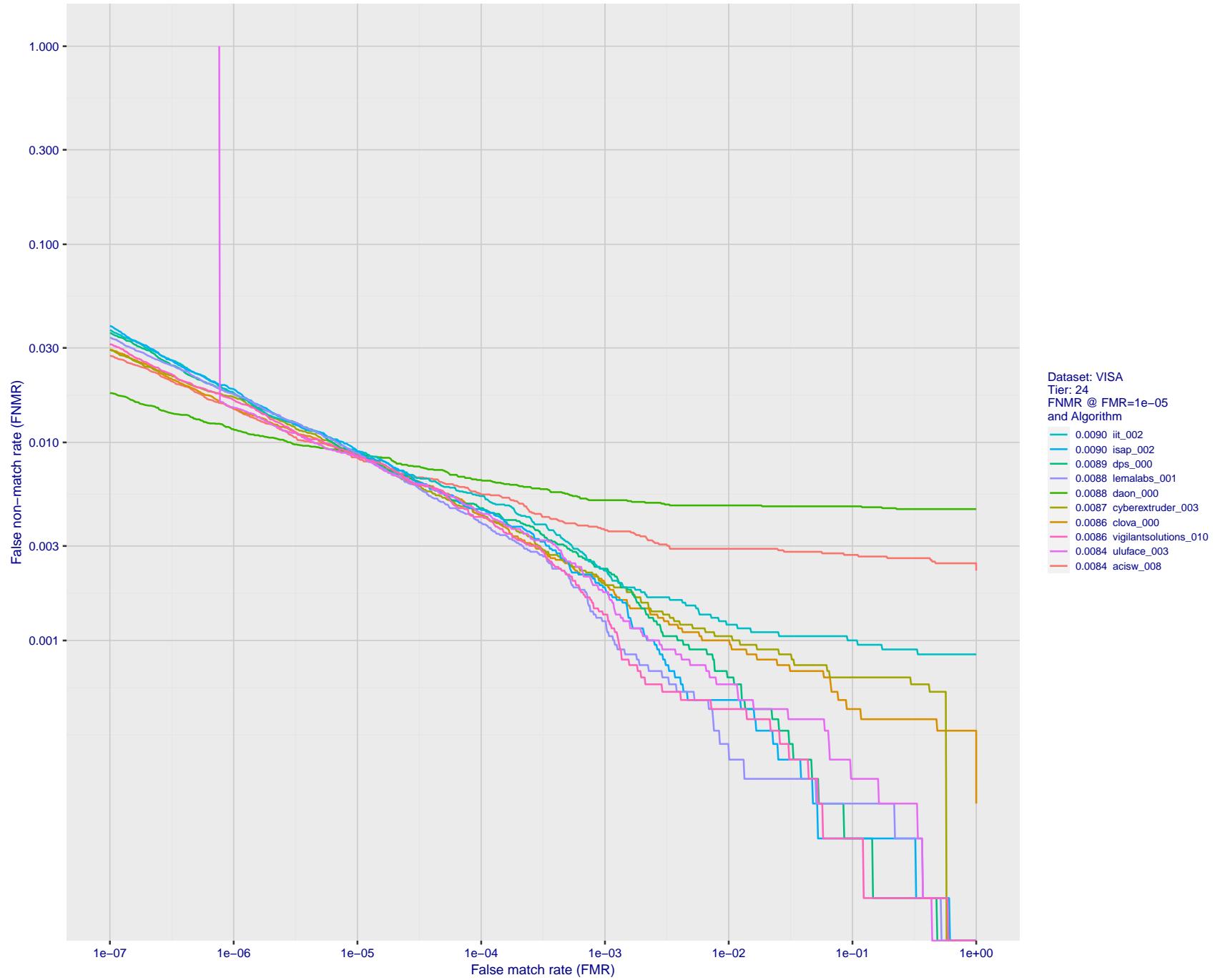


Figure 45: For the visa images, detection error tradeoff (DET) characteristics showing false non-match rate vs. false match rate plotted parametrically on threshold,  $T$ . The scales are logarithmic in order to show many decades of FMR.

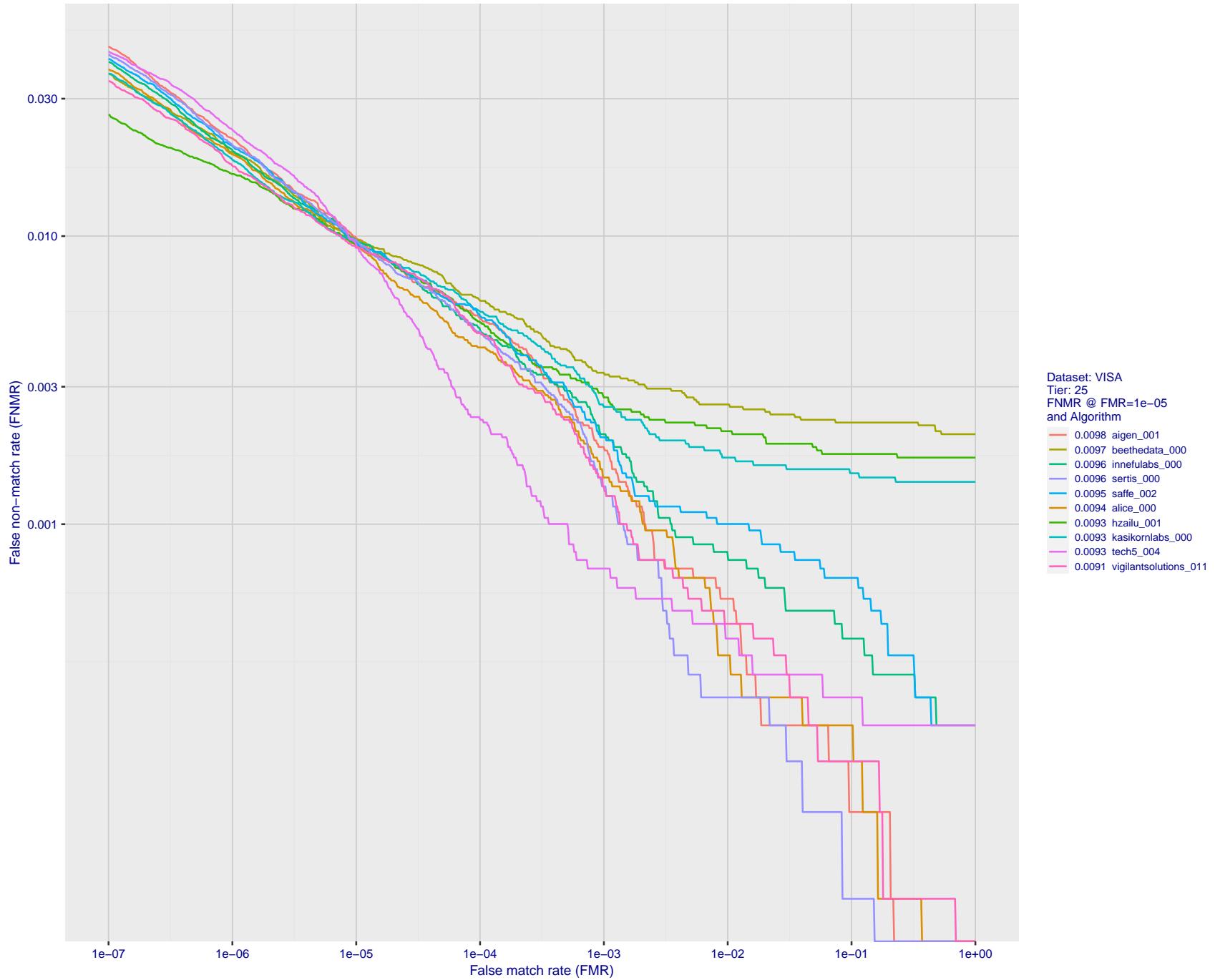


Figure 46: For the visa images, detection error tradeoff (DET) characteristics showing false non-match rate vs. false match rate plotted parametrically on threshold,  $T$ . The scales are logarithmic in order to show many decades of FMR.

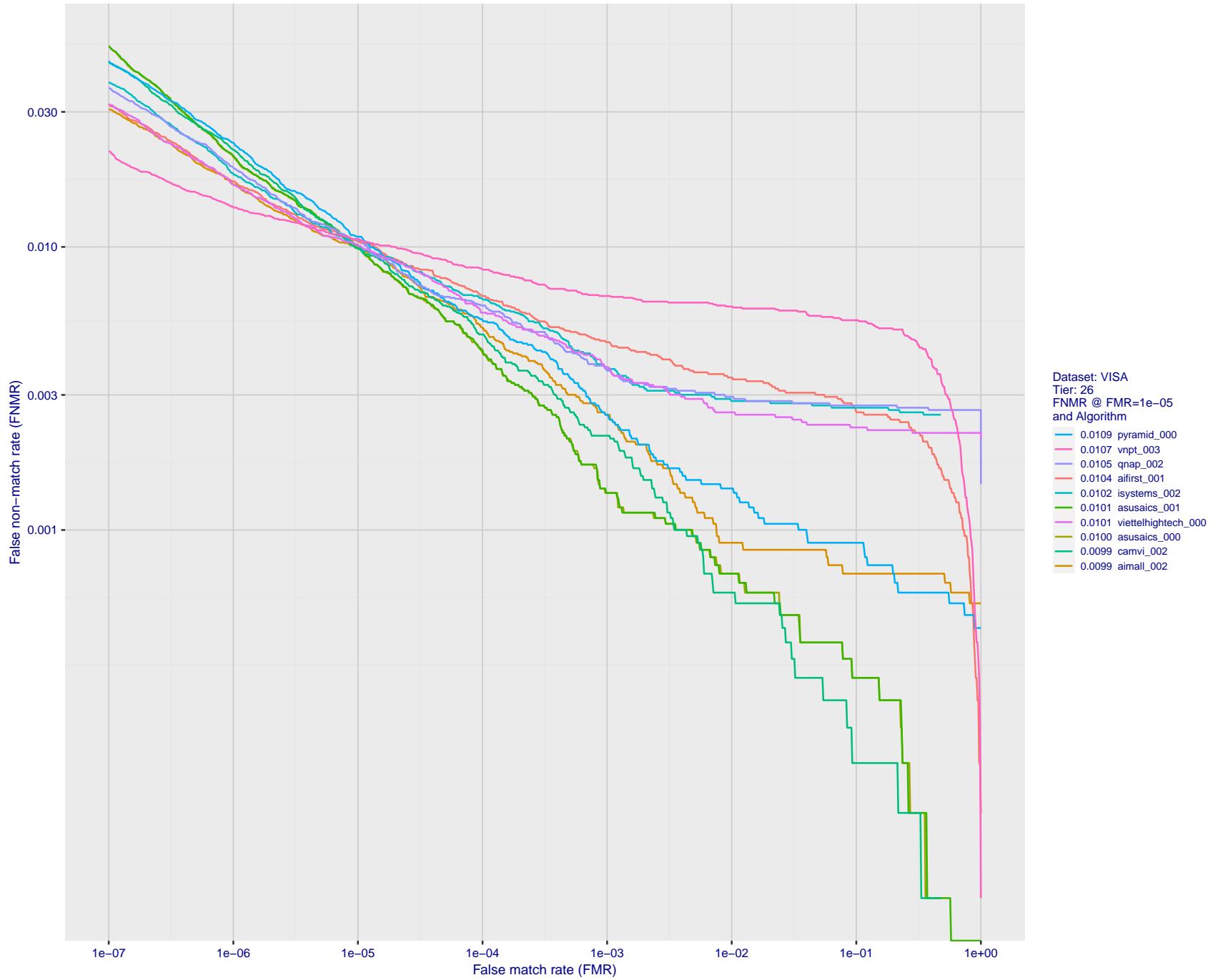


Figure 47: For the visa images, detection error tradeoff (DET) characteristics showing false non-match rate vs. false match rate plotted parametrically on threshold,  $T$ . The scales are logarithmic in order to show many decades of FMR.

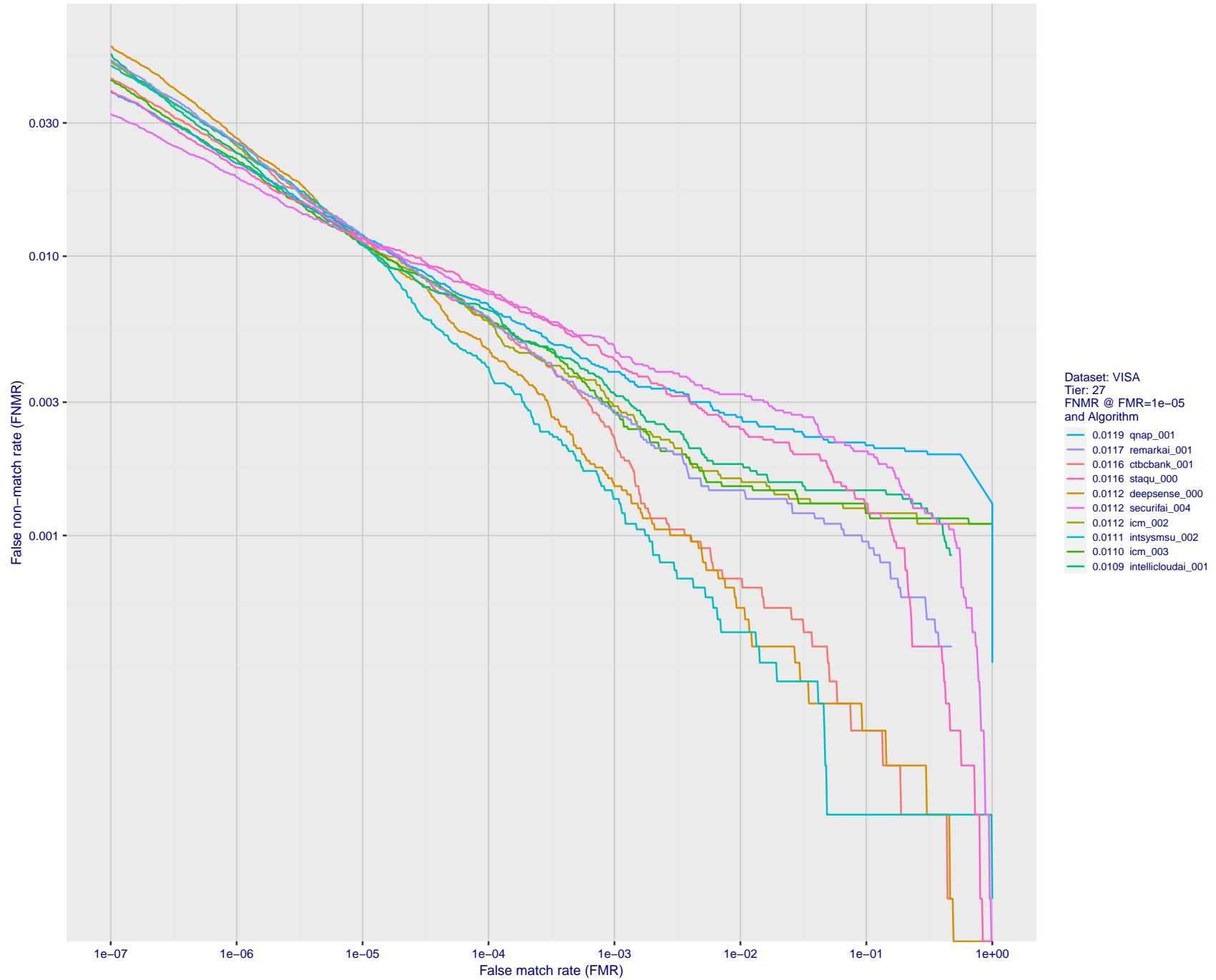


Figure 48: For the visa images, detection error tradeoff (DET) characteristics showing false non-match rate vs. false match rate plotted parametrically on threshold,  $T$ . The scales are logarithmic in order to show many decades of FMR.

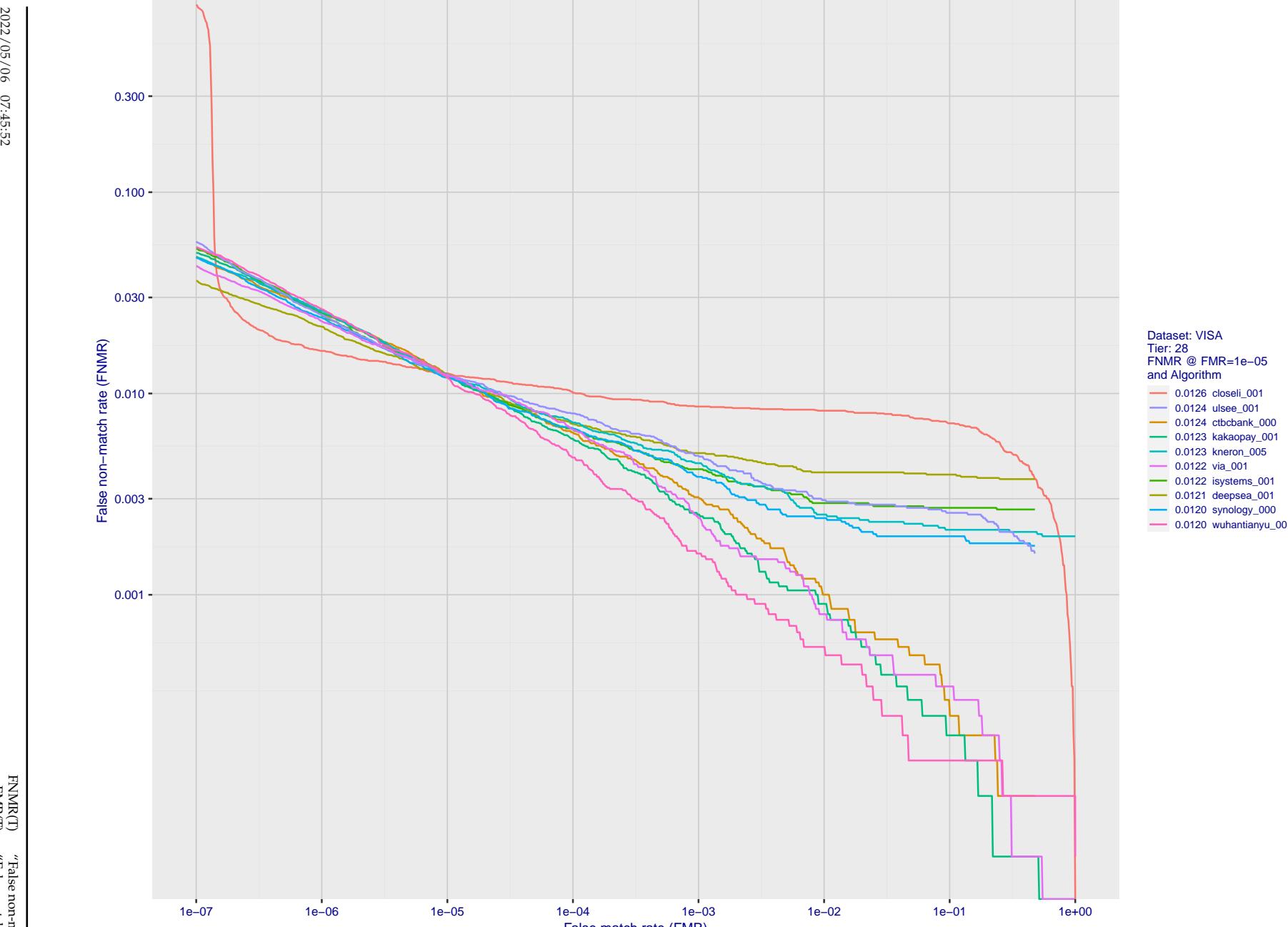


Figure 49: For the visa images, detection error tradeoff (DET) characteristics showing false non-match rate vs. false match rate plotted parametrically on threshold,  $T$ . The scales are logarithmic in order to show many decades of FMR.

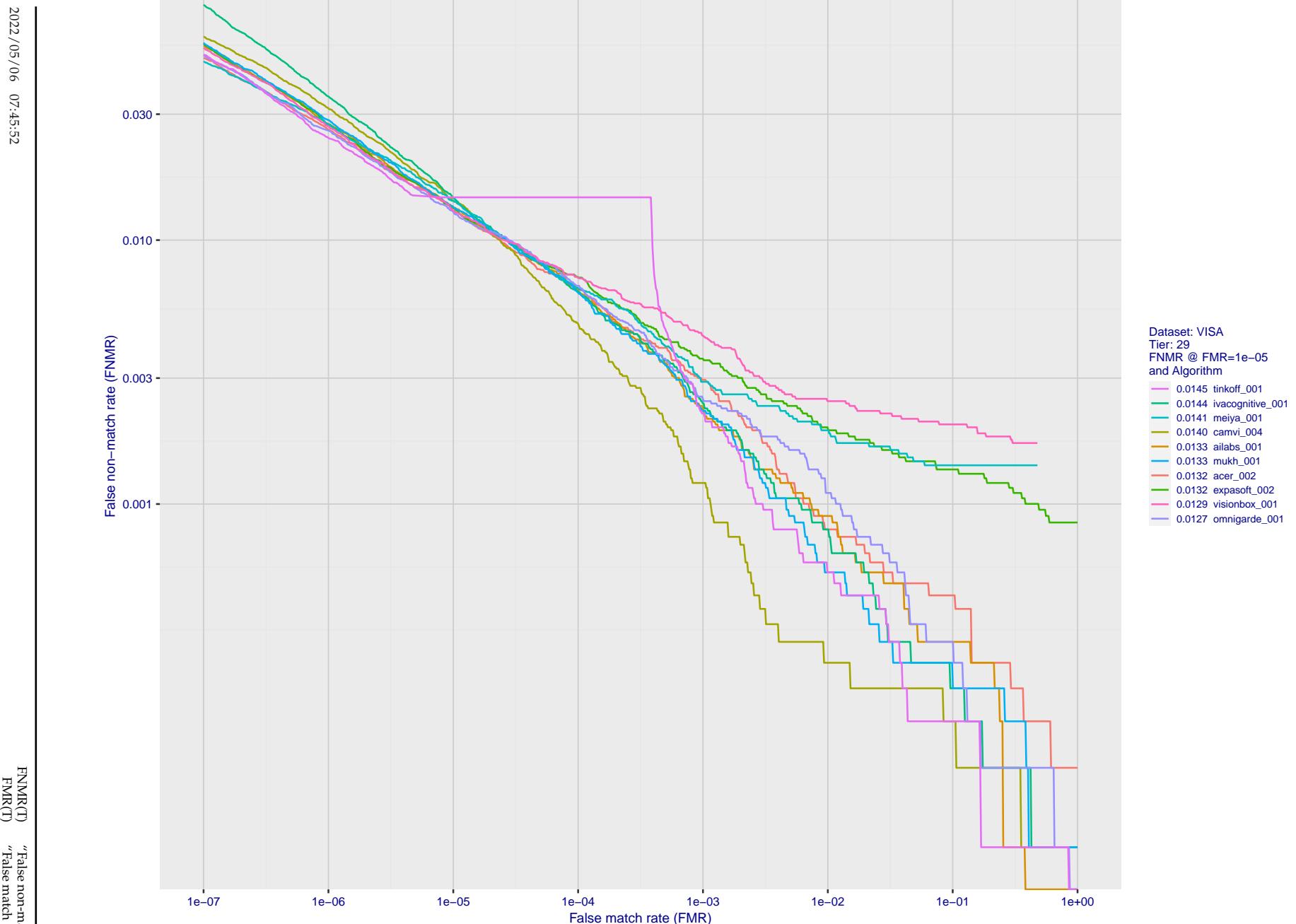


Figure 50: For the visa images, detection error tradeoff (DET) characteristics showing false non-match rate vs. false match rate plotted parametrically on threshold,  $T$ . The scales are logarithmic in order to show many decades of FMR.

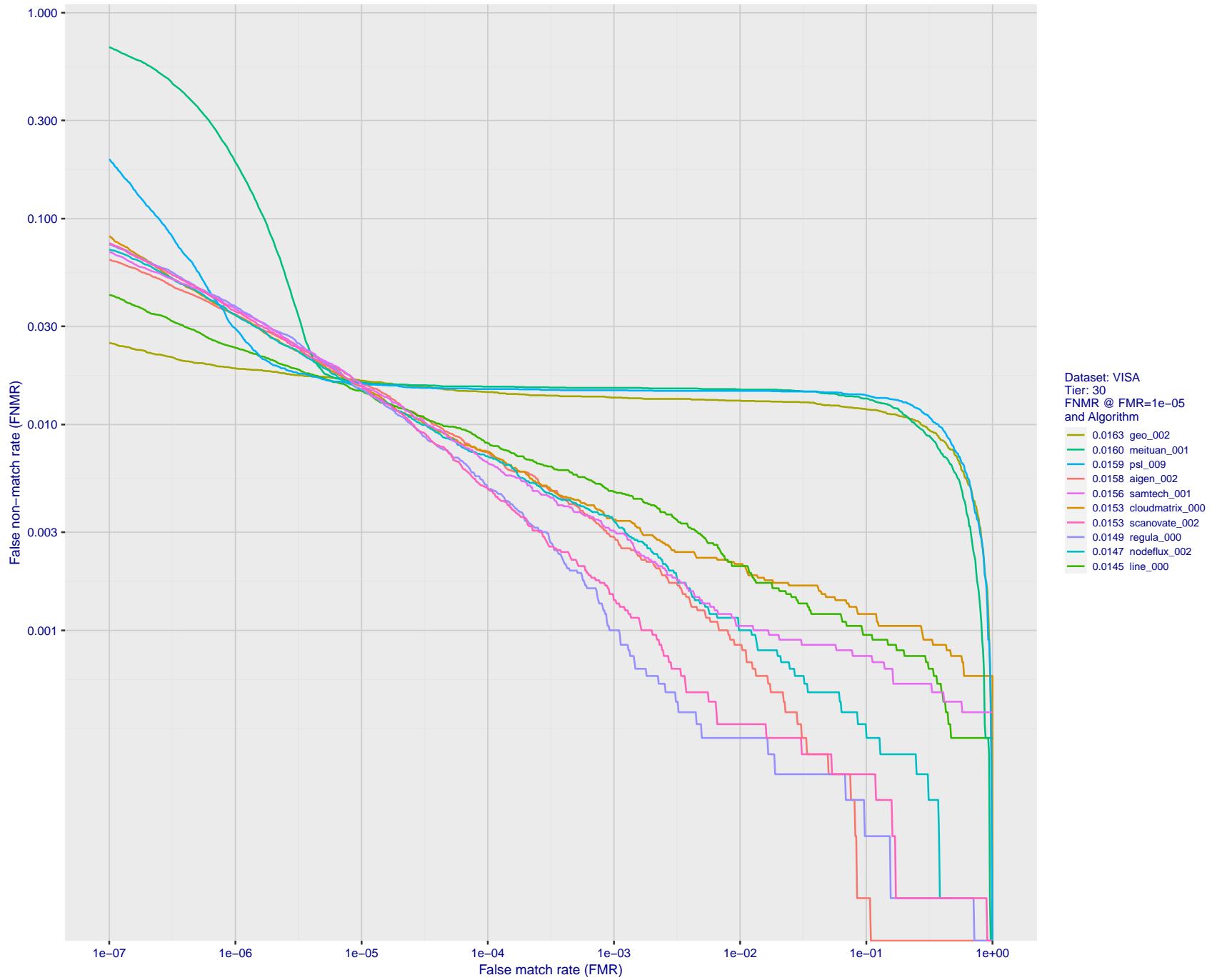


Figure 51: For the visa images, detection error tradeoff (DET) characteristics showing false non-match rate vs. false match rate plotted parametrically on threshold,  $T$ . The scales are logarithmic in order to show many decades of FMR.

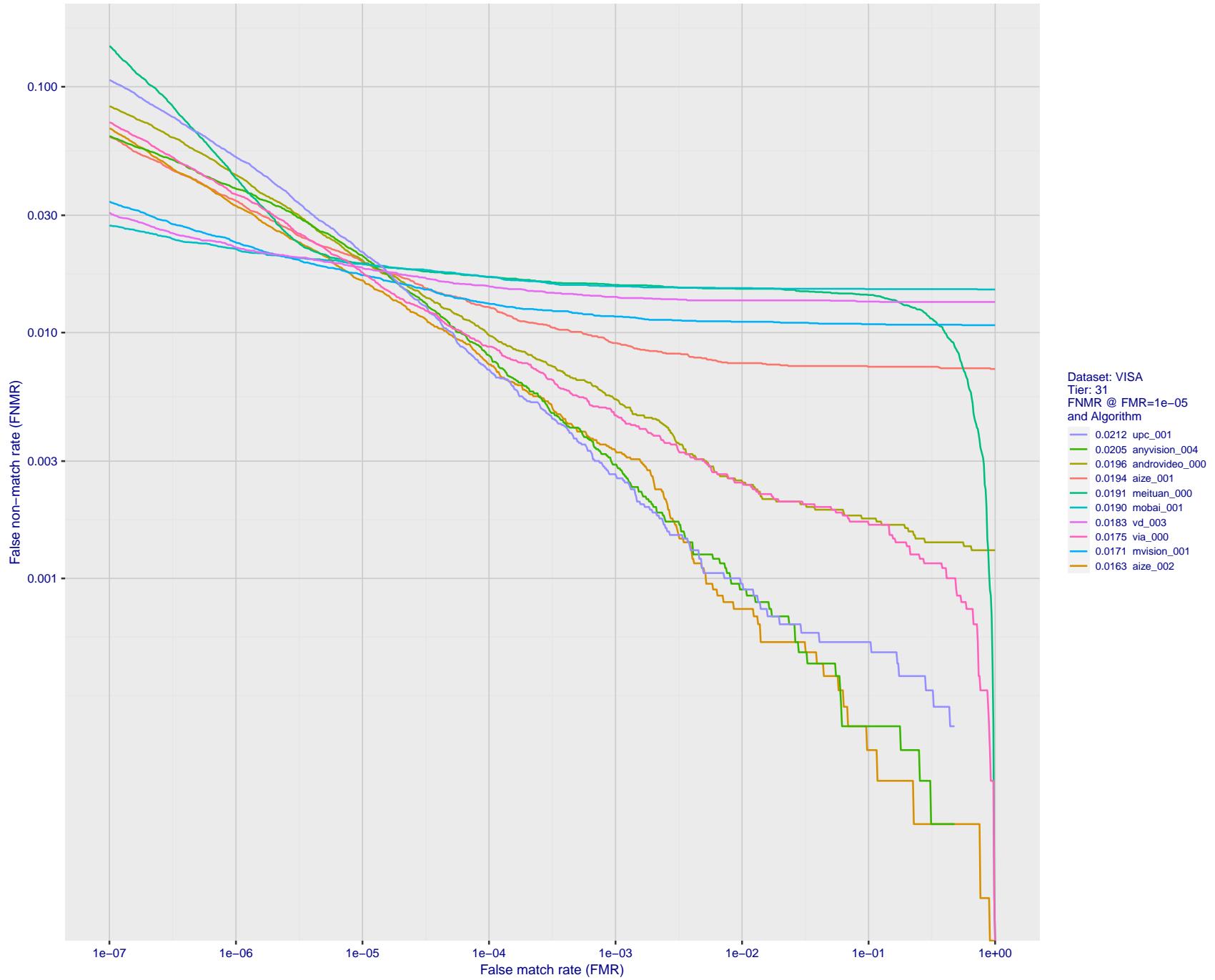


Figure 52: For the visa images, detection error tradeoff (DET) characteristics showing false non-match rate vs. false match rate plotted parametrically on threshold,  $T$ . The scales are logarithmic in order to show many decades of FMR.

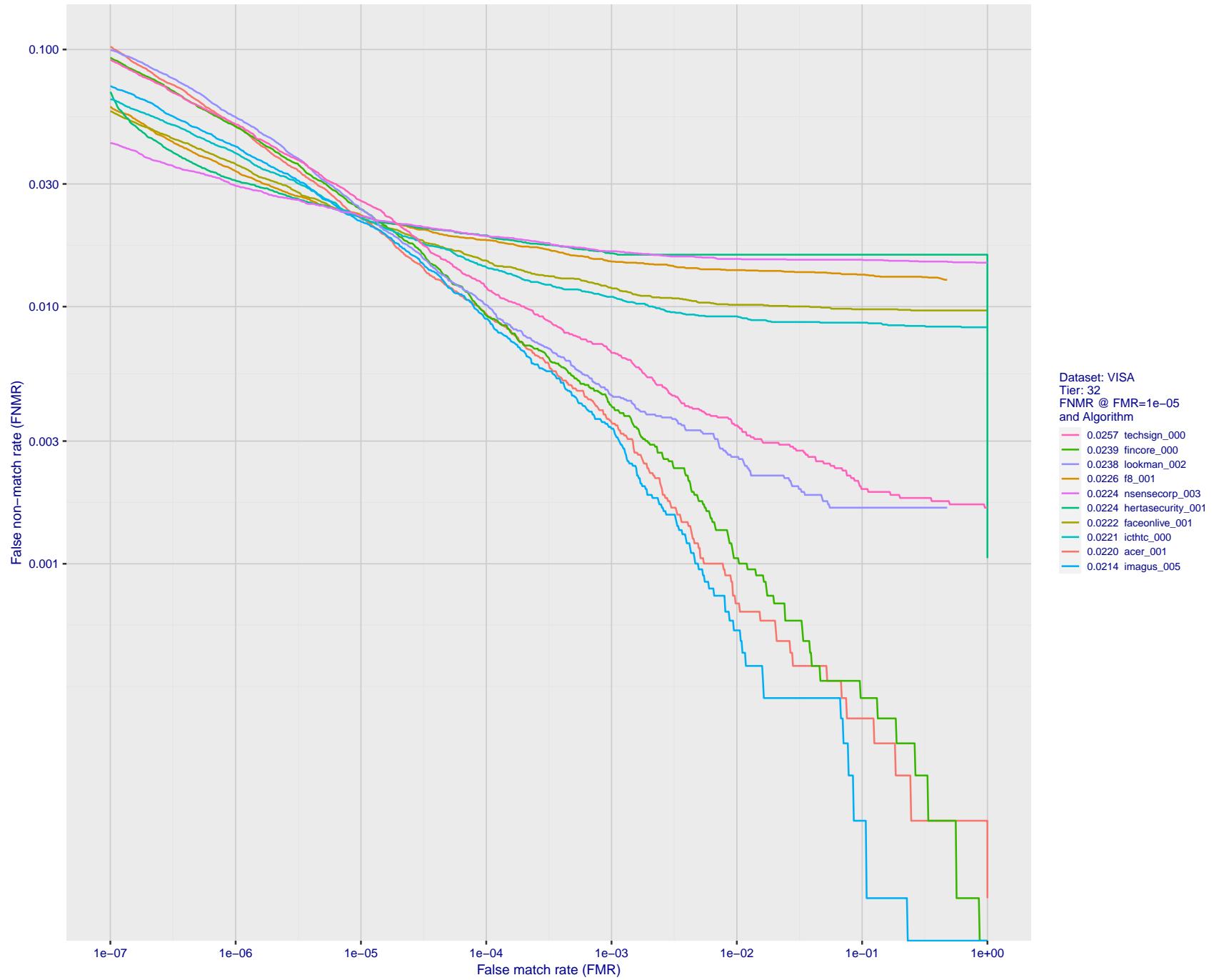


Figure 53: For the visa images, detection error tradeoff (DET) characteristics showing false non-match rate vs. false match rate plotted parametrically on threshold,  $T$ . The scales are logarithmic in order to show many decades of FMR.

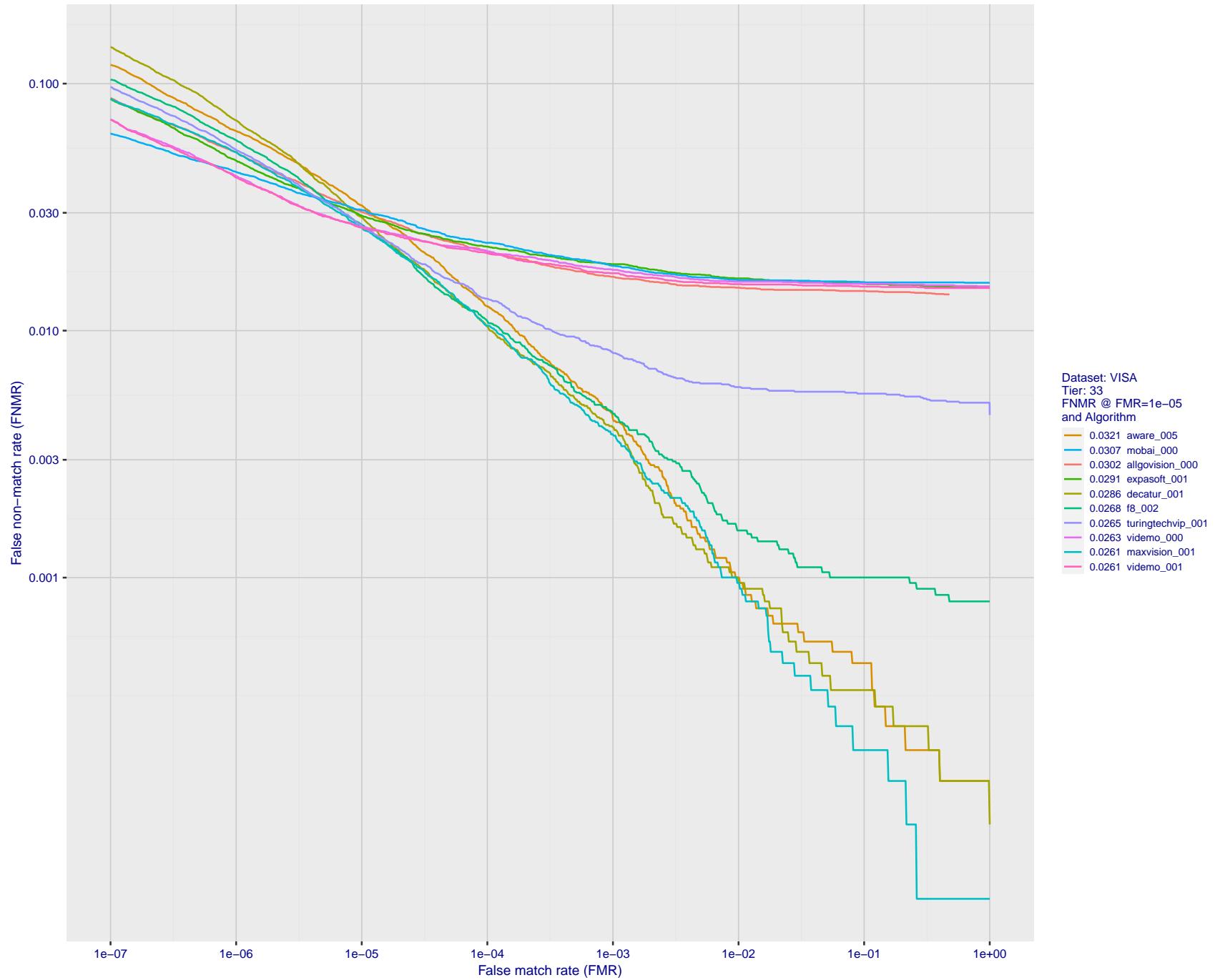


Figure 54: For the visa images, detection error tradeoff (DET) characteristics showing false non-match rate vs. false match rate plotted parametrically on threshold,  $T$ . The scales are logarithmic in order to show many decades of FMR.

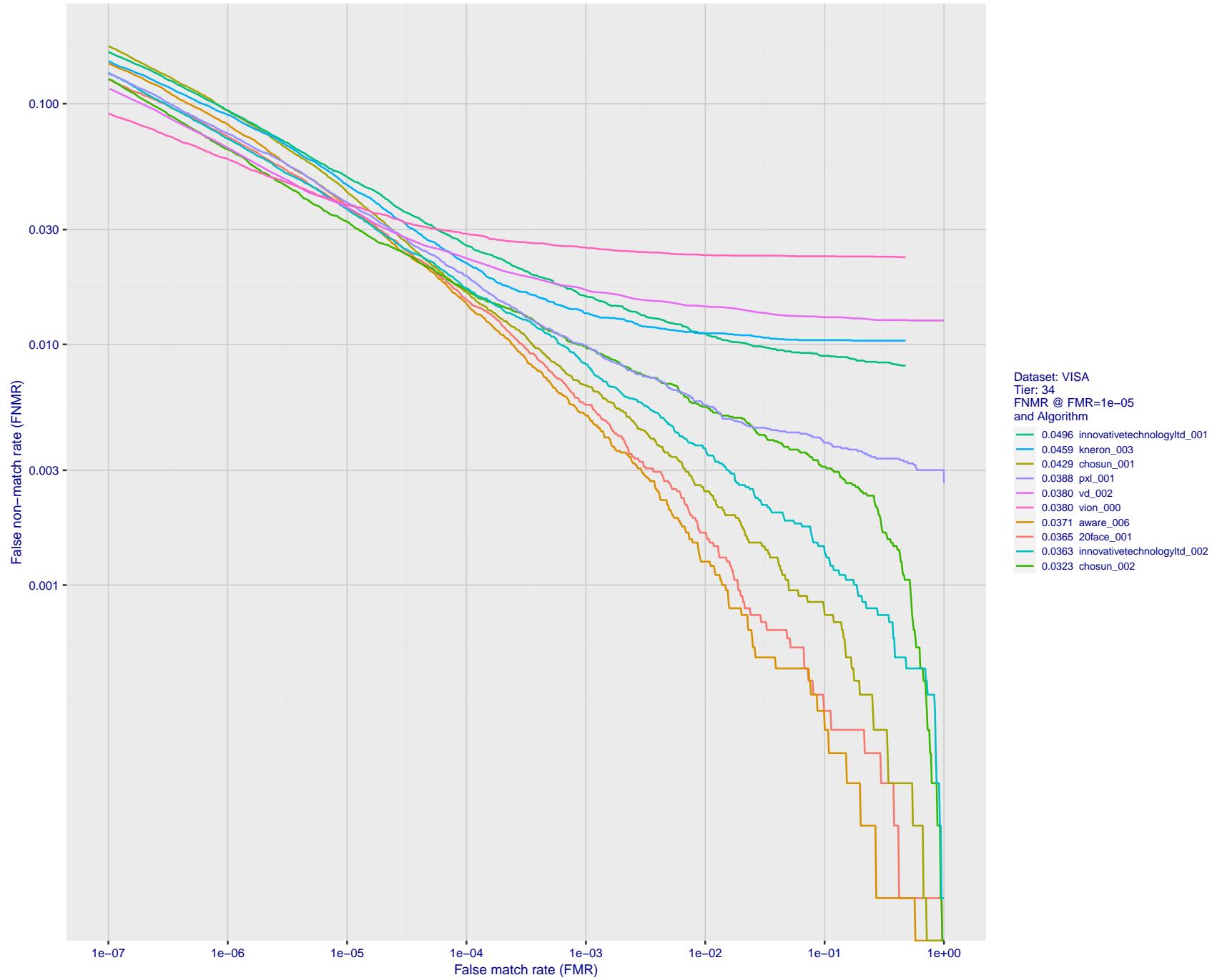


Figure 55: For the visa images, detection error tradeoff (DET) characteristics showing false non-match rate vs. false match rate plotted parametrically on threshold,  $T$ . The scales are logarithmic in order to show many decades of FMR.

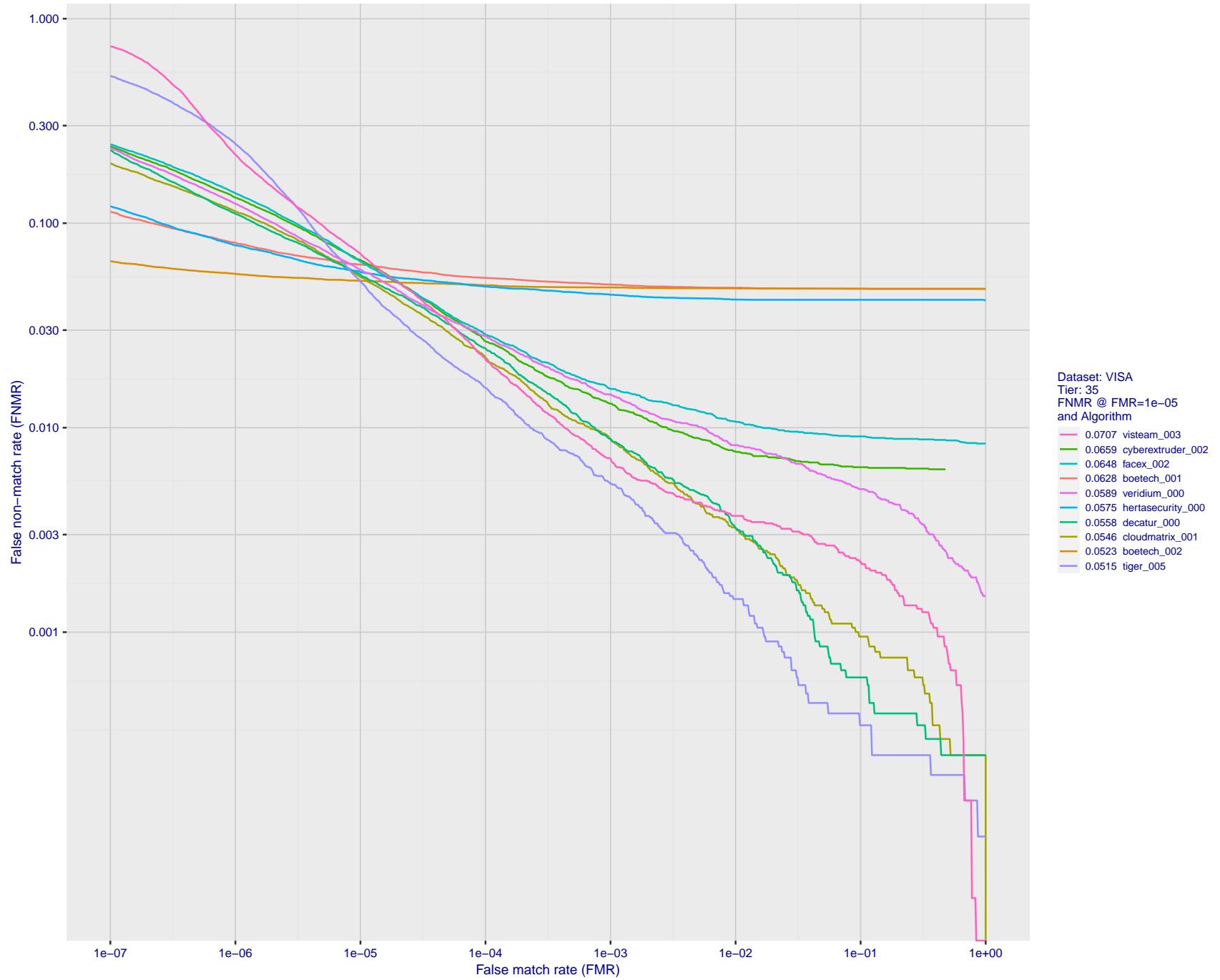


Figure 56: For the visa images, detection error tradeoff (DET) characteristics showing false non-match rate vs. false match rate plotted parametrically on threshold,  $T$ . The scales are logarithmic in order to show many decades of FMR.

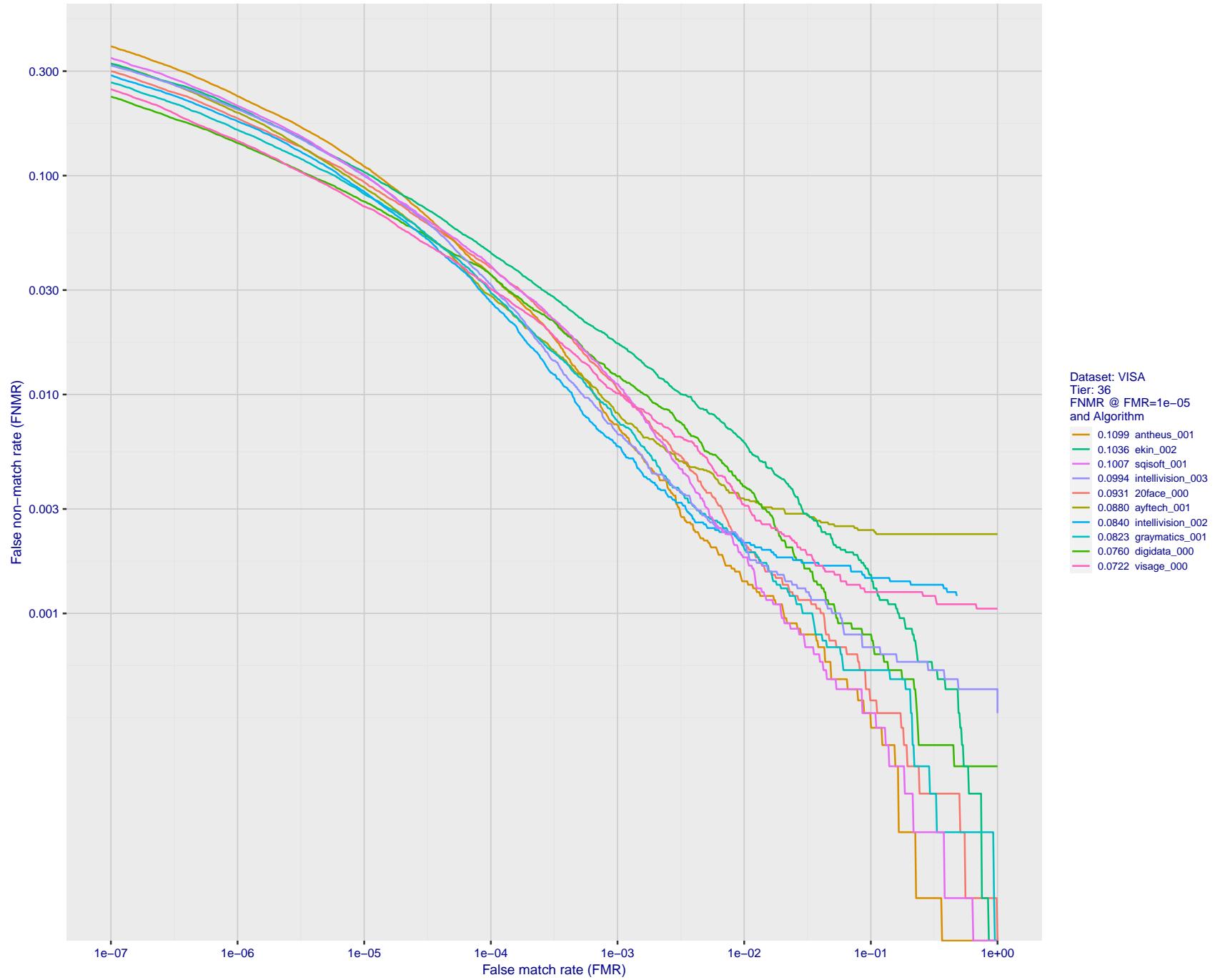


Figure 57: For the visa images, detection error tradeoff (DET) characteristics showing false non-match rate vs. false match rate plotted parametrically on threshold,  $T$ . The scales are logarithmic in order to show many decades of FMR.

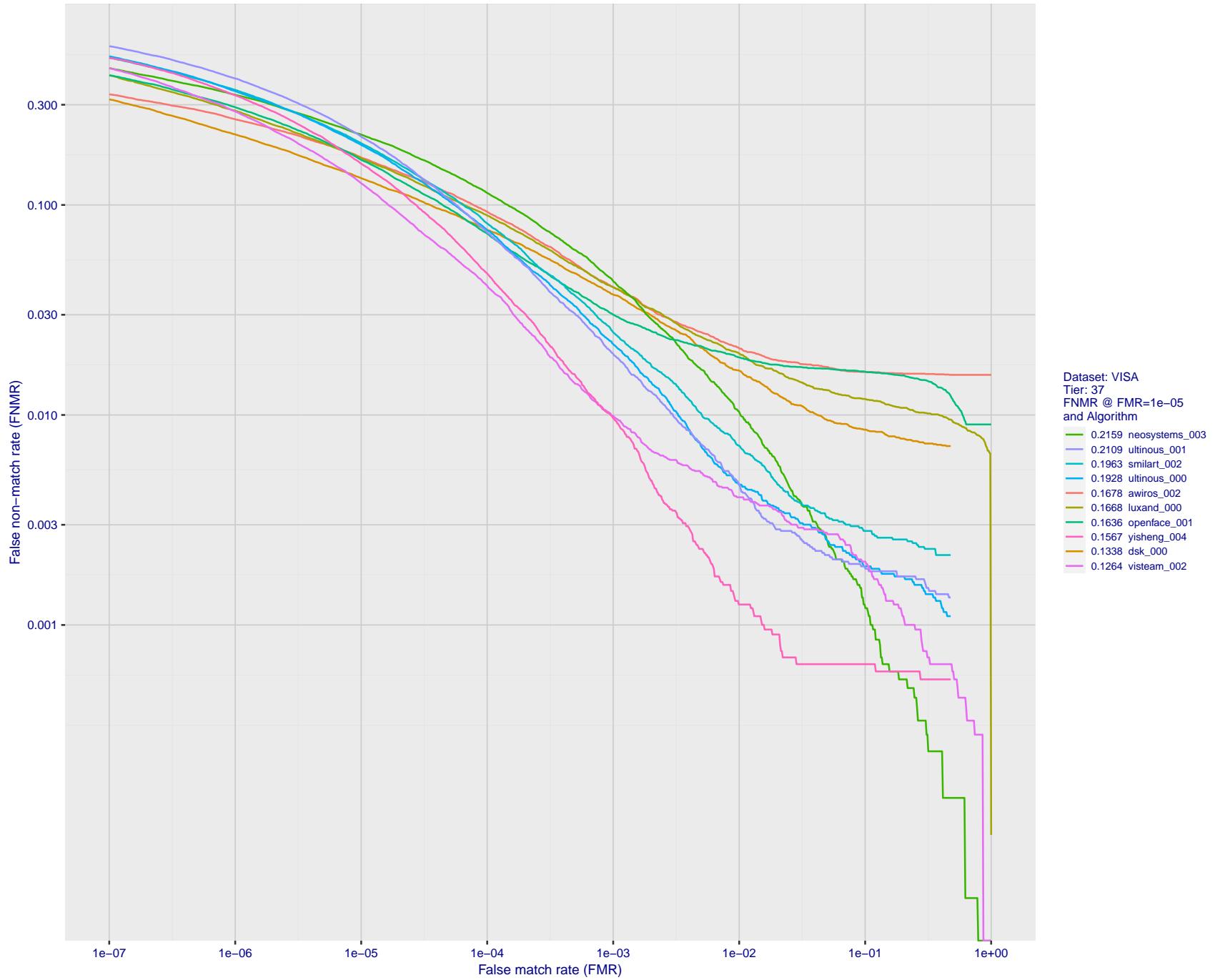


Figure 58: For the visa images, detection error tradeoff (DET) characteristics showing false non-match rate vs. false match rate plotted parametrically on threshold,  $T$ . The scales are logarithmic in order to show many decades of FMR.

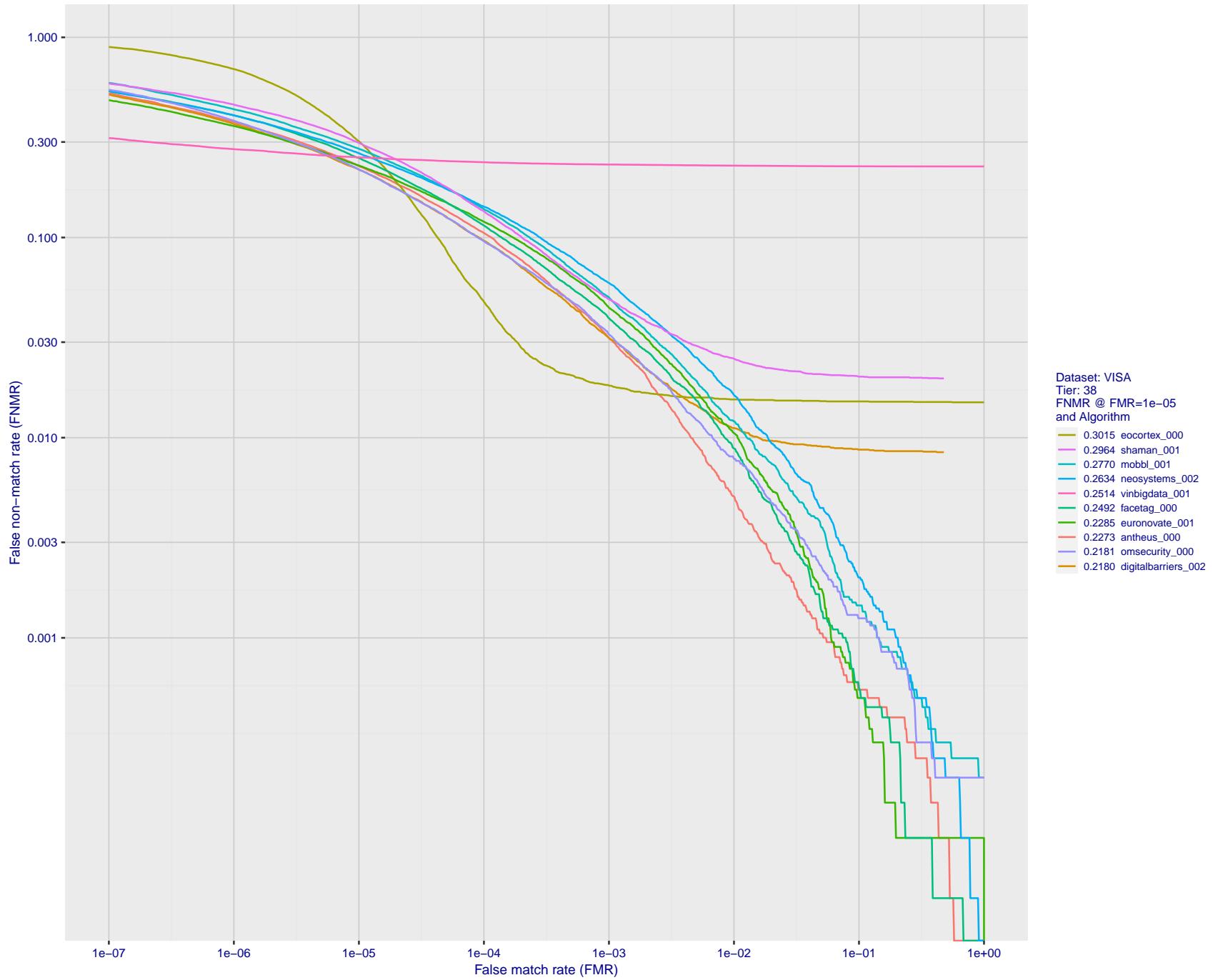


Figure 59: For the visa images, detection error tradeoff (DET) characteristics showing false non-match rate vs. false match rate plotted parametrically on threshold,  $T$ . The scales are logarithmic in order to show many decades of FMR.

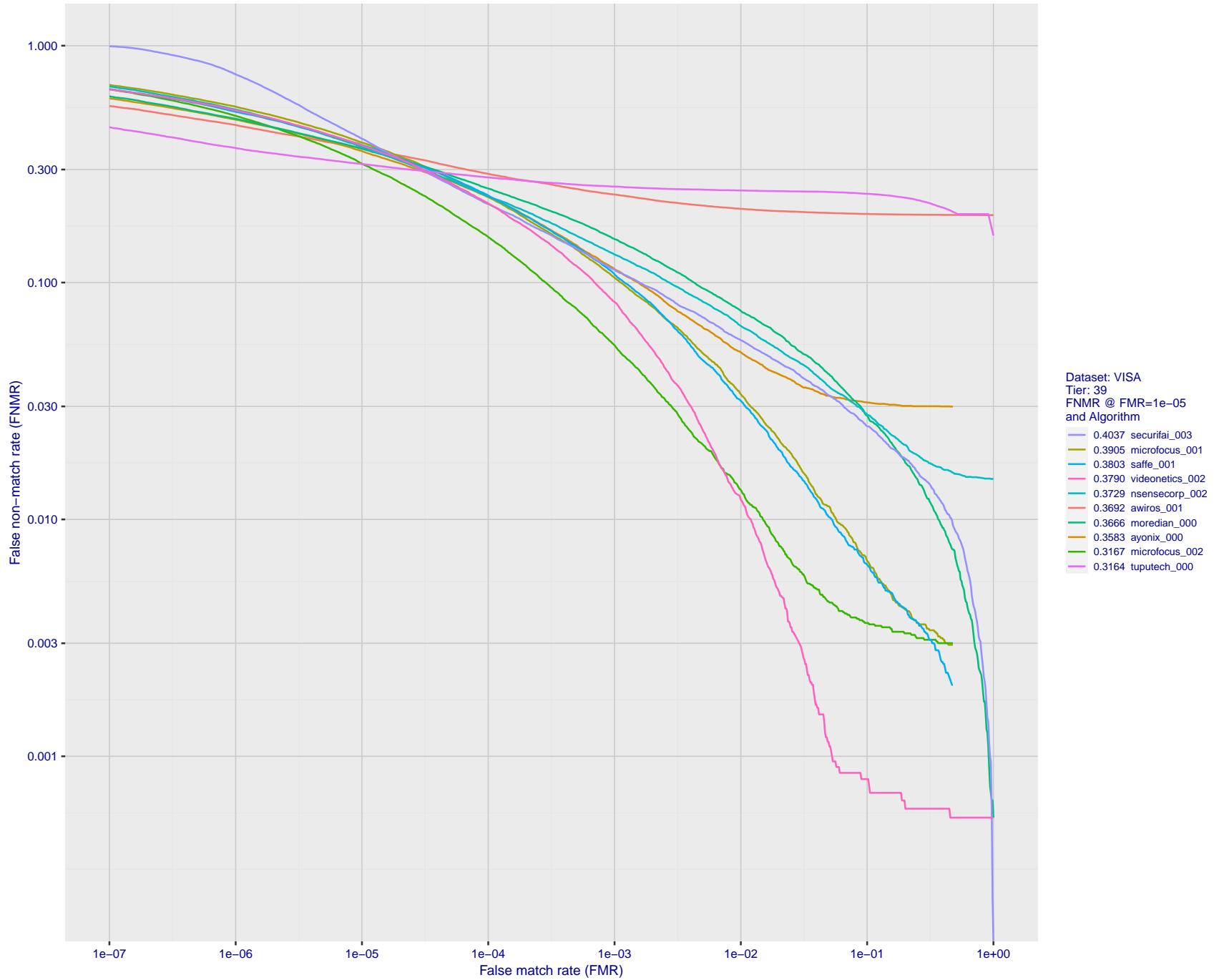


Figure 60: For the visa images, detection error tradeoff (DET) characteristics showing false non-match rate vs. false match rate plotted parametrically on threshold,  $T$ . The scales are logarithmic in order to show many decades of FMR.

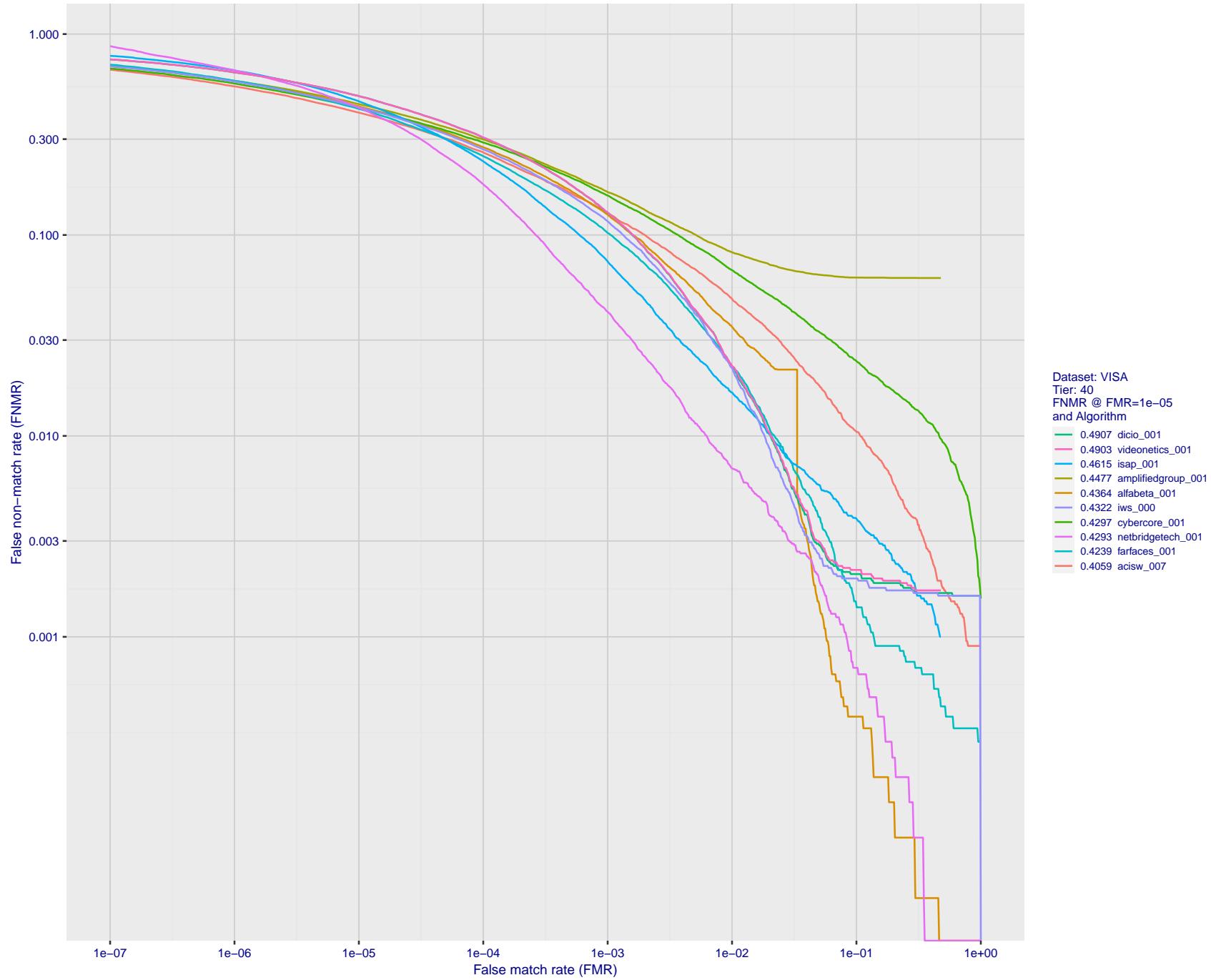


Figure 61: For the visa images, detection error tradeoff (DET) characteristics showing false non-match rate vs. false match rate plotted parametrically on threshold,  $T$ . The scales are logarithmic in order to show many decades of FMR.

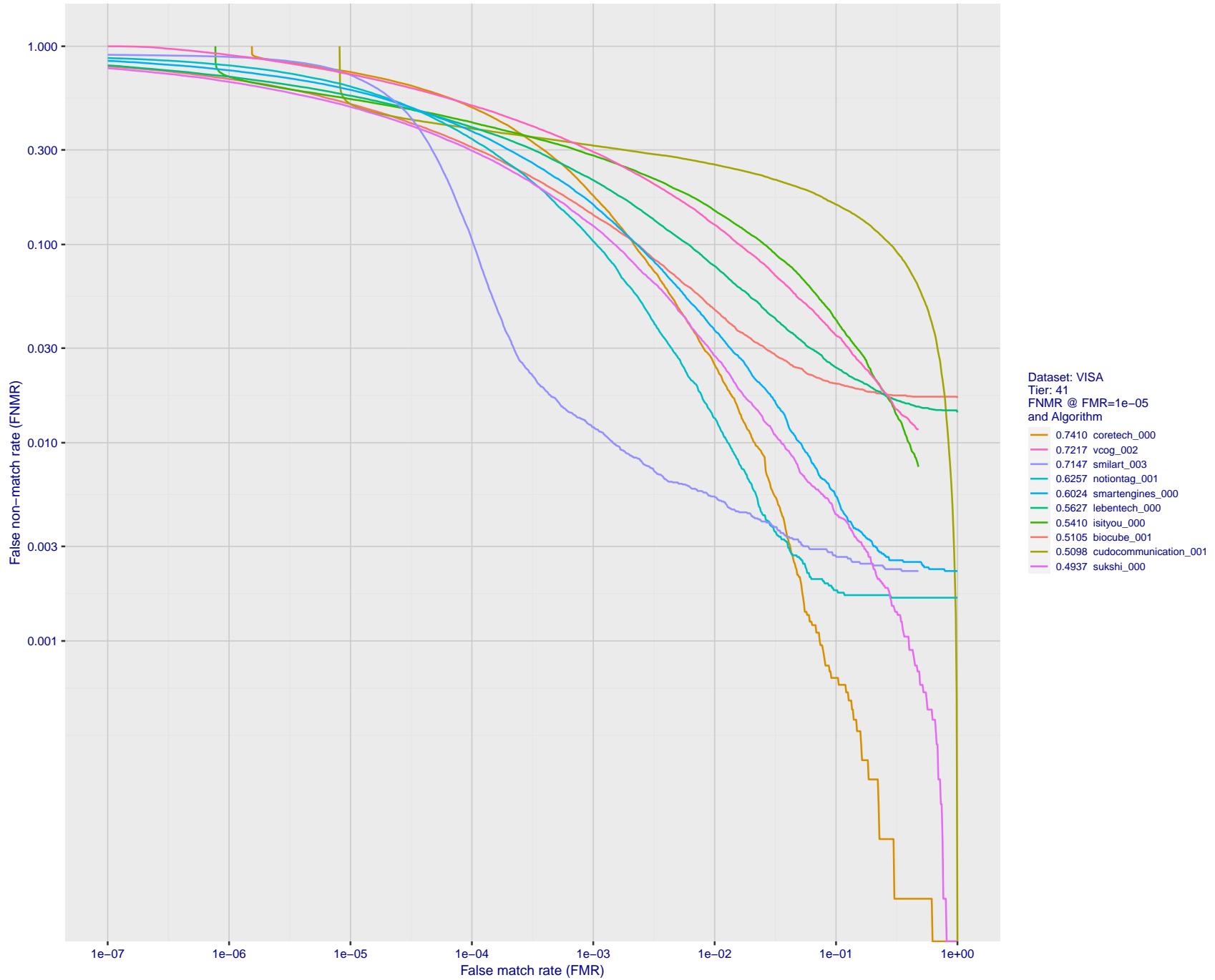


Figure 62: For the visa images, detection error tradeoff (DET) characteristics showing false non-match rate vs. false match rate plotted parametrically on threshold,  $T$ . The scales are logarithmic in order to show many decades of FMR.

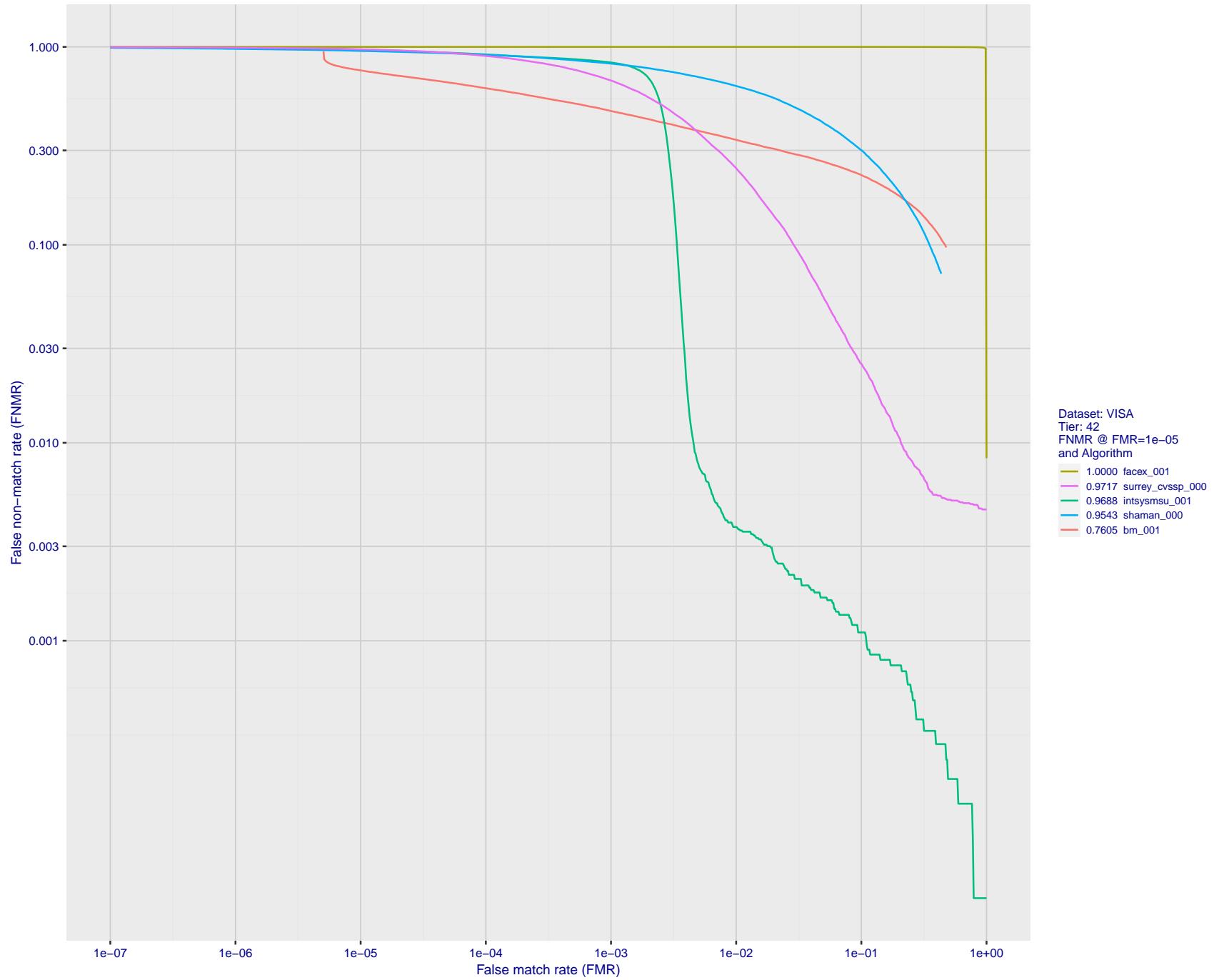


Figure 63: For the visa images, detection error tradeoff (DET) characteristics showing false non-match rate vs. false match rate plotted parametrically on threshold,  $T$ . The scales are logarithmic in order to show many decades of FMR.

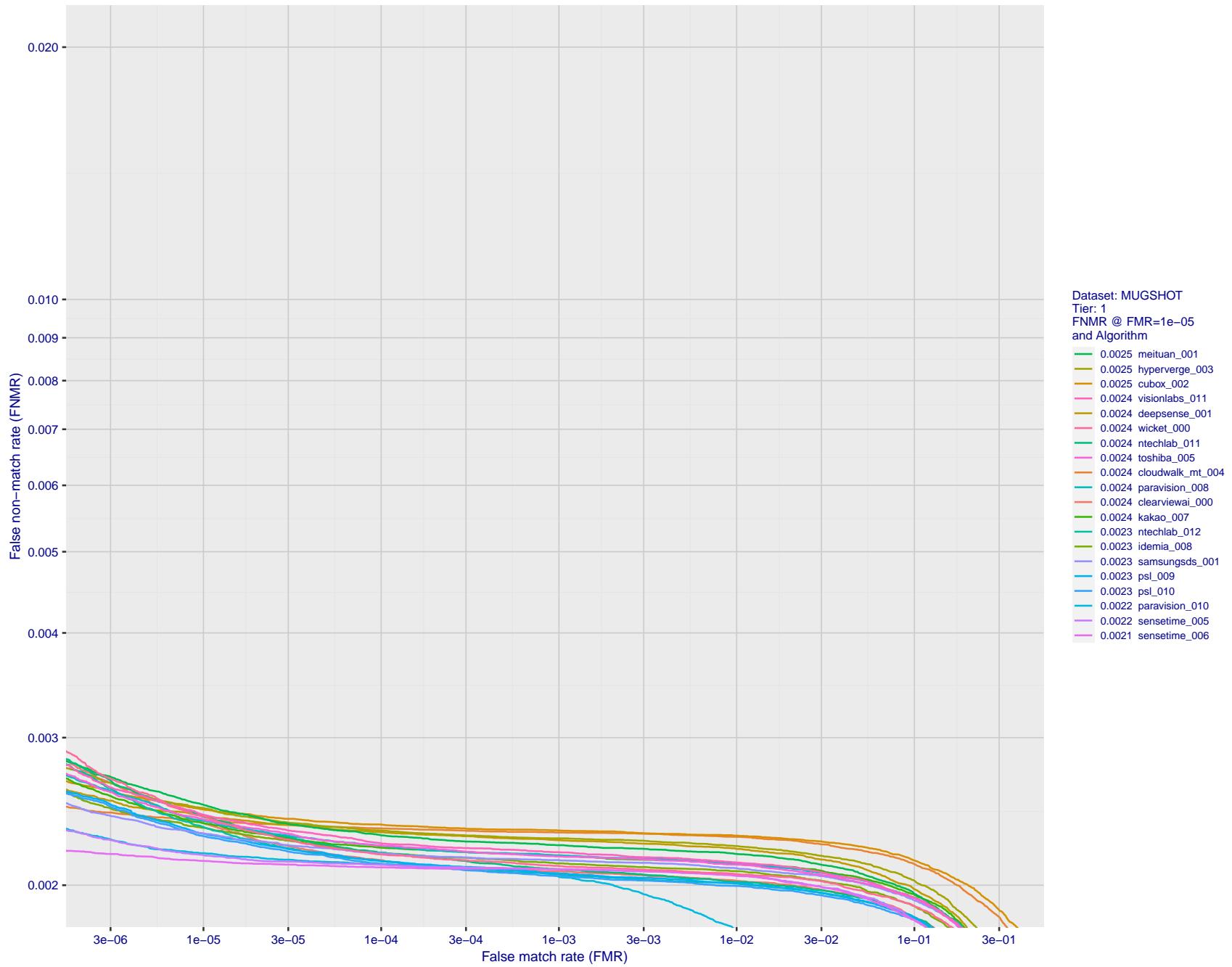


Figure 64: For the mugshot images, detection error tradeoff (DET) characteristics showing false non-match rate vs. false match rate plotted parametrically on threshold,  $T$ . The scales are logarithmic in order to show decades of FMR.

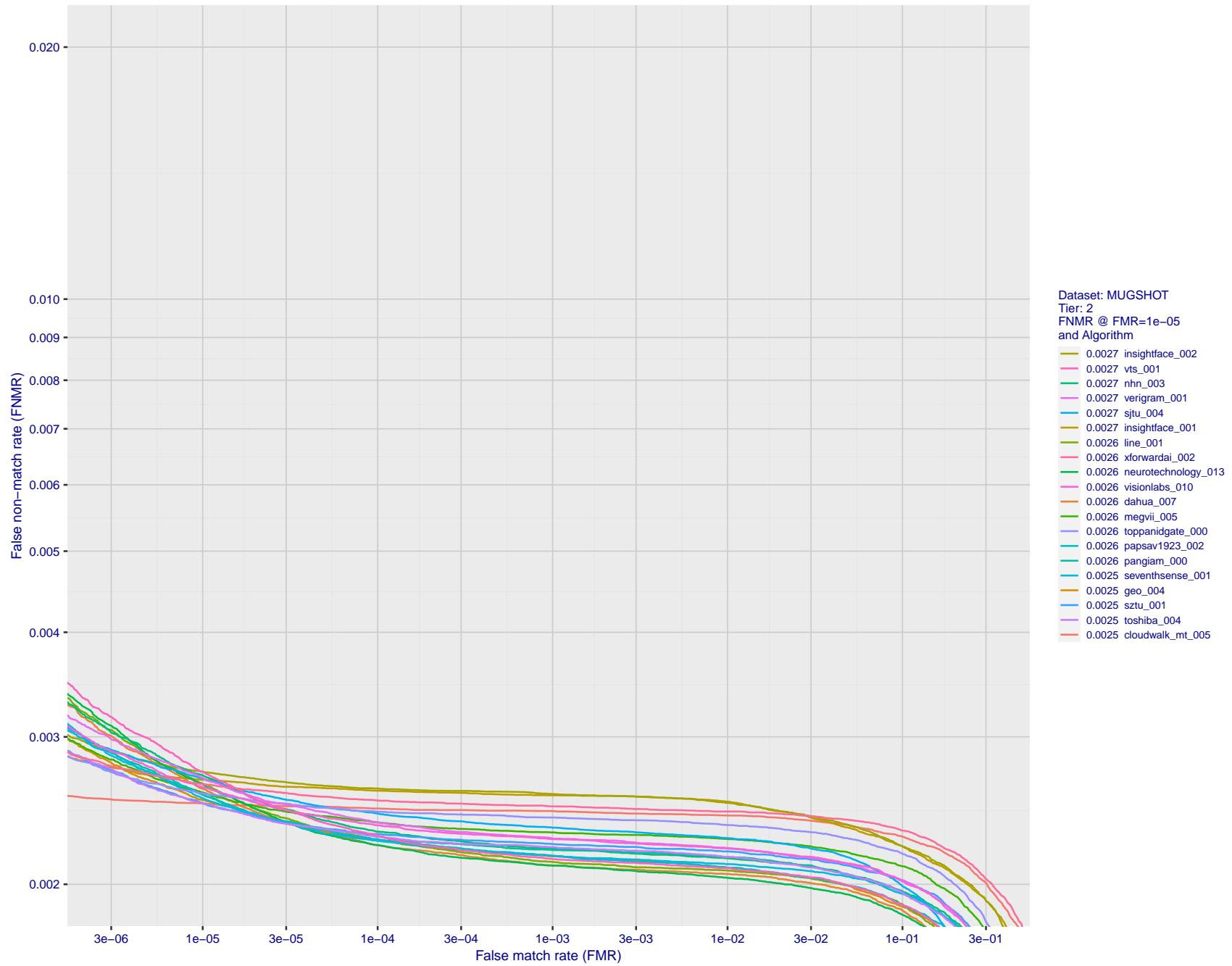


Figure 65: For the mugshot images, detection error tradeoff (DET) characteristics showing false non-match rate vs. false match rate plotted parametrically on threshold,  $T$ . The scales are logarithmic in order to show decades of FMR.

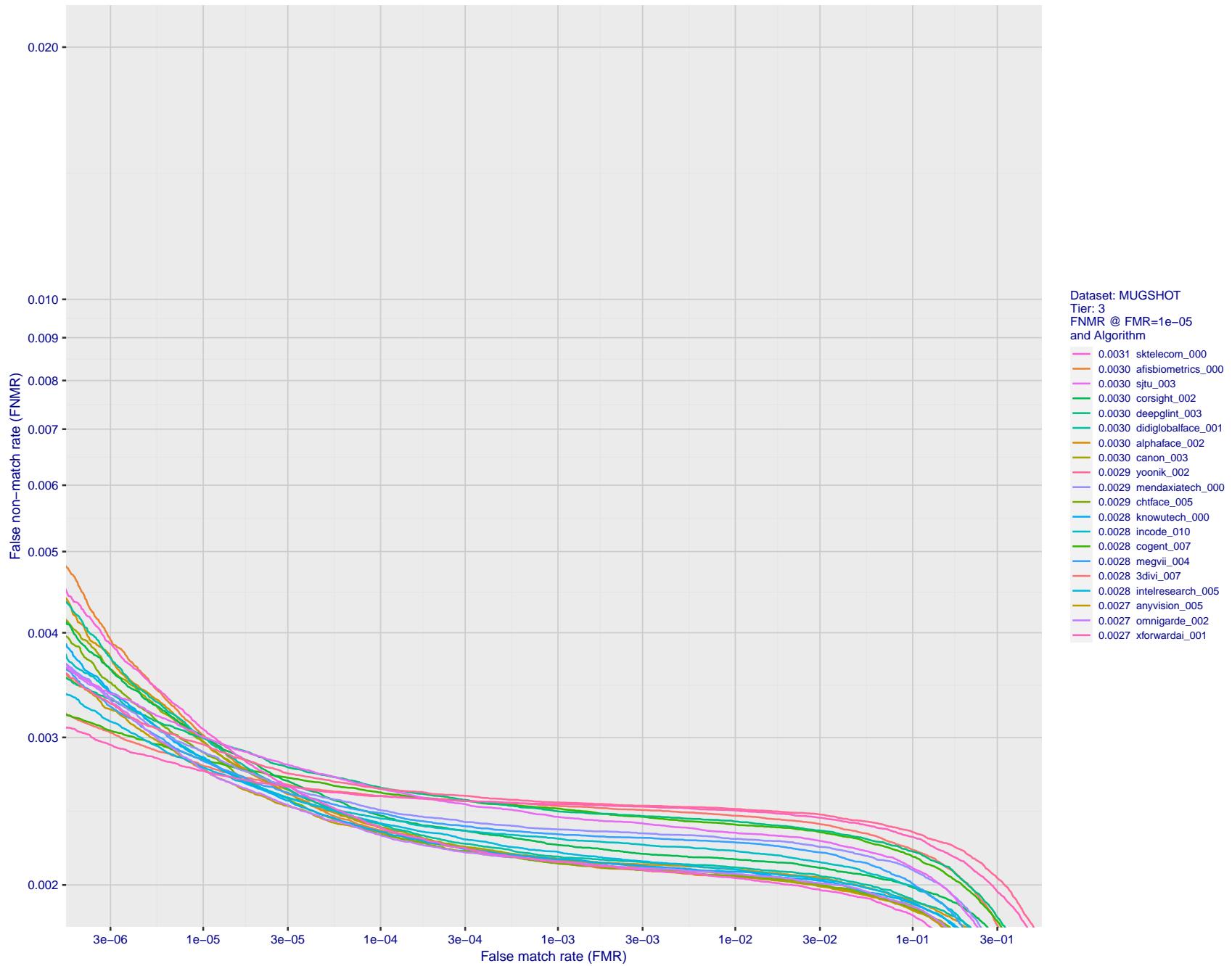


Figure 66: For the mugshot images, detection error tradeoff (DET) characteristics showing false non-match rate vs. false match rate plotted parametrically on threshold,  $T$ . The scales are logarithmic in order to show decades of FMR.

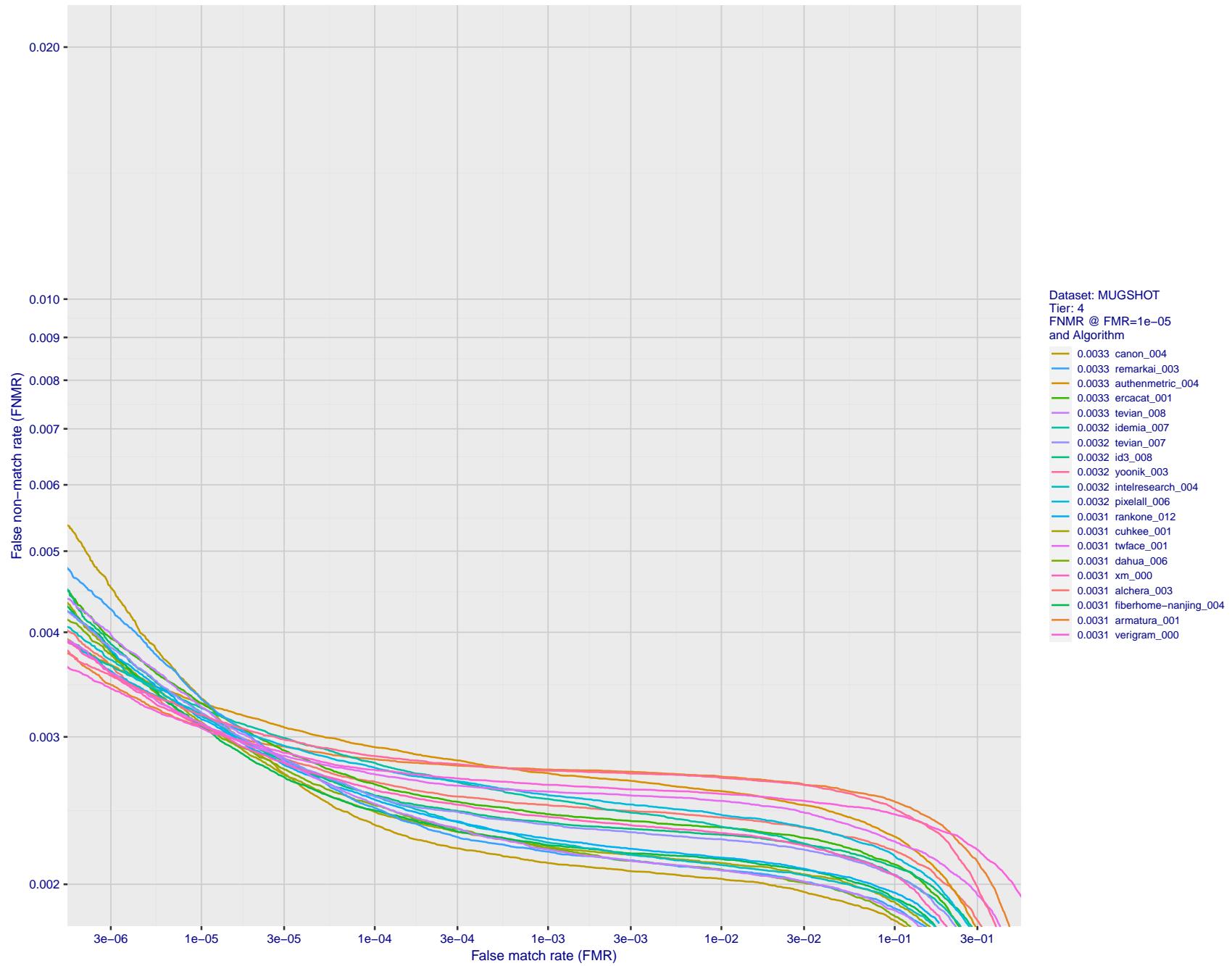


Figure 67: For the mugshot images, detection error tradeoff (DET) characteristics showing false non-match rate vs. false match rate plotted parametrically on threshold,  $T$ . The scales are logarithmic in order to show decades of FMR.

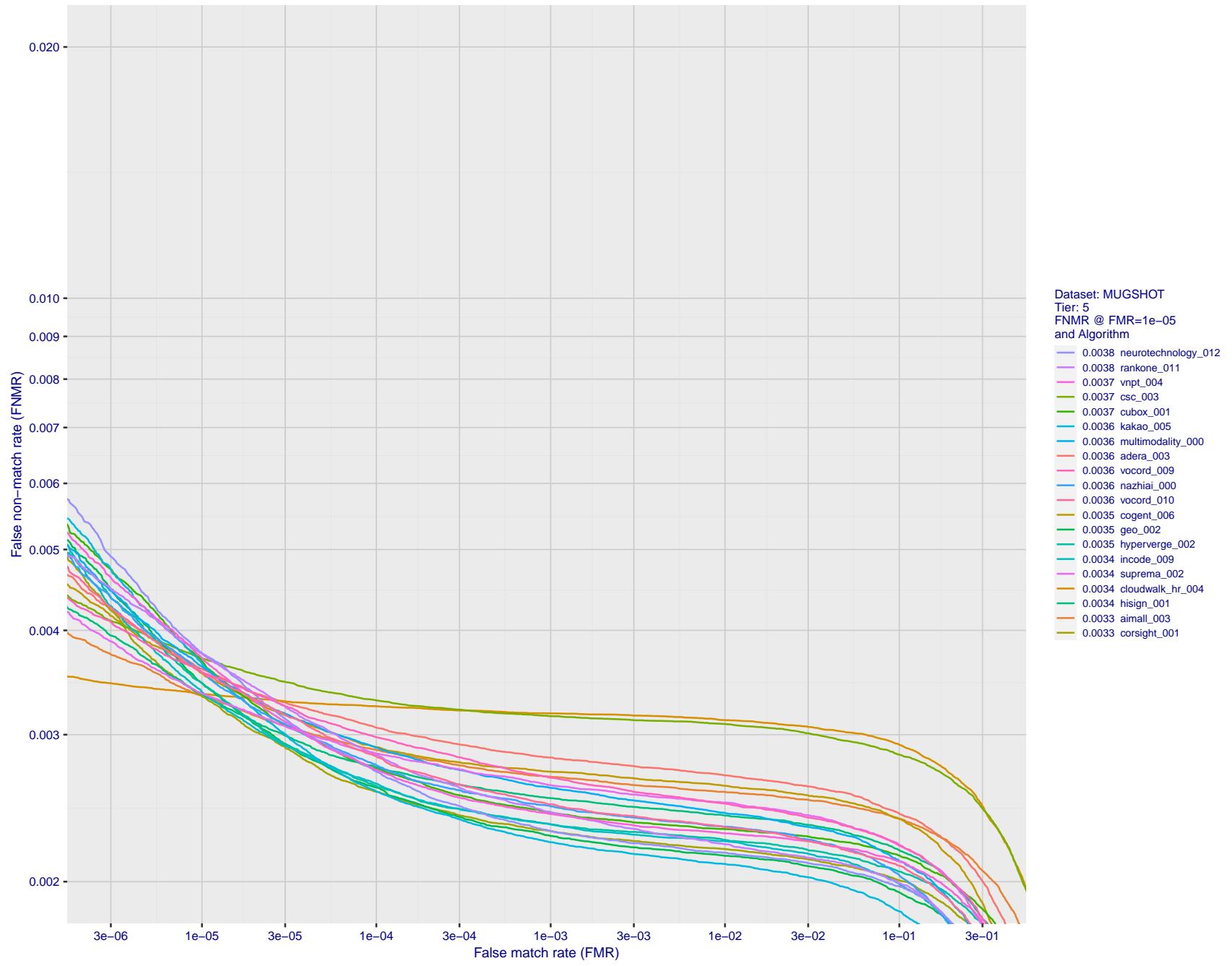


Figure 68: For the mugshot images, detection error tradeoff (DET) characteristics showing false non-match rate vs. false match rate plotted parametrically on threshold,  $T$ . The scales are logarithmic in order to show decades of FMR.

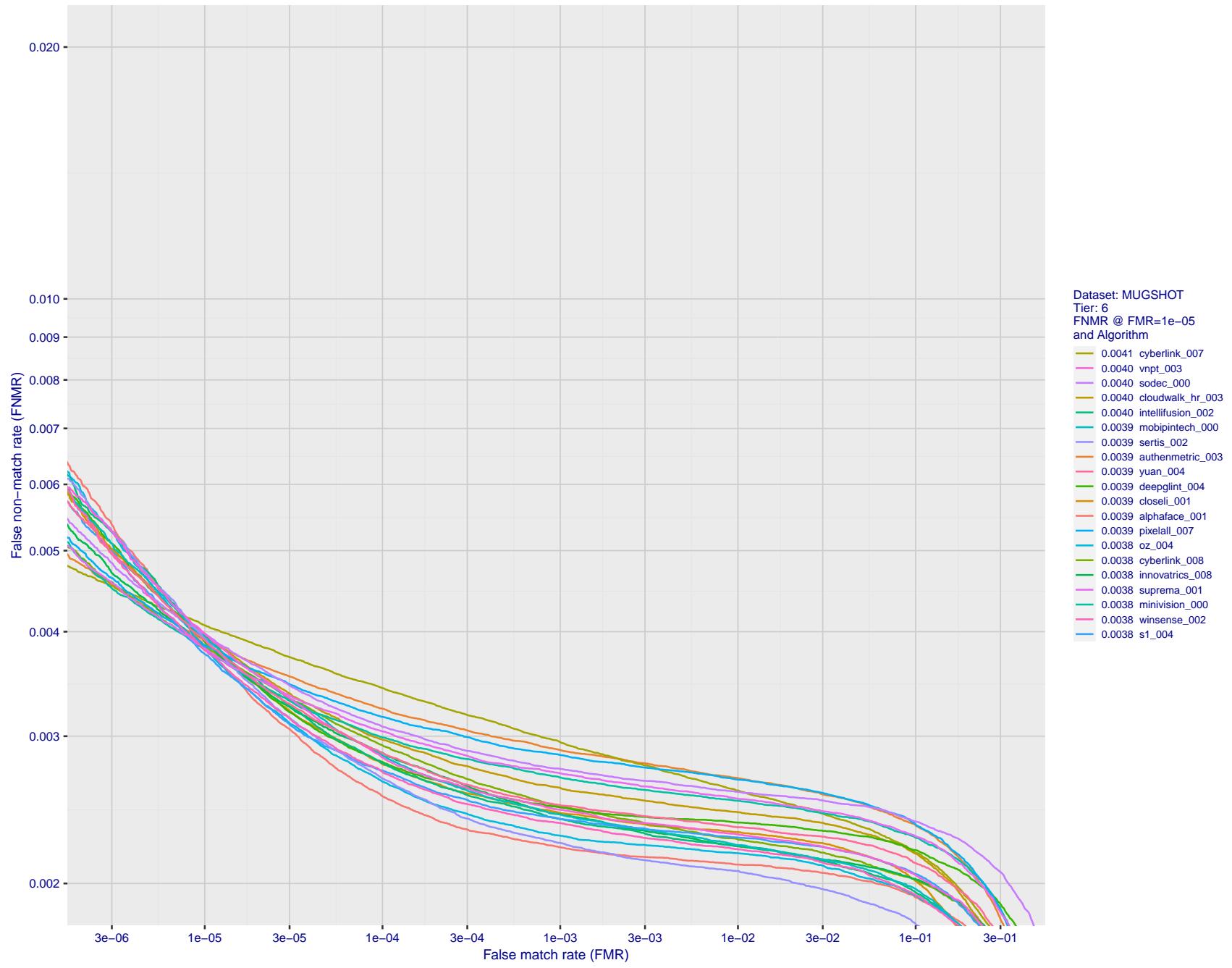


Figure 69: For the mugshot images, detection error tradeoff (DET) characteristics showing false non-match rate vs. false match rate plotted parametrically on threshold,  $T$ . The scales are logarithmic in order to show decades of FMR.

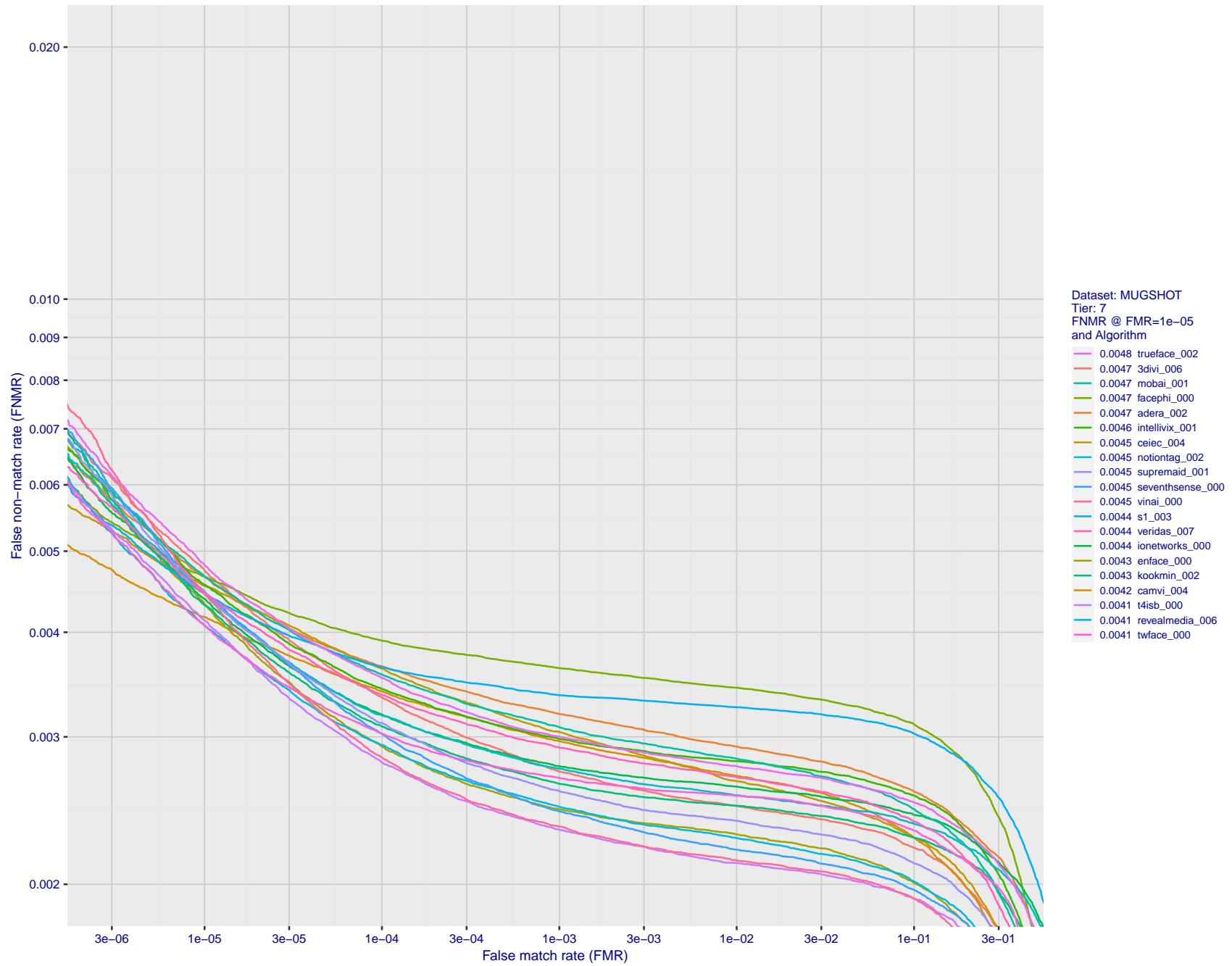


Figure 70: For the mugshot images, detection error tradeoff (DET) characteristics showing false non-match rate vs. false match rate plotted parametrically on threshold,  $T$ . The scales are logarithmic in order to show decades of FMR.

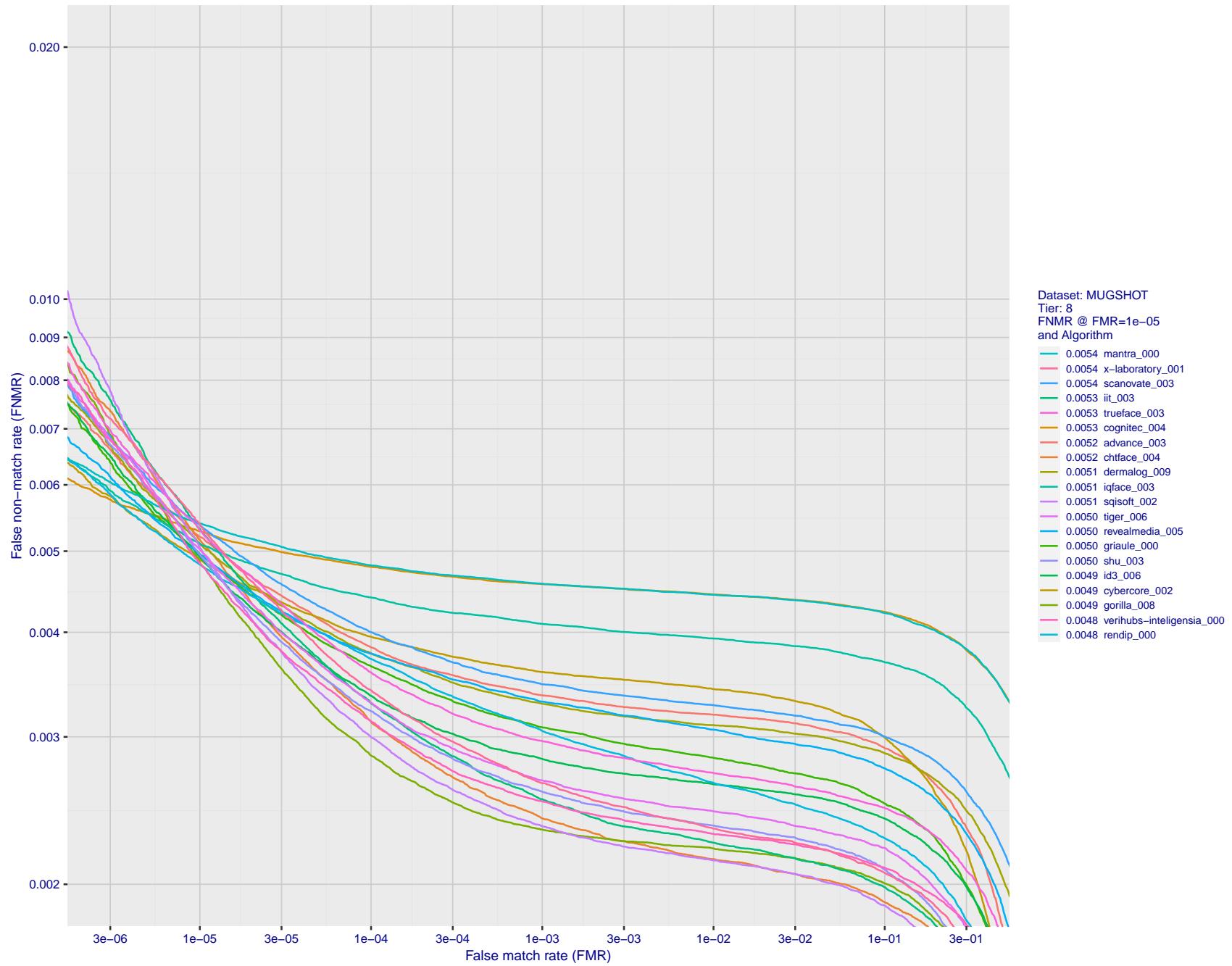


Figure 71: For the mugshot images, detection error tradeoff (DET) characteristics showing false non-match rate vs. false match rate plotted parametrically on threshold,  $T$ . The scales are logarithmic in order to show decades of FMR.

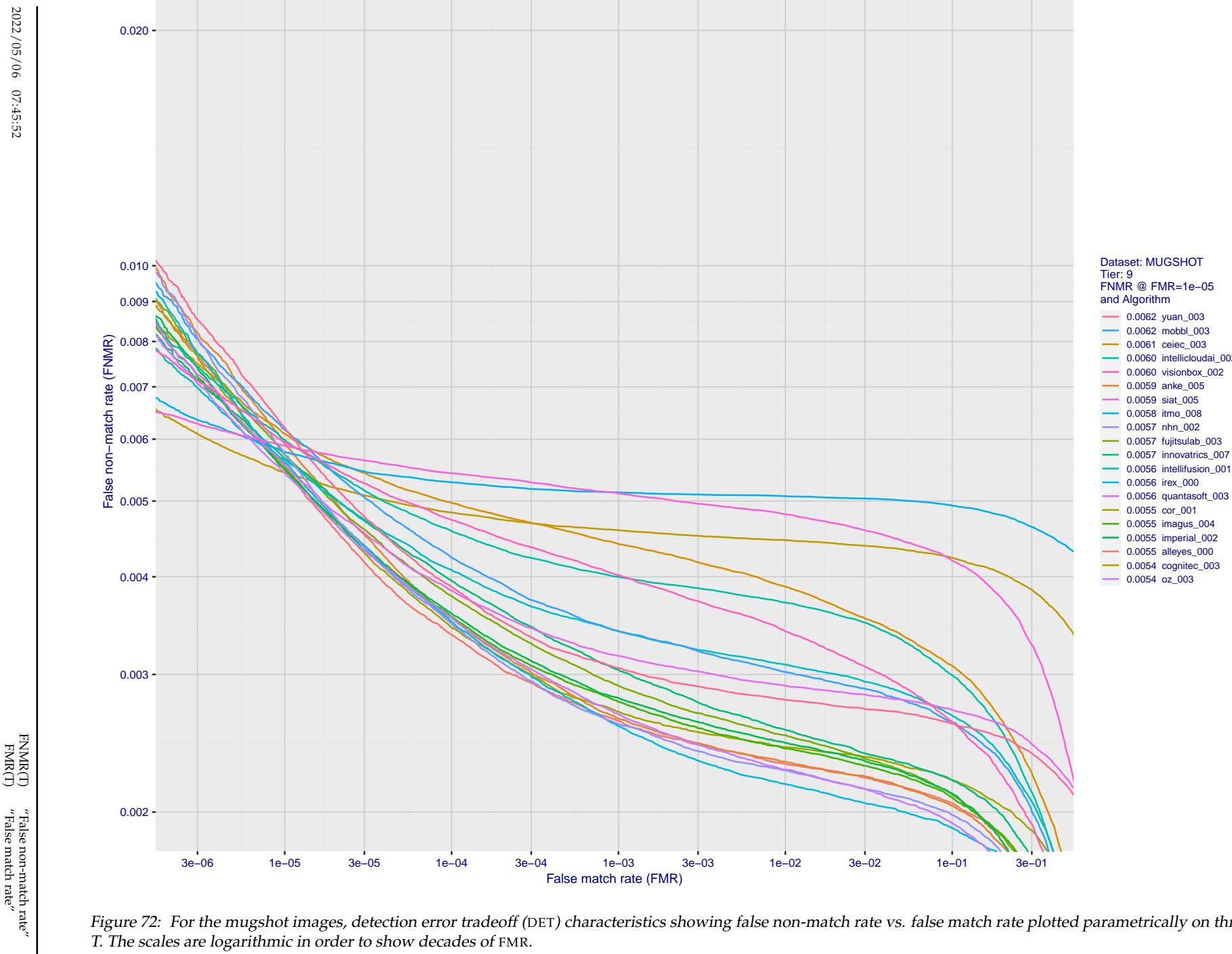


Figure 72: For the mugshot images, detection error tradeoff (DET) characteristics showing false non-match rate vs. false match rate plotted parametrically on threshold,  $T$ . The scales are logarithmic in order to show decades of FMR.

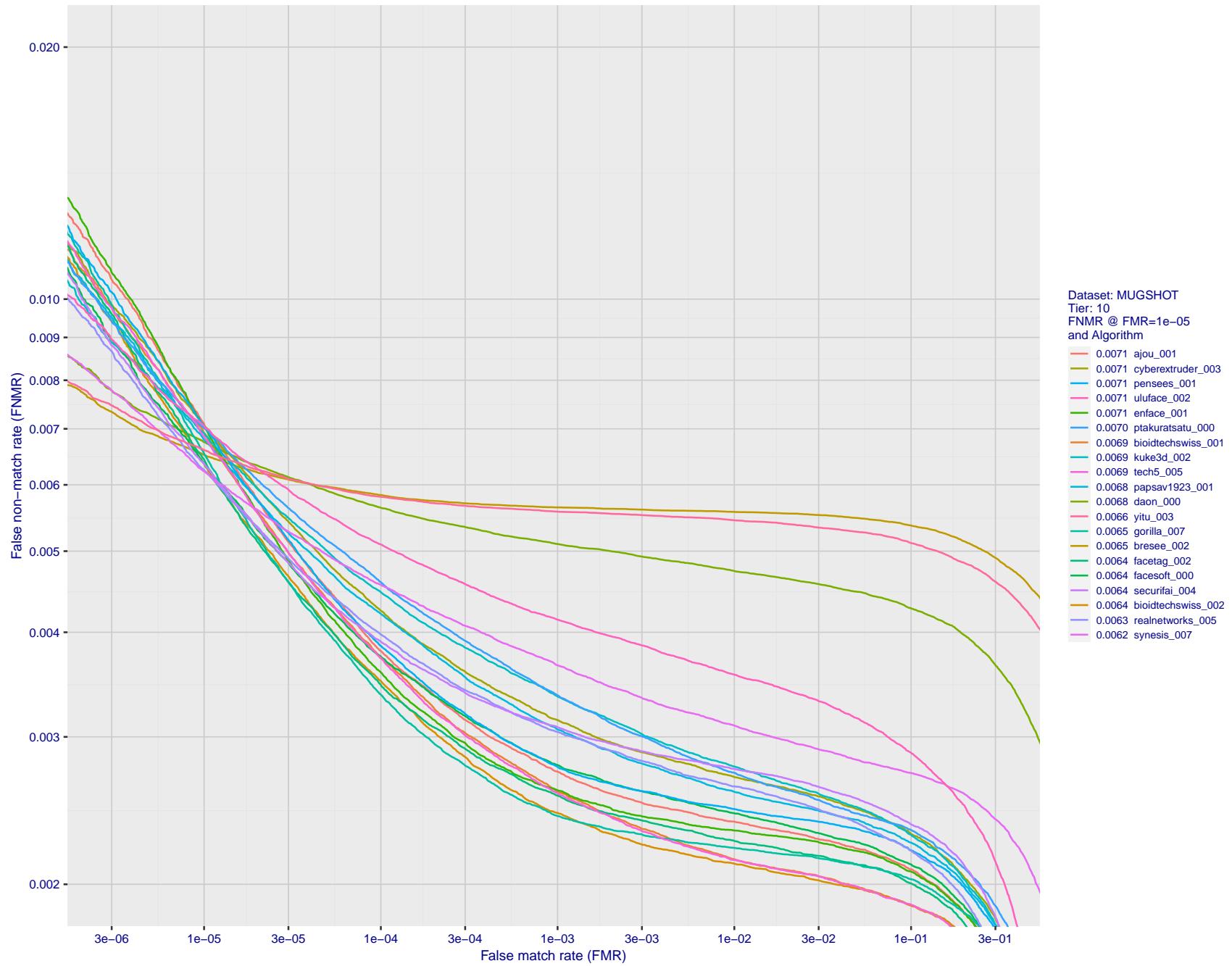


Figure 73: For the mugshot images, detection error tradeoff (DET) characteristics showing false non-match rate vs. false match rate plotted parametrically on threshold,  $T$ . The scales are logarithmic in order to show decades of FMR.

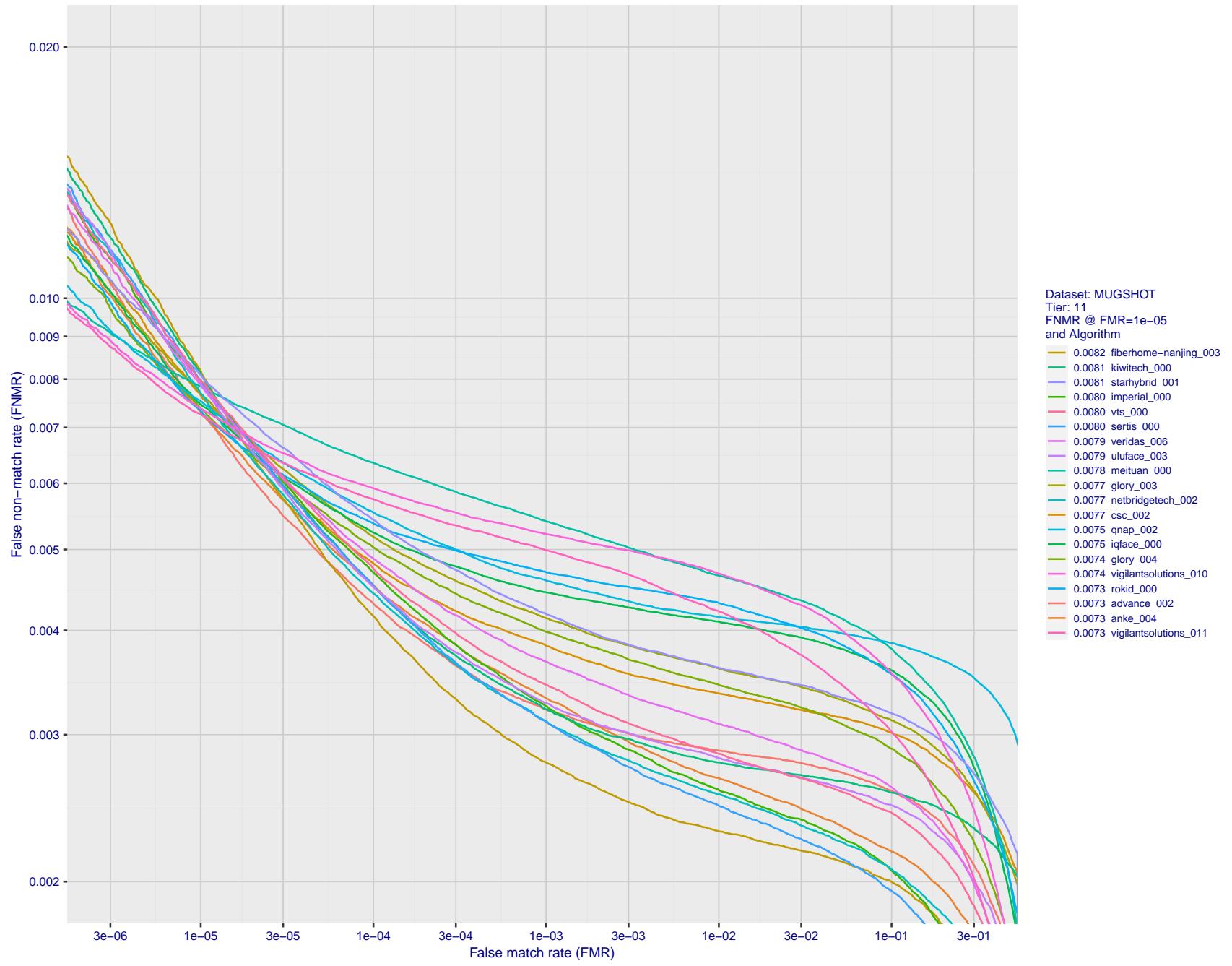


Figure 74: For the mugshot images, detection error tradeoff (DET) characteristics showing false non-match rate vs. false match rate plotted parametrically on threshold,  $T$ . The scales are logarithmic in order to show decades of FMR.

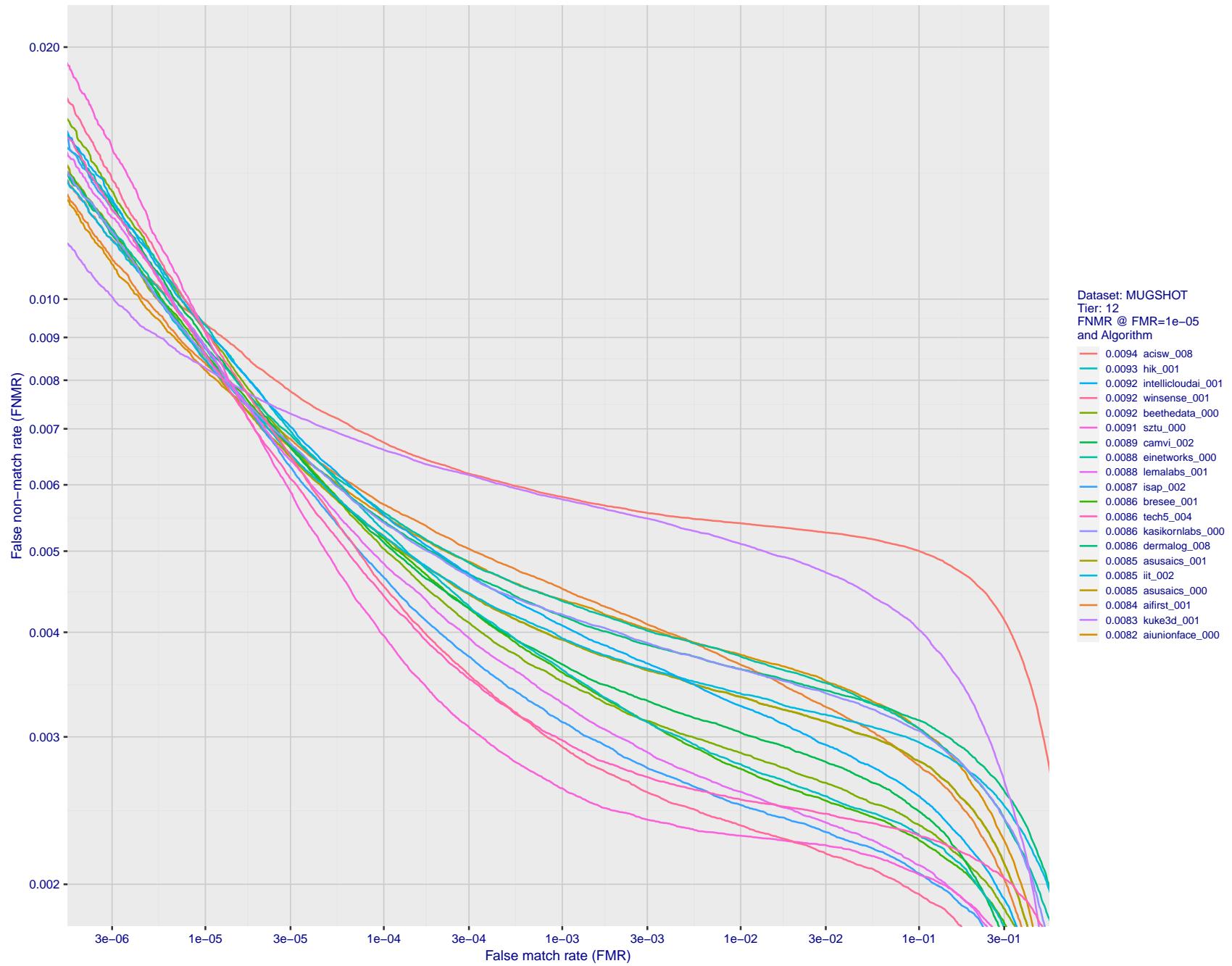


Figure 75: For the mugshot images, detection error tradeoff (DET) characteristics showing false non-match rate vs. false match rate plotted parametrically on threshold, T. The scales are logarithmic in order to show decades of FMR.

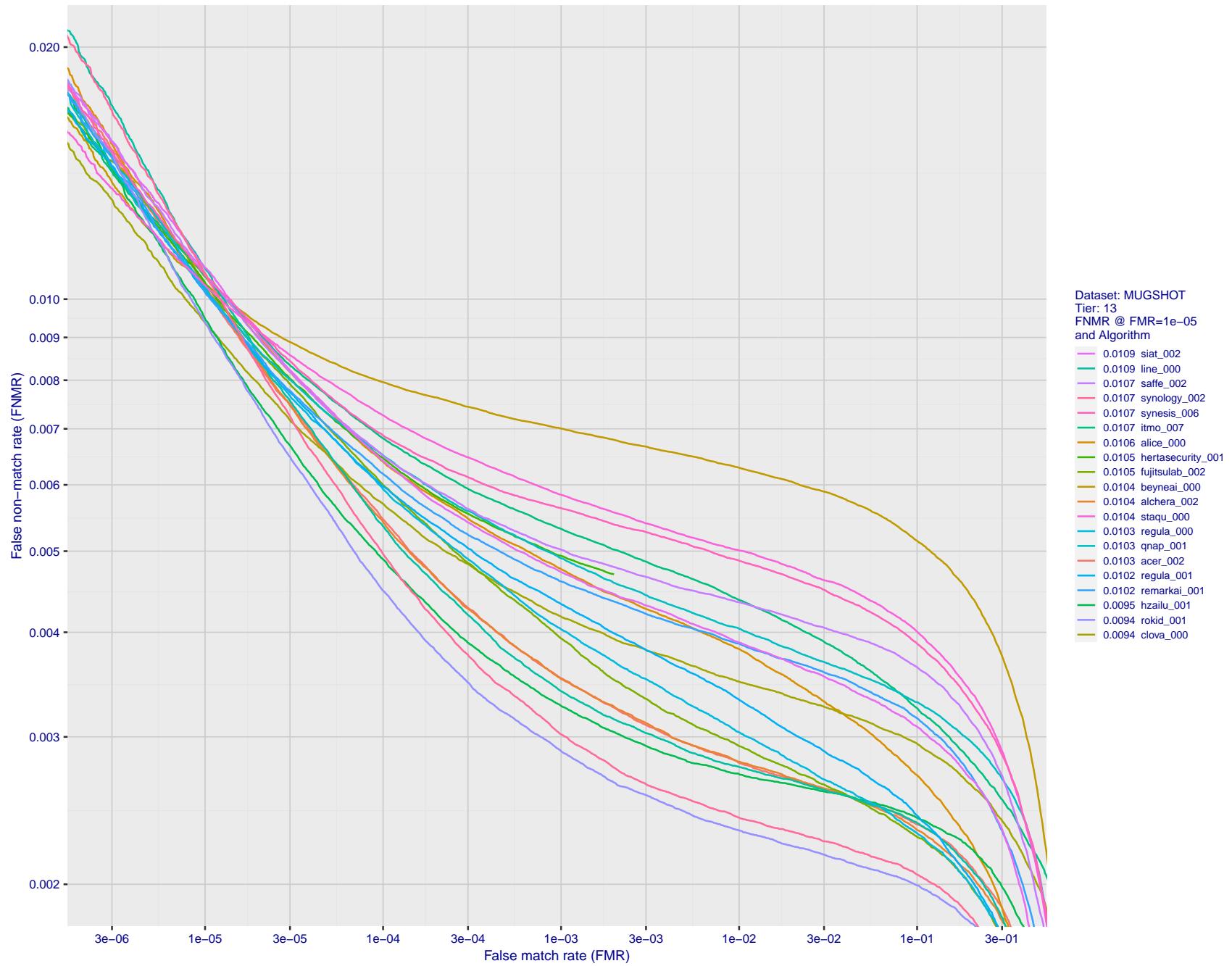


Figure 76: For the mugshot images, detection error tradeoff (DET) characteristics showing false non-match rate vs. false match rate plotted parametrically on threshold,  $T$ . The scales are logarithmic in order to show decades of FMR.

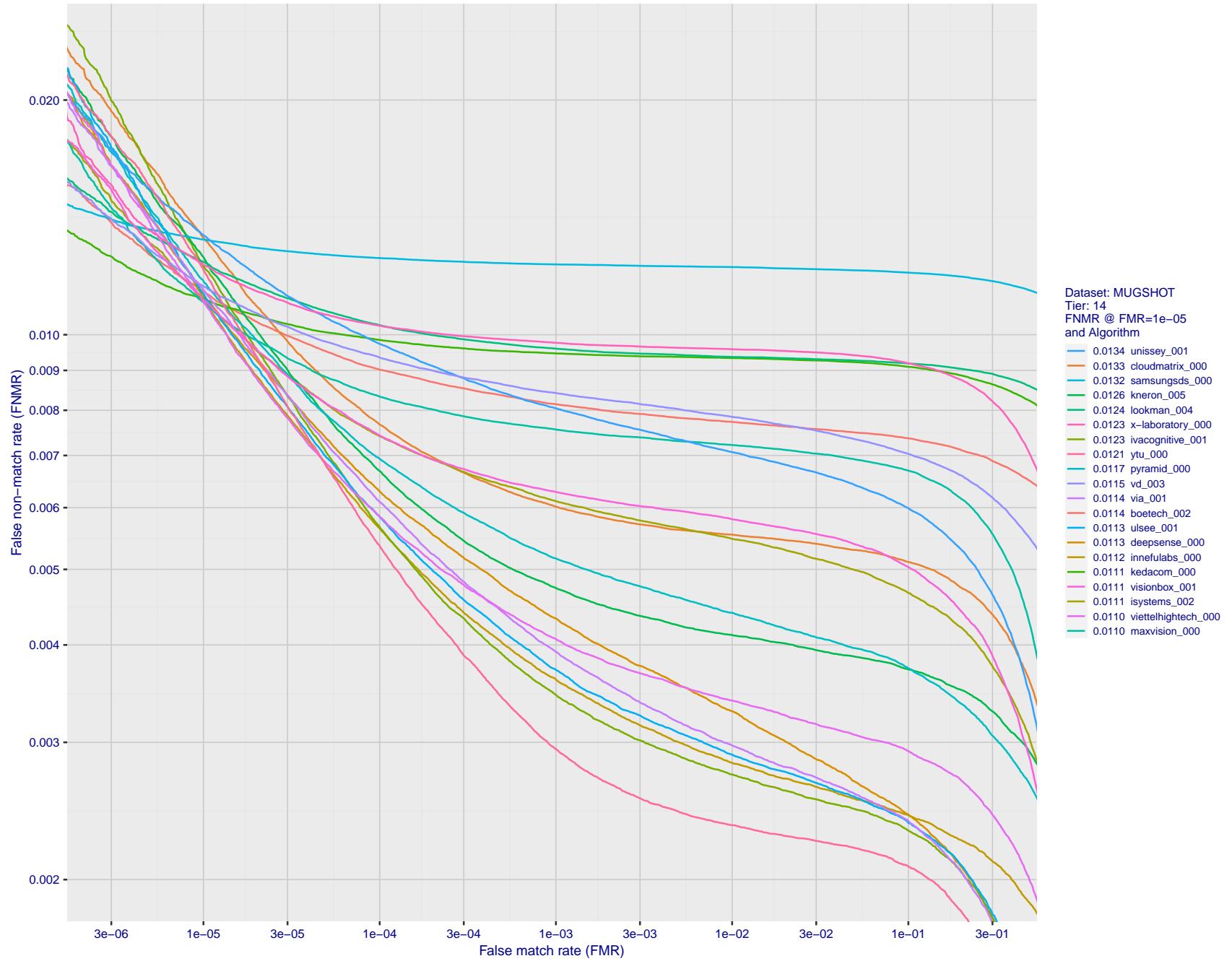


Figure 77: For the mugshot images, detection error tradeoff (DET) characteristics showing false non-match rate vs. false match rate plotted parametrically on threshold,  $T$ . The scales are logarithmic in order to show decades of FMR.

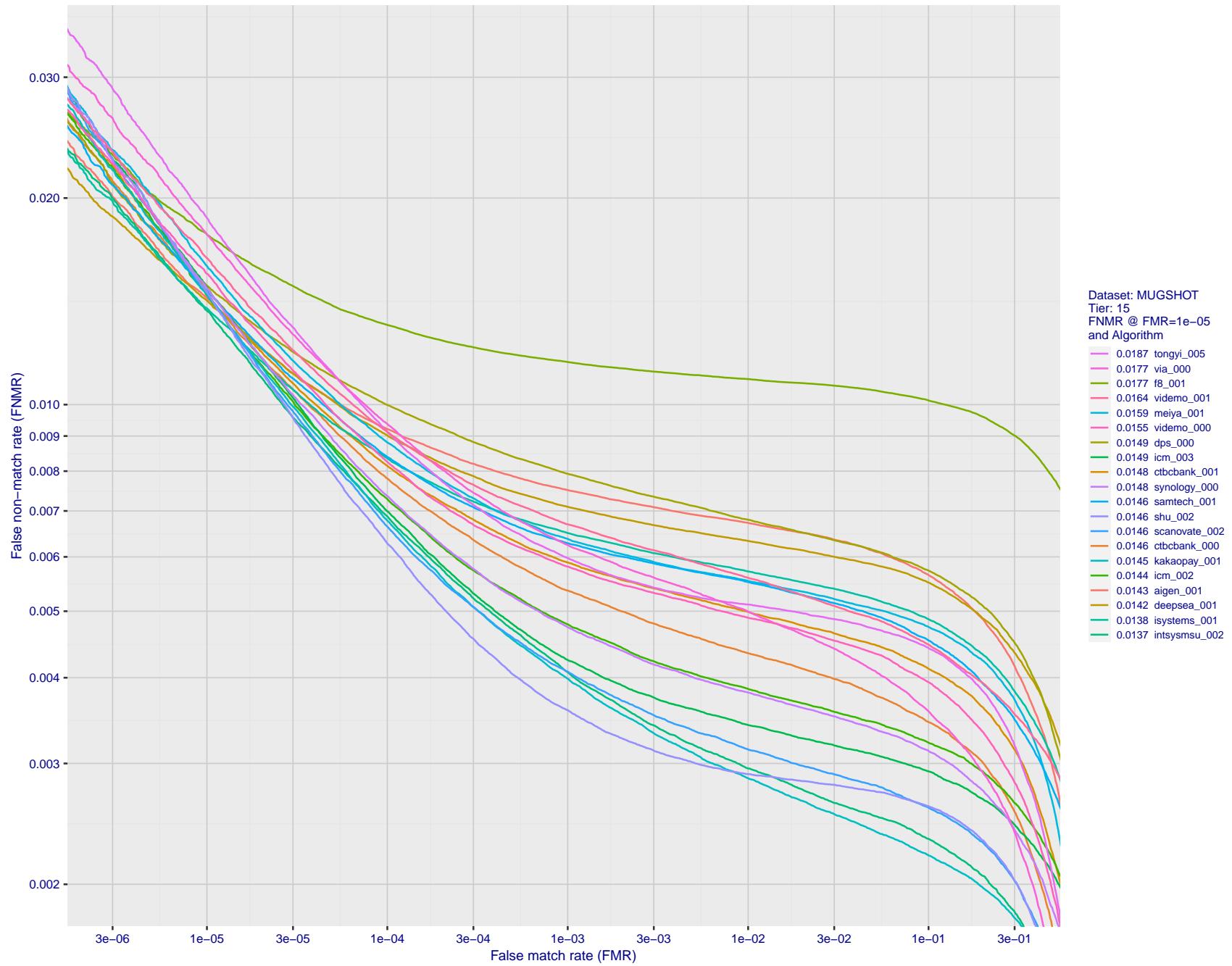


Figure 78: For the mugshot images, detection error tradeoff (DET) characteristics showing false non-match rate vs. false match rate plotted parametrically on threshold,  $T$ . The scales are logarithmic in order to show decades of FMR.

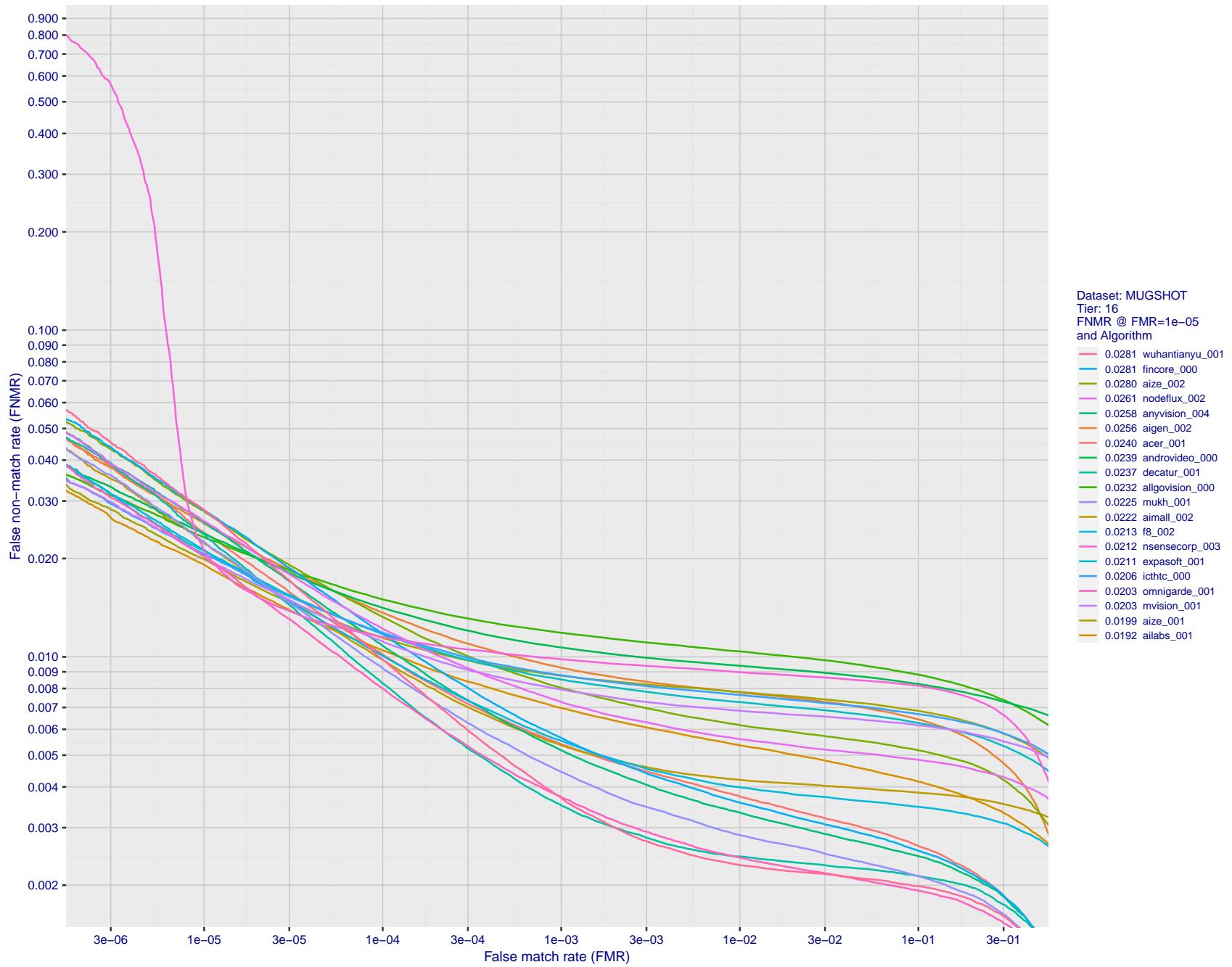


Figure 79: For the mugshot images, detection error tradeoff (DET) characteristics showing false non-match rate vs. false match rate plotted parametrically on threshold,  $T$ . The scales are logarithmic in order to show decades of FMR.

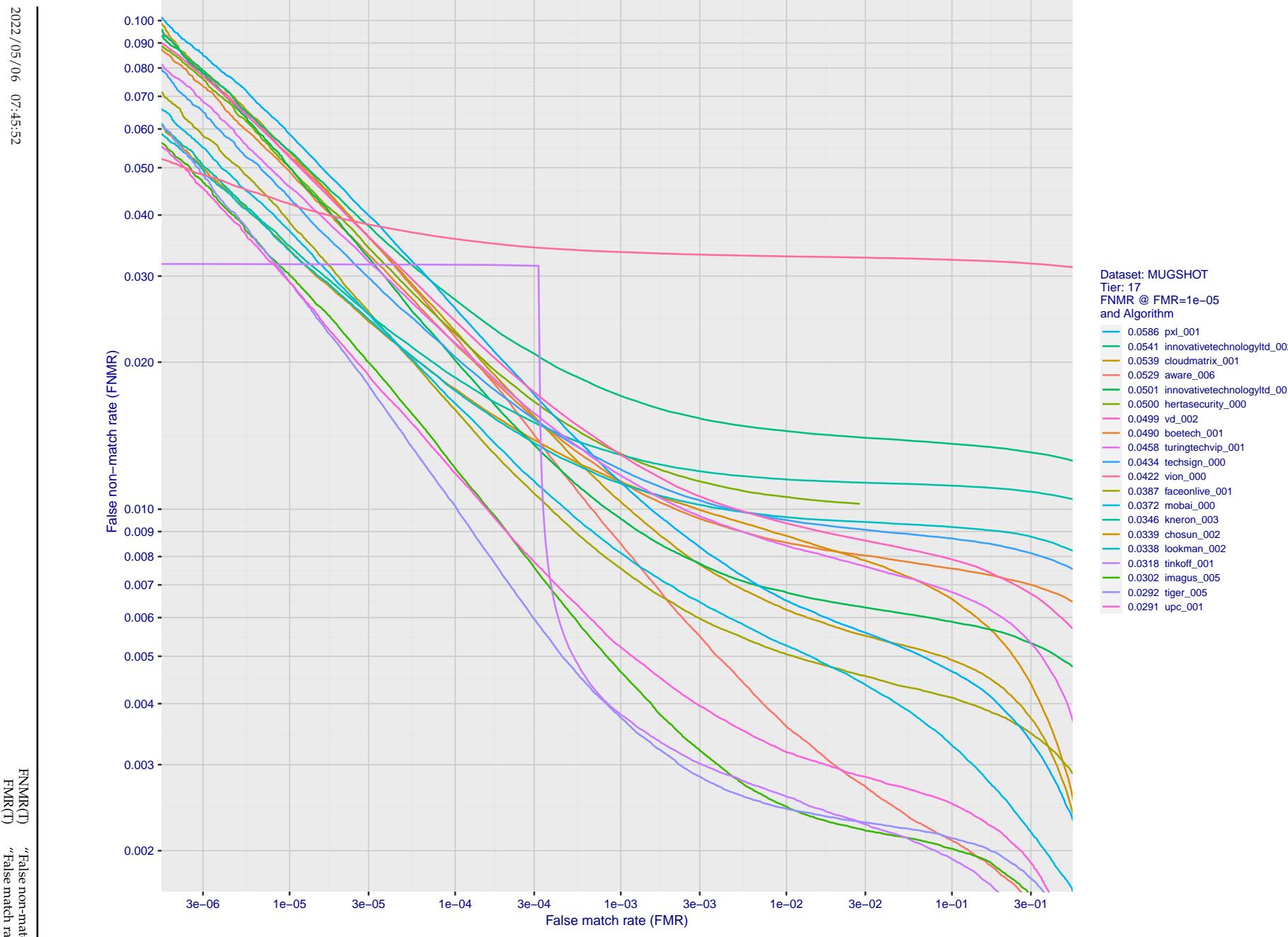


Figure 80: For the mugshot images, detection error tradeoff (DET) characteristics showing false non-match rate vs. false match rate plotted parametrically on threshold,  $T$ . The scales are logarithmic in order to show decades of FMR.

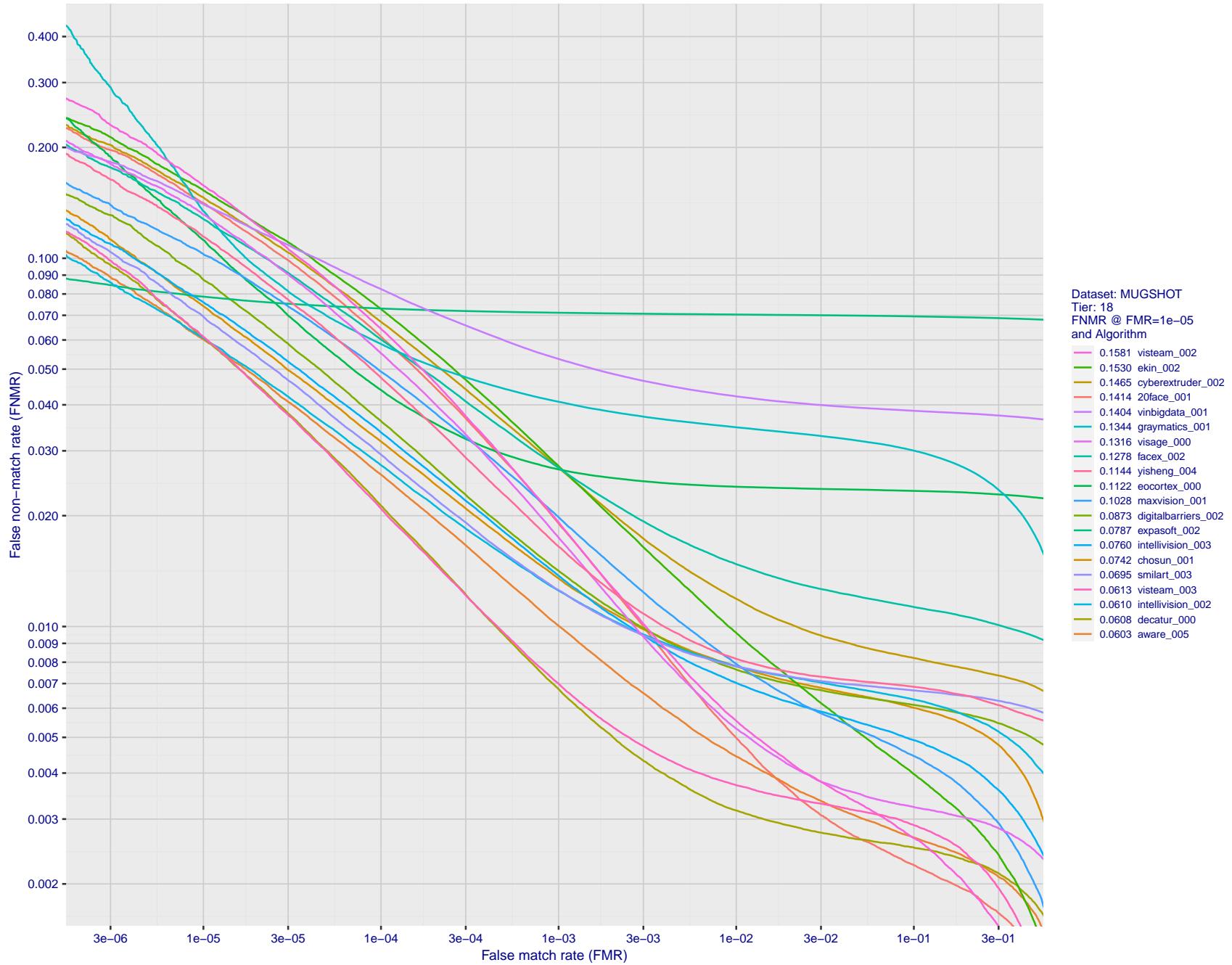


Figure 81: For the mugshot images, detection error tradeoff (DET) characteristics showing false non-match rate vs. false match rate plotted parametrically on threshold,  $T$ . The scales are logarithmic in order to show decades of FMR.

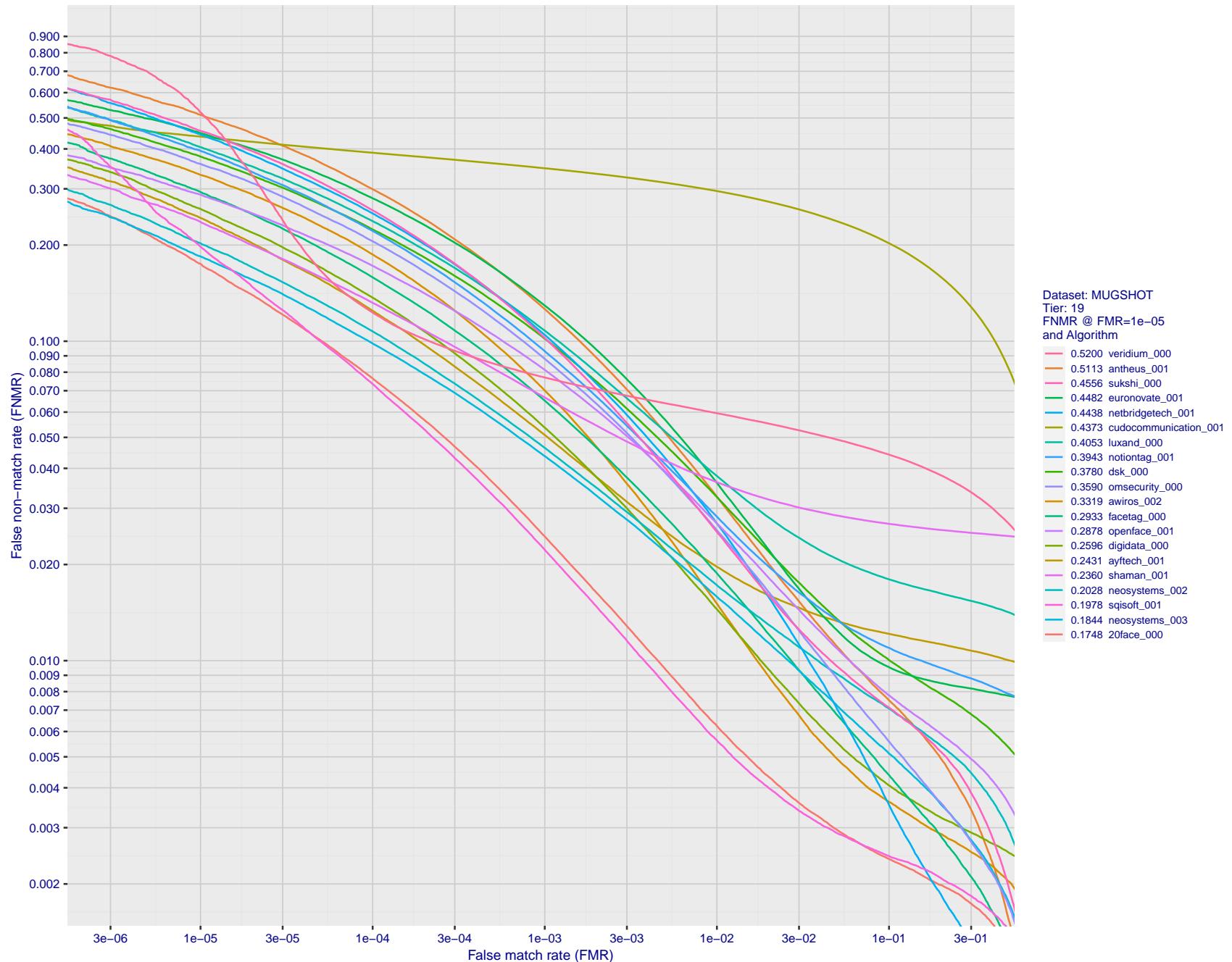


Figure 82: For the mugshot images, detection error tradeoff (DET) characteristics showing false non-match rate vs. false match rate plotted parametrically on threshold,  $T$ . The scales are logarithmic in order to show decades of FMR.

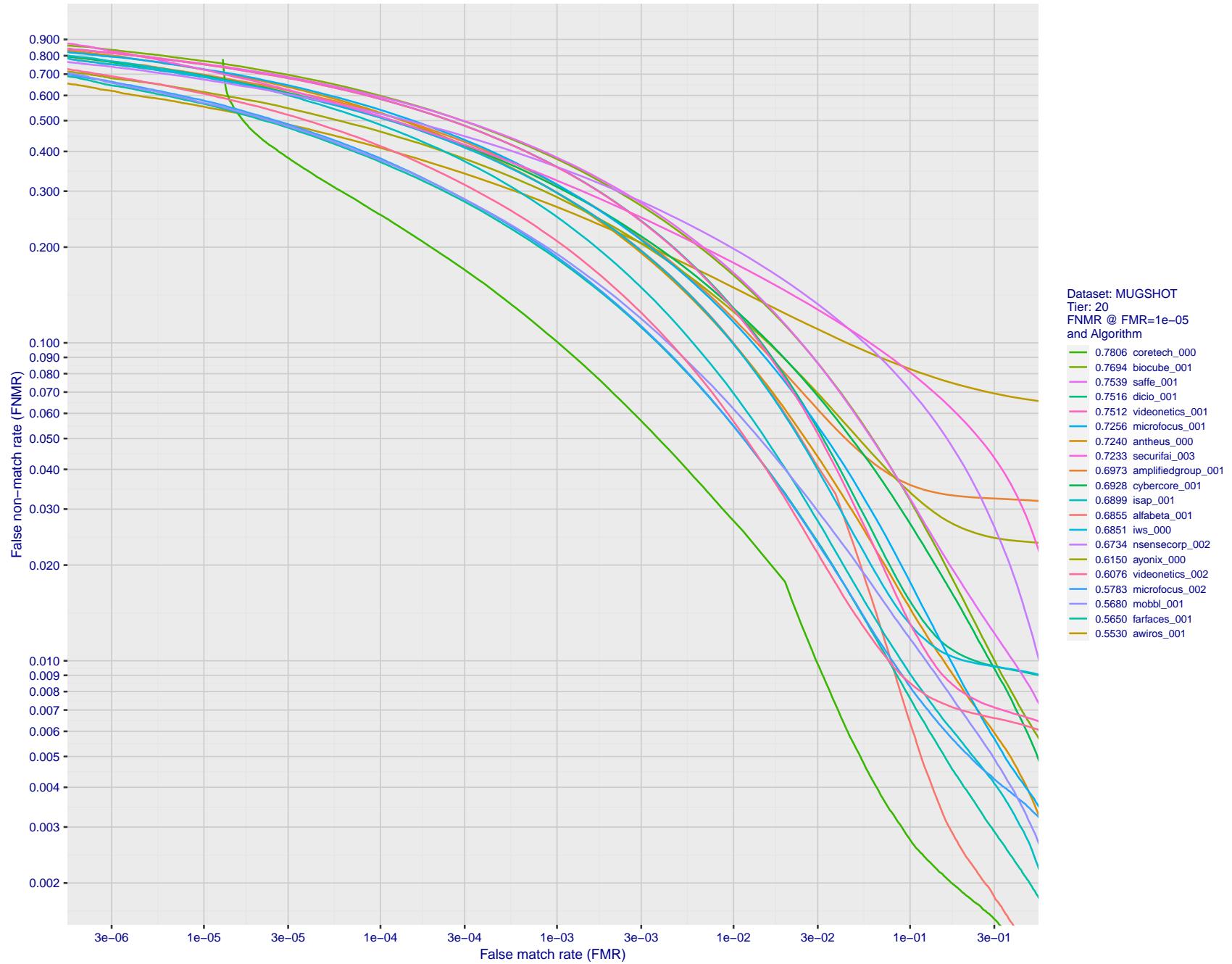


Figure 83: For the mugshot images, detection error tradeoff (DET) characteristics showing false non-match rate vs. false match rate plotted parametrically on threshold,  $T$ . The scales are logarithmic in order to show decades of FMR.

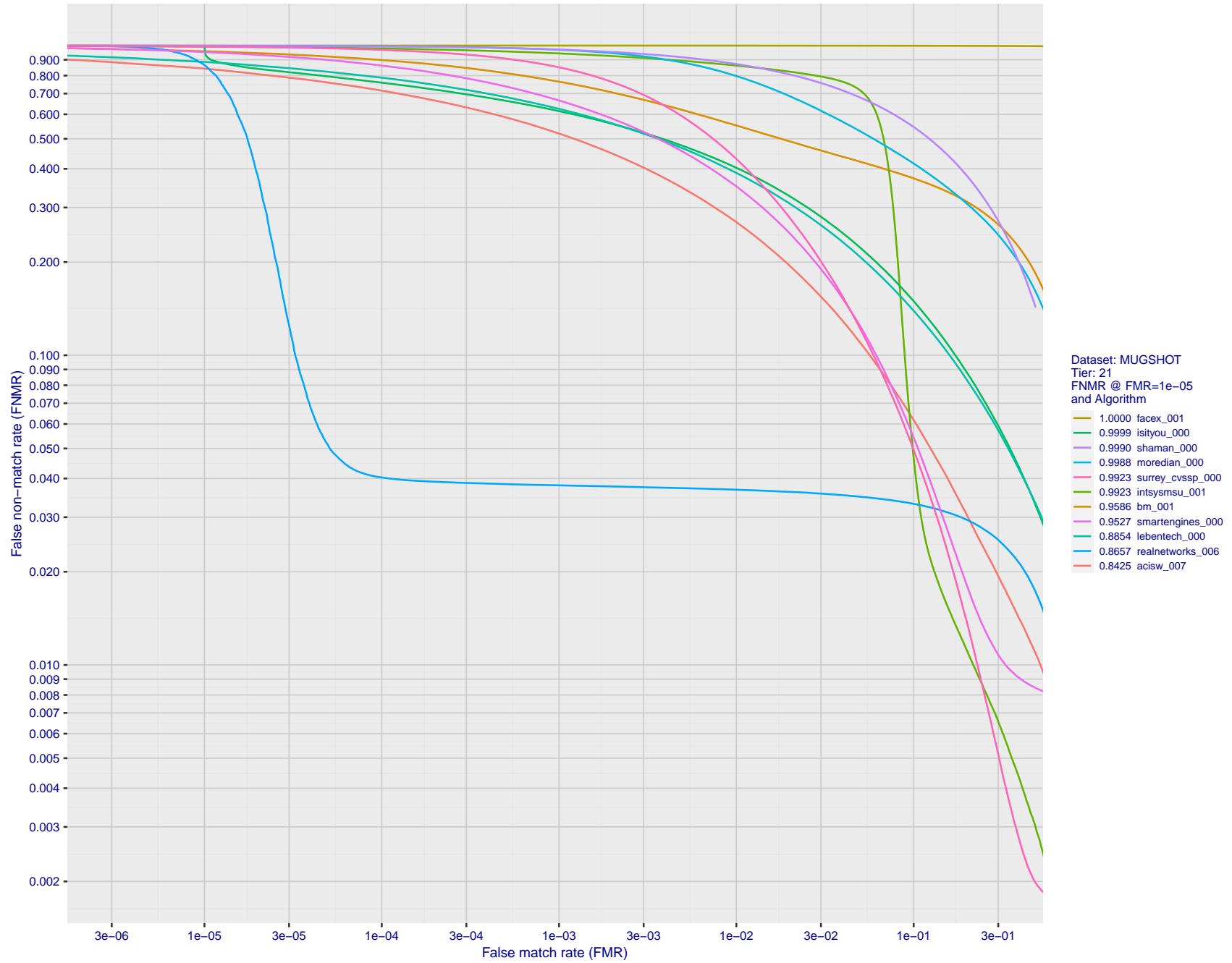


Figure 84: For the mugshot images, detection error tradeoff (DET) characteristics showing false non-match rate vs. false match rate plotted parametrically on threshold,  $T$ . The scales are logarithmic in order to show decades of FMR.

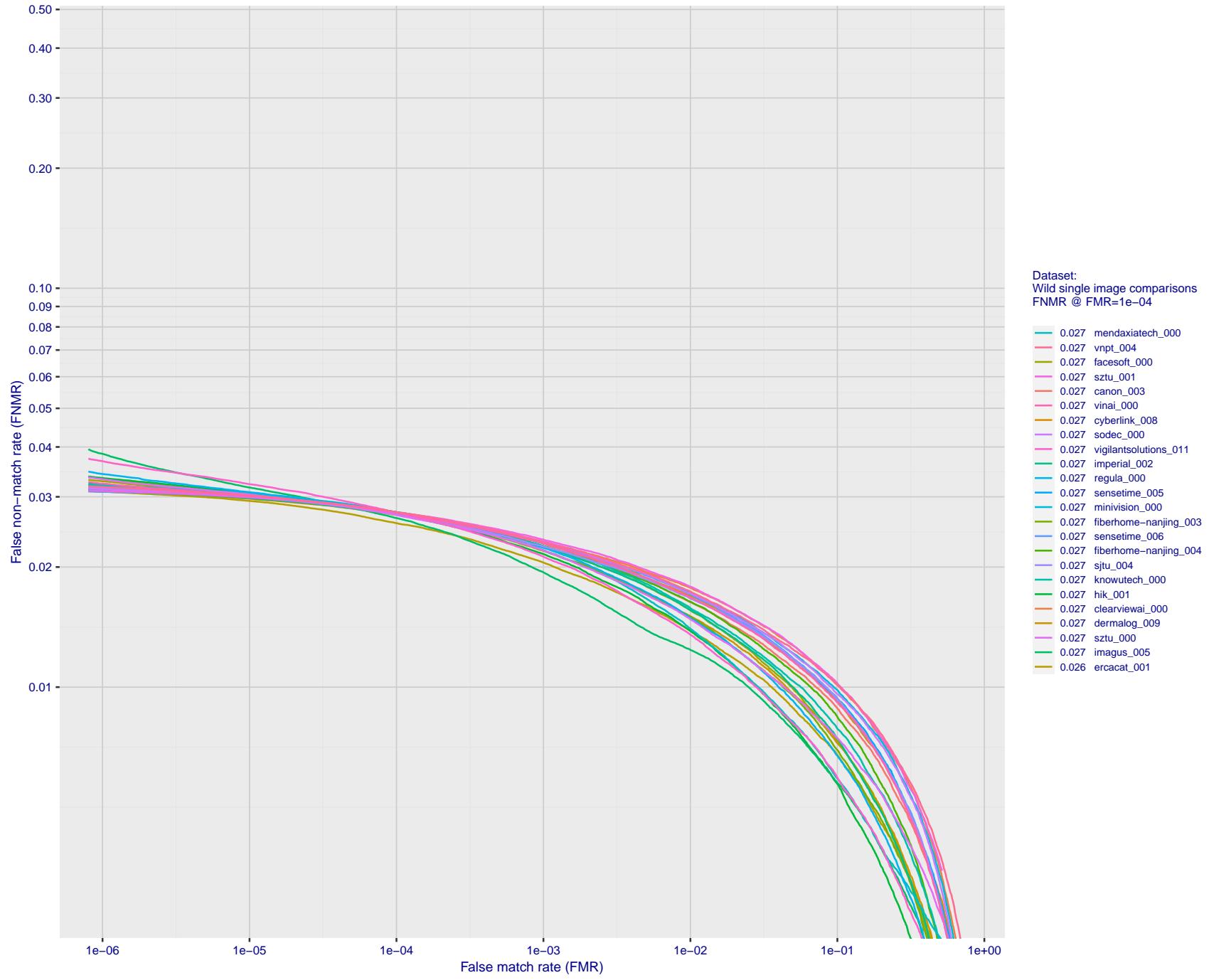


Figure 85: For the 2018 wild image comparisons, detection error tradeoff (DET) characteristics showing false non-match rate vs. false match rate plotted parametrically on threshold,  $T$ . The scales are logarithmic in order to show several decades of FMR.

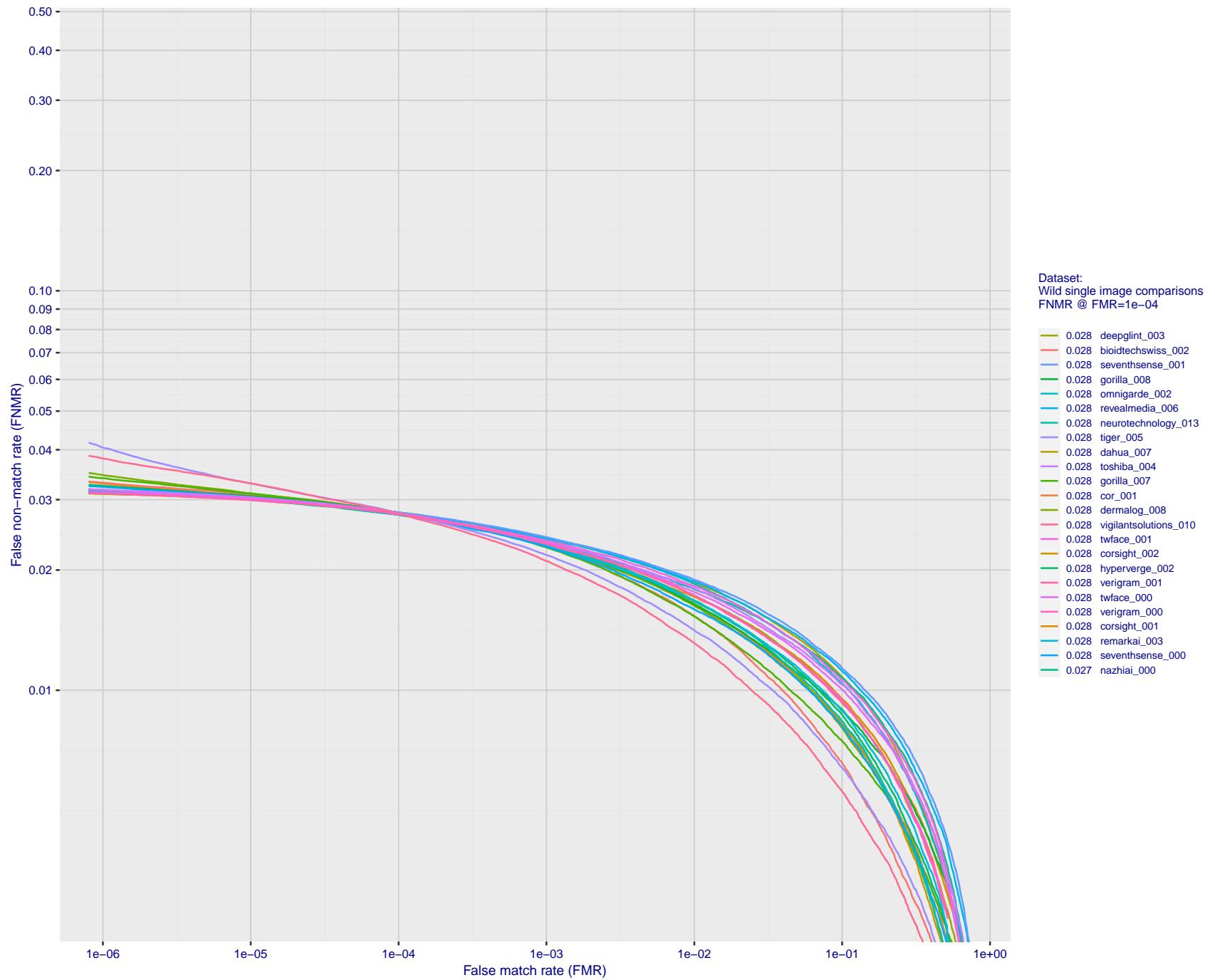


Figure 86: For the 2018 wild image comparisons, detection error tradeoff (DET) characteristics showing false non-match rate vs. false match rate plotted parametrically on threshold,  $T$ . The scales are logarithmic in order to show several decades of FMR.

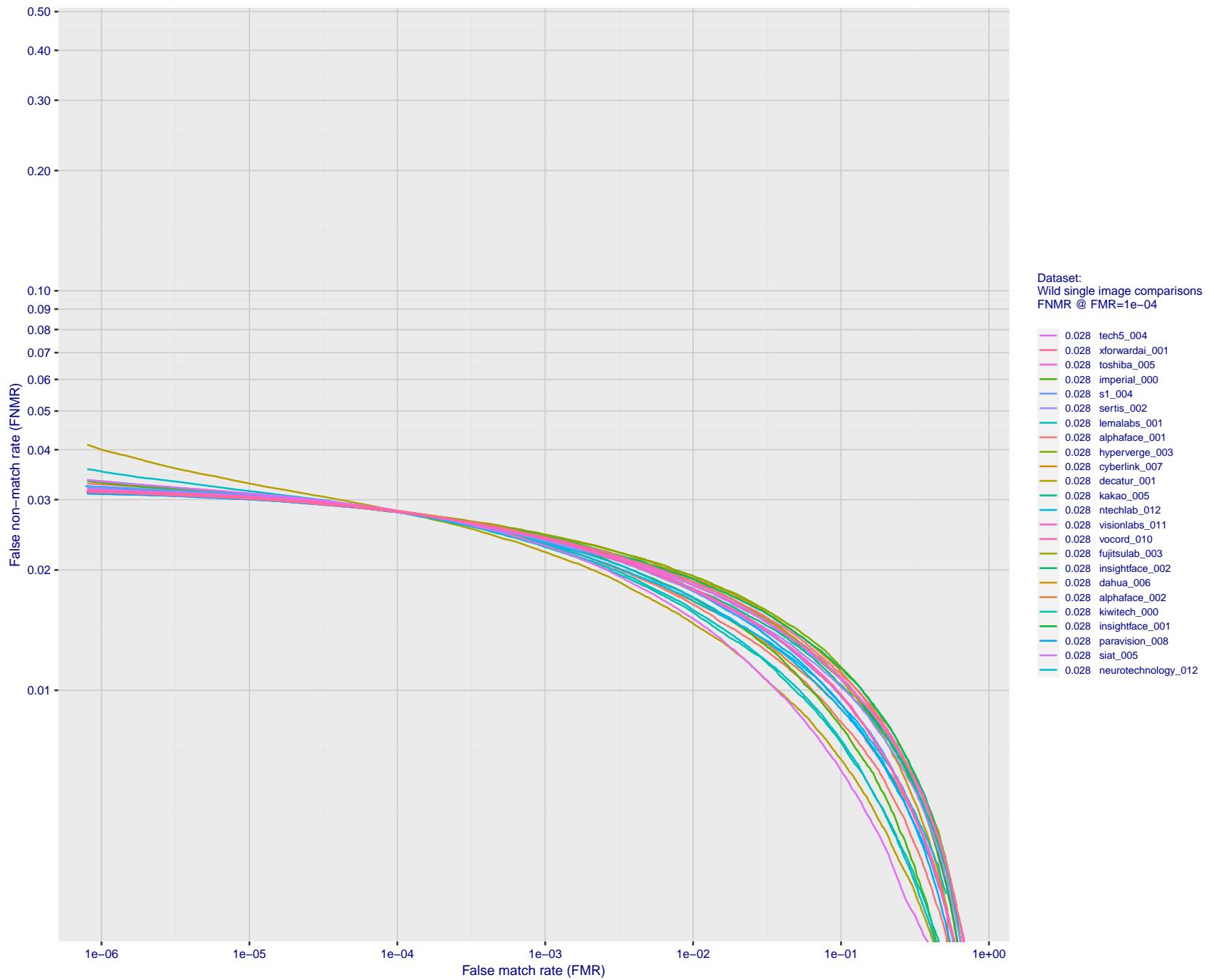


Figure 87: For the 2018 wild image comparisons, detection error tradeoff (DET) characteristics showing false non-match rate vs. false match rate plotted parametrically on threshold,  $T$ . The scales are logarithmic in order to show several decades of FMR.

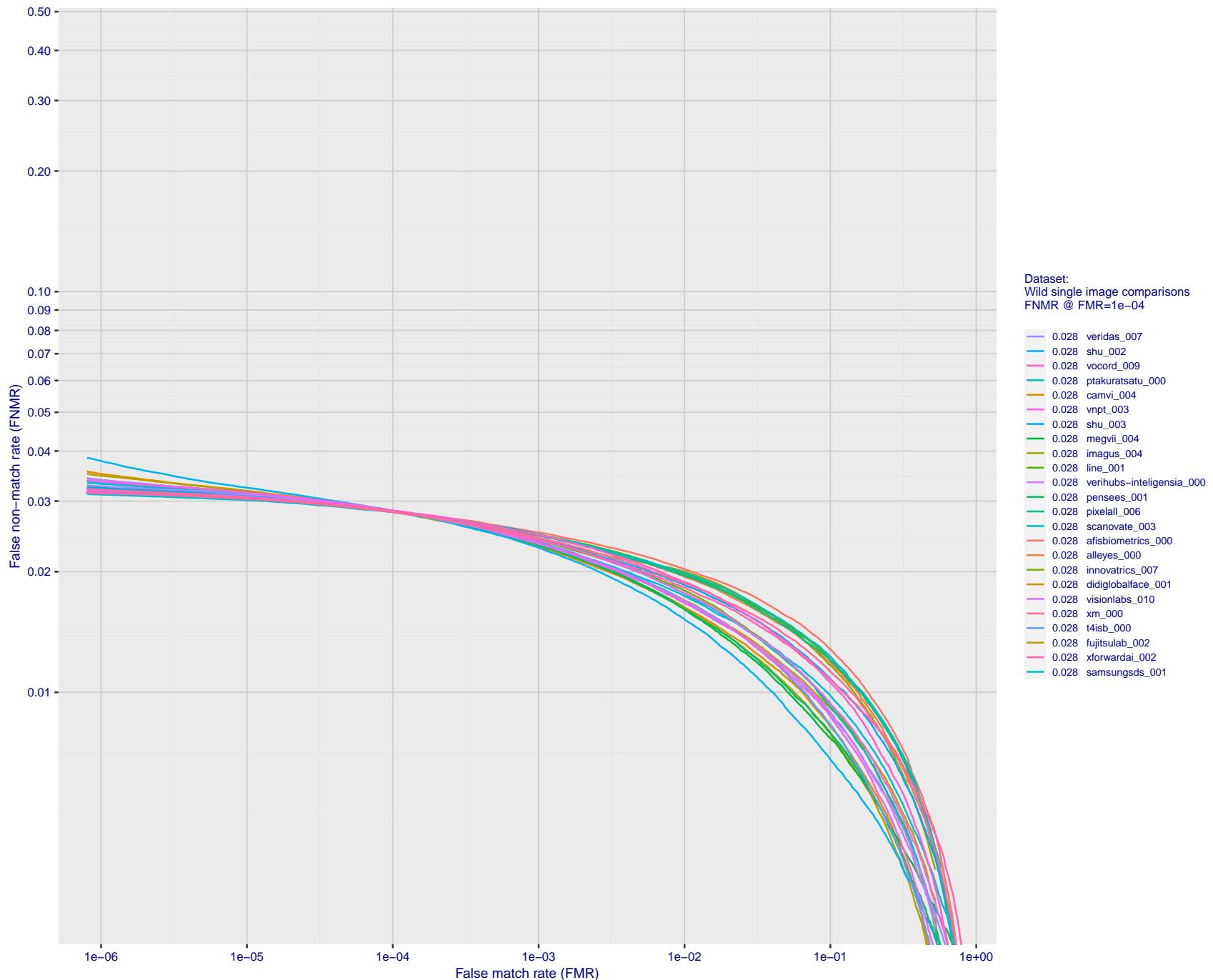


Figure 88: For the 2018 wild image comparisons, detection error tradeoff (DET) characteristics showing false non-match rate vs. false match rate plotted parametrically on threshold,  $T$ . The scales are logarithmic in order to show several decades of FMR.

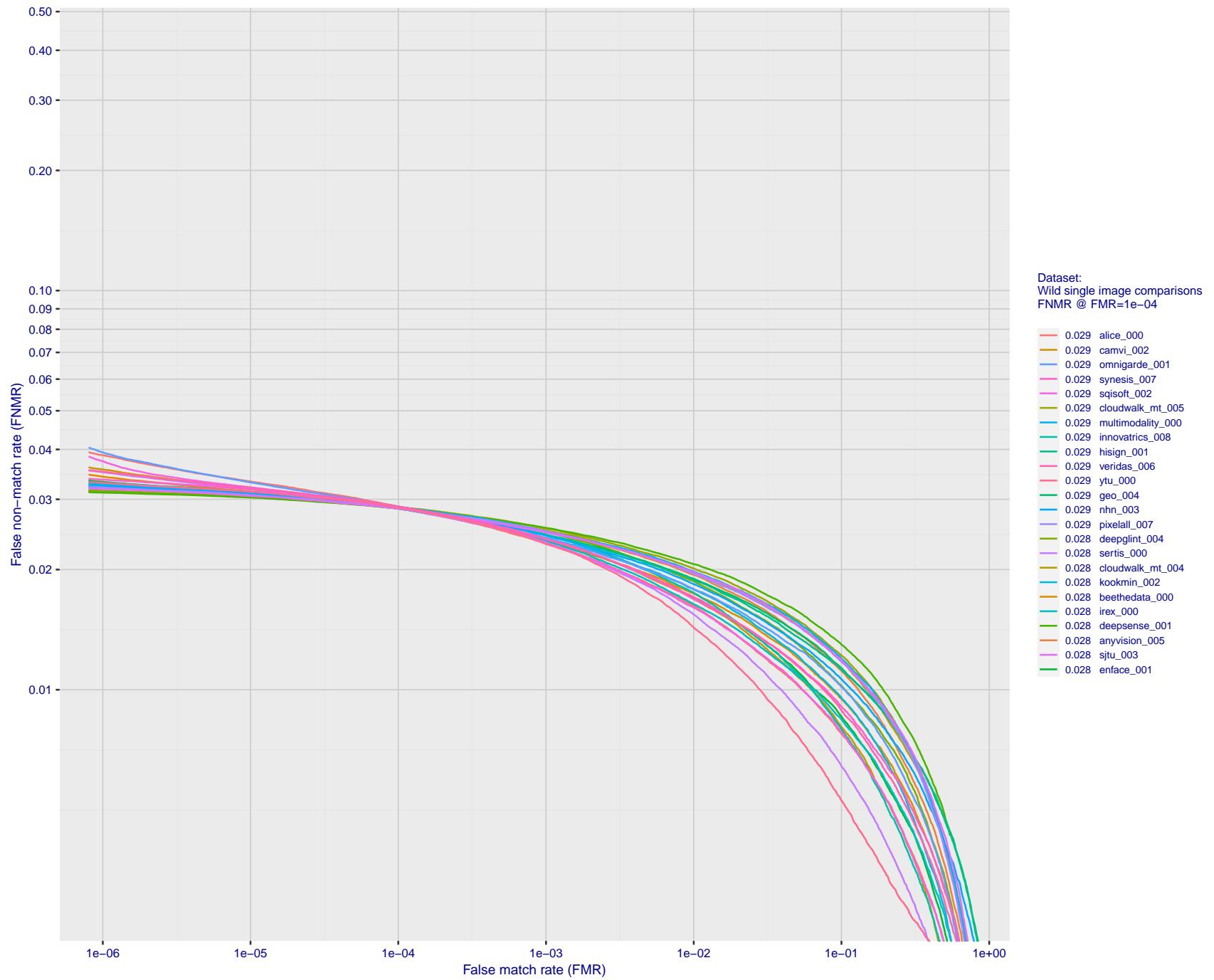


Figure 89: For the 2018 wild image comparisons, detection error tradeoff (DET) characteristics showing false non-match rate vs. false match rate plotted parametrically on threshold,  $T$ . The scales are logarithmic in order to show several decades of FMR.

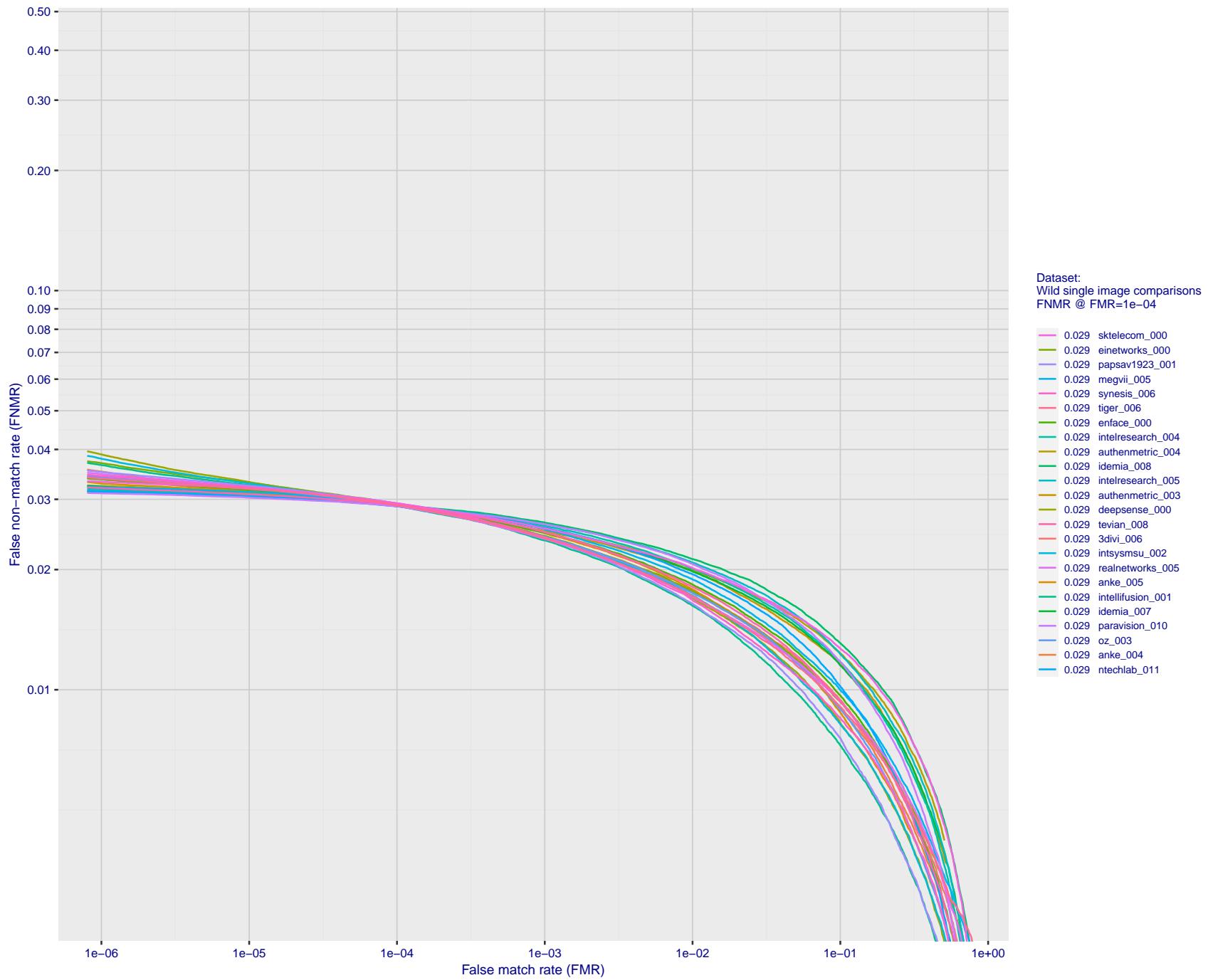


Figure 90: For the 2018 wild image comparisons, detection error tradeoff (DET) characteristics showing false non-match rate vs. false match rate plotted parametrically on threshold,  $T$ . The scales are logarithmic in order to show several decades of FMR.

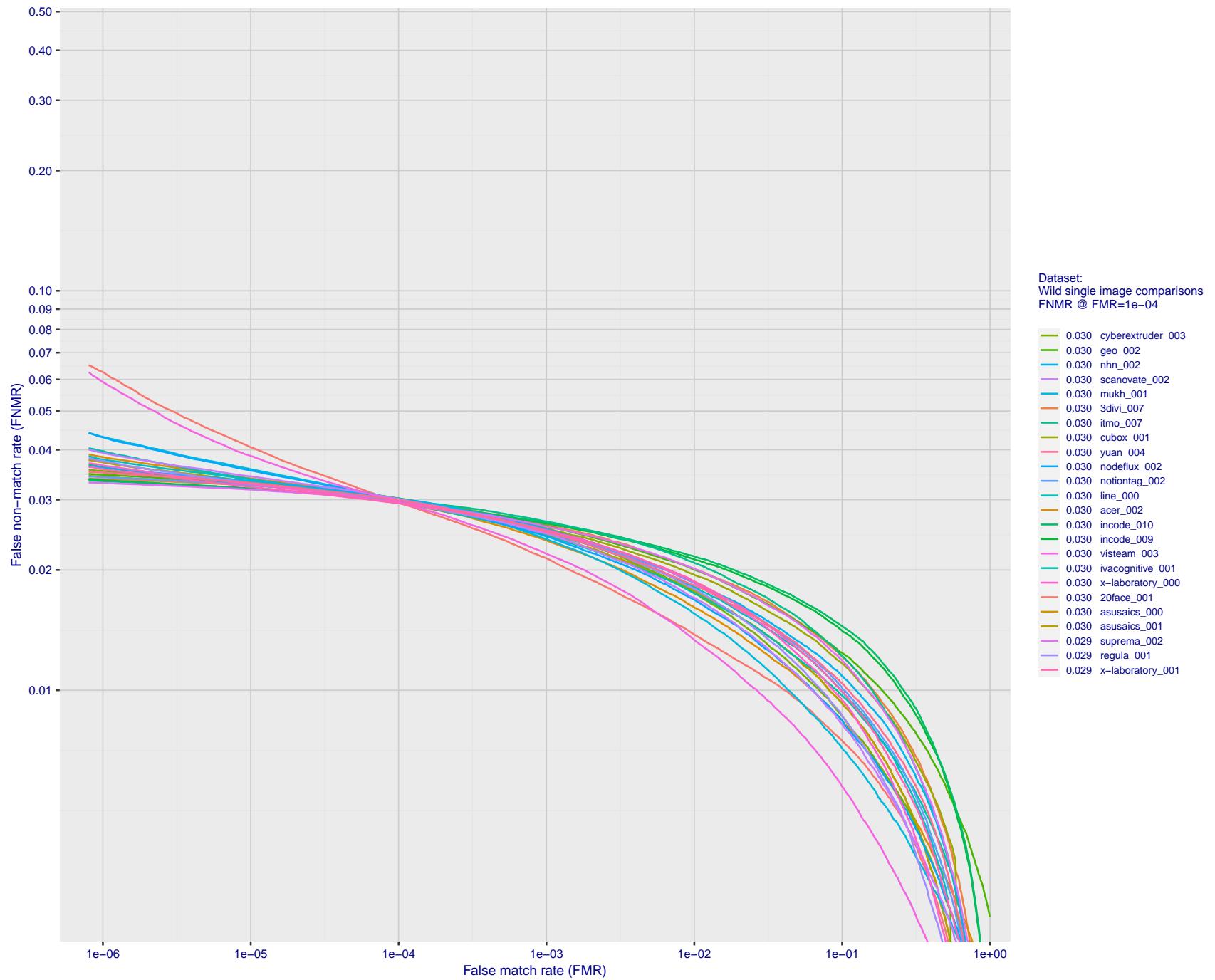


Figure 91: For the 2018 wild image comparisons, detection error tradeoff (DET) characteristics showing false non-match rate vs. false match rate plotted parametrically on threshold,  $T$ . The scales are logarithmic in order to show several decades of FMR.

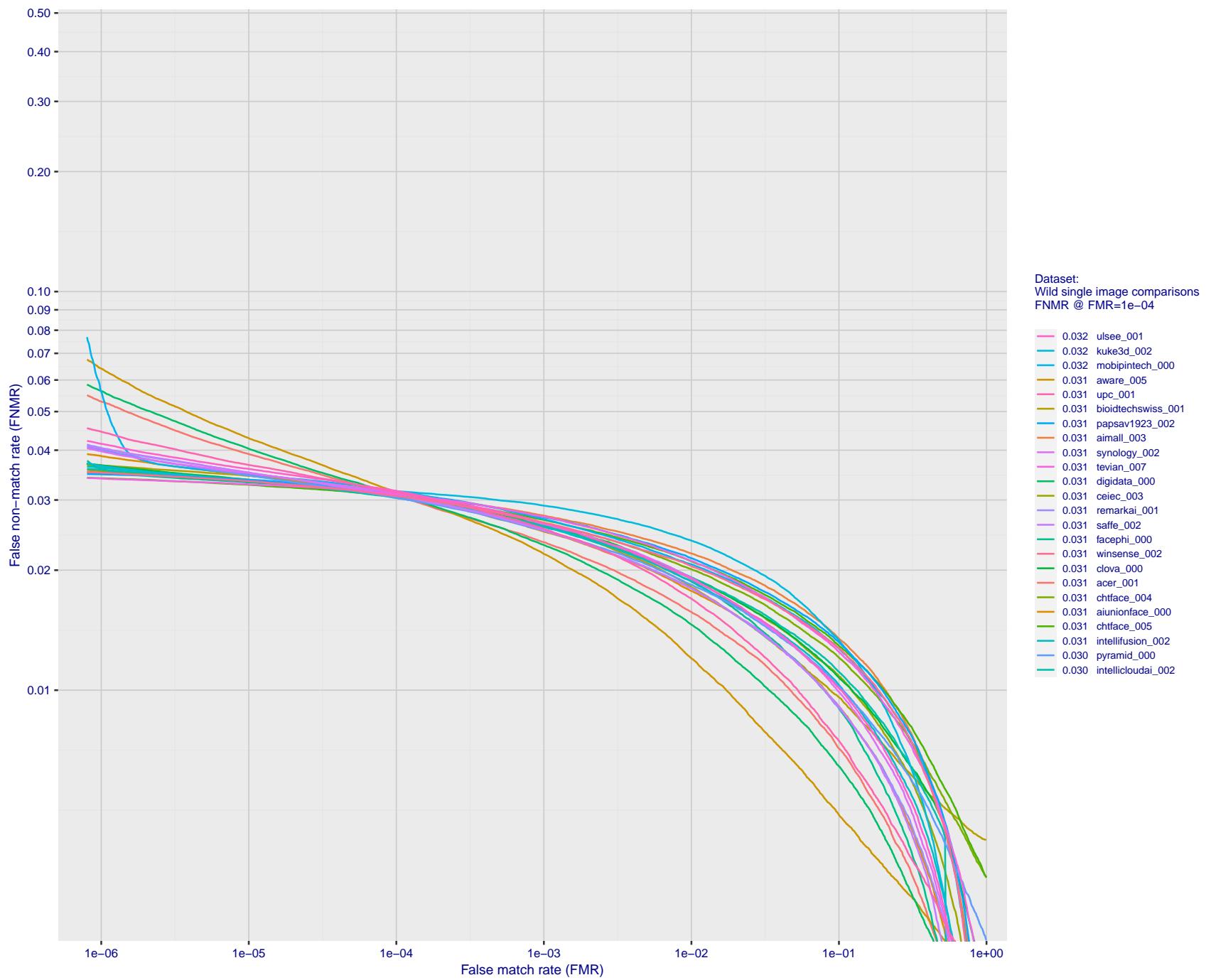


Figure 92: For the 2018 wild image comparisons, detection error tradeoff (DET) characteristics showing false non-match rate vs. false match rate plotted parametrically on threshold,  $T$ . The scales are logarithmic in order to show several decades of FMR.

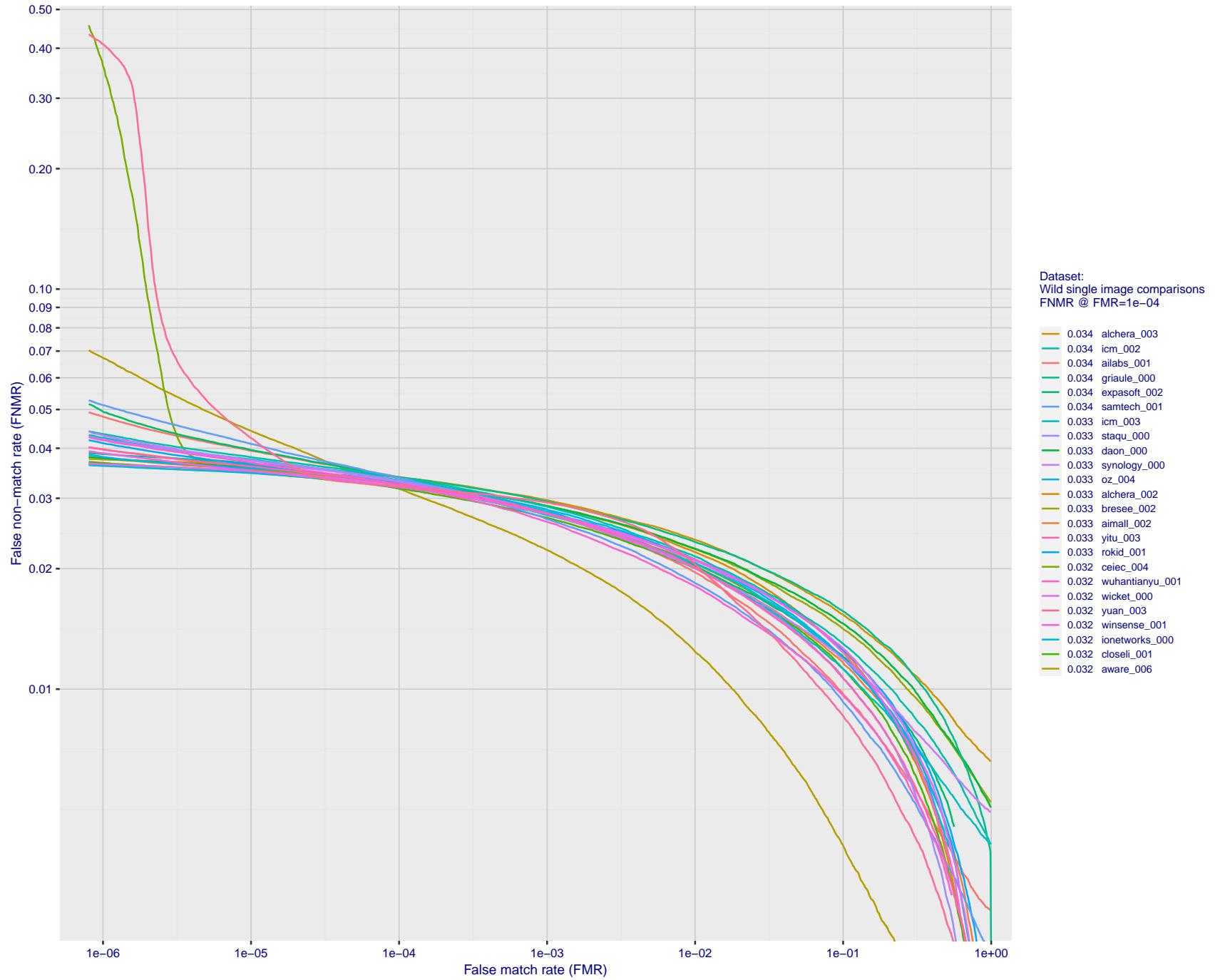


Figure 93: For the 2018 wild image comparisons, detection error tradeoff (DET) characteristics showing false non-match rate vs. false match rate plotted parametrically on threshold,  $T$ . The scales are logarithmic in order to show several decades of FMR.

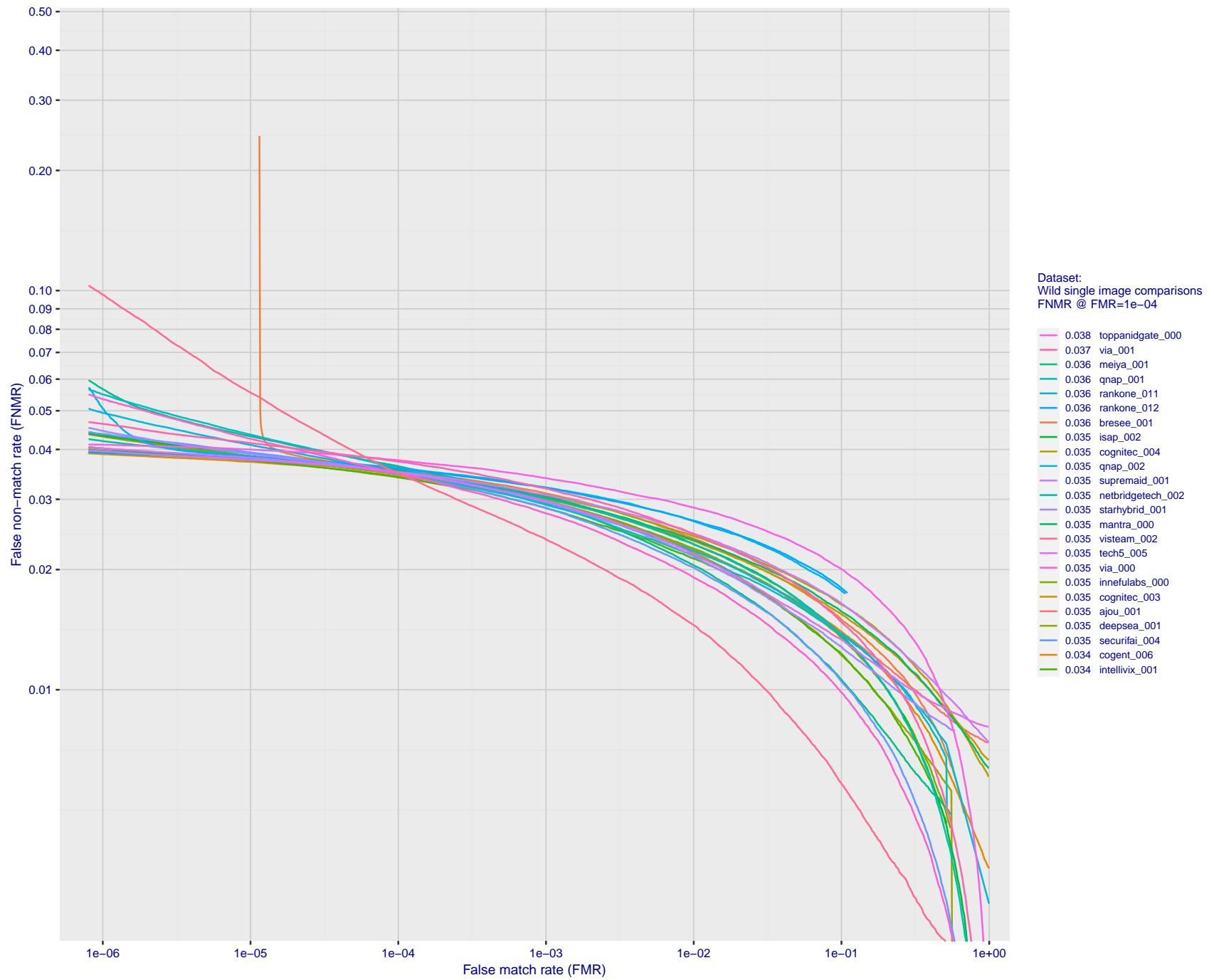


Figure 94: For the 2018 wild image comparisons, detection error tradeoff (DET) characteristics showing false non-match rate vs. false match rate plotted parametrically on threshold,  $T$ . The scales are logarithmic in order to show several decades of FMR.

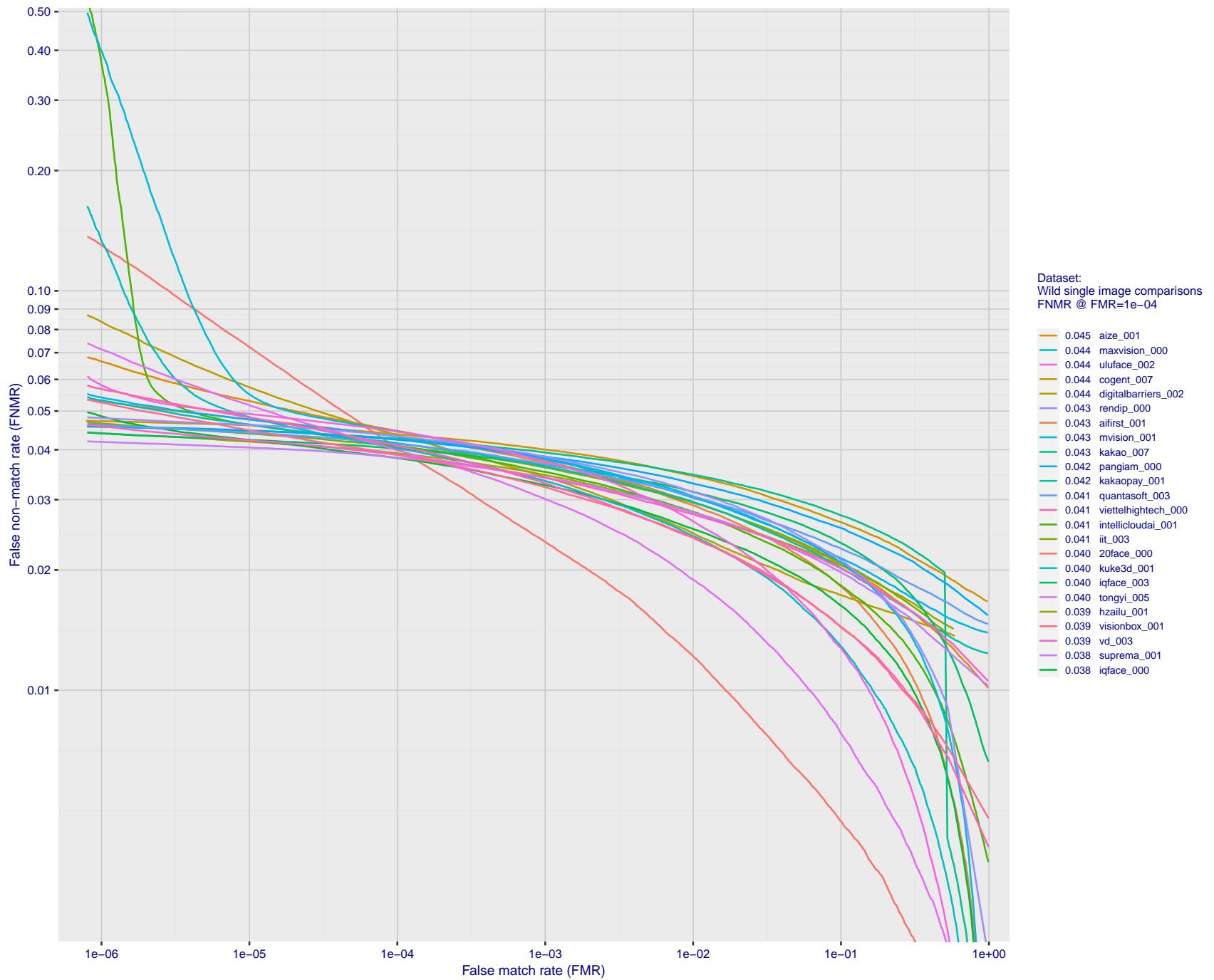


Figure 95: For the 2018 wild image comparisons, detection error tradeoff (DET) characteristics showing false non-match rate vs. false match rate plotted parametrically on threshold,  $T$ . The scales are logarithmic in order to show several decades of FMR.

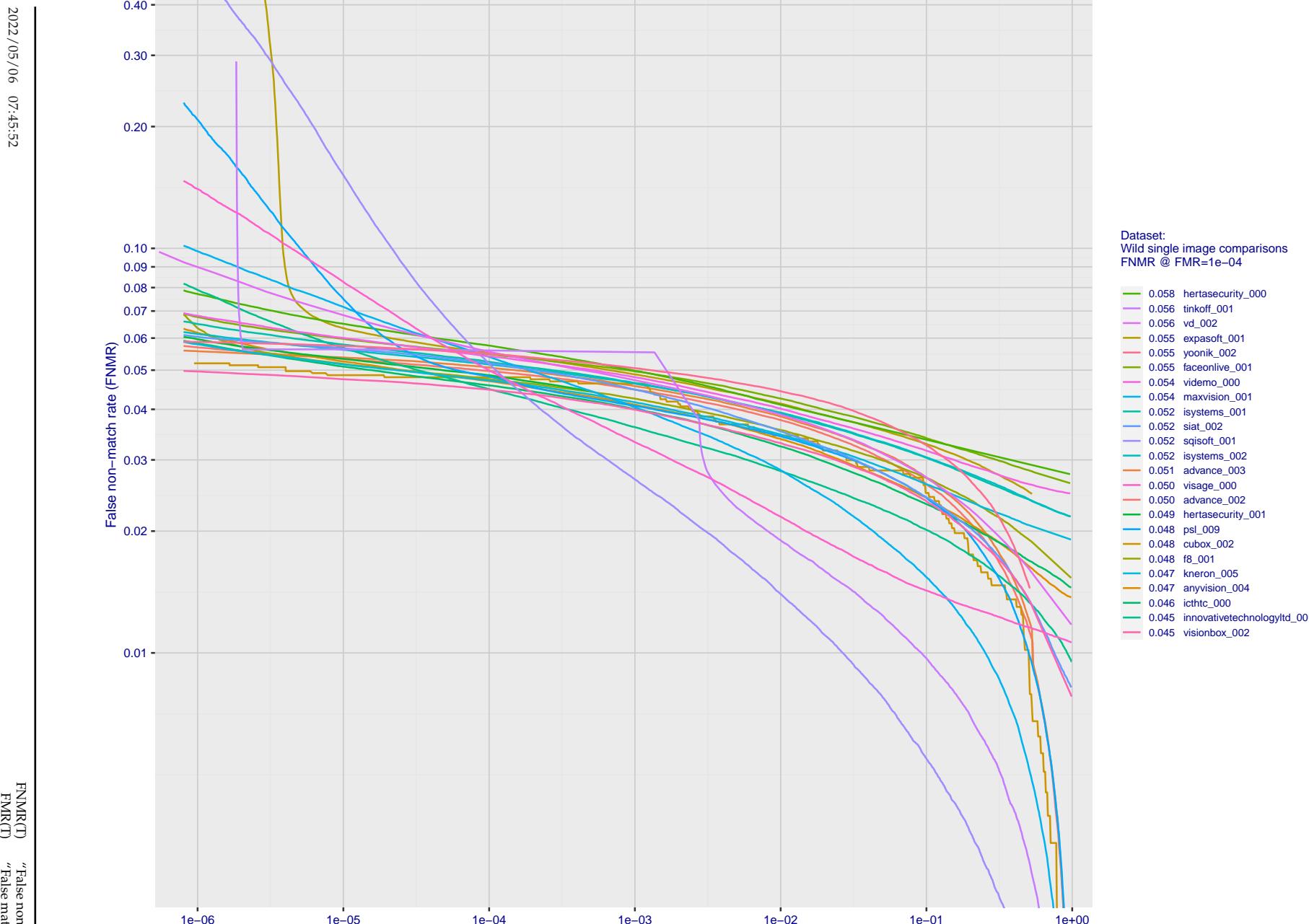


Figure 96: For the 2018 wild image comparisons, detection error tradeoff (DET) characteristics showing false non-match rate vs. false match rate plotted parametrically on threshold,  $T$ . The scales are logarithmic in order to show several decades of FMR.

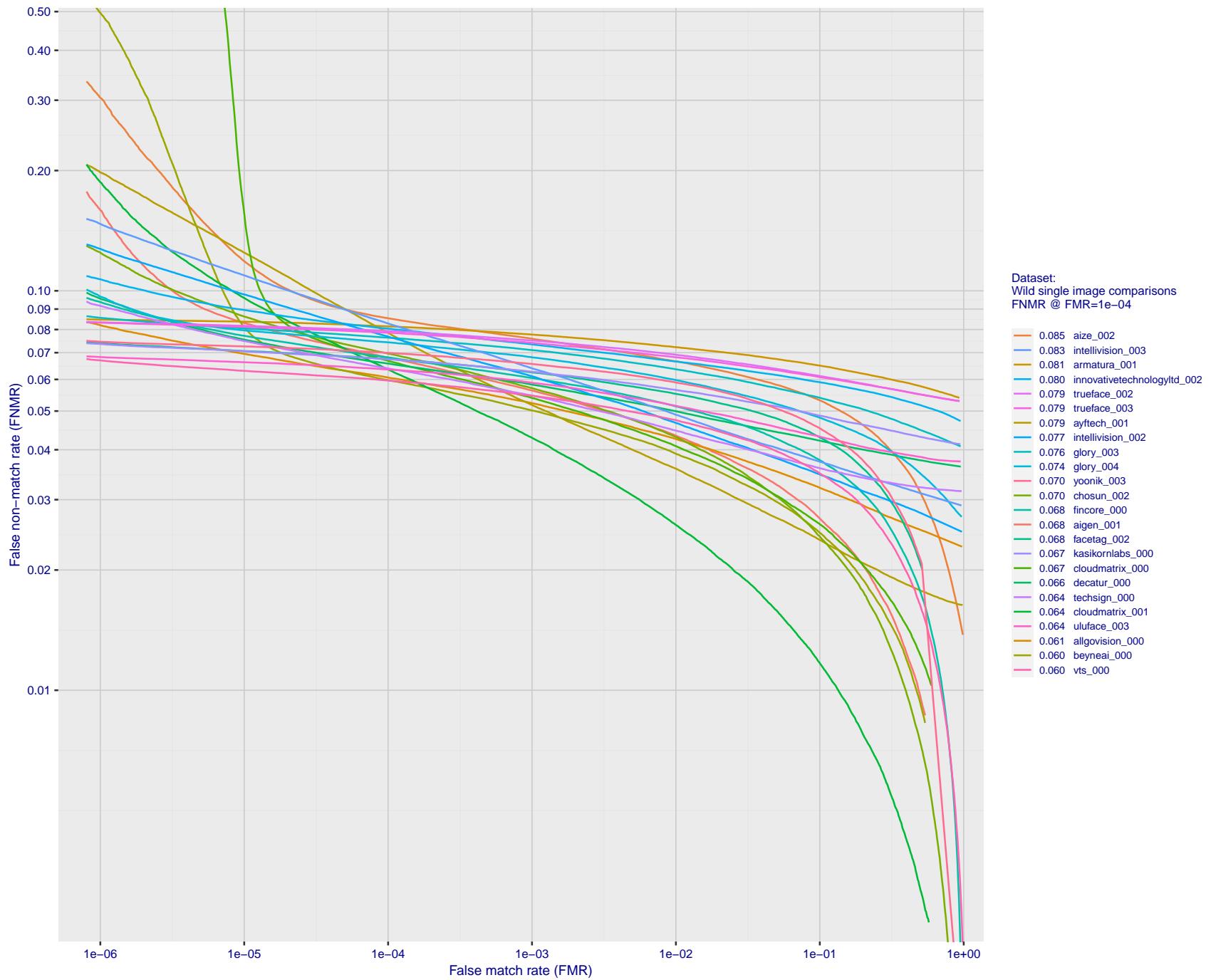


Figure 97: For the 2018 wild image comparisons, detection error tradeoff (DET) characteristics showing false non-match rate vs. false match rate plotted parametrically on threshold,  $T$ . The scales are logarithmic in order to show several decades of FMR.

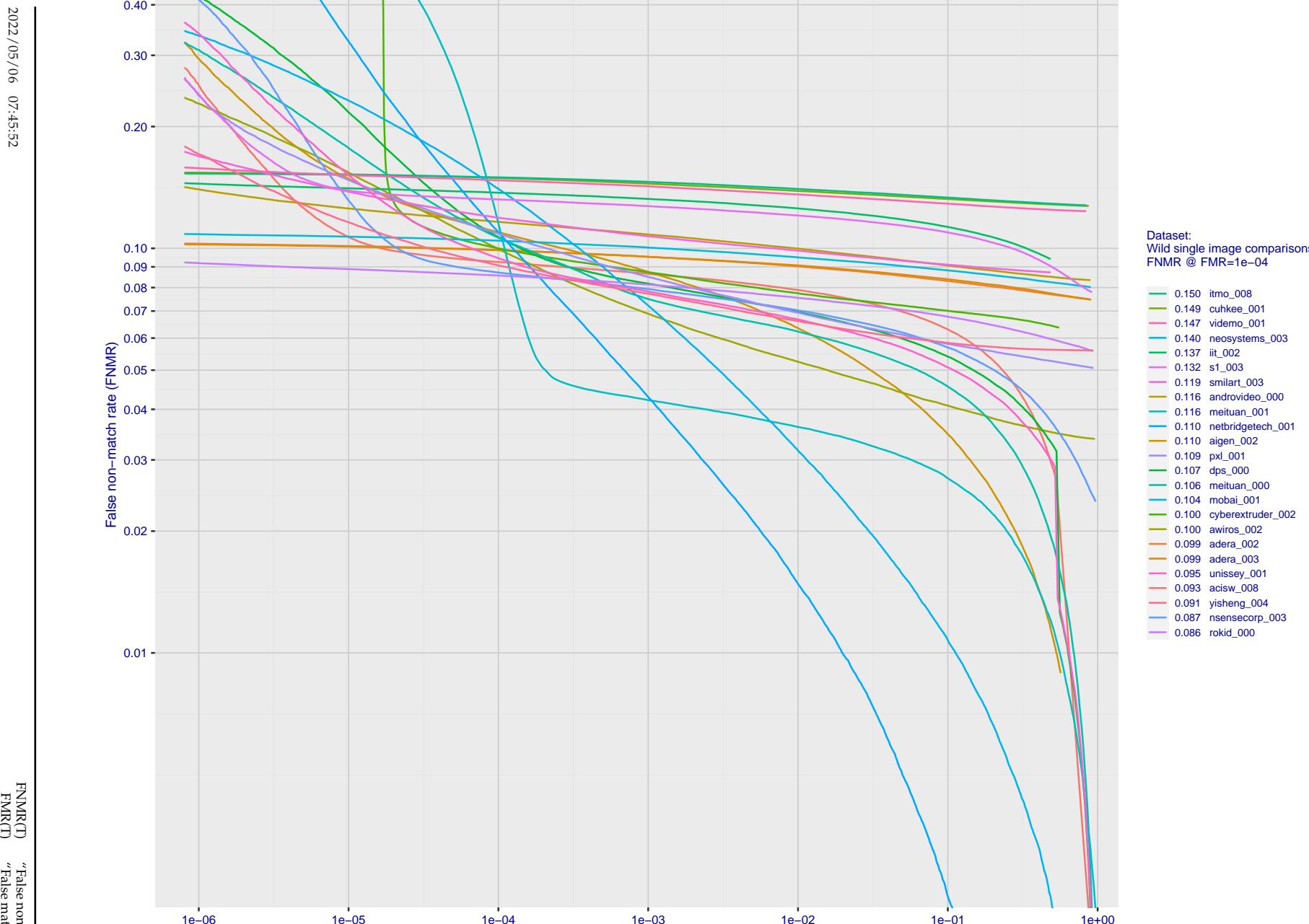


Figure 98: For the 2018 wild image comparisons, detection error tradeoff (DET) characteristics showing false non-match rate vs. false match rate plotted parametrically on threshold,  $T$ . The scales are logarithmic in order to show several decades of FMR.

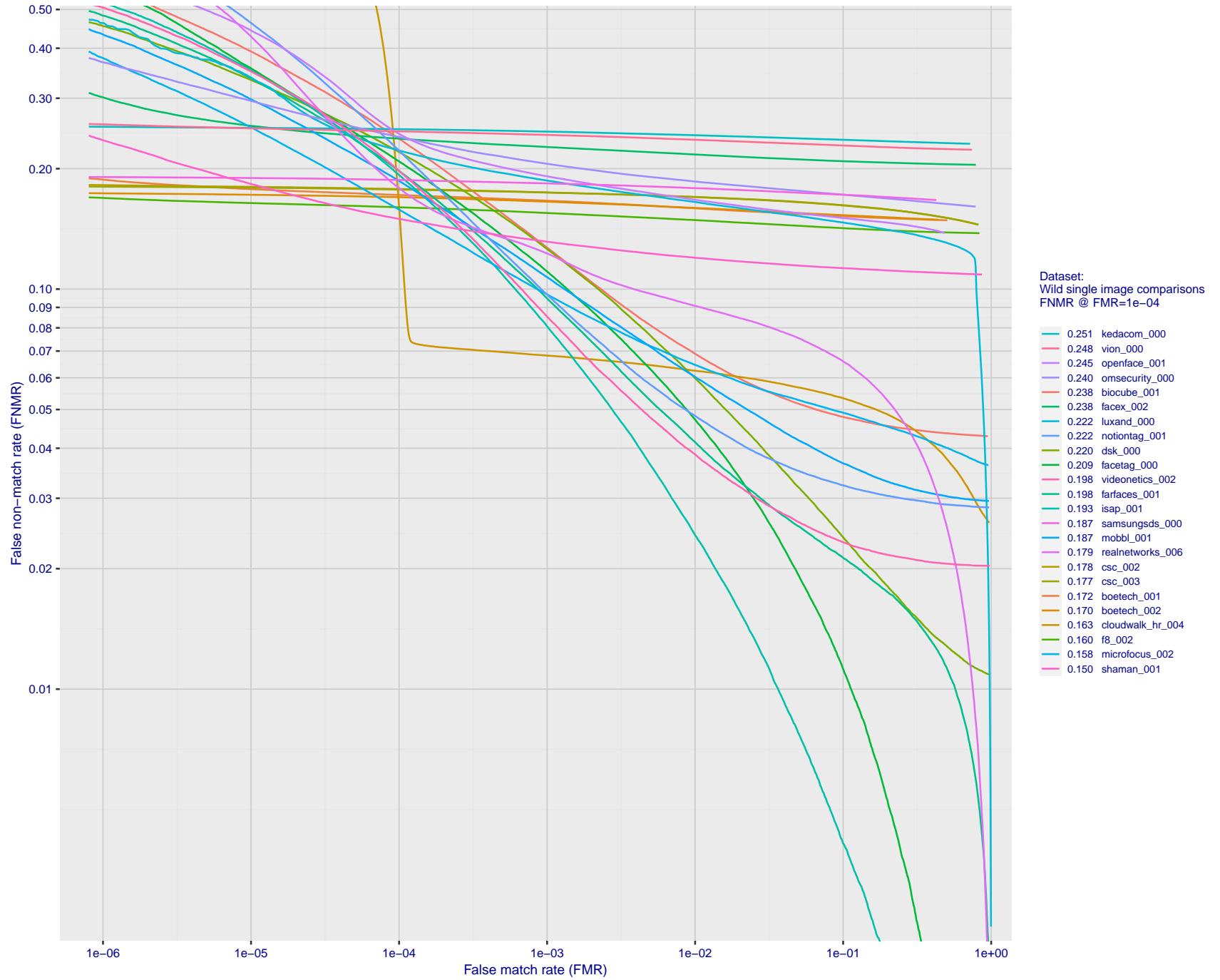


Figure 99: For the 2018 wild image comparisons, detection error tradeoff (DET) characteristics showing false non-match rate vs. false match rate plotted parametrically on threshold, T. The scales are logarithmic in order to show several decades of FMR.

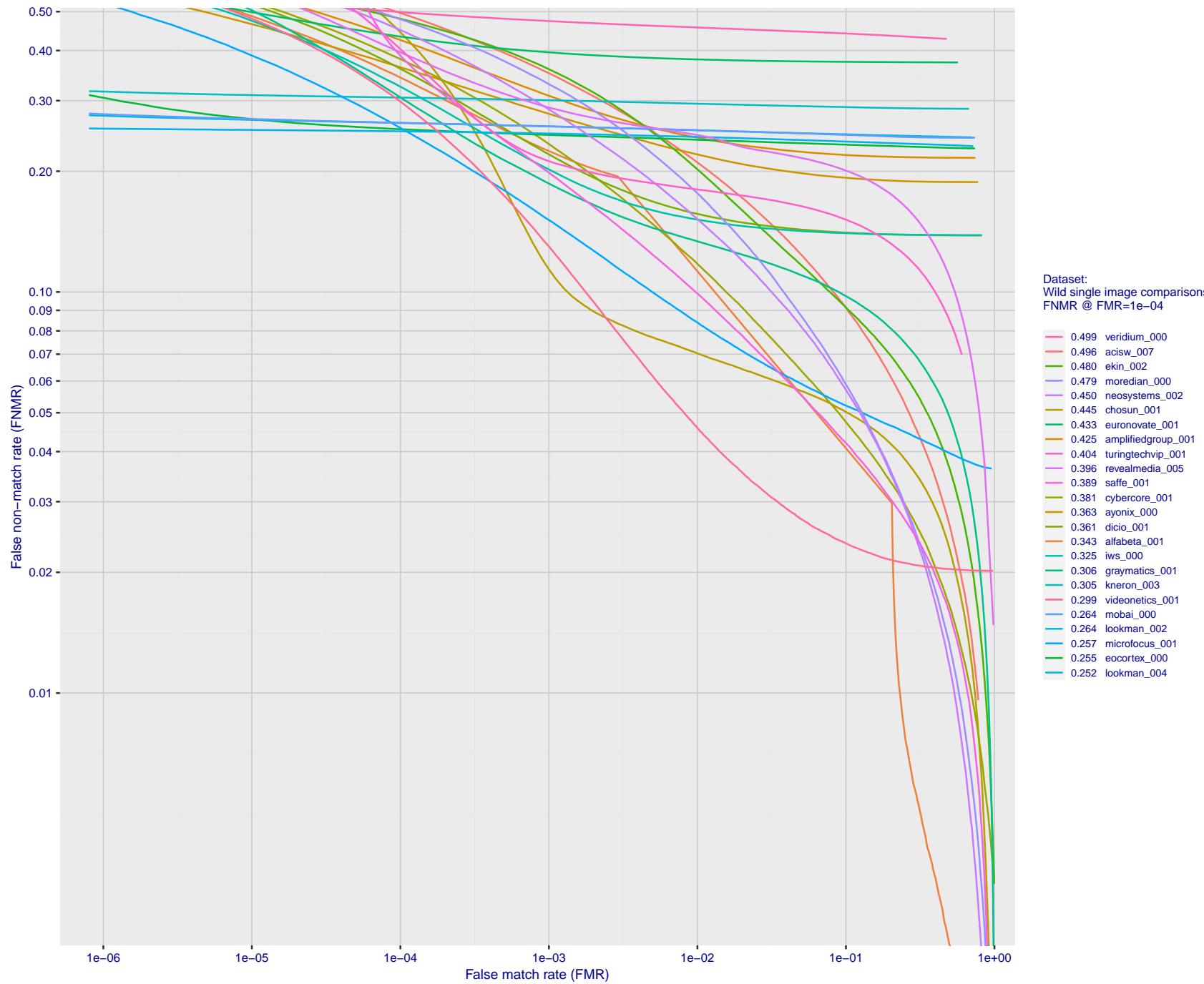


Figure 100: For the 2018 wild image comparisons, detection error tradeoff (DET) characteristics showing false non-match rate vs. false match rate plotted parametrically on threshold,  $T$ . The scales are logarithmic in order to show several decades of FMR.

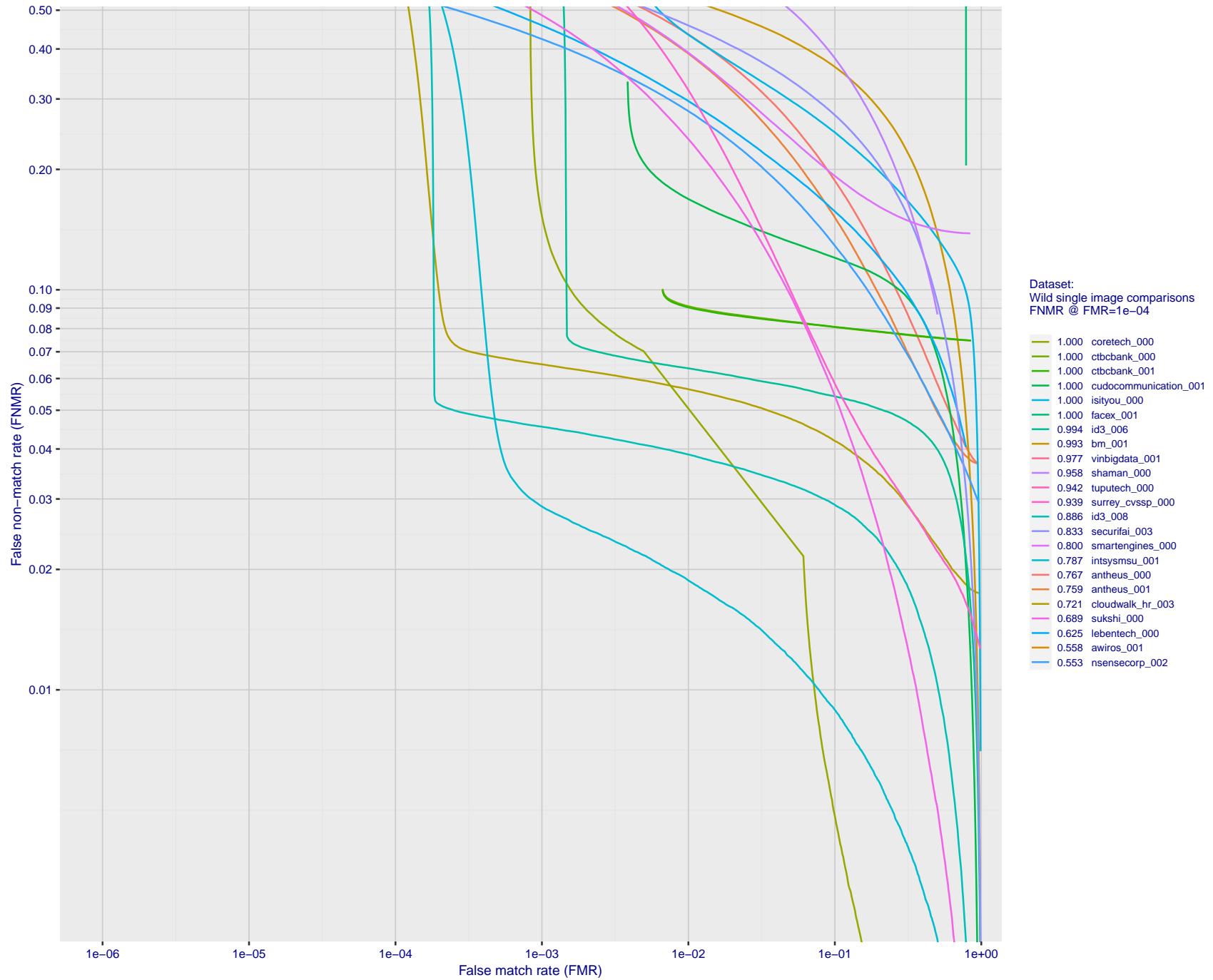


Figure 101: For the 2018 wild image comparisons, detection error tradeoff (DET) characteristics showing false non-match rate vs. false match rate plotted parametrically on threshold,  $T$ . The scales are logarithmic in order to show several decades of FMR.

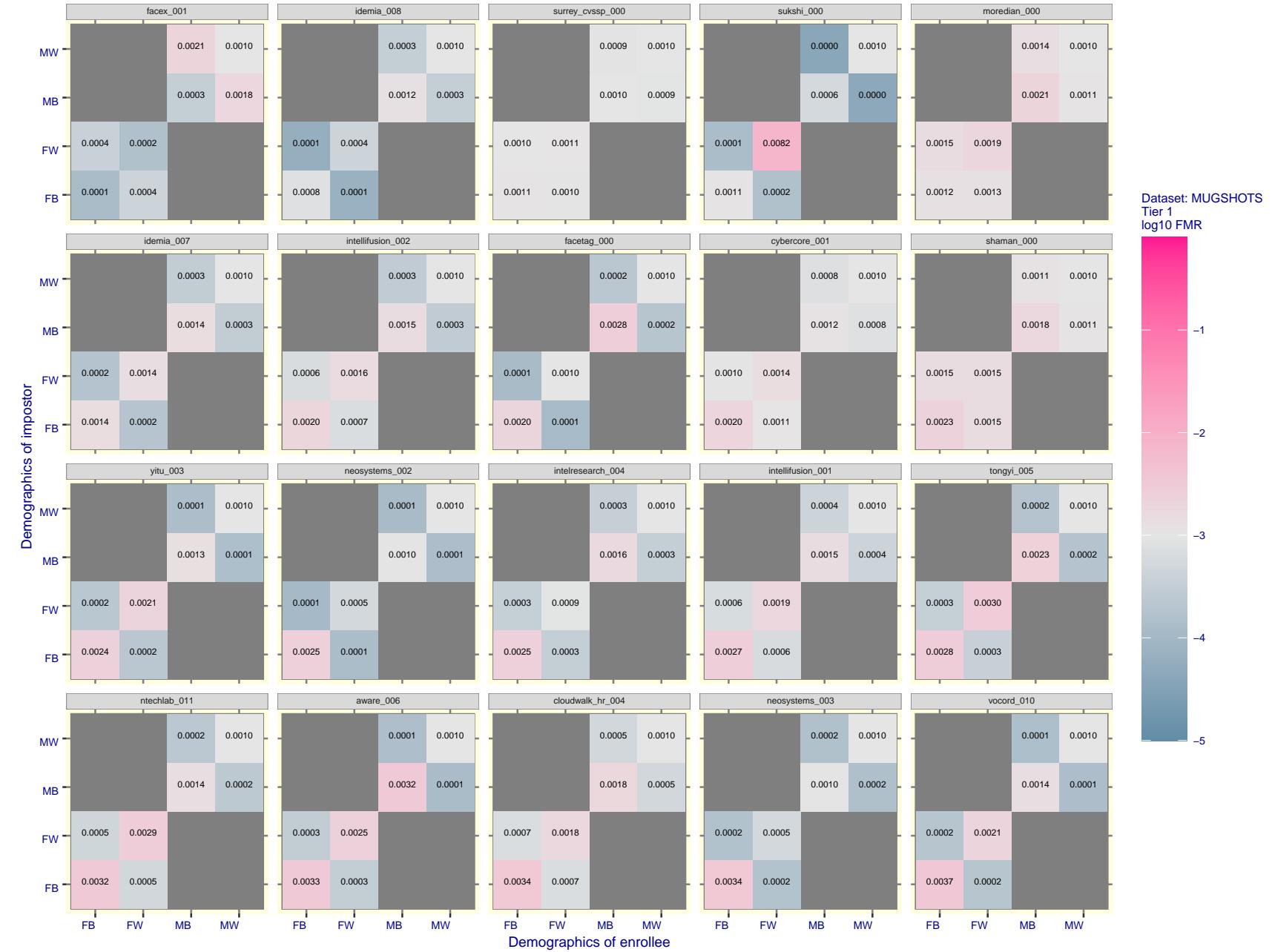


Figure 102: For the mugshot images, FMR for same-sex impostor pairs of images annotated with codes for black female, black male, white female, white male. The threshold is set for each algorithm to give FMR = 0.001 for white males which is the demographic that usually gives the lowest FMR. This means the top right box is the same color in all panels. The panels are sorted over multiple pages in order of FMR on black females, which is the demographic that usually gives the highest FMR.

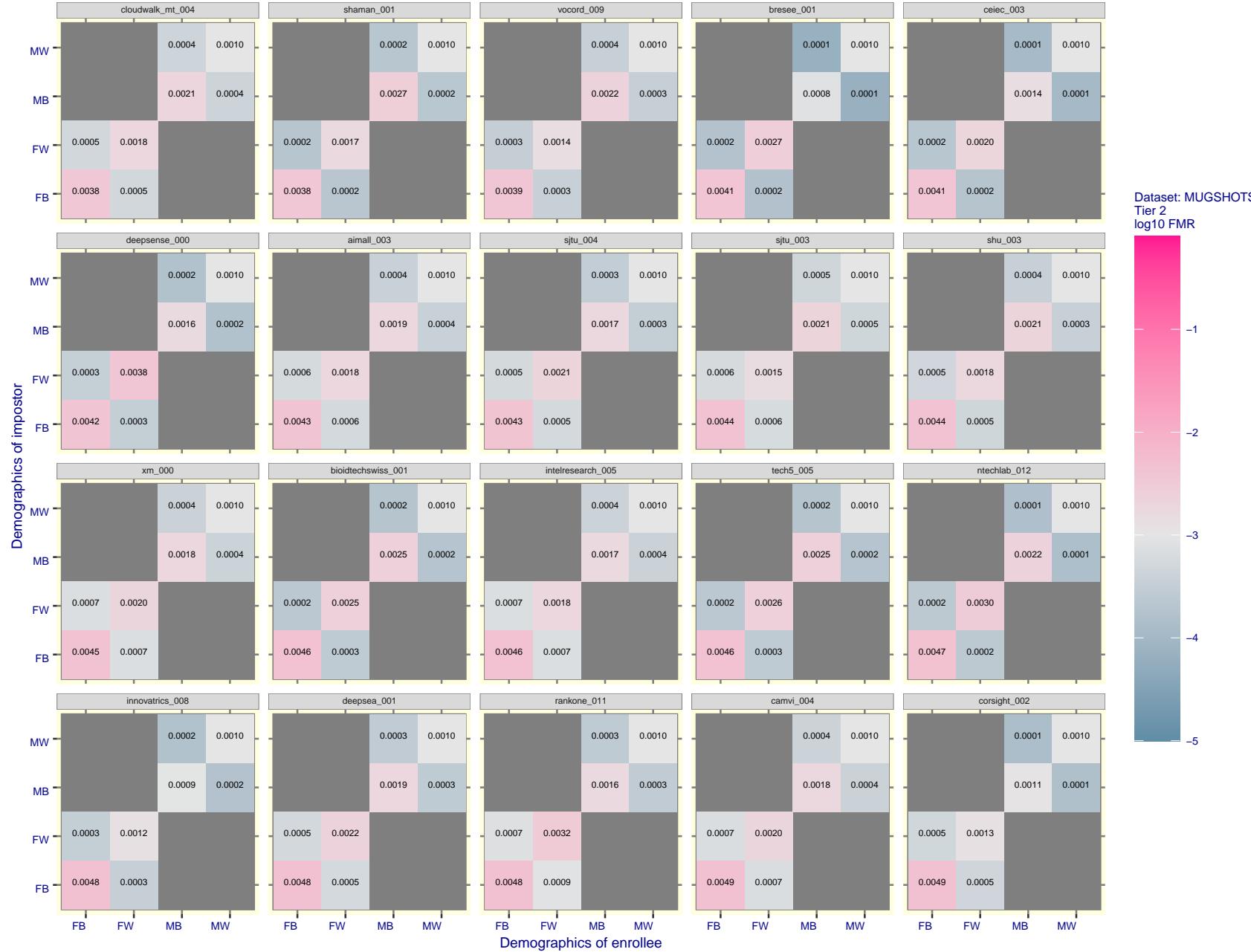


Figure 103: For the mugshot images, FMR for same-sex impostor pairs of images annotated with codes for black female, black male, white female, white male. The threshold is set for each algorithm to give  $FMR = 0.001$  for white males which is the demographic that usually gives the lowest FMR. This means the top right box is the same color in all panels. The panels are sorted over multiple pages in order of FMR on black females, which is the demographic that usually gives the highest FMR.

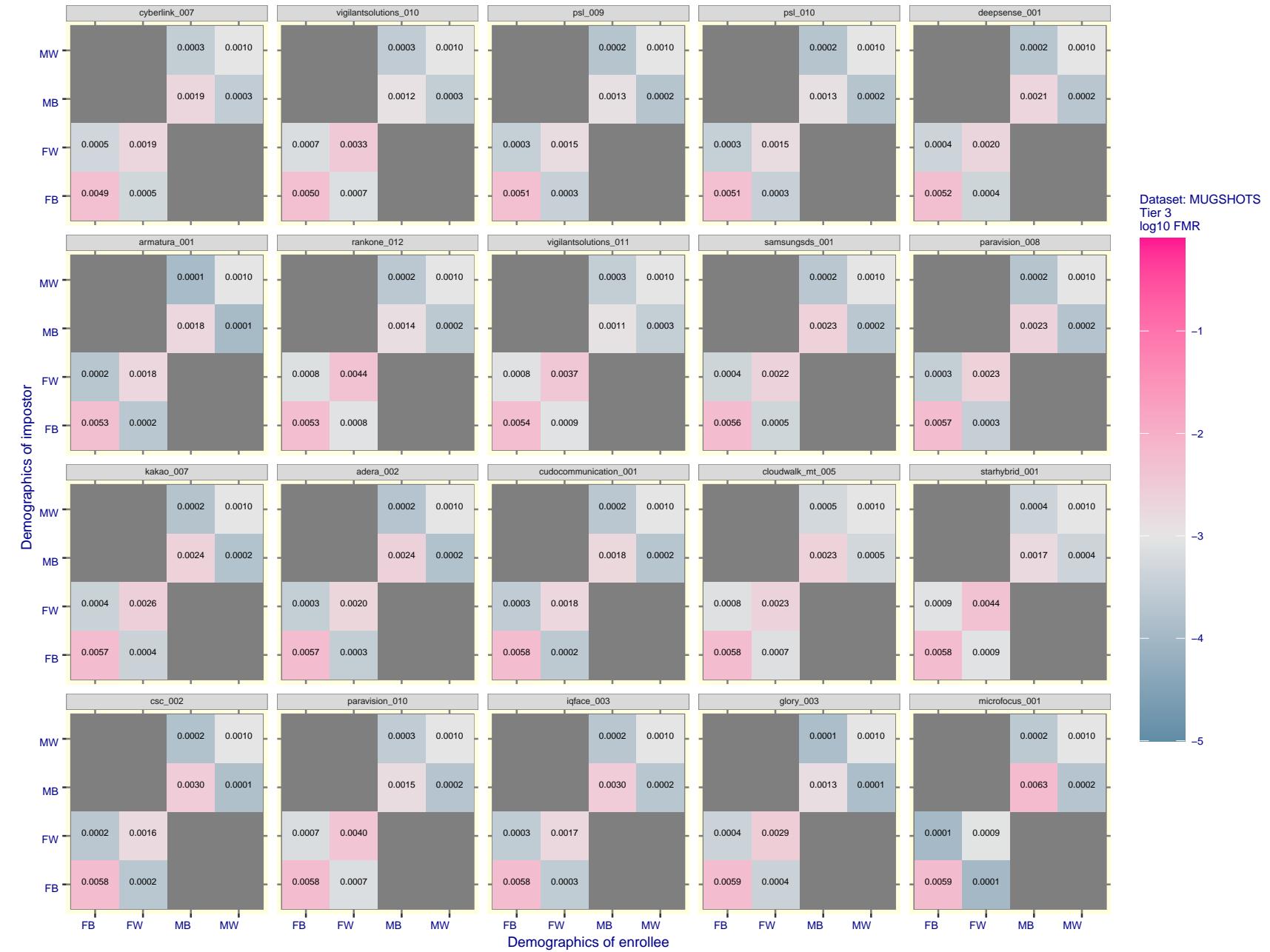


Figure 104: For the mugshot images, FMR for same-sex impostor pairs of images annotated with codes for black female, black male, white female, white male. The threshold is set for each algorithm to give  $FMR = 0.001$  for white males which is the demographic that usually gives the lowest FMR. This means the top right box is the same color in all panels. The panels are sorted over multiple pages in order of FMR on black females, which is the demographic that usually gives the highest FMR.

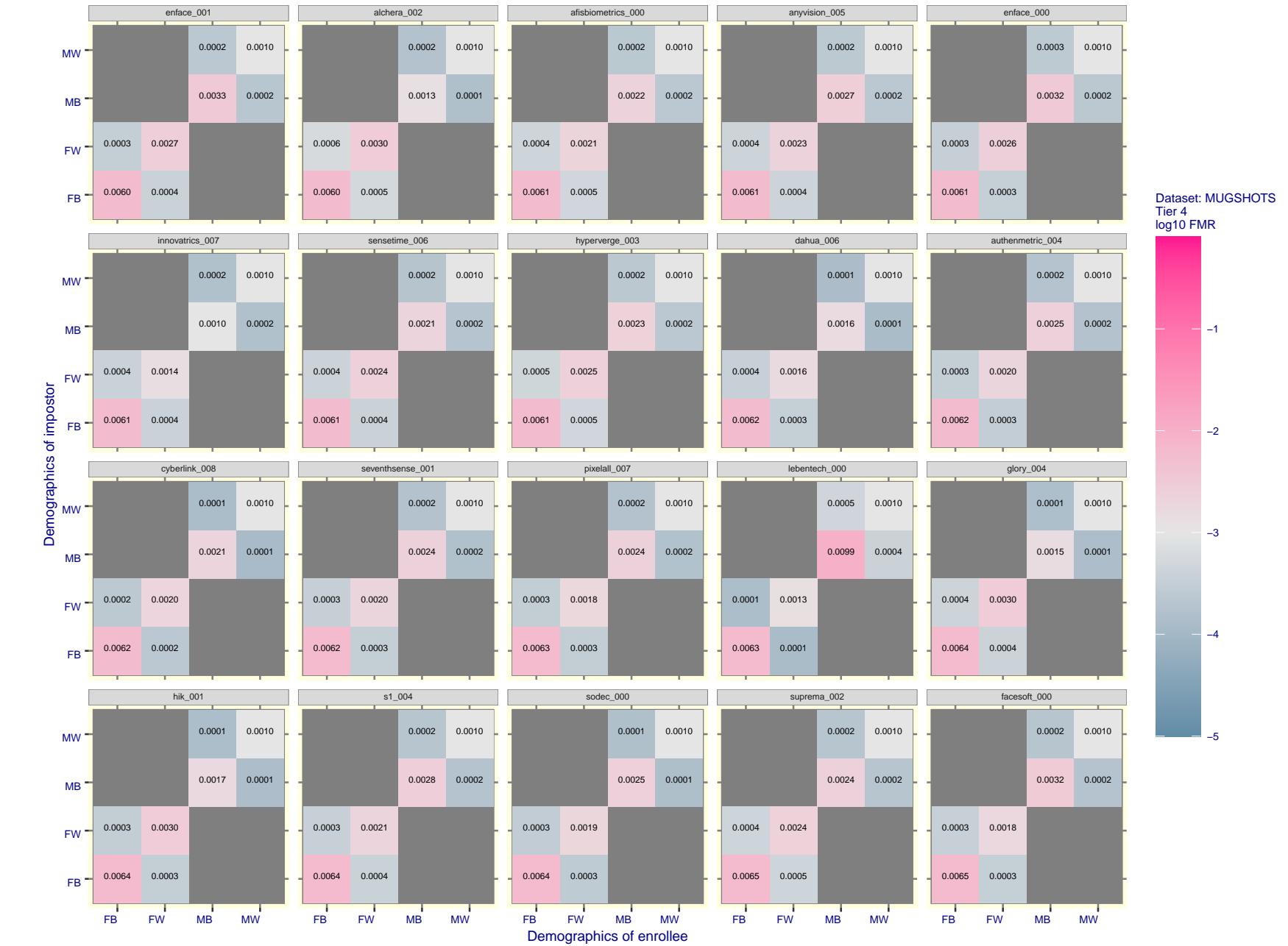


Figure 105: For the mugshot images, FMR for same-sex impostor pairs of images annotated with codes for black female, black male, white female, white male. The threshold is set for each algorithm to give FMR = 0.001 for white males which is the demographic that usually gives the lowest FMR. This means the top right box is the same color in all panels. The panels are sorted over multiple pages in order of FMR on black females, which is the demographic that usually gives the highest FMR.

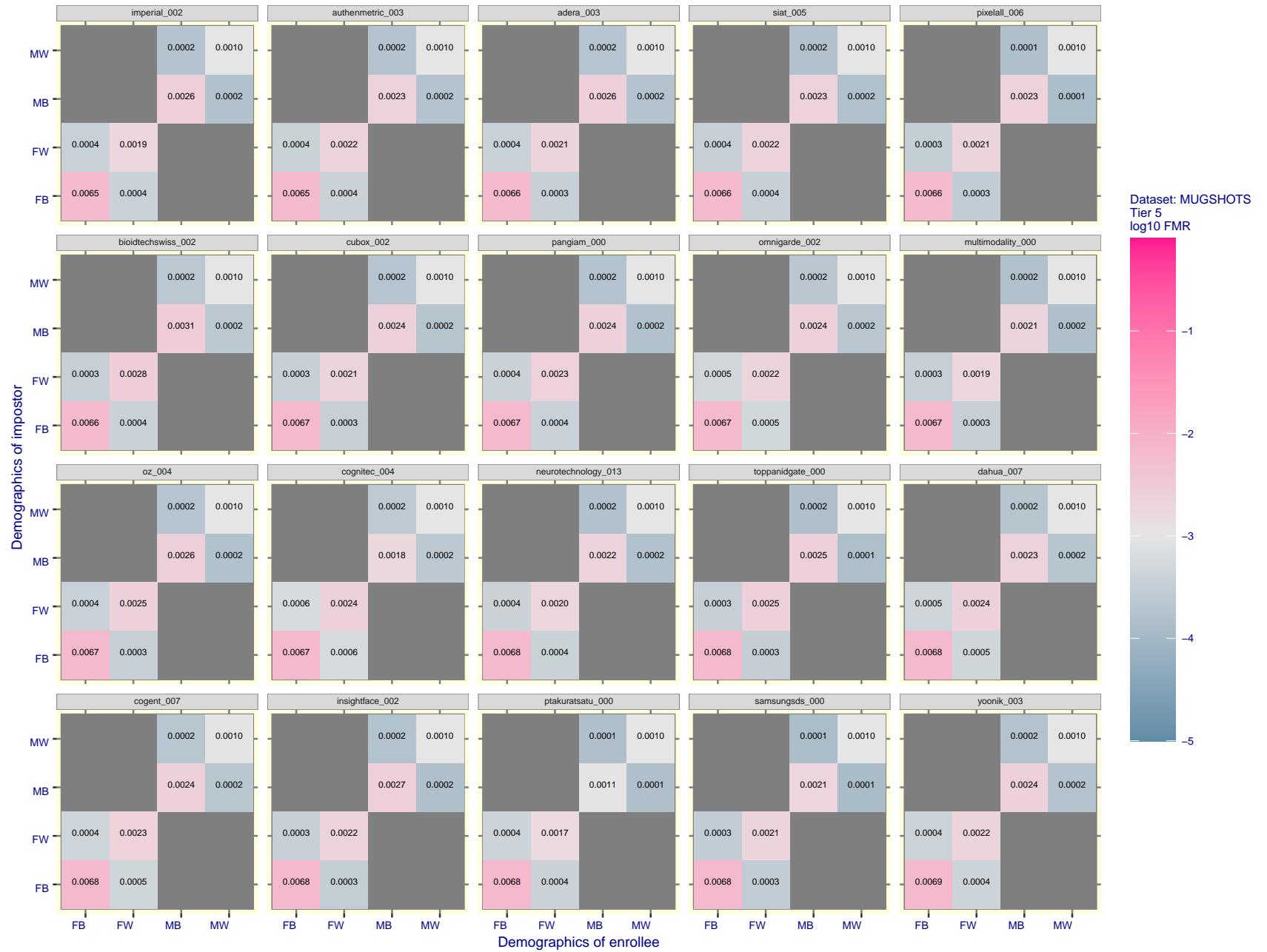


Figure 106: For the mugshot images, FMR for same-sex impostor pairs of images annotated with codes for black female, black male, white female, white male. The threshold is set for each algorithm to give FMR = 0.001 for white males which is the demographic that usually gives the lowest FMR. This means the top right box is the same color in all panels. The panels are sorted over multiple pages in order of FMR on black females, which is the demographic that usually gives the highest FMR.

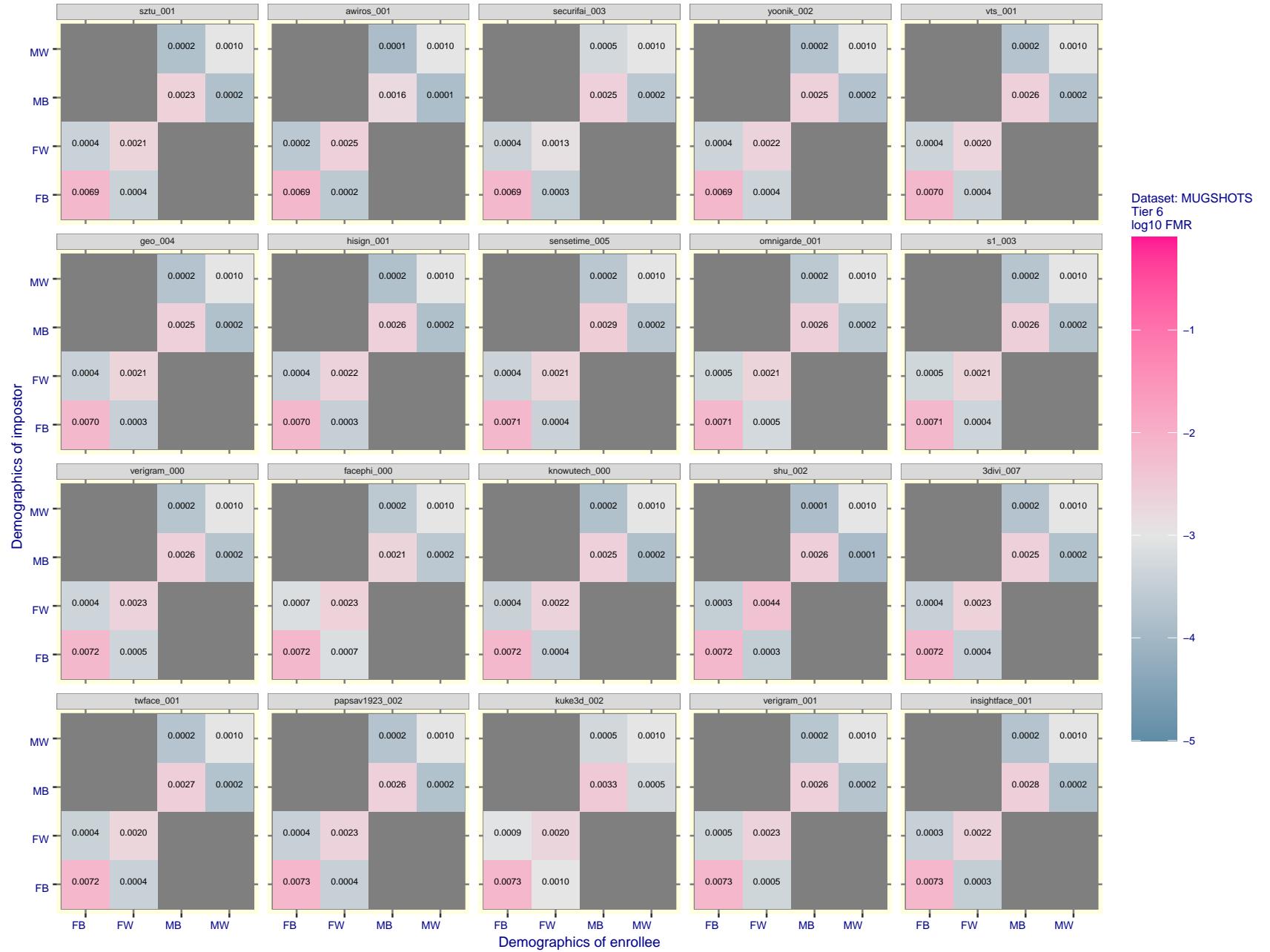


Figure 107: For the mugshot images, FMR for same-sex impostor pairs of images annotated with codes for black female, black male, white female, white male. The threshold is set for each algorithm to give  $FMR = 0.001$  for white males which is the demographic that usually gives the lowest FMR. This means the top right box is the same color in all panels. The panels are sorted over multiple pages in order of FMR on black females, which is the demographic that usually gives the highest FMR.

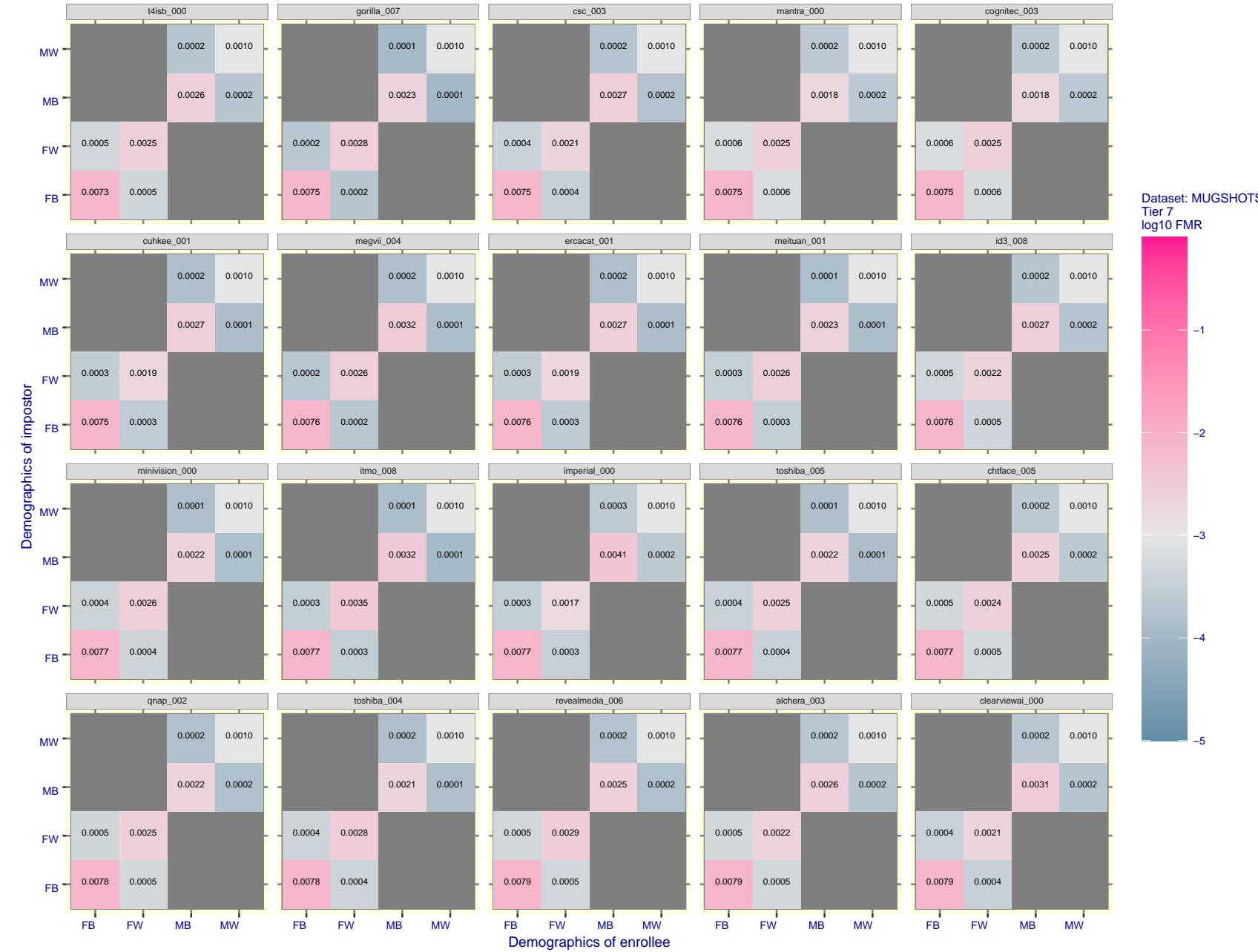


Figure 108: For the mugshot images, FMR for same-sex impostor pairs of images annotated with codes for black female, black male, white female, white male. The threshold is set for each algorithm to give FMR = 0.001 for white males which is the demographic that usually gives the lowest FMR. This means the top right box is the same color in all panels. The panels are sorted over multiple pages in order of FMR on black females, which is the demographic that usually gives the highest FMR.

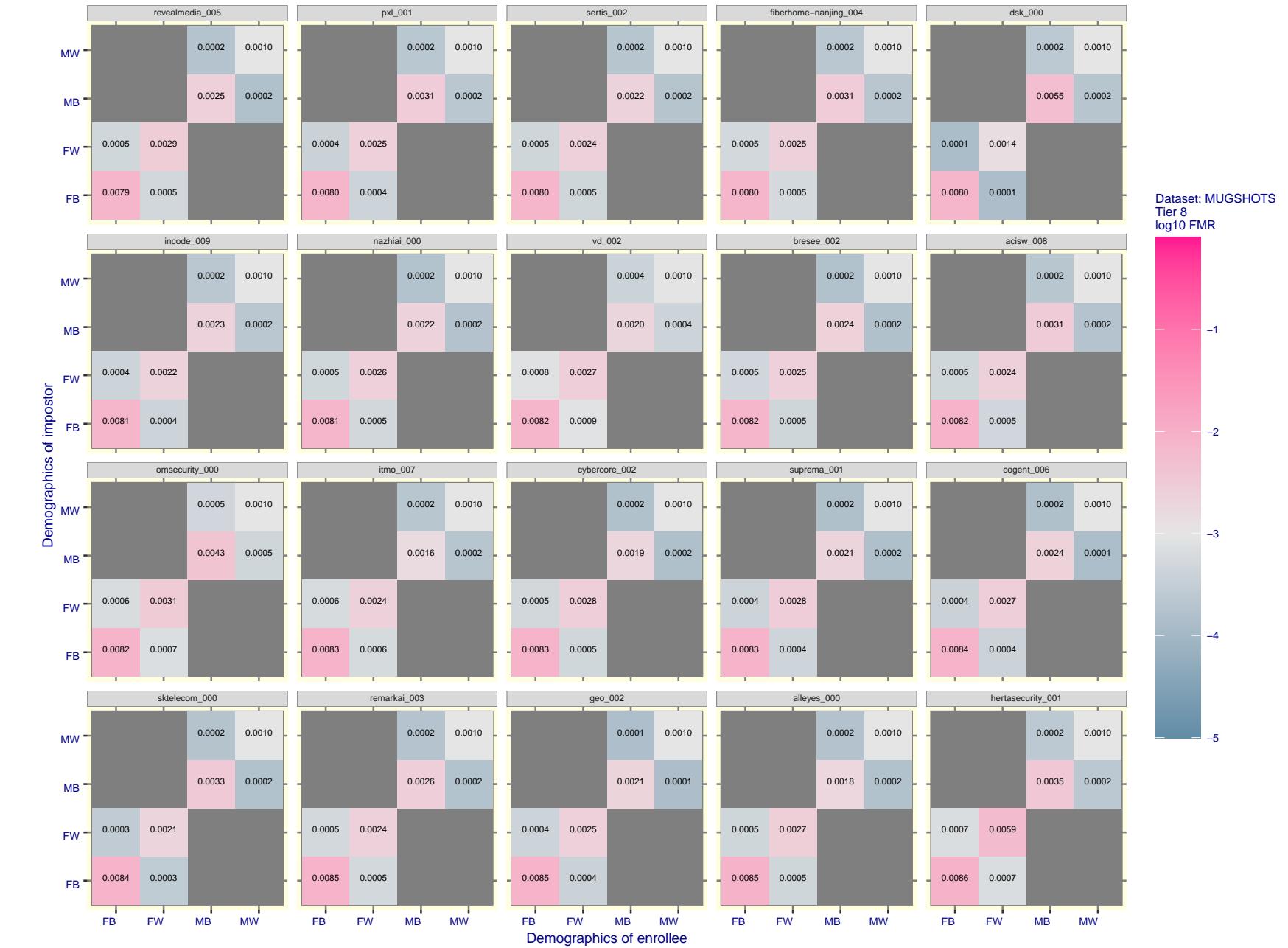


Figure 109: For the mugshot images, FMR for same-sex impostor pairs of images annotated with codes for black female, black male, white female, white male. The threshold is set for each algorithm to give FMR = 0.001 for white males which is the demographic that usually gives the lowest FMR. This means the top right box is the same color in all panels. The panels are sorted over multiple pages in order of FMR on black females, which is the demographic that usually gives the highest FMR.

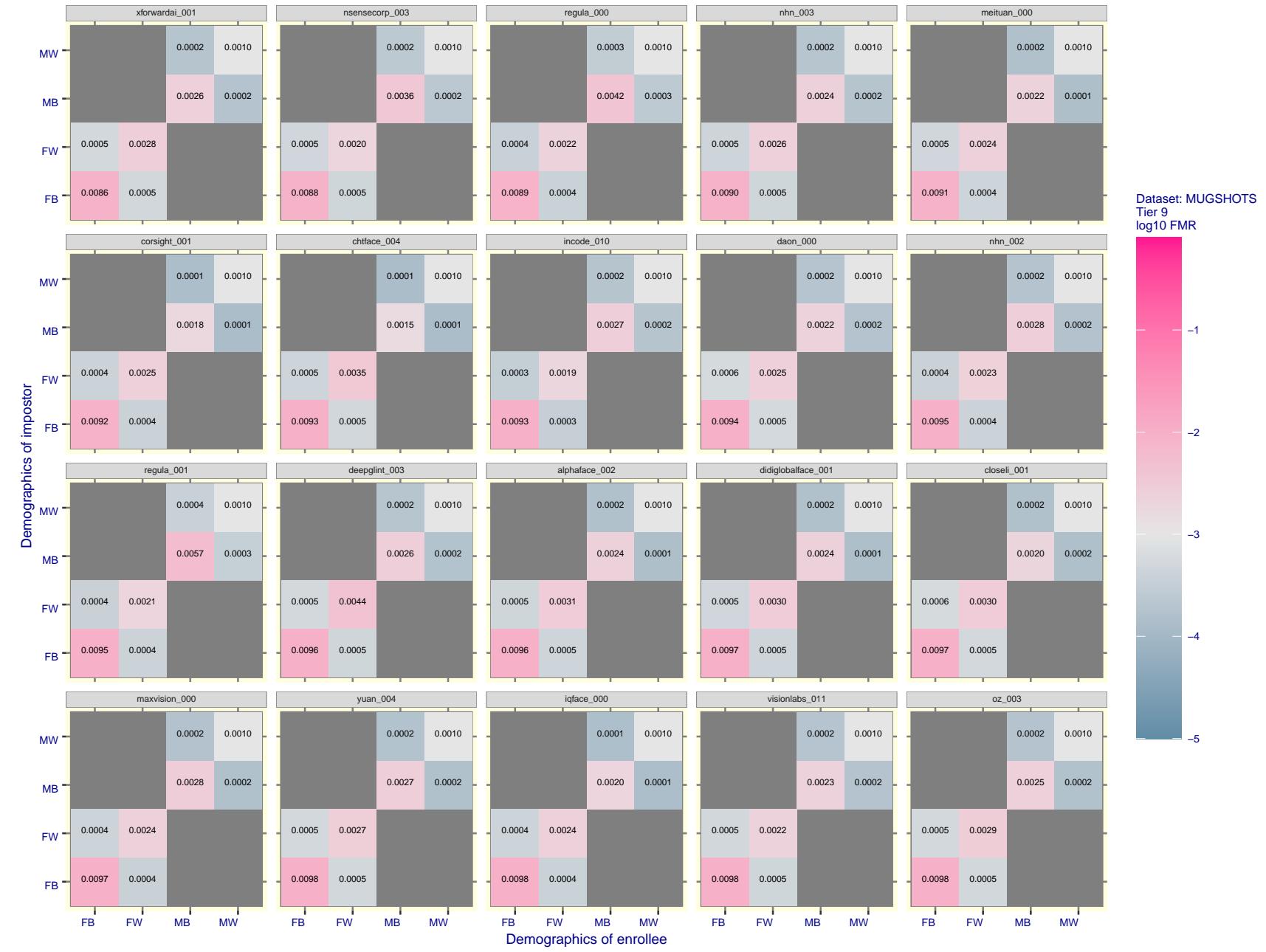


Figure 110: For the mugshot images, FMR for same-sex impostor pairs of images annotated with codes for black female, black male, white female, white male. The threshold is set for each algorithm to give FMR = 0.001 for white males which is the demographic that usually gives the lowest FMR. This means the top right box is the same color in all panels. The panels are sorted over multiple pages in order of FMR on black females, which is the demographic that usually gives the highest FMR.

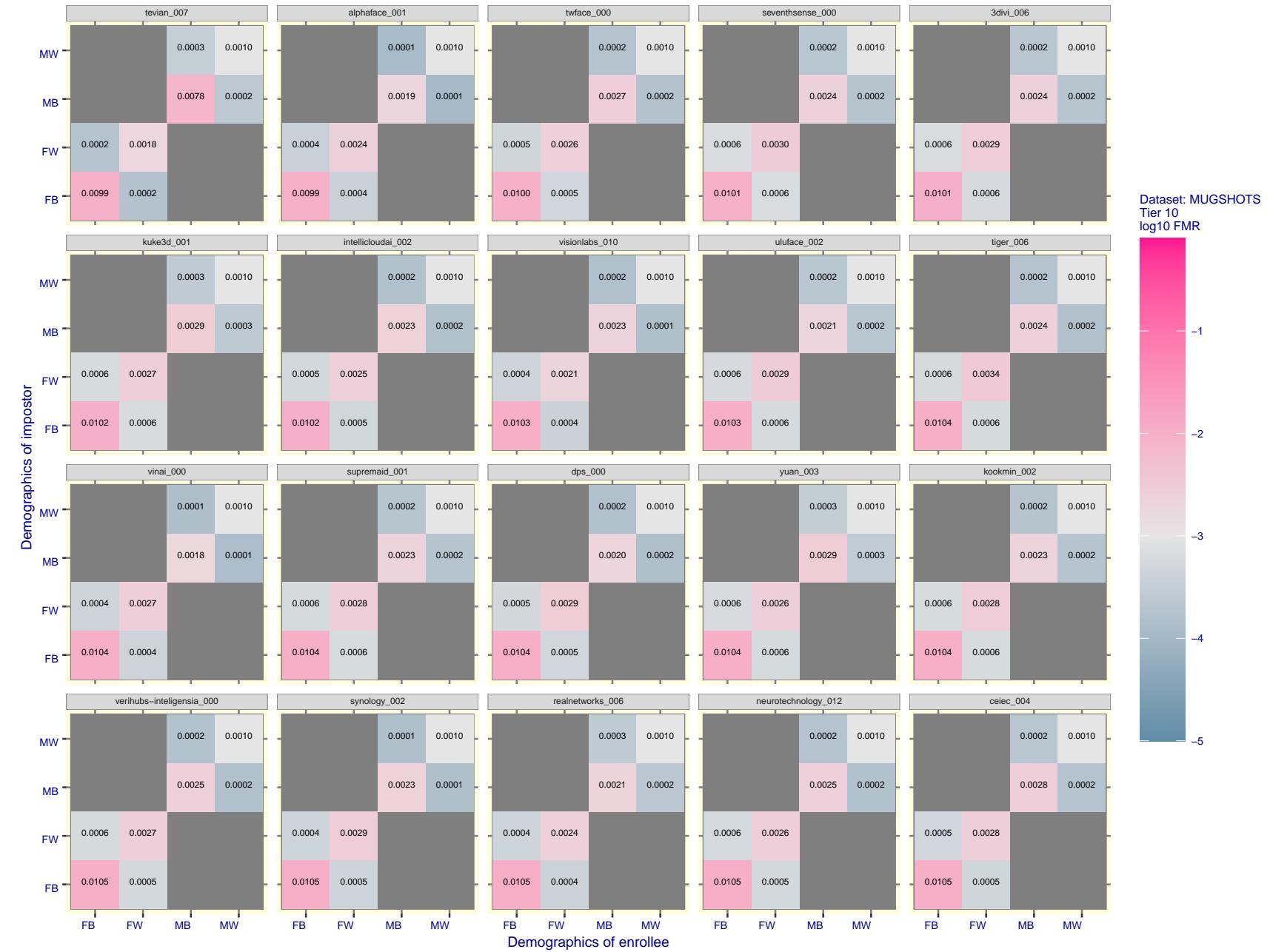


Figure 111: For the mugshot images, FMR for same-sex impostor pairs of images annotated with codes for black female, black male, white female, white male. The threshold is set for each algorithm to give FMR = 0.001 for white males which is the demographic that usually gives the lowest FMR. This means the top right box is the same color in all panels. The panels are sorted over multiple pages in order of FMR on black females, which is the demographic that usually gives the highest FMR.

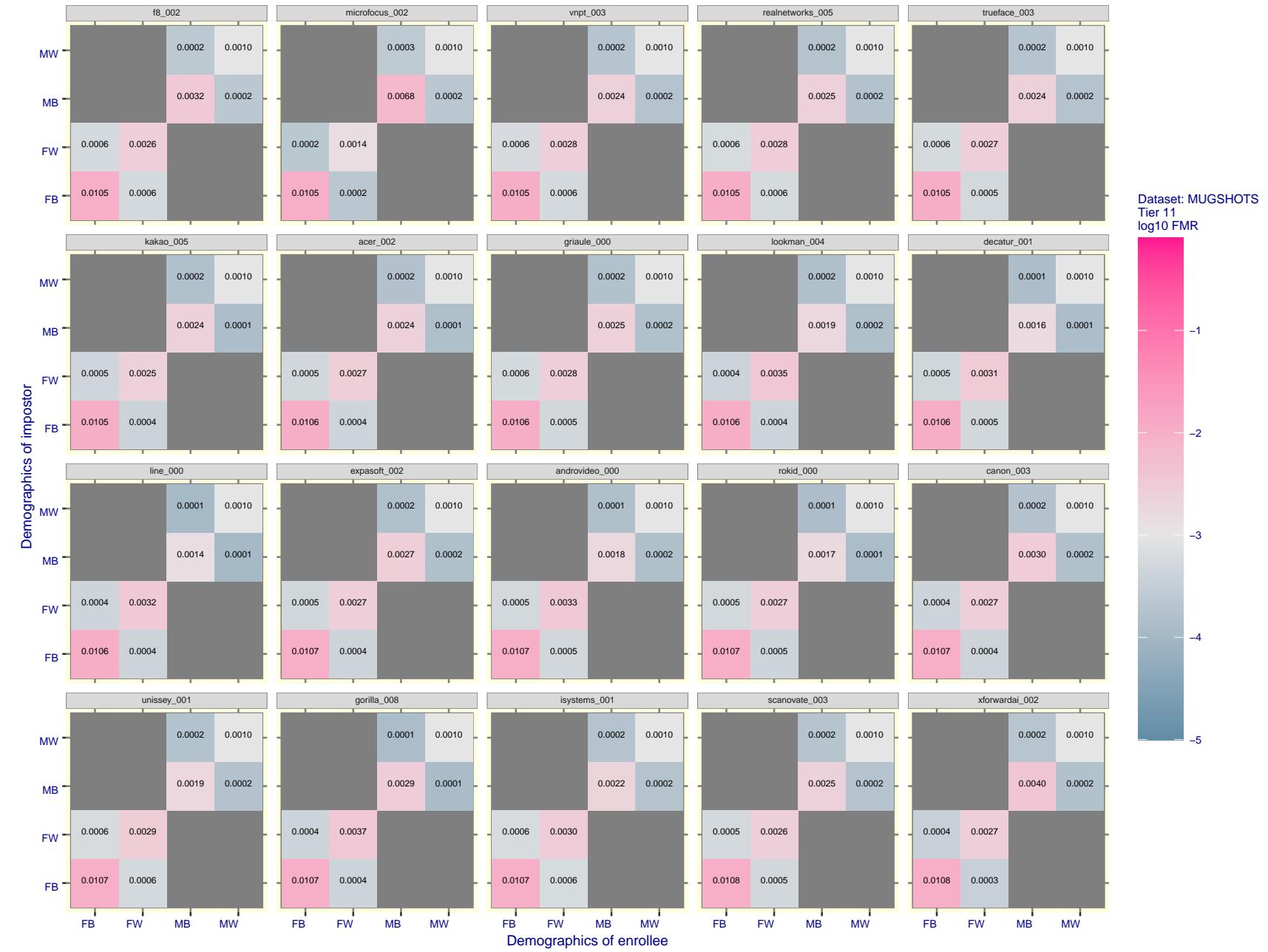


Figure 112: For the mugshot images, FMR for same-sex impostor pairs of images annotated with codes for black female, black male, white female, white male. The threshold is set for each algorithm to give FMR = 0.001 for white males which is the demographic that usually gives the lowest FMR. This means the top right box is the same color in all panels. The panels are sorted over multiple pages in order of FMR on black females, which is the demographic that usually gives the highest FMR.

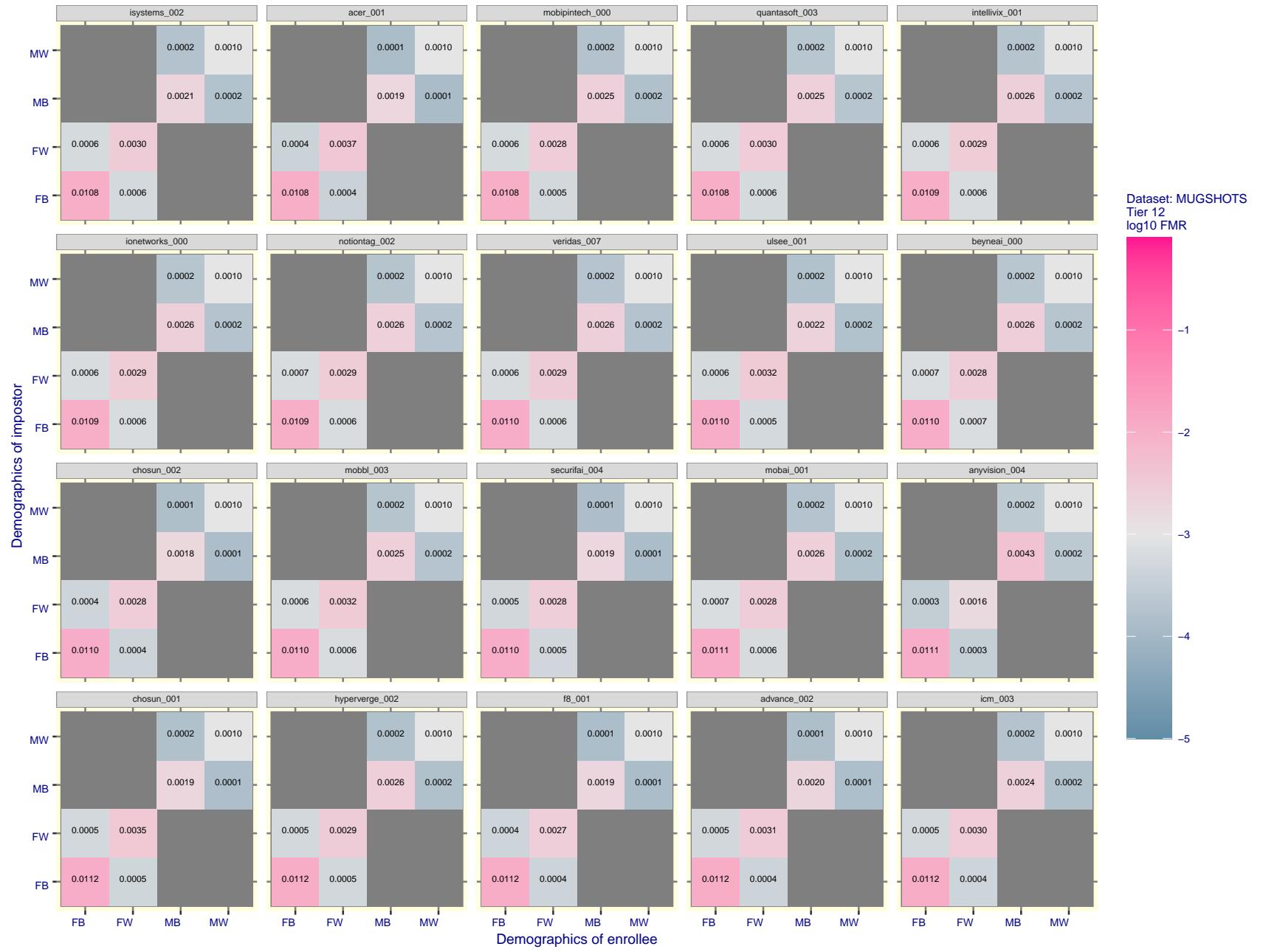


Figure 113: For the mugshot images, FMR for same-sex impostor pairs of images annotated with codes for black female, black male, white female, white male. The threshold is set for each algorithm to give FMR = 0.001 for white males which is the demographic that usually gives the lowest FMR. This means the top right box is the same color in all panels. The panels are sorted over multiple pages in order of FMR on black females, which is the demographic that usually gives the highest FMR.

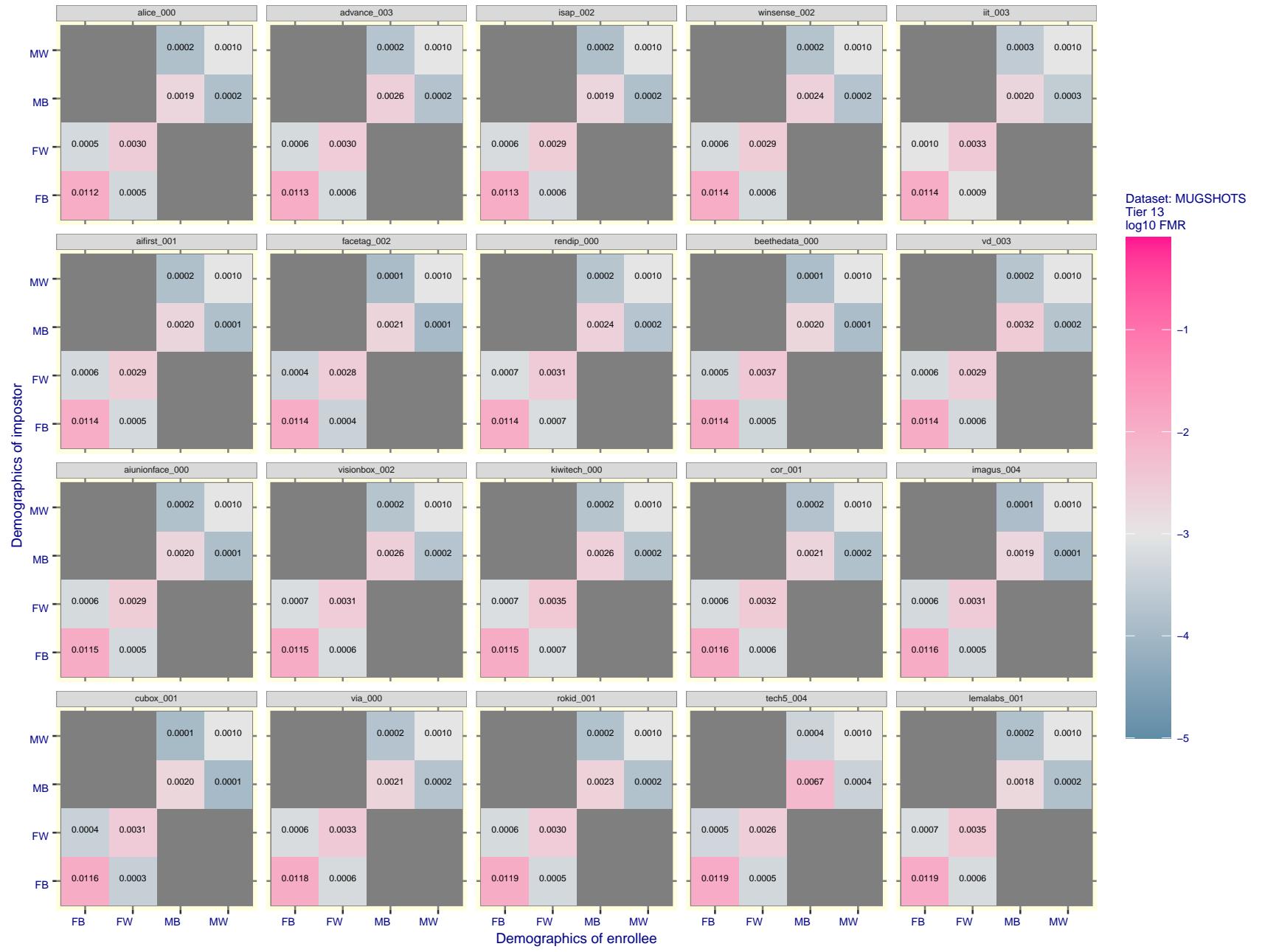


Figure 114: For the mugshot images, FMR for same-sex impostor pairs of images annotated with codes for black female, black male, white female, white male. The threshold is set for each algorithm to give FMR = 0.001 for white males which is the demographic that usually gives the lowest FMR. This means the top right box is the same color in all panels. The panels are sorted over multiple pages in order of FMR on black females, which is the demographic that usually gives the highest FMR.

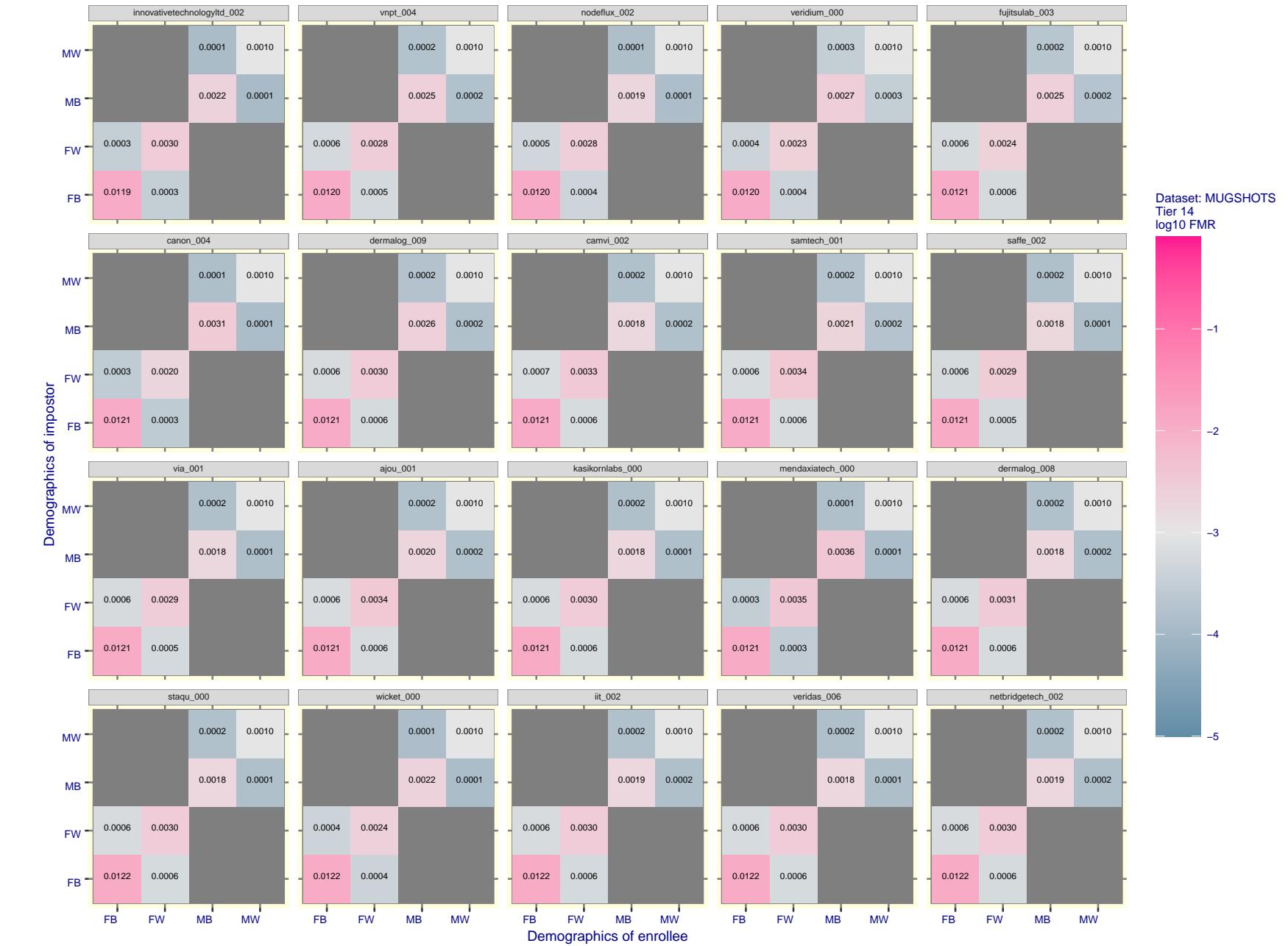


Figure 115: For the mugshot images, FMR for same-sex impostor pairs of images annotated with codes for black female, black male, white female, white male. The threshold is set for each algorithm to give FMR = 0.001 for white males which is the demographic that usually gives the lowest FMR. This means the top right box is the same color in all panels. The panels are sorted over multiple pages in order of FMR on black females, which is the demographic that usually gives the highest FMR.

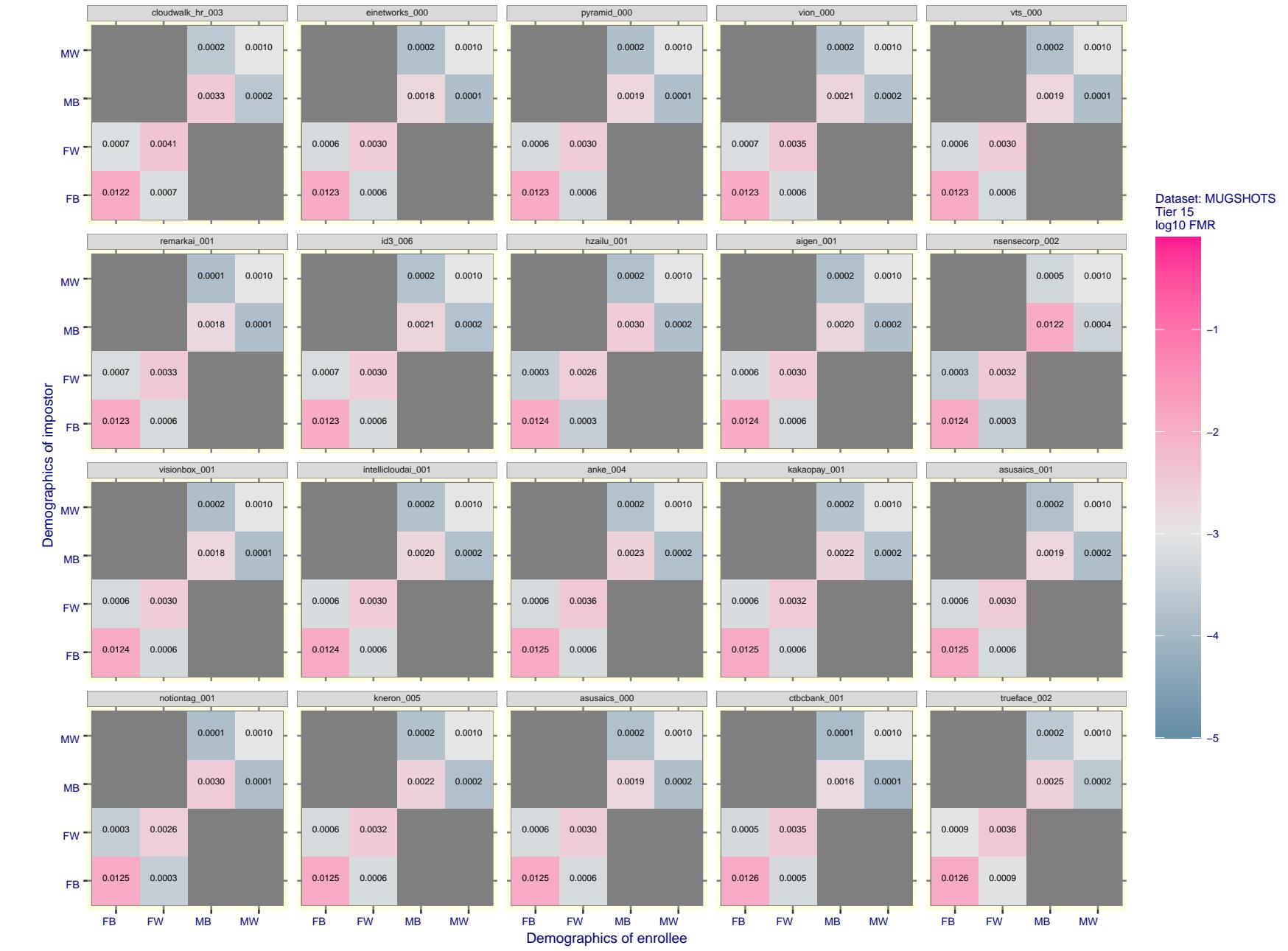


Figure 116: For the mugshot images, FMR for same-sex impostor pairs of images annotated with codes for black female, black male, white female, white male. The threshold is set for each algorithm to give  $FMR = 0.001$  for white males which is the demographic that usually gives the lowest FMR. This means the top right box is the same color in all panels. The panels are sorted over multiple pages in order of FMR on black females, which is the demographic that usually gives the highest FMR.

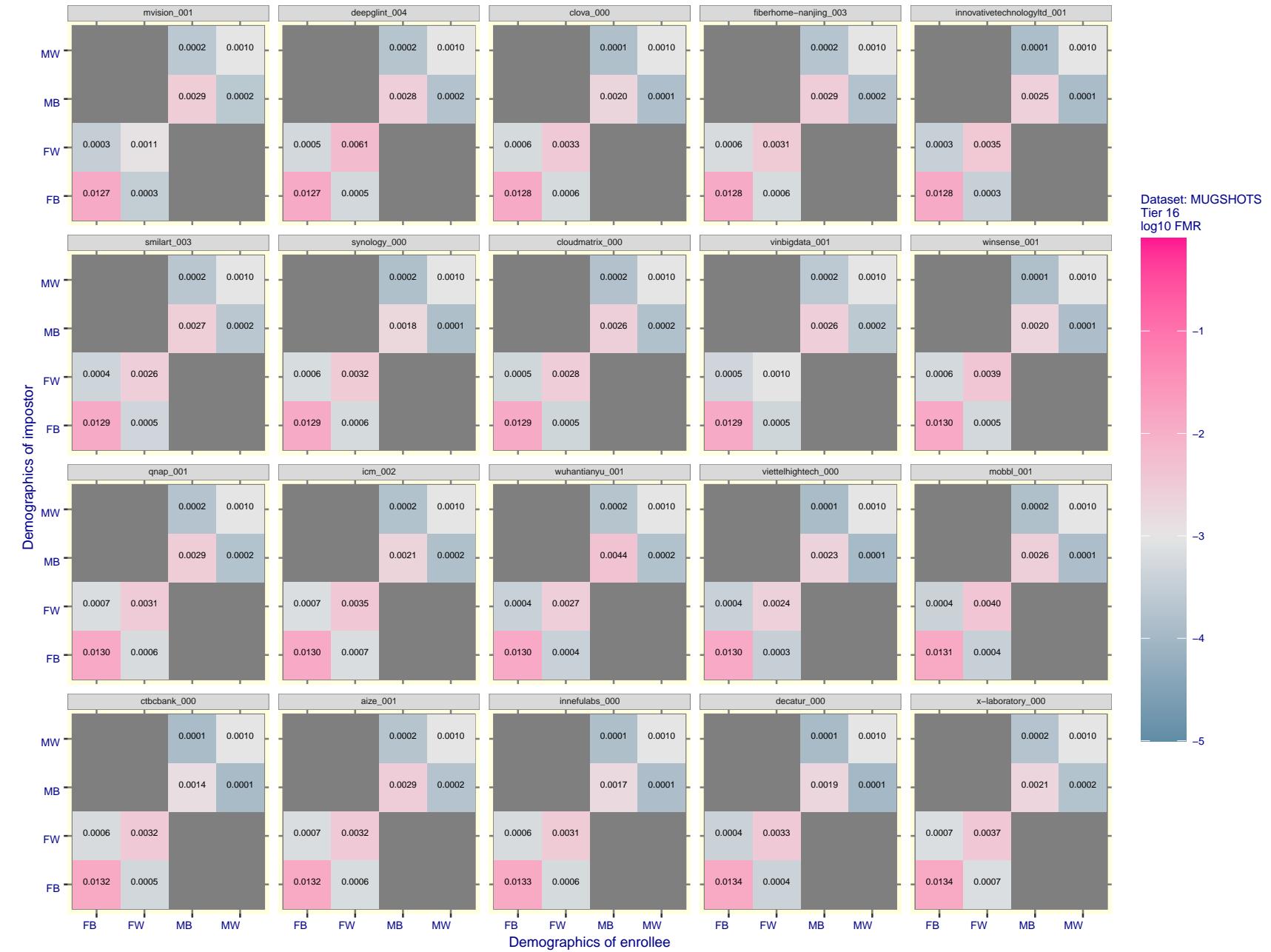


Figure 117: For the mugshot images, FMR for same-sex impostor pairs of images annotated with codes for black female, black male, white female, white male. The threshold is set for each algorithm to give FMR = 0.001 for white males which is the demographic that usually gives the lowest FMR. This means the top right box is the same color in all panels. The panels are sorted over multiple pages in order of FMR on black females, which is the demographic that usually gives the highest FMR.

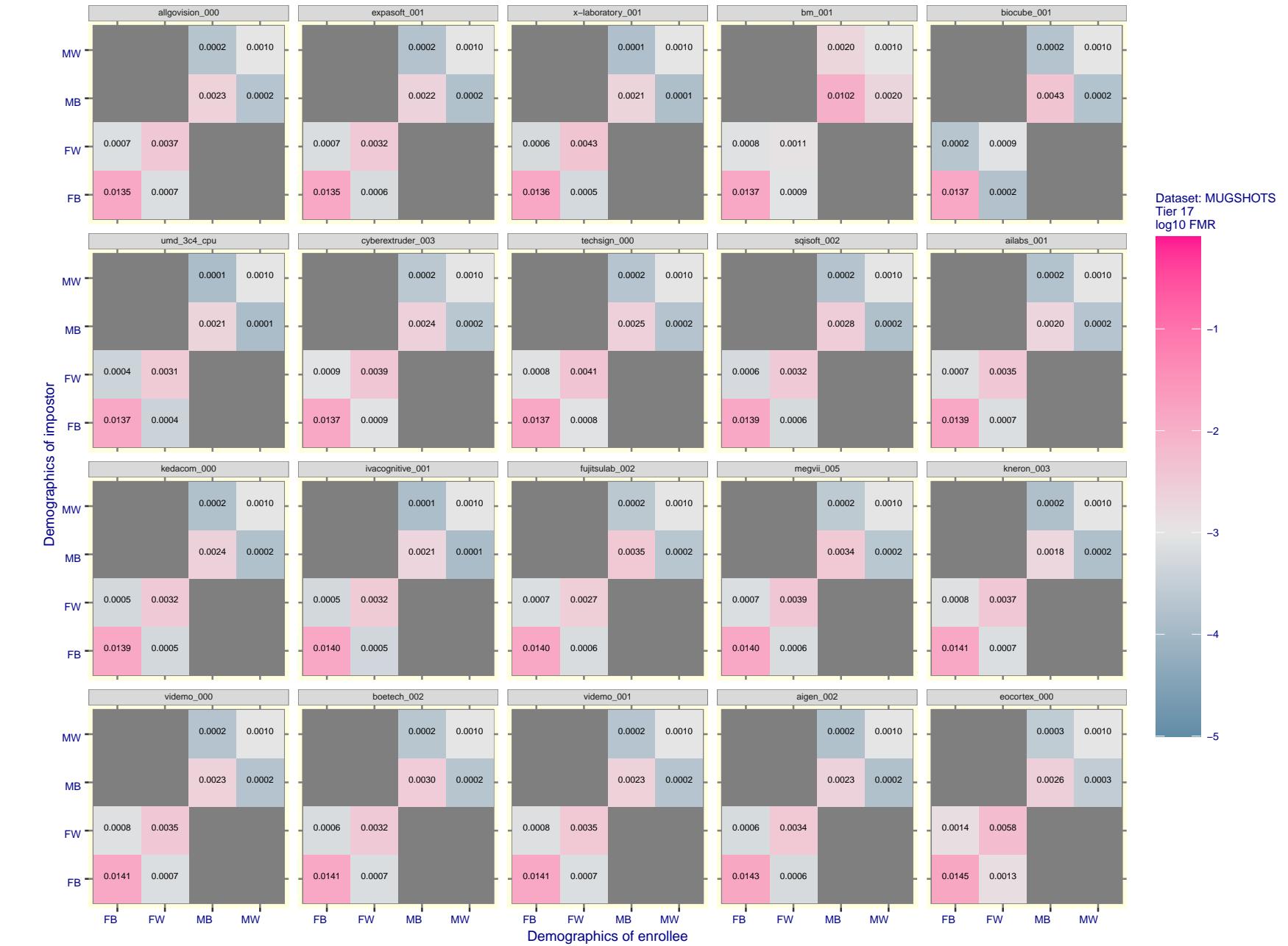


Figure 118: For the mugshot images, FMR for same-sex impostor pairs of images annotated with codes for black female, black male, white female, white male. The threshold is set for each algorithm to give FMR = 0.001 for white males which is the demographic that usually gives the lowest FMR. This means the top right box is the same color in all panels. The panels are sorted over multiple pages in order of FMR on black females, which is the demographic that usually gives the highest FMR.

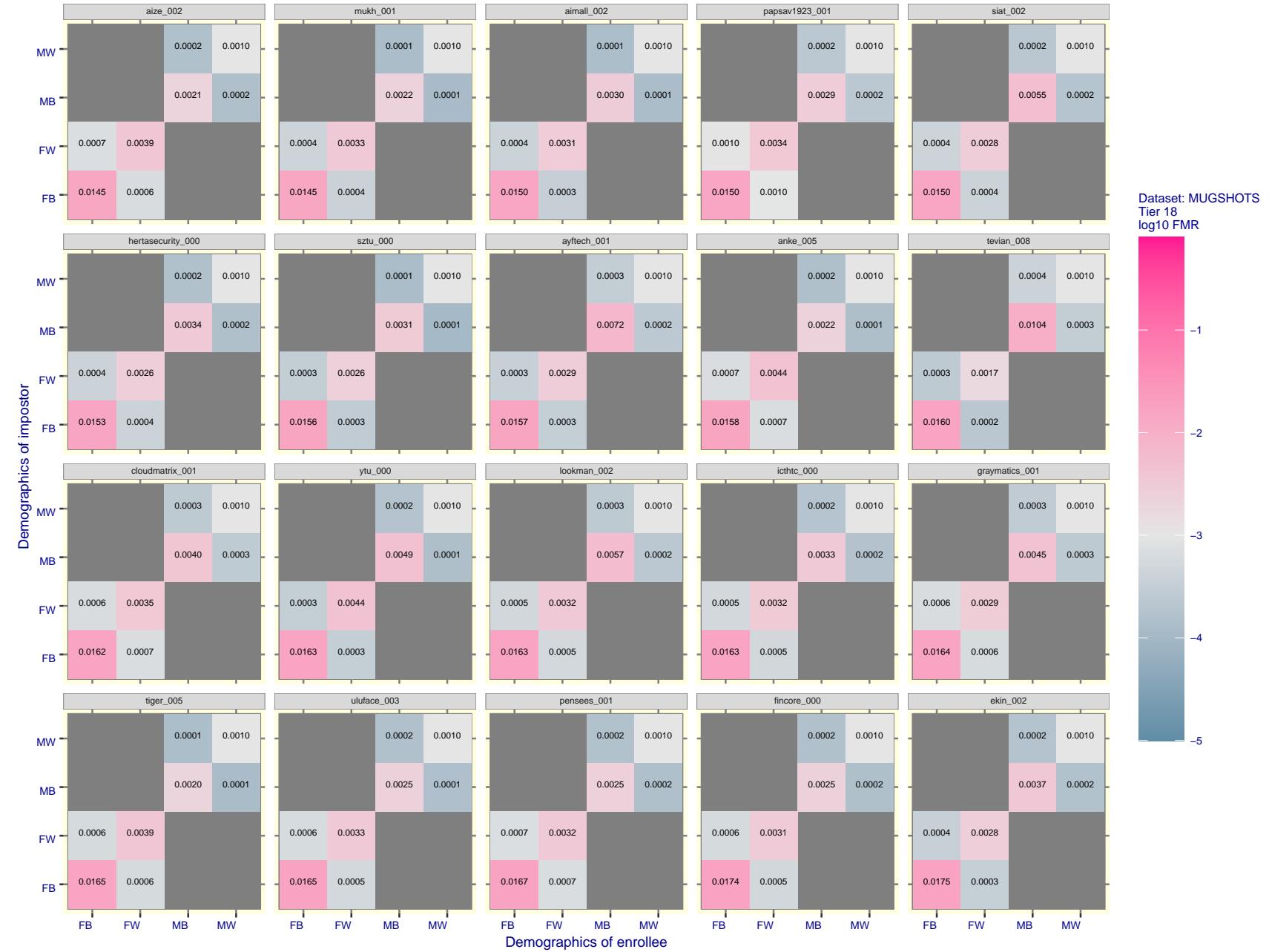


Figure 119: For the mugshot images, FMR for same-sex impostor pairs of images annotated with codes for black female, black male, white female, white male. The threshold is set for each algorithm to give FMR = 0.001 for white males which is the demographic that usually gives the lowest FMR. This means the top right box is the same color in all panels. The panels are sorted over multiple pages in order of FMR on black females, which is the demographic that usually gives the highest FMR.

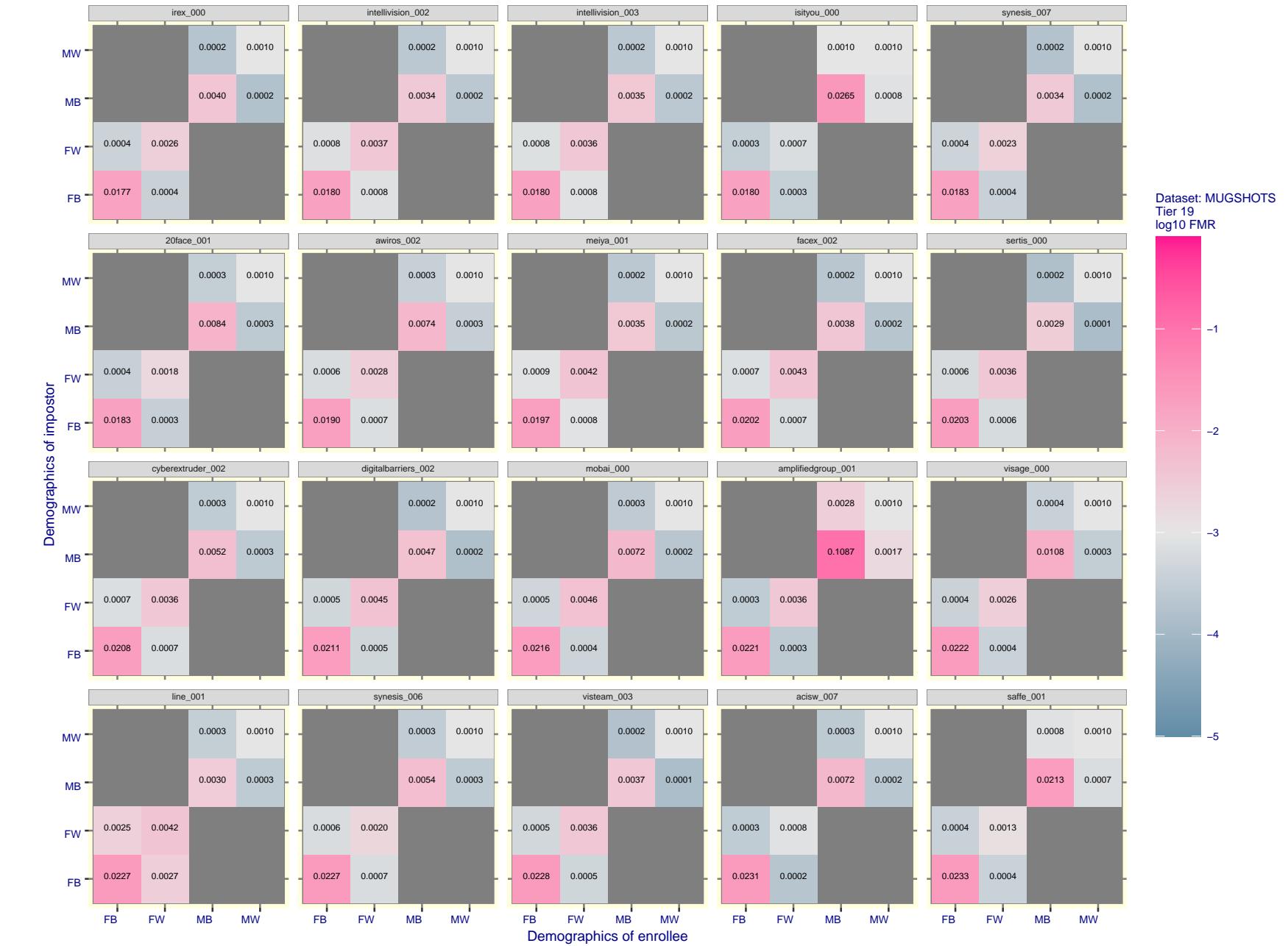


Figure 120: For the mugshot images, FMR for same-sex impostor pairs of images annotated with codes for black female, black male, white female, white male. The threshold is set for each algorithm to give FMR = 0.001 for white males which is the demographic that usually gives the lowest FMR. This means the top right box is the same color in all panels. The panels are sorted over multiple pages in order of FMR on black females, which is the demographic that usually gives the highest FMR.

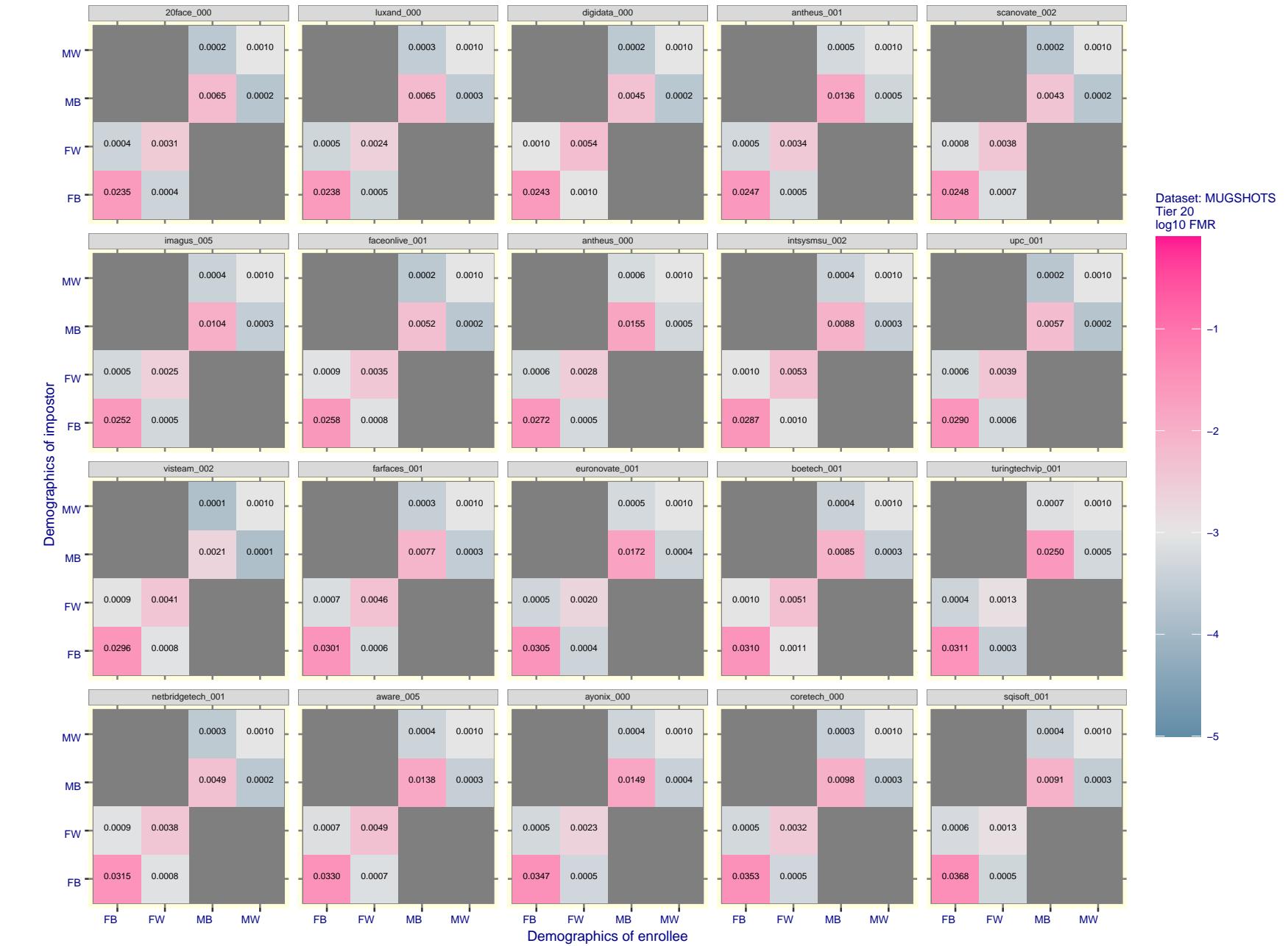


Figure 121: For the mugshot images, FMR for same-sex impostor pairs of images annotated with codes for black female, black male, white female, white male. The threshold is set for each algorithm to give FMR = 0.001 for white males which is the demographic that usually gives the lowest FMR. This means the top right box is the same color in all panels. The panels are sorted over multiple pages in order of FMR on black females, which is the demographic that usually gives the highest FMR.



Figure 122: For the mugshot images, FMR for same-sex impostor pairs of images annotated with codes for black female, black male, white female, white male. The threshold is set for each algorithm to give  $FMR = 0.001$  for white males which is the demographic that usually gives the lowest FMR. This means the top right box is the same color in all panels. The panels are sorted over multiple pages in order of FMR on black females, which is the demographic that usually gives the highest FMR.

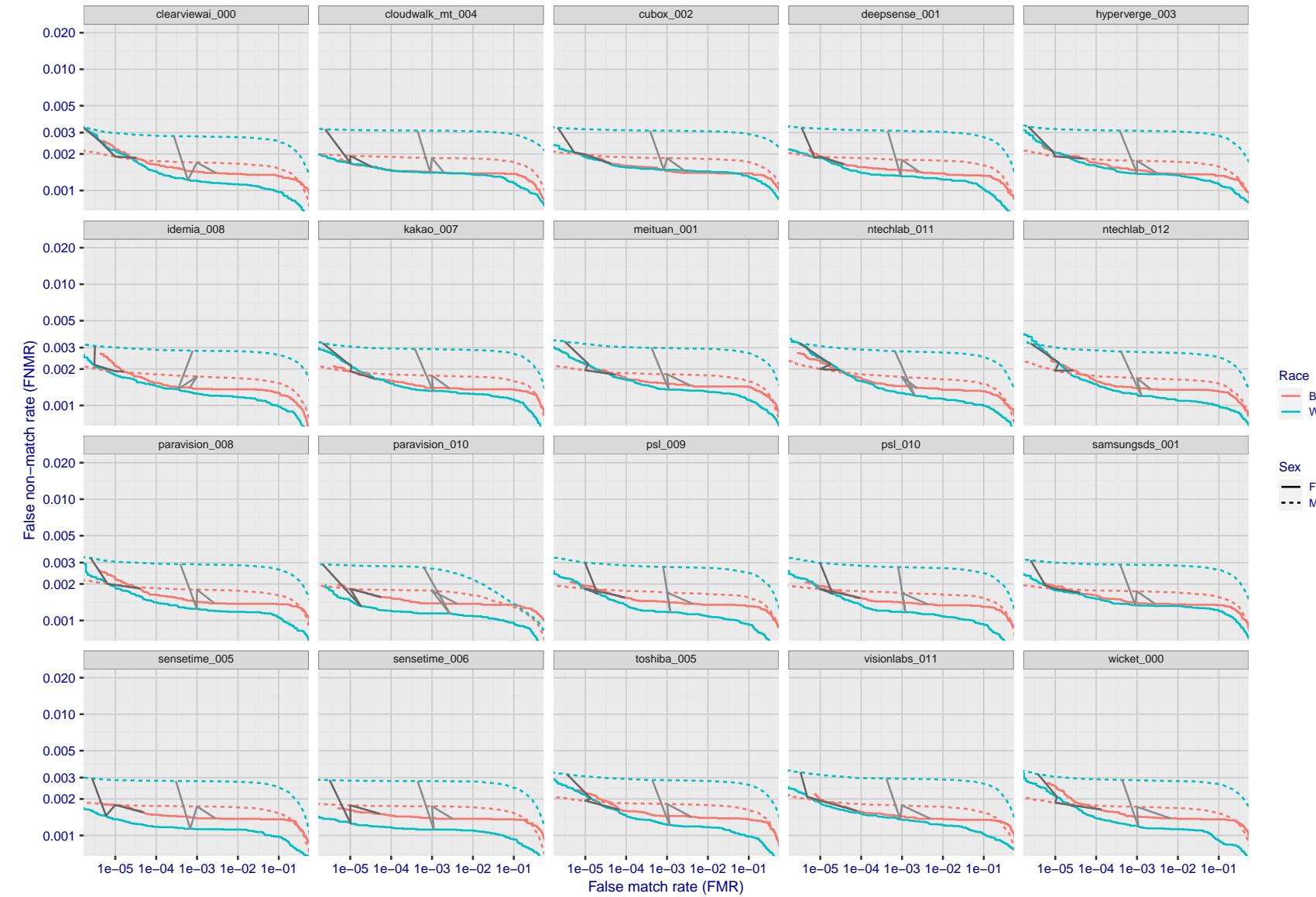


Figure 123: For the mugshot images, error tradeoff characteristics for white females, black females, black males and white males. The Z-shaped grey lines correspond to fixed thresholds, showing both FNMR and FMR vary at one  $T$  value. Note: Many of the plots will naively be read as saying women gives worse error rates than men because the solid traces lie above the dotted ones. However, this is misleading and incomplete: The grey lines show the traces reveal horizontal shifts. Thus for the cogent-003 algorithm FNMR for men is higher than for women at a fixed threshold but, at the same time, FMR is higher for women - see Figure 199. As access control systems almost always operate at a fixed threshold, the naive interpretation is incorrect.

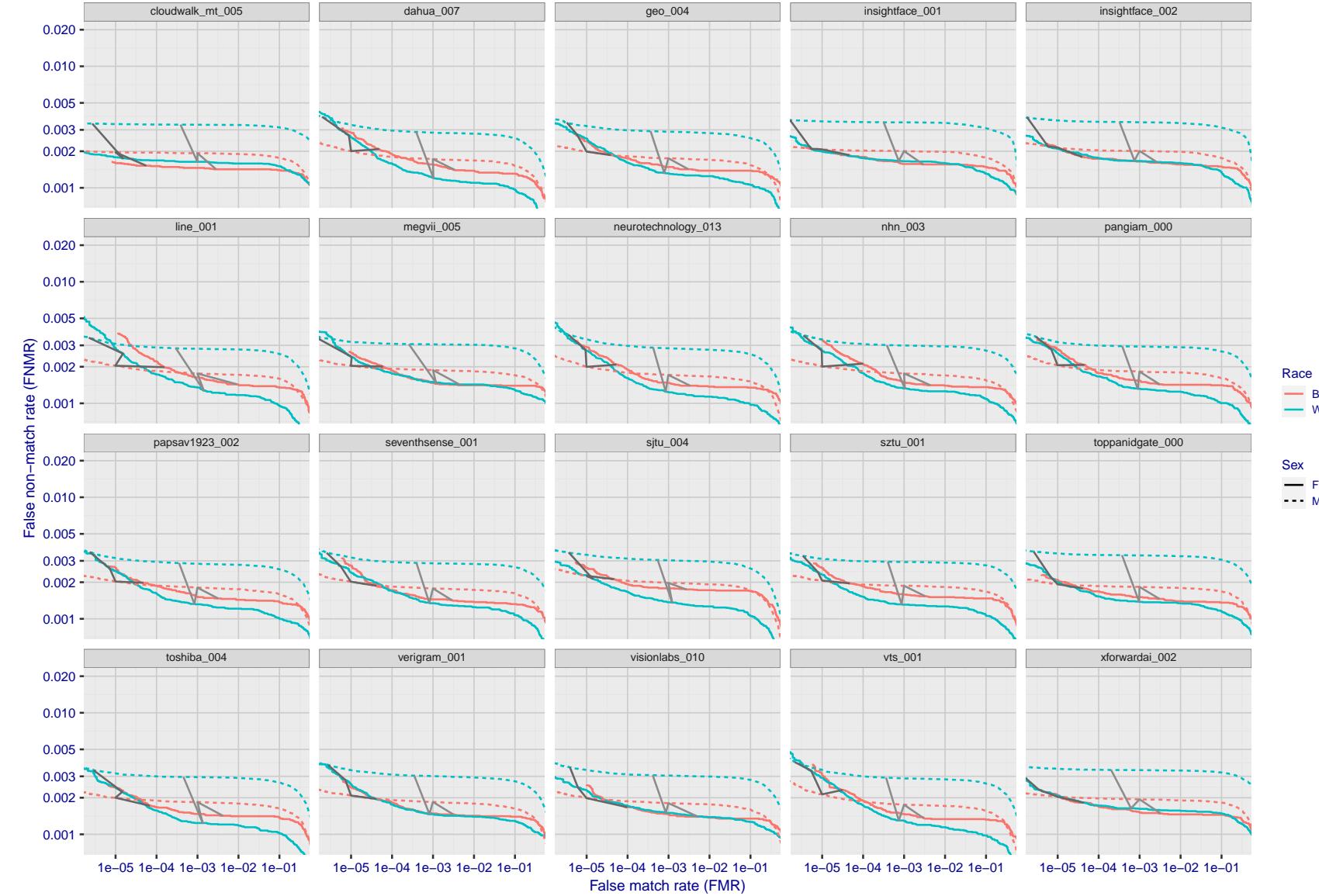


Figure 124: For the mugshot images, error tradeoff characteristics for white females, black females, black males and white males. The Z-shaped grey lines correspond to fixed thresholds, showing both FNMR and FMR vary at one T value. Note: Many of the plots will naively be read as saying women gives worse error rates than men because the solid traces lie above the dotted ones. However, this is misleading and incomplete: The grey lines show the traces reveal horizontal shifts. Thus for the cogent-003 algorithm FNMR for men is higher than for women at a fixed threshold but, at the same time, FMR is higher for women - see Figure 199. As access control systems almost always operate at a fixed threshold, the naive interpretation is incorrect.

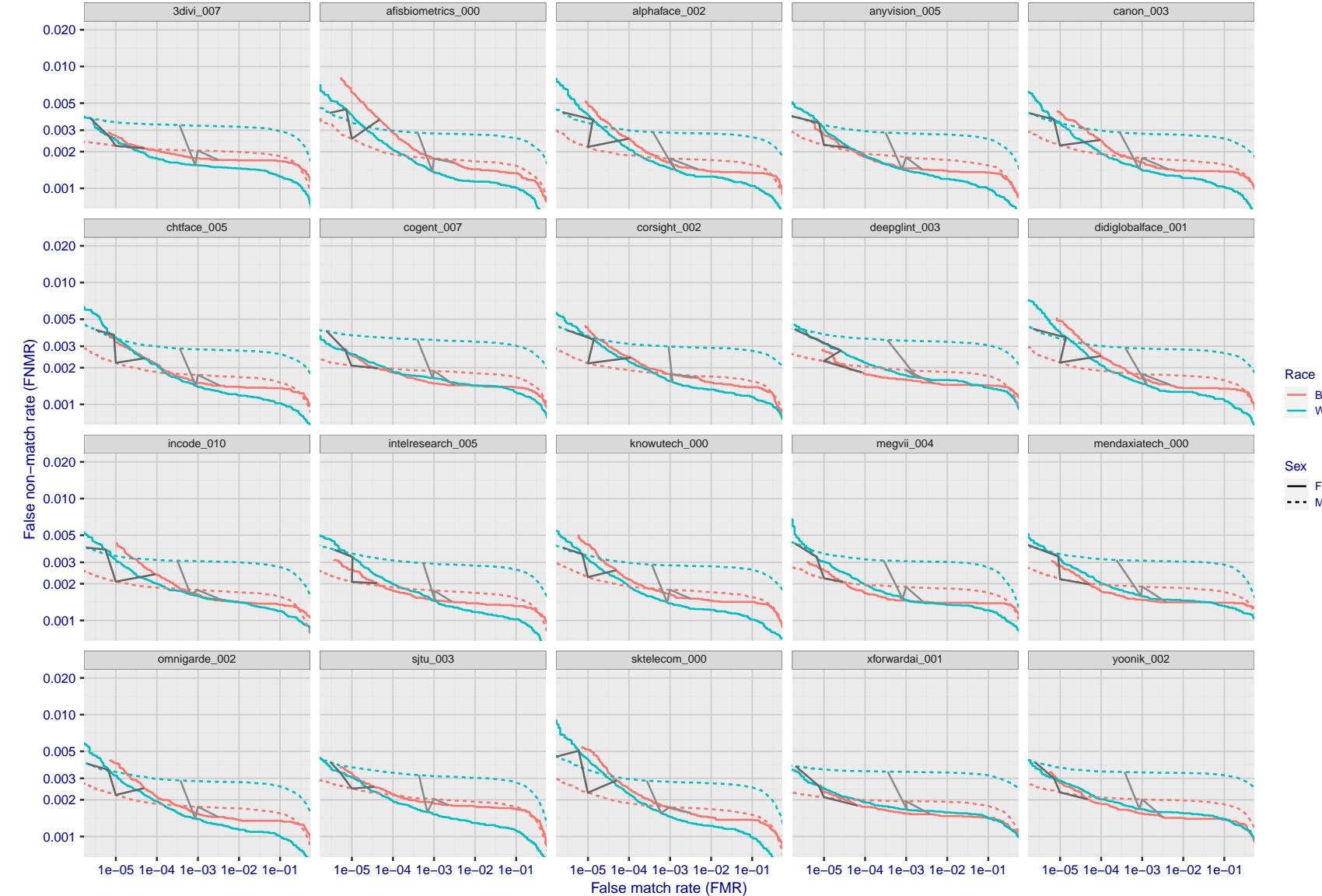


Figure 125: For the mugshot images, error tradeoff characteristics for white females, black females, black males and white males. The Z-shaped grey lines correspond to fixed thresholds, showing both FNMR and FMR vary at one  $T$  value. Note: Many of the plots will naively be read as saying women gives worse error rates than men because the solid traces lie above the dotted ones. However, this is misleading and incomplete: The grey lines show the traces reveal horizontal shifts. Thus for the cogent-003 algorithm FNMR for men is higher than for women at a fixed threshold but, at the same time, FMR is higher for women - see Figure 199. As access control systems almost always operate at a fixed threshold, the naive interpretation is incorrect.

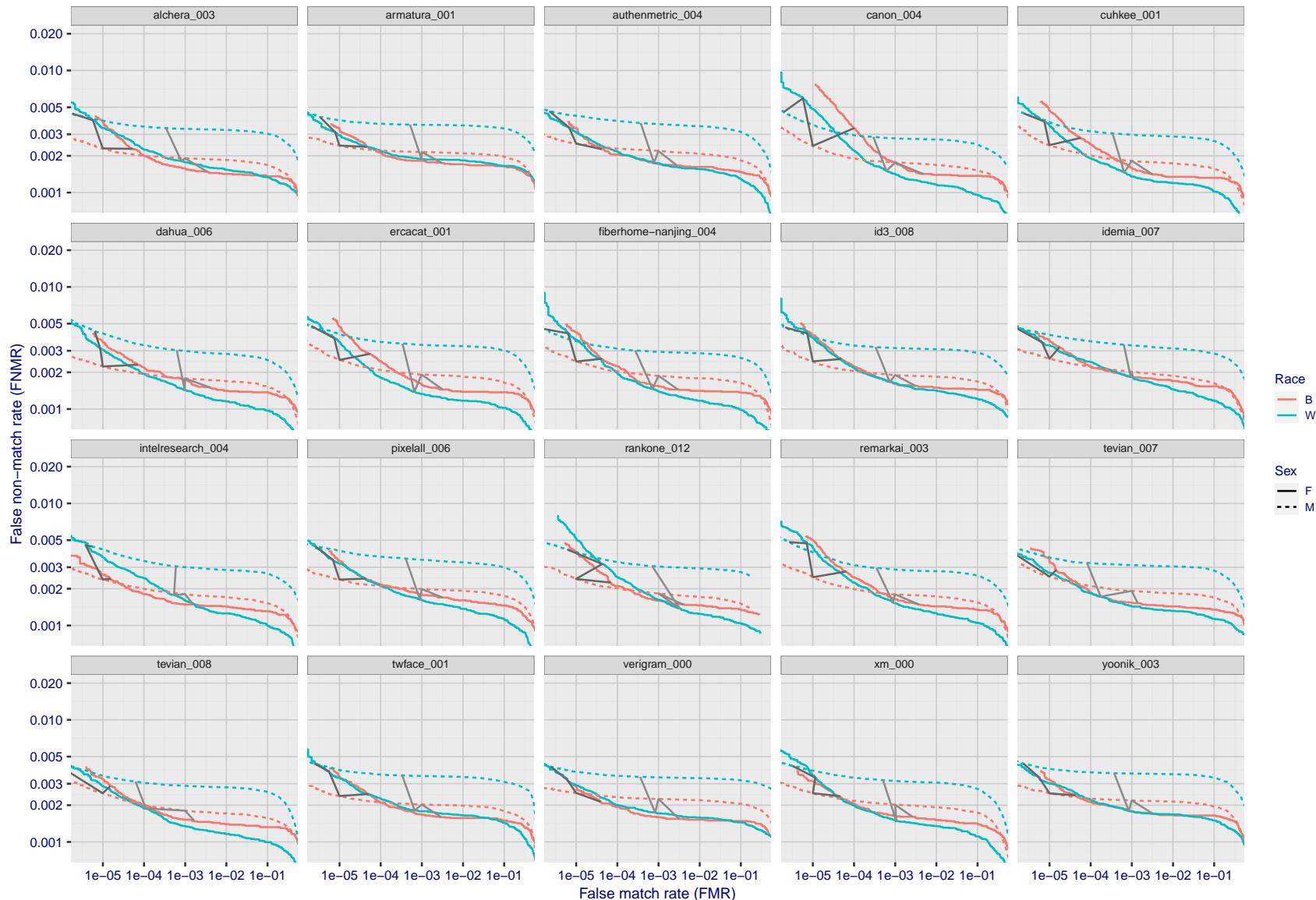


Figure 126: For the mugshot images, error tradeoff characteristics for white females, black females, black males and white males. The Z-shaped grey lines correspond to fixed thresholds, showing both FNMR and FMR vary at one T value. Note: Many of the plots will naively be read as saying women gives worse error rates than men because the solid traces lie above the dotted ones. However, this is misleading and incomplete: The grey lines show the traces reveal horizontal shifts. Thus for the cogent-003 algorithm FNMR for men is higher than for women at a fixed threshold but, at the same time, FMR is higher for women - see Figure 199. As access control systems almost always operate at a fixed threshold, the naive interpretation is incorrect.

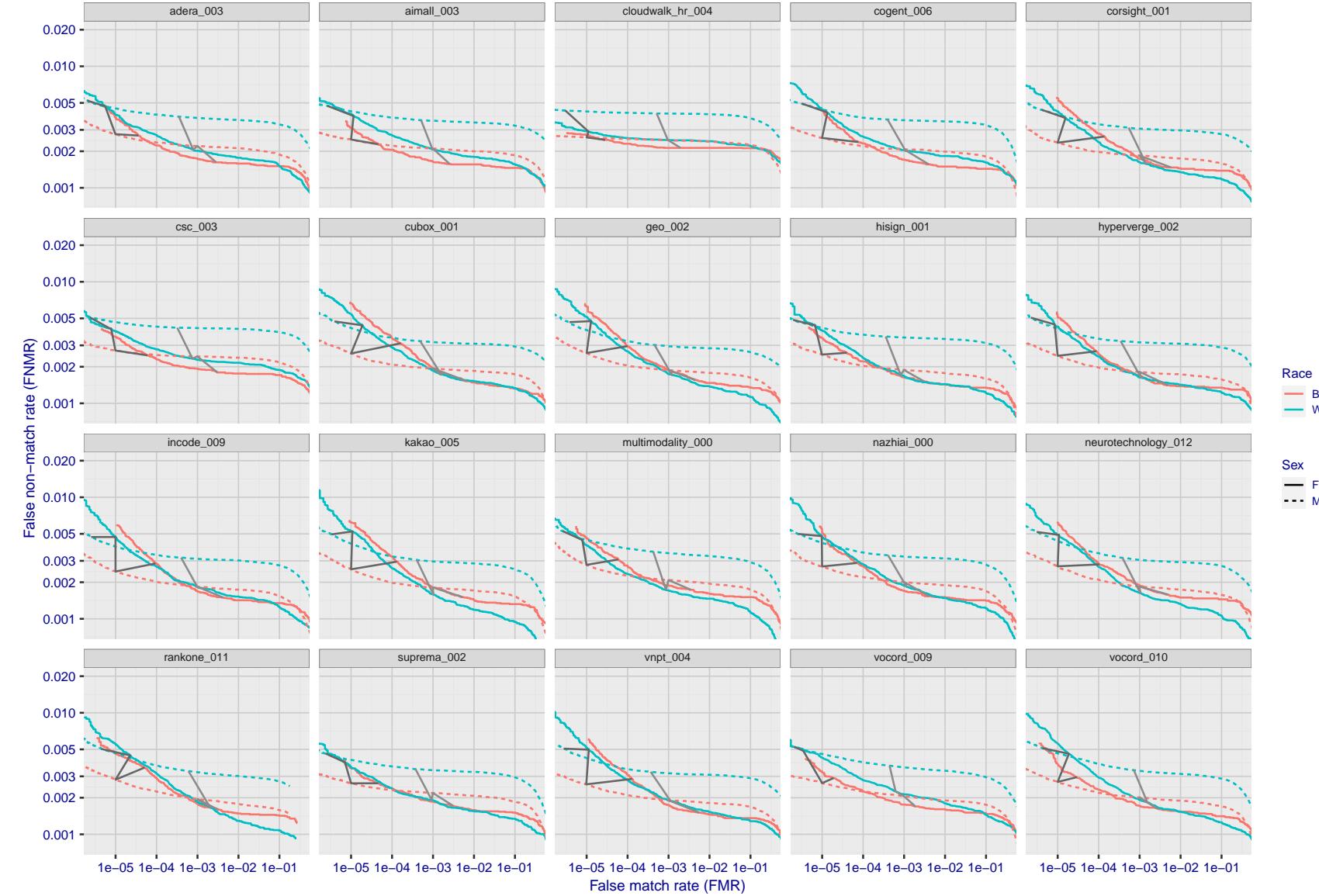


Figure 127: For the mugshot images, error tradeoff characteristics for white females, black females, black males and white males. The Z-shaped grey lines correspond to fixed thresholds, showing both FNMR and FMR vary at one T value. Note: Many of the plots will naively be read as saying women gives worse error rates than men because the solid traces lie above the dotted ones. However, this is misleading and incomplete: The grey lines show the traces reveal horizontal shifts. Thus for the cogent-003 algorithm FNMR for men is higher than for women at a fixed threshold but, at the same time, FMR is higher for women - see Figure 199. As access control systems almost always operate at a fixed threshold, the naive interpretation is incorrect.

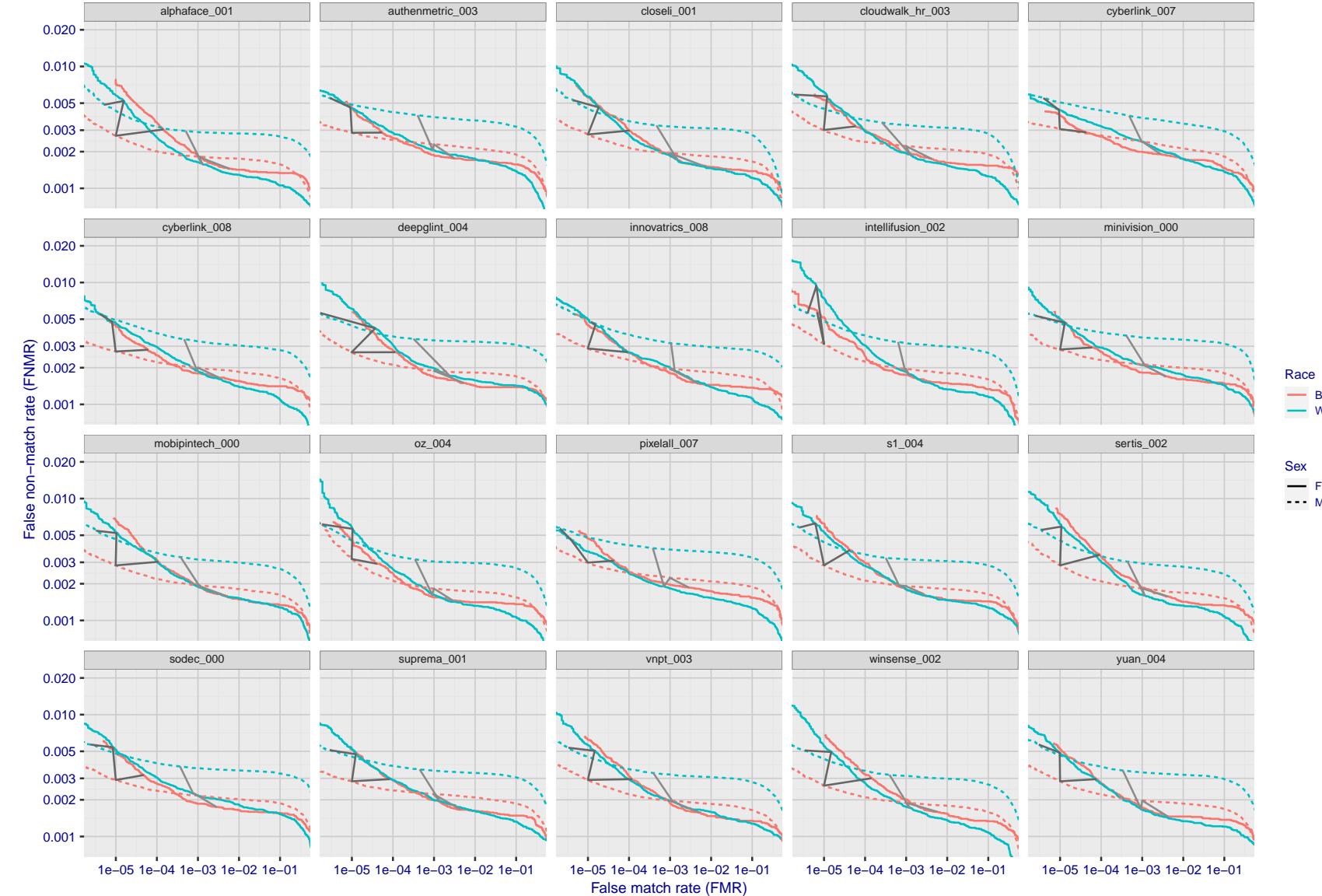


Figure 128: For the mugshot images, error tradeoff characteristics for white females, black females, black males and white males. The Z-shaped grey lines correspond to fixed thresholds, showing both FNMR and FMR vary at one  $T$  value. Note: Many of the plots will naively be read as saying women gives worse error rates than men because the solid traces lie above the dotted ones. However, this is misleading and incomplete: The grey lines show the traces reveal horizontal shifts. Thus for the cogent-003 algorithm FNMR for men is higher than for women at a fixed threshold but, at the same time, FMR is higher for women - see Figure 199. As access control systems almost always operate at a fixed threshold, the naive interpretation is incorrect.

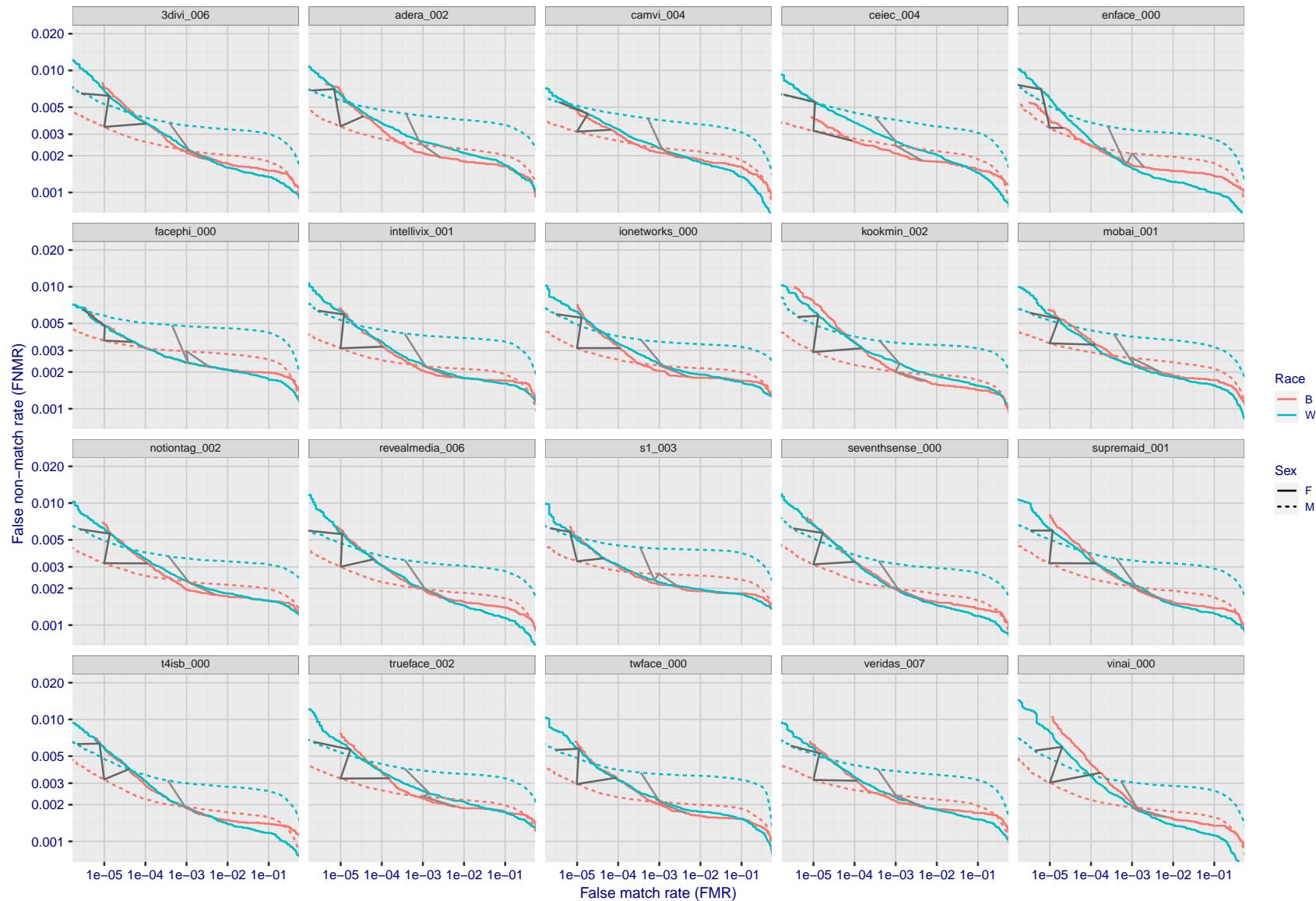


Figure 129: For the mugshot images, error tradeoff characteristics for white females, black females, black males and white males. The Z-shaped grey lines correspond to fixed thresholds, showing both FNMR and FMR vary at one  $T$  value. Note: Many of the plots will naively be read as saying women gives worse error rates than men because the solid traces lie above the dotted ones. However, this is misleading and incomplete: The grey lines show the traces reveal horizontal shifts. Thus for the cogent-003 algorithm FNMR for men is higher than for women at a fixed threshold but, at the same time, FMR is higher for women - see Figure 199. As access control systems almost always operate at a fixed threshold, the naive interpretation is incorrect.

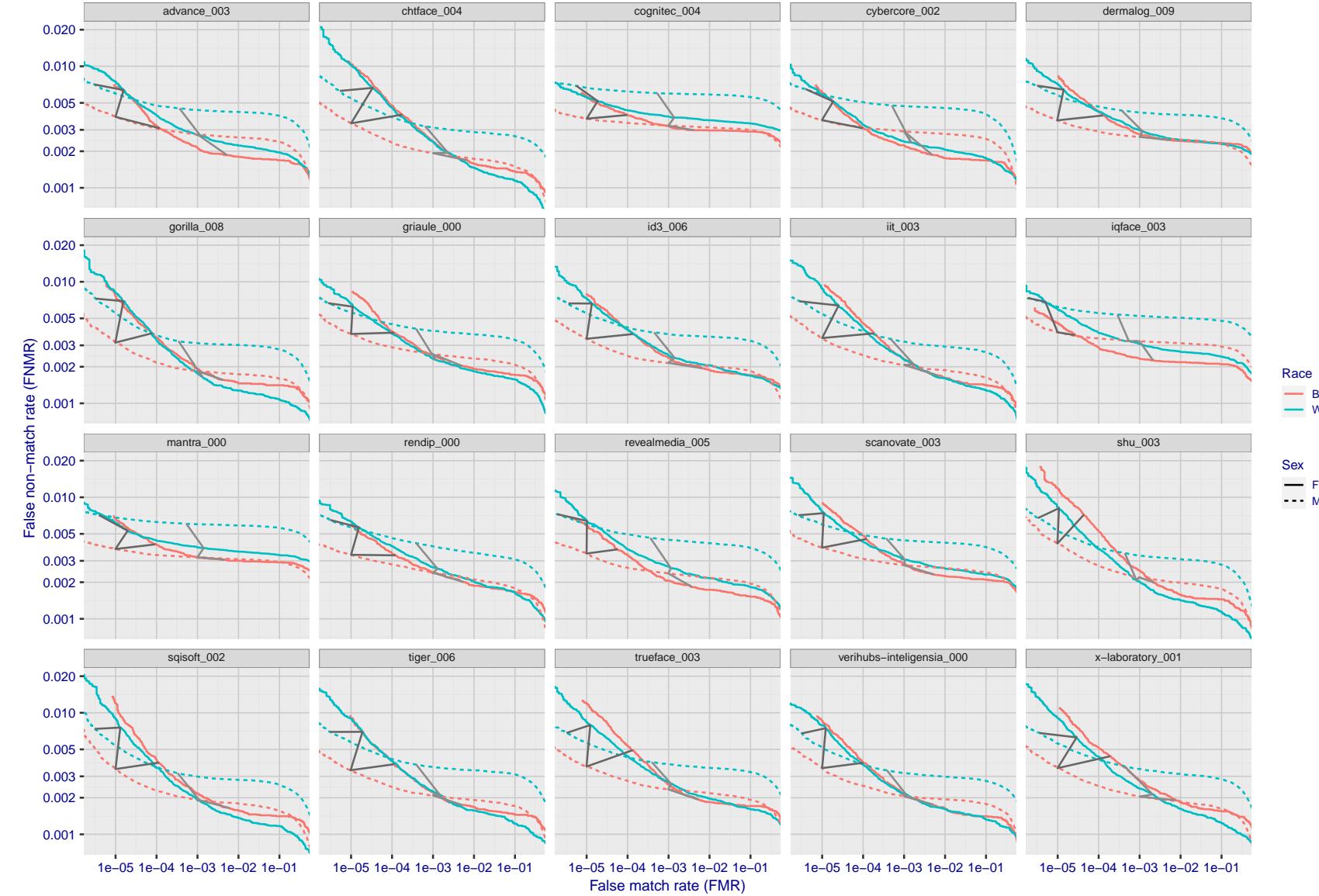


Figure 130: For the mugshot images, error tradeoff characteristics for white females, black females, black males and white males. The Z-shaped grey lines correspond to fixed thresholds, showing both FNMR and FMR vary at one T value. Note: Many of the plots will naively be read as saying women gives worse error rates than men because the solid traces lie above the dotted ones. However, this is misleading and incomplete: The grey lines show the traces reveal horizontal shifts. Thus for the cogent-003 algorithm FNMR for men is higher than for women at a fixed threshold but, at the same time, FMR is higher for women - see Figure 199. As access control systems almost always operate at a fixed threshold, the naive interpretation is incorrect.

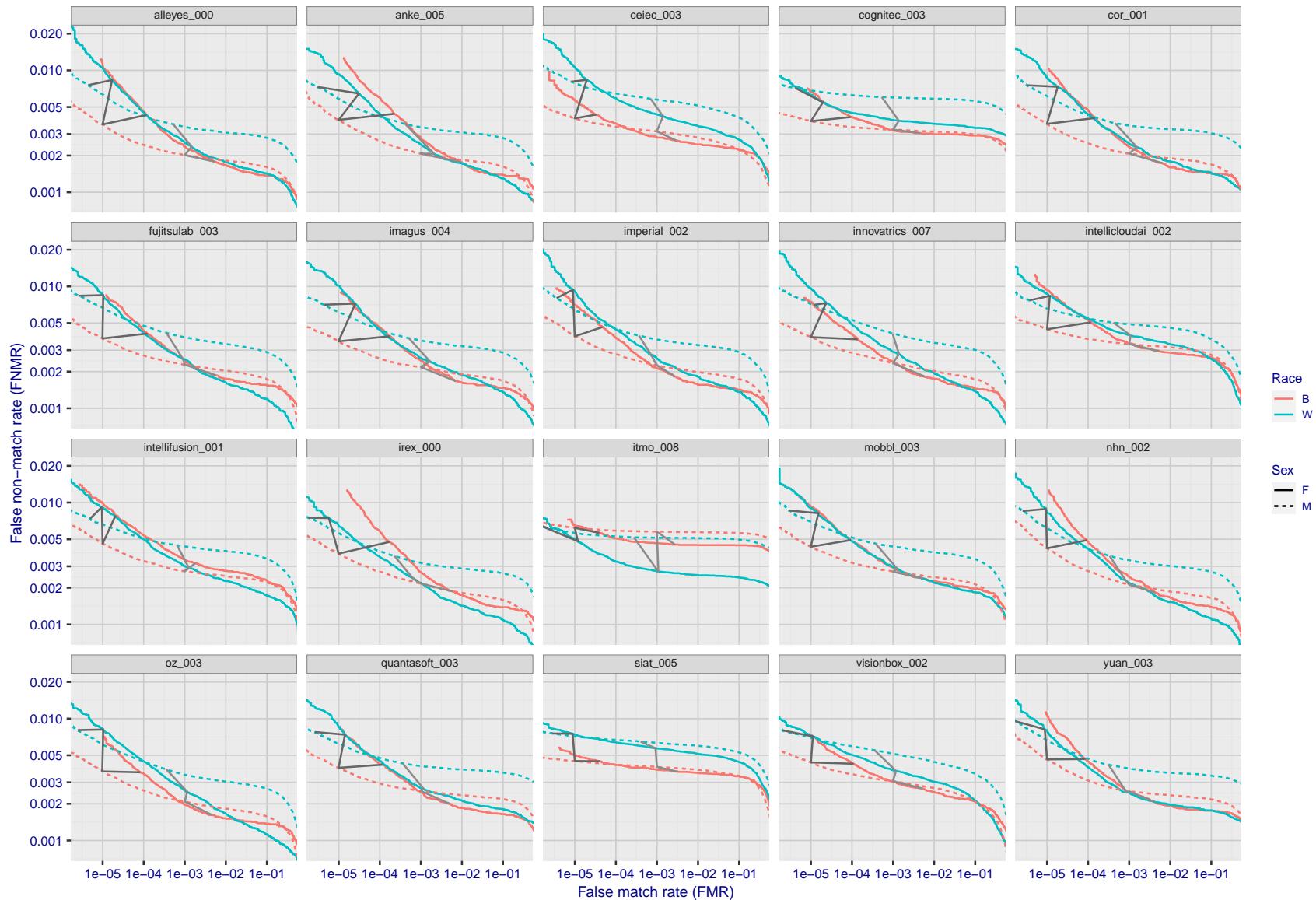


Figure 131: For the mugshot images, error tradeoff characteristics for white females, black females, black males and white males. The Z-shaped grey lines correspond to fixed thresholds, showing both FNMR and FMR vary at one T value. Note: Many of the plots will naively be read as saying women gives worse error rates than men because the solid traces lie above the dotted ones. However, this is misleading and incomplete: The grey lines show the traces reveal horizontal shifts. Thus for the cogent-003 algorithm FNMR for men is higher than for women at a fixed threshold but, at the same time, FMR is higher for women - see Figure 199. As access control systems almost always operate at a fixed threshold, the naive interpretation is incorrect.

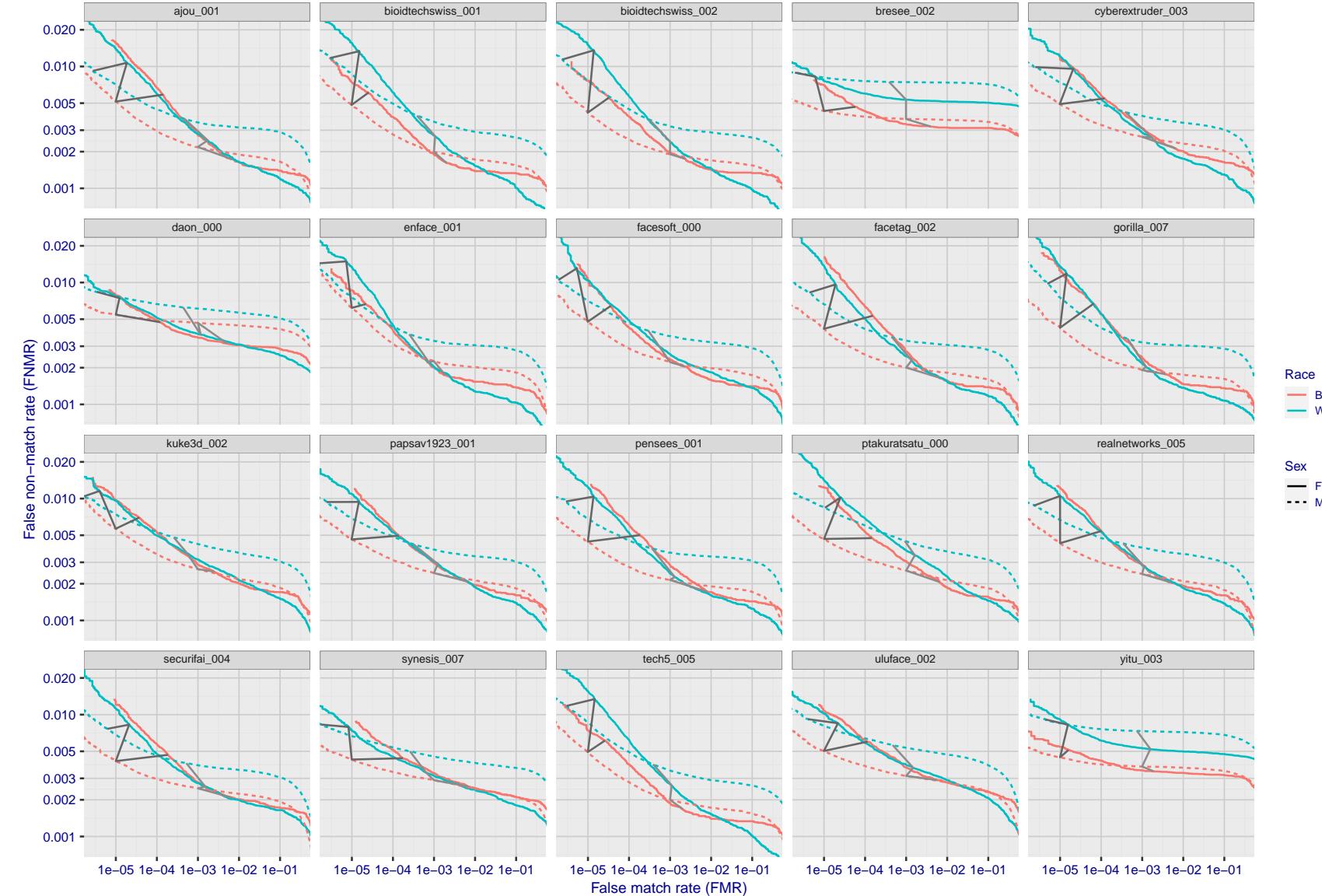


Figure 132: For the mugshot images, error tradeoff characteristics for white females, black females, black males and white males. The Z-shaped grey lines correspond to fixed thresholds, showing both FNMR and FMR vary at one T value. Note: Many of the plots will naively be read as saying women gives worse error rates than men because the solid traces lie above the dotted ones. However, this is misleading and incomplete: The grey lines show the traces reveal horizontal shifts. Thus for the cogent-003 algorithm FNMR for men is higher than for women at a fixed threshold but, at the same time, FMR is higher for women - see Figure 199. As access control systems almost always operate at a fixed threshold, the naive interpretation is incorrect.

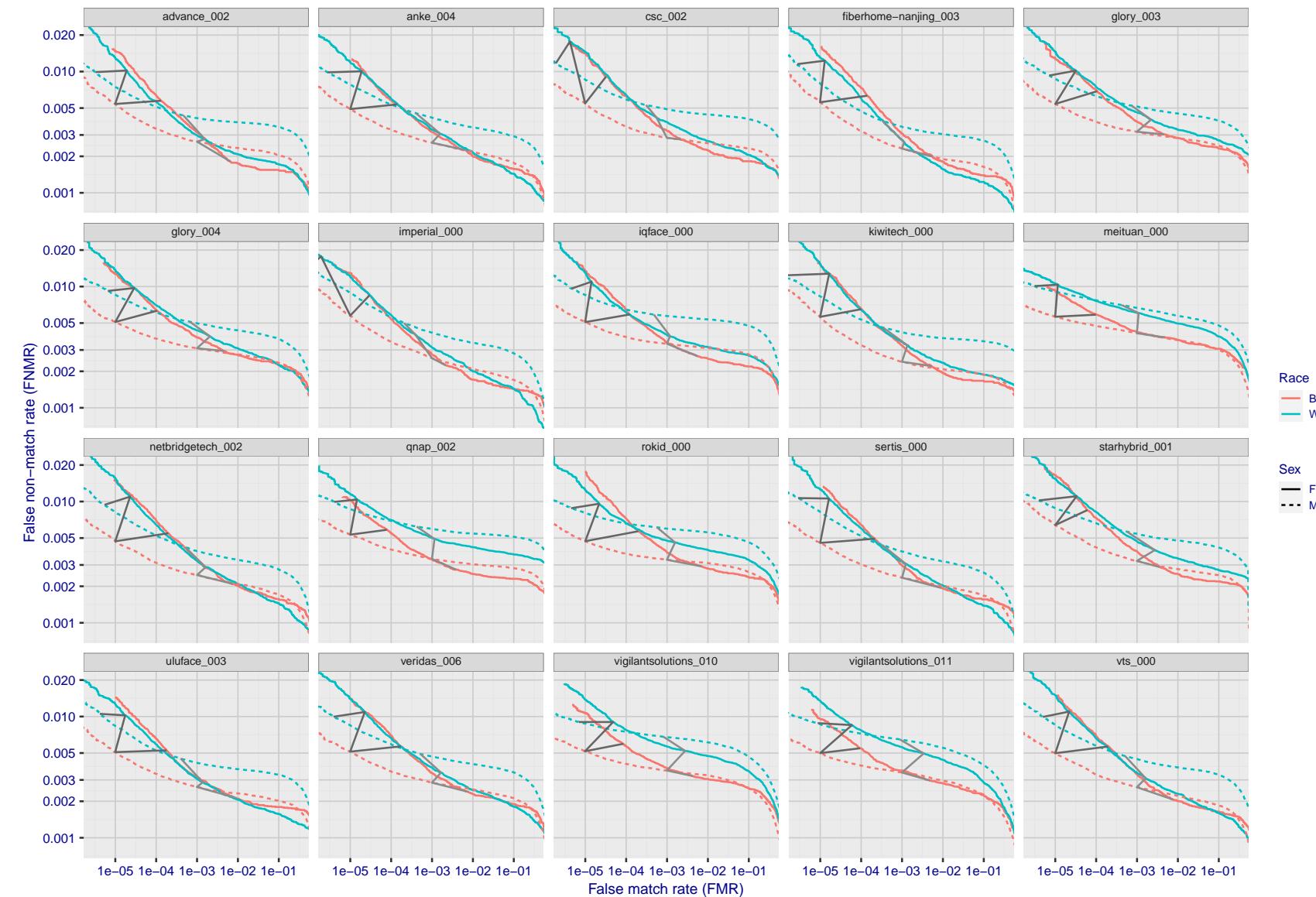


Figure 133: For the mugshot images, error tradeoff characteristics for white females, black females, black males and white males. The Z-shaped grey lines correspond to fixed thresholds, showing both FNMR and FMR vary at one  $T$  value. Note: Many of the plots will naively be read as saying women gives worse error rates than men because the solid traces lie above the dotted ones. However, this is misleading and incomplete: The grey lines show the traces reveal horizontal shifts. Thus for the cogent-003 algorithm FNMR for men is higher than for women at a fixed threshold but, at the same time, FMR is higher for women - see Figure 199. As access control systems almost always operate at a fixed threshold, the naive interpretation is incorrect.

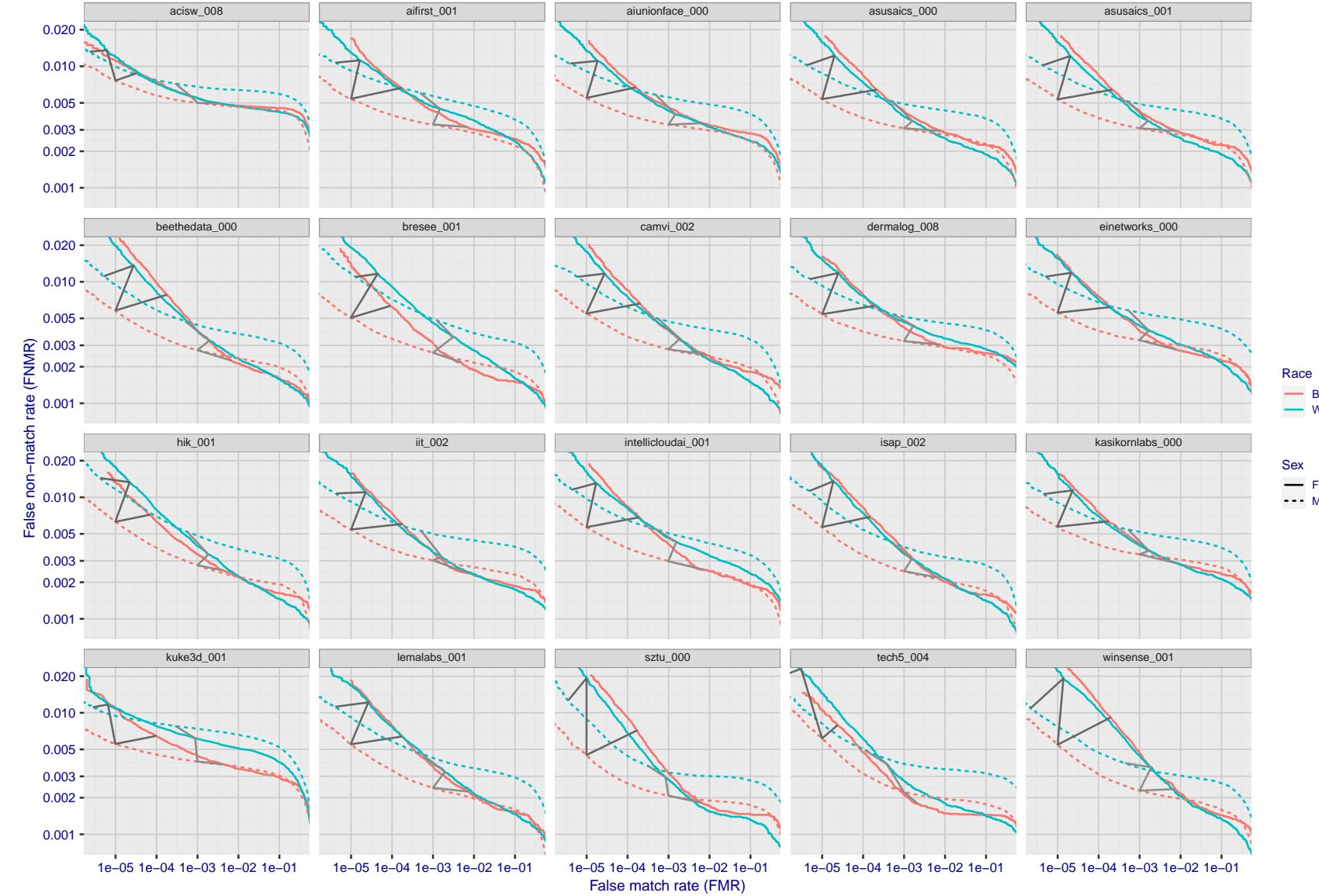


Figure 134: For the mugshot images, error tradeoff characteristics for white females, black females, black males and white males. The Z-shaped grey lines correspond to fixed thresholds, showing both FNMR and FMR vary at one T value. Note: Many of the plots will naively be read as saying women gives worse error rates than men because the solid traces lie above the dotted ones. However, this is misleading and incomplete: The grey lines show the traces reveal horizontal shifts. Thus for the cogent-003 algorithm FNMR for men is higher than for women at a fixed threshold but, at the same time, FMR is higher for women - see Figure 199. As access control systems almost always operate at a fixed threshold, the naive interpretation is incorrect.

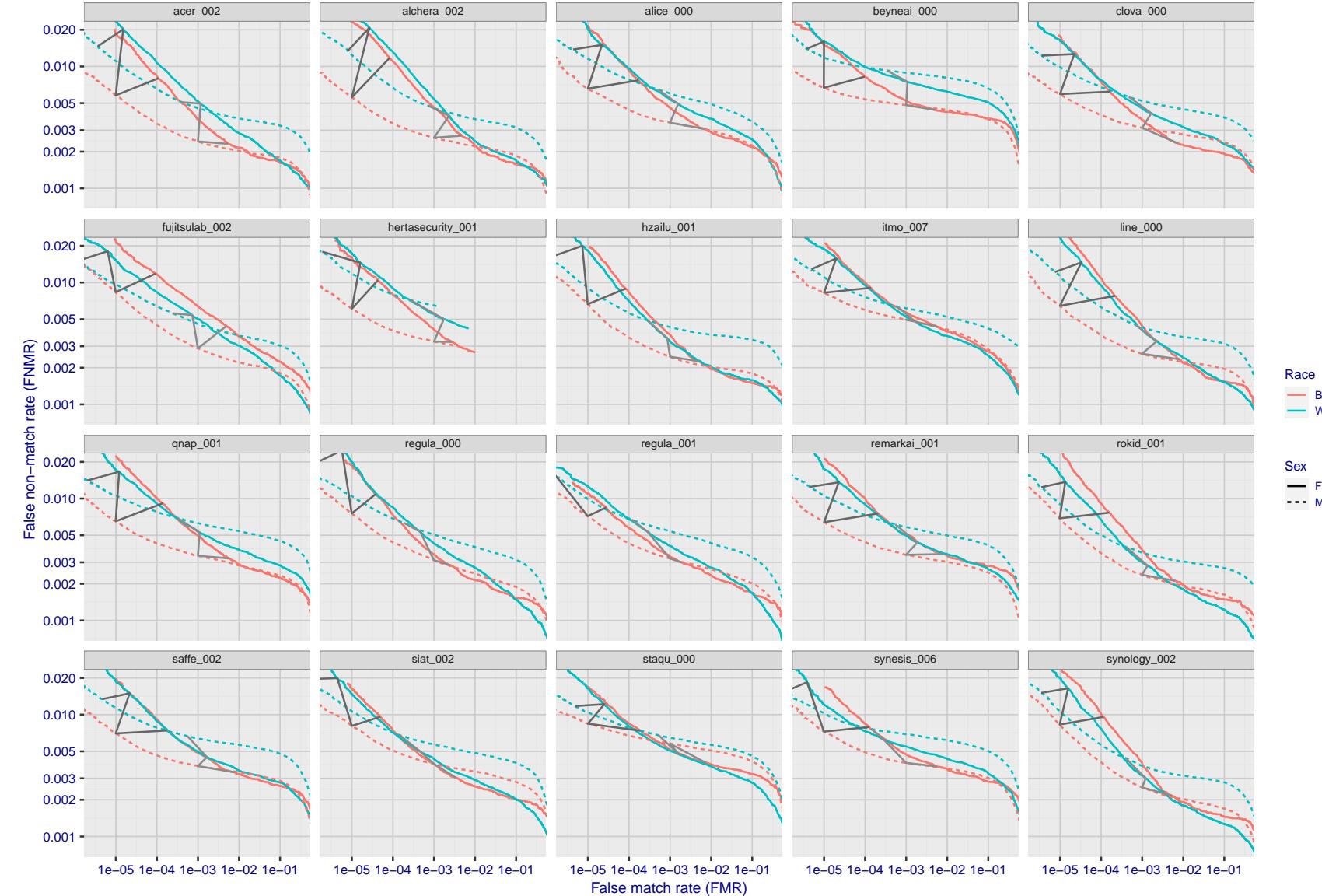


Figure 135: For the mugshot images, error tradeoff characteristics for white females, black females, black males and white males. The Z-shaped grey lines correspond to fixed thresholds, showing both FNMR and FMR vary at one T value. Note: Many of the plots will naively be read as saying women gives worse error rates than men because the solid traces lie above the dotted ones. However, this is misleading and incomplete: The grey lines show the traces reveal horizontal shifts. Thus for the cogent-003 algorithm FNMR for men is higher than for women at a fixed threshold but, at the same time, FMR is higher for women - see Figure 199. As access control systems almost always operate at a fixed threshold, the naive interpretation is incorrect.

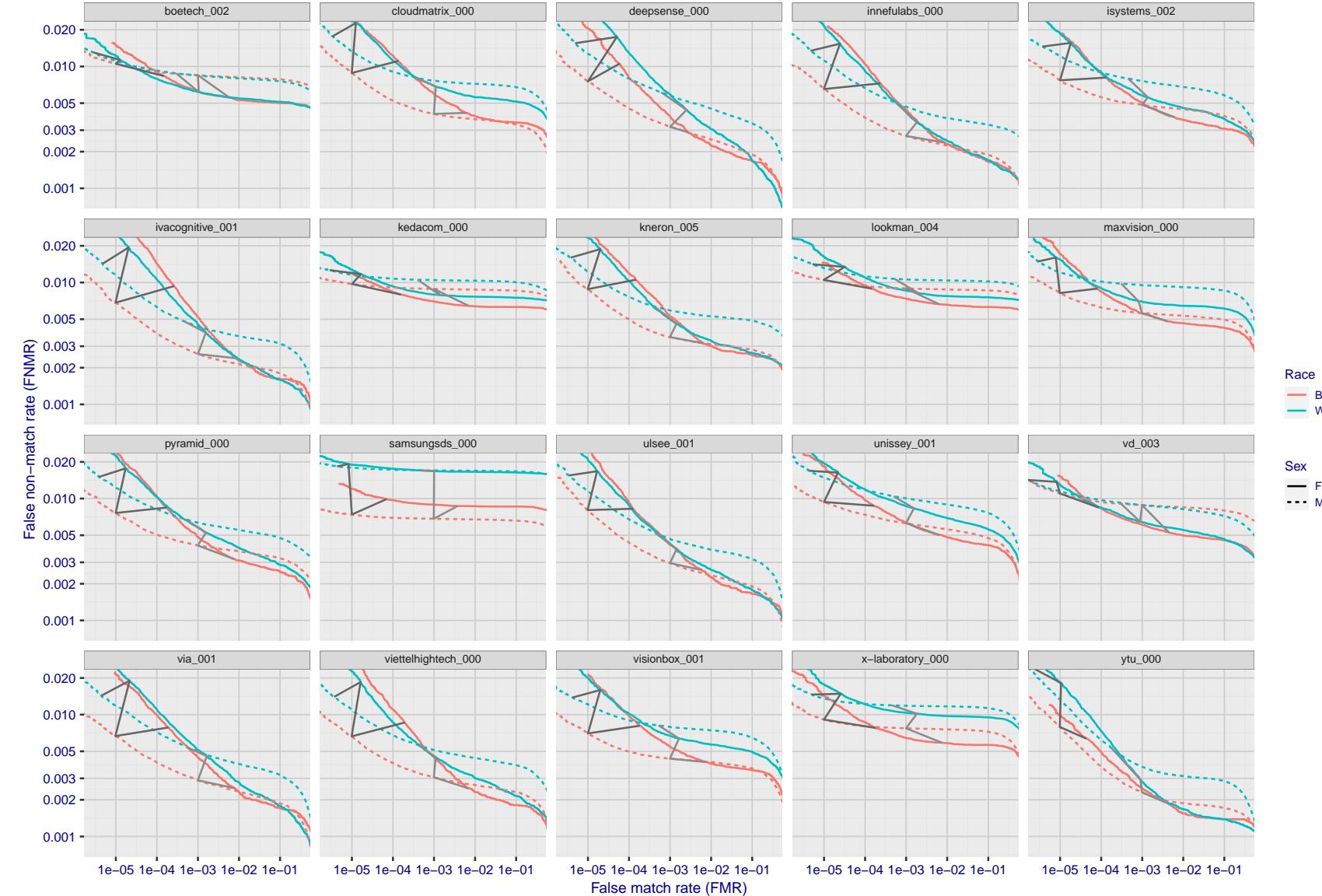


Figure 136: For the mugshot images, error tradeoff characteristics for white females, black females, black males and white males. The Z-shaped grey lines correspond to fixed thresholds, showing both FNMR and FMR vary at one  $T$  value. Note: Many of the plots will naively be read as saying women gives worse error rates than men because the solid traces lie above the dotted ones. However, this is misleading and incomplete: The grey lines show the traces reveal horizontal shifts. Thus for the cogent-003 algorithm FNMR for men is higher than for women at a fixed threshold but, at the same time, FMR is higher for women - see Figure 199. As access control systems almost always operate at a fixed threshold, the naive interpretation is incorrect.

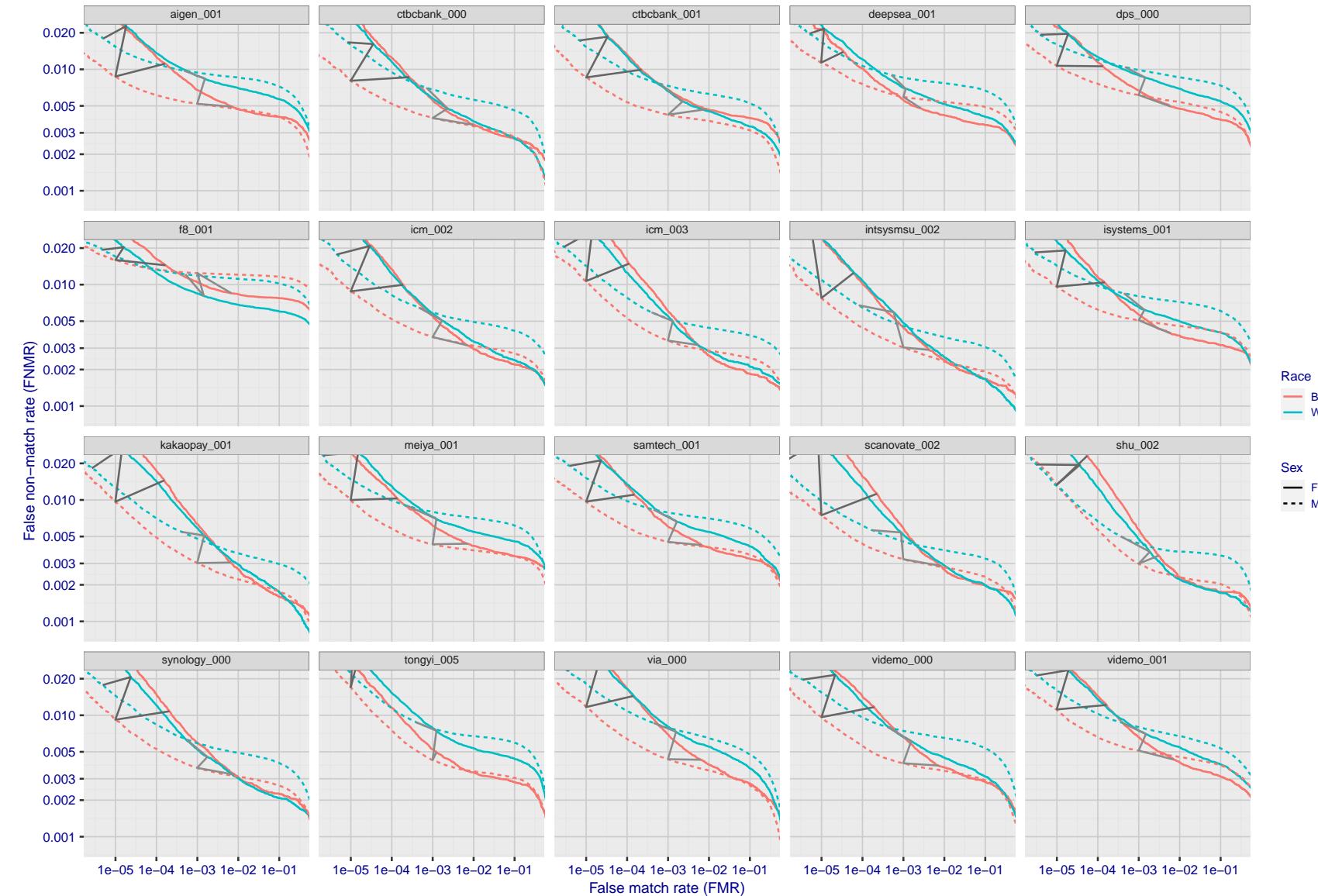


Figure 137: For the mugshot images, error tradeoff characteristics for white females, black females, black males and white males. The Z-shaped grey lines correspond to fixed thresholds, showing both FNMR and FMR vary at one T value. Note: Many of the plots will naively be read as saying women gives worse error rates than men because the solid traces lie above the dotted ones. However, this is misleading and incomplete: The grey lines show the traces reveal horizontal shifts. Thus for the cogent-003 algorithm FNMR for men is higher than for women at a fixed threshold but, at the same time, FMR is higher for women - see Figure 199. As access control systems almost always operate at a fixed threshold, the naive interpretation is incorrect.

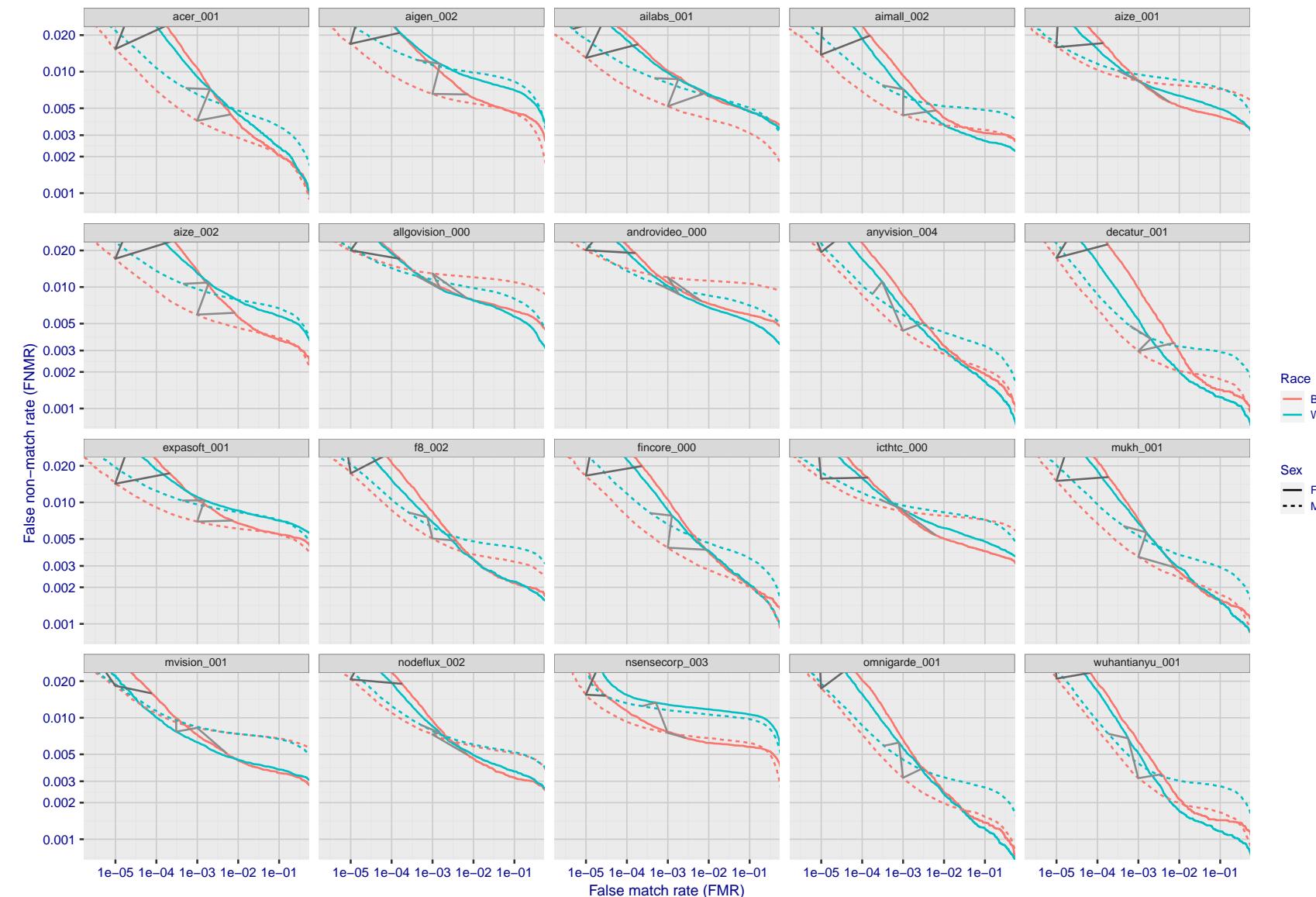


Figure 138: For the mugshot images, error tradeoff characteristics for white females, black females, black males and white males. The Z-shaped grey lines correspond to fixed thresholds, showing both FNMR and FMR vary at one T value. Note: Many of the plots will naively be read as saying women gives worse error rates than men because the solid traces lie above the dotted ones. However, this is misleading and incomplete: The grey lines show the traces reveal horizontal shifts. Thus for the cogent-003 algorithm FNMR for men is higher than for women at a fixed threshold but, at the same time, FMR is higher for women - see Figure 199. As access control systems almost always operate at a fixed threshold, the naive interpretation is incorrect.

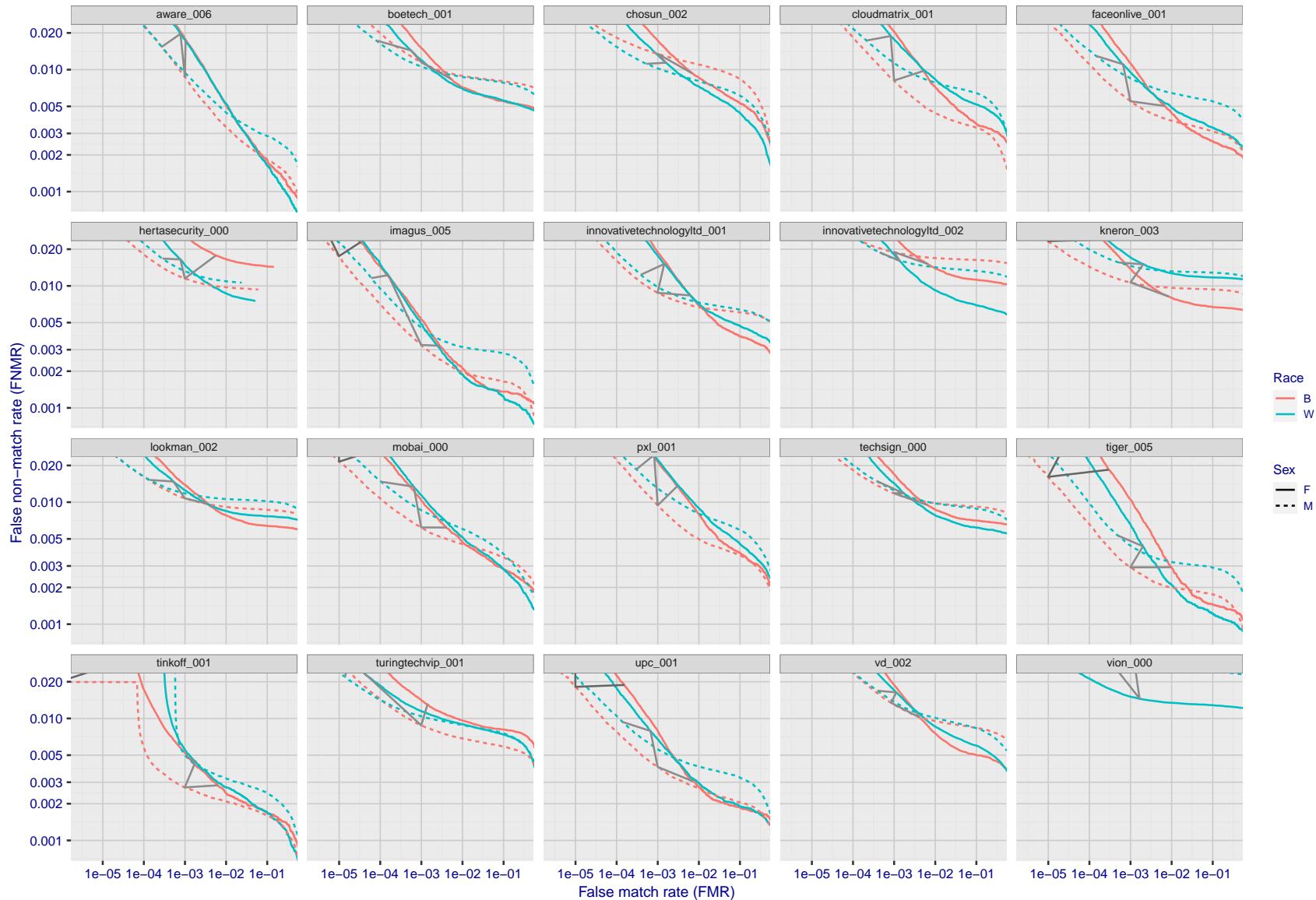


Figure 139: For the mugshot images, error tradeoff characteristics for white females, black females, black males and white males. The Z-shaped grey lines correspond to fixed thresholds, showing both FNMR and FMR vary at one  $T$  value. Note: Many of the plots will naively be read as saying women gives worse error rates than men because the solid traces lie above the dotted ones. However, this is misleading and incomplete: The grey lines show the traces reveal horizontal shifts. Thus for the cogent-003 algorithm FNMR for men is higher than for women at a fixed threshold but, at the same time, FMR is higher for women - see Figure 199. As access control systems almost always operate at a fixed threshold, the naive interpretation is incorrect.

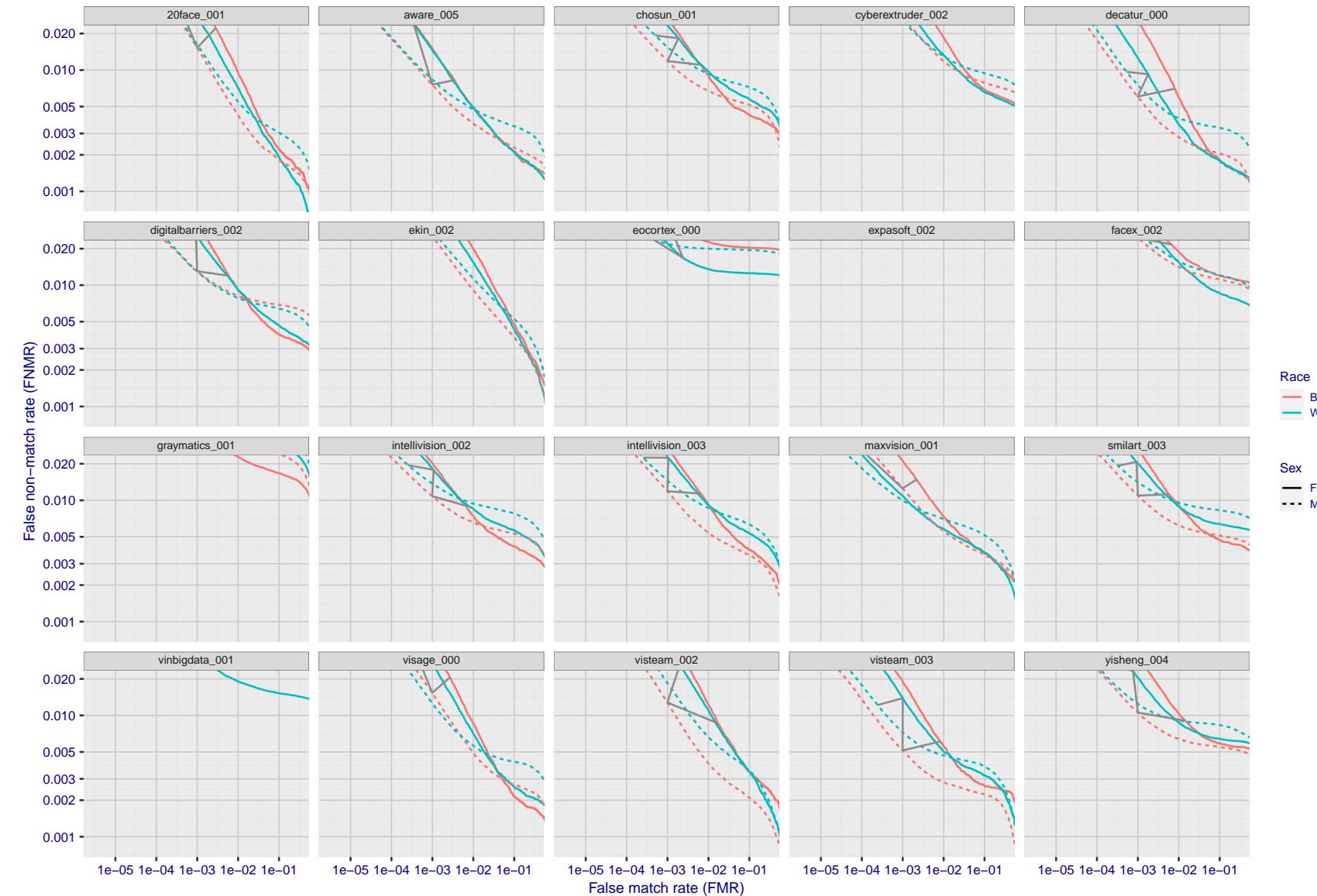


Figure 140: For the mugshot images, error tradeoff characteristics for white females, black females, black males and white males. The Z-shaped grey lines correspond to fixed thresholds, showing both FNMR and FMR vary at one T value. Note: Many of the plots will naively be read as saying women gives worse error rates than men because the solid traces lie above the dotted ones. However, this is misleading and incomplete: The grey lines show the traces reveal horizontal shifts. Thus for the cogent-003 algorithm FNMR for men is higher than for women at a fixed threshold but, at the same time, FMR is higher for women - see Figure 199. As access control systems almost always operate at a fixed threshold, the naive interpretation is incorrect.

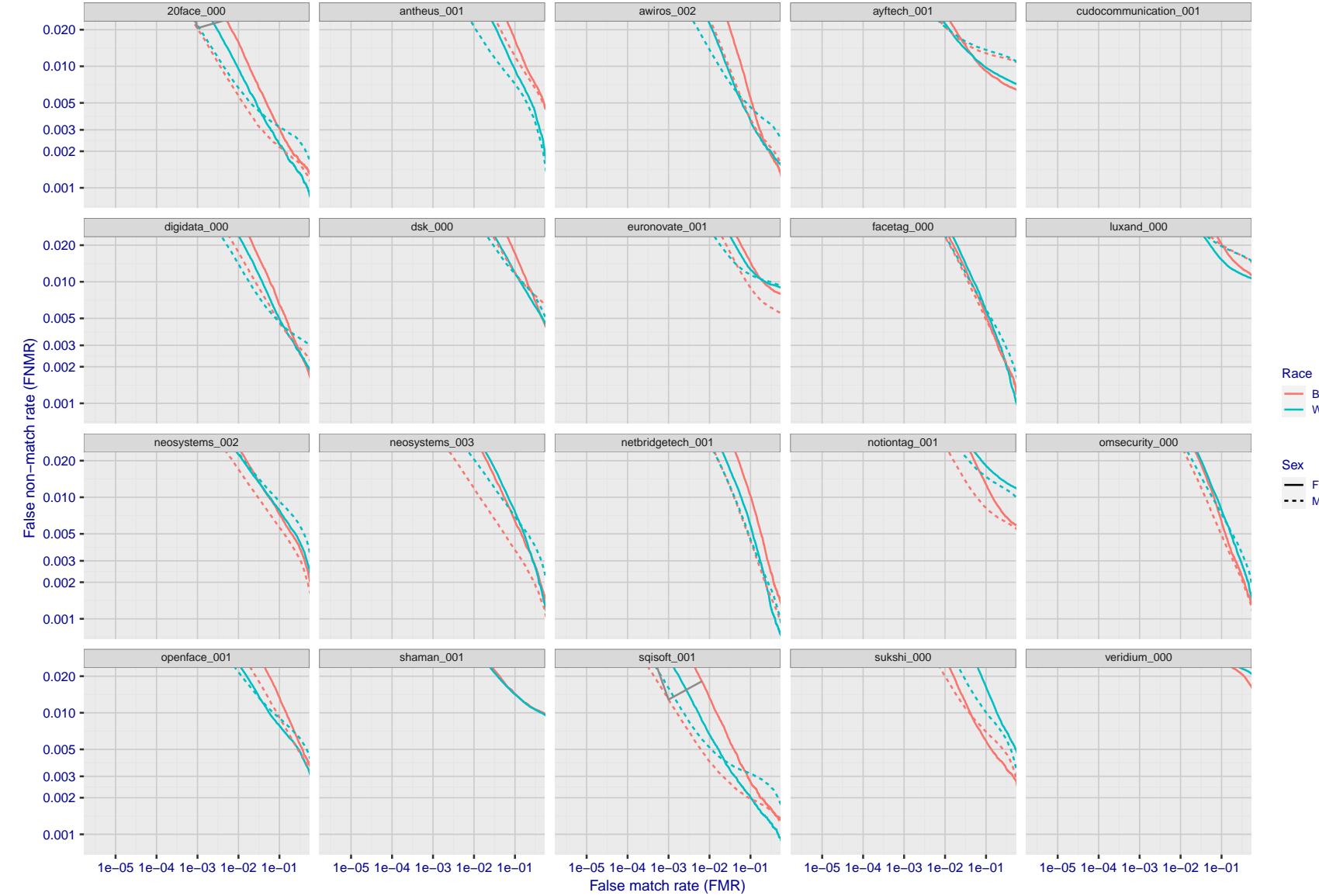


Figure 141: For the mugshot images, error tradeoff characteristics for white females, black females, black males and white males. The Z-shaped grey lines correspond to fixed thresholds, showing both FNMR and FMR vary at one  $T$  value. Note: Many of the plots will naively be read as saying women gives worse error rates than men because the solid traces lie above the dotted ones. However, this is misleading and incomplete: The grey lines show the traces reveal horizontal shifts. Thus for the cogent-003 algorithm FNMR for men is higher than for women at a fixed threshold but, at the same time, FMR is higher for women - see Figure 199. As access control systems almost always operate at a fixed threshold, the naive interpretation is incorrect.

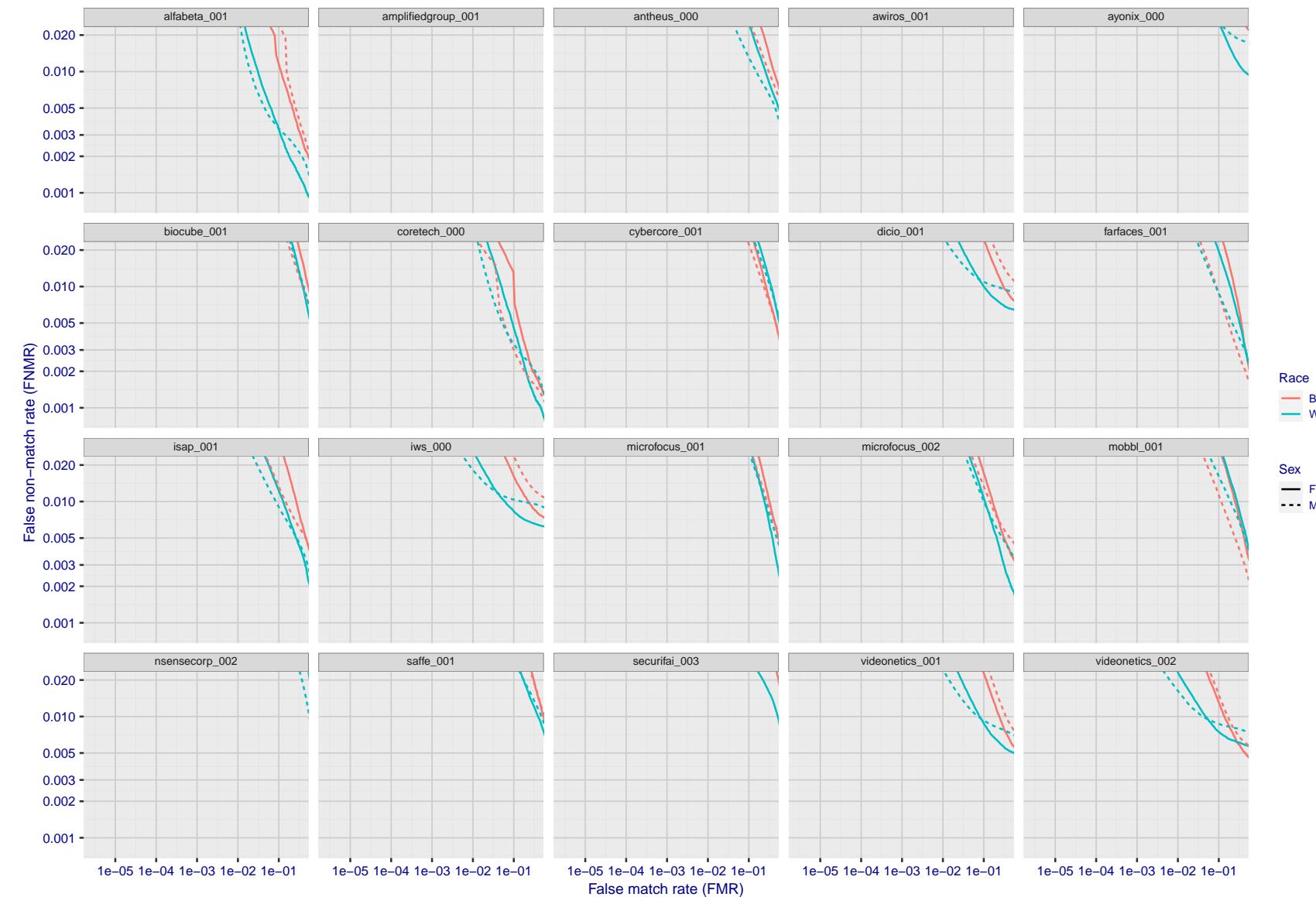


Figure 142: For the mugshot images, error tradeoff characteristics for white females, black females, black males and white males. The Z-shaped grey lines correspond to fixed thresholds, showing both FNMR and FMR vary at one T value. Note: Many of the plots will naively be read as saying women gives worse error rates than men because the solid traces lie above the dotted ones. However, this is misleading and incomplete: The grey lines show the traces reveal horizontal shifts. Thus for the cogent-003 algorithm FNMR for men is higher than for women at a fixed threshold but, at the same time, FMR is higher for women - see Figure 199. As access control systems almost always operate at a fixed threshold, the naive interpretation is incorrect.

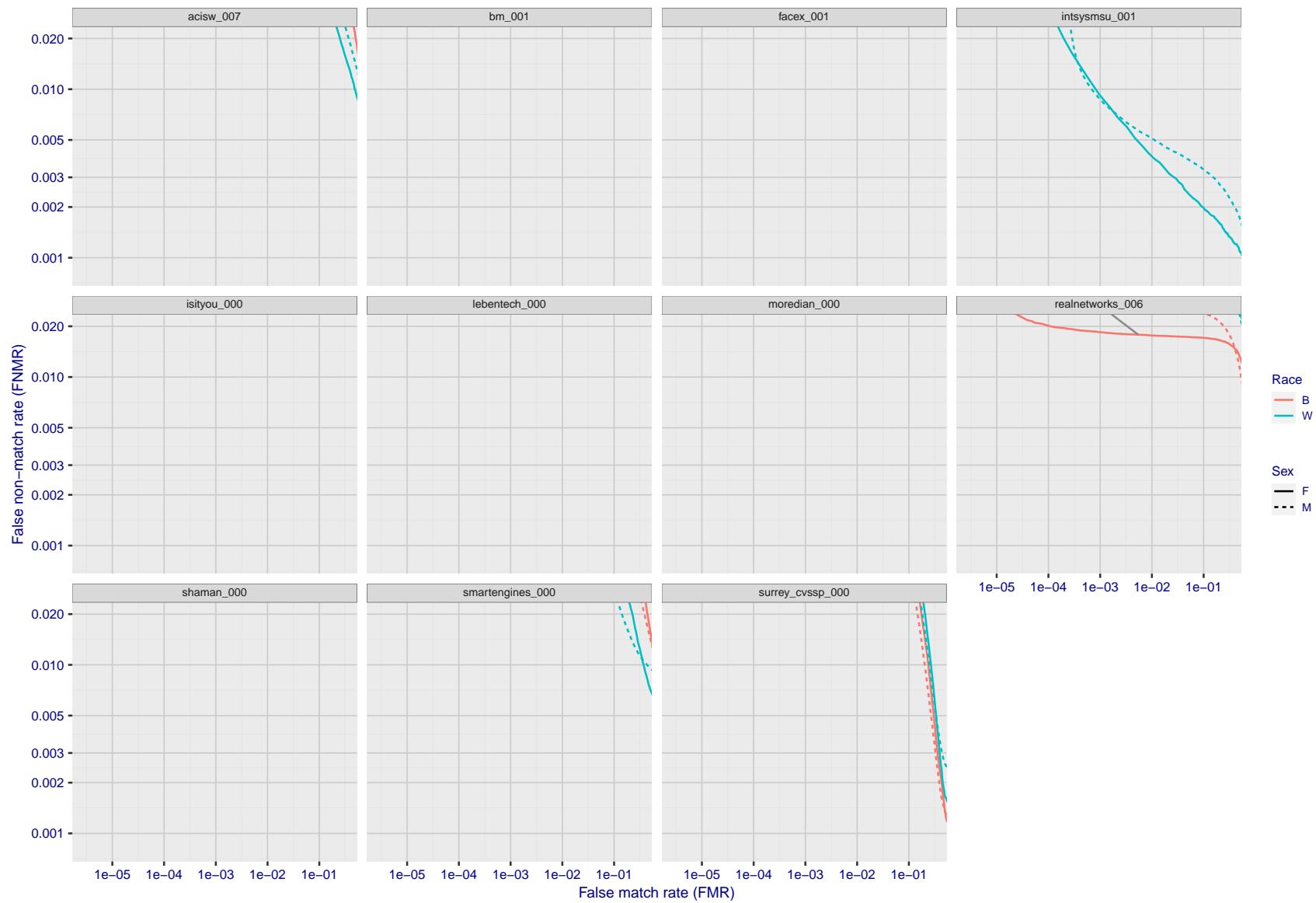


Figure 143: For the mugshot images, error tradeoff characteristics for white females, black females, black males and white males. The Z-shaped grey lines correspond to fixed thresholds, showing both FNMR and FMR vary at one T value. Note: Many of the plots will naively be read as saying women gives worse error rates than men because the solid traces lie above the dotted ones. However, this is misleading and incomplete: The grey lines show the traces reveal horizontal shifts. Thus for the cogent-003 algorithm FNMR for men is higher than for women at a fixed threshold but, at the same time, FMR is higher for women - see Figure 199. As access control systems almost always operate at a fixed threshold, the naive interpretation is incorrect.

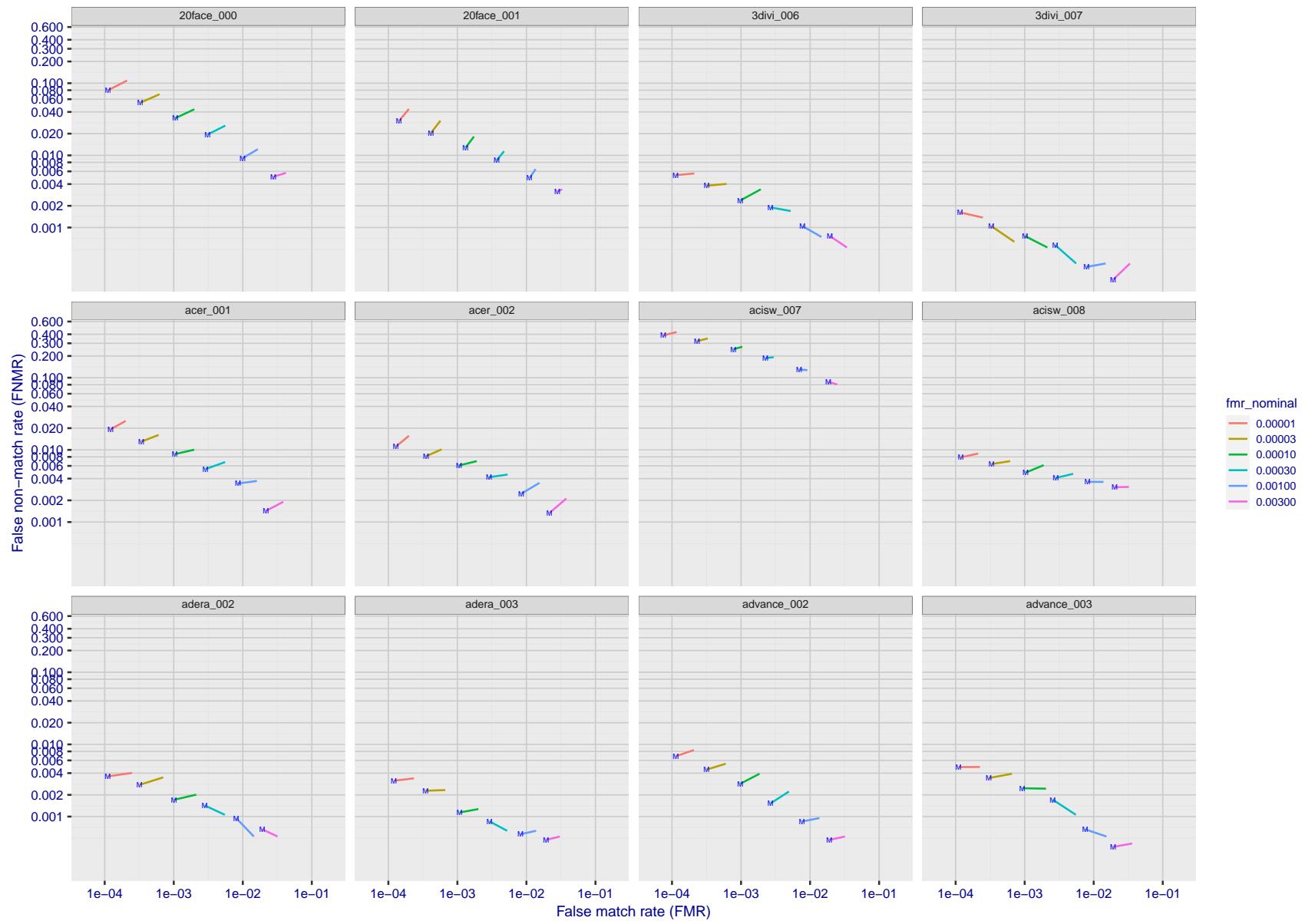


Figure 144: For the visa images, FNMR and FMR at six operating points along the DET characteristic. At each point a line is drawn between  $(FMR, FNMR)_{MALE}$  and  $(FMR, FNMR)_{FEMALE}$  showing how which sex has lower FMR and/or FNMR. The "M" label denotes male, the other end of the line corresponds to female. The six operating thresholds are selected to give the nominal false match rates given in the legend, and are computed over all impostor pairs regardless of age, sex, and place of birth. The plotted FMR values are broadly an order of magnitude larger than the nominal rates because FMR is computed over demographically-matched impostor pairs i.e individuals of the same sex, from the same geographic region (see section 3.6.1), and the same age group (see section 3.6.2).

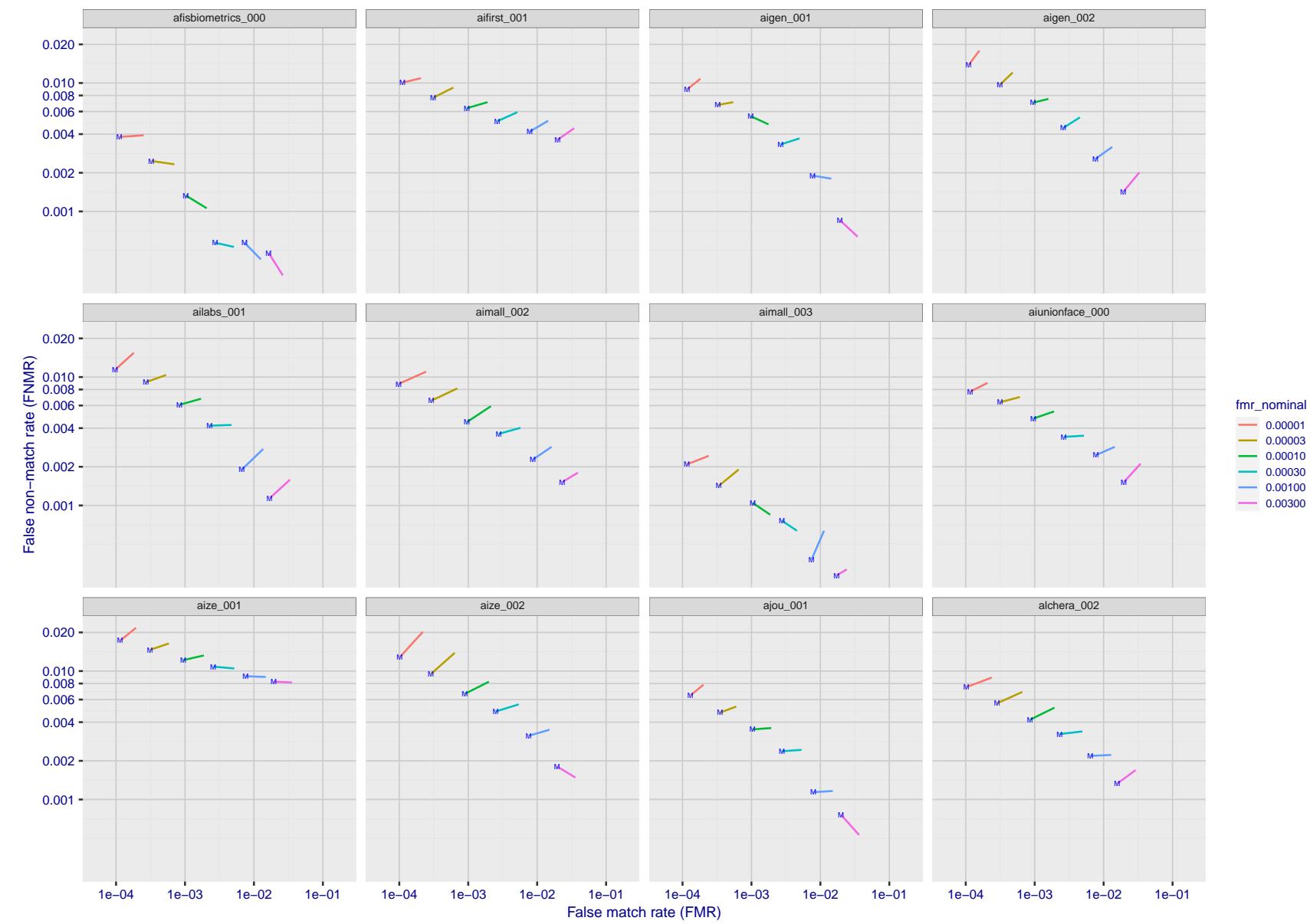


Figure 145: For the visa images, FNMR and FMR at six operating points along the DET characteristic. At each point a line is drawn between  $(FMR, FNMR)_{MALE}$  and  $(FMR, FNMR)_{FEMALE}$  showing how which sex has lower FMR and/or FNMR. The "M" label denotes male, the other end of the line corresponds to female. The six operating thresholds are selected to give the nominal false match rates given in the legend, and are computed over all impostor pairs regardless of age, sex, and place of birth. The plotted FMR values are broadly an order of magnitude larger than the nominal rates because FMR is computed over demographically-matched impostor pairs i.e individuals of the same sex, from the same geographic region (see section 3.6.1), and the same age group (see section 3.6.2).

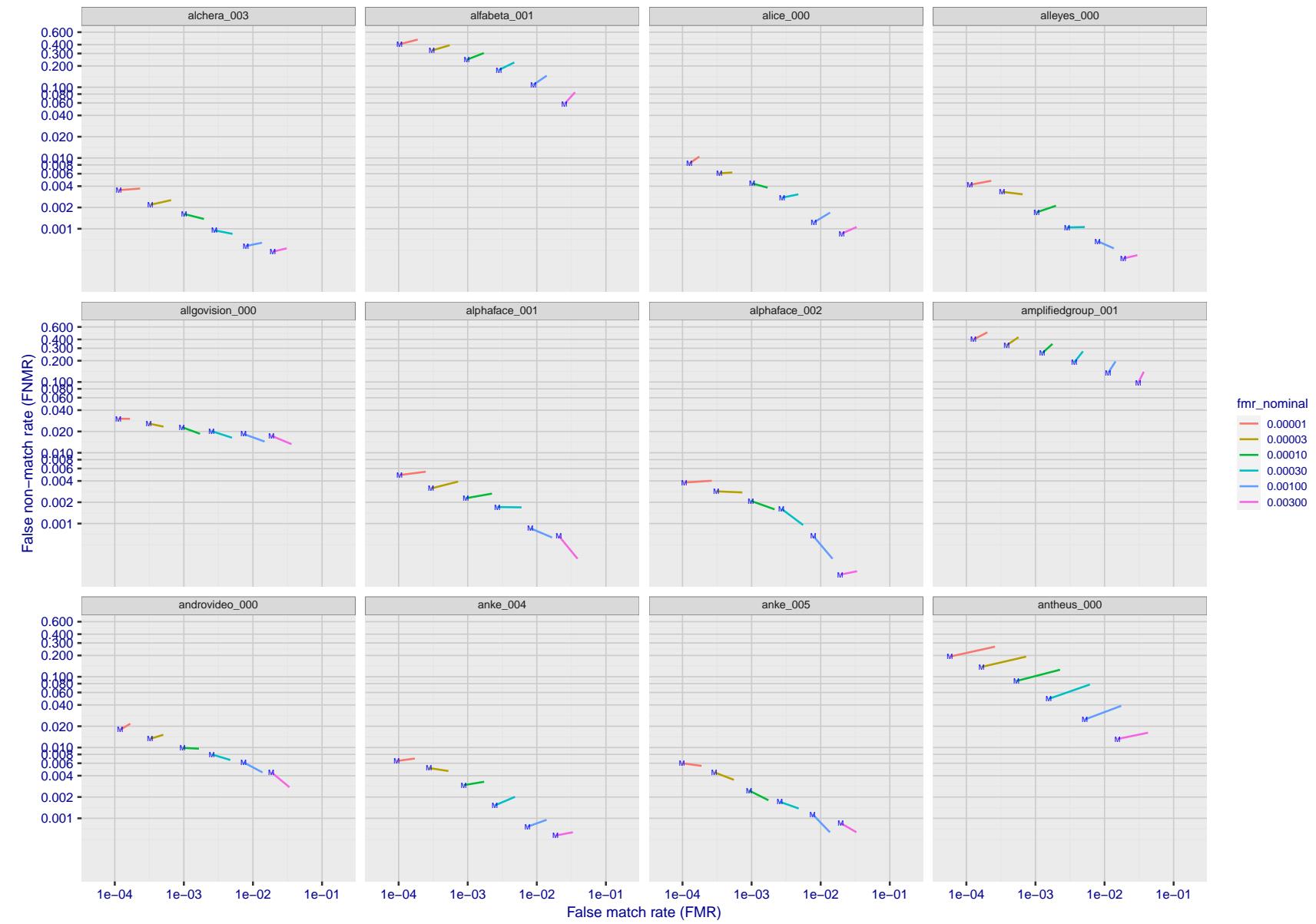


Figure 146: For the visa images, FNMR and FMR at six operating points along the DET characteristic. At each point a line is drawn between  $(FMR, FNMR)_{MALE}$  and  $(FMR, FNMR)_{FEMALE}$  showing how which sex has lower FMR and/or FNMR. The "M" label denotes male, the other end of the line corresponds to female. The six operating thresholds are selected to give the nominal false match rates given in the legend, and are computed over all impostor pairs regardless of age, sex, and place of birth. The plotted FMR values are broadly an order of magnitude larger than the nominal rates because FMR is computed over demographically-matched impostor pairs i.e individuals of the same sex, from the same geographic region (see section 3.6.1), and the same age group (see section 3.6.2).

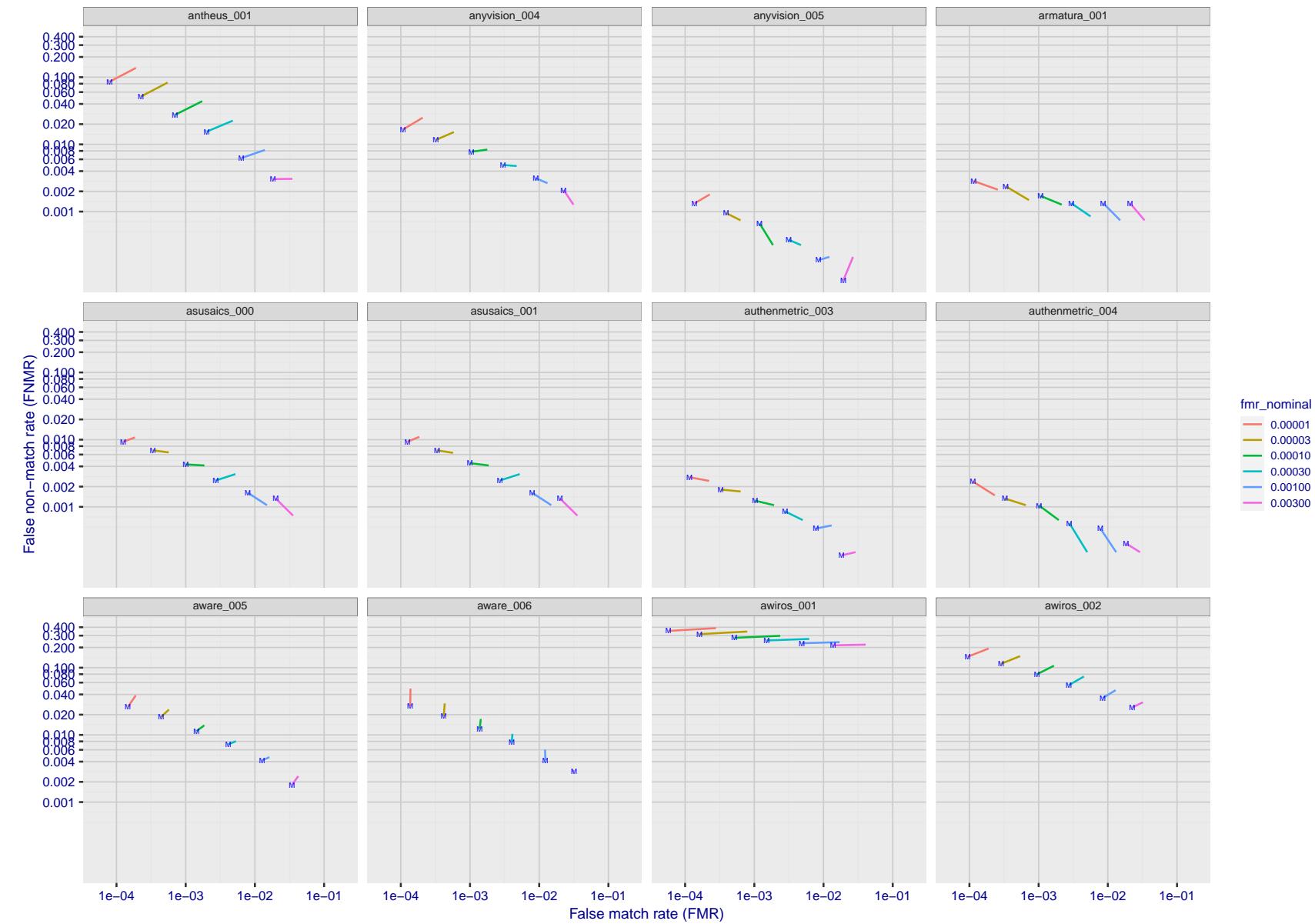


Figure 147: For the visa images, FNMR and FMR at six operating points along the DET characteristic. At each point a line is drawn between  $(FMR, FNMR)_{MALE}$  and  $(FMR, FNMR)_{FEMALE}$  showing how which sex has lower FMR and/or FNMR. The "M" label denotes male, the other end of the line corresponds to female. The six operating thresholds are selected to give the nominal false match rates given in the legend, and are computed over all impostor pairs regardless of age, sex, and place of birth. The plotted FMR values are broadly an order of magnitude larger than the nominal rates because FMR is computed over demographically-matched impostor pairs i.e individuals of the same sex, from the same geographic region (see section 3.6.1), and the same age group (see section 3.6.2).

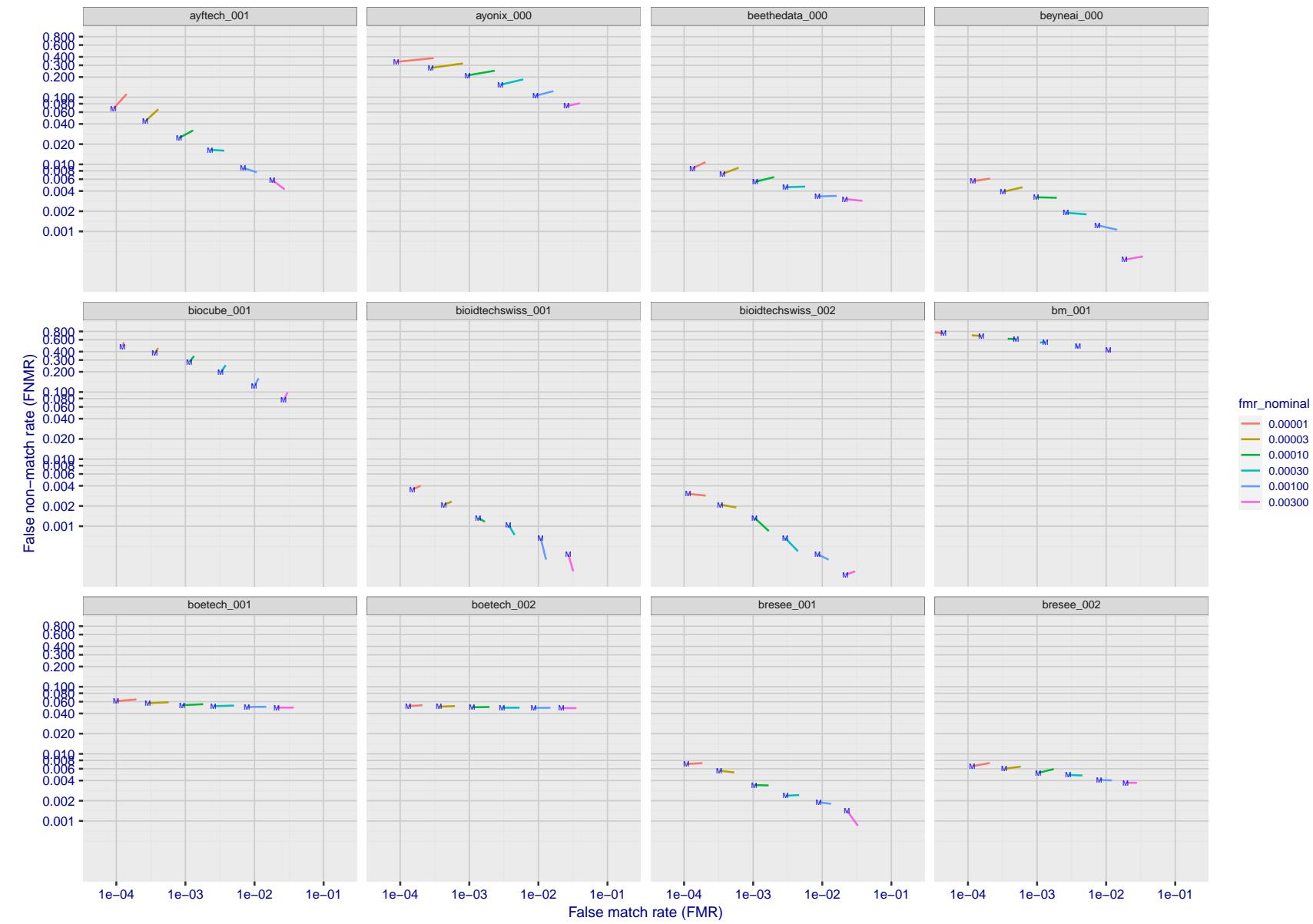


Figure 148: For the visa images, FNMR and FMR at six operating points along the DET characteristic. At each point a line is drawn between  $(FMR, FNMR)_{MALE}$  and  $(FMR, FNMR)_{FEMALE}$  showing how which sex has lower FMR and/or FNMR. The "M" label denotes male, the other end of the line corresponds to female. The six operating thresholds are selected to give the nominal false match rates given in the legend, and are computed over all impostor pairs regardless of age, sex, and place of birth. The plotted FMR values are broadly an order of magnitude larger than the nominal rates because FMR is computed over demographically-matched impostor pairs i.e individuals of the same sex, from the same geographic region (see section 3.6.1), and the same age group (see section 3.6.2).

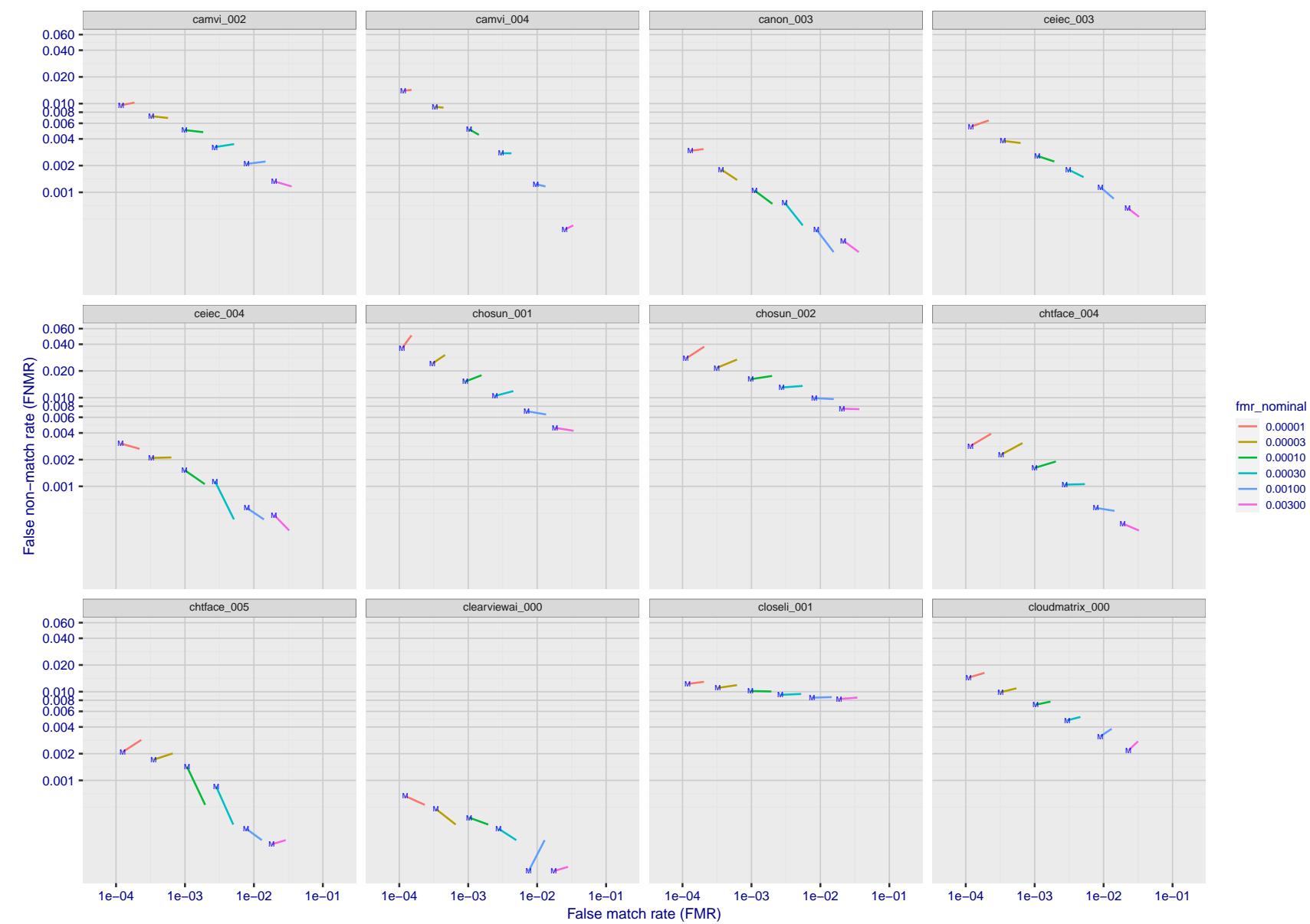


Figure 149: For the visa images, FNMR and FMR at six operating points along the DET characteristic. At each point a line is drawn between  $(FMR, FNMR)_{MALE}$  and  $(FMR, FNMR)_{FEMALE}$  showing how which sex has lower FMR and/or FNMR. The "M" label denotes male, the other end of the line corresponds to female. The six operating thresholds are selected to give the nominal false match rates given in the legend, and are computed over all impostor pairs regardless of age, sex, and place of birth. The plotted FMR values are broadly an order of magnitude larger than the nominal rates because FMR is computed over demographically-matched impostor pairs i.e individuals of the same sex, from the same geographic region (see section 3.6.1), and the same age group (see section 3.6.2).

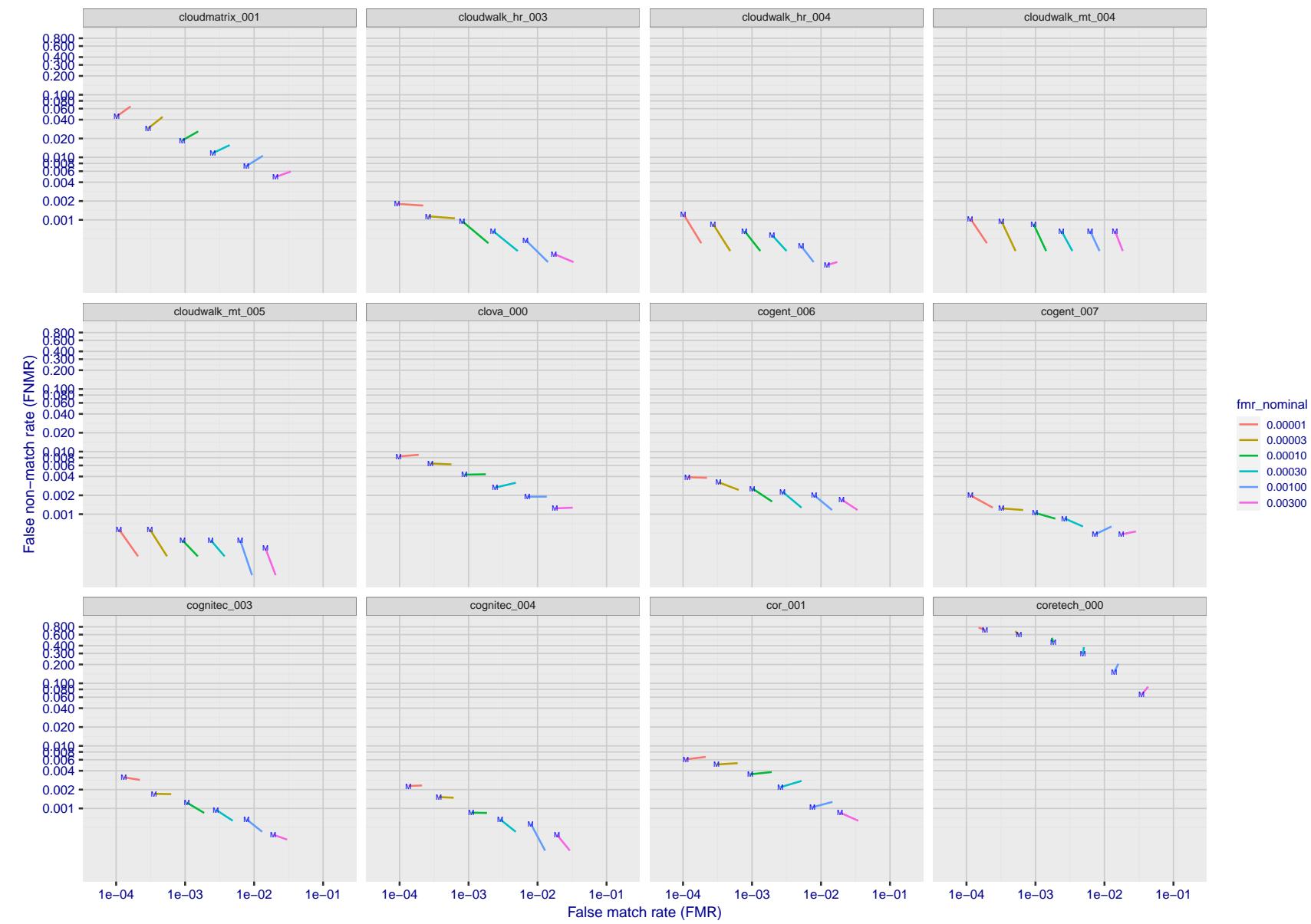


Figure 150: For the visa images, FNMR and FMR at six operating points along the DET characteristic. At each point a line is drawn between  $(FMR, FNMR)_{MALE}$  and  $(FMR, FNMR)_{FEMALE}$  showing how which sex has lower FMR and/or FNMR. The "M" label denotes male, the other end of the line corresponds to female. The six operating thresholds are selected to give the nominal false match rates given in the legend, and are computed over all impostor pairs regardless of age, sex, and place of birth. The plotted FMR values are broadly an order of magnitude larger than the nominal rates because FMR is computed over demographically-matched impostor pairs i.e individuals of the same sex, from the same geographic region (see section 3.6.1), and the same age group (see section 3.6.2).

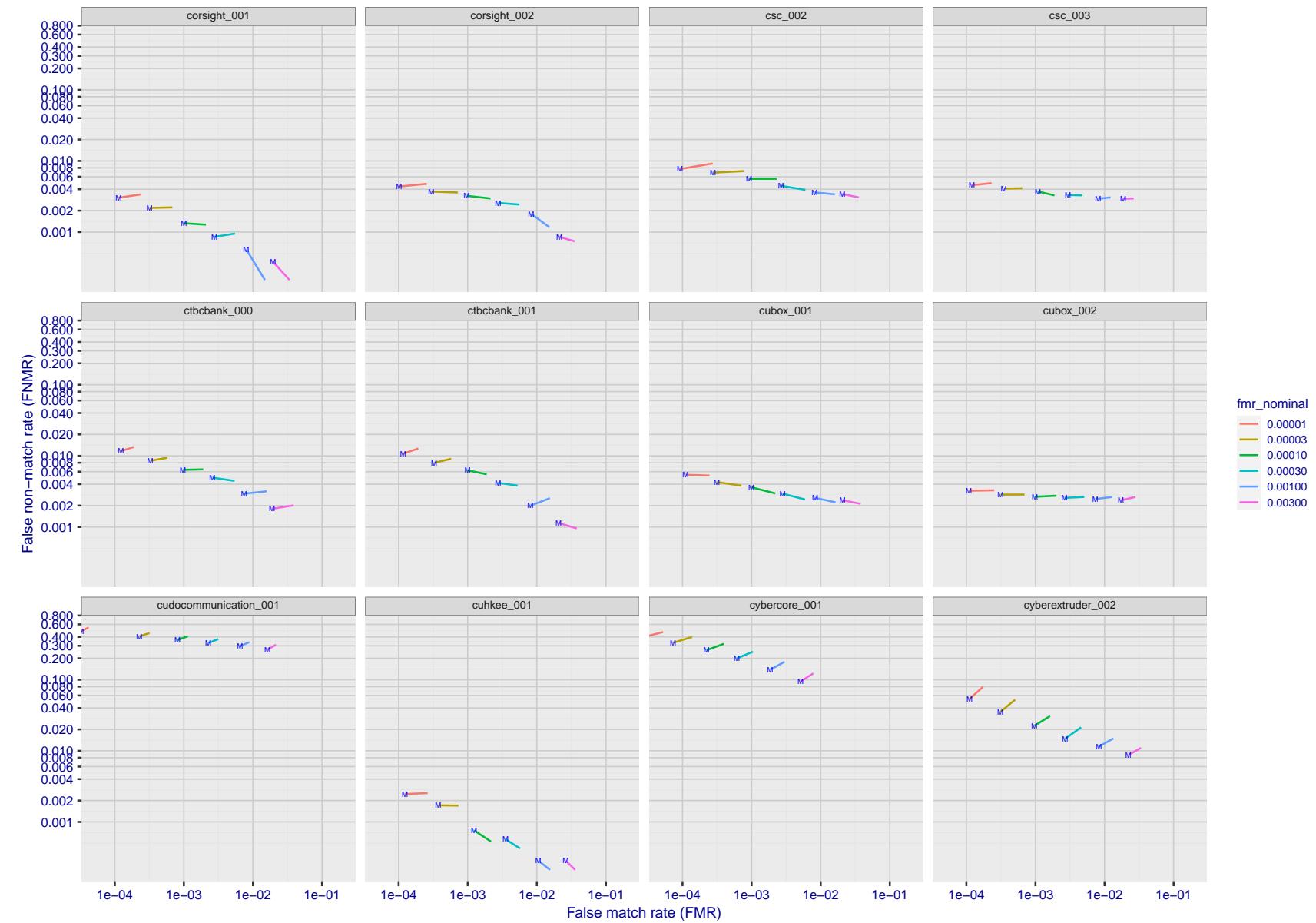


Figure 151: For the visa images, FNMR and FMR at six operating points along the DET characteristic. At each point a line is drawn between  $(FMR, FNMR)_{MALE}$  and  $(FMR, FNMR)_{FEMALE}$  showing how which sex has lower FMR and/or FNMR. The "M" label denotes male, the other end of the line corresponds to female. The six operating thresholds are selected to give the nominal false match rates given in the legend, and are computed over all impostor pairs regardless of age, sex, and place of birth. The plotted FMR values are broadly an order of magnitude larger than the nominal rates because FMR is computed over demographically-matched impostor pairs i.e individuals of the same sex, from the same geographic region (see section 3.6.1), and the same age group (see section 3.6.2).

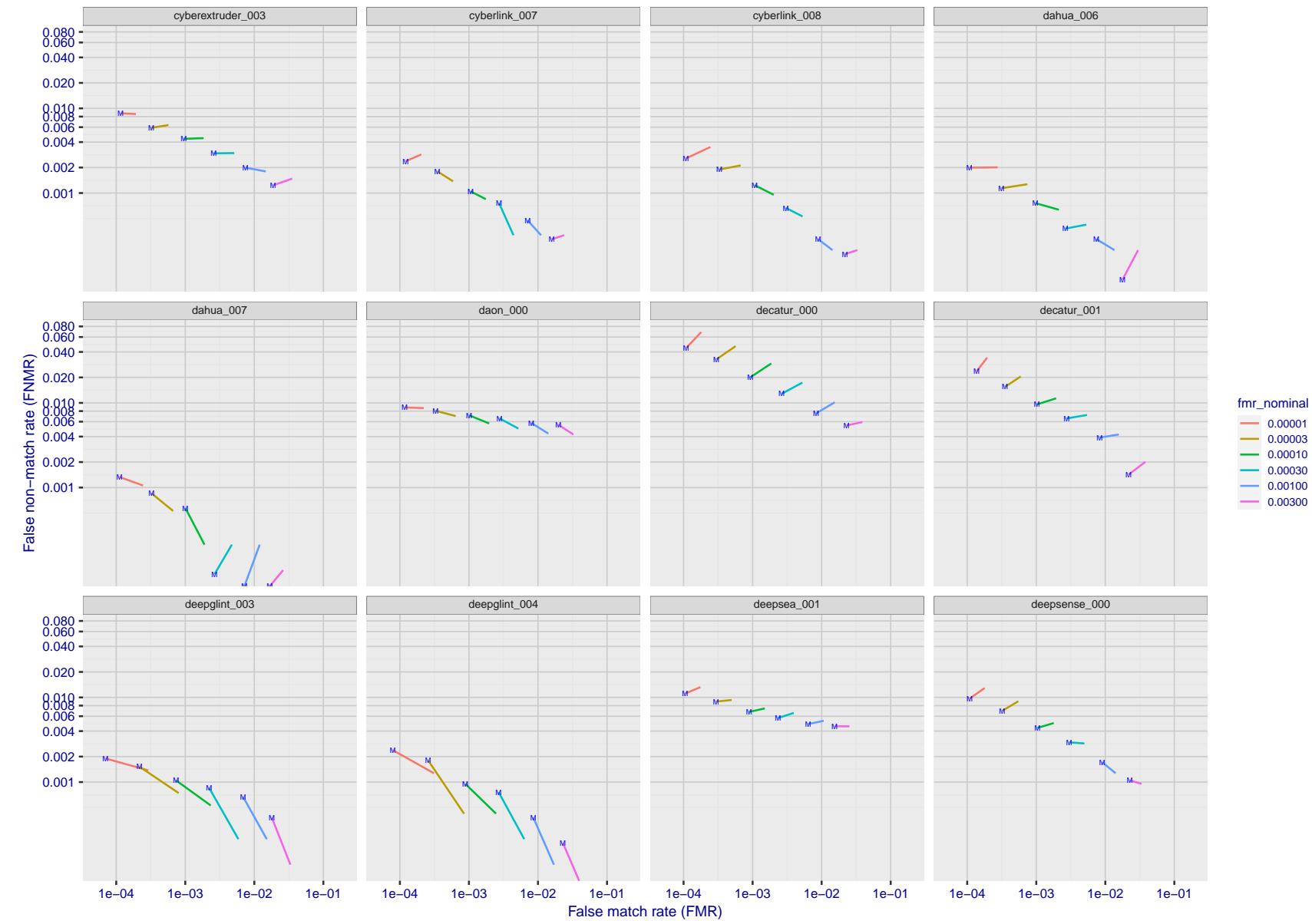


Figure 152: For the visa images, FNMR and FMR at six operating points along the DET characteristic. At each point a line is drawn between  $(FMR, FNMR)_{MALE}$  and  $(FMR, FNMR)_{FEMALE}$  showing how which sex has lower FMR and/or FNMR. The "M" label denotes male, the other end of the line corresponds to female. The six operating thresholds are selected to give the nominal false match rates given in the legend, and are computed over all impostor pairs regardless of age, sex, and place of birth. The plotted FMR values are broadly an order of magnitude larger than the nominal rates because FMR is computed over demographically-matched impostor pairs i.e individuals of the same sex, from the same geographic region (see section 3.6.1), and the same age group (see section 3.6.2).

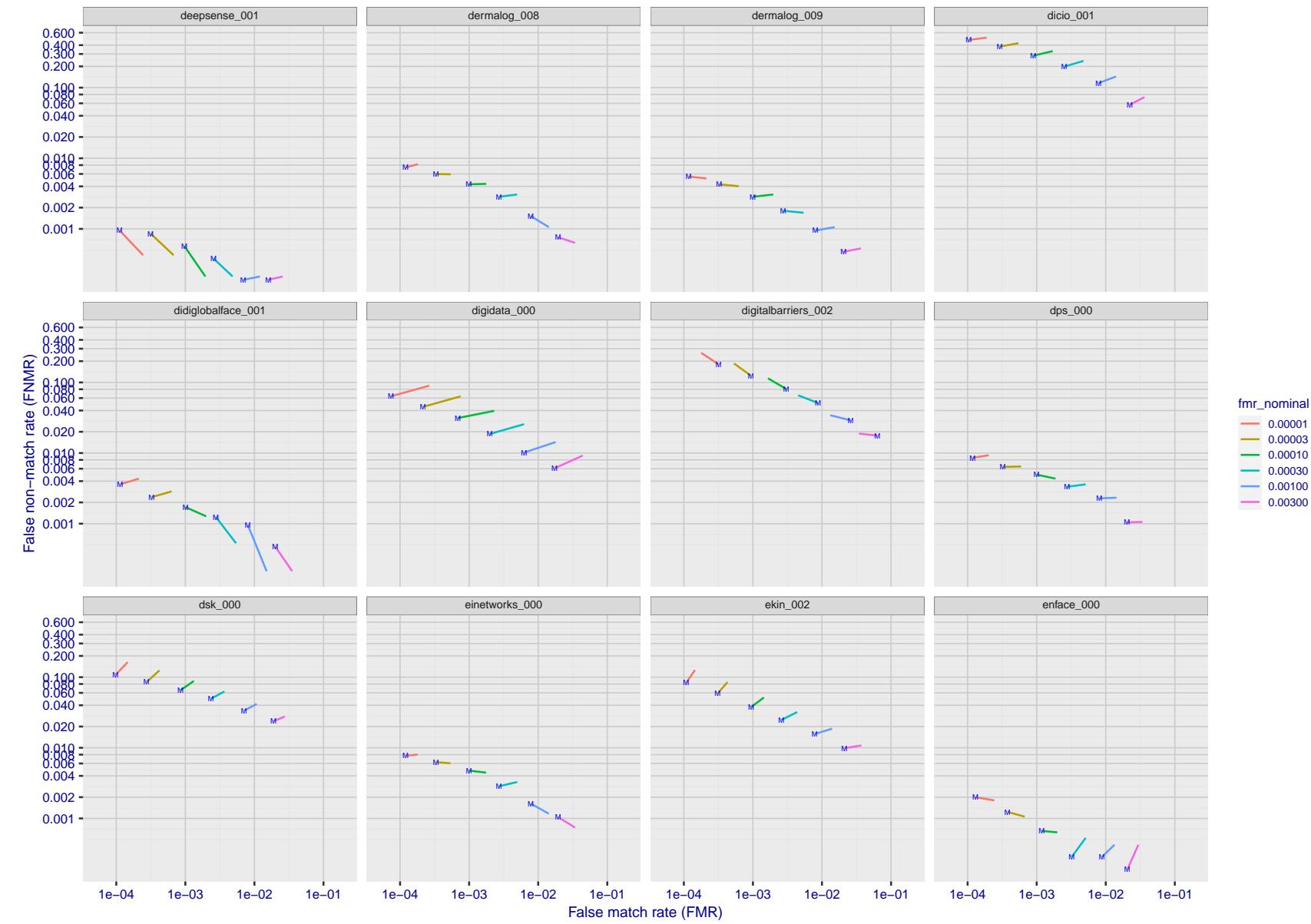


Figure 153: For the visa images, FNMR and FMR at six operating points along the DET characteristic. At each point a line is drawn between  $(FMR, FNMR)_{MALE}$  and  $(FMR, FNMR)_{FEMALE}$  showing how which sex has lower FMR and/or FNMR. The "M" label denotes male, the other end of the line corresponds to female. The six operating thresholds are selected to give the nominal false match rates given in the legend, and are computed over all impostor pairs regardless of age, sex, and place of birth. The plotted FMR values are broadly an order of magnitude larger than the nominal rates because FMR is computed over demographically-matched impostor pairs i.e individuals of the same sex, from the same geographic region (see section 3.6.1), and the same age group (see section 3.6.2).

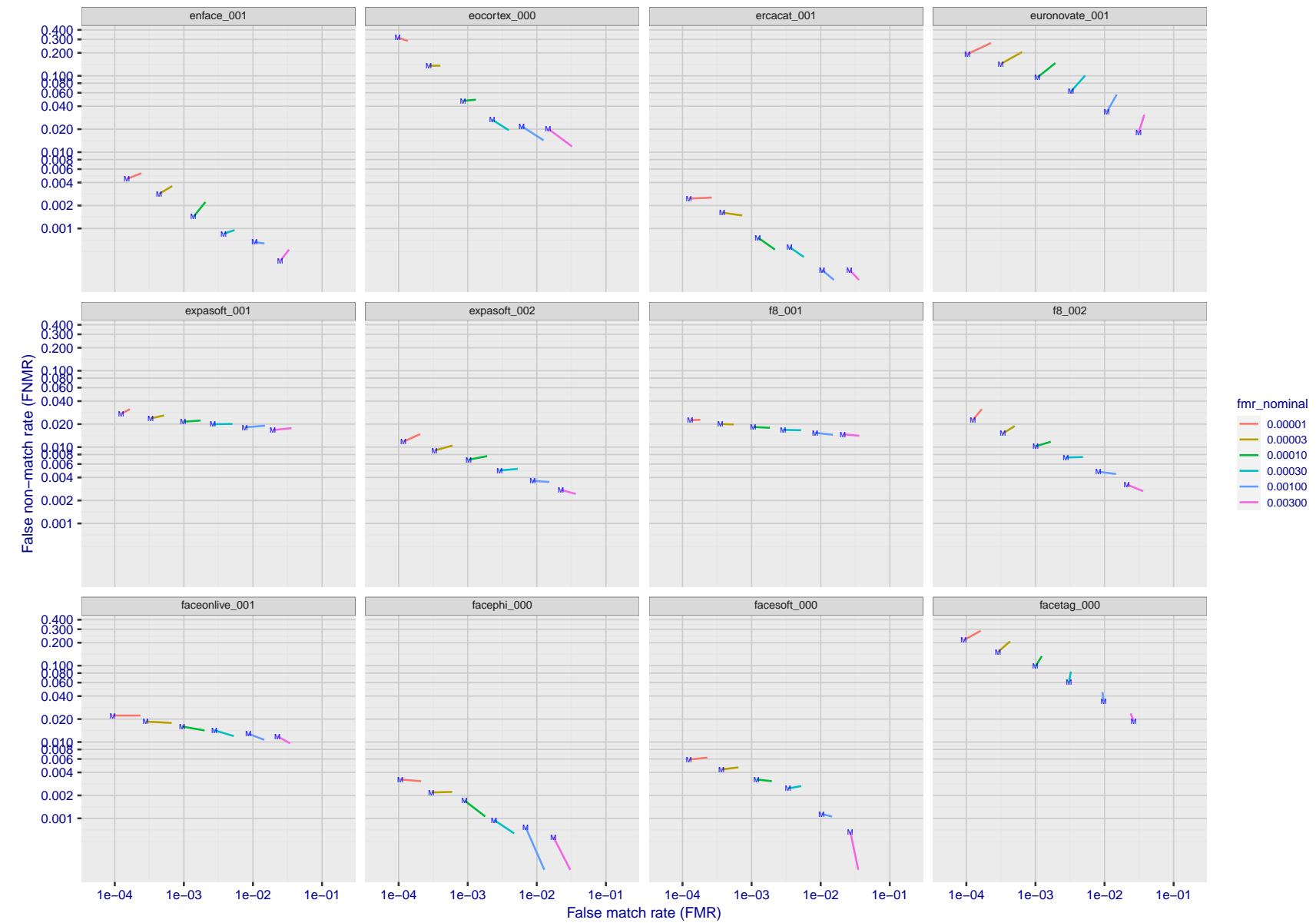


Figure 154: For the visa images, FNMR and FMR at six operating points along the DET characteristic. At each point a line is drawn between  $(FMR, FNMR)_{MALE}$  and  $(FMR, FNMR)_{FEMALE}$  showing how which sex has lower FMR and/or FNMR. The "M" label denotes male, the other end of the line corresponds to female. The six operating thresholds are selected to give the nominal false match rates given in the legend, and are computed over all impostor pairs regardless of age, sex, and place of birth. The plotted FMR values are broadly an order of magnitude larger than the nominal rates because FMR is computed over demographically-matched impostor pairs i.e individuals of the same sex, from the same geographic region (see section 3.6.1), and the same age group (see section 3.6.2).

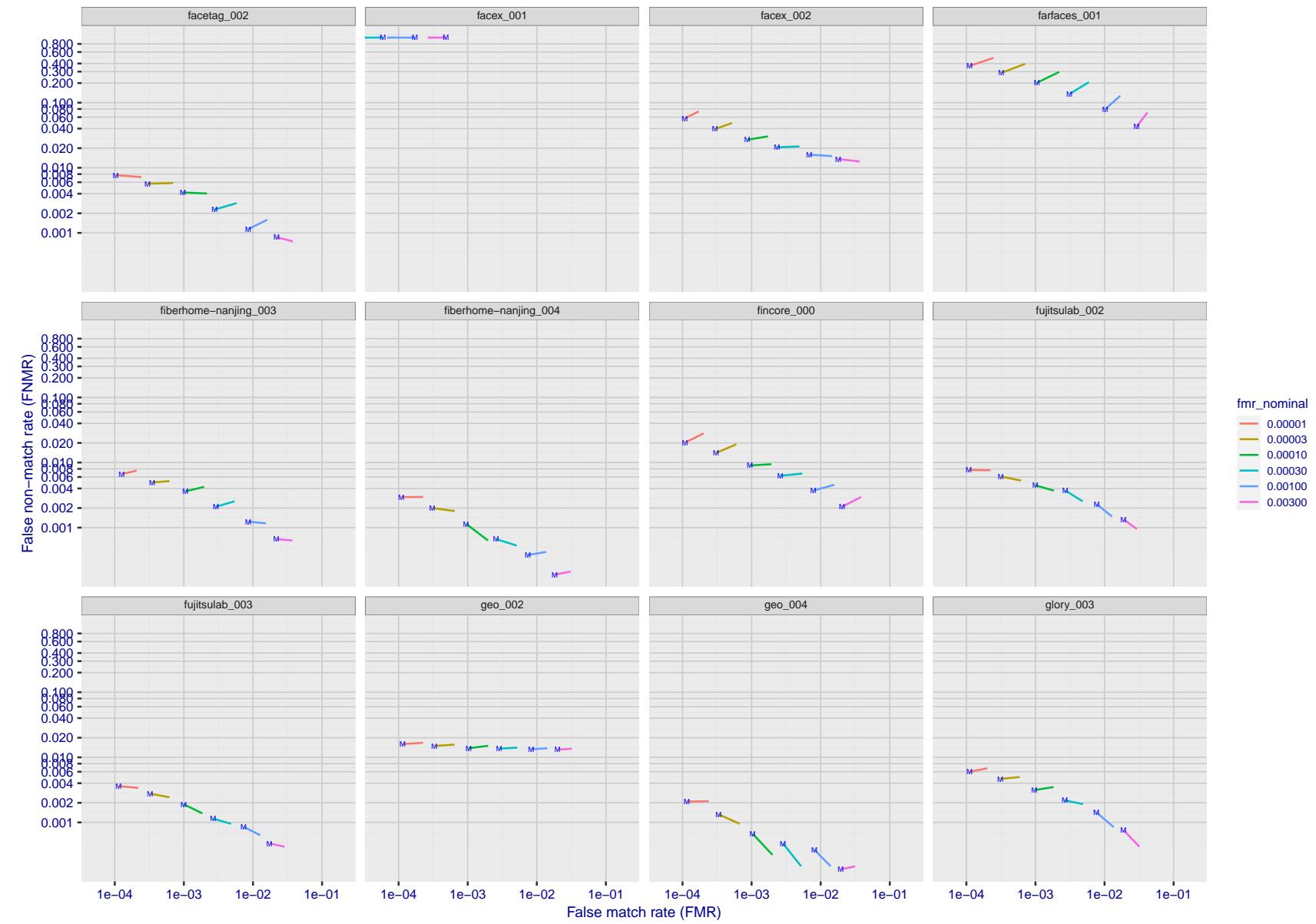


Figure 155: For the visa images, FNMR and FMR at six operating points along the DET characteristic. At each point a line is drawn between  $(FMR, FNMR)_{MALE}$  and  $(FMR, FNMR)_{FEMALE}$  showing how which sex has lower FMR and/or FNMR. The "M" label denotes male, the other end of the line corresponds to female. The six operating thresholds are selected to give the nominal false match rates given in the legend, and are computed over all impostor pairs regardless of age, sex, and place of birth. The plotted FMR values are broadly an order of magnitude larger than the nominal rates because FMR is computed over demographically-matched impostor pairs i.e individuals of the same sex, from the same geographic region (see section 3.6.1), and the same age group (see section 3.6.2).

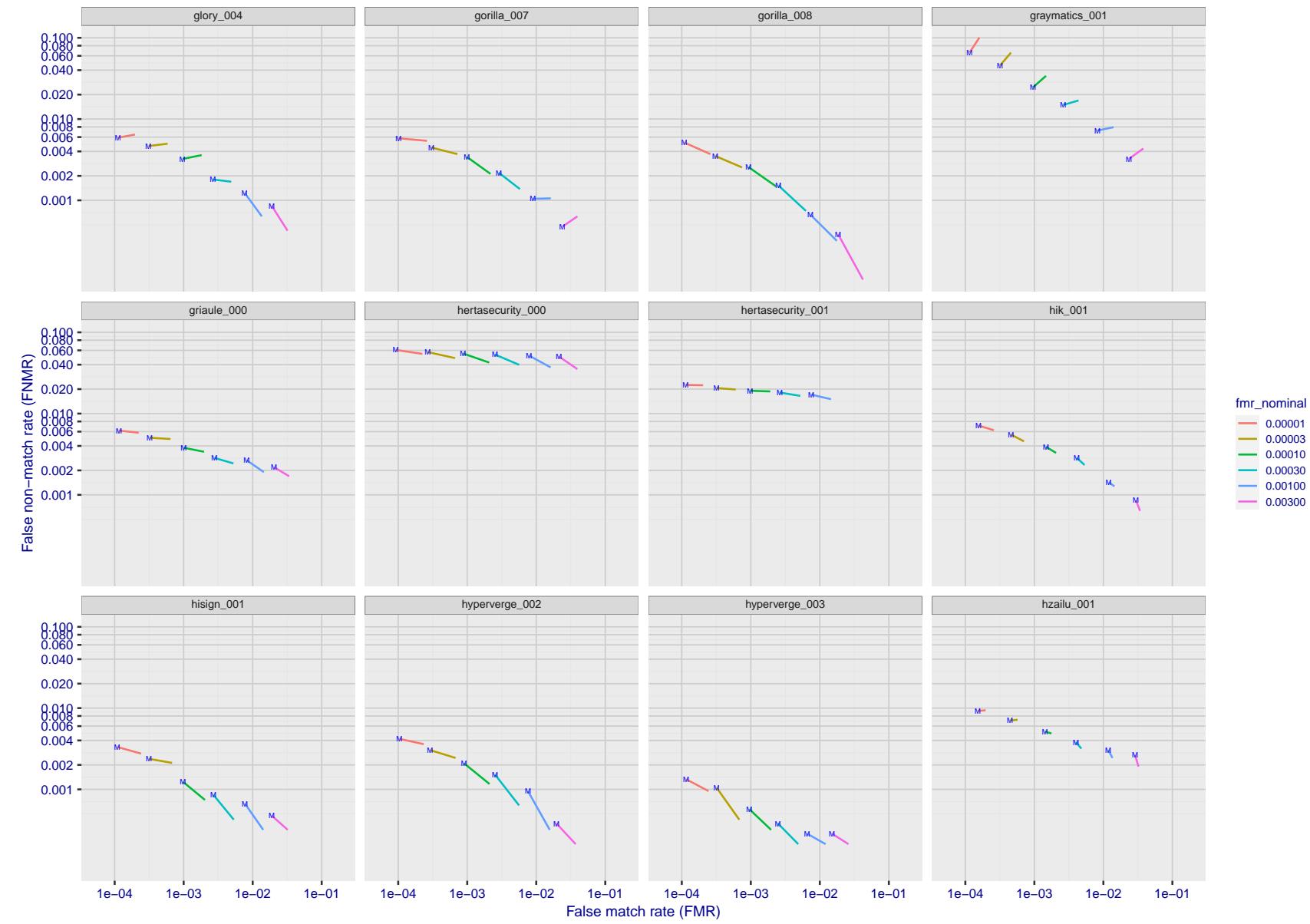


Figure 156: For the visa images, FNMR and FMR at six operating points along the DET characteristic. At each point a line is drawn between  $(FMR, FNMR)_{MALE}$  and  $(FMR, FNMR)_{FEMALE}$  showing how which sex has lower FMR and/or FNMR. The "M" label denotes male, the other end of the line corresponds to female. The six operating thresholds are selected to give the nominal false match rates given in the legend, and are computed over all impostor pairs regardless of age, sex, and place of birth. The plotted FMR values are broadly an order of magnitude larger than the nominal rates because FMR is computed over demographically-matched impostor pairs i.e individuals of the same sex, from the same geographic region (see section 3.6.1), and the same age group (see section 3.6.2).

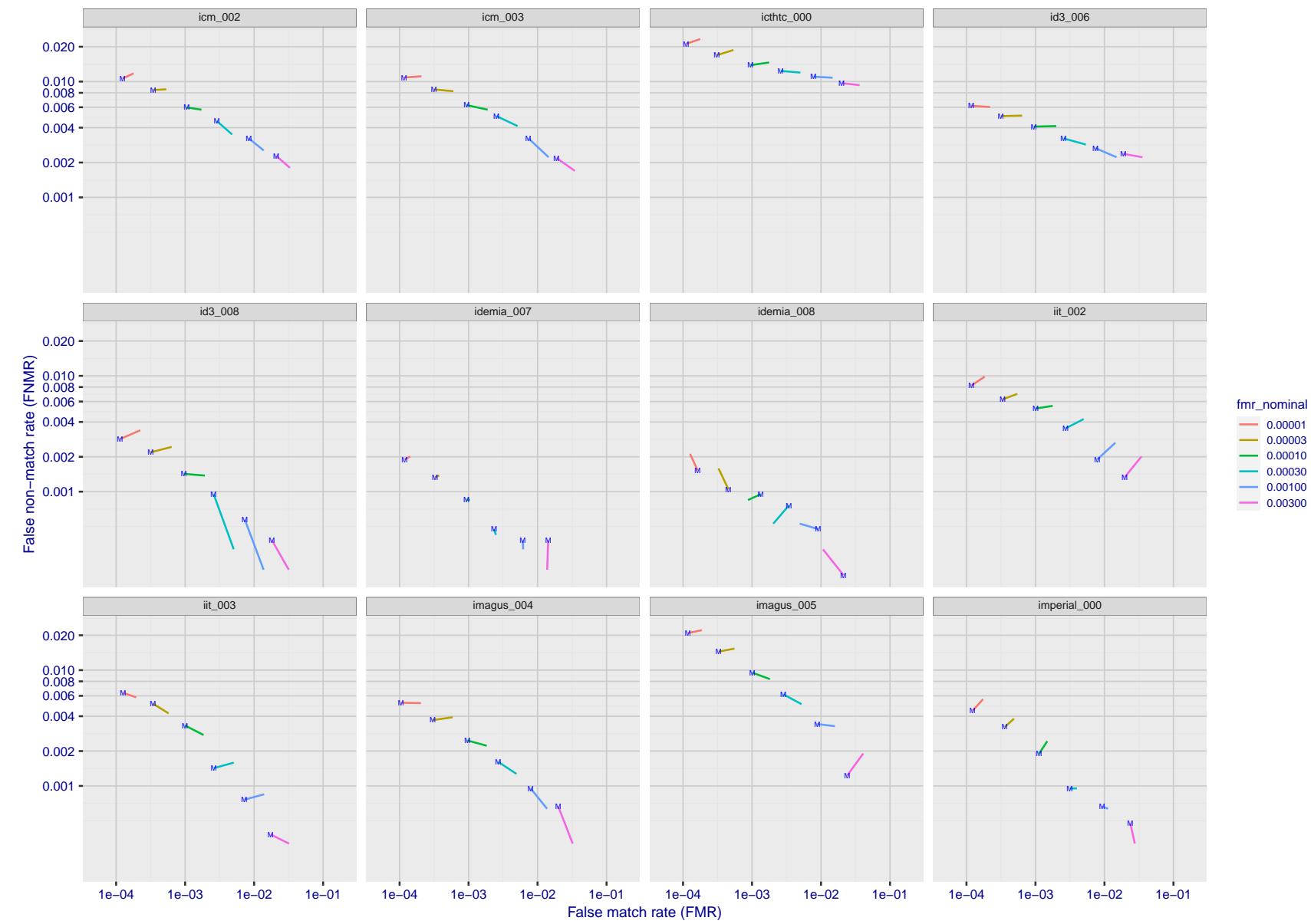


Figure 157: For the visa images, FNMR and FMR at six operating points along the DET characteristic. At each point a line is drawn between  $(FMR, FNMR)_{MALE}$  and  $(FMR, FNMR)_{FEMALE}$  showing how which sex has lower FMR and/or FNMR. The "M" label denotes male, the other end of the line corresponds to female. The six operating thresholds are selected to give the nominal false match rates given in the legend, and are computed over all impostor pairs regardless of age, sex, and place of birth. The plotted FMR values are broadly an order of magnitude larger than the nominal rates because FMR is computed over demographically-matched impostor pairs i.e individuals of the same sex, from the same geographic region (see section 3.6.1), and the same age group (see section 3.6.2).

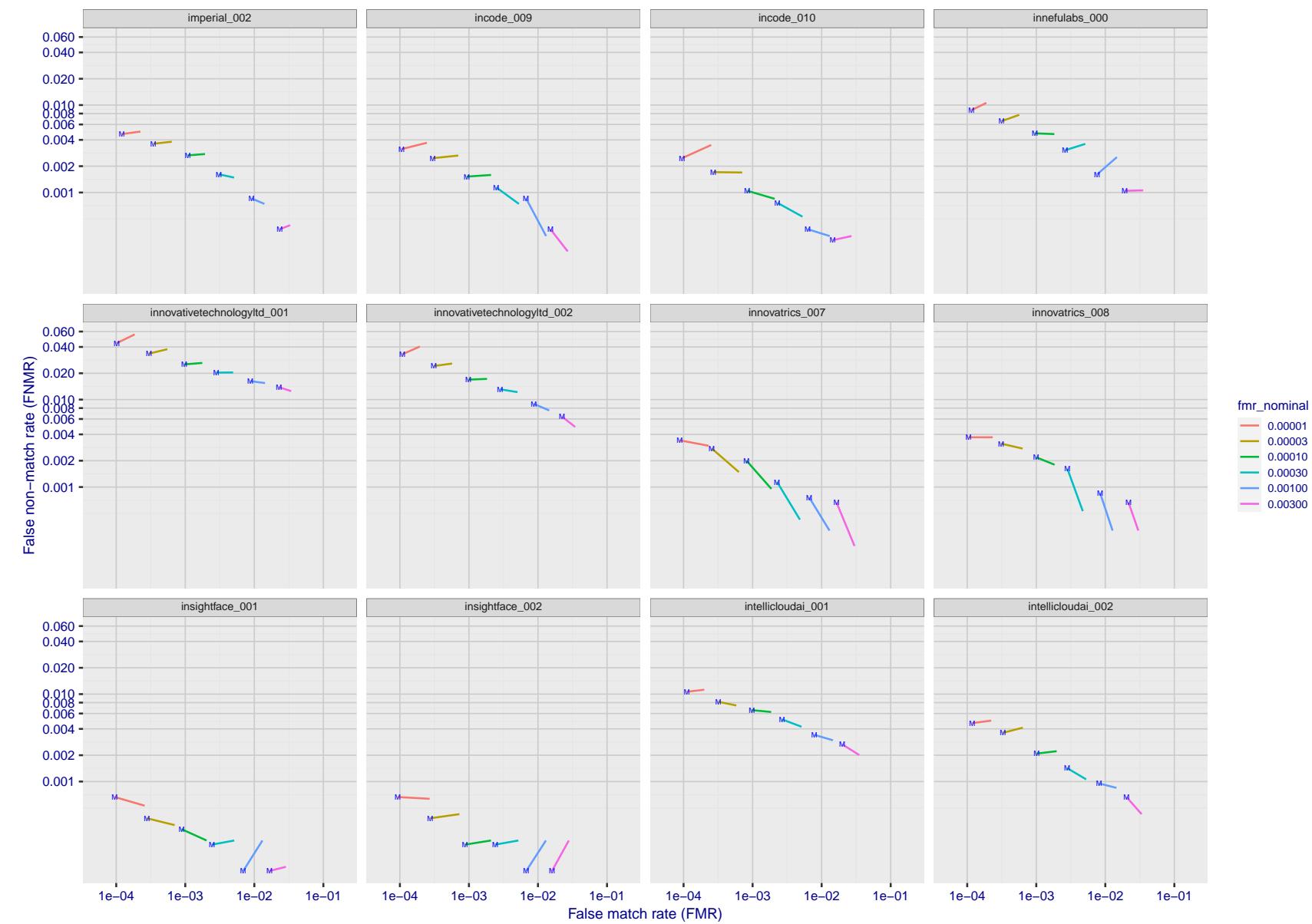


Figure 158: For the visa images, FNMR and FMR at six operating points along the DET characteristic. At each point a line is drawn between  $(FMR, FNMR)_{MALE}$  and  $(FMR, FNMR)_{FEMALE}$  showing how which sex has lower FMR and/or FNMR. The "M" label denotes male, the other end of the line corresponds to female. The six operating thresholds are selected to give the nominal false match rates given in the legend, and are computed over all impostor pairs regardless of age, sex, and place of birth. The plotted FMR values are broadly an order of magnitude larger than the nominal rates because FMR is computed over demographically-matched impostor pairs i.e individuals of the same sex, from the same geographic region (see section 3.6.1), and the same age group (see section 3.6.2).

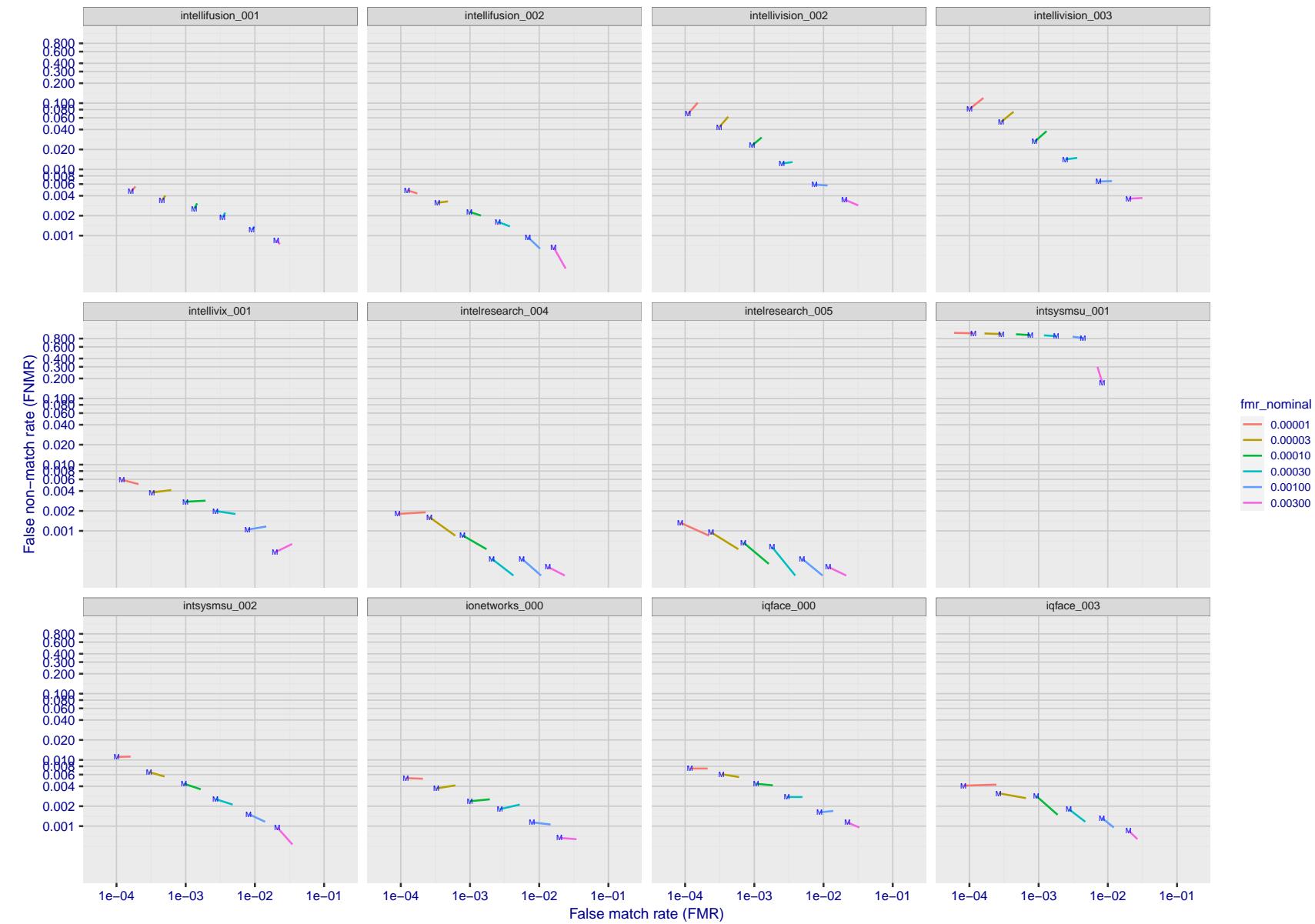


Figure 159: For the visa images, FNMR and FMR at six operating points along the DET characteristic. At each point a line is drawn between  $(FMR, FNMR)_{MALE}$  and  $(FMR, FNMR)_{FEMALE}$  showing how which sex has lower FMR and/or FNMR. The "M" label denotes male, the other end of the line corresponds to female. The six operating thresholds are selected to give the nominal false match rates given in the legend, and are computed over all impostor pairs regardless of age, sex, and place of birth. The plotted FMR values are broadly an order of magnitude larger than the nominal rates because FMR is computed over demographically-matched impostor pairs i.e individuals of the same sex, from the same geographic region (see section 3.6.1), and the same age group (see section 3.6.2).

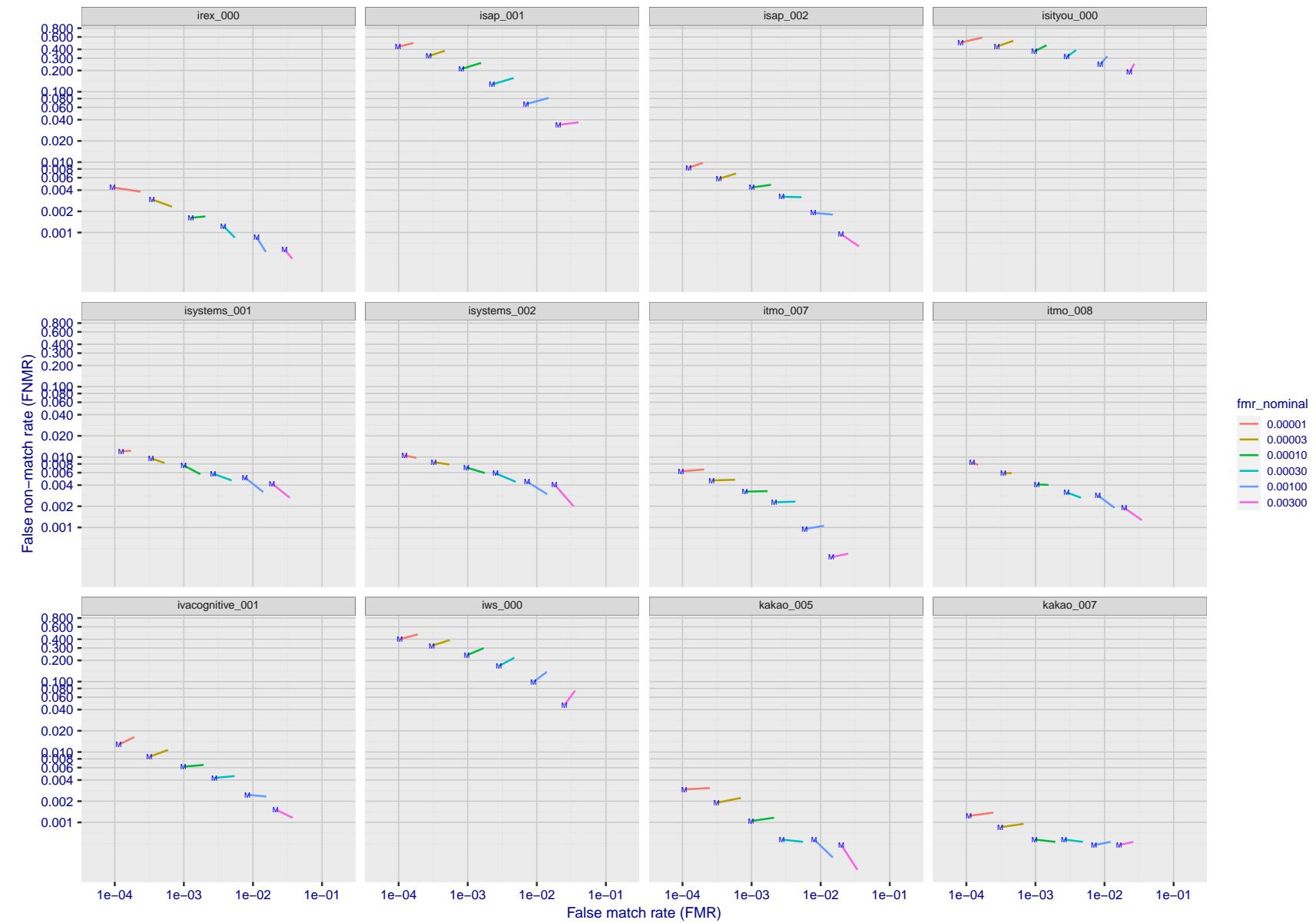


Figure 160: For the visa images, FNMR and FMR at six operating points along the DET characteristic. At each point a line is drawn between  $(FMR, FNMR)_{MALE}$  and  $(FMR, FNMR)_{FEMALE}$  showing how which sex has lower FMR and/or FNMR. The "M" label denotes male, the other end of the line corresponds to female. The six operating thresholds are selected to give the nominal false match rates given in the legend, and are computed over all impostor pairs regardless of age, sex, and place of birth. The plotted FMR values are broadly an order of magnitude larger than the nominal rates because FMR is computed over demographically-matched impostor pairs i.e individuals of the same sex, from the same geographic region (see section 3.6.1), and the same age group (see section 3.6.2).

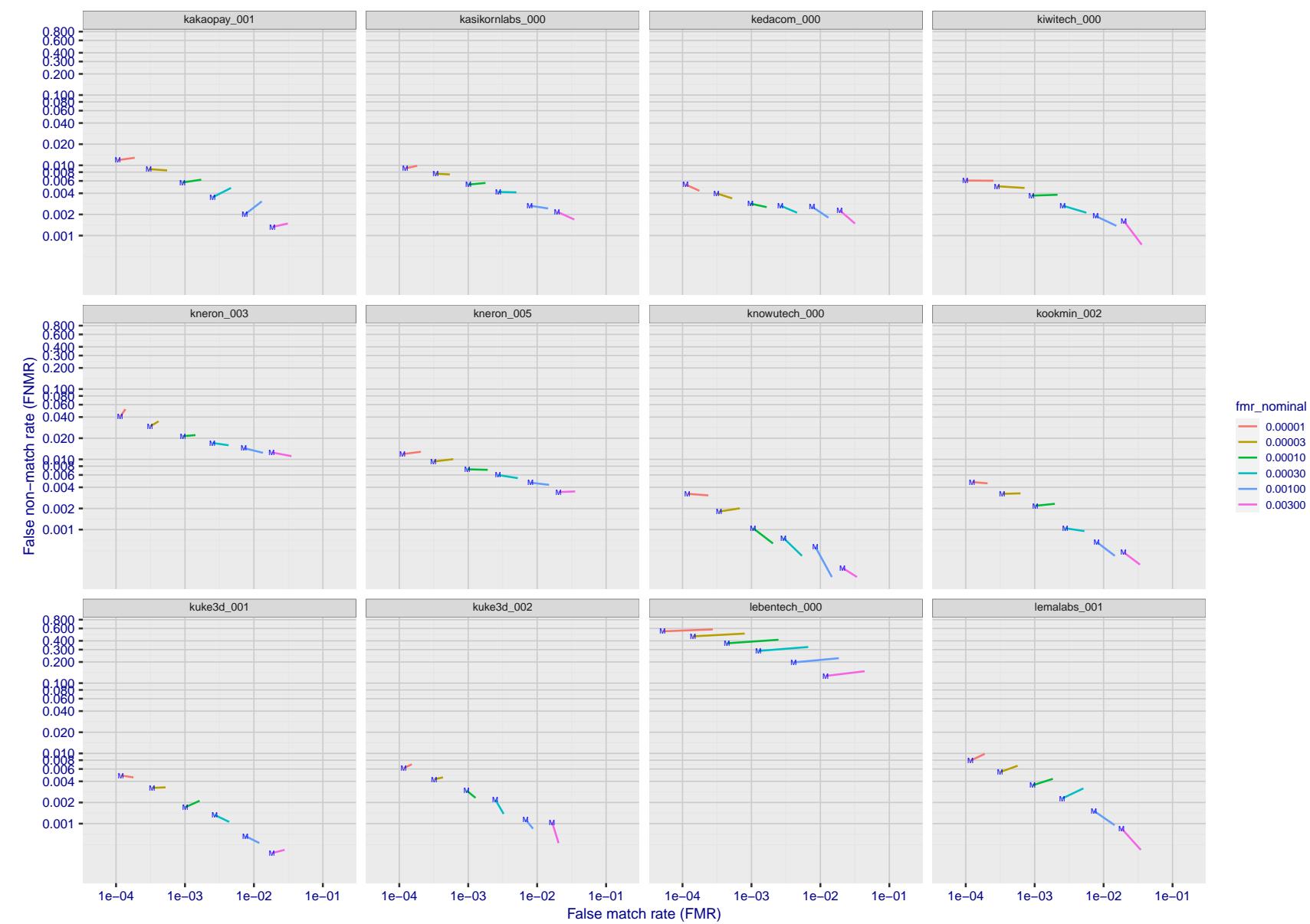


Figure 161: For the visa images, FNMR and FMR at six operating points along the DET characteristic. At each point a line is drawn between  $(FMR, FNMR)_{MALE}$  and  $(FMR, FNMR)_{FEMALE}$  showing how which sex has lower FMR and/or FNMR. The "M" label denotes male, the other end of the line corresponds to female. The six operating thresholds are selected to give the nominal false match rates given in the legend, and are computed over all impostor pairs regardless of age, sex, and place of birth. The plotted FMR values are broadly an order of magnitude larger than the nominal rates because FMR is computed over demographically-matched impostor pairs i.e individuals of the same sex, from the same geographic region (see section 3.6.1), and the same age group (see section 3.6.2).

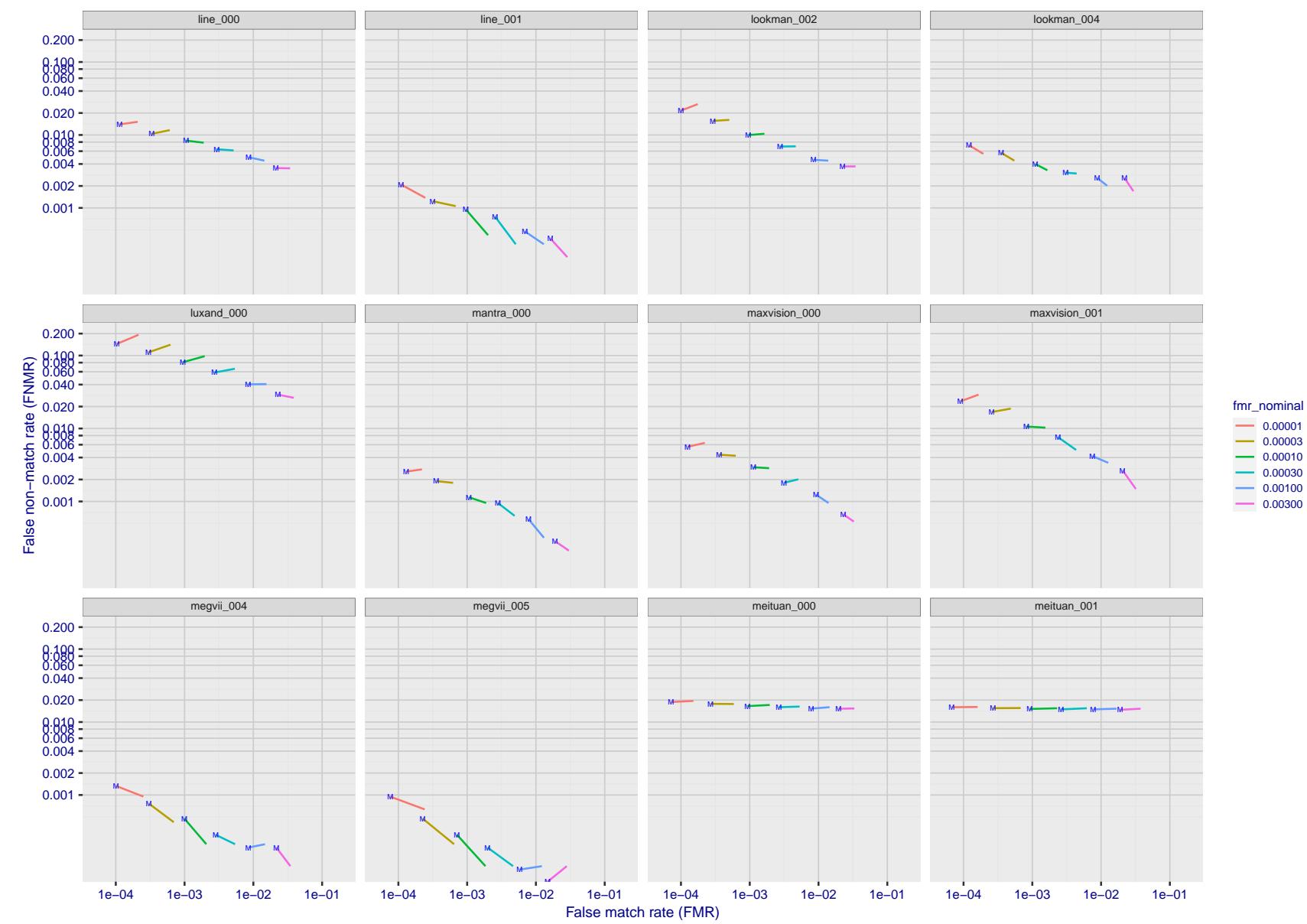


Figure 162: For the visa images, FNMR and FMR at six operating points along the DET characteristic. At each point a line is drawn between  $(FMR, FNMR)_{MALE}$  and  $(FMR, FNMR)_{FEMALE}$  showing how which sex has lower FMR and/or FNMR. The "M" label denotes male, the other end of the line corresponds to female. The six operating thresholds are selected to give the nominal false match rates given in the legend, and are computed over all impostor pairs regardless of age, sex, and place of birth. The plotted FMR values are broadly an order of magnitude larger than the nominal rates because FMR is computed over demographically-matched impostor pairs i.e individuals of the same sex, from the same geographic region (see section 3.6.1), and the same age group (see section 3.6.2).

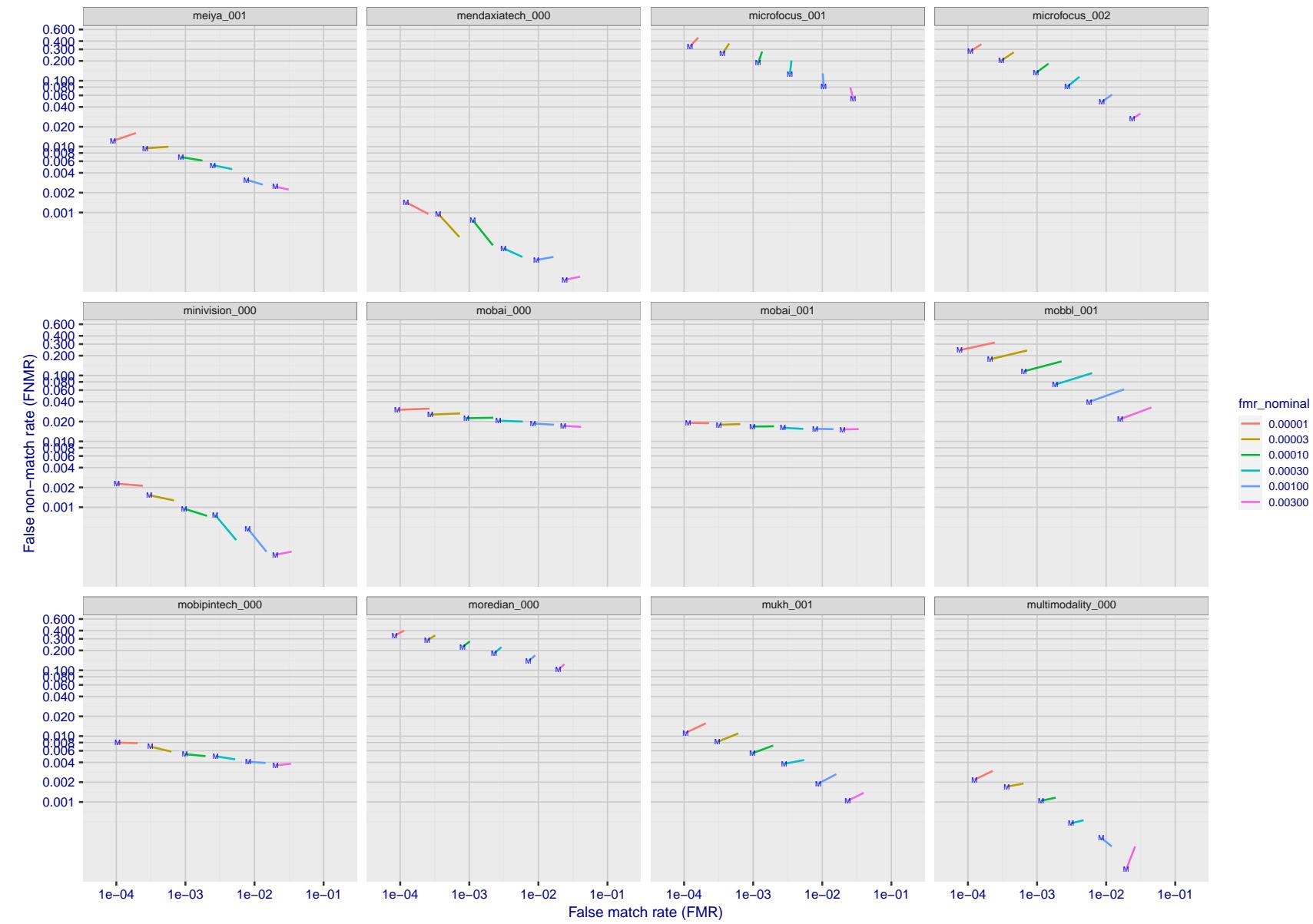


Figure 163: For the visa images, FNMR and FMR at six operating points along the DET characteristic. At each point a line is drawn between  $(FMR, FNMR)_{MALE}$  and  $(FMR, FNMR)_{FEMALE}$  showing how which sex has lower FMR and/or FNMR. The "M" label denotes male, the other end of the line corresponds to female. The six operating thresholds are selected to give the nominal false match rates given in the legend, and are computed over all impostor pairs regardless of age, sex, and place of birth. The plotted FMR values are broadly an order of magnitude larger than the nominal rates because FMR is computed over demographically-matched impostor pairs i.e individuals of the same sex, from the same geographic region (see section 3.6.1), and the same age group (see section 3.6.2).

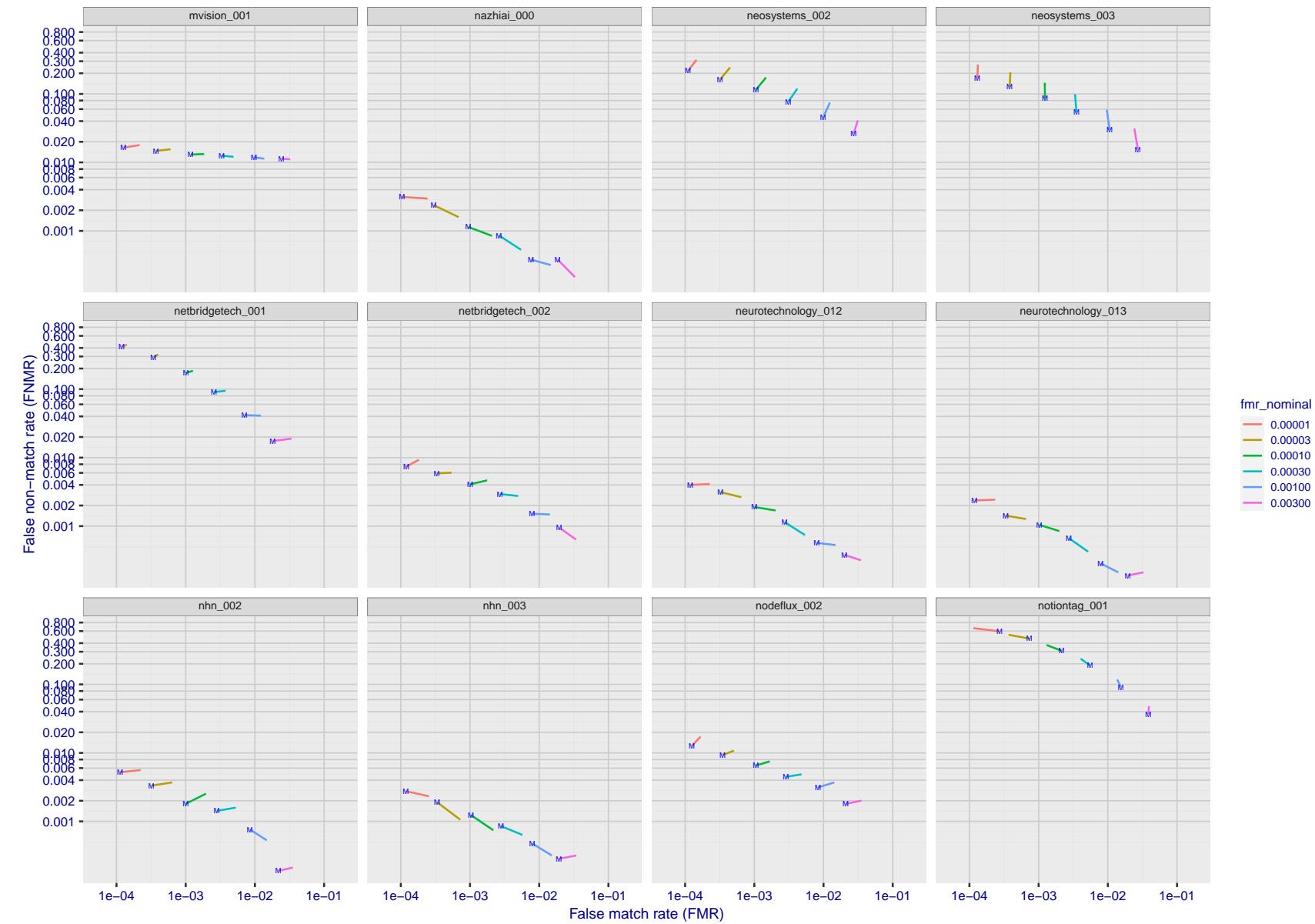


Figure 164: For the visa images, FNMR and FMR at six operating points along the DET characteristic. At each point a line is drawn between  $(FMR, FNMR)_{MALE}$  and  $(FMR, FNMR)_{FEMALE}$  showing how which sex has lower FMR and/or FNMR. The "M" label denotes male, the other end of the line corresponds to female. The six operating thresholds are selected to give the nominal false match rates given in the legend, and are computed over all impostor pairs regardless of age, sex, and place of birth. The plotted FMR values are broadly an order of magnitude larger than the nominal rates because FMR is computed over demographically-matched impostor pairs i.e individuals of the same sex, from the same geographic region (see section 3.6.1), and the same age group (see section 3.6.2).

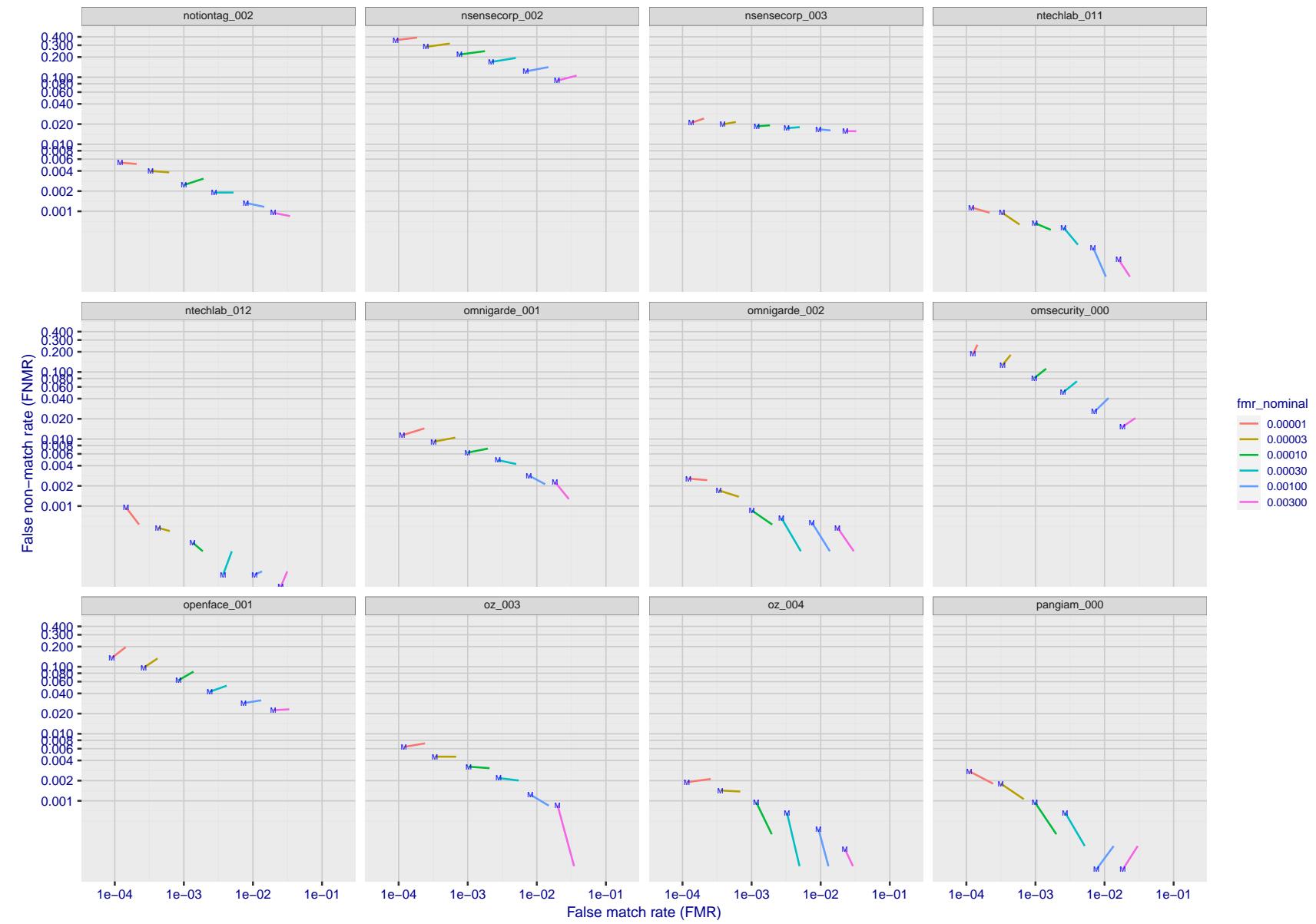


Figure 165: For the visa images, FNMR and FMR at six operating points along the DET characteristic. At each point a line is drawn between  $(FMR, FNMR)_{MALE}$  and  $(FMR, FNMR)_{FEMALE}$  showing how which sex has lower FMR and/or FNMR. The "M" label denotes male, the other end of the line corresponds to female. The six operating thresholds are selected to give the nominal false match rates given in the legend, and are computed over all impostor pairs regardless of age, sex, and place of birth. The plotted FMR values are broadly an order of magnitude larger than the nominal rates because FMR is computed over demographically-matched impostor pairs i.e individuals of the same sex, from the same geographic region (see section 3.6.1), and the same age group (see section 3.6.2).

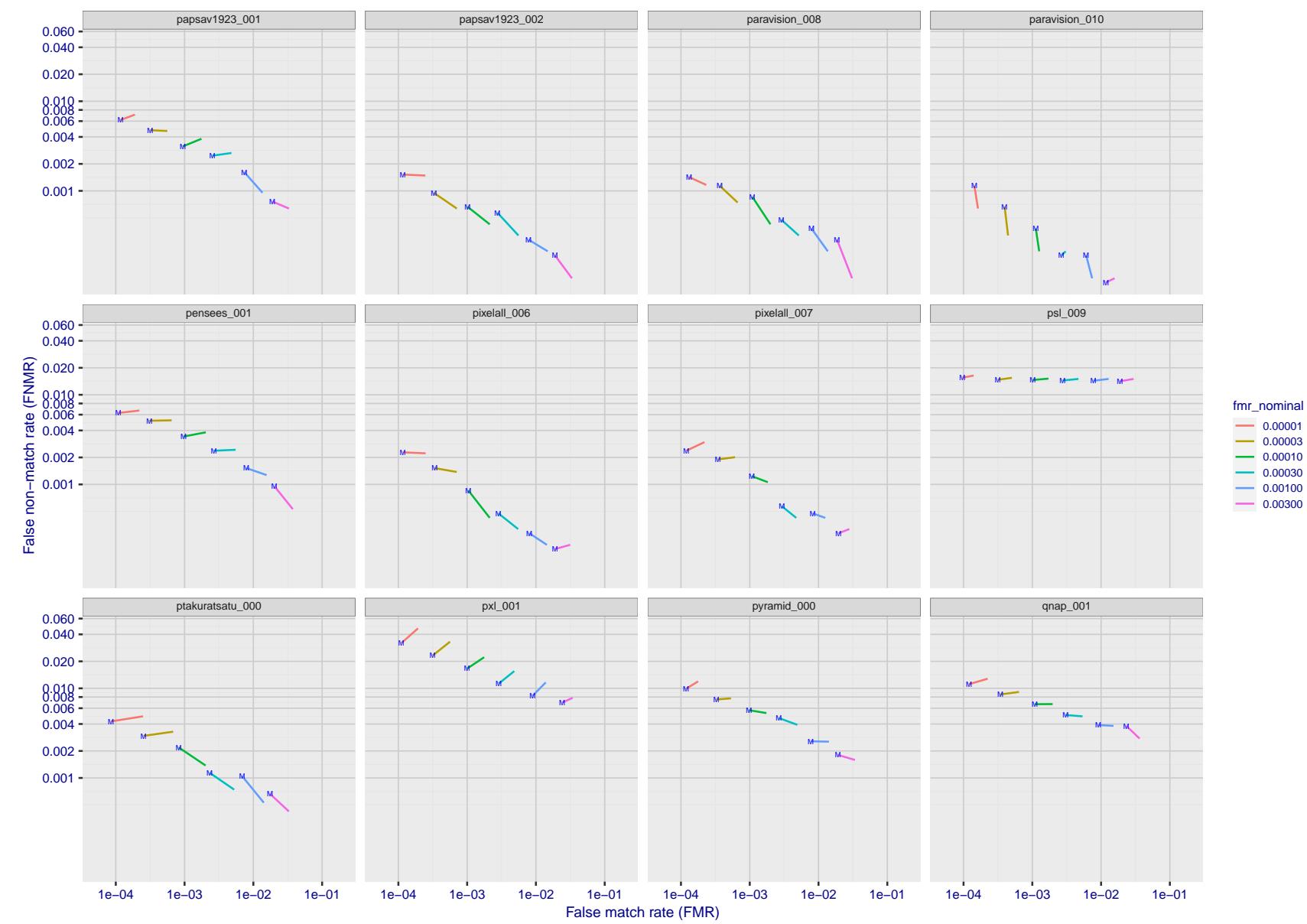


Figure 166: For the visa images, FNMR and FMR at six operating points along the DET characteristic. At each point a line is drawn between  $(FMR, FNMR)_{MALE}$  and  $(FMR, FNMR)_{FEMALE}$  showing how which sex has lower FMR and/or FNMR. The "M" label denotes male, the other end of the line corresponds to female. The six operating thresholds are selected to give the nominal false match rates given in the legend, and are computed over all impostor pairs regardless of age, sex, and place of birth. The plotted FMR values are broadly an order of magnitude larger than the nominal rates because FMR is computed over demographically-matched impostor pairs i.e individuals of the same sex, from the same geographic region (see section 3.6.1), and the same age group (see section 3.6.2).

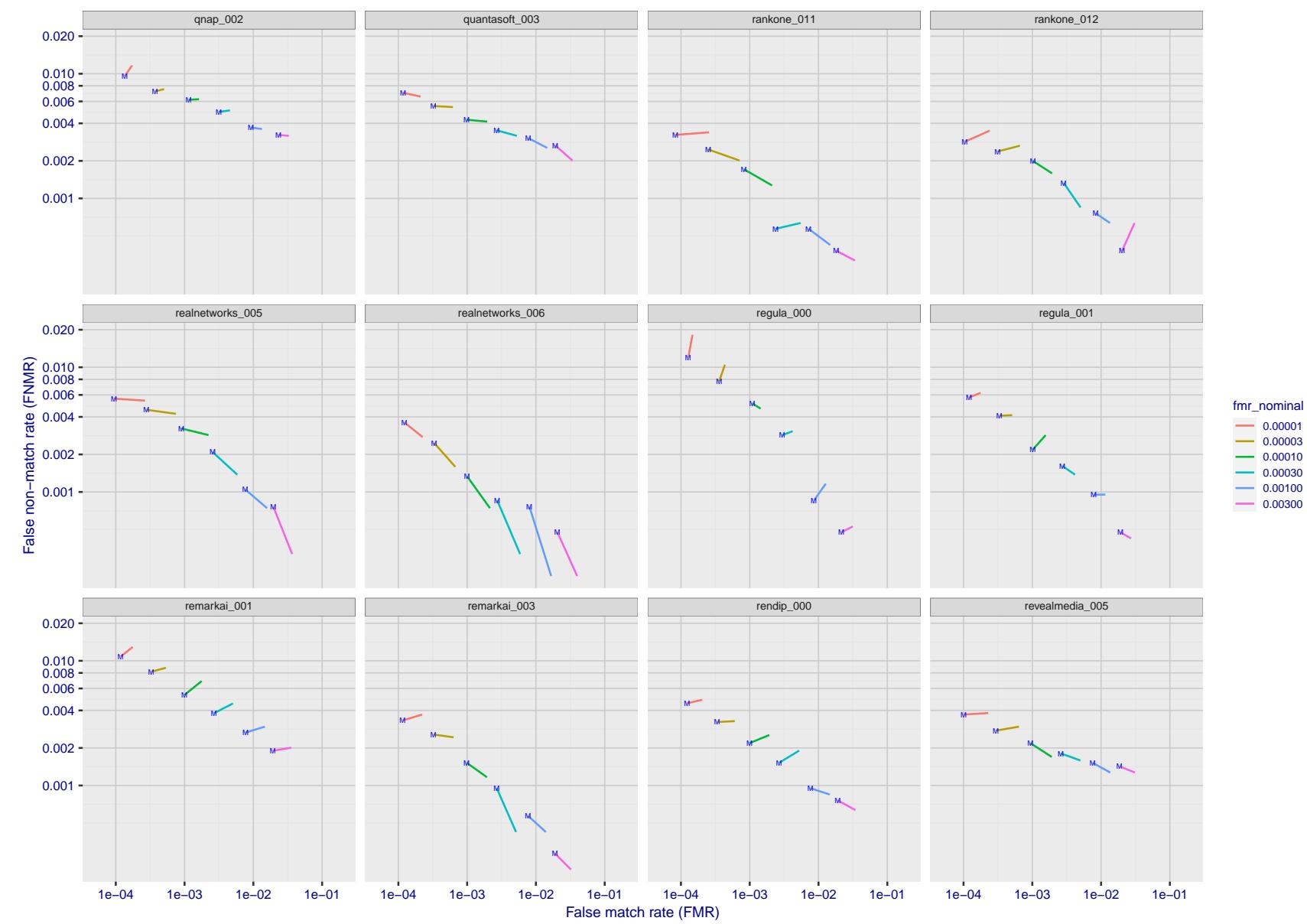


Figure 167: For the visa images, FNMR and FMR at six operating points along the DET characteristic. At each point a line is drawn between  $(FMR, FNMR)_{MALE}$  and  $(FMR, FNMR)_{FEMALE}$  showing how which sex has lower FMR and/or FNMR. The "M" label denotes male, the other end of the line corresponds to female. The six operating thresholds are selected to give the nominal false match rates given in the legend, and are computed over all impostor pairs regardless of age, sex, and place of birth. The plotted FMR values are broadly an order of magnitude larger than the nominal rates because FMR is computed over demographically-matched impostor pairs i.e individuals of the same sex, from the same geographic region (see section 3.6.1), and the same age group (see section 3.6.2).

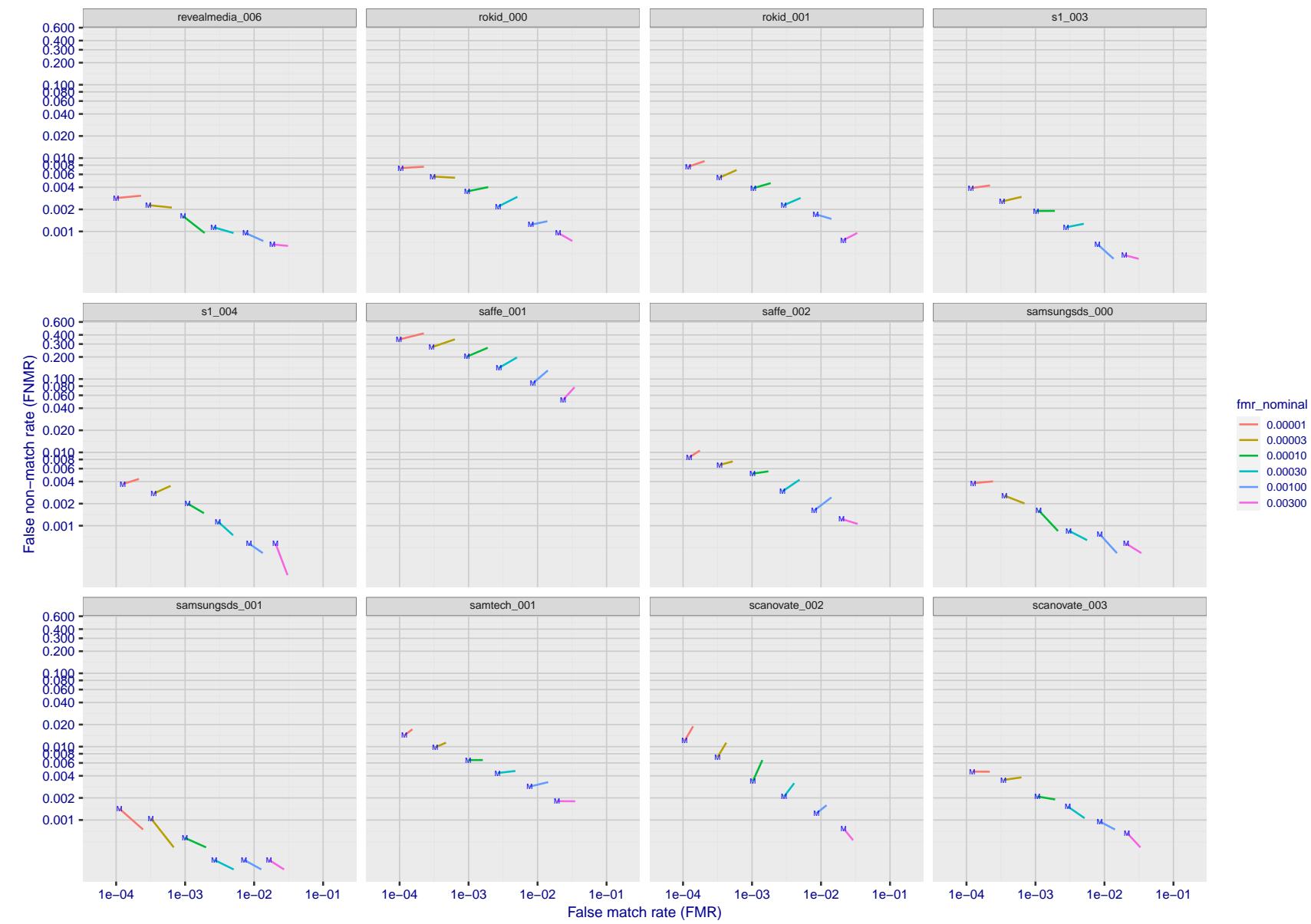


Figure 168: For the visa images, FNMR and FMR at six operating points along the DET characteristic. At each point a line is drawn between  $(FMR, FNMR)_{MALE}$  and  $(FMR, FNMR)_{FEMALE}$  showing how which sex has lower FMR and/or FNMR. The "M" label denotes male, the other end of the line corresponds to female. The six operating thresholds are selected to give the nominal false match rates given in the legend, and are computed over all impostor pairs regardless of age, sex, and place of birth. The plotted FMR values are broadly an order of magnitude larger than the nominal rates because FMR is computed over demographically-matched impostor pairs i.e individuals of the same sex, from the same geographic region (see section 3.6.1), and the same age group (see section 3.6.2).

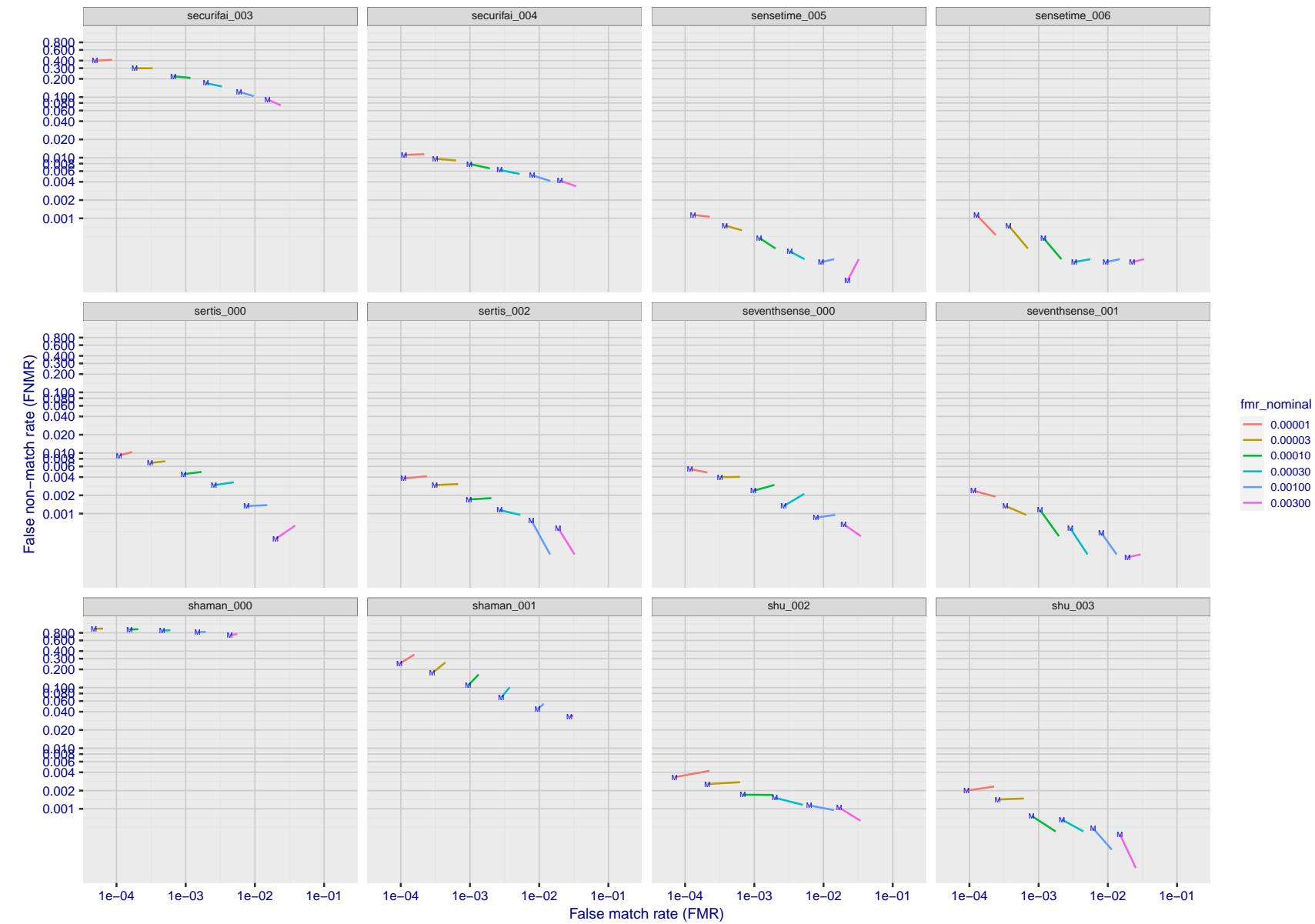


Figure 169: For the visa images, FNMR and FMR at six operating points along the DET characteristic. At each point a line is drawn between  $(FMR, FNMR)_{MALE}$  and  $(FMR, FNMR)_{FEMALE}$  showing how which sex has lower FMR and/or FNMR. The "M" label denotes male, the other end of the line corresponds to female. The six operating thresholds are selected to give the nominal false match rates given in the legend, and are computed over all impostor pairs regardless of age, sex, and place of birth. The plotted FMR values are broadly an order of magnitude larger than the nominal rates because FMR is computed over demographically-matched impostor pairs i.e individuals of the same sex, from the same geographic region (see section 3.6.1), and the same age group (see section 3.6.2).

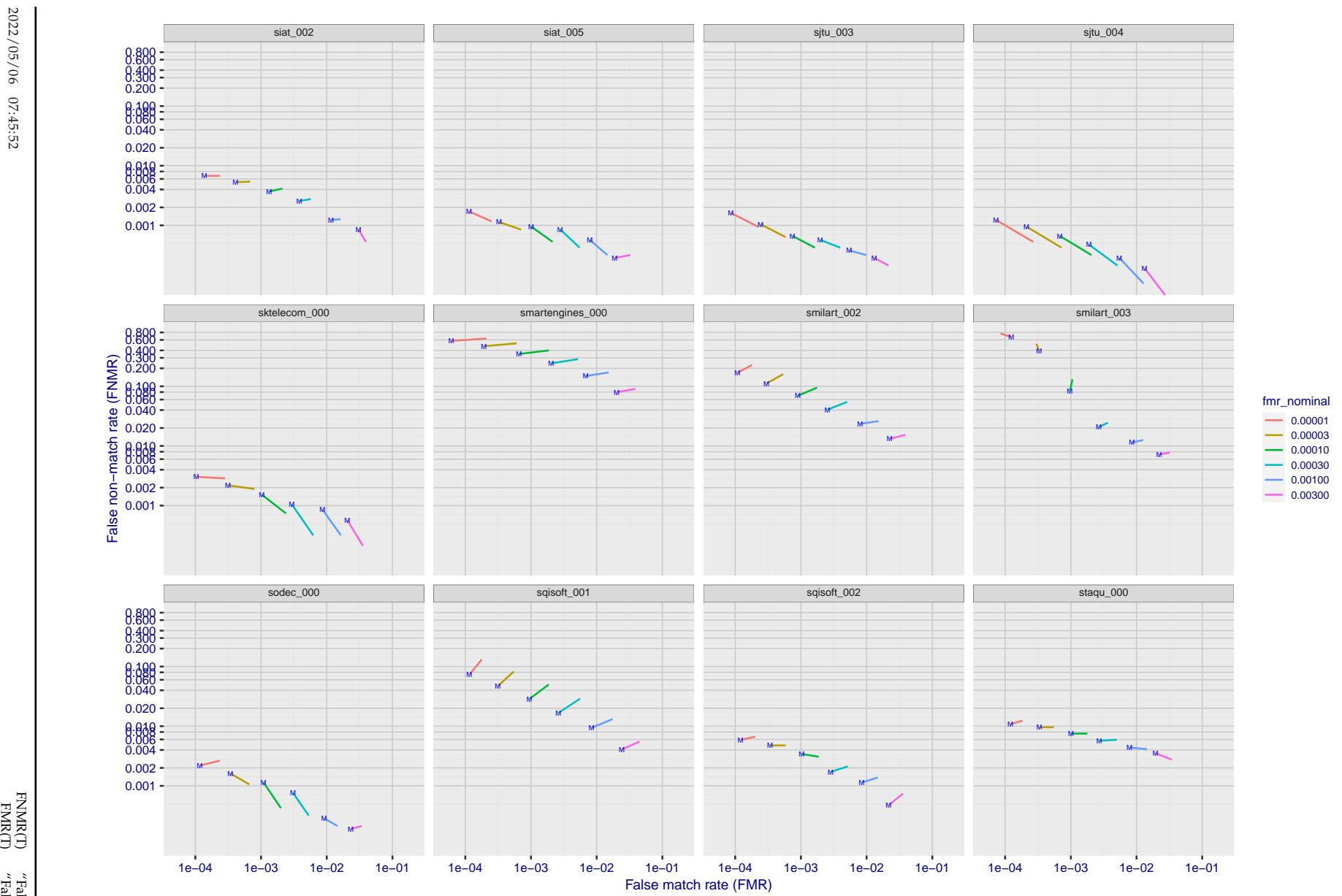


Figure 170: For the visa images, FNMR and FMR at six operating points along the DET characteristic. At each point a line is drawn between  $(FMR, FNMR)_{MALE}$  and  $(FMR, FNMR)_{FEMALE}$  showing how which sex has lower FMR and/or FNMR. The "M" label denotes male, the other end of the line corresponds to female. The six operating thresholds are selected to give the nominal false match rates given in the legend, and are computed over all impostor pairs regardless of age, sex, and place of birth. The plotted FMR values are broadly an order of magnitude larger than the nominal rates because FMR is computed over demographically-matched impostor pairs i.e individuals of the same sex, from the same geographic region (see section 3.6.1), and the same age group (see section 3.6.2).

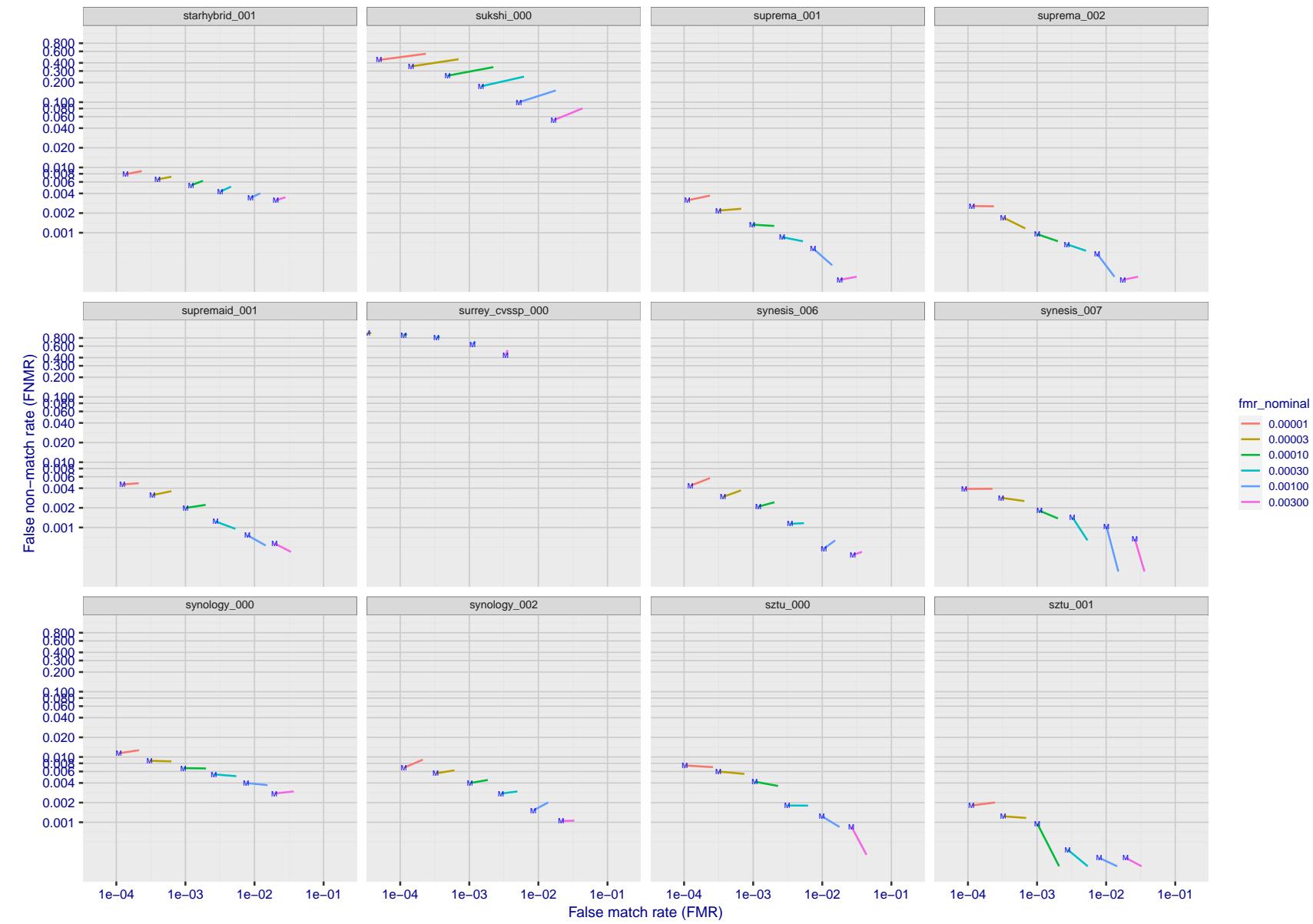


Figure 171: For the visa images, FNMR and FMR at six operating points along the DET characteristic. At each point a line is drawn between  $(FMR, FNMR)_{MALE}$  and  $(FMR, FNMR)_{FEMALE}$  showing how which sex has lower FMR and/or FNMR. The "M" label denotes male, the other end of the line corresponds to female. The six operating thresholds are selected to give the nominal false match rates given in the legend, and are computed over all impostor pairs regardless of age, sex, and place of birth. The plotted FMR values are broadly an order of magnitude larger than the nominal rates because FMR is computed over demographically-matched impostor pairs i.e individuals of the same sex, from the same geographic region (see section 3.6.1), and the same age group (see section 3.6.2).

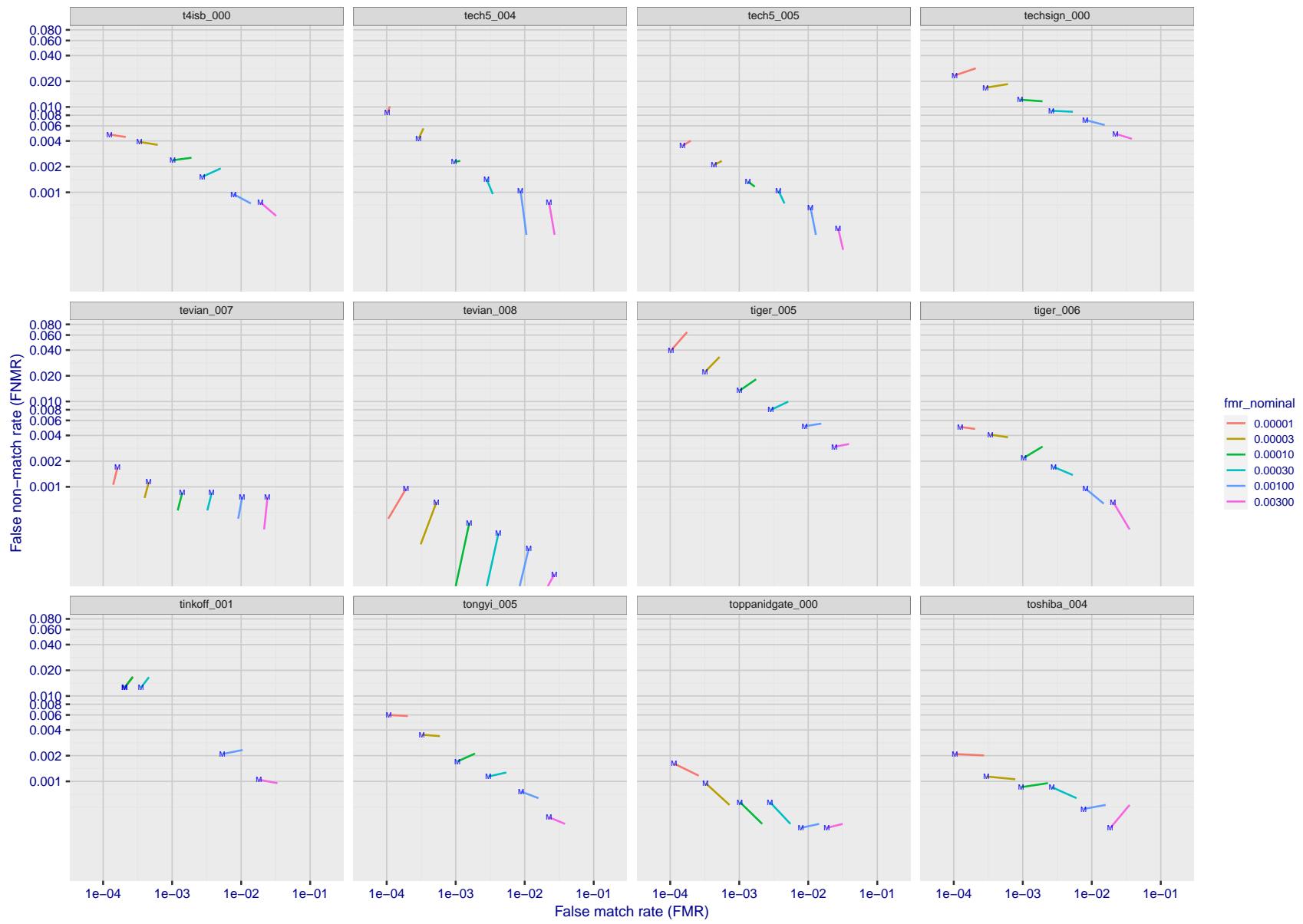


Figure 172: For the visa images, FNMR and FMR at six operating points along the DET characteristic. At each point a line is drawn between  $(FMR, FNMR)_{MALE}$  and  $(FMR, FNMR)_{FEMALE}$  showing how which sex has lower FMR and/or FNMR. The "M" label denotes male, the other end of the line corresponds to female. The six operating thresholds are selected to give the nominal false match rates given in the legend, and are computed over all impostor pairs regardless of age, sex, and place of birth. The plotted FMR values are broadly an order of magnitude larger than the nominal rates because FMR is computed over demographically-matched impostor pairs i.e individuals of the same sex, from the same geographic region (see section 3.6.1), and the same age group (see section 3.6.2).

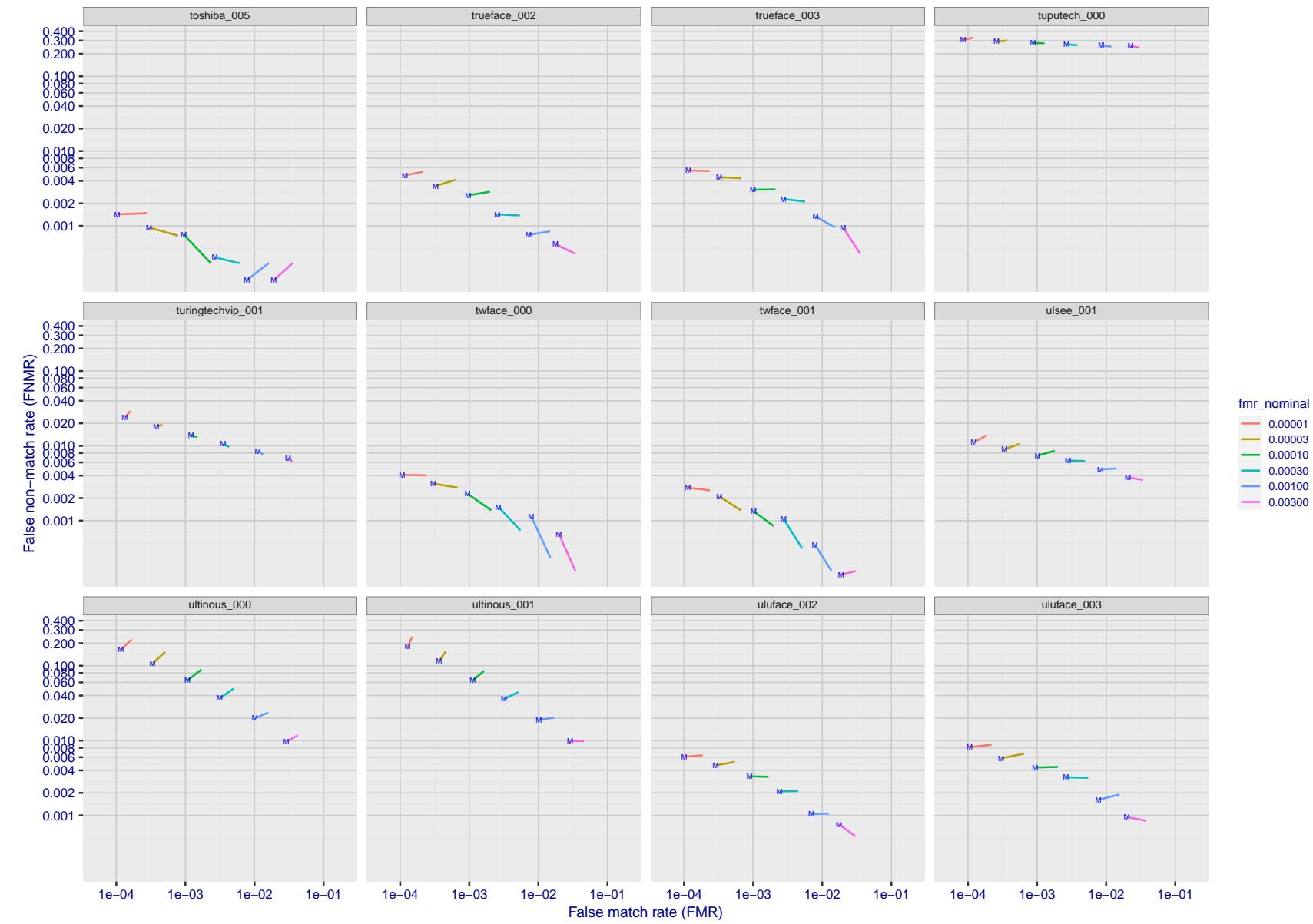


Figure 173: For the visa images, FNMR and FMR at six operating points along the DET characteristic. At each point a line is drawn between  $(FMR, FNMR)_{MALE}$  and  $(FMR, FNMR)_{FEMALE}$  showing how which sex has lower FMR and/or FNMR. The "M" label denotes male, the other end of the line corresponds to female. The six operating thresholds are selected to give the nominal false match rates given in the legend, and are computed over all impostor pairs regardless of age, sex, and place of birth. The plotted FMR values are broadly an order of magnitude larger than the nominal rates because FMR is computed over demographically-matched impostor pairs i.e individuals of the same sex, from the same geographic region (see section 3.6.1), and the same age group (see section 3.6.2).

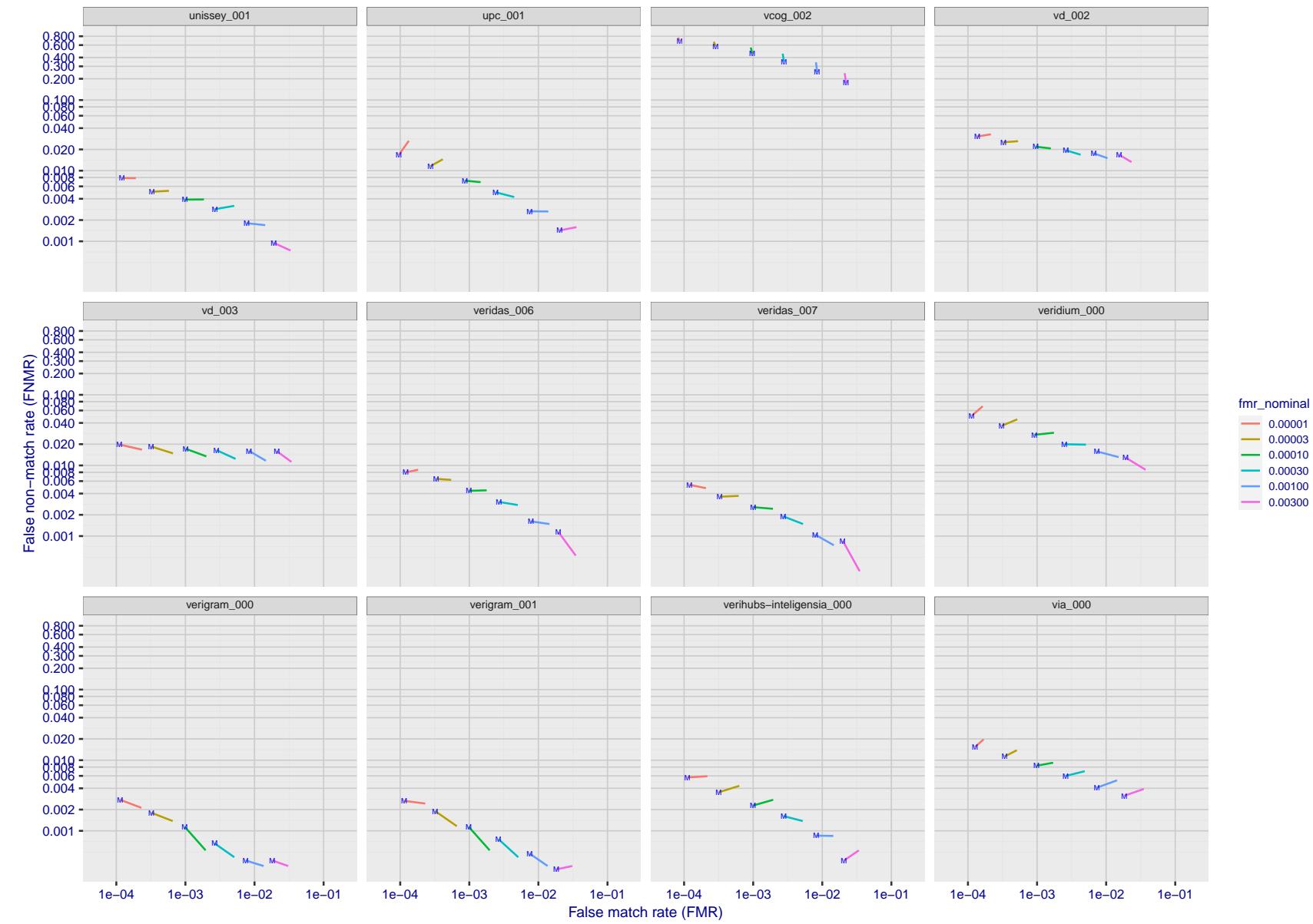


Figure 174: For the visa images, FNMR and FMR at six operating points along the DET characteristic. At each point a line is drawn between  $(FMR, FNMR)_{MALE}$  and  $(FMR, FNMR)_{FEMALE}$  showing how which sex has lower FMR and/or FNMR. The "M" label denotes male, the other end of the line corresponds to female. The six operating thresholds are selected to give the nominal false match rates given in the legend, and are computed over all impostor pairs regardless of age, sex, and place of birth. The plotted FMR values are broadly an order of magnitude larger than the nominal rates because FMR is computed over demographically-matched impostor pairs i.e individuals of the same sex, from the same geographic region (see section 3.6.1), and the same age group (see section 3.6.2).

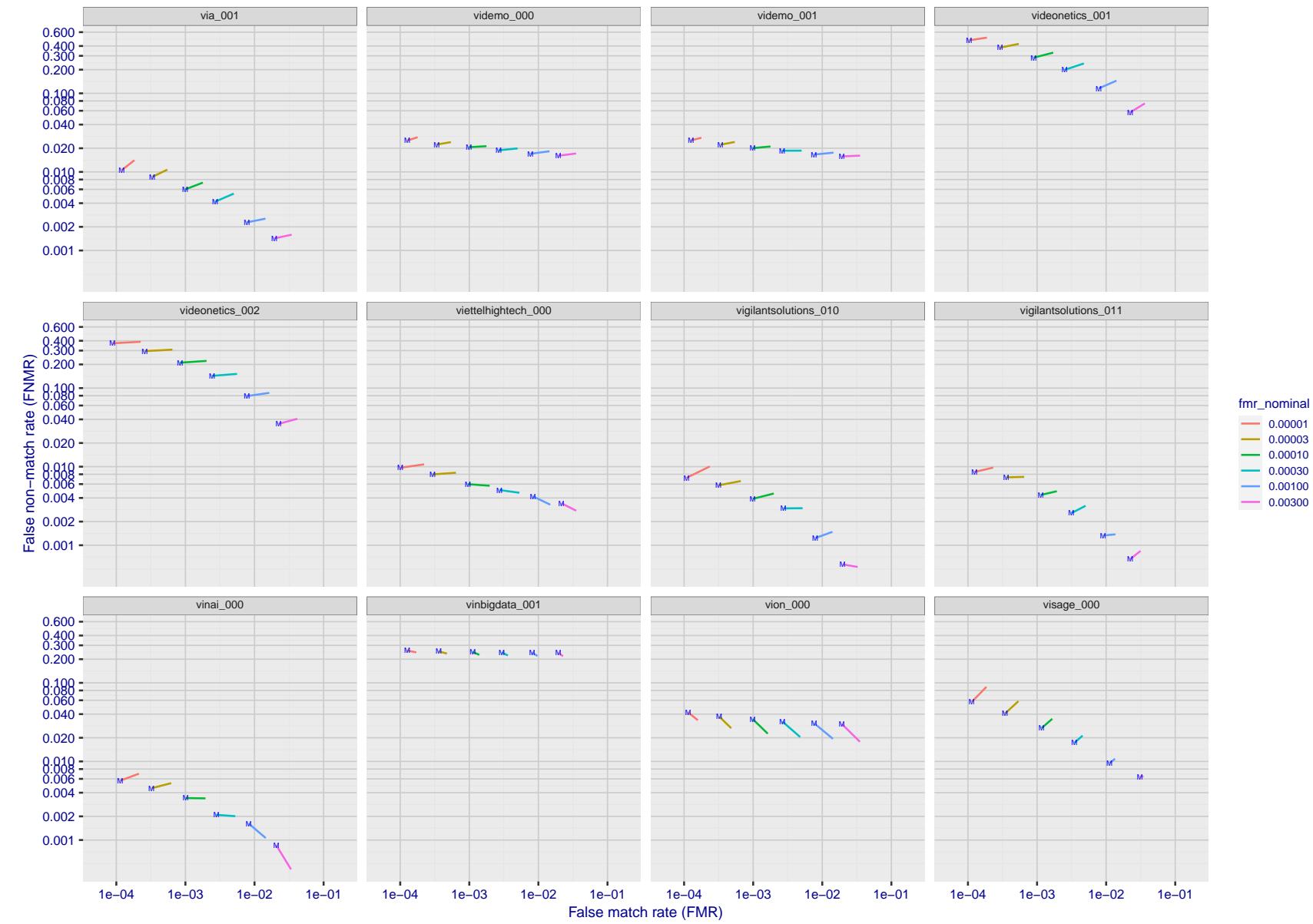


Figure 175: For the visa images, FNMR and FMR at six operating points along the DET characteristic. At each point a line is drawn between  $(FMR, FNMR)_{MALE}$  and  $(FMR, FNMR)_{FEMALE}$  showing how which sex has lower FMR and/or FNMR. The "M" label denotes male, the other end of the line corresponds to female. The six operating thresholds are selected to give the nominal false match rates given in the legend, and are computed over all impostor pairs regardless of age, sex, and place of birth. The plotted FMR values are broadly an order of magnitude larger than the nominal rates because FMR is computed over demographically-matched impostor pairs i.e individuals of the same sex, from the same geographic region (see section 3.6.1), and the same age group (see section 3.6.2).

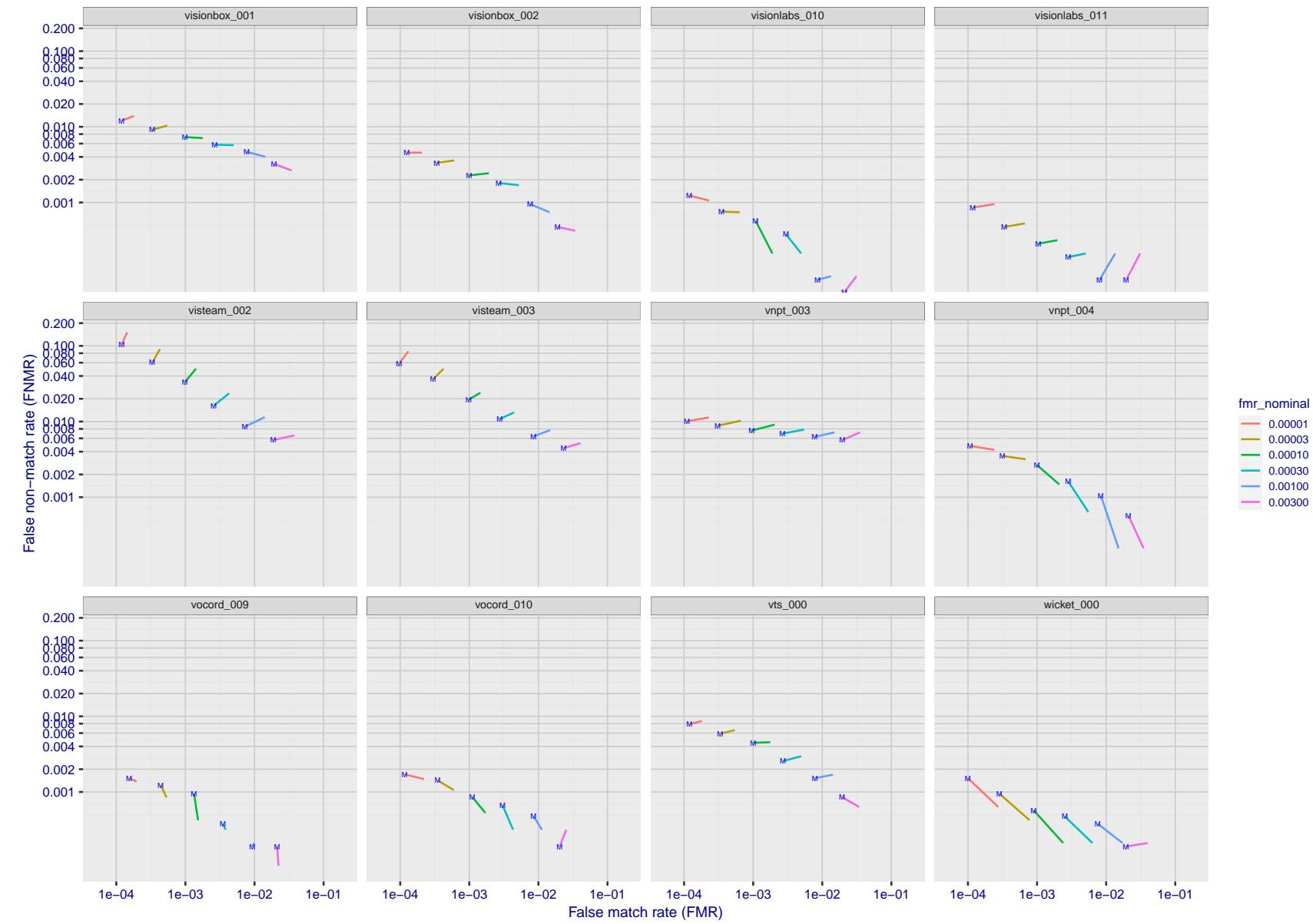


Figure 176: For the visa images, FNMR and FMR at six operating points along the DET characteristic. At each point a line is drawn between  $(FMR, FNMR)_{MALE}$  and  $(FMR, FNMR)_{FEMALE}$  showing how which sex has lower FMR and/or FNMR. The "M" label denotes male, the other end of the line corresponds to female. The six operating thresholds are selected to give the nominal false match rates given in the legend, and are computed over all impostor pairs regardless of age, sex, and place of birth. The plotted FMR values are broadly an order of magnitude larger than the nominal rates because FMR is computed over demographically-matched impostor pairs i.e individuals of the same sex, from the same geographic region (see section 3.6.1), and the same age group (see section 3.6.2).

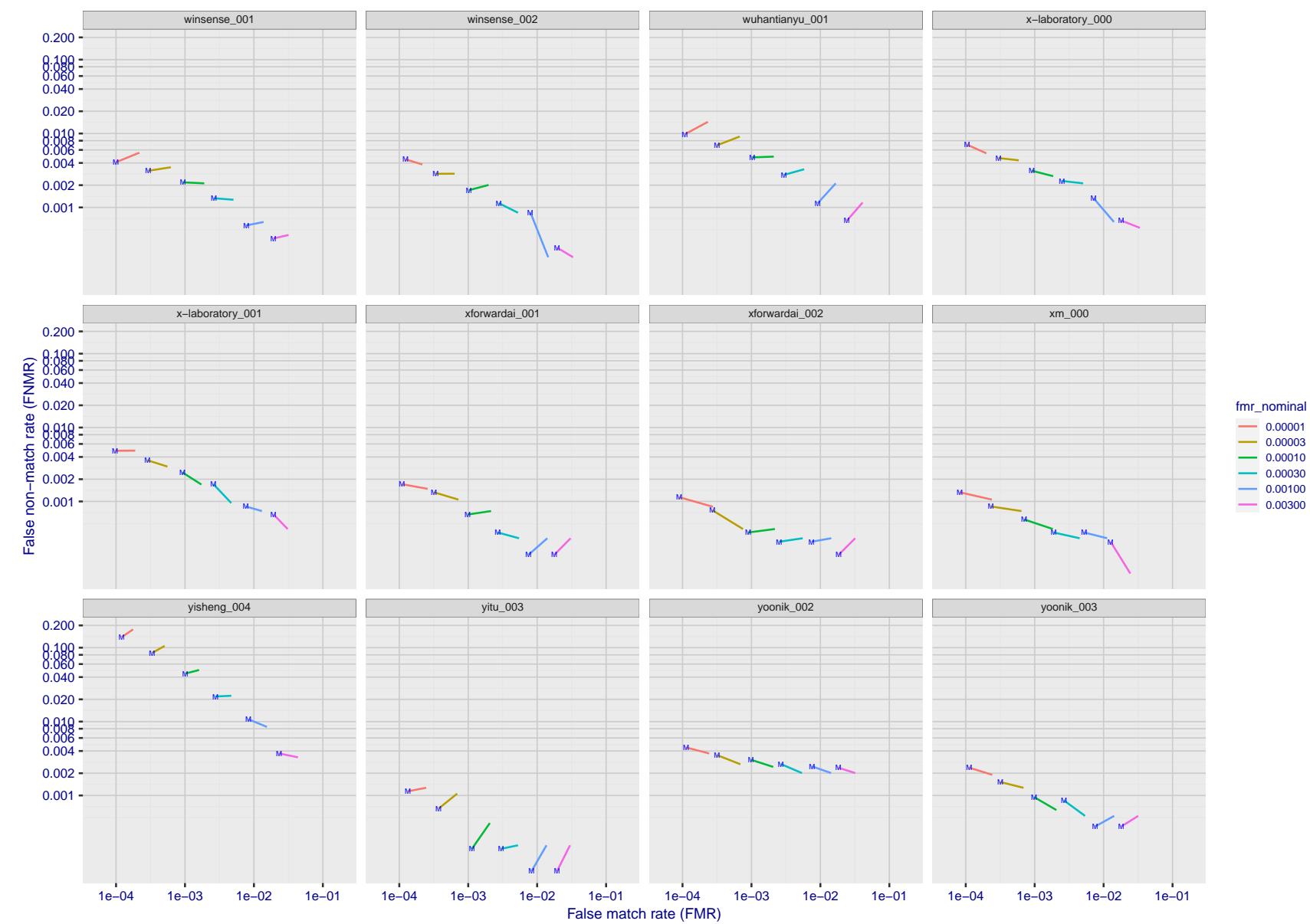


Figure 177: For the visa images, FNMR and FMR at six operating points along the DET characteristic. At each point a line is drawn between  $(FMR, FNMR)_{MALE}$  and  $(FMR, FNMR)_{FEMALE}$  showing how which sex has lower FMR and/or FNMR. The "M" label denotes male, the other end of the line corresponds to female. The six operating thresholds are selected to give the nominal false match rates given in the legend, and are computed over all impostor pairs regardless of age, sex, and place of birth. The plotted FMR values are broadly an order of magnitude larger than the nominal rates because FMR is computed over demographically-matched impostor pairs i.e individuals of the same sex, from the same geographic region (see section 3.6.1), and the same age group (see section 3.6.2).

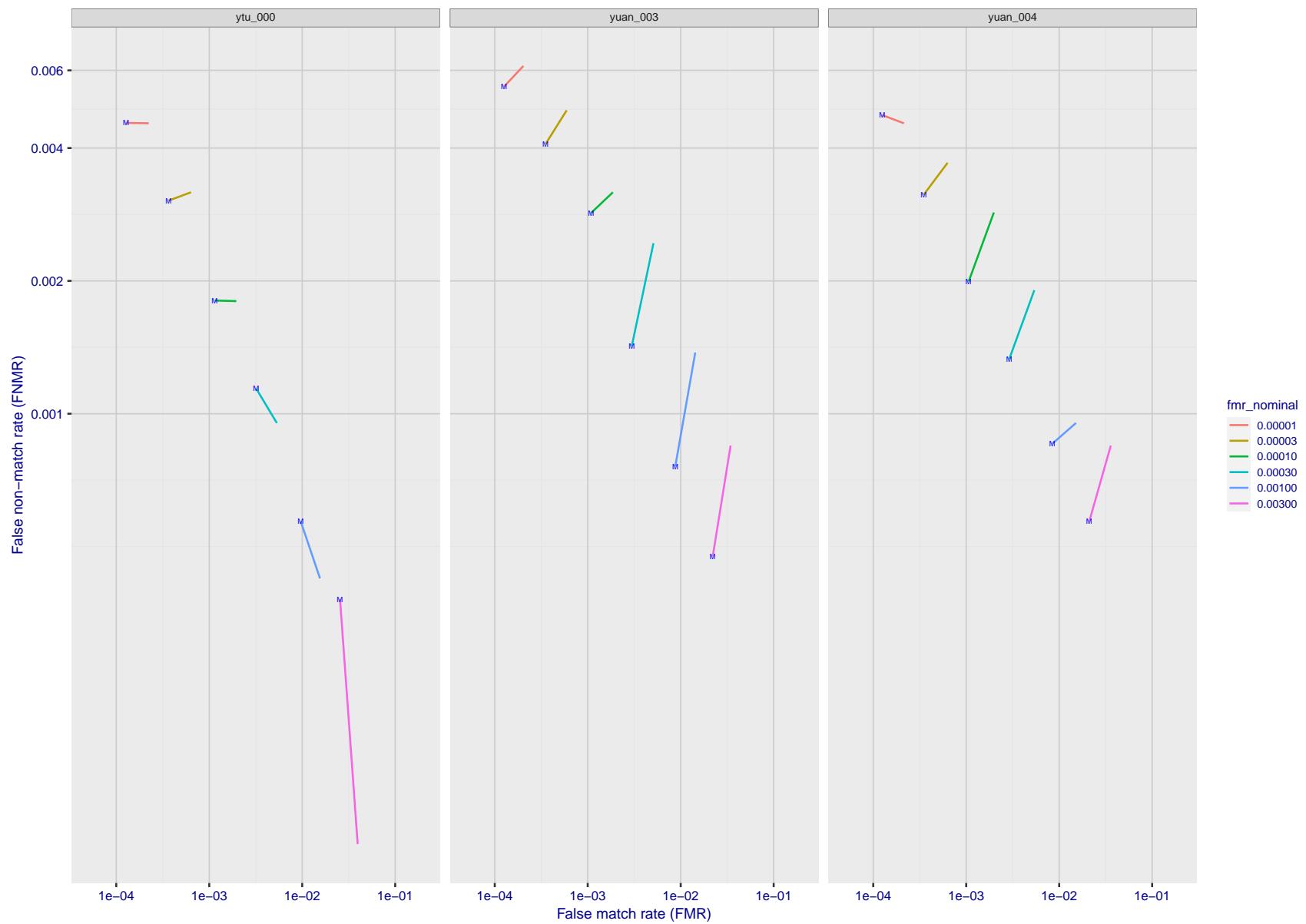


Figure 178: For the visa images, FNMR and FMR at six operating points along the DET characteristic. At each point a line is drawn between  $(FMR, FNMR)_{MALE}$  and  $(FMR, FNMR)_{FEMALE}$  showing how which sex has lower FMR and/or FNMR. The "M" label denotes male, the other end of the line corresponds to female. The six operating thresholds are selected to give the nominal false match rates given in the legend, and are computed over all impostor pairs regardless of age, sex, and place of birth. The plotted FMR values are broadly an order of magnitude larger than the nominal rates because FMR is computed over demographically-matched impostor pairs i.e individuals of the same sex, from the same geographic region (see section 3.6.1), and the same age group (see section 3.6.2).

2022/05/06 07:45:52

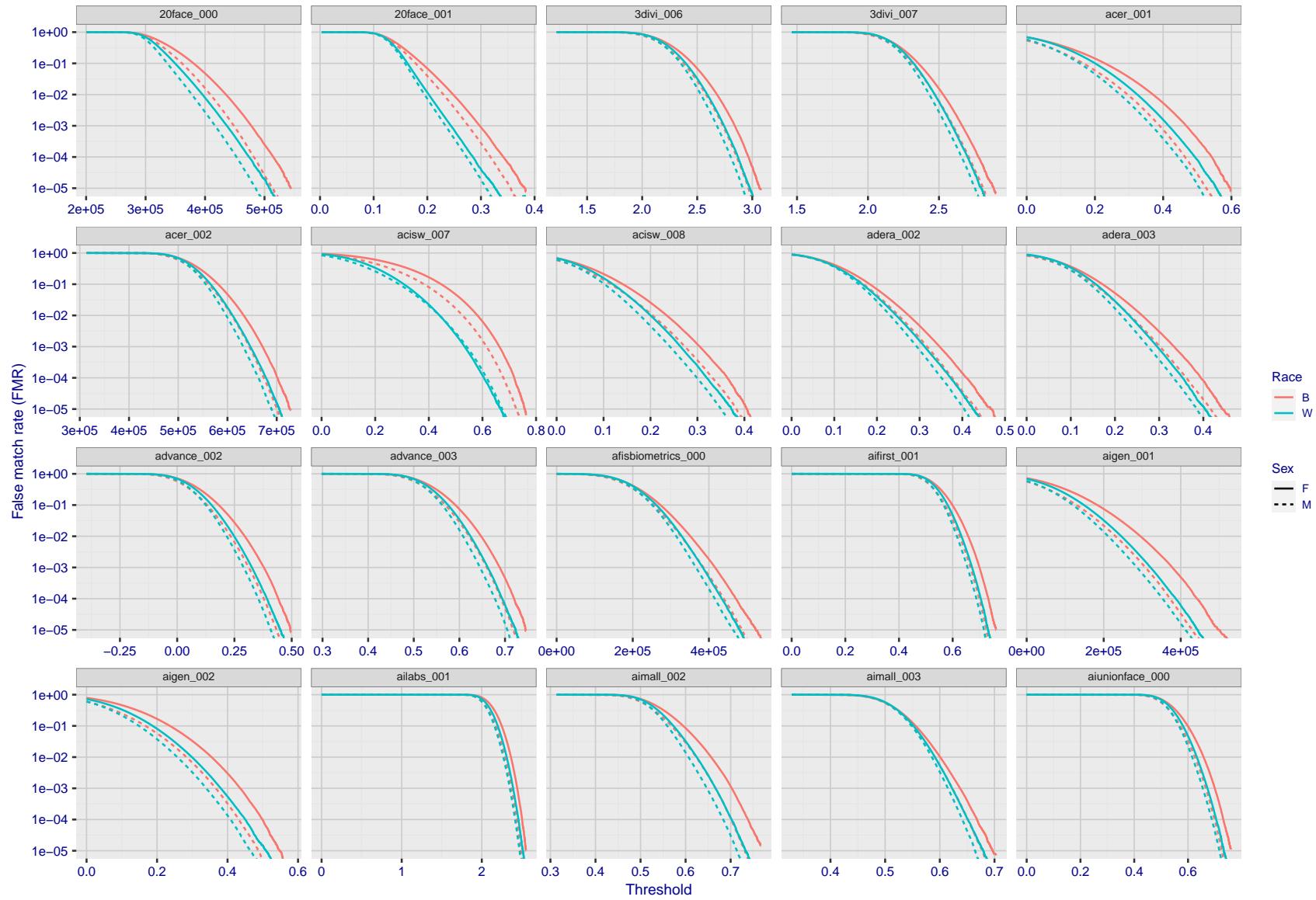


Figure 179: For the mugshot images, the false match calibration curves show false match rate vs. threshold. Separate curves appear for white females, black females, black males and white males.

FNMR(T)  
"False non-match rate"  
"False match rate"

2022/05/06 07:45:52

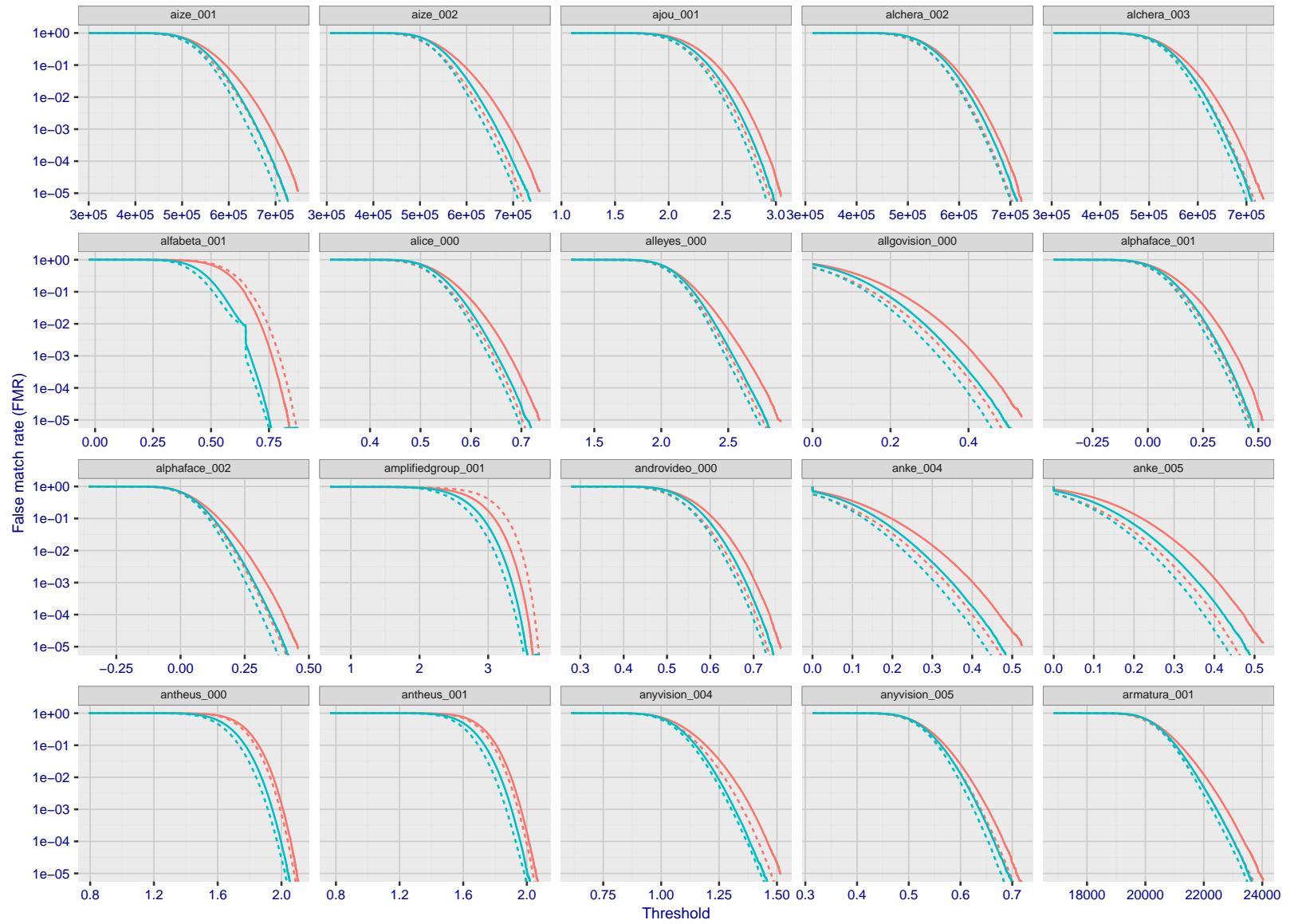


Figure 180: For the mugshot images, the false match calibration curves show false match rate vs. threshold. Separate curves appear for white females, black females, black males and white males.

FNMR(T)

"False non-match rate"

FMR(T)

"False match rate"

2022/05/06 07:45:52

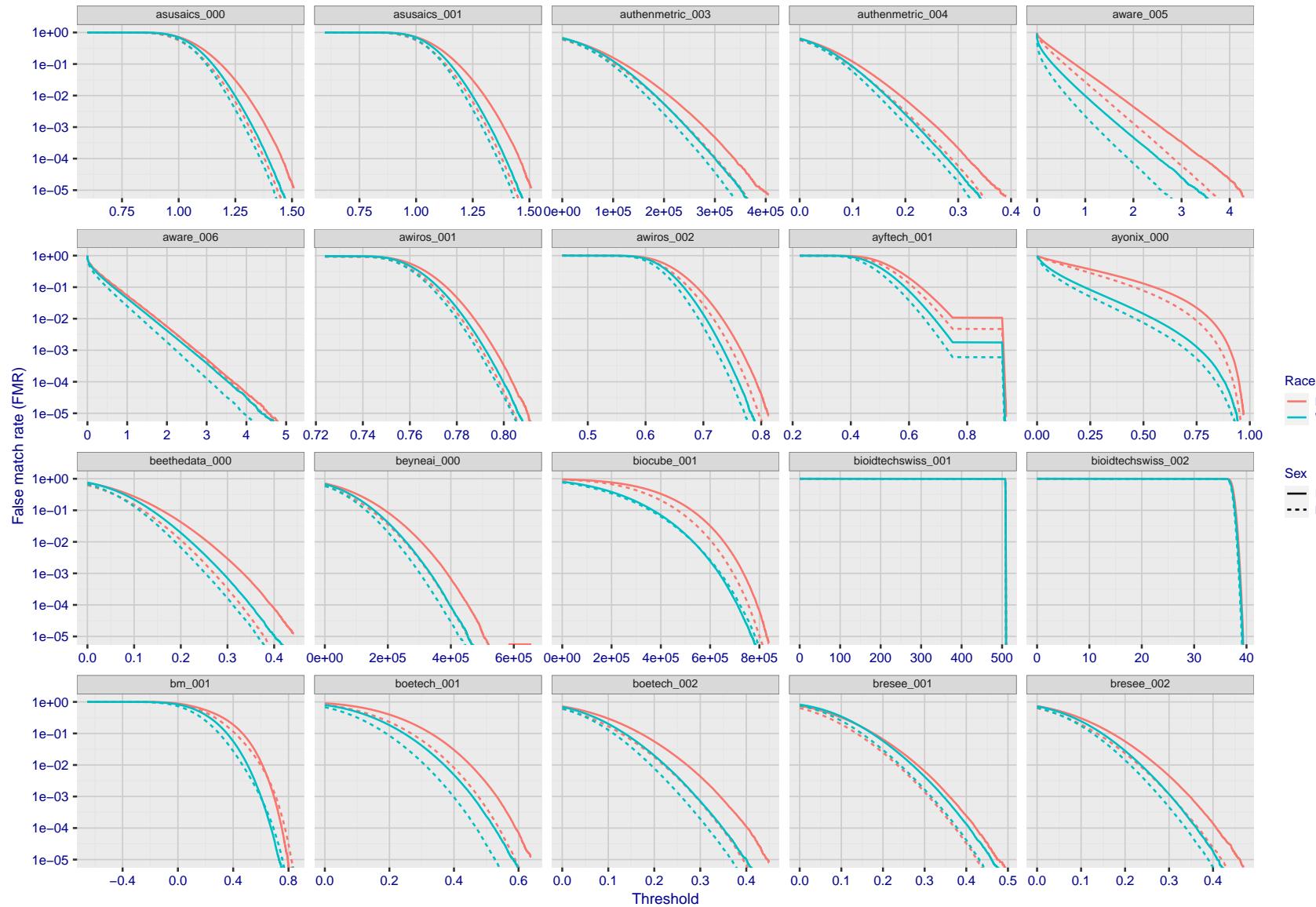


Figure 181: For the mugshot images, the false match calibration curves show false match rate vs. threshold. Separate curves appear for white females, black females, black males and white males.

FNMR(T)  
FMR(T)  
"False non-match rate"  
"False match rate"

2022/05/06 07:45:52

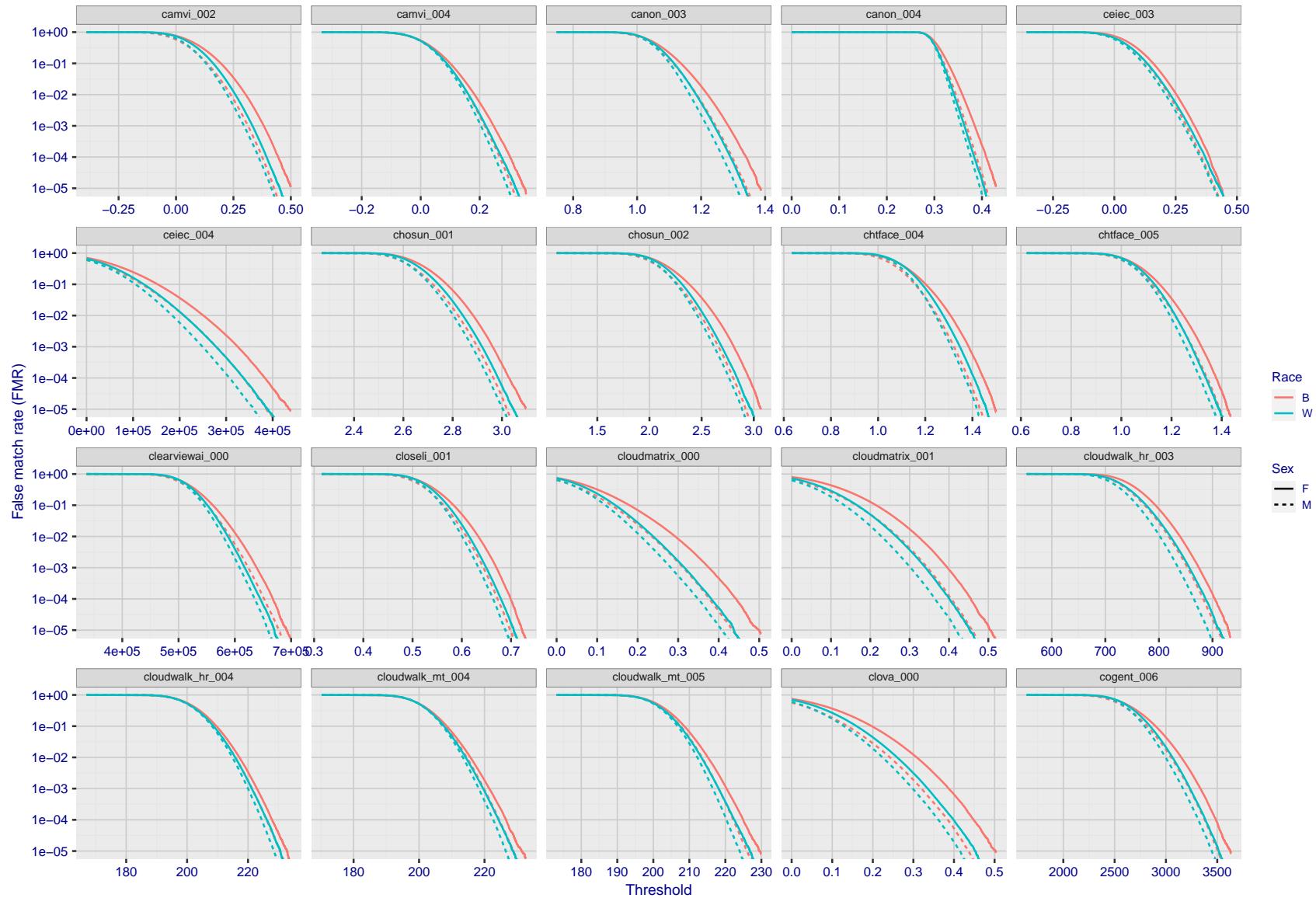


Figure 182: For the mugshot images, the false match calibration curves show false match rate vs. threshold. Separate curves appear for white females, black females, black males and white males.

2022/05/06 07:45:52

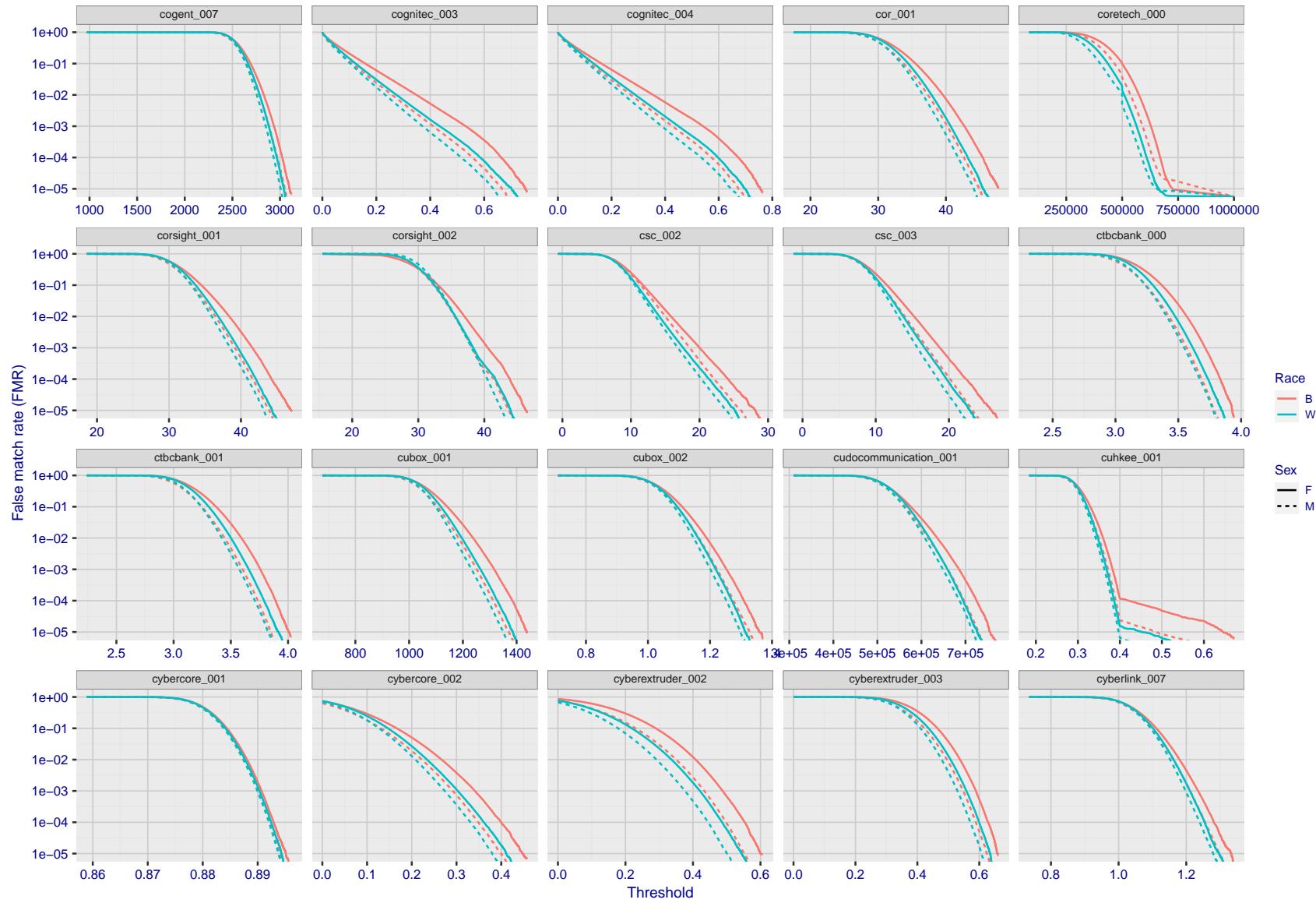


Figure 183: For the mugshot images, the false match calibration curves show false match rate vs. threshold. Separate curves appear for white females, black females, black males and white males.

FNMR(T)  
"False non-match rate"  
"False match rate"

2022/05/06 07:45:52

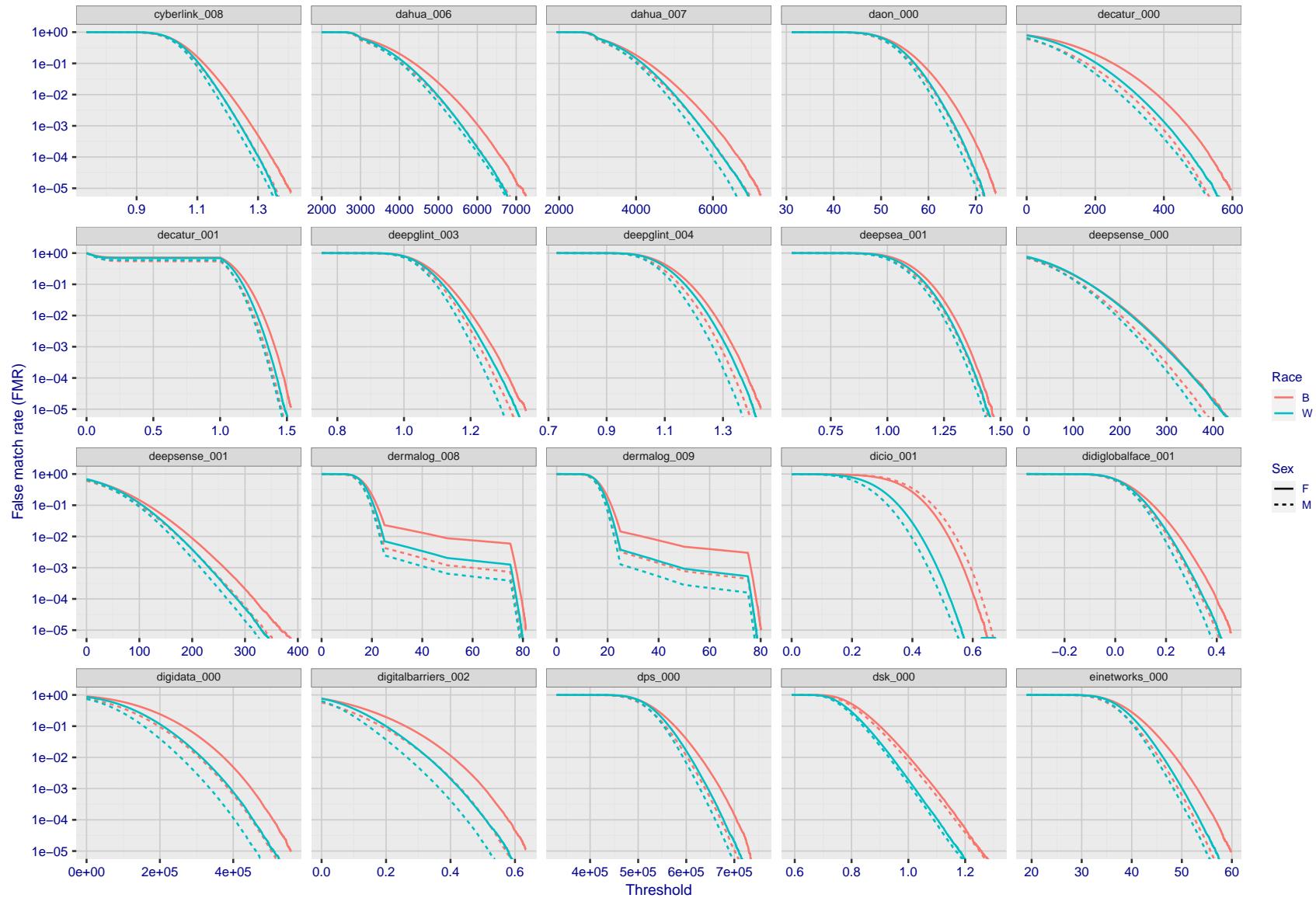


Figure 184: For the mugshot images, the false match calibration curves show false match rate vs. threshold. Separate curves appear for white females, black females, black males and white males.

2022/05/06 07:45:52

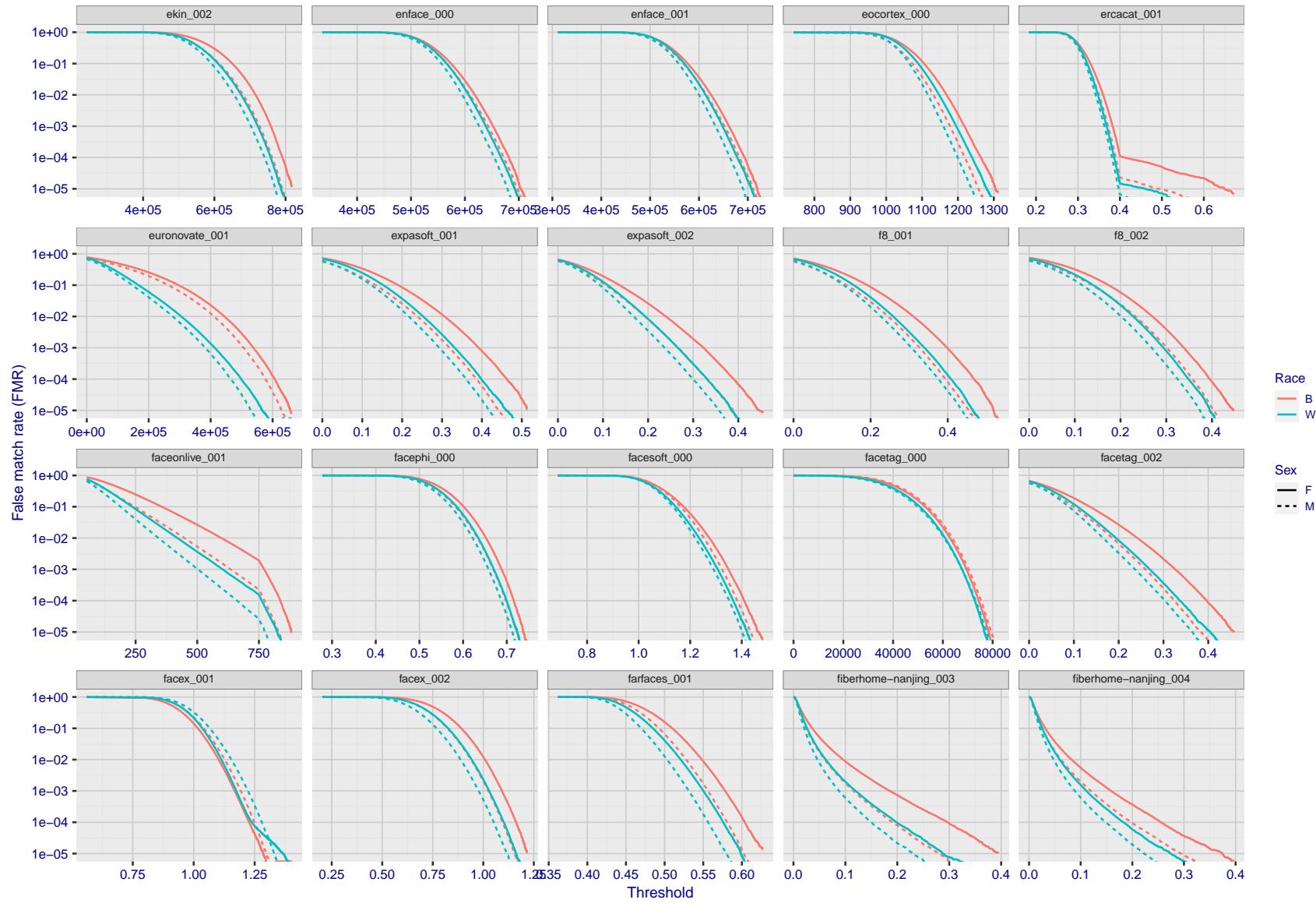


Figure 185: For the mugshot images, the false match calibration curves show false match rate vs. threshold. Separate curves appear for white females, black females, black males and white males.

FNMR(T)  
"False non-match rate"  
"False match rate"

2022/05/06 07:45:52

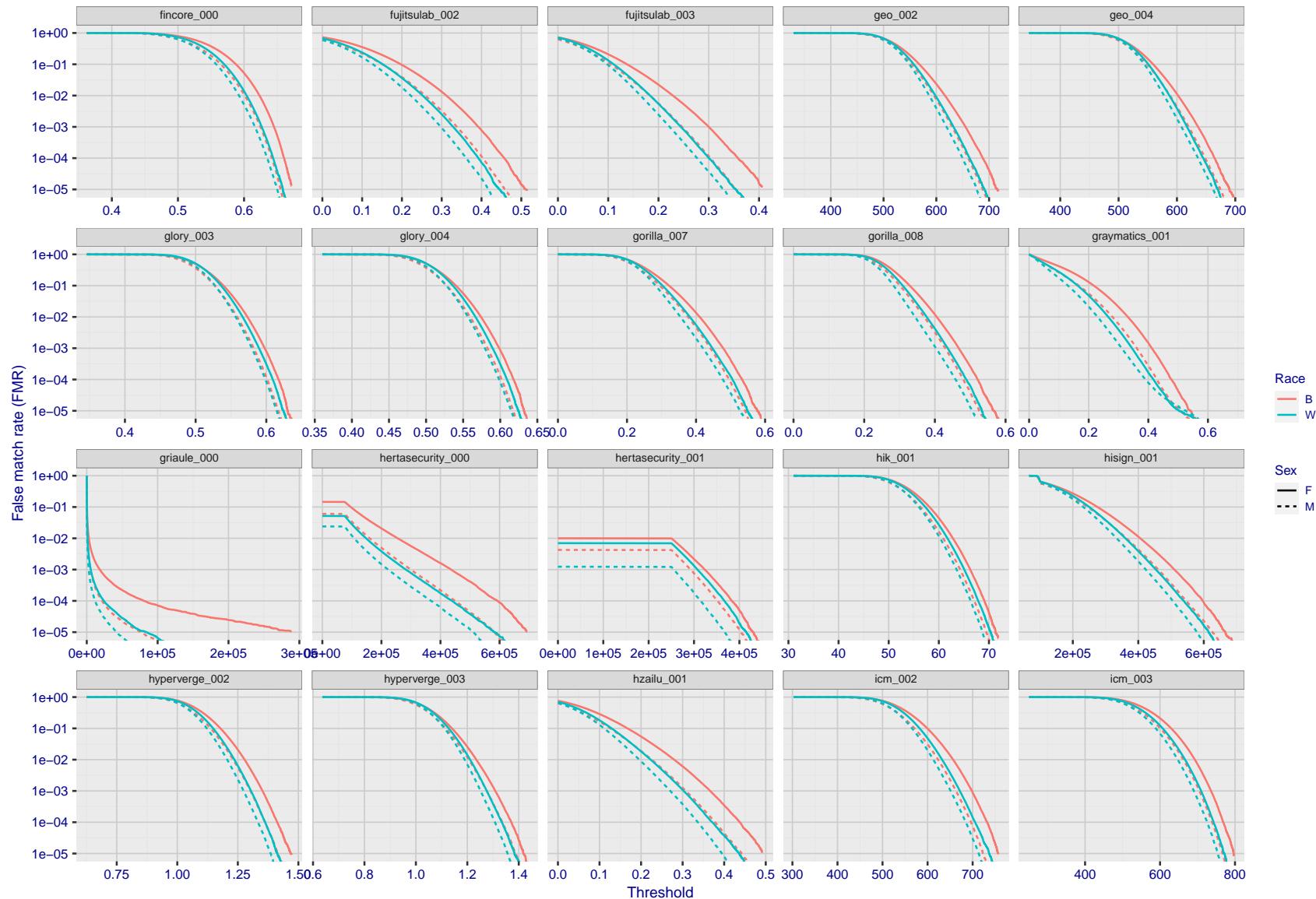


Figure 186: For the mugshot images, the false match calibration curves show false match rate vs. threshold. Separate curves appear for white females, black females, black males and white males.

FNMR(T)  
"False non-match rate"  
"False match rate"

2022/05/06 07:45:52

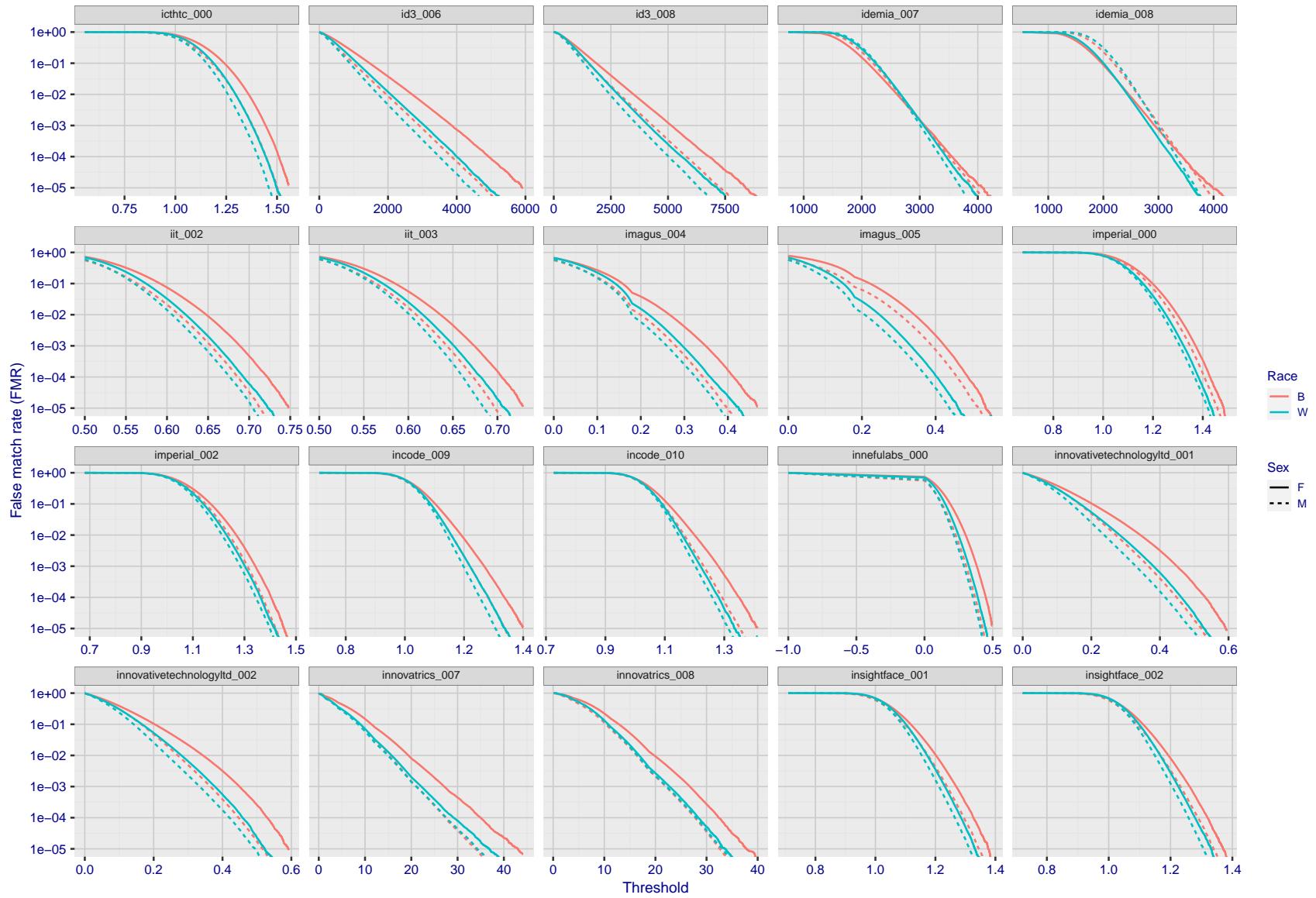


Figure 187: For the mugshot images, the false match calibration curves show false match rate vs. threshold. Separate curves appear for white females, black females, black males and white males.

2022/05/06 07:45:52

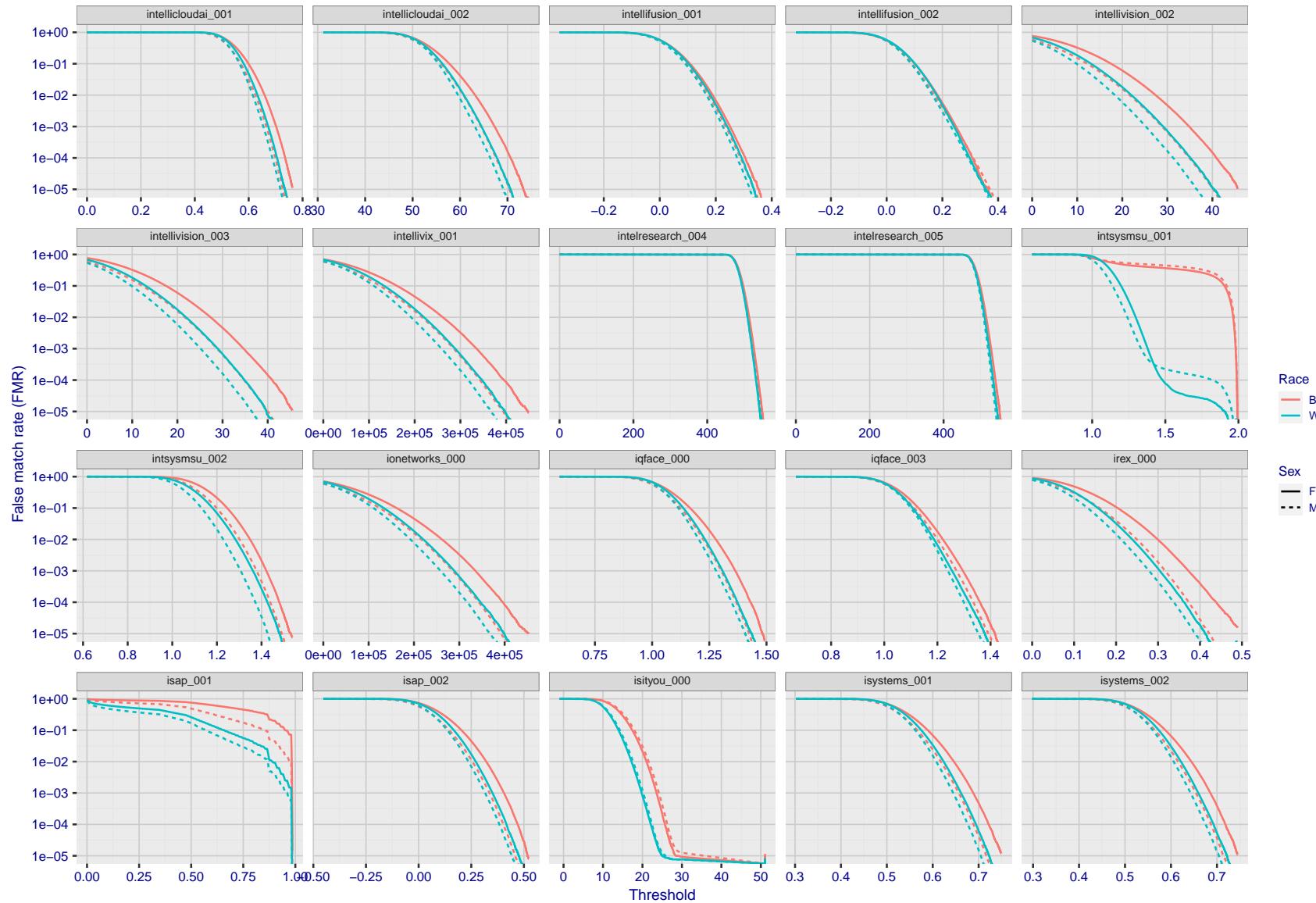


Figure 188: For the mugshot images, the false match calibration curves show false match rate vs. threshold. Separate curves appear for white females, black females, black males and white males.

2022/05/06 07:45:52

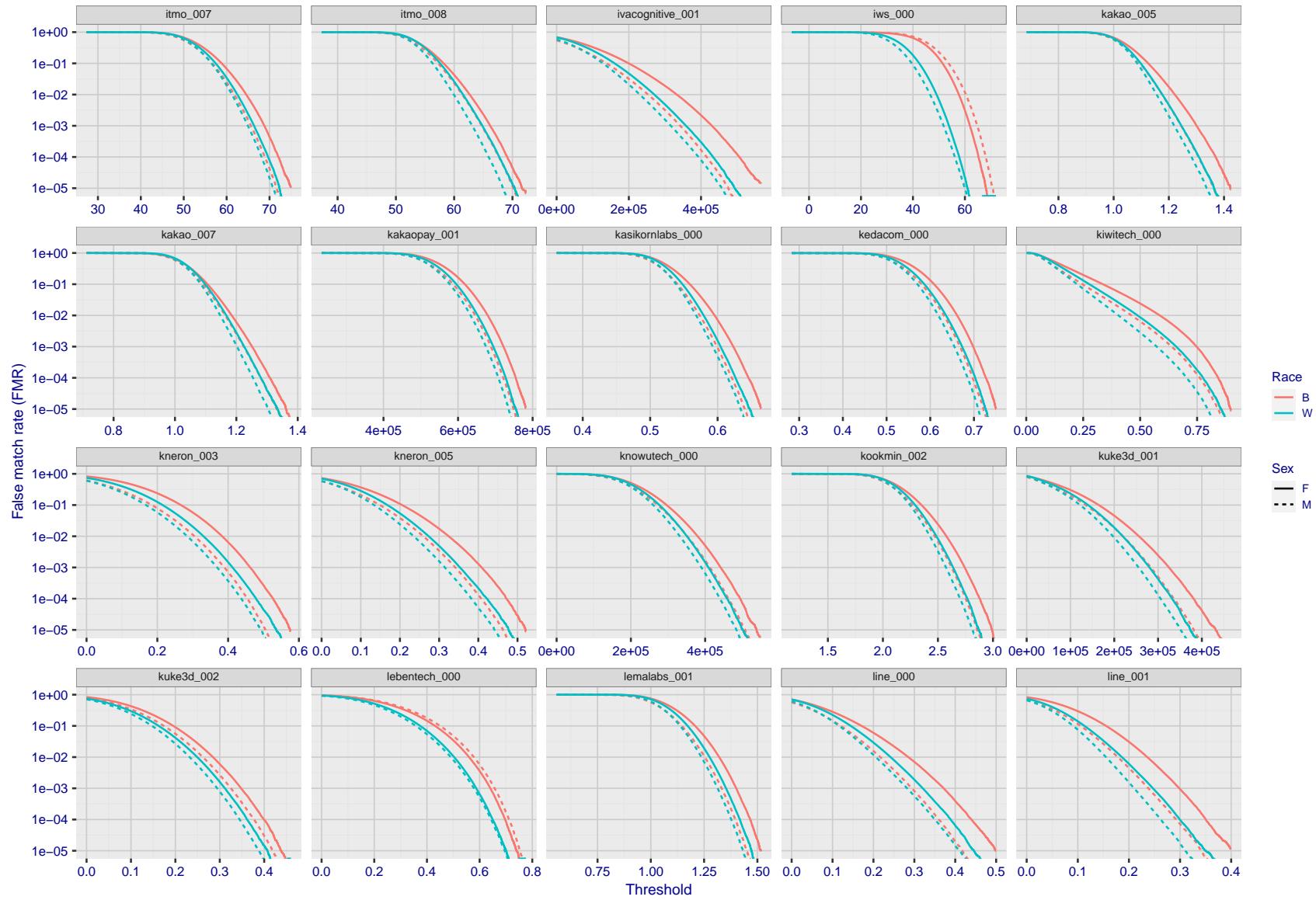


Figure 189: For the mugshot images, the false match calibration curves show false match rate vs. threshold. Separate curves appear for white females, black females, black males and white males.

2022/05/06 07:45:52

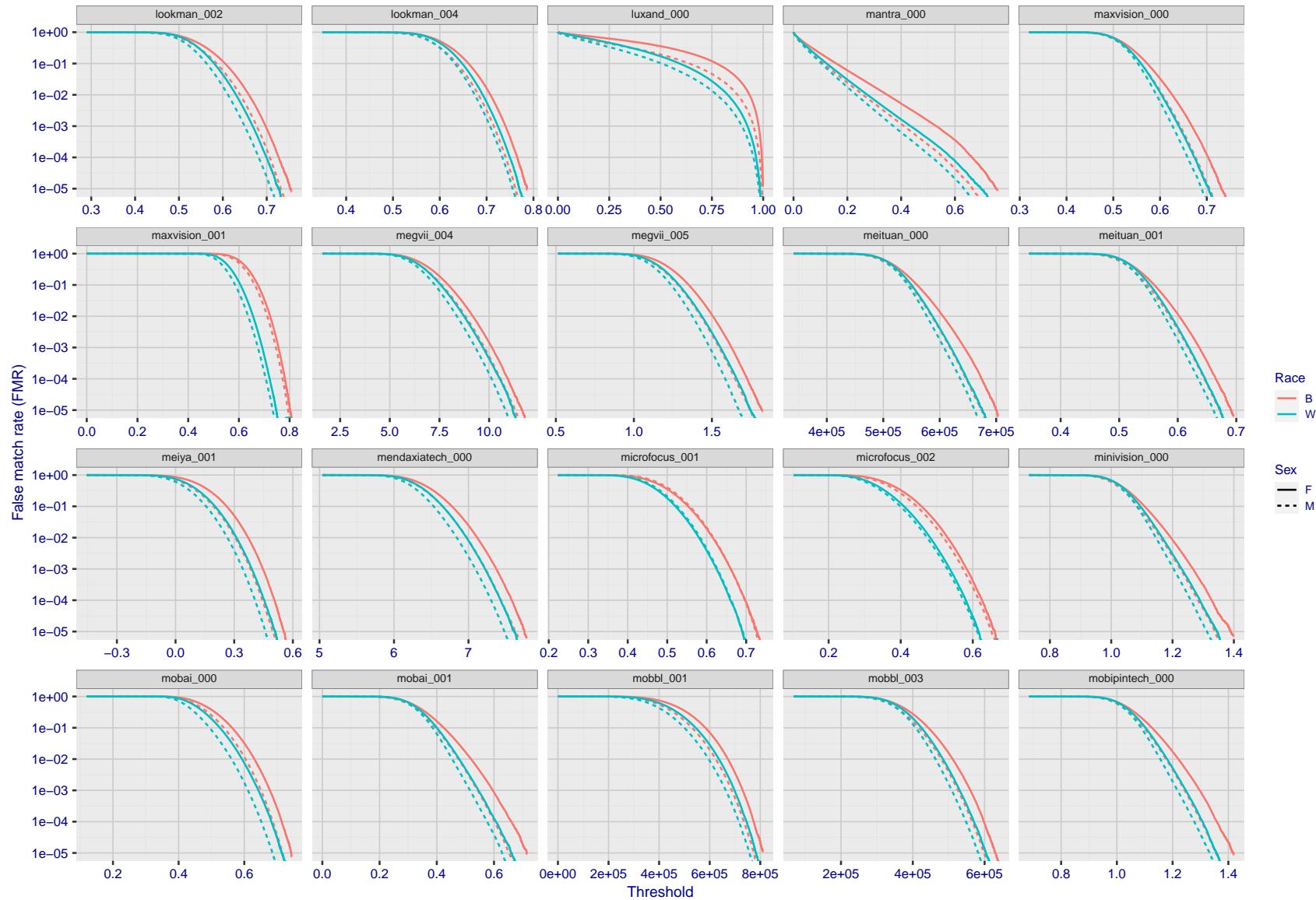


Figure 190: For the mugshot images, the false match calibration curves show false match rate vs. threshold. Separate curves appear for white females, black females, black males and white males.

2022/05/06 07:45:52

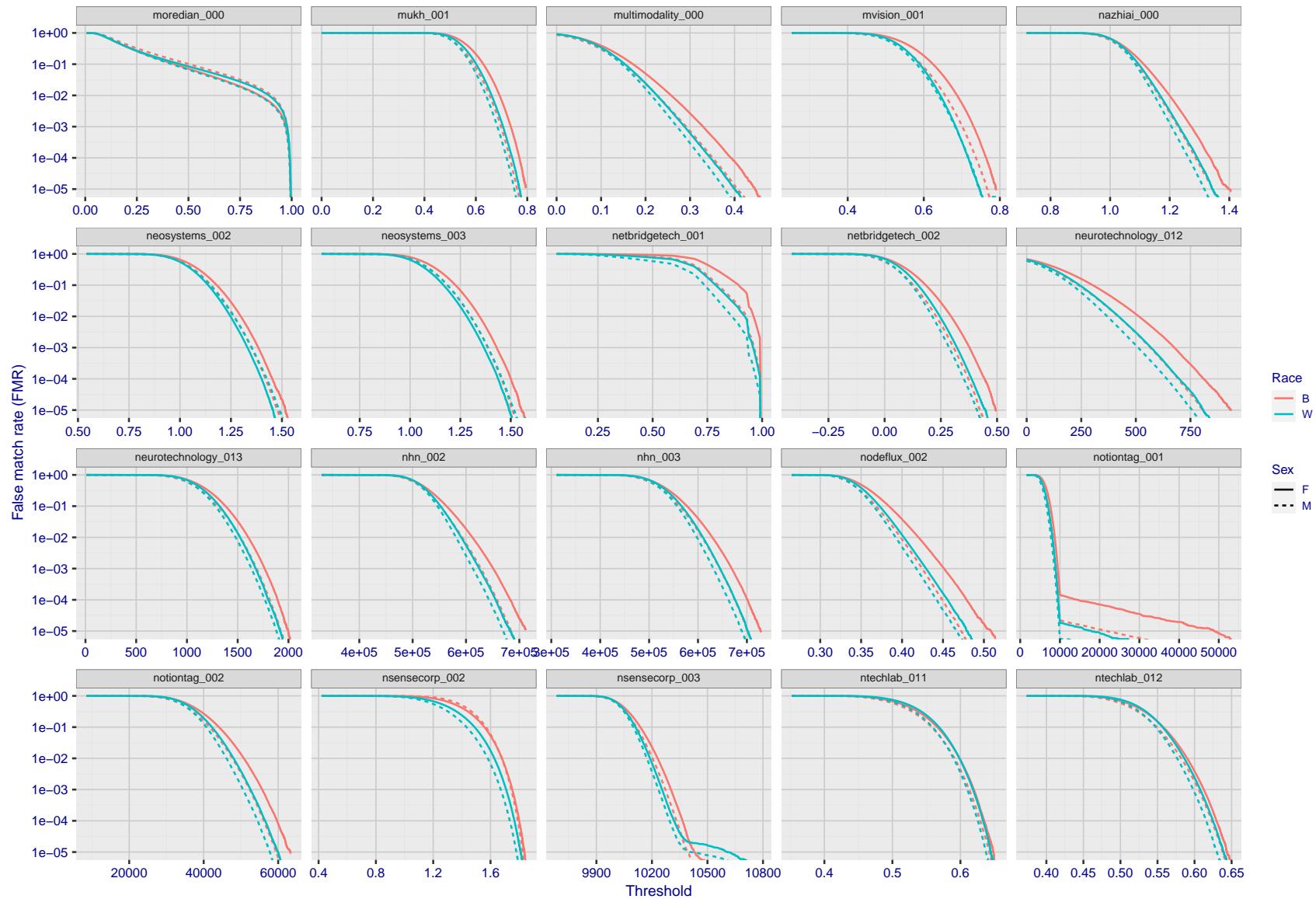


Figure 191: For the mugshot images, the false match calibration curves show false match rate vs. threshold. Separate curves appear for white females, black females, black males and white males.

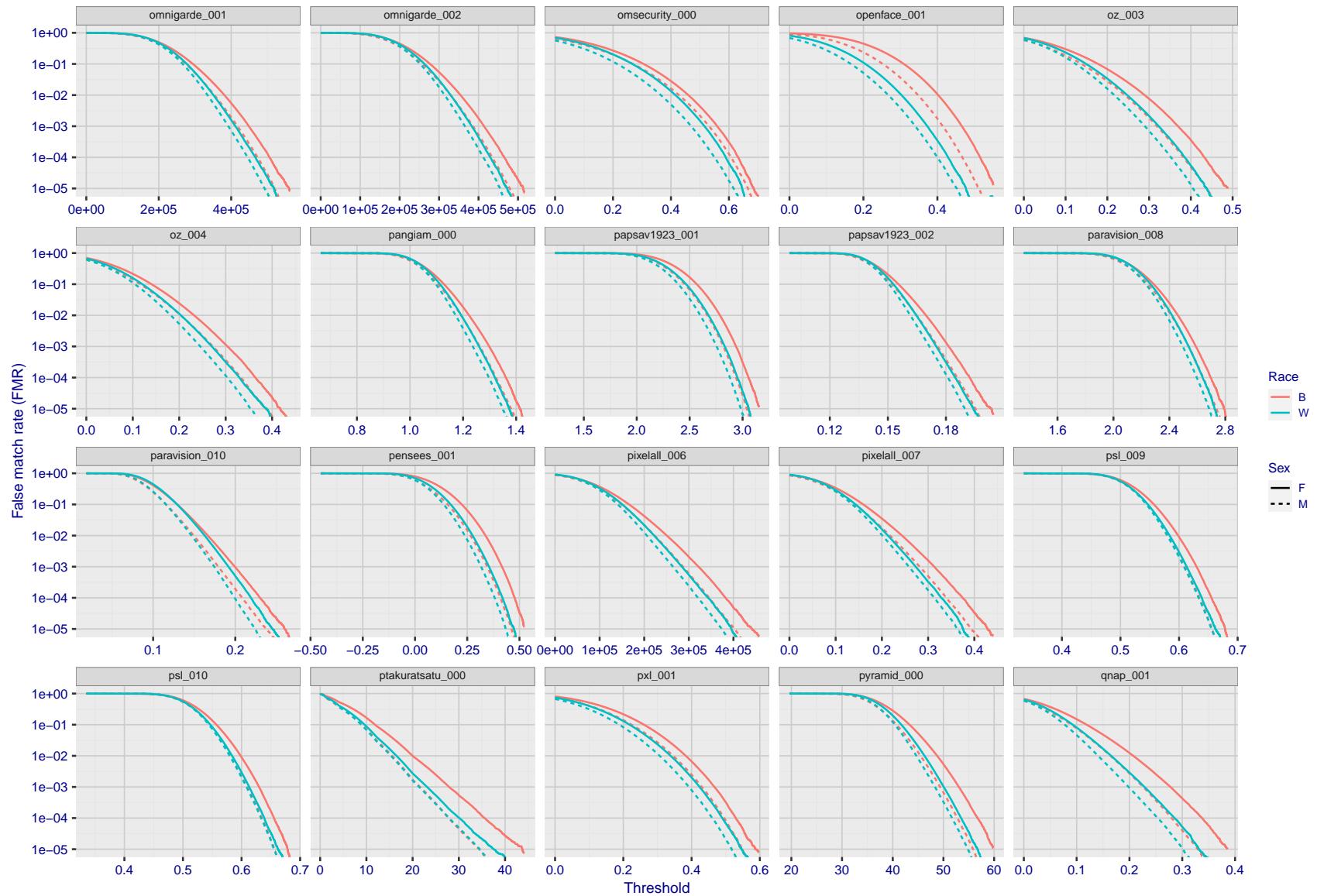


Figure 192: For the mugshot images, the false match calibration curves show false match rate vs. threshold. Separate curves appear for white females, black females, black males and white males.

2022/05/06 07:45:52

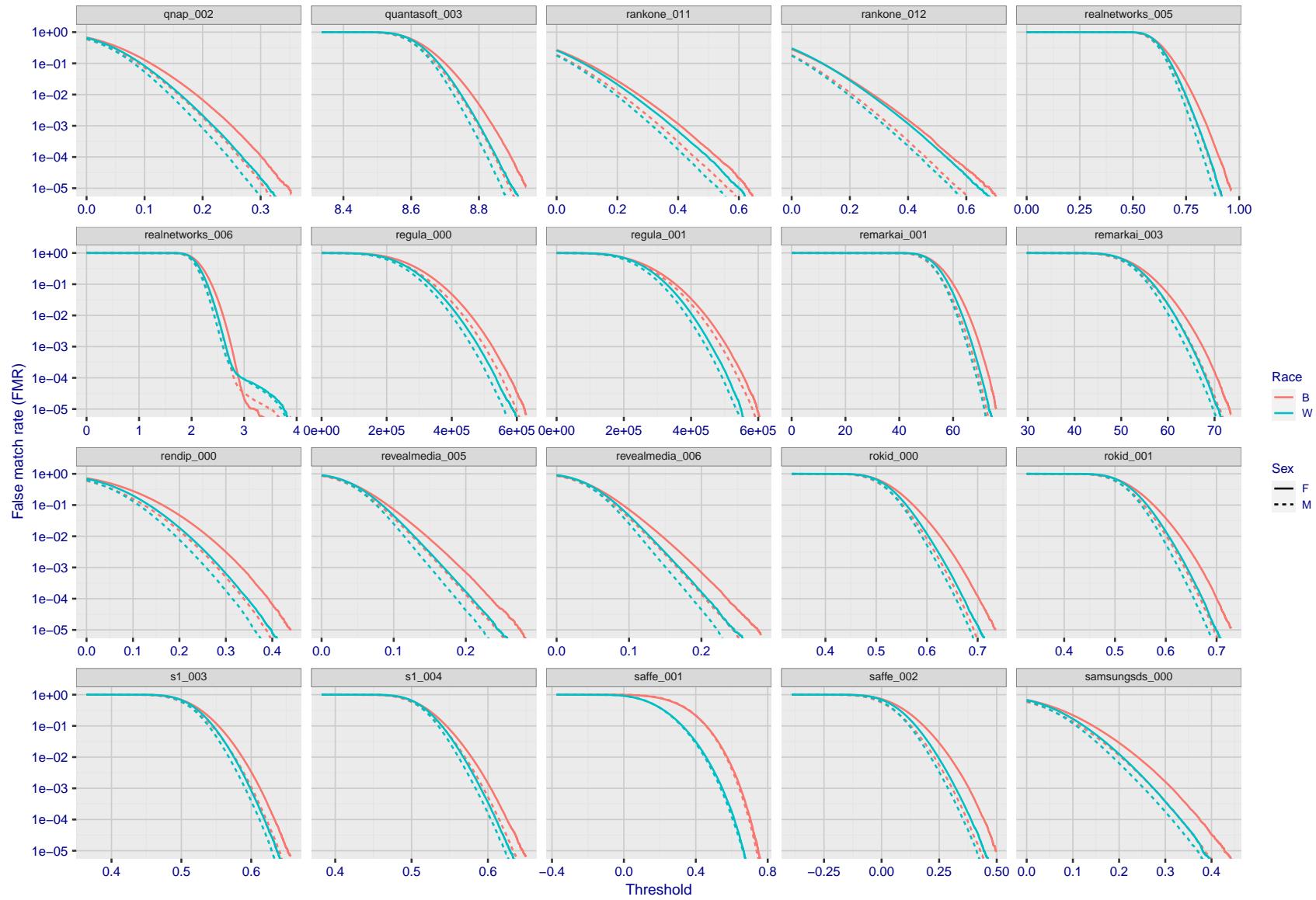


Figure 193: For the mugshot images, the false match calibration curves show false match rate vs. threshold. Separate curves appear for white females, black females, black males and white males.

2022/05/06 07:45:52

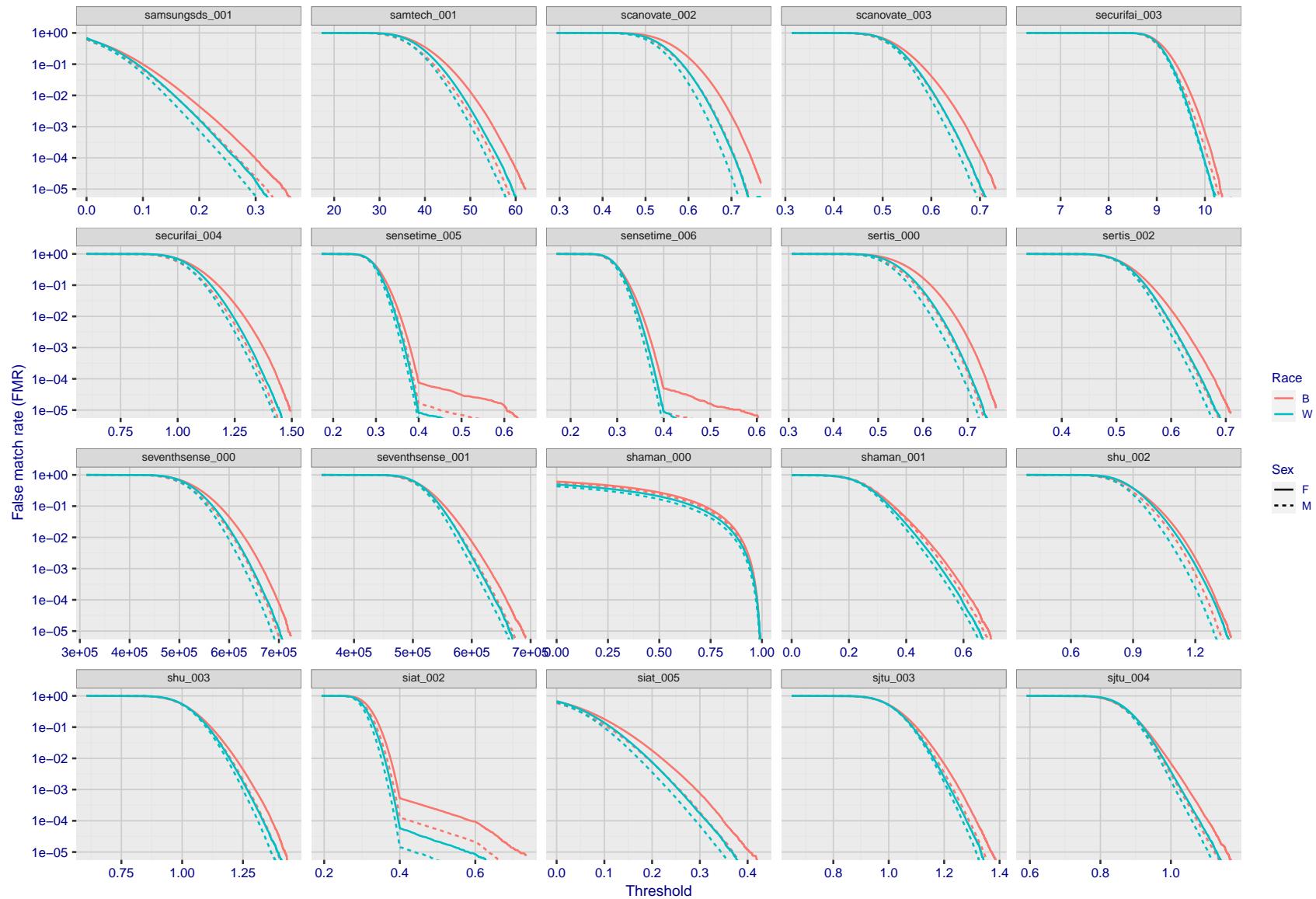


Figure 194: For the mugshot images, the false match calibration curves show false match rate vs. threshold. Separate curves appear for white females, black females, black males and white males.

2022/05/06 07:45:52

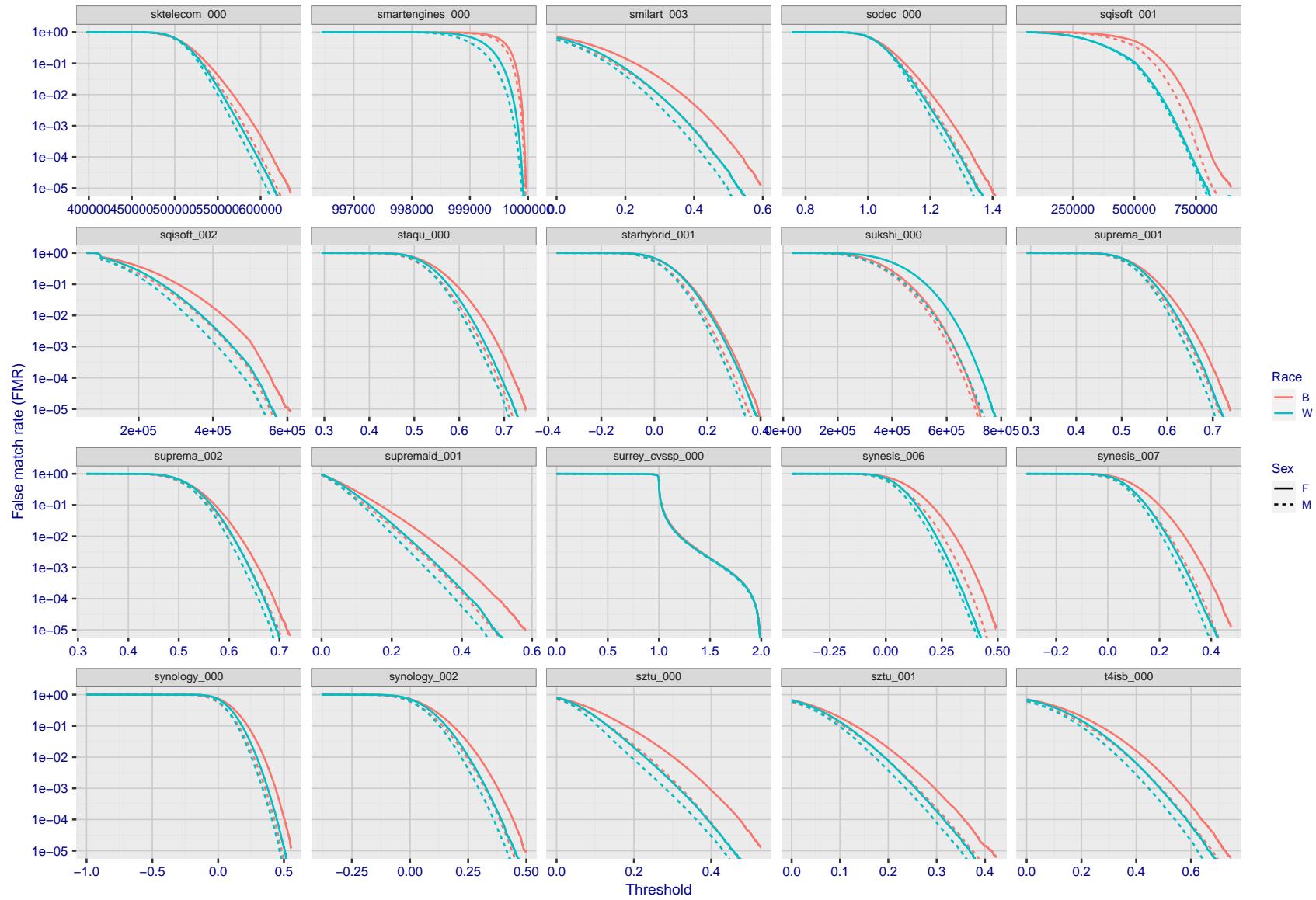


Figure 195: For the mugshot images, the false match calibration curves show false match rate vs. threshold. Separate curves appear for white females, black females, black males and white males.

2022/05/06 07:45:52

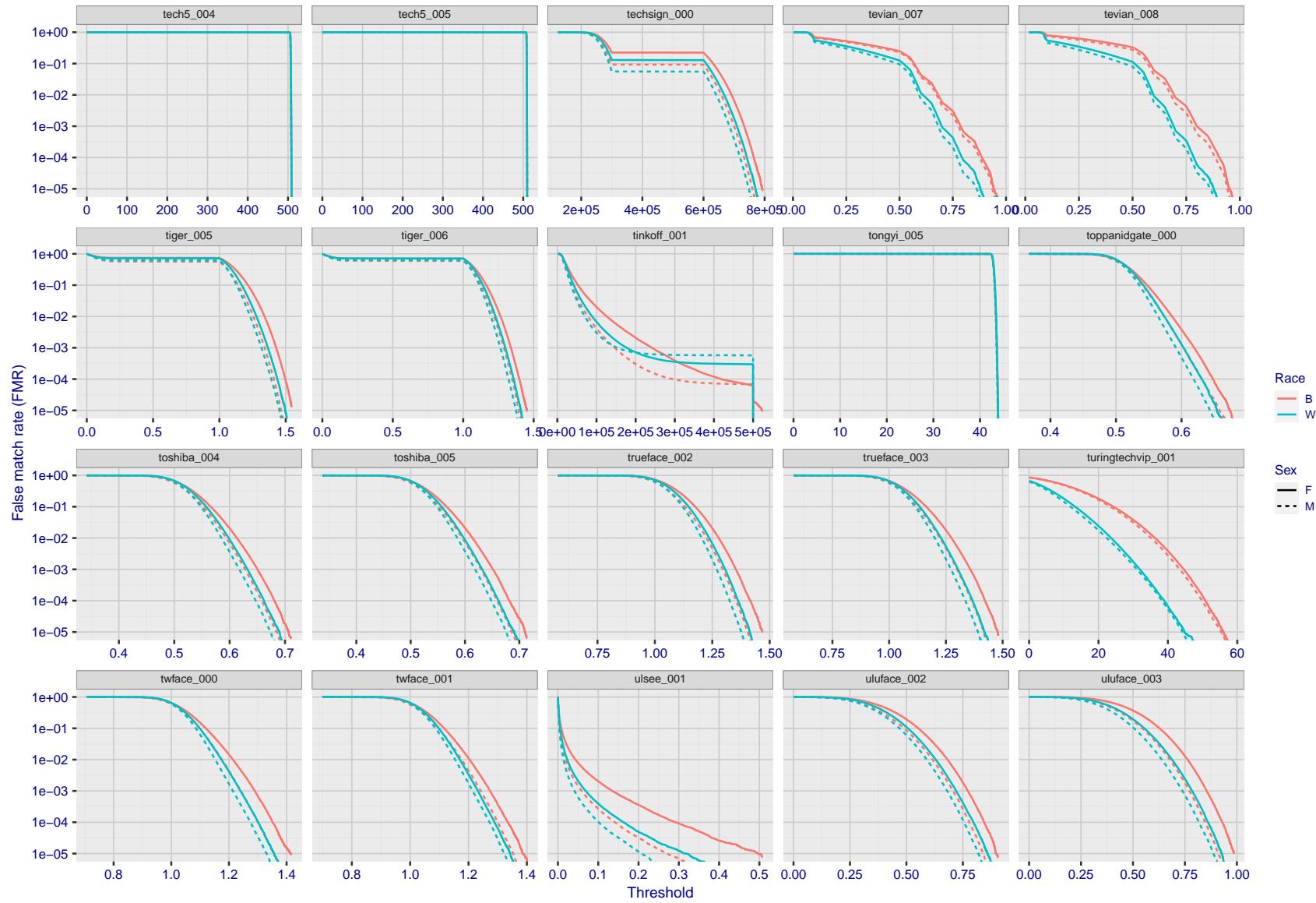


Figure 196: For the mugshot images, the false match calibration curves show false match rate vs. threshold. Separate curves appear for white females, black females, black males and white males.

2022/05/06 07:45:52

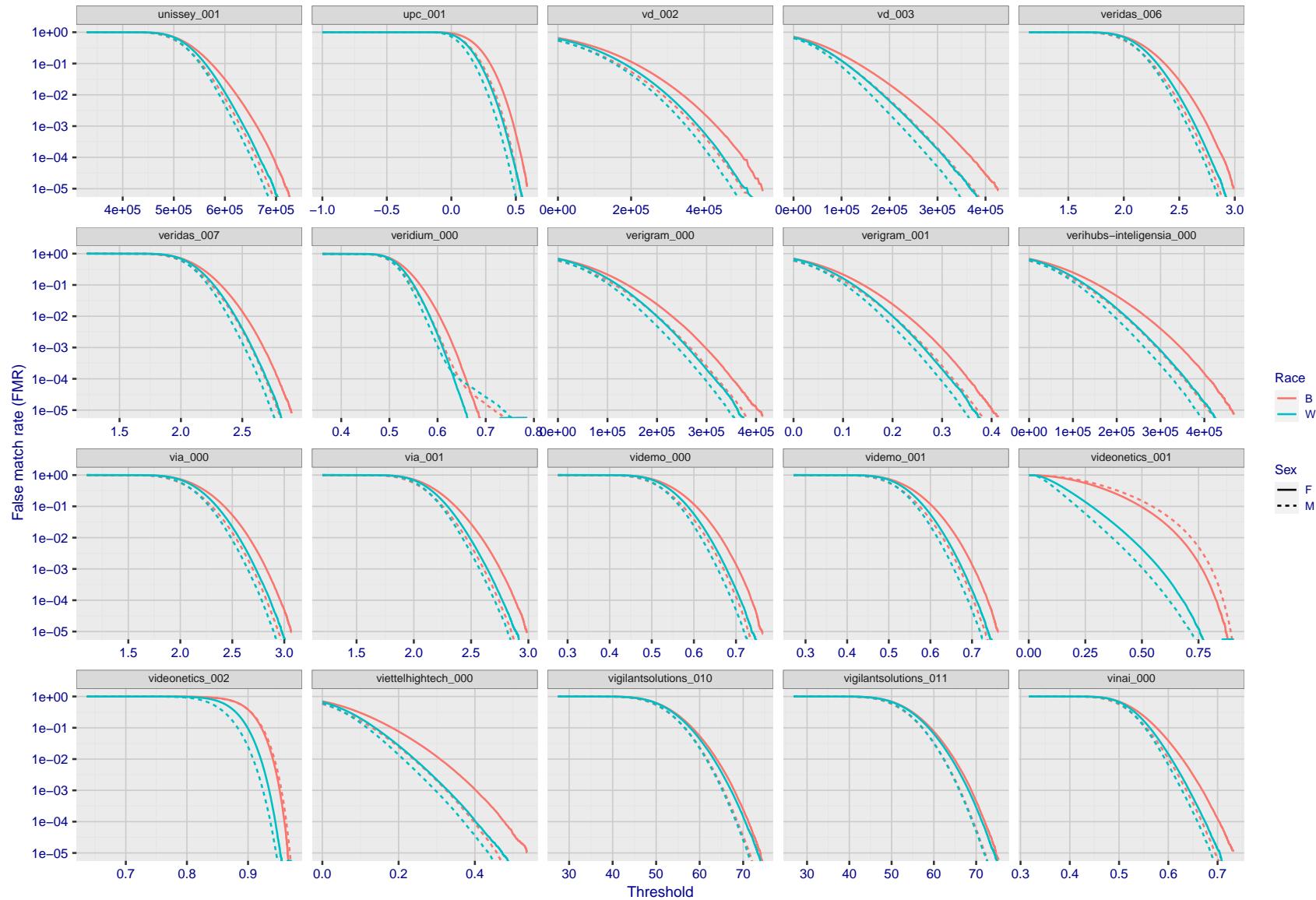


Figure 197: For the mugshot images, the false match calibration curves show false match rate vs. threshold. Separate curves appear for white females, black females, black males and white males.

2022/05/06 07:45:52

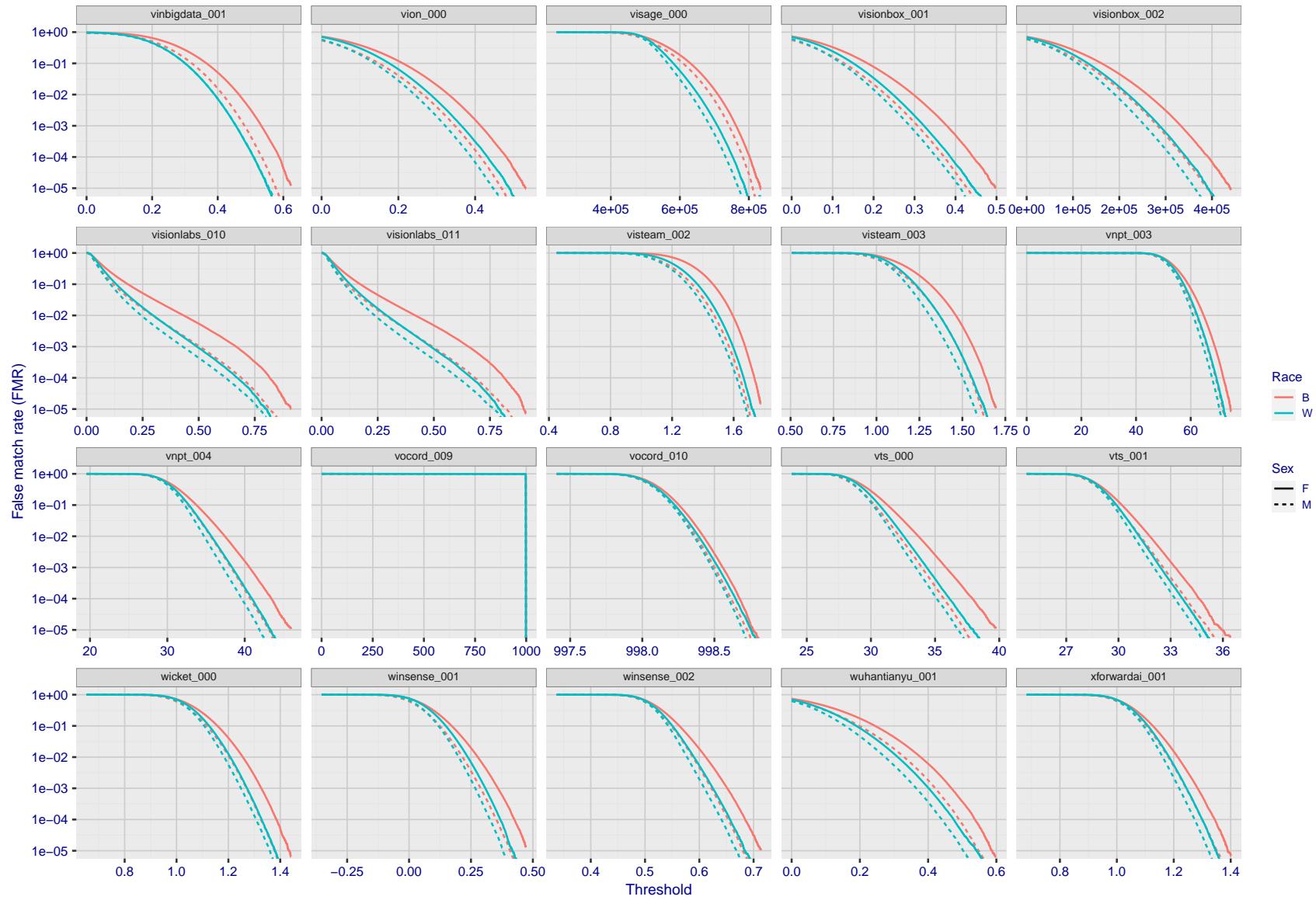


Figure 198: For the mugshot images, the false match calibration curves show false match rate vs. threshold. Separate curves appear for white females, black females, black males and white males.

2022/05/06 07:45:52

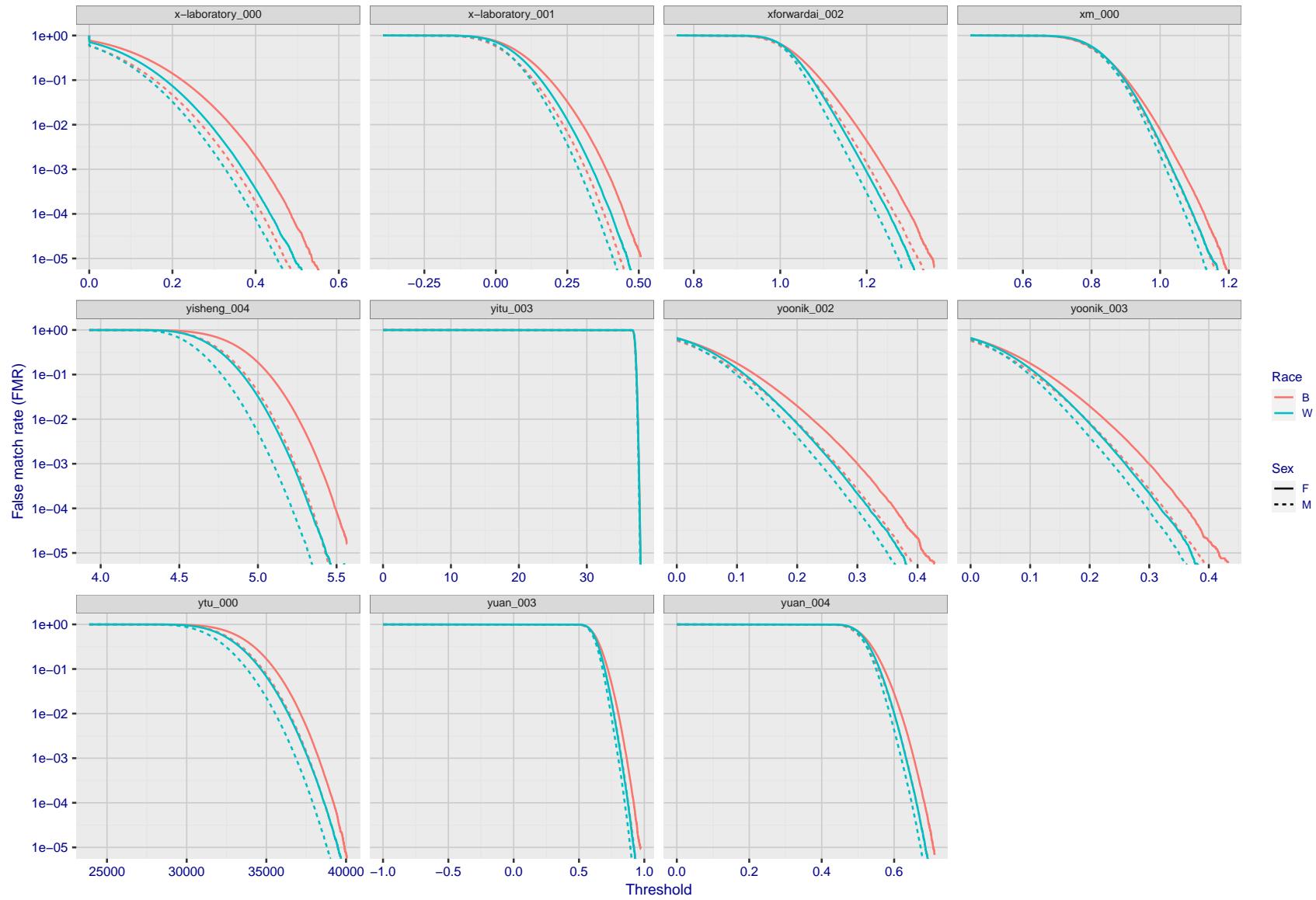


Figure 199: For the mugshot images, the false match calibration curves show false match rate vs. threshold. Separate curves appear for white females, black females, black males and white males.

FNMR(T)

"False non-match rate"

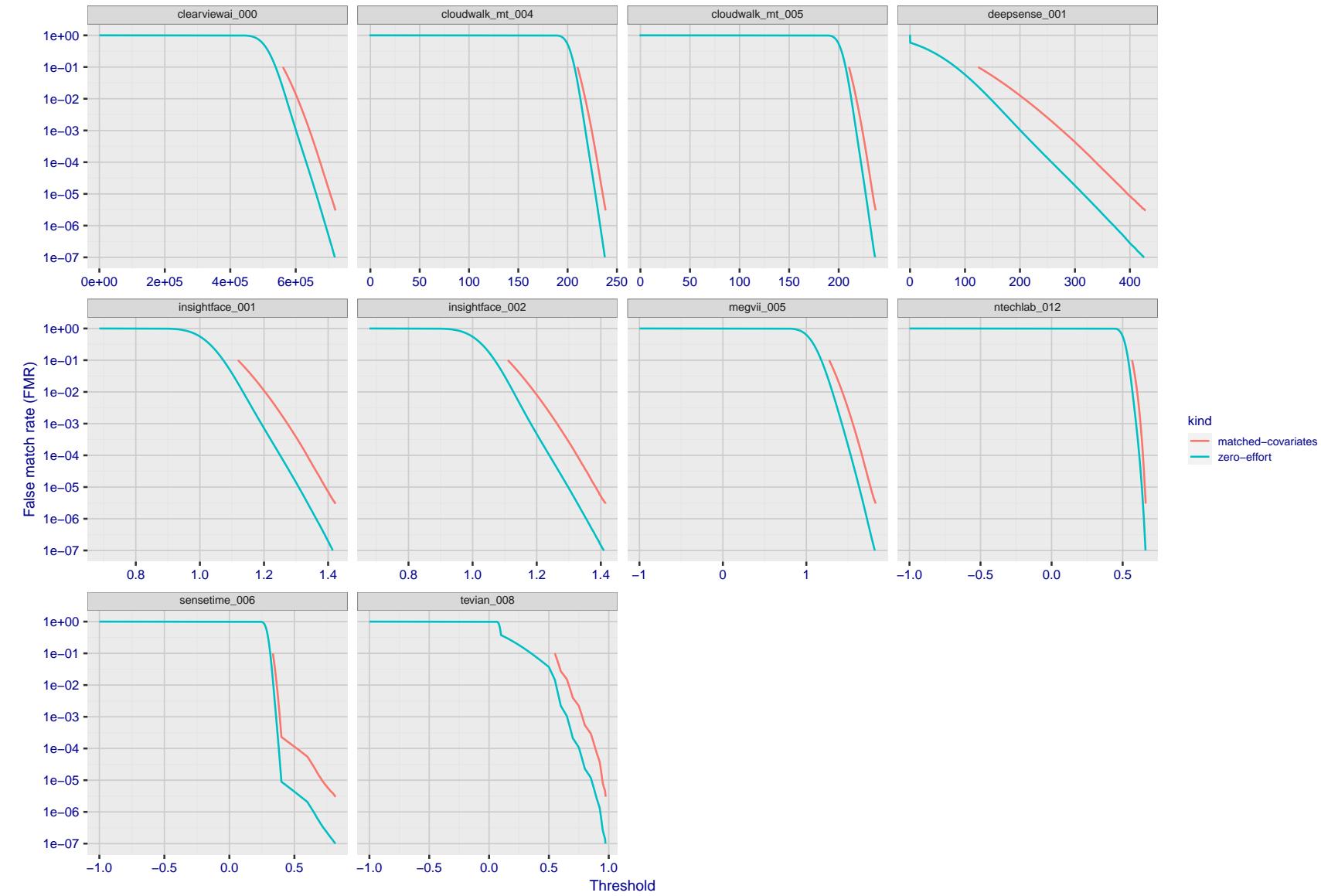


Figure 200: For the visa images, the false match calibration curves show FMR vs. threshold,  $T$ . The blue (lower) curves are for zero-effort impostors (i.e. comparing all images against all). The red (upper) curves are for persons of the same-sex, same-age, and same national-origin. This shows that FMR is underestimated (by a factor of 10 or more) by using a zero-effort impostor calculation to calibrate  $T$ . As shown later (sec. 3.6), FMR is higher for demographic-matched impostors.

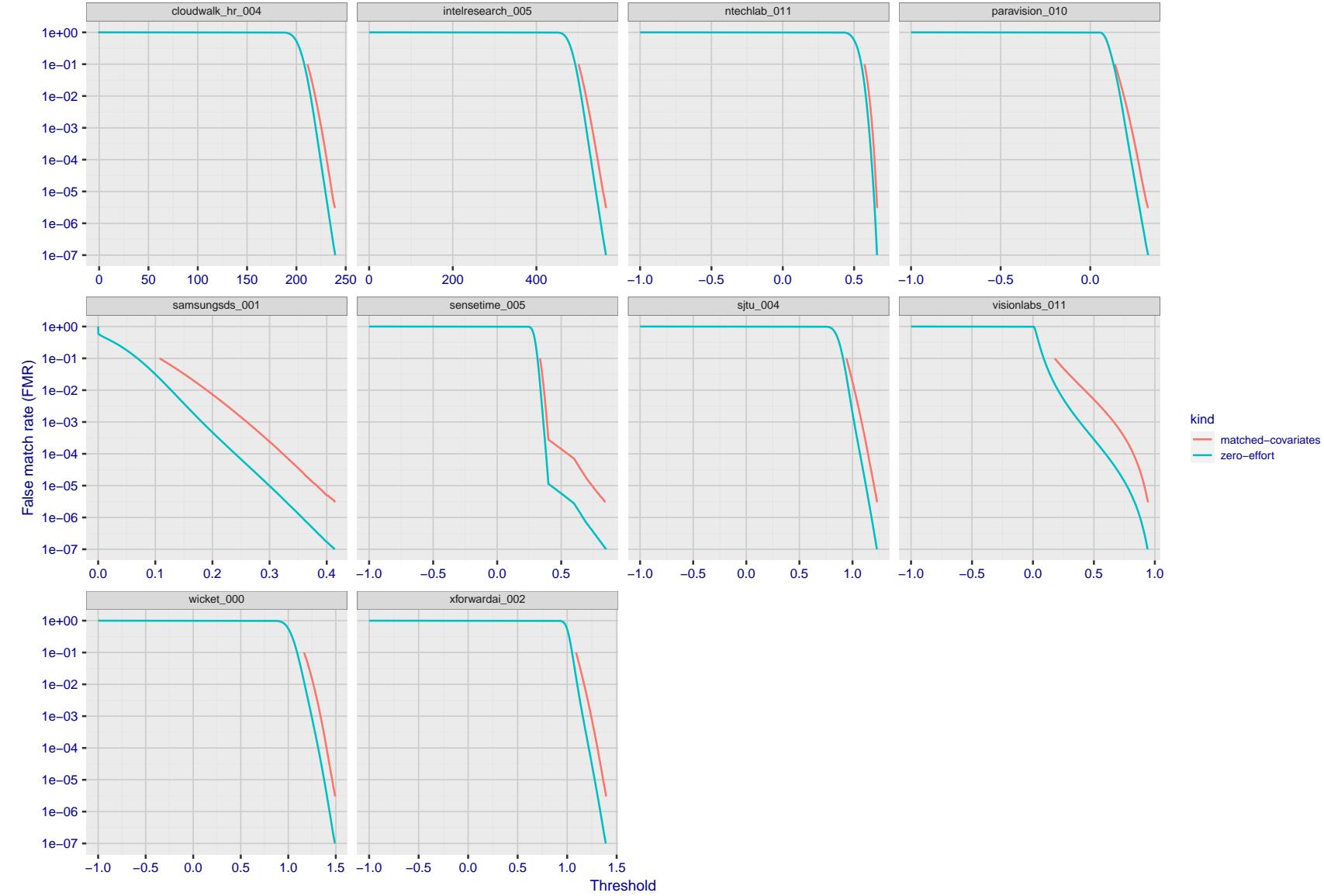


Figure 201: For the visa images, the false match calibration curves show FMR vs. threshold,  $T$ . The blue (lower) curves are for zero-effort impostors (i.e. comparing all images against all). The red (upper) curves are for persons of the same-sex, same-age, and same national-origin. This shows that FMR is underestimated (by a factor of 10 or more) by using a zero-effort impostor calculation to calibrate  $T$ . As shown later (sec. 3.6), FMR is higher for demographic-matched impostors.

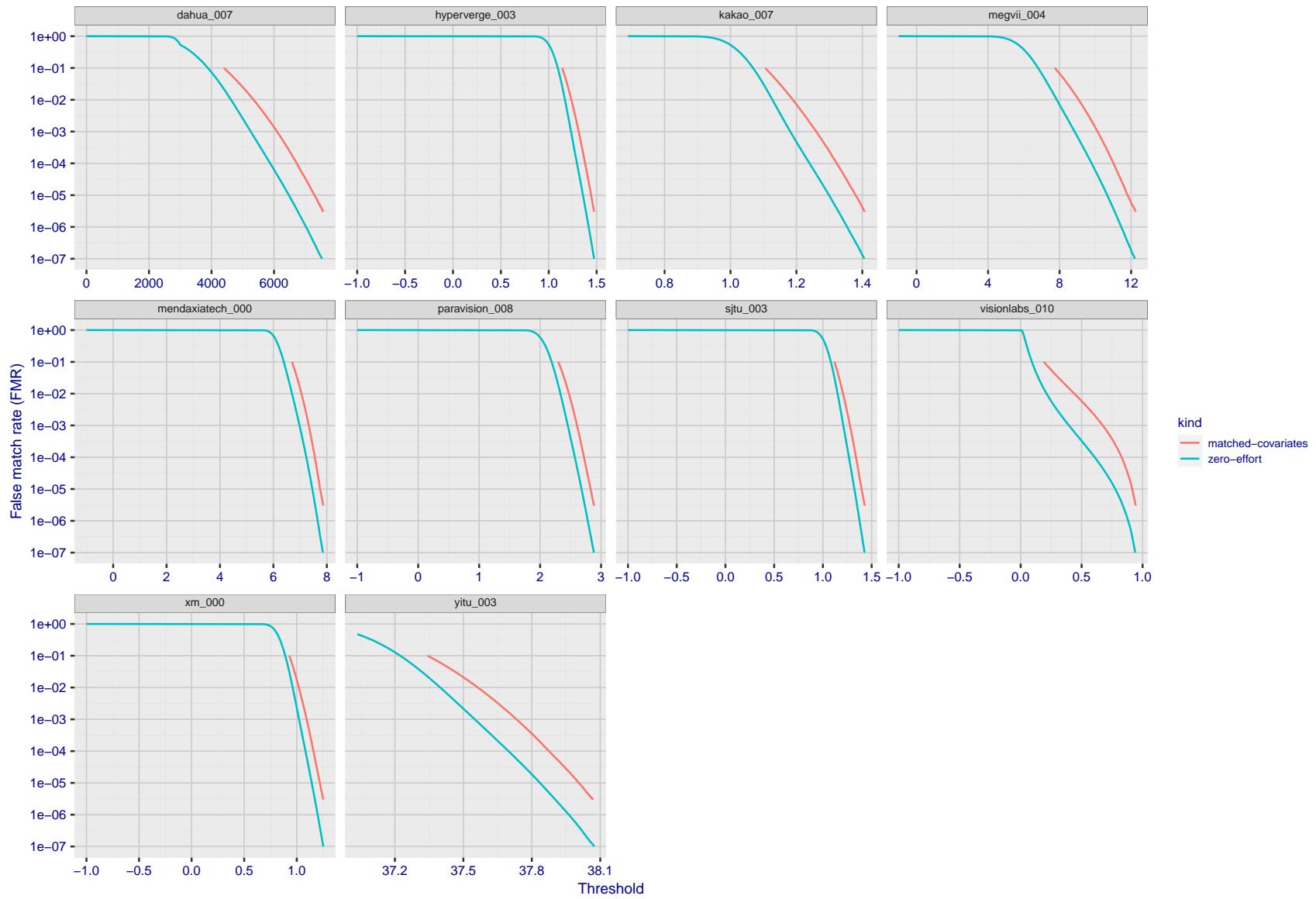


Figure 202: For the visa images, the false match calibration curves show FMR vs. threshold,  $T$ . The blue (lower) curves are for zero-effort impostors (i.e. comparing all images against all). The red (upper) curves are for persons of the same-sex, same-age, and same national-origin. This shows that FMR is underestimated (by a factor of 10 or more) by using a zero-effort impostor calculation to calibrate  $T$ . As shown later (sec. 3.6), FMR is higher for demographic-matched impostors.

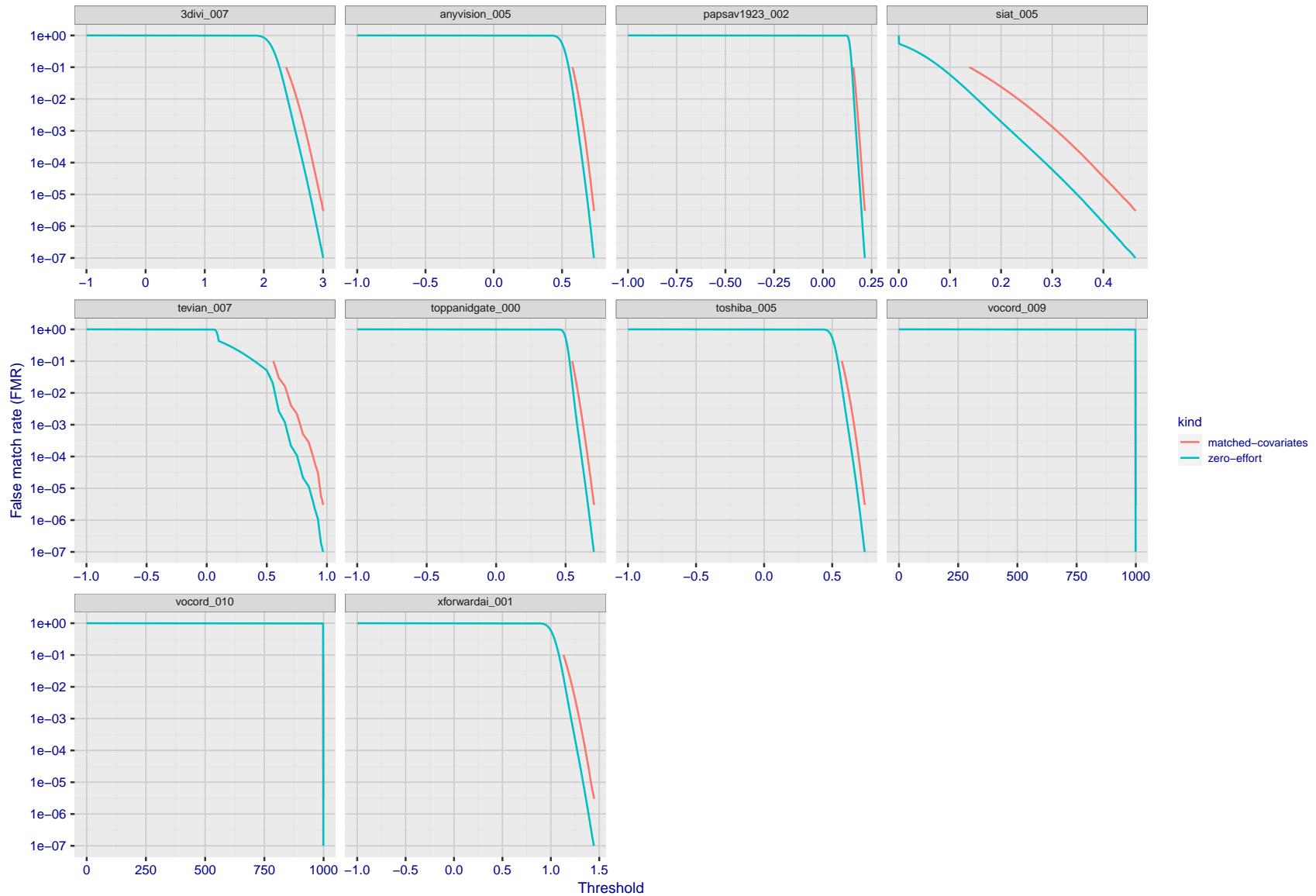


Figure 203: For the visa images, the false match calibration curves show FMR vs. threshold,  $T$ . The blue (lower) curves are for zero-effort impostors (i.e. comparing all images against all). The red (upper) curves are for persons of the same-sex, same-age, and same national-origin. This shows that FMR is underestimated (by a factor of 10 or more) by using a zero-effort impostor calculation to calibrate  $T$ . As shown later (sec. 3.6), FMR is higher for demographic-matched impostors.

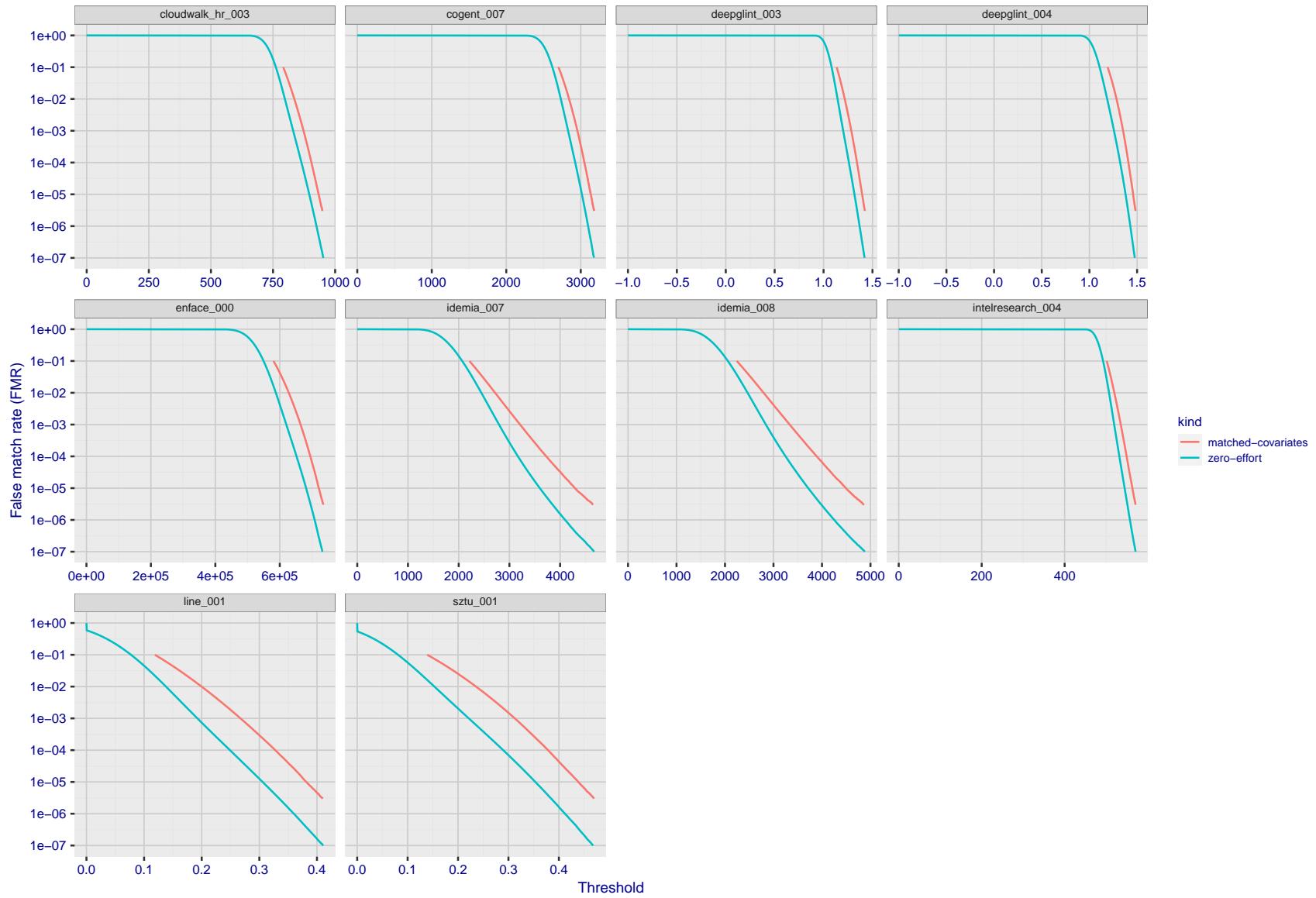


Figure 204: For the visa images, the false match calibration curves show FMR vs. threshold,  $T$ . The blue (lower) curves are for zero-effort impostors (i.e. comparing all images against all). The red (upper) curves are for persons of the same-sex, same-age, and same national-origin. This shows that FMR is underestimated (by a factor of 10 or more) by using a zero-effort impostor calculation to calibrate  $T$ . As shown later (sec. 3.6), FMR is higher for demographic-matched impostors.

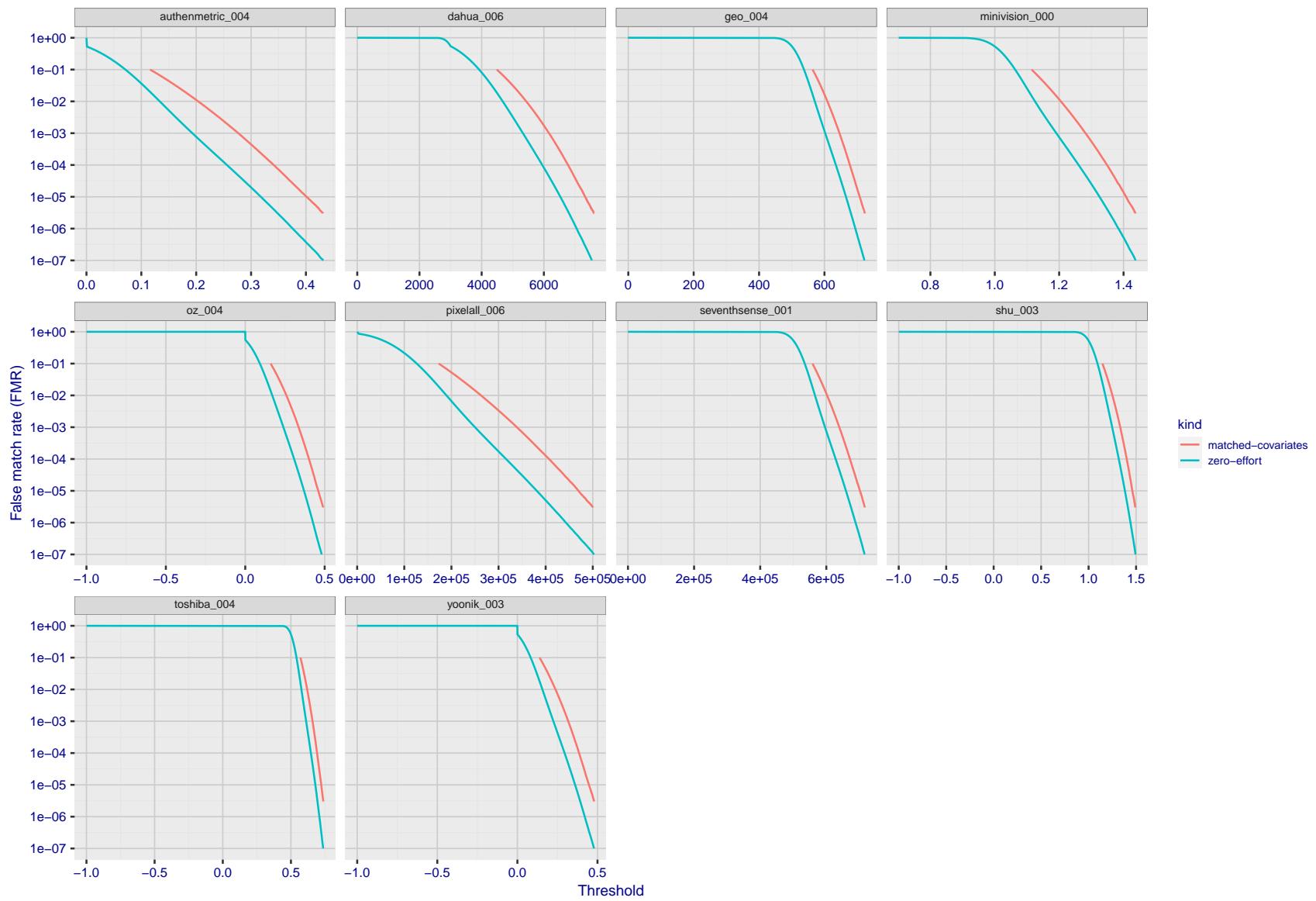


Figure 205: For the visa images, the false match calibration curves show FMR vs. threshold,  $T$ . The blue (lower) curves are for zero-effort impostors (i.e. comparing all images against all). The red (upper) curves are for persons of the same-sex, same-age, and same national-origin. This shows that FMR is underestimated (by a factor of 10 or more) by using a zero-effort impostor calculation to calibrate  $T$ . As shown later (sec. 3.6), FMR is higher for demographic-matched impostors.

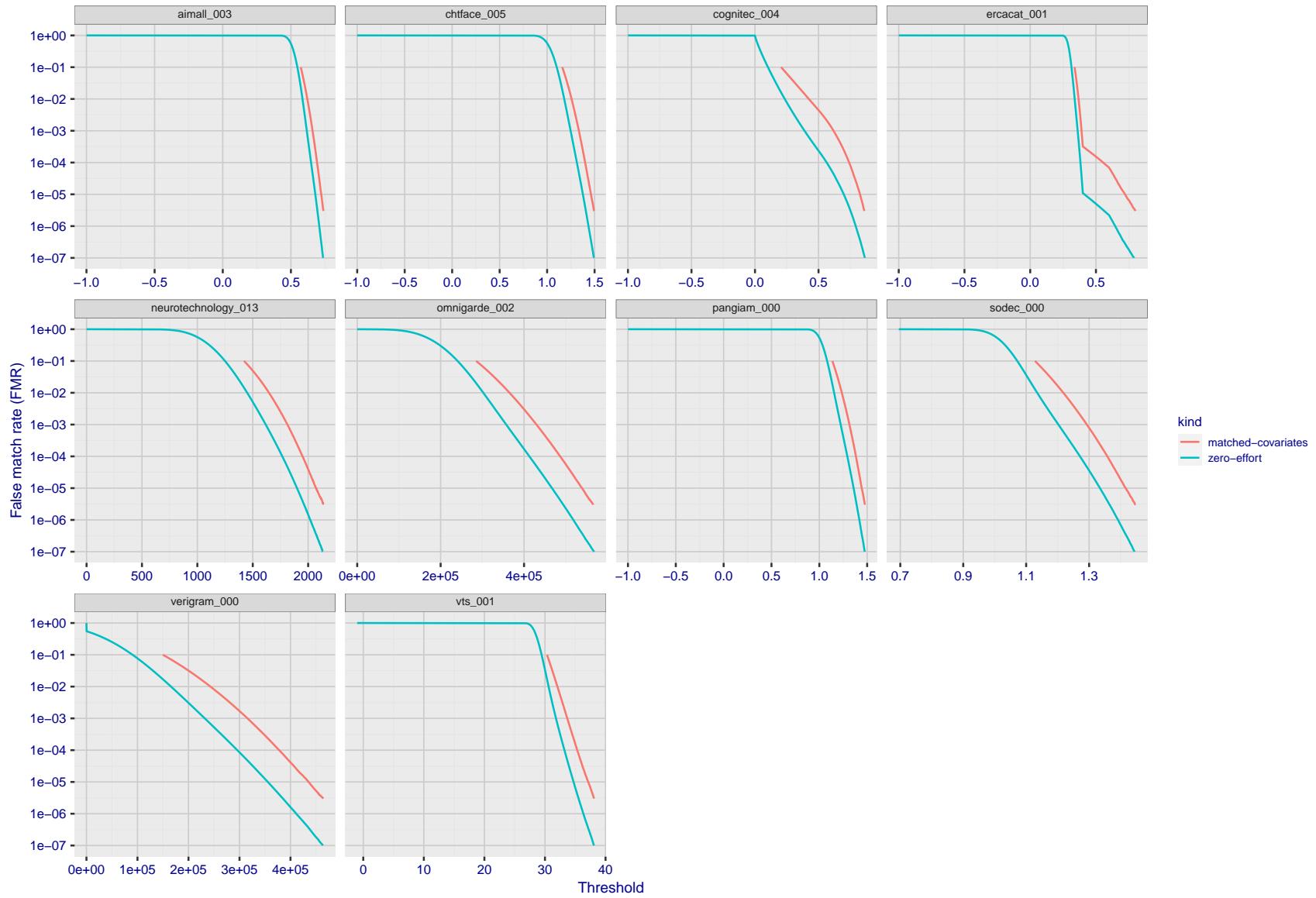


Figure 206: For the visa images, the false match calibration curves show FMR vs. threshold,  $T$ . The blue (lower) curves are for zero-effort impostors (i.e. comparing all images against all). The red (upper) curves are for persons of the same-sex, same-age, and same national-origin. This shows that FMR is underestimated (by a factor of 10 or more) by using a zero-effort impostor calculation to calibrate  $T$ . As shown later (sec. 3.6), FMR is higher for demographic-matched impostors.

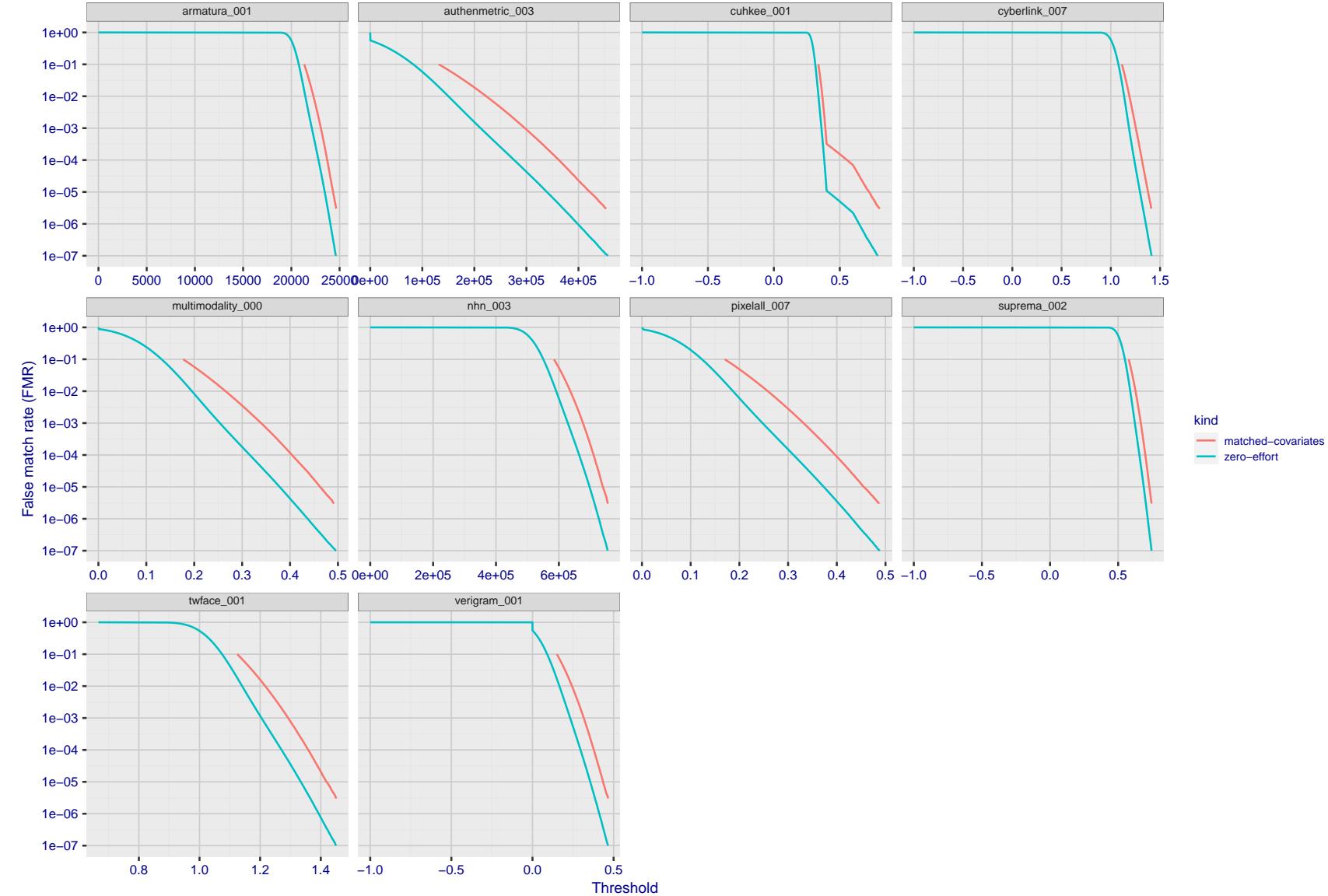


Figure 207: For the visa images, the false match calibration curves show FMR vs. threshold,  $T$ . The blue (lower) curves are for zero-effort impostors (i.e. comparing all images against all). The red (upper) curves are for persons of the same-sex, same-age, and same national-origin. This shows that FMR is underestimated (by a factor of 10 or more) by using a zero-effort impostor calculation to calibrate  $T$ . As shown later (sec. 3.6), FMR is higher for demographic-matched impostors.

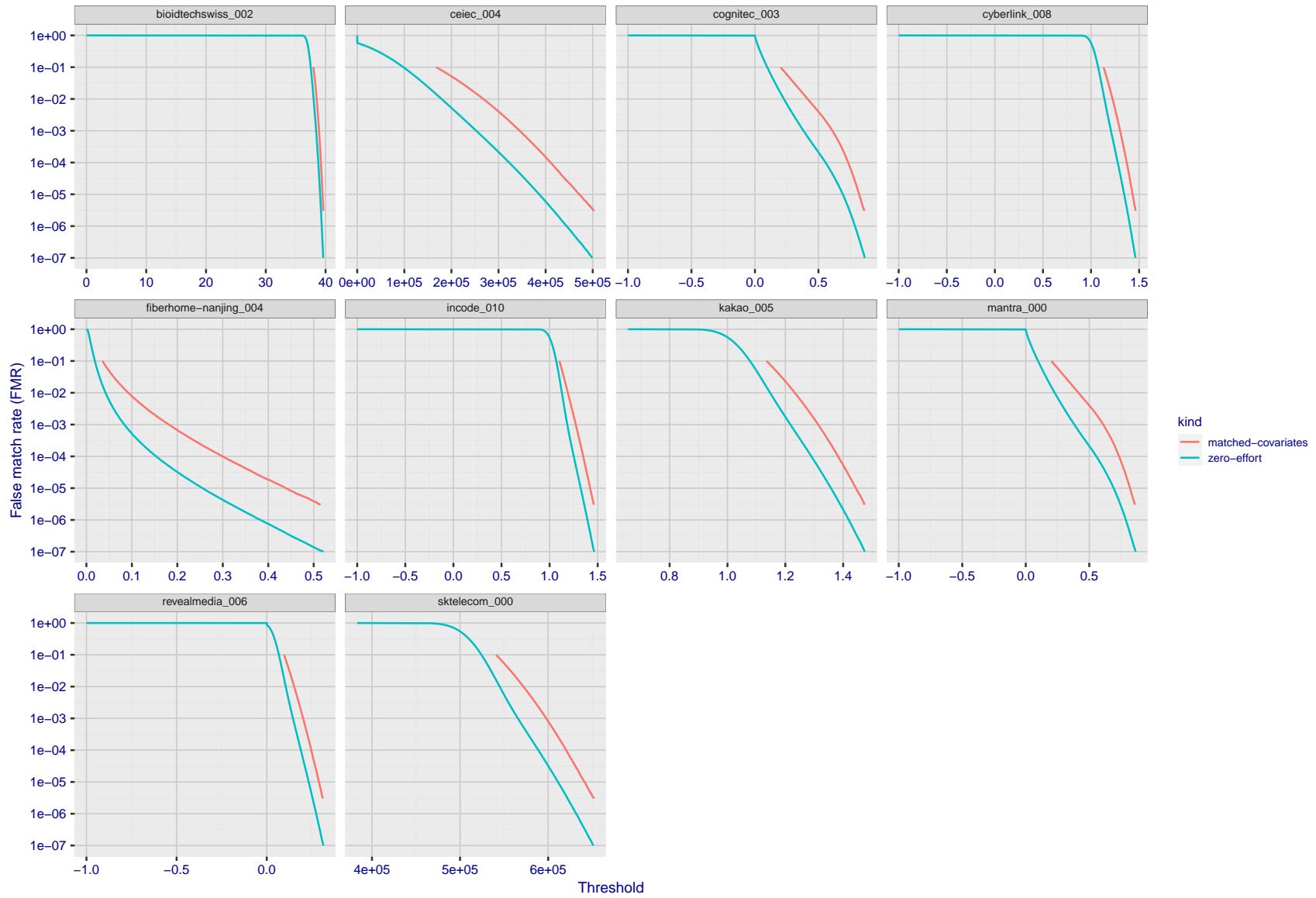


Figure 208: For the visa images, the false match calibration curves show FMR vs. threshold,  $T$ . The blue (lower) curves are for zero-effort impostors (i.e. comparing all images against all). The red (upper) curves are for persons of the same-sex, same-age, and same national-origin. This shows that FMR is underestimated (by a factor of 10 or more) by using a zero-effort impostor calculation to calibrate  $T$ . As shown later (sec. 3.6), FMR is higher for demographic-matched impostors.

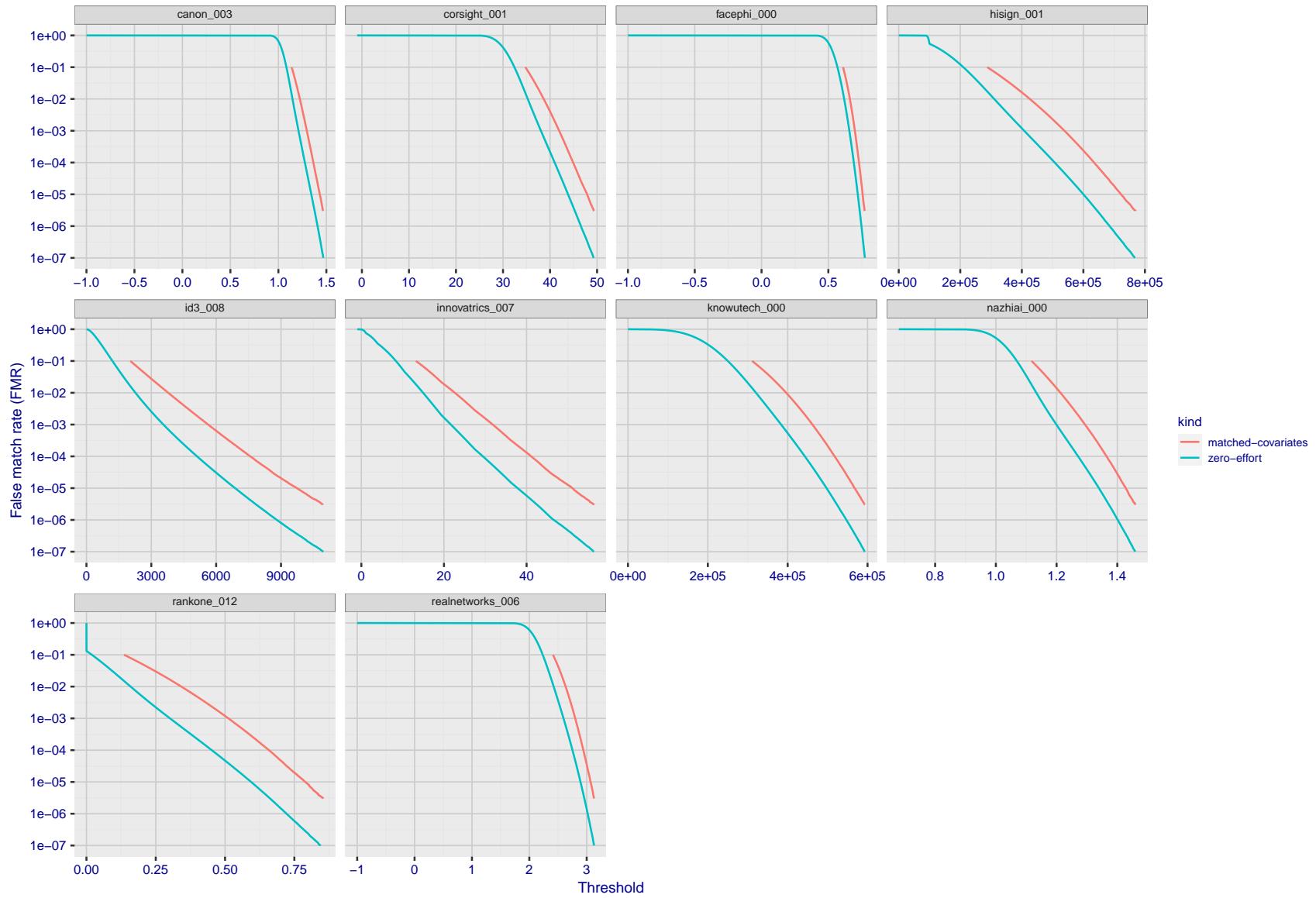


Figure 209: For the visa images, the false match calibration curves show FMR vs. threshold,  $T$ . The blue (lower) curves are for zero-effort impostors (i.e. comparing all images against all). The red (upper) curves are for persons of the same-sex, same-age, and same national-origin. This shows that FMR is underestimated (by a factor of 10 or more) by using a zero-effort impostor calculation to calibrate  $T$ . As shown later (sec. 3.6), FMR is higher for demographic-matched impostors.

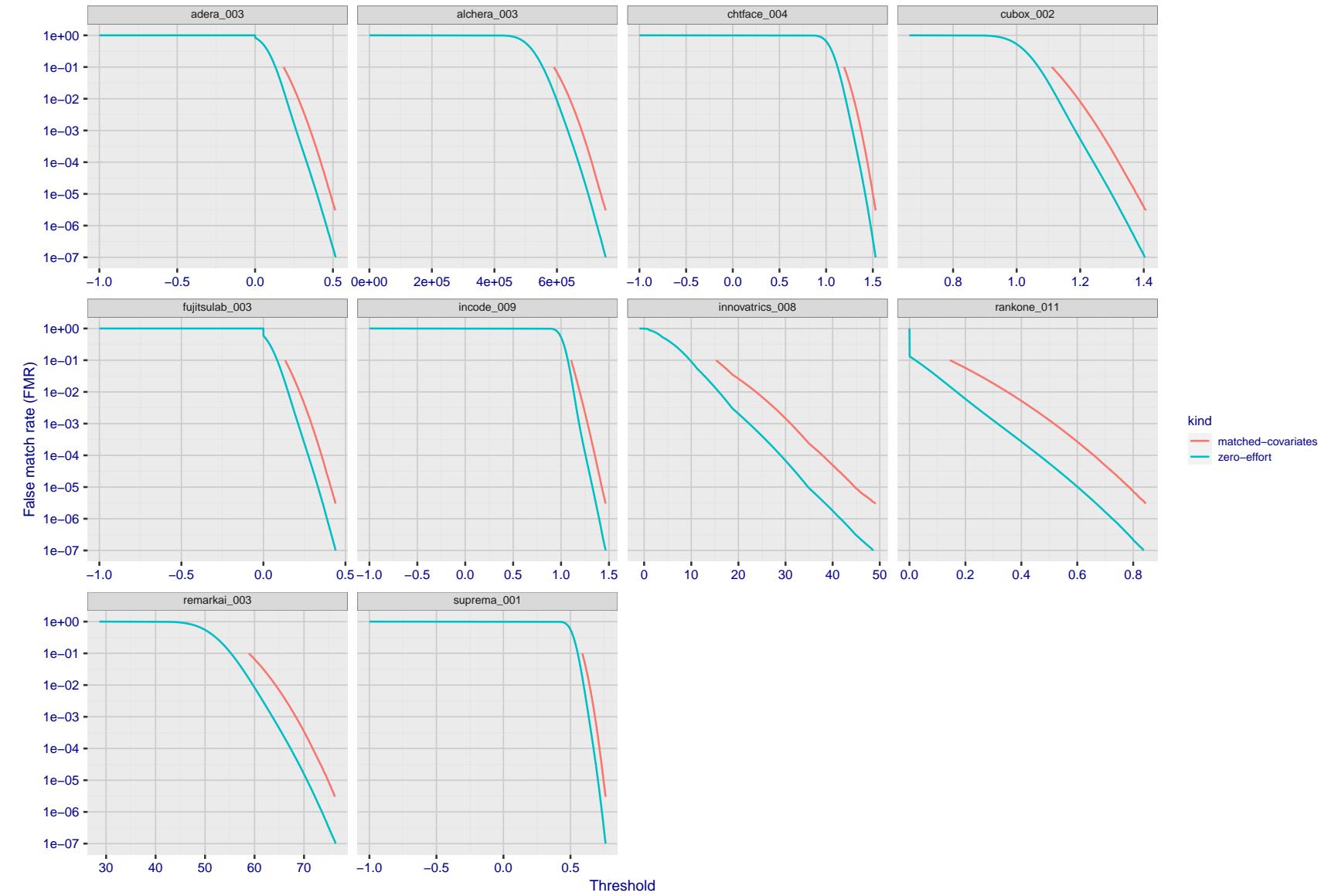


Figure 210: For the visa images, the false match calibration curves show FMR vs. threshold,  $T$ . The blue (lower) curves are for zero-effort impostors (i.e. comparing all images against all). The red (upper) curves are for persons of the same-sex, same-age, and same national-origin. This shows that FMR is underestimated (by a factor of 10 or more) by using a zero-effort impostor calculation to calibrate  $T$ . As shown later (sec. 3.6), FMR is higher for demographic-matched impostors.

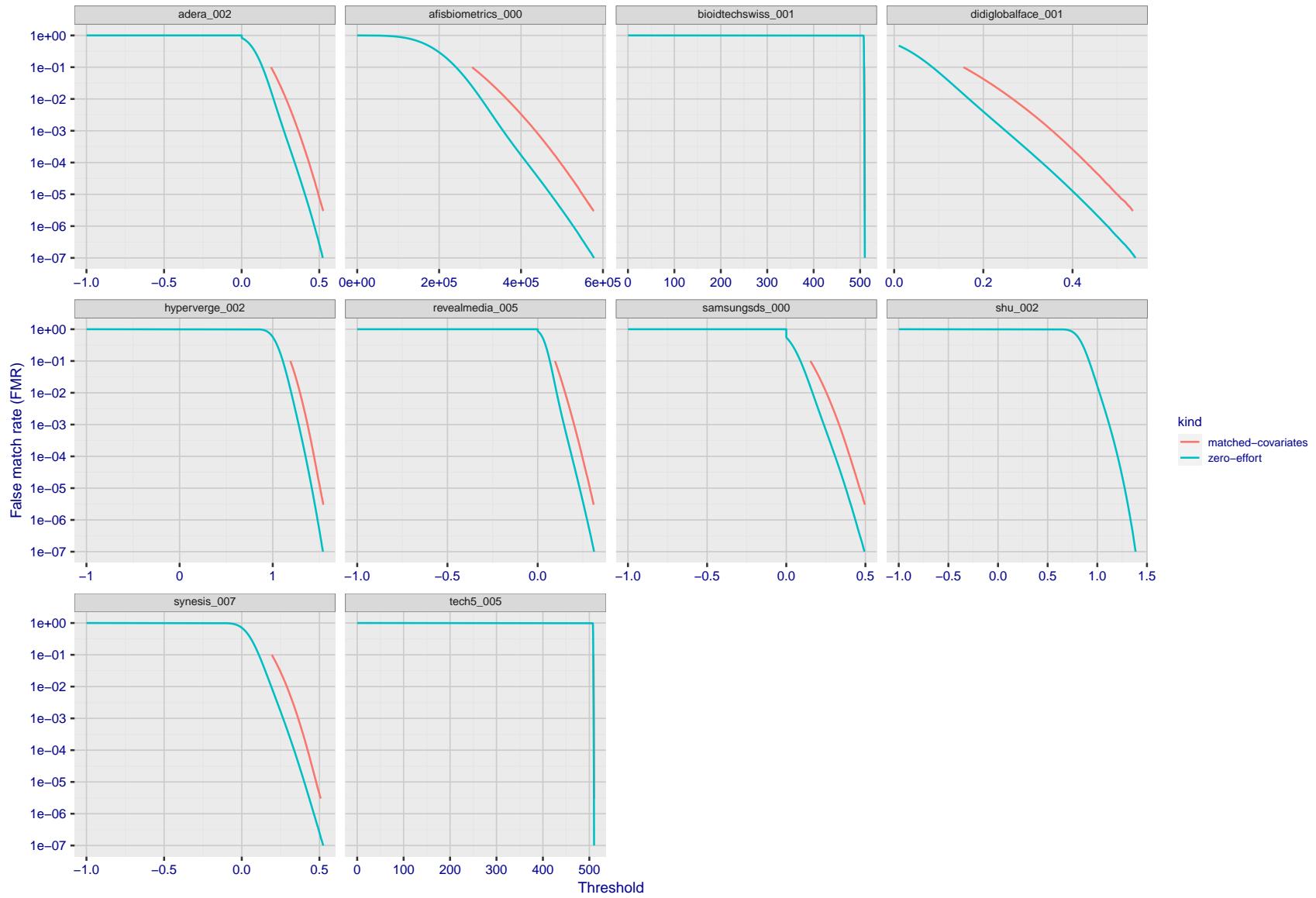


Figure 211: For the visa images, the false match calibration curves show FMR vs. threshold,  $T$ . The blue (lower) curves are for zero-effort impostors (i.e. comparing all images against all). The red (upper) curves are for persons of the same-sex, same-age, and same national-origin. This shows that FMR is underestimated (by a factor of 10 or more) by using a zero-effort impostor calculation to calibrate  $T$ . As shown later (sec. 3.6), FMR is higher for demographic-matched impostors.

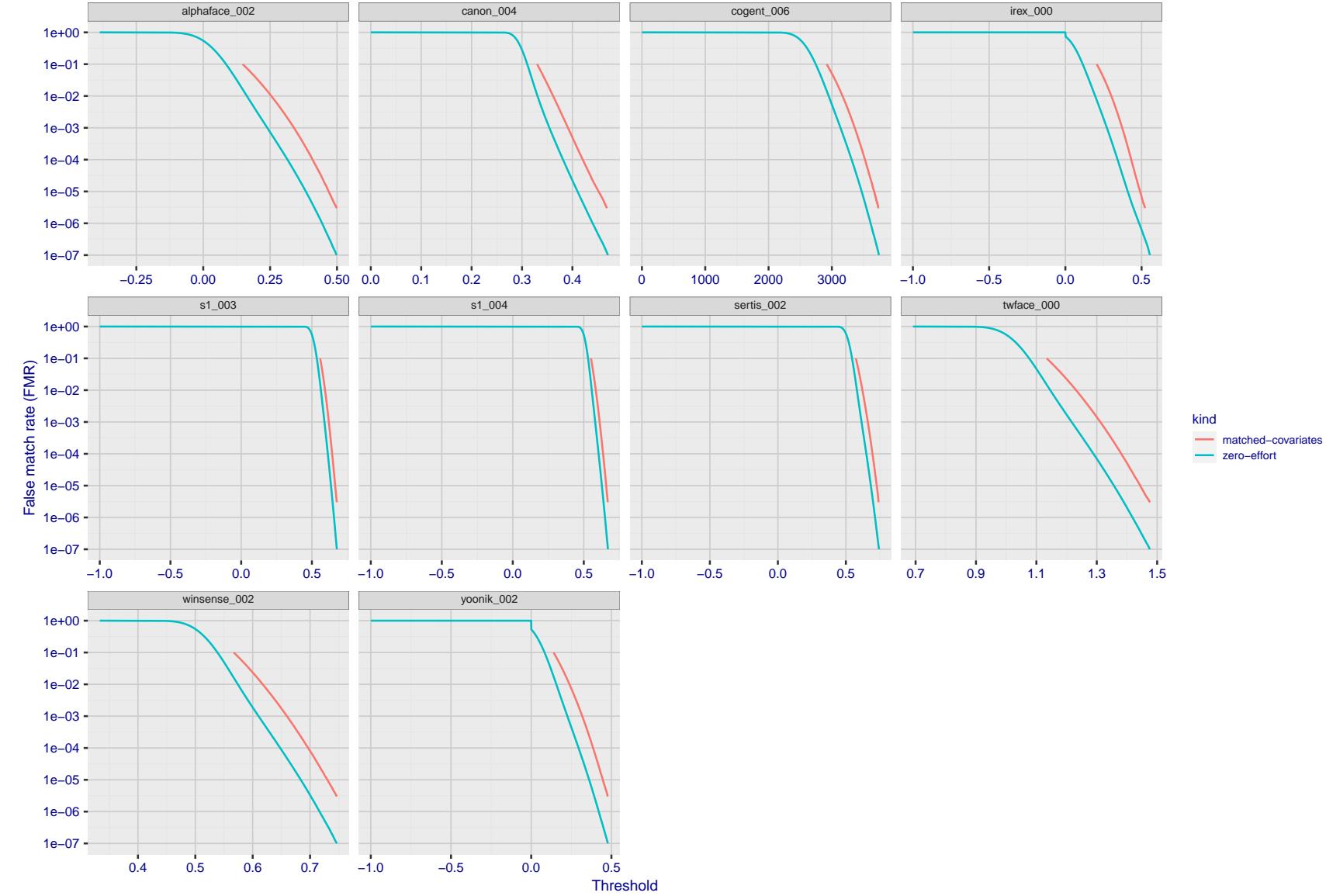


Figure 212: For the visa images, the false match calibration curves show FMR vs. threshold,  $T$ . The blue (lower) curves are for zero-effort impostors (i.e. comparing all images against all). The red (upper) curves are for persons of the same-sex, same-age, and same national-origin. This shows that FMR is underestimated (by a factor of 10 or more) by using a zero-effort impostor calculation to calibrate  $T$ . As shown later (sec. 3.6), FMR is higher for demographic-matched impostors.

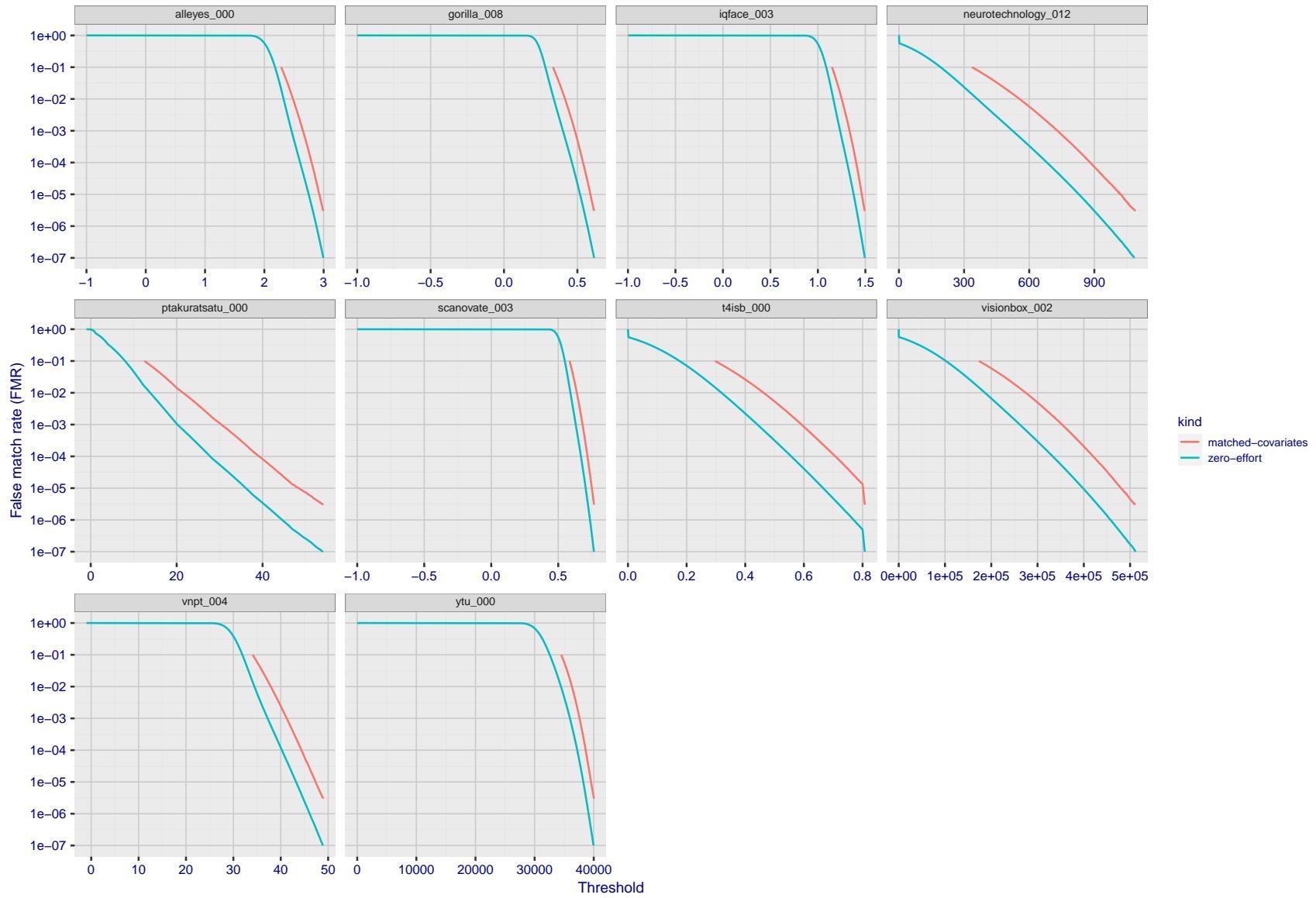


Figure 213: For the visa images, the false match calibration curves show FMR vs. threshold,  $T$ . The blue (lower) curves are for zero-effort impostors (i.e. comparing all images against all). The red (upper) curves are for persons of the same-sex, same-age, and same national-origin. This shows that FMR is underestimated (by a factor of 10 or more) by using a zero-effort impostor calculation to calibrate  $T$ . As shown later (sec. 3.6), FMR is higher for demographic-matched impostors.

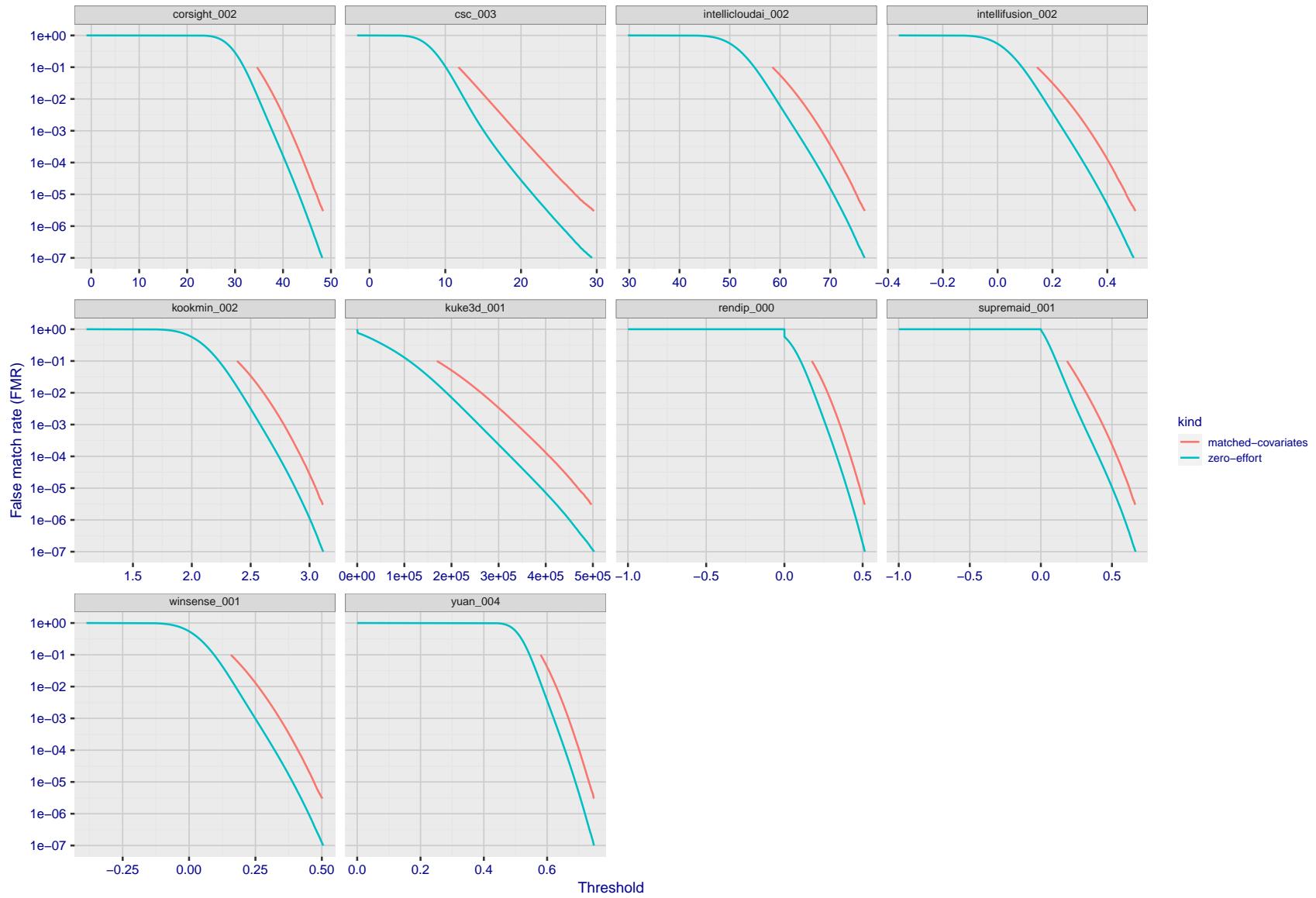


Figure 214: For the visa images, the false match calibration curves show FMR vs. threshold,  $T$ . The blue (lower) curves are for zero-effort impostors (i.e. comparing all images against all). The red (upper) curves are for persons of the same-sex, same-age, and same national-origin. This shows that FMR is underestimated (by a factor of 10 or more) by using a zero-effort impostor calculation to calibrate  $T$ . As shown later (sec. 3.6), FMR is higher for demographic-matched impostors.

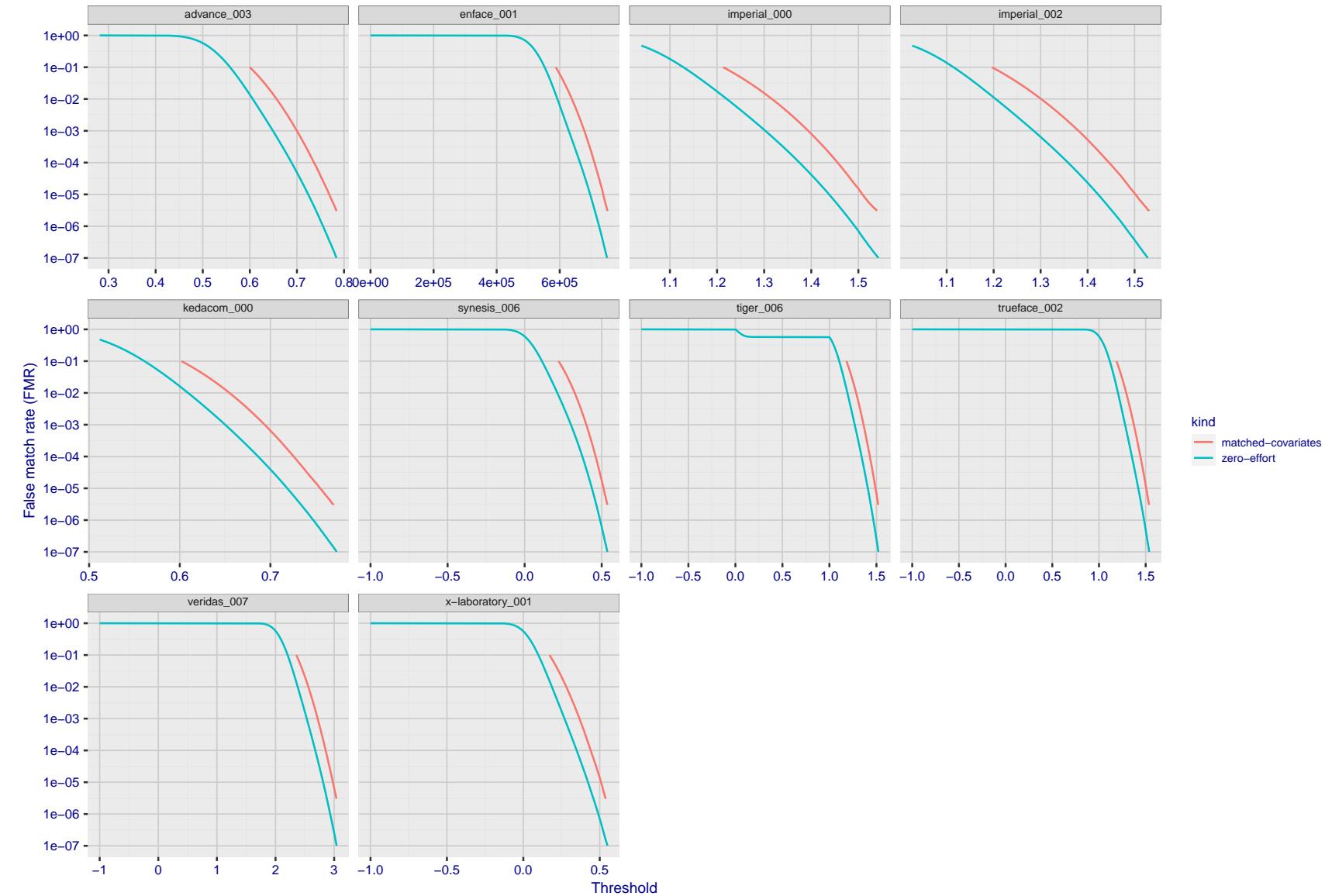


Figure 215: For the visa images, the false match calibration curves show FMR vs. threshold,  $T$ . The blue (lower) curves are for zero-effort impostors (i.e. comparing all images against all). The red (upper) curves are for persons of the same-sex, same-age, and same national-origin. This shows that FMR is underestimated (by a factor of 10 or more) by using a zero-effort impostor calculation to calibrate  $T$ . As shown later (sec. 3.6), FMR is higher for demographic-matched impostors.

2022/05/06 07:45:52

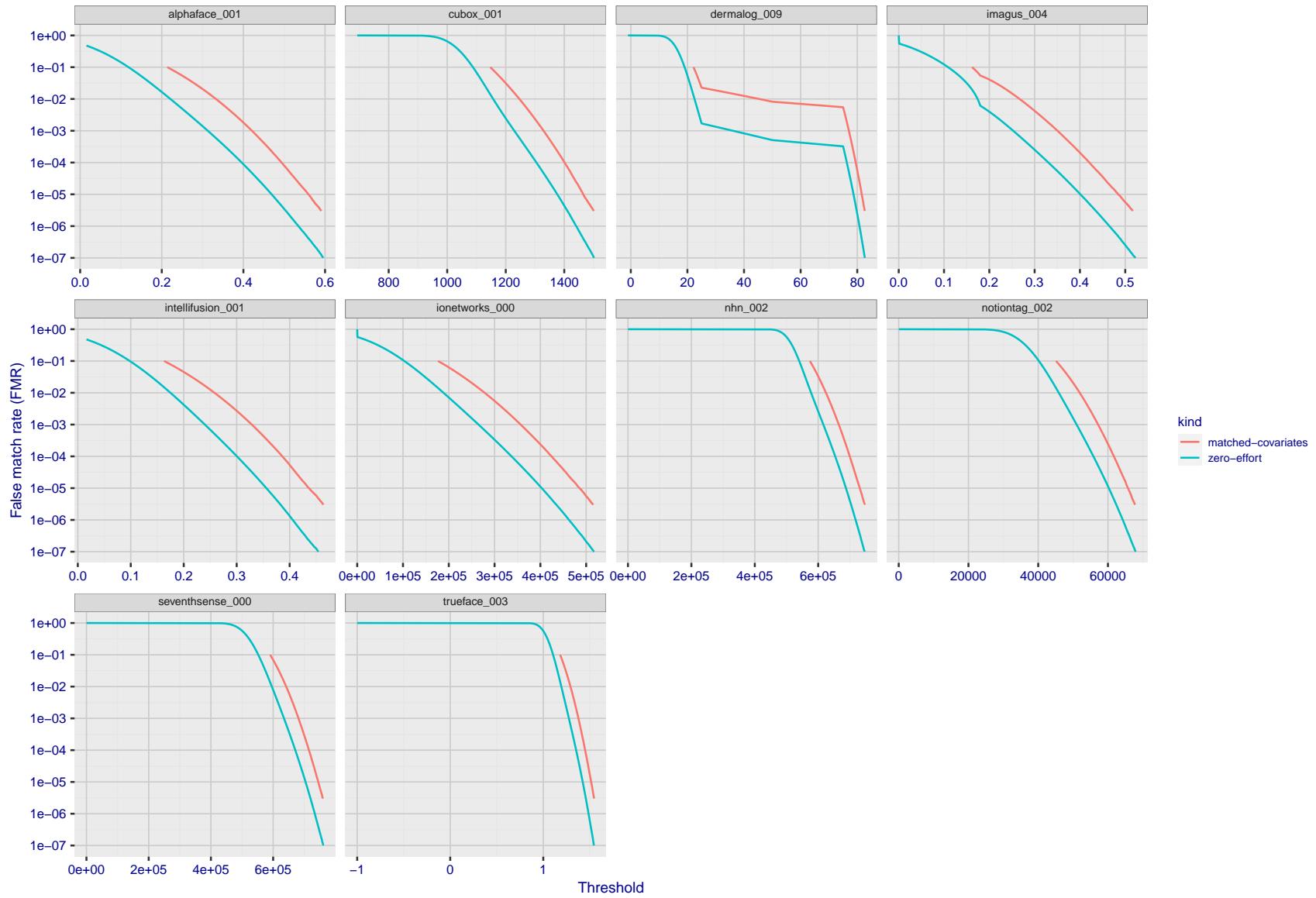


Figure 216: For the visa images, the false match calibration curves show FMR vs. threshold,  $T$ . The blue (lower) curves are for zero-effort impostors (i.e. comparing all images against all). The red (upper) curves are for persons of the same-sex, same-age, and same national-origin. This shows that FMR is underestimated (by a factor of 10 or more) by using a zero-effort impostor calculation to calibrate  $T$ . As shown later (sec. 3.6), FMR is higher for demographic-matched impostors.

FNMR( $T$ )  
"False non-match rate"  
"False match rate"

2022/05/06 07:45:52

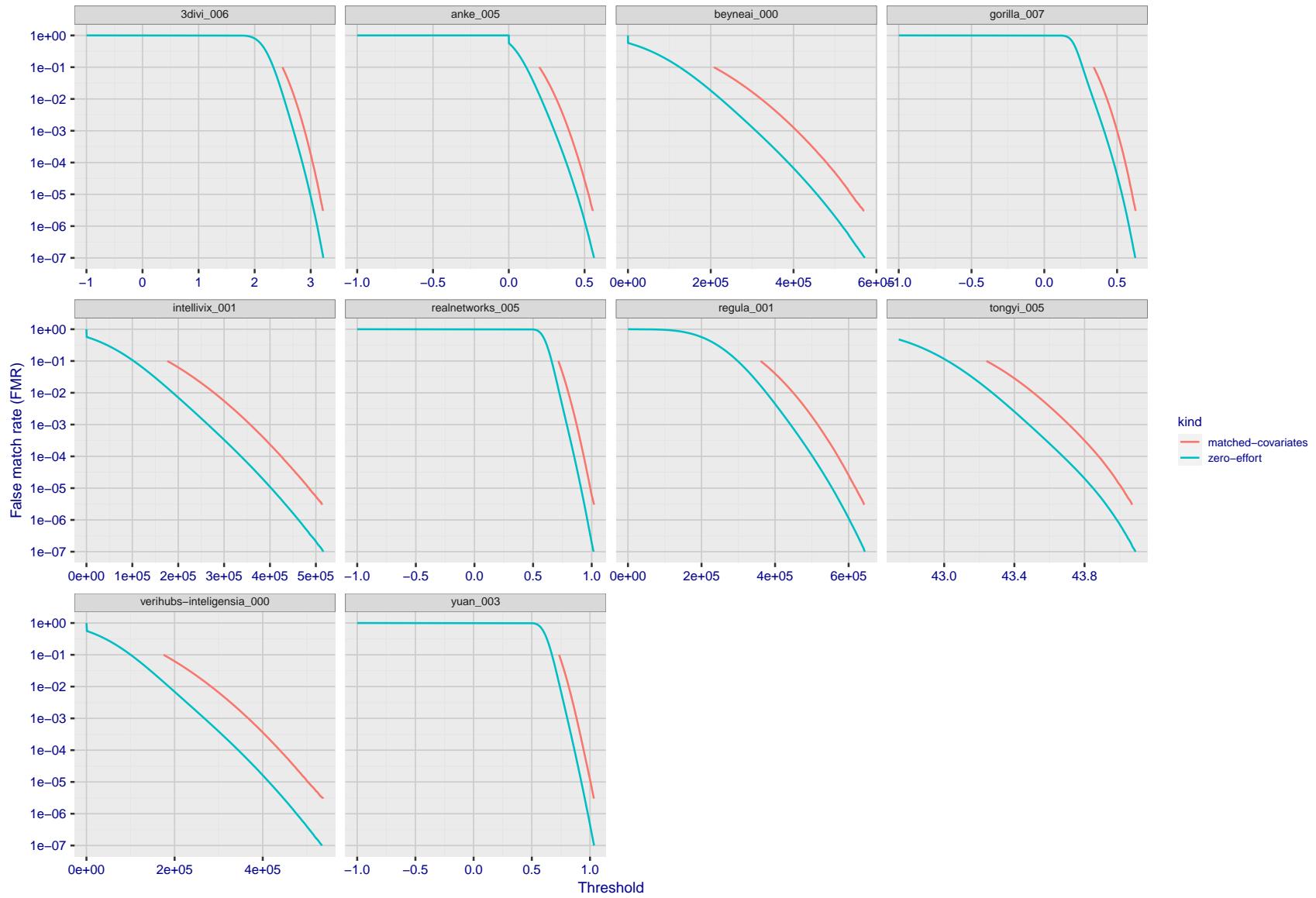


Figure 217: For the visa images, the false match calibration curves show FMR vs. threshold,  $T$ . The blue (lower) curves are for zero-effort impostors (i.e. comparing all images against all). The red (upper) curves are for persons of the same-sex, same-age, and same national-origin. This shows that FMR is underestimated (by a factor of 10 or more) by using a zero-effort impostor calculation to calibrate  $T$ . As shown later (sec. 3.6), FMR is higher for demographic-matched impostors.

FNMR( $T$ )  
"False non-match rate"  
"False match rate"

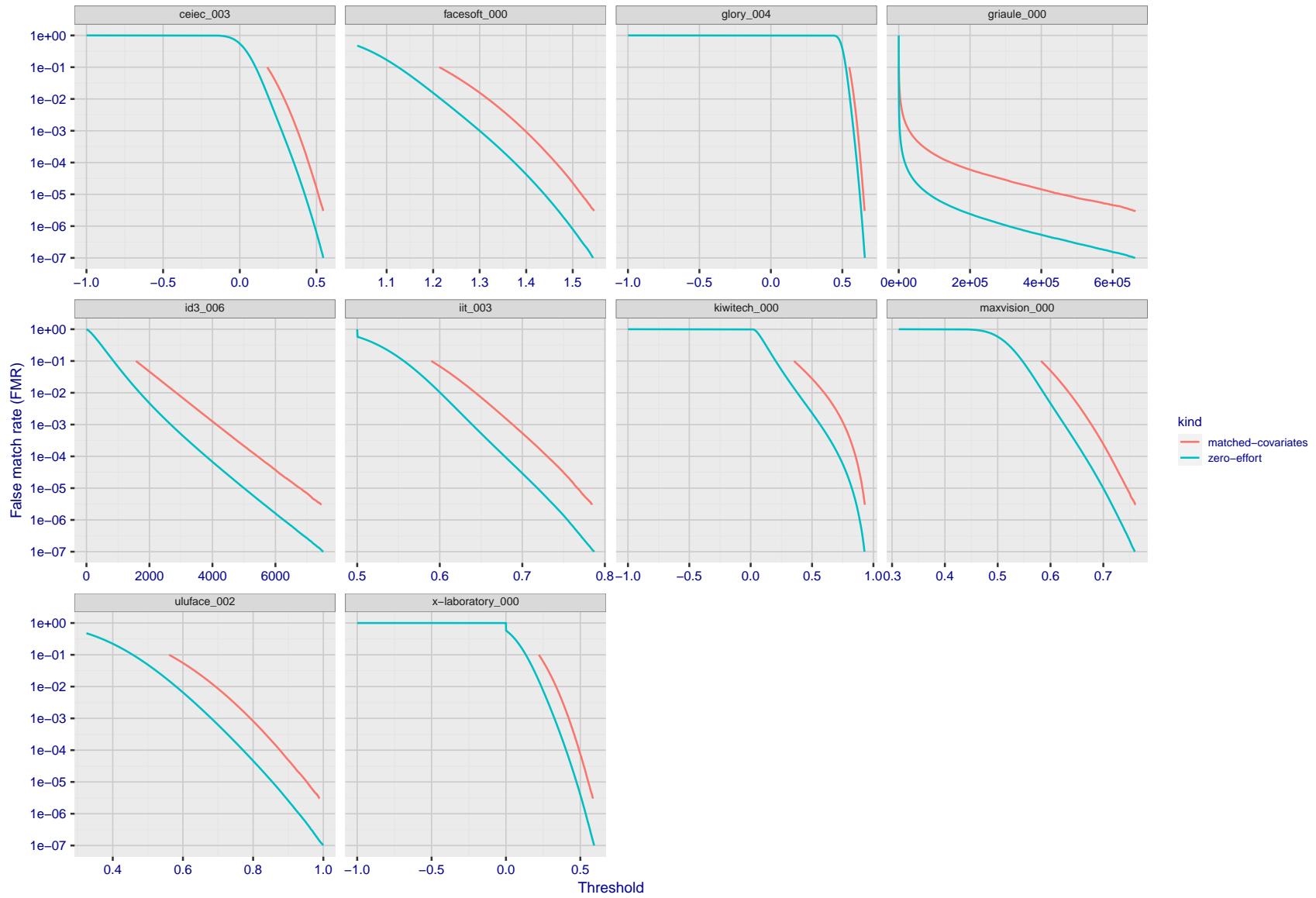


Figure 218: For the visa images, the false match calibration curves show FMR vs. threshold,  $T$ . The blue (lower) curves are for zero-effort impostors (i.e. comparing all images against all). The red (upper) curves are for persons of the same-sex, same-age, and same national-origin. This shows that FMR is underestimated (by a factor of 10 or more) by using a zero-effort impostor calculation to calibrate  $T$ . As shown later (sec. 3.6), FMR is higher for demographic-matched impostors.

2022/05/06 07:45:52

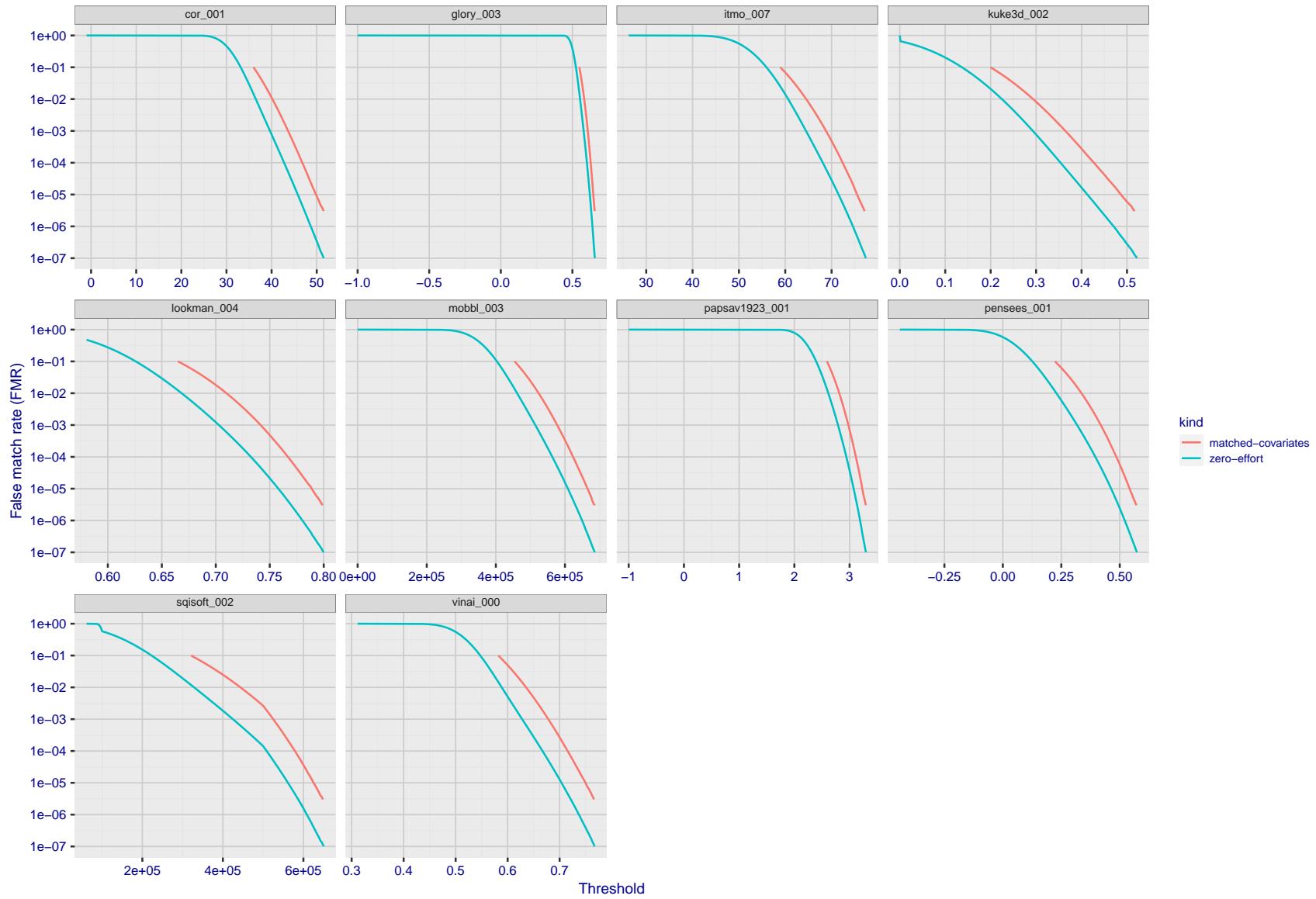


Figure 219: For the visa images, the false match calibration curves show FMR vs. threshold,  $T$ . The blue (lower) curves are for zero-effort impostors (i.e. comparing all images against all). The red (upper) curves are for persons of the same-sex, same-age, and same national-origin. This shows that FMR is underestimated (by a factor of 10 or more) by using a zero-effort impostor calculation to calibrate  $T$ . As shown later (sec. 3.6), FMR is higher for demographic-matched impostors.

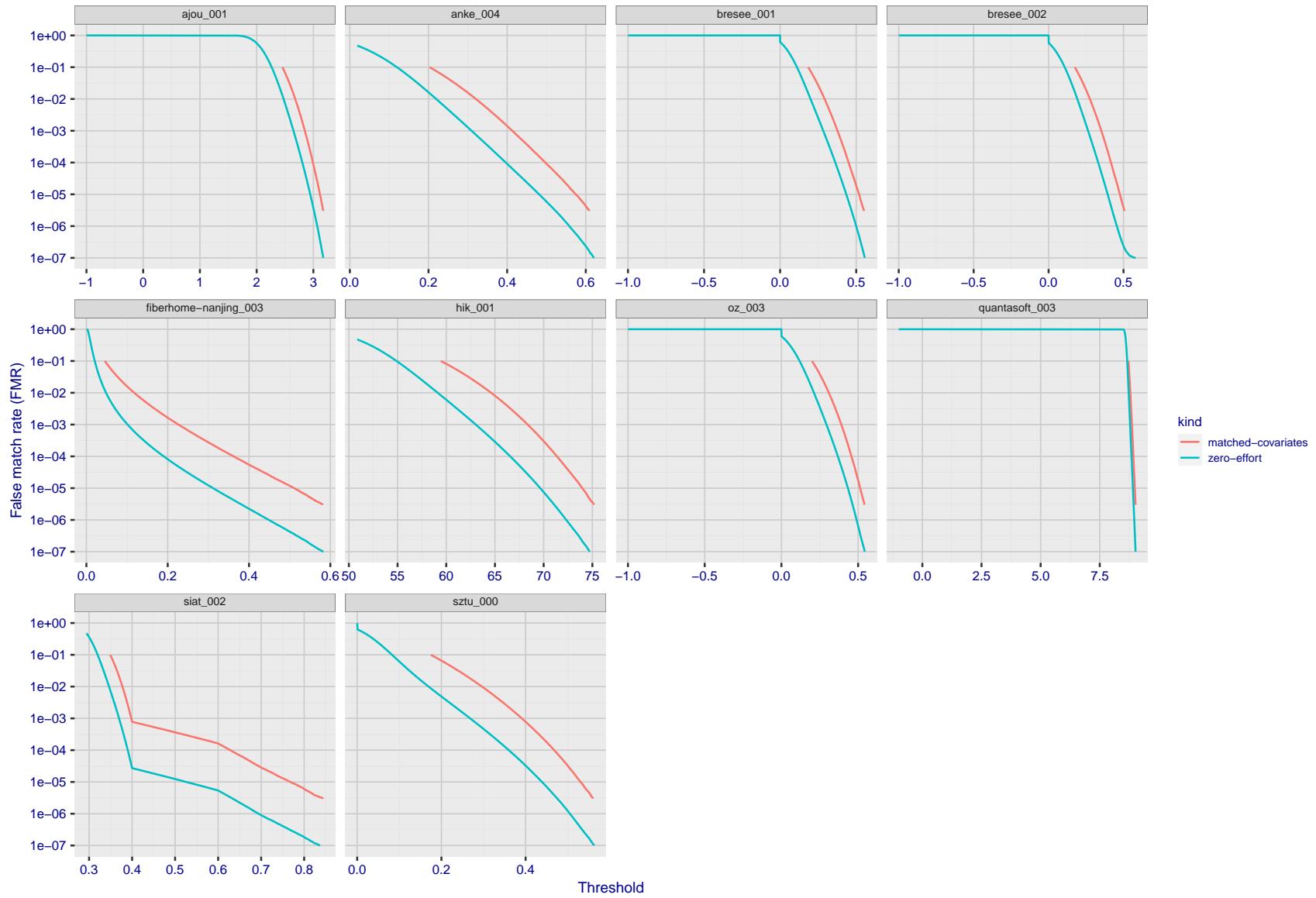


Figure 220: For the visa images, the false match calibration curves show FMR vs. threshold,  $T$ . The blue (lower) curves are for zero-effort impostors (i.e. comparing all images against all). The red (upper) curves are for persons of the same-sex, same-age, and same national-origin. This shows that FMR is underestimated (by a factor of 10 or more) by using a zero-effort impostor calculation to calibrate  $T$ . As shown later (sec. 3.6), FMR is higher for demographic-matched impostors.

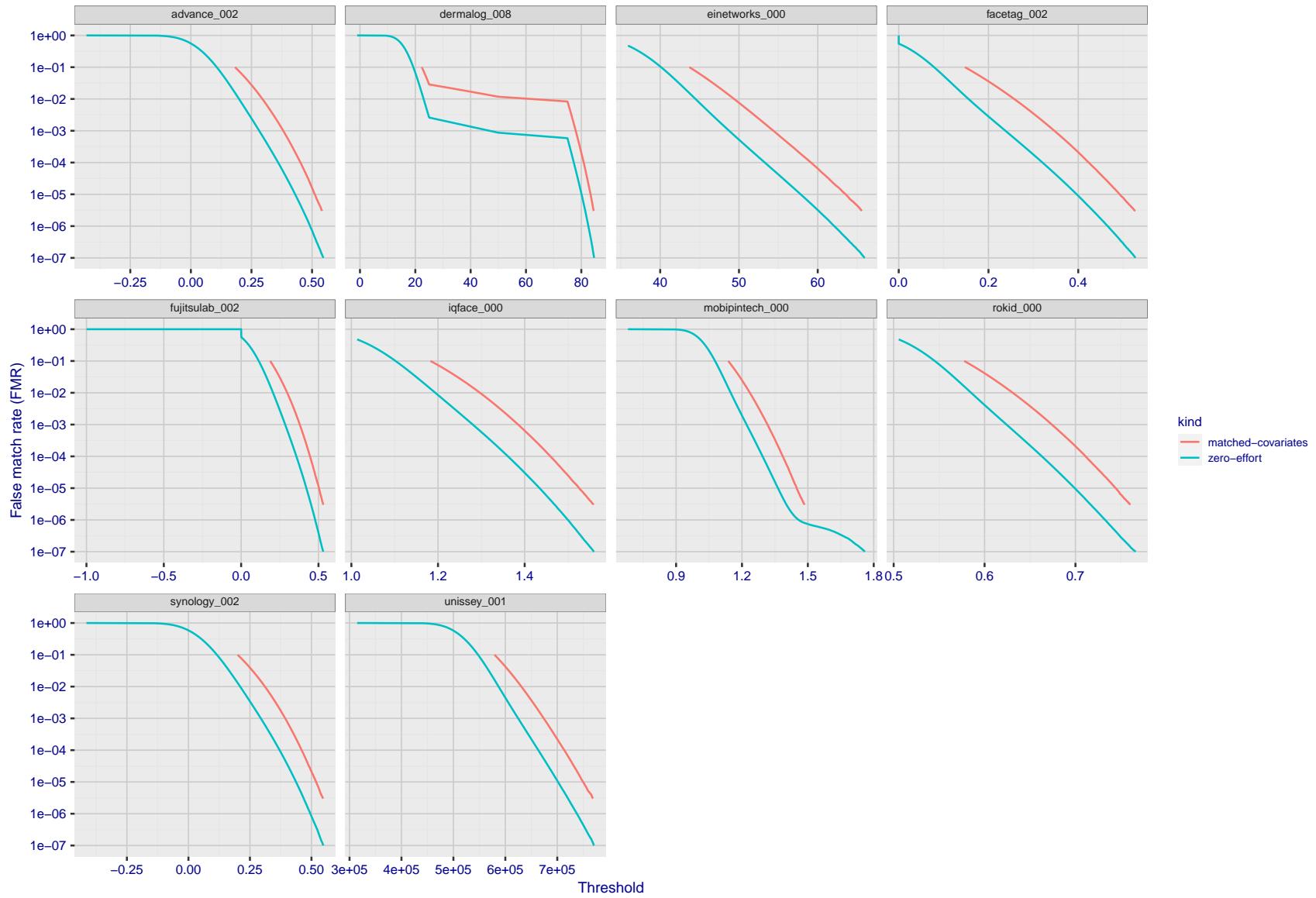


Figure 221: For the visa images, the false match calibration curves show FMR vs. threshold,  $T$ . The blue (lower) curves are for zero-effort impostors (i.e. comparing all images against all). The red (upper) curves are for persons of the same-sex, same-age, and same national-origin. This shows that FMR is underestimated (by a factor of 10 or more) by using a zero-effort impostor calculation to calibrate  $T$ . As shown later (sec. 3.6), FMR is higher for demographic-matched impostors.

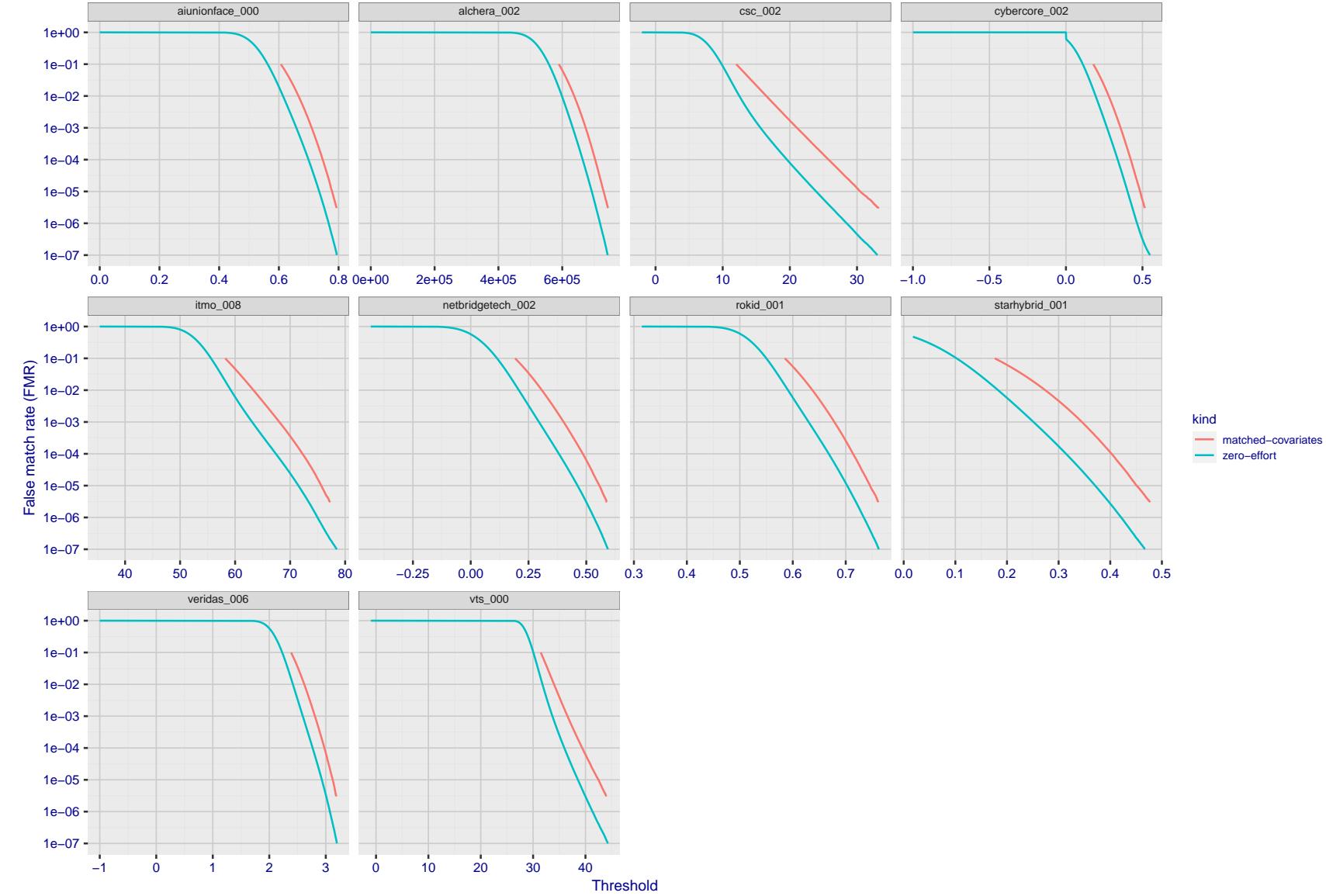


Figure 222: For the visa images, the false match calibration curves show FMR vs. threshold,  $T$ . The blue (lower) curves are for zero-effort impostors (i.e. comparing all images against all). The red (upper) curves are for persons of the same-sex, same-age, and same national-origin. This shows that FMR is underestimated (by a factor of 10 or more) by using a zero-effort impostor calculation to calibrate  $T$ . As shown later (sec. 3.6), FMR is higher for demographic-matched impostors.

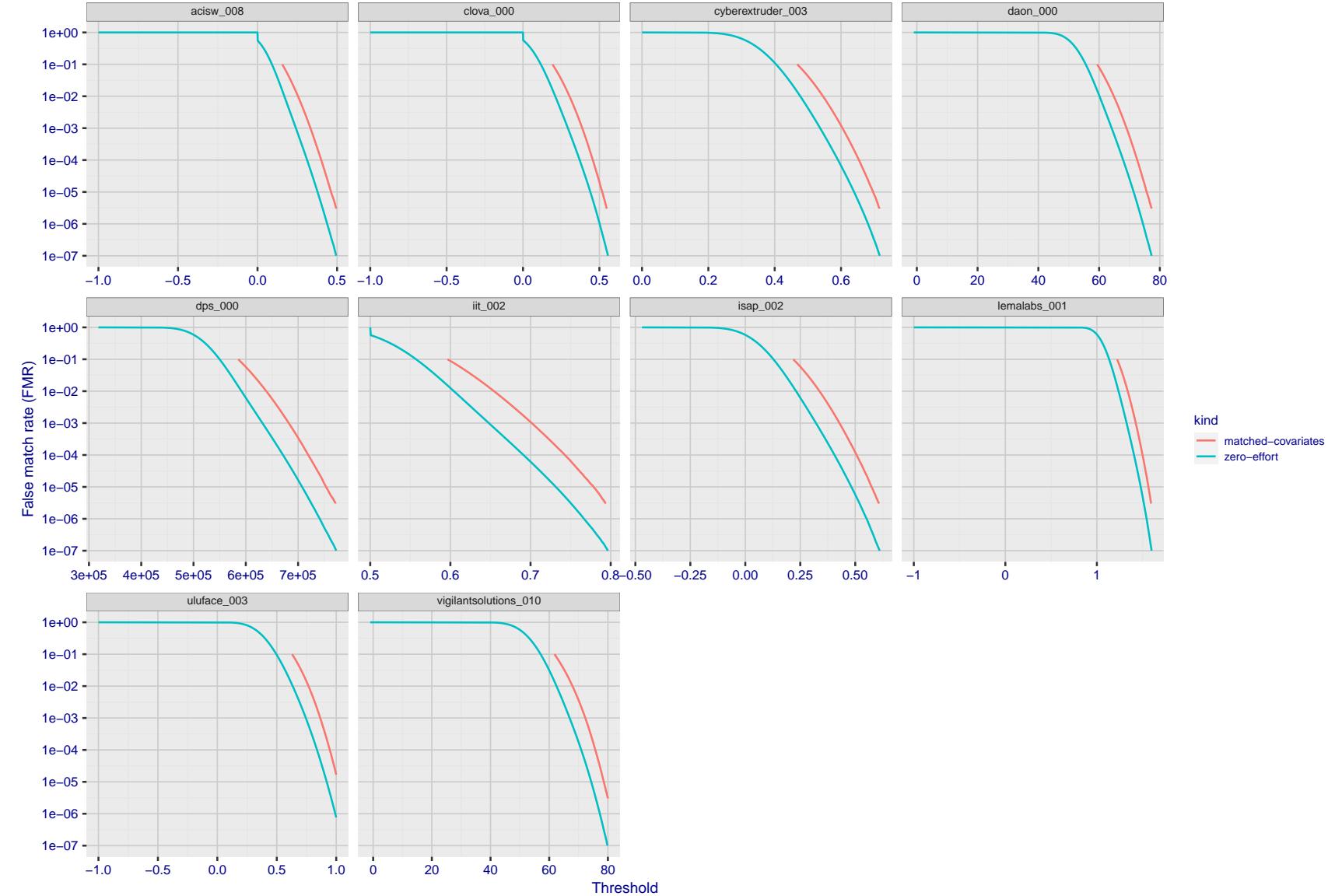


Figure 223: For the visa images, the false match calibration curves show FMR vs. threshold,  $T$ . The blue (lower) curves are for zero-effort impostors (i.e. comparing all images against all). The red (upper) curves are for persons of the same-sex, same-age, and same national-origin. This shows that FMR is underestimated (by a factor of 10 or more) by using a zero-effort impostor calculation to calibrate  $T$ . As shown later (sec. 3.6), FMR is higher for demographic-matched impostors.

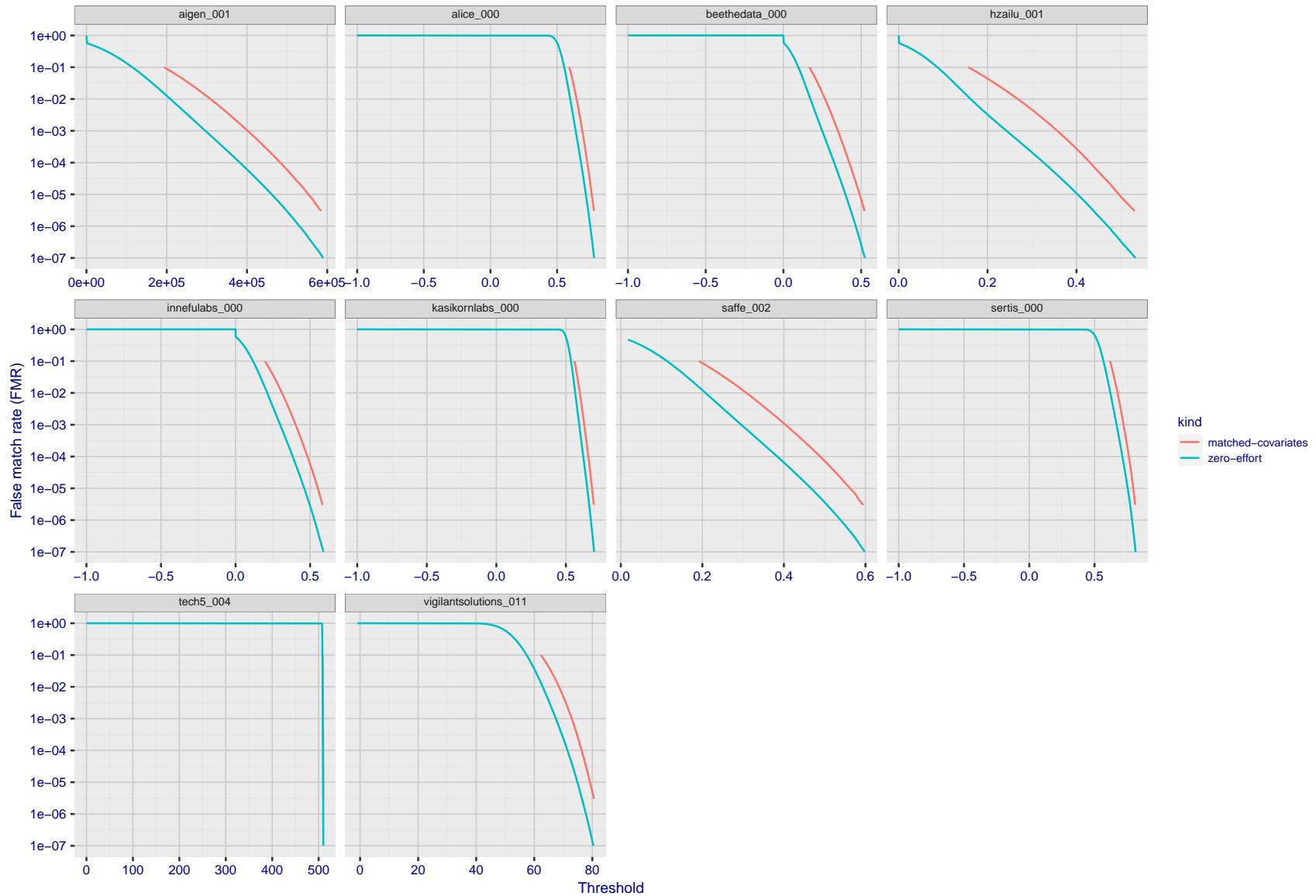


Figure 224: For the visa images, the false match calibration curves show FMR vs. threshold,  $T$ . The blue (lower) curves are for zero-effort impostors (i.e. comparing all images against all). The red (upper) curves are for persons of the same-sex, same-age, and same national-origin. This shows that FMR is underestimated (by a factor of 10 or more) by using a zero-effort impostor calculation to calibrate  $T$ . As shown later (sec. 3.6), FMR is higher for demographic-matched impostors.

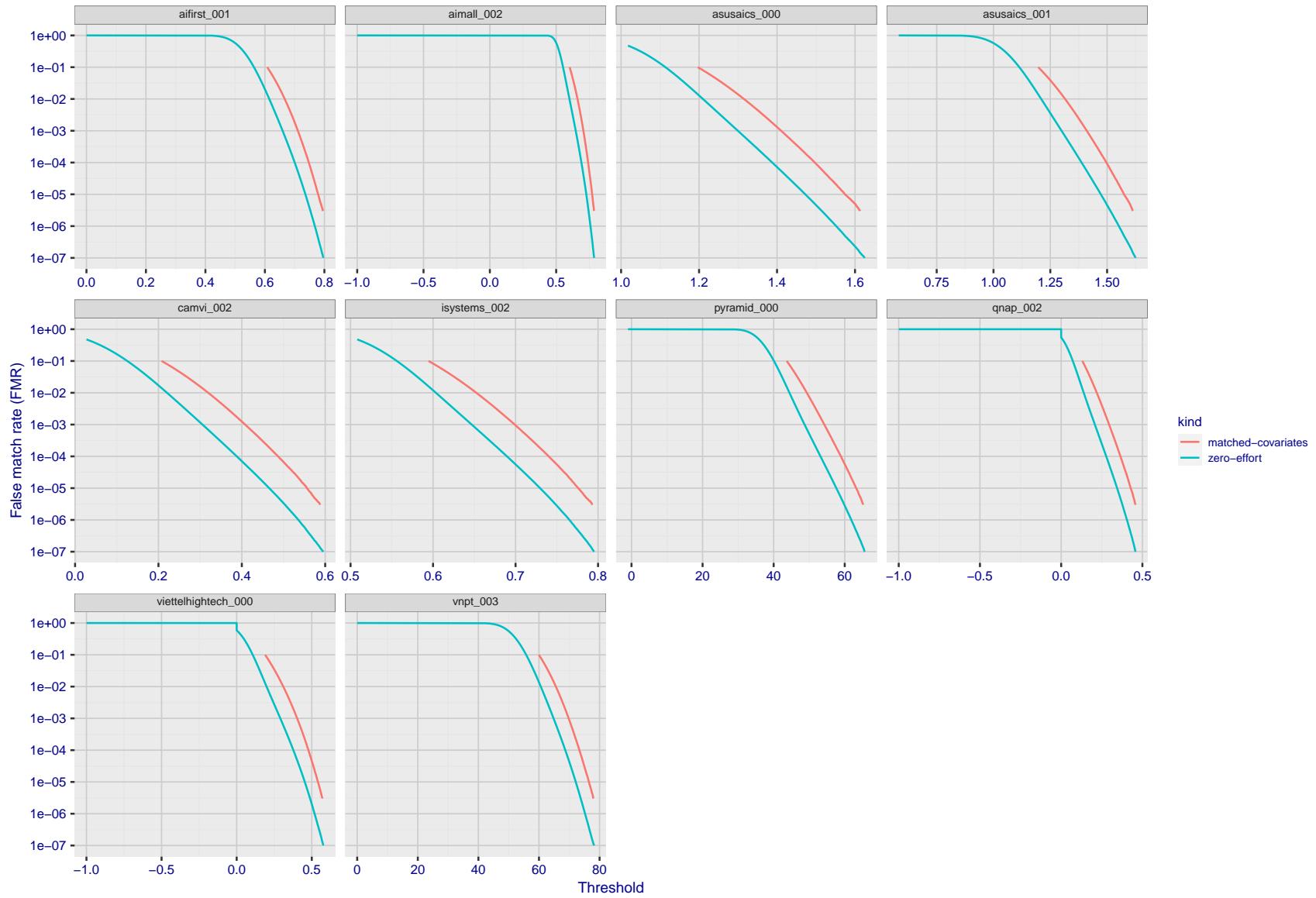


Figure 225: For the visa images, the false match calibration curves show FMR vs. threshold,  $T$ . The blue (lower) curves are for zero-effort impostors (i.e. comparing all images against all). The red (upper) curves are for persons of the same-sex, same-age, and same national-origin. This shows that FMR is underestimated (by a factor of 10 or more) by using a zero-effort impostor calculation to calibrate  $T$ . As shown later (sec. 3.6), FMR is higher for demographic-matched impostors.

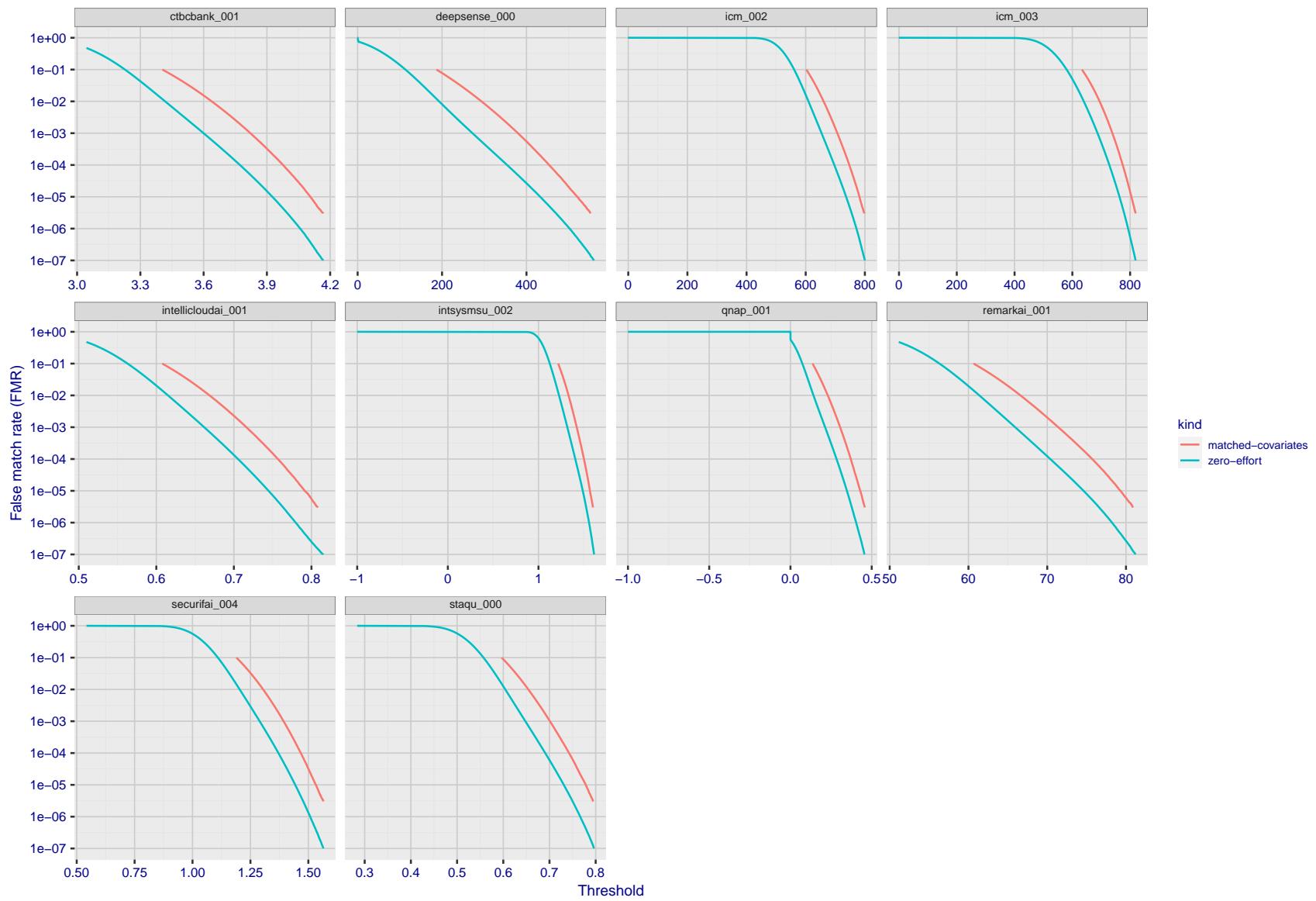


Figure 226: For the visa images, the false match calibration curves show FMR vs. threshold,  $T$ . The blue (lower) curves are for zero-effort impostors (i.e. comparing all images against all). The red (upper) curves are for persons of the same-sex, same-age, and same national-origin. This shows that FMR is underestimated (by a factor of 10 or more) by using a zero-effort impostor calculation to calibrate  $T$ . As shown later (sec. 3.6), FMR is higher for demographic-matched impostors.

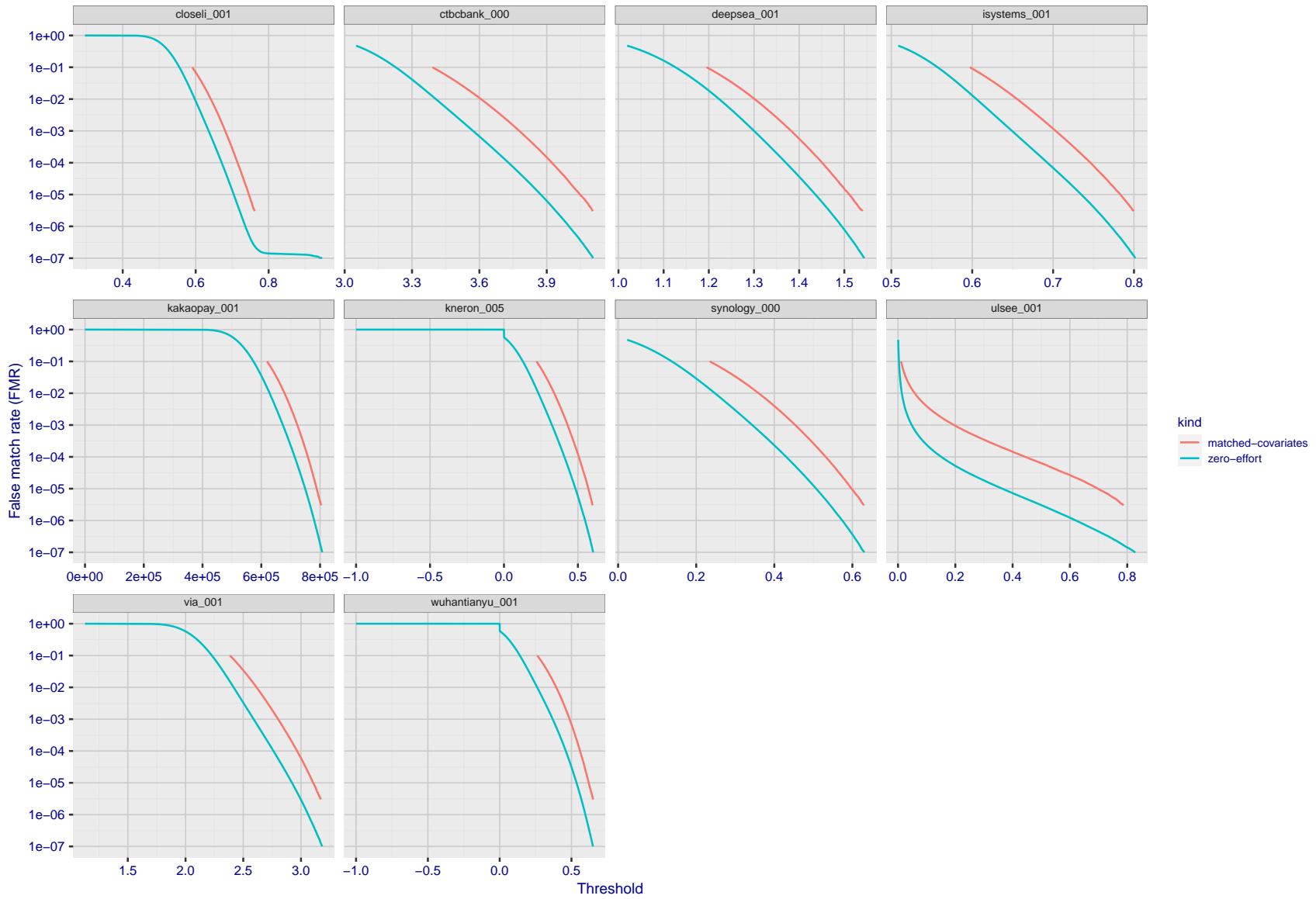


Figure 227: For the visa images, the false match calibration curves show FMR vs. threshold,  $T$ . The blue (lower) curves are for zero-effort impostors (i.e. comparing all images against all). The red (upper) curves are for persons of the same-sex, same-age, and same national-origin. This shows that FMR is underestimated (by a factor of 10 or more) by using a zero-effort impostor calculation to calibrate  $T$ . As shown later (sec. 3.6), FMR is higher for demographic-matched impostors.

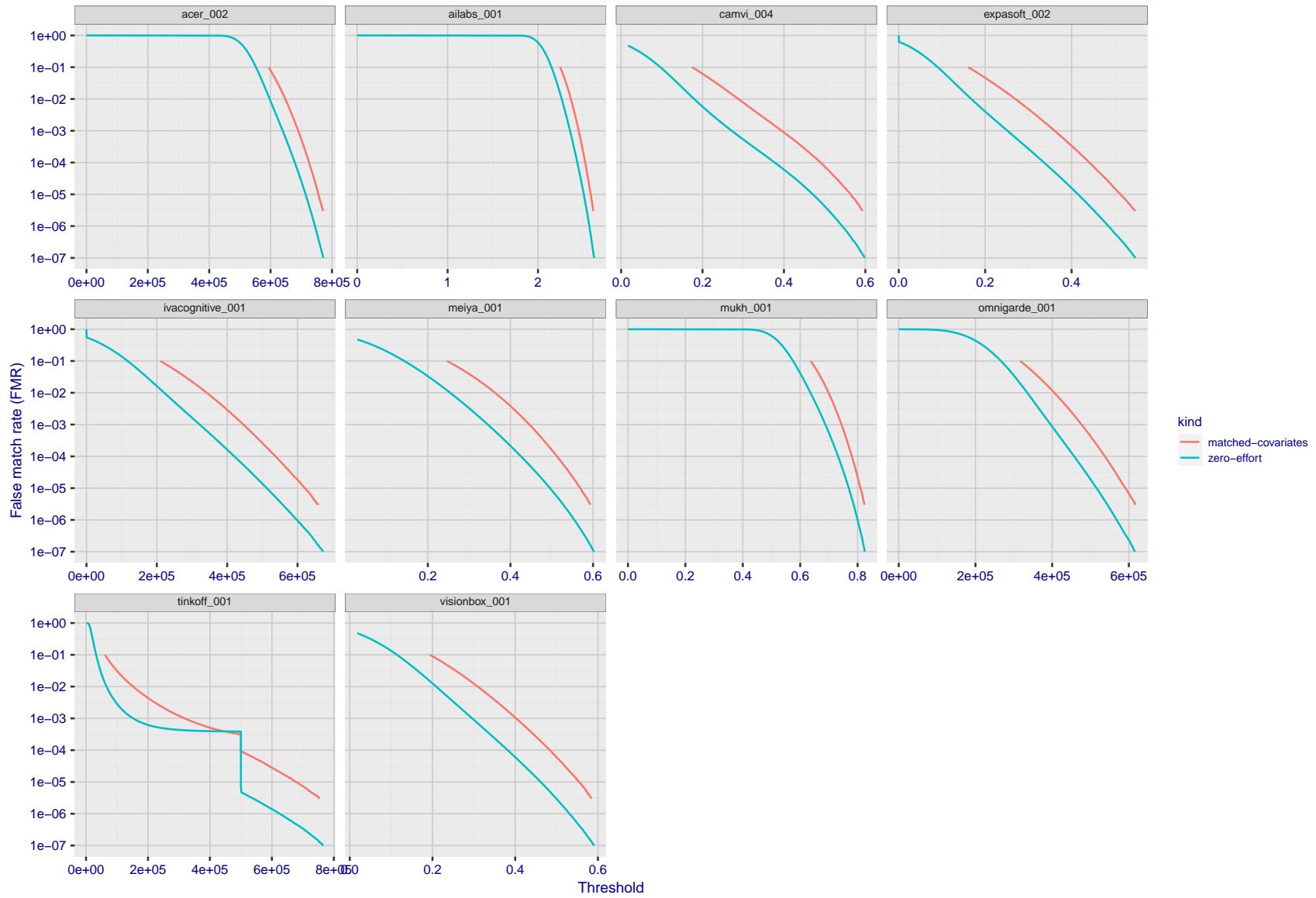


Figure 228: For the visa images, the false match calibration curves show FMR vs. threshold,  $T$ . The blue (lower) curves are for zero-effort impostors (i.e. comparing all images against all). The red (upper) curves are for persons of the same-sex, same-age, and same national-origin. This shows that FMR is underestimated (by a factor of 10 or more) by using a zero-effort impostor calculation to calibrate  $T$ . As shown later (sec. 3.6), FMR is higher for demographic-matched impostors.

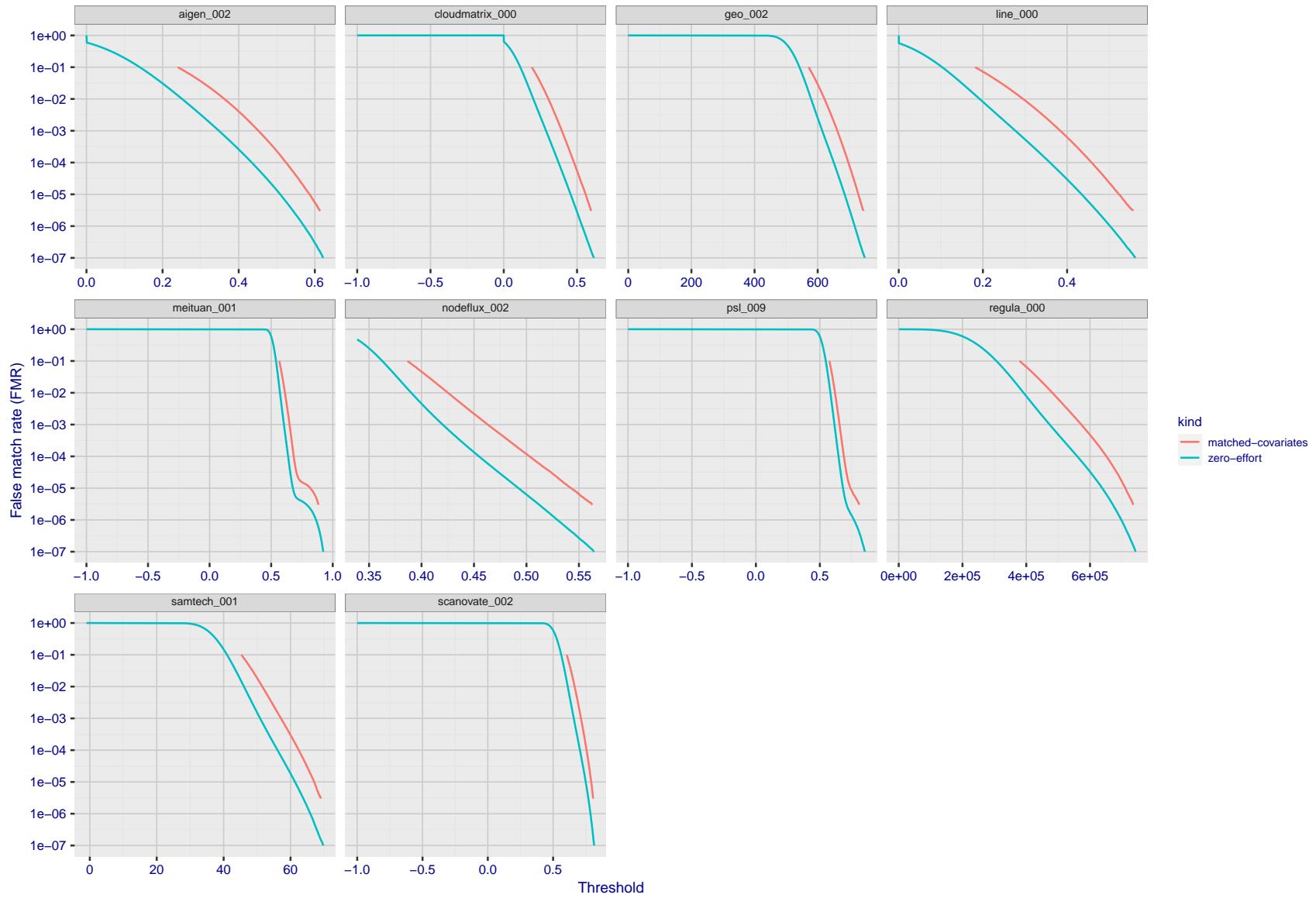


Figure 229: For the visa images, the false match calibration curves show FMR vs. threshold,  $T$ . The blue (lower) curves are for zero-effort impostors (i.e. comparing all images against all). The red (upper) curves are for persons of the same-sex, same-age, and same national-origin. This shows that FMR is underestimated (by a factor of 10 or more) by using a zero-effort impostor calculation to calibrate  $T$ . As shown later (sec. 3.6), FMR is higher for demographic-matched impostors.

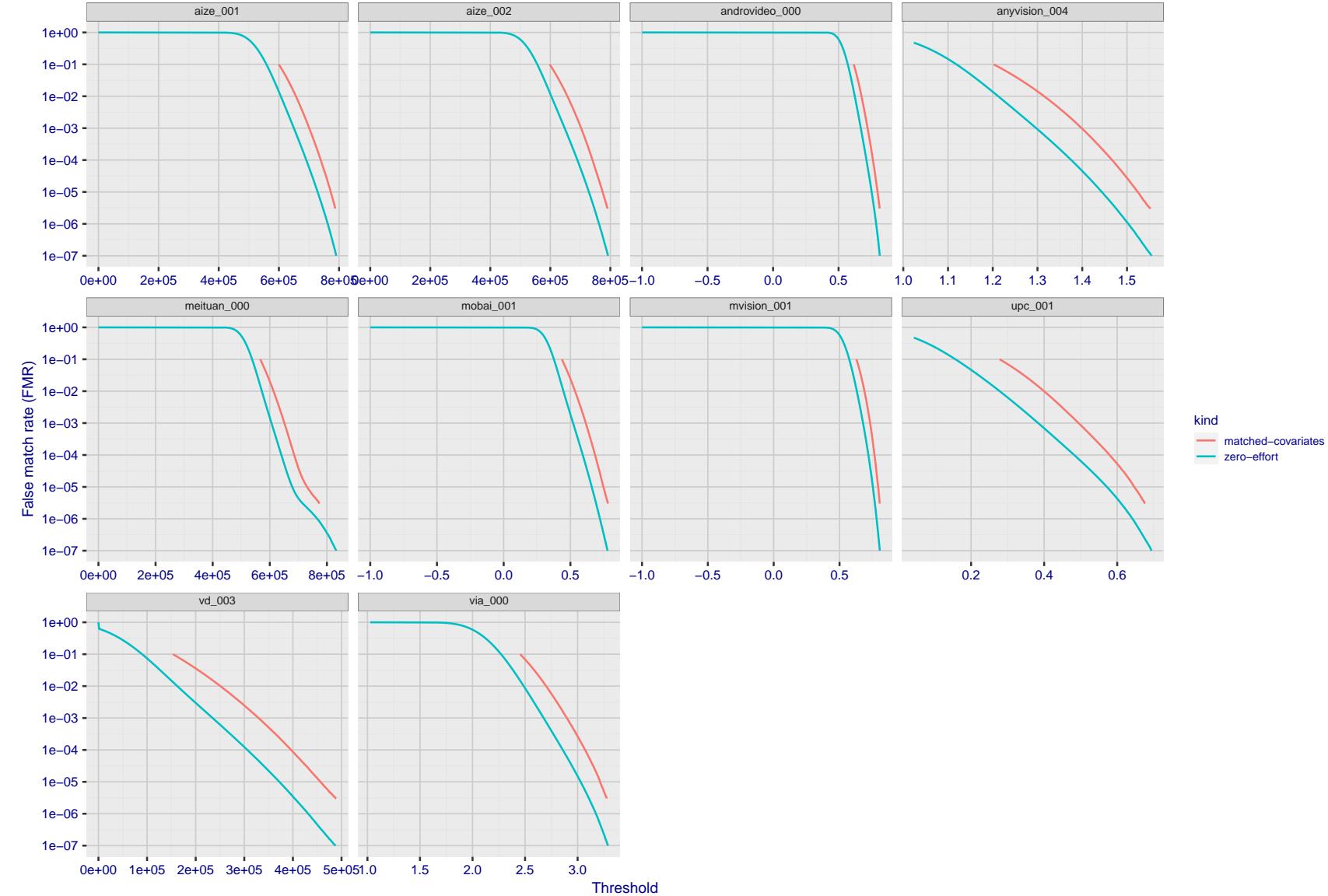


Figure 230: For the visa images, the false match calibration curves show FMR vs. threshold,  $T$ . The blue (lower) curves are for zero-effort impostors (i.e. comparing all images against all). The red (upper) curves are for persons of the same-sex, same-age, and same national-origin. This shows that FMR is underestimated (by a factor of 10 or more) by using a zero-effort impostor calculation to calibrate  $T$ . As shown later (sec. 3.6), FMR is higher for demographic-matched impostors.

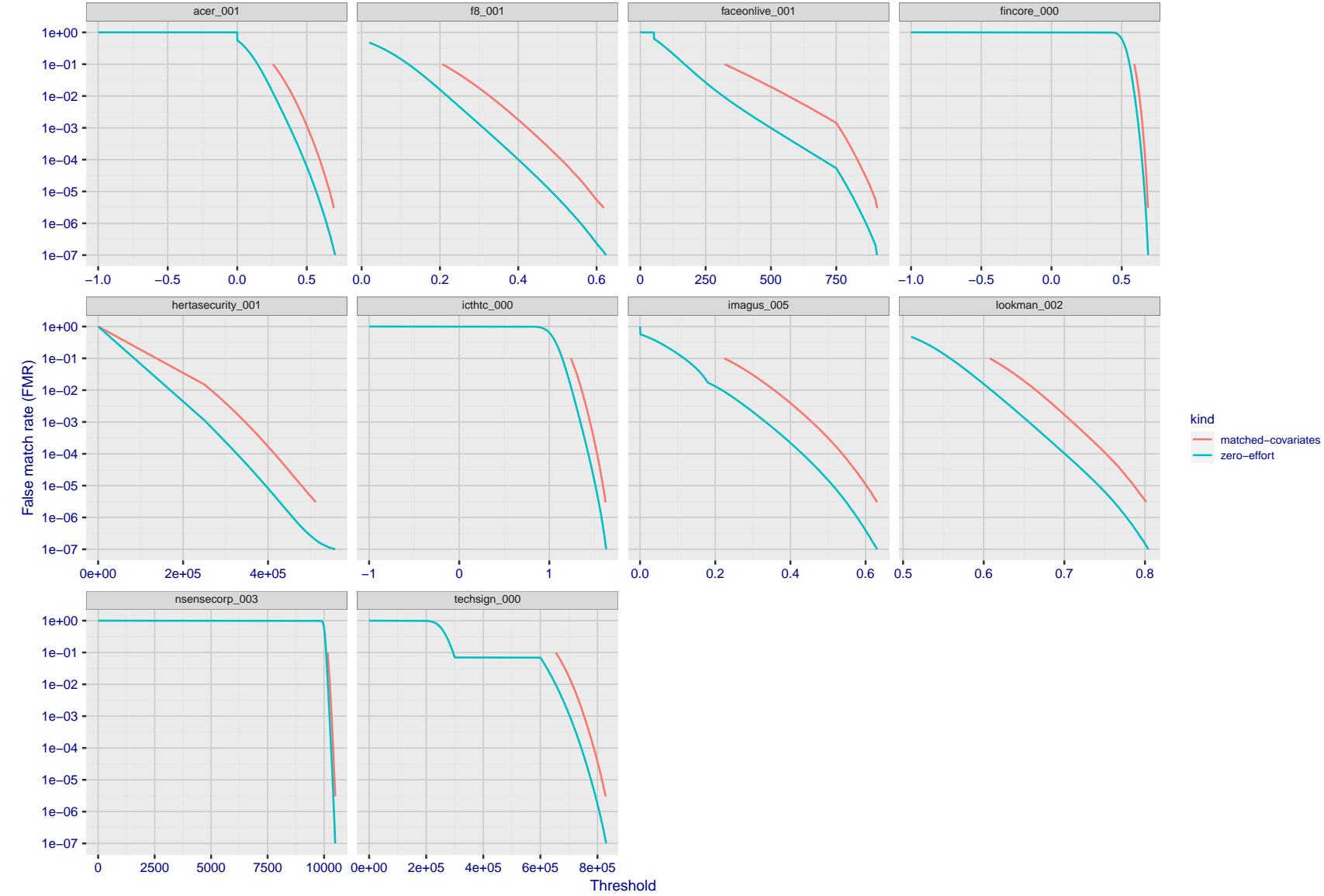


Figure 231: For the visa images, the false match calibration curves show FMR vs. threshold,  $T$ . The blue (lower) curves are for zero-effort impostors (i.e. comparing all images against all). The red (upper) curves are for persons of the same-sex, same-age, and same national-origin. This shows that FMR is underestimated (by a factor of 10 or more) by using a zero-effort impostor calculation to calibrate  $T$ . As shown later (sec. 3.6), FMR is higher for demographic-matched impostors.

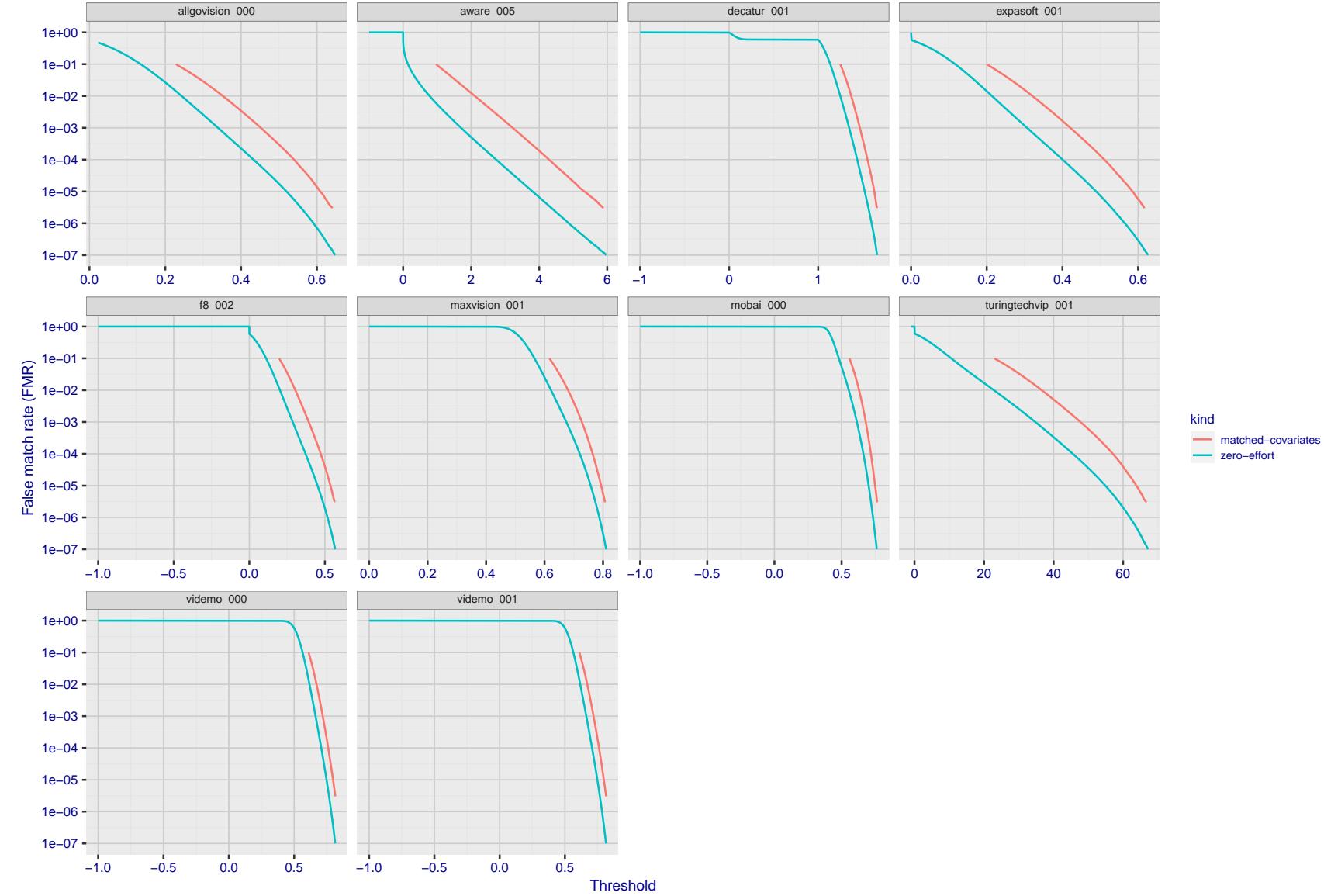


Figure 232: For the visa images, the false match calibration curves show FMR vs. threshold,  $T$ . The blue (lower) curves are for zero-effort impostors (i.e. comparing all images against all). The red (upper) curves are for persons of the same-sex, same-age, and same national-origin. This shows that FMR is underestimated (by a factor of 10 or more) by using a zero-effort impostor calculation to calibrate  $T$ . As shown later (sec. 3.6), FMR is higher for demographic-matched impostors.

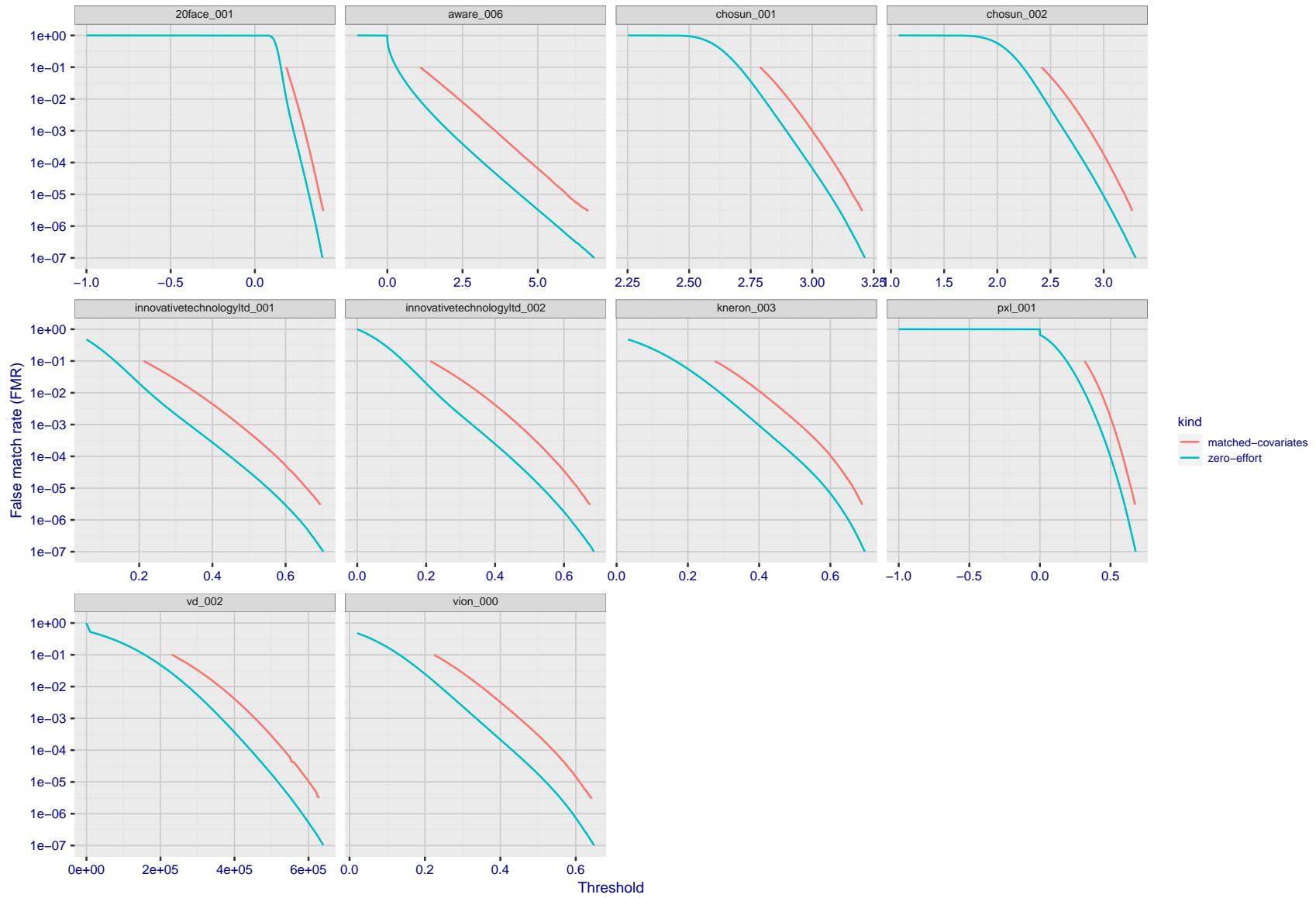


Figure 233: For the visa images, the false match calibration curves show FMR vs. threshold,  $T$ . The blue (lower) curves are for zero-effort impostors (i.e. comparing all images against all). The red (upper) curves are for persons of the same-sex, same-age, and same national-origin. This shows that FMR is underestimated (by a factor of 10 or more) by using a zero-effort impostor calculation to calibrate  $T$ . As shown later (sec. 3.6), FMR is higher for demographic-matched impostors.

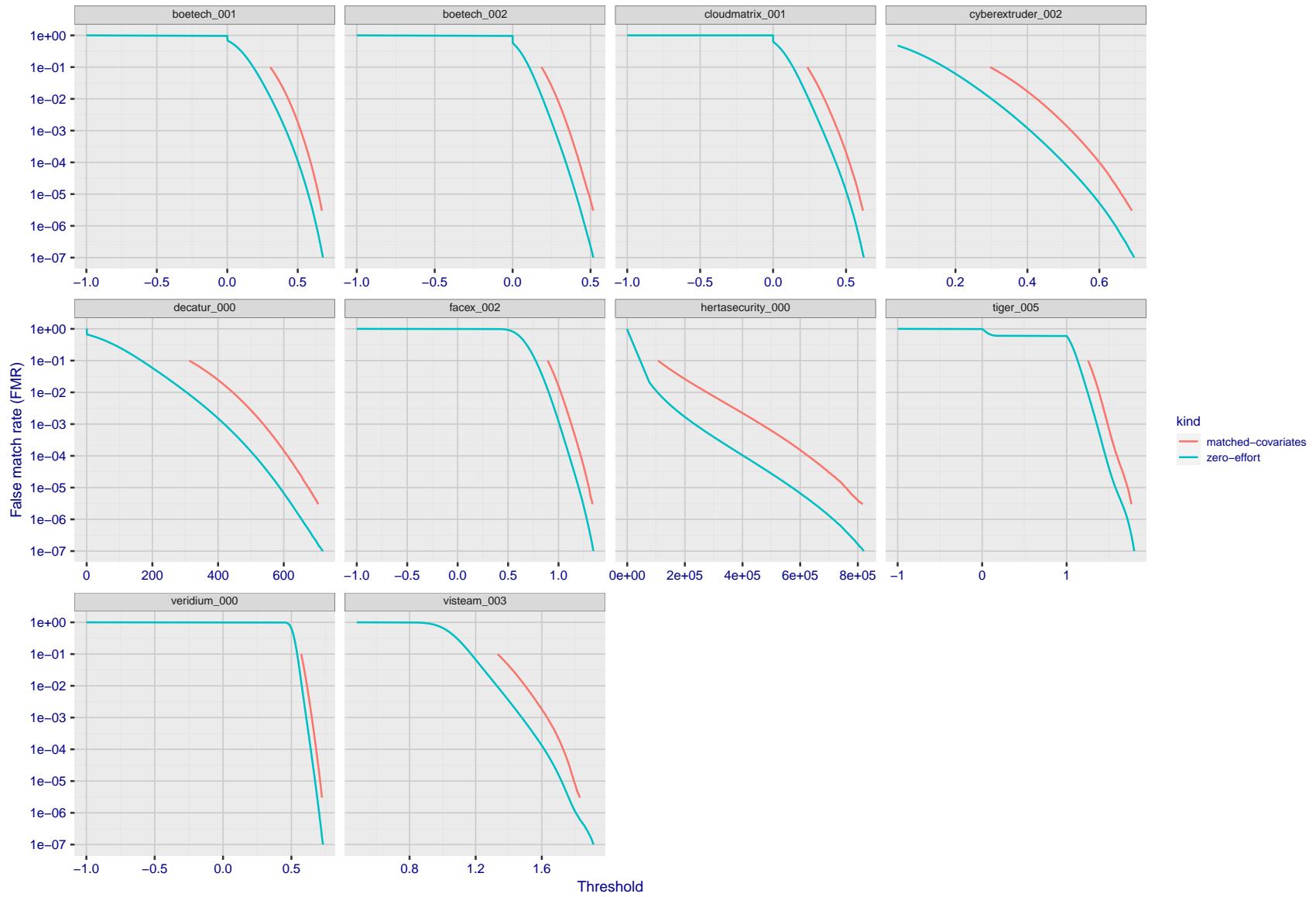


Figure 234: For the visa images, the false match calibration curves show FMR vs. threshold,  $T$ . The blue (lower) curves are for zero-effort impostors (i.e. comparing all images against all). The red (upper) curves are for persons of the same-sex, same-age, and same national-origin. This shows that FMR is underestimated (by a factor of 10 or more) by using a zero-effort impostor calculation to calibrate  $T$ . As shown later (sec. 3.6), FMR is higher for demographic-matched impostors.

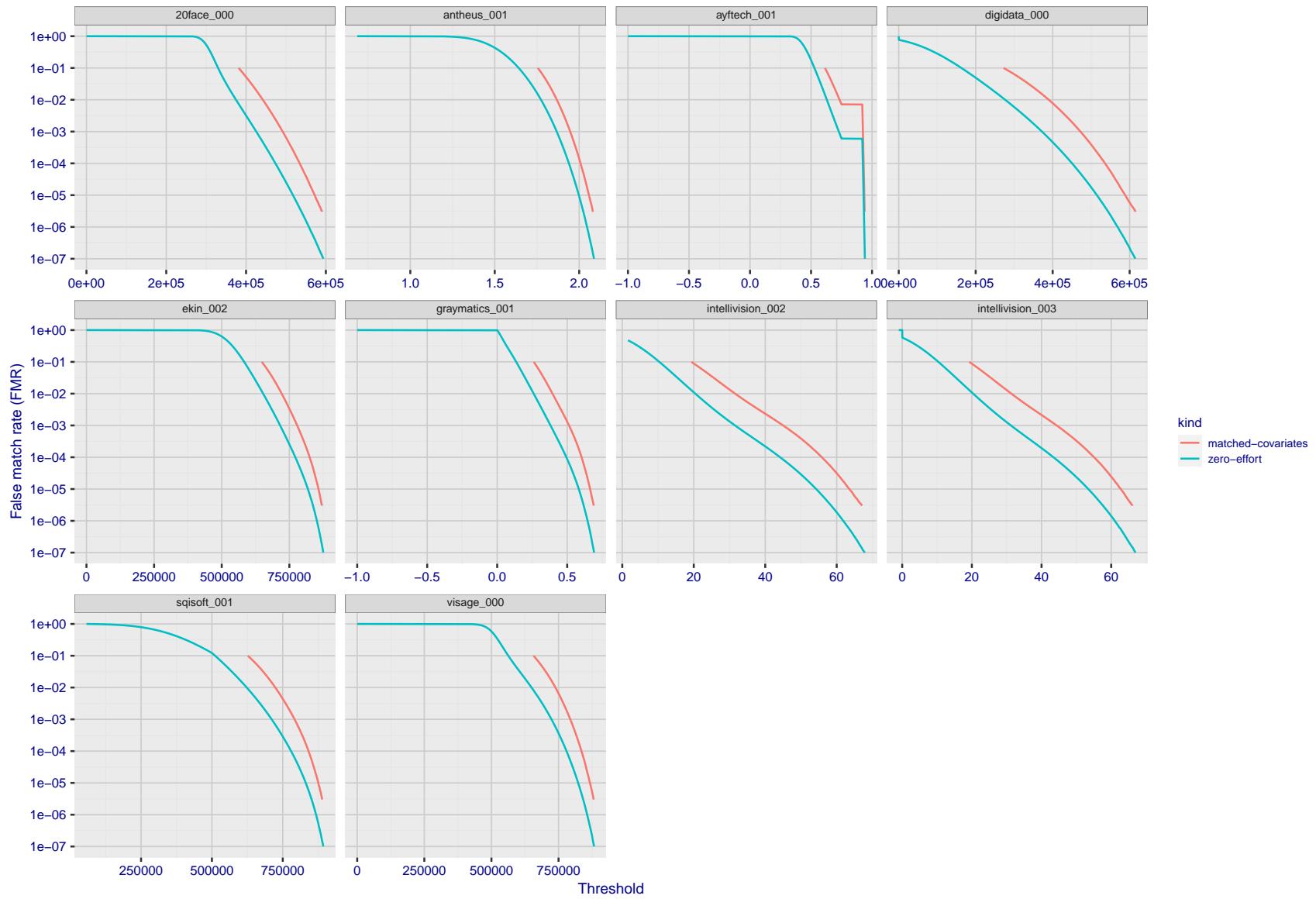


Figure 235: For the visa images, the false match calibration curves show FMR vs. threshold,  $T$ . The blue (lower) curves are for zero-effort impostors (i.e. comparing all images against all). The red (upper) curves are for persons of the same-sex, same-age, and same national-origin. This shows that FMR is underestimated (by a factor of 10 or more) by using a zero-effort impostor calculation to calibrate  $T$ . As shown later (sec. 3.6), FMR is higher for demographic-matched impostors.

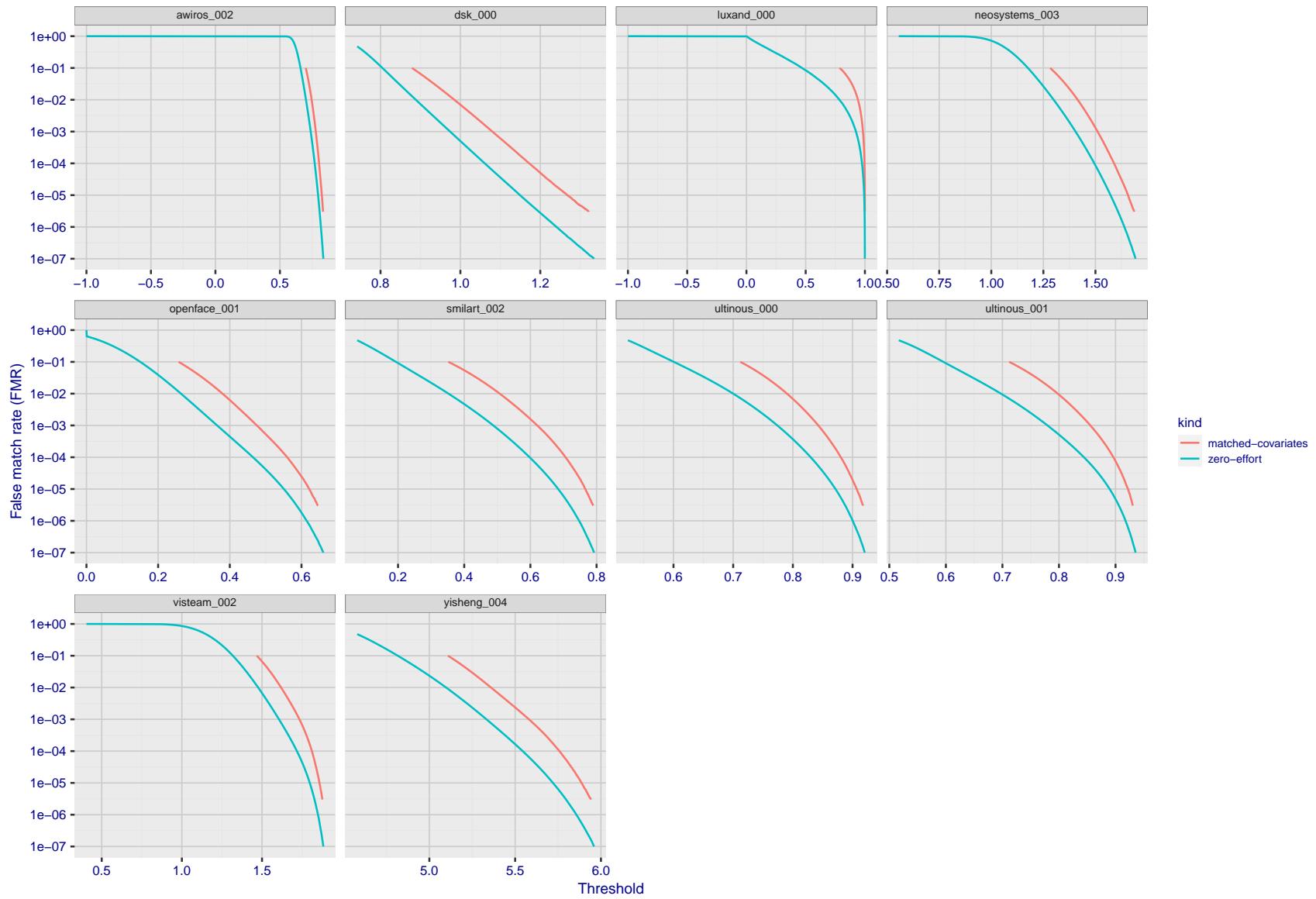


Figure 236: For the visa images, the false match calibration curves show FMR vs. threshold,  $T$ . The blue (lower) curves are for zero-effort impostors (i.e. comparing all images against all). The red (upper) curves are for persons of the same-sex, same-age, and same national-origin. This shows that FMR is underestimated (by a factor of 10 or more) by using a zero-effort impostor calculation to calibrate  $T$ . As shown later (sec. 3.6), FMR is higher for demographic-matched impostors.

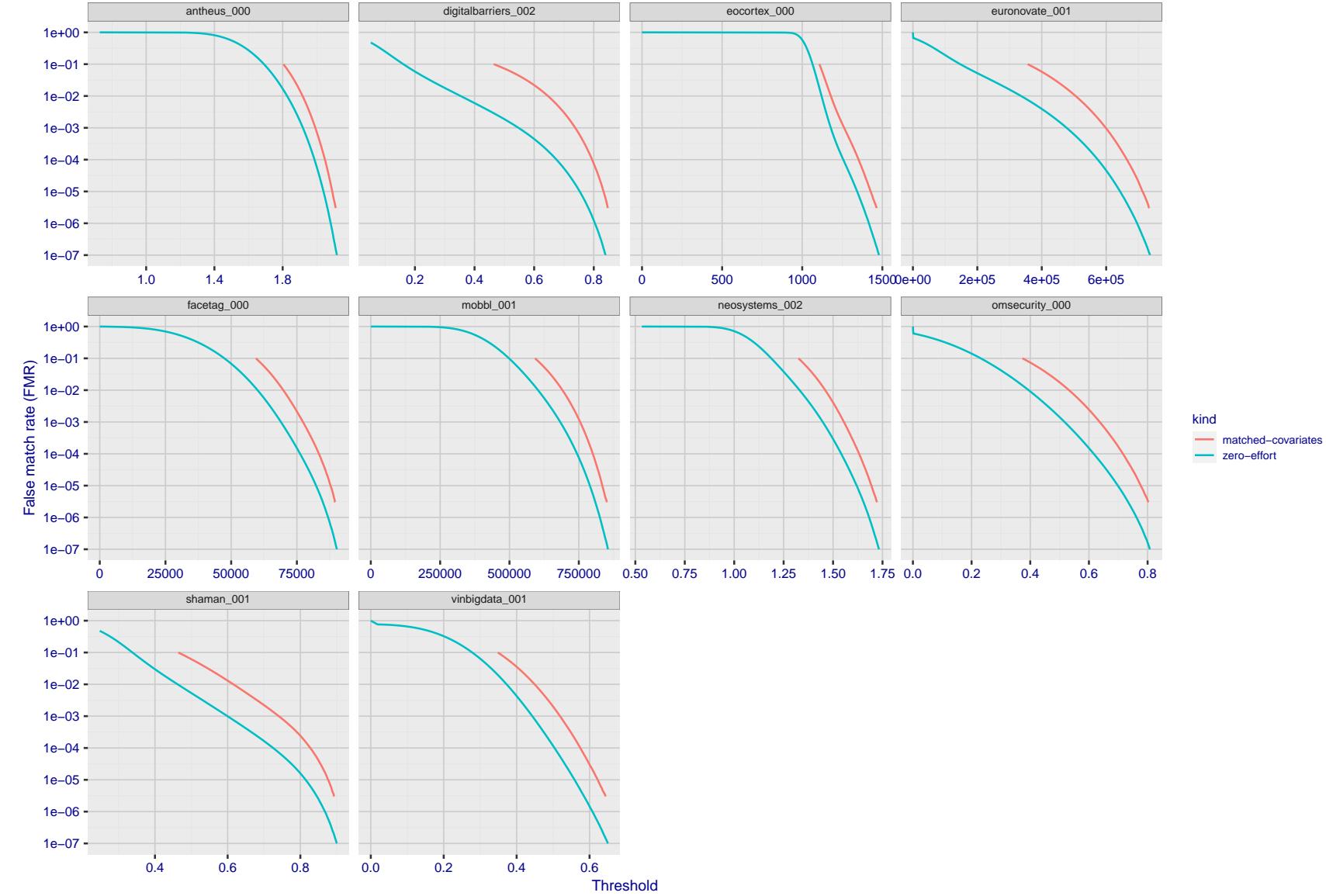


Figure 237: For the visa images, the false match calibration curves show FMR vs. threshold,  $T$ . The blue (lower) curves are for zero-effort impostors (i.e. comparing all images against all). The red (upper) curves are for persons of the same-sex, same-age, and same national-origin. This shows that FMR is underestimated (by a factor of 10 or more) by using a zero-effort impostor calculation to calibrate  $T$ . As shown later (sec. 3.6), FMR is higher for demographic-matched impostors.

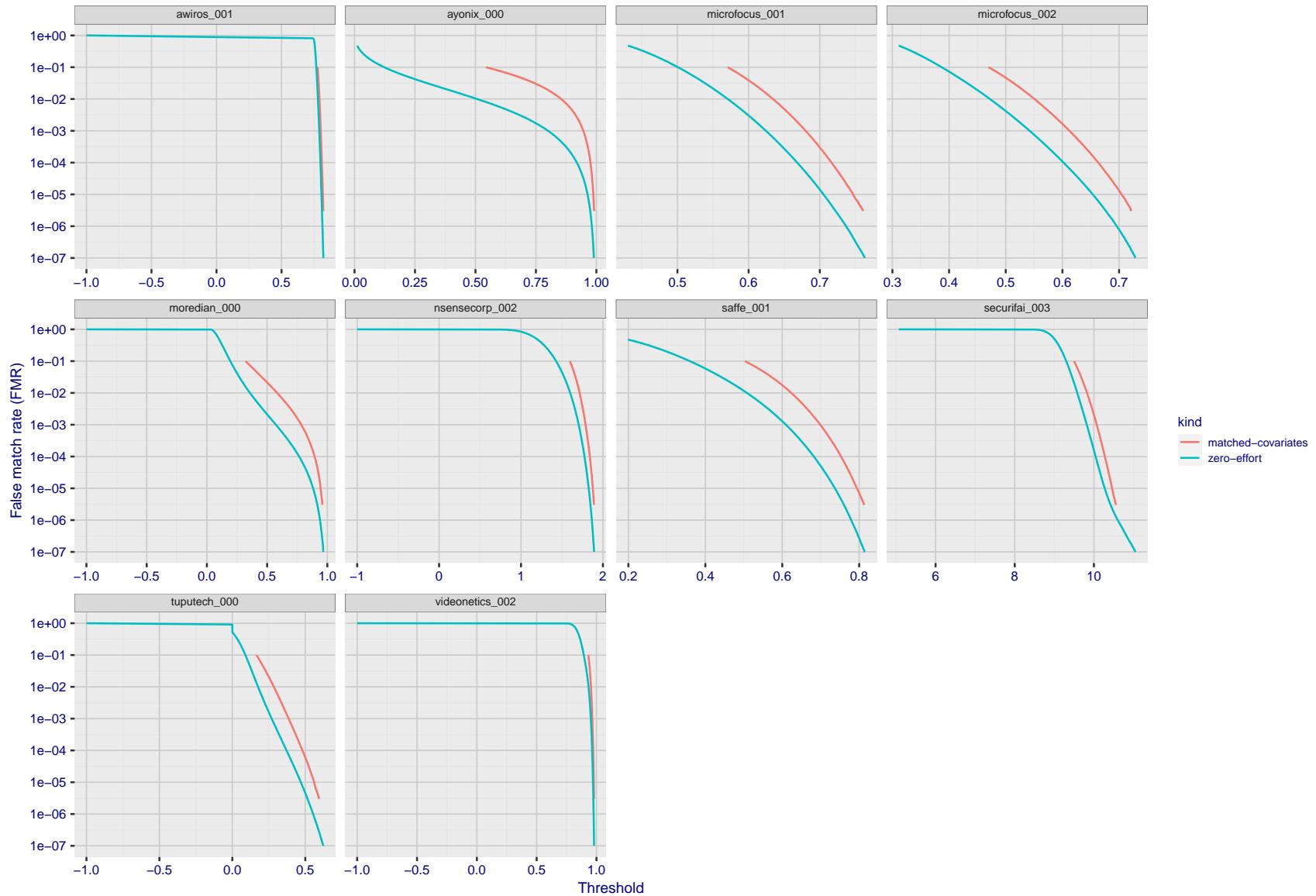


Figure 238: For the visa images, the false match calibration curves show FMR vs. threshold,  $T$ . The blue (lower) curves are for zero-effort impostors (i.e. comparing all images against all). The red (upper) curves are for persons of the same-sex, same-age, and same national-origin. This shows that FMR is underestimated (by a factor of 10 or more) by using a zero-effort impostor calculation to calibrate  $T$ . As shown later (sec. 3.6), FMR is higher for demographic-matched impostors.

2022/05/06 07:45:52

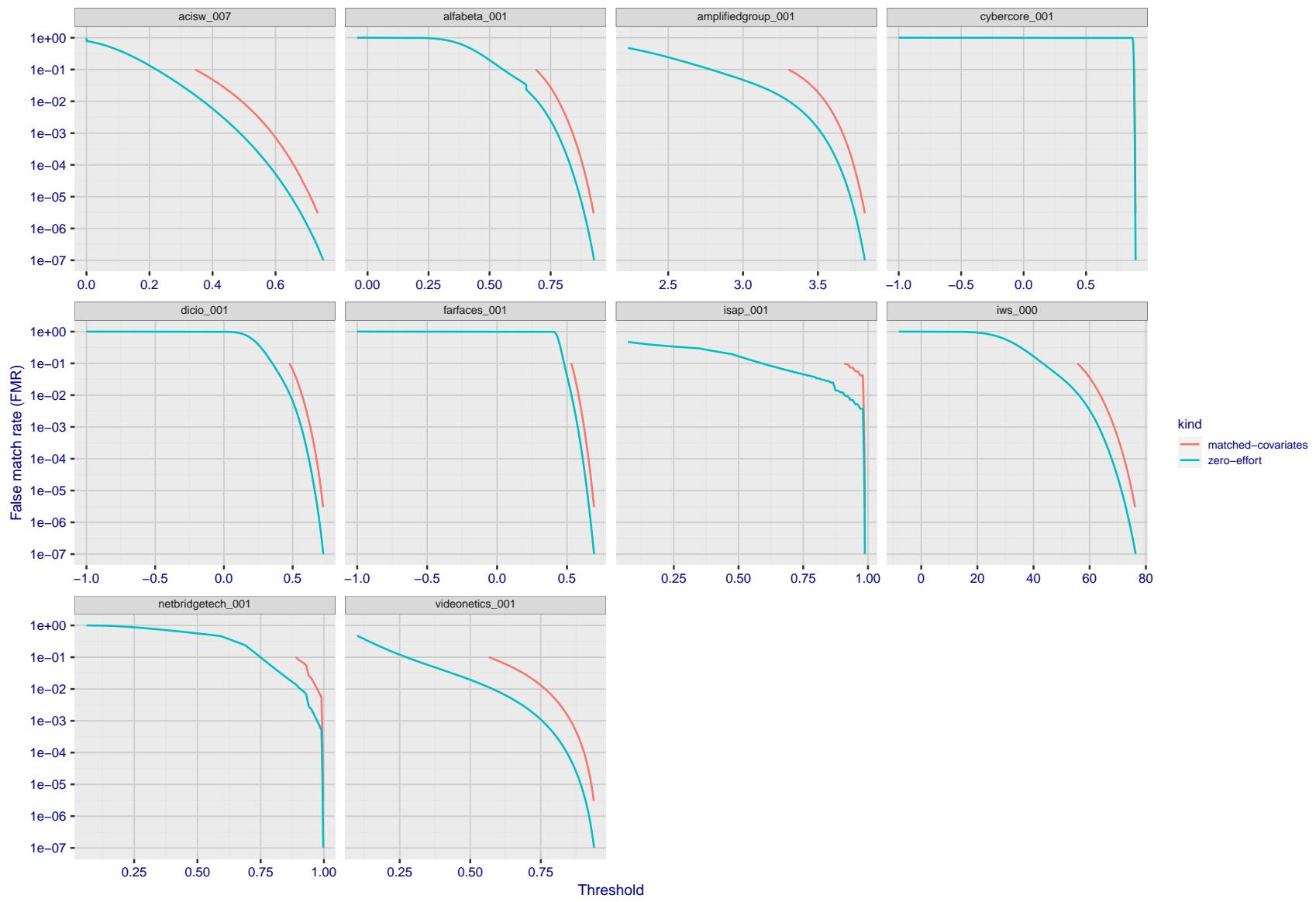


Figure 239: For the visa images, the false match calibration curves show FMR vs. threshold,  $T$ . The blue (lower) curves are for zero-effort impostors (i.e. comparing all images against all). The red (upper) curves are for persons of the same-sex, same-age, and same national-origin. This shows that FMR is underestimated (by a factor of 10 or more) by using a zero-effort impostor calculation to calibrate  $T$ . As shown later (sec. 3.6), FMR is higher for demographic-matched impostors.

FNMR( $T$ )

"False non-match rate"

"False match rate"

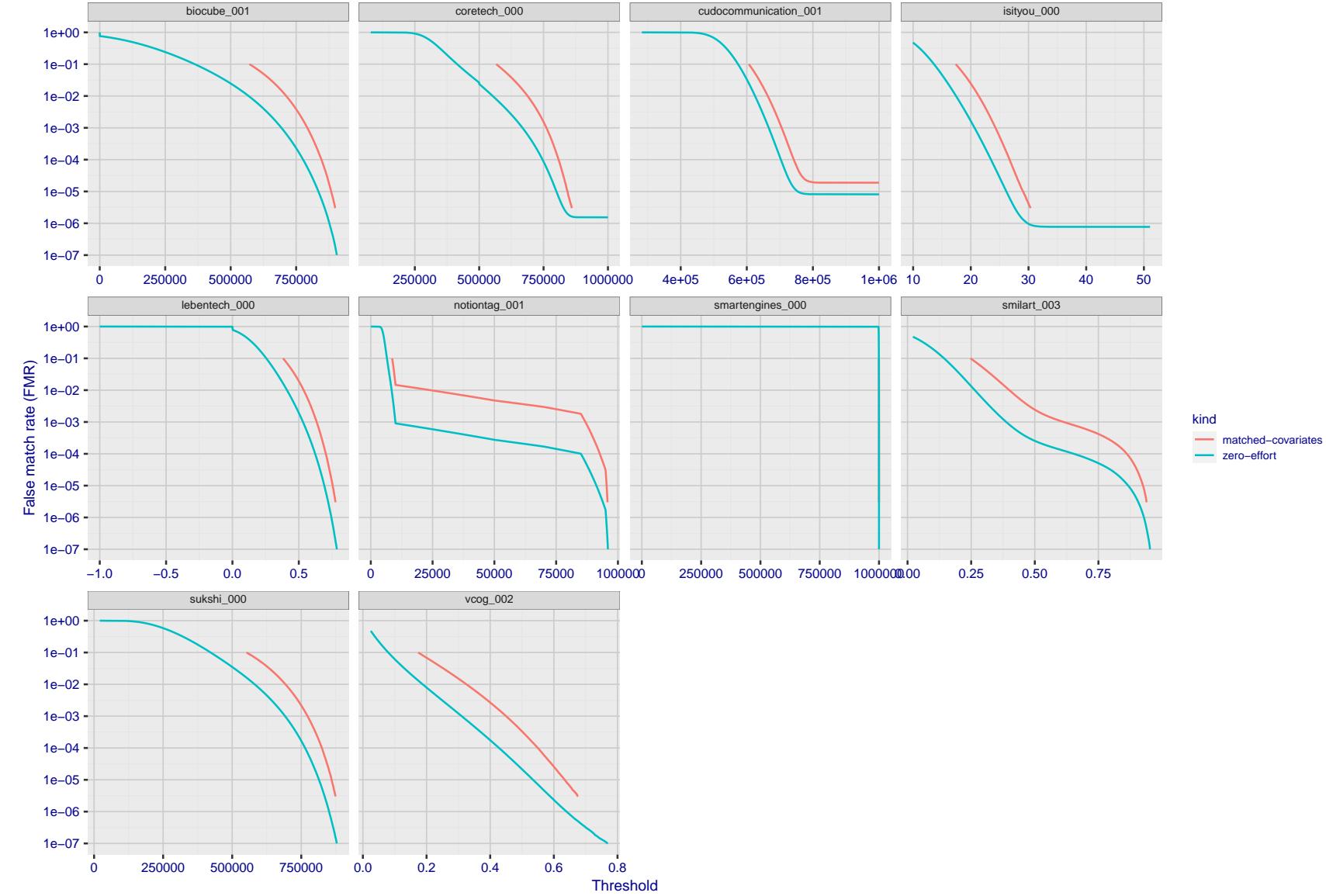


Figure 240: For the visa images, the false match calibration curves show FMR vs. threshold,  $T$ . The blue (lower) curves are for zero-effort impostors (i.e. comparing all images against all). The red (upper) curves are for persons of the same-sex, same-age, and same national-origin. This shows that FMR is underestimated (by a factor of 10 or more) by using a zero-effort impostor calculation to calibrate  $T$ . As shown later (sec. 3.6), FMR is higher for demographic-matched impostors.

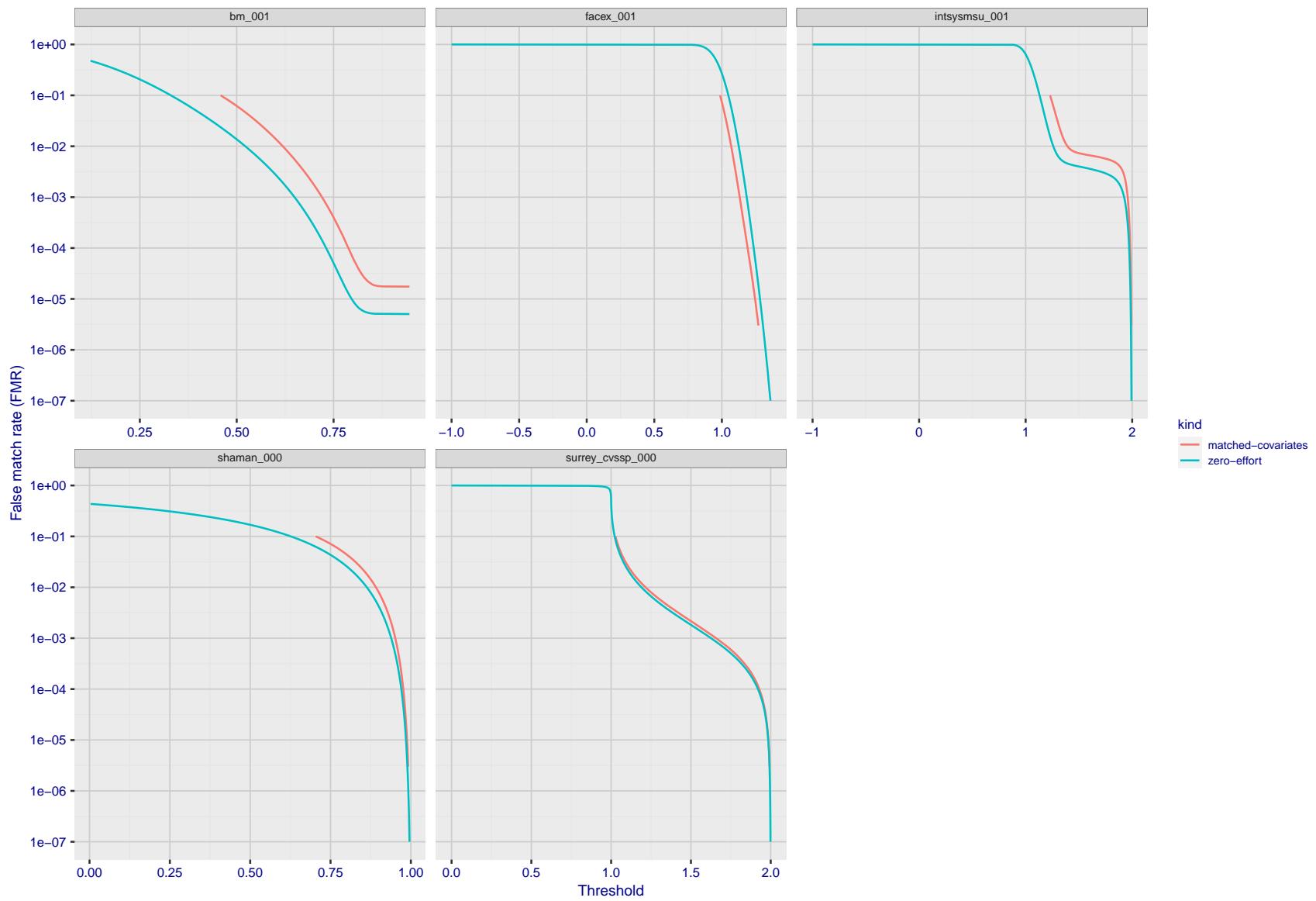


Figure 241: For the visa images, the false match calibration curves show FMR vs. threshold,  $T$ . The blue (lower) curves are for zero-effort impostors (i.e. comparing all images against all). The red (upper) curves are for persons of the same-sex, same-age, and same national-origin. This shows that FMR is underestimated (by a factor of 10 or more) by using a zero-effort impostor calculation to calibrate  $T$ . As shown later (sec. 3.6), FMR is higher for demographic-matched impostors.

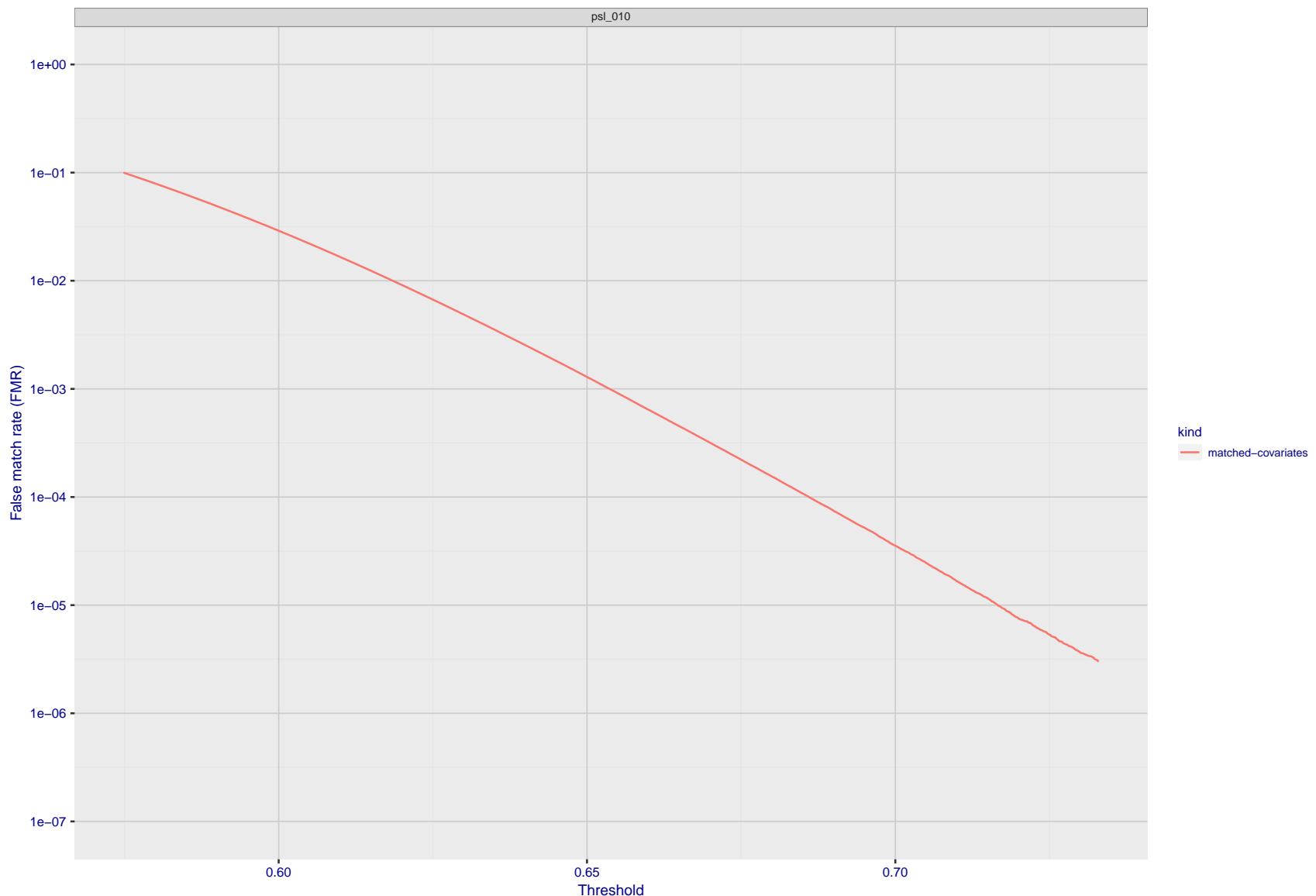


Figure 242: For the visa images, the false match calibration curves show FMR vs. threshold,  $T$ . The blue (lower) curves are for zero-effort impostors (i.e. comparing all images against all). The red (upper) curves are for persons of the same-sex, same-age, and same national-origin. This shows that FMR is underestimated (by a factor of 10 or more) by using a zero-effort impostor calculation to calibrate  $T$ . As shown later (sec. 3.6), FMR is higher for demographic-matched impostors.

## 3.5 Genuine distribution stability

### 3.5.1 Effect of birth place on the genuine distribution

**Background:** Both skin tone and bone structure vary geographically. Prior studies have reported variations in FNMR and FMR.

**Goal:** To measure false non-match rate (FNMR) variation with country of birth.

**Methods:** Thresholds are determined that give  $FMR = \{0.001, 0.0001\}$  over the entire impostor set. Then FNMR is measured over 1000 bootstrap replications of the genuine scores. Only those countries with at least 140 individuals are included in the analysis.

**Results:** Figure 277 shows FNMR by country of birth for the two thresholds.

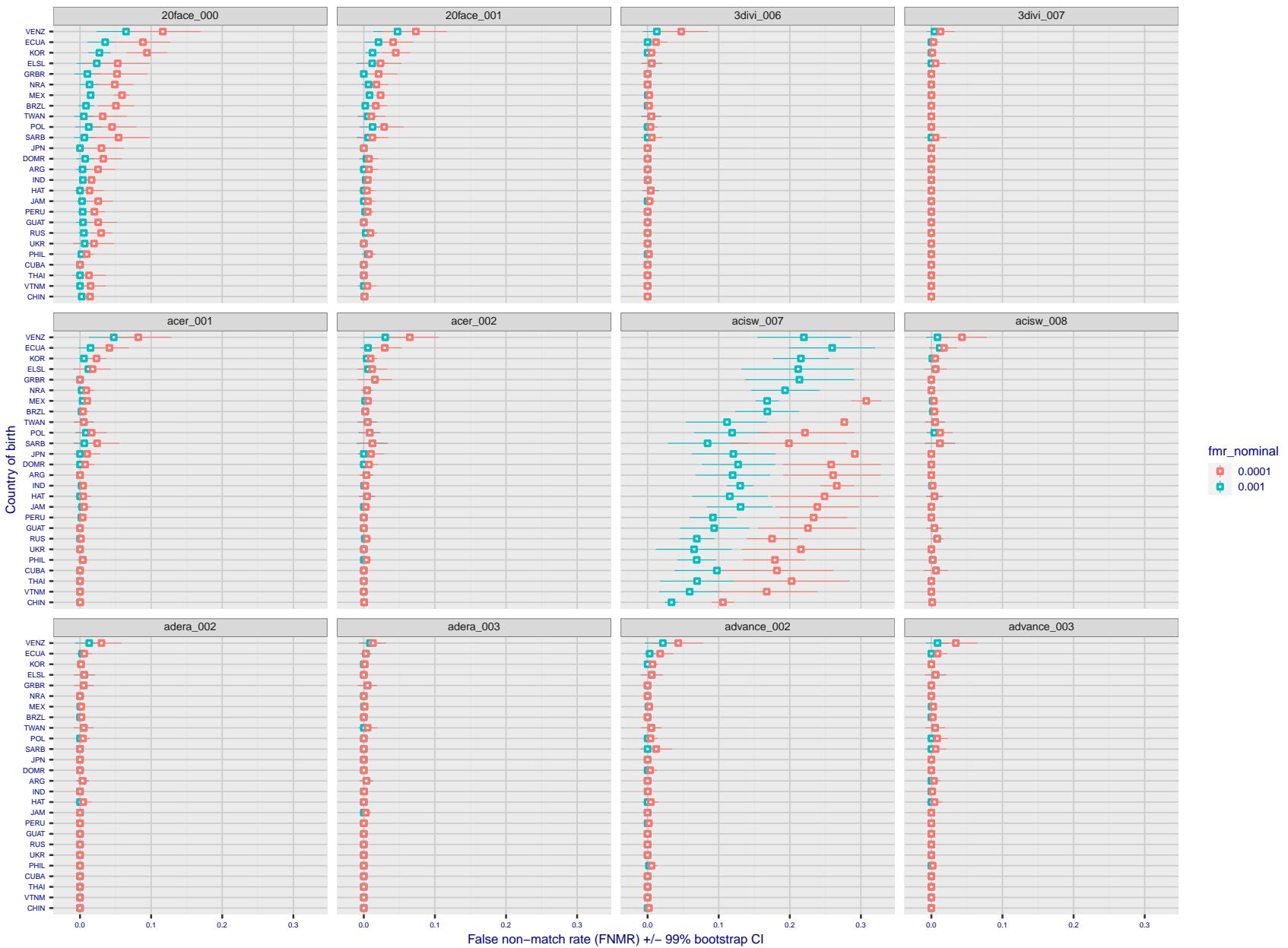


Figure 243: For the visa images, the dots show FNMR by country of birth for two globally set operating thresholds corresponding to  $FMR = \{0.001, 0.0001\}$  computed over all on the order of  $10^{10}$  impostor scores. The FMR in each bin will vary also - see subsequent impostor heatmaps in sec. 3.6.1. The figures shows an order of magnitude variation in FNMR across country of birth; these effects are likely due quality variations, then demographics like age and race. The error rates in some cases are zero, and in others the DET is flat so the error rates at the two thresholds are identical. The lines span 1% and 99% of bootstrap replicated FNMR estimates.

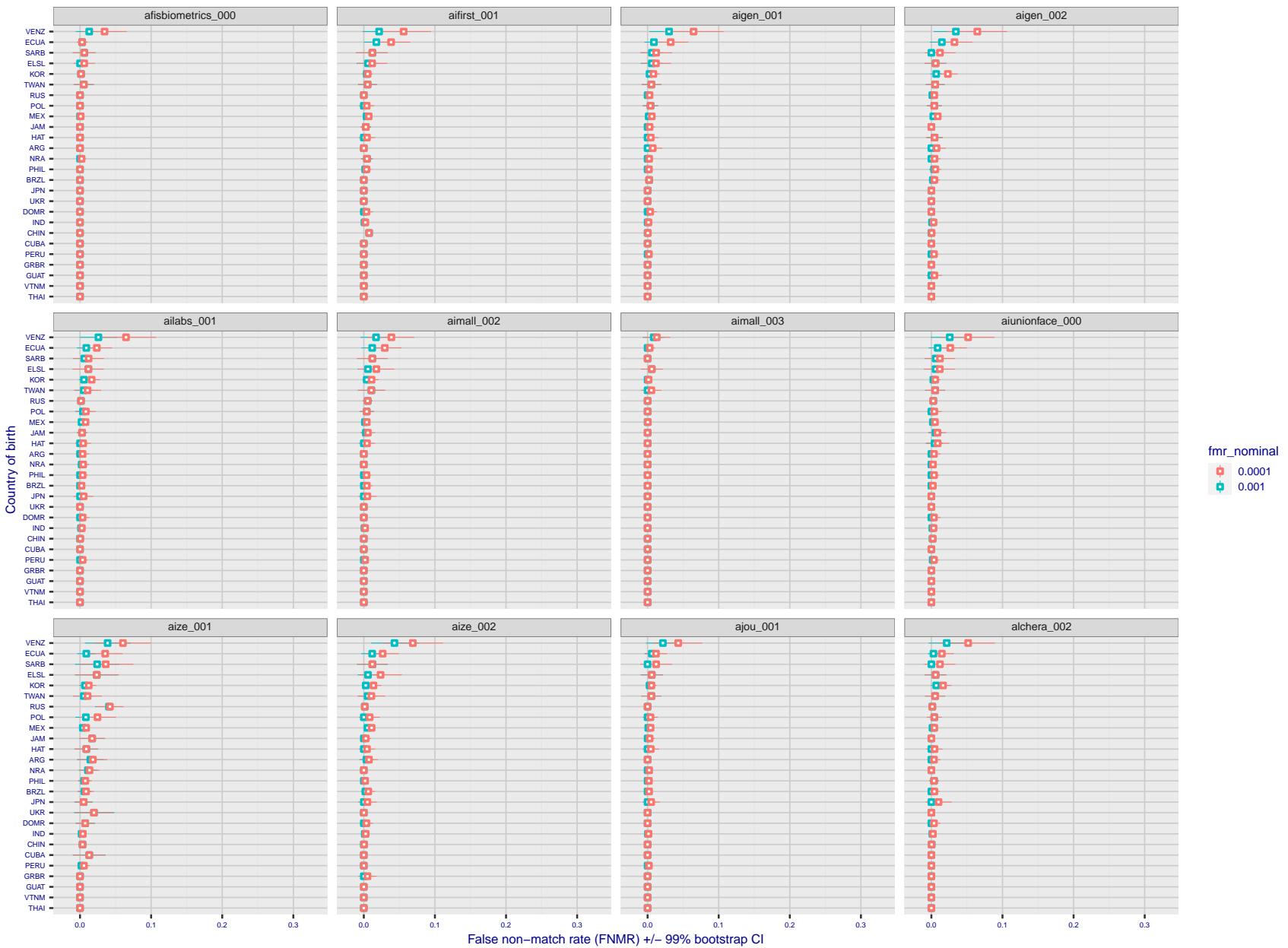


Figure 244: For the visa images, the dots show FNMR by country of birth for two globally set operating thresholds corresponding to  $FMR = \{0.001, 0.0001\}$  computed over all on the order of  $10^{10}$  impostor scores. The FMR in each bin will vary also - see subsequent impostor heatmaps in sec. 3.6.1. The figures shows an order of magnitude variation in FNMR across country of birth; these effects are likely due quality variations, then demographics like age and race. The error rates in some cases are zero, and in others the DET is flat so the error rates at the two thresholds are identical. The lines span 1% and 99% of bootstrap replicated FNMR estimates.

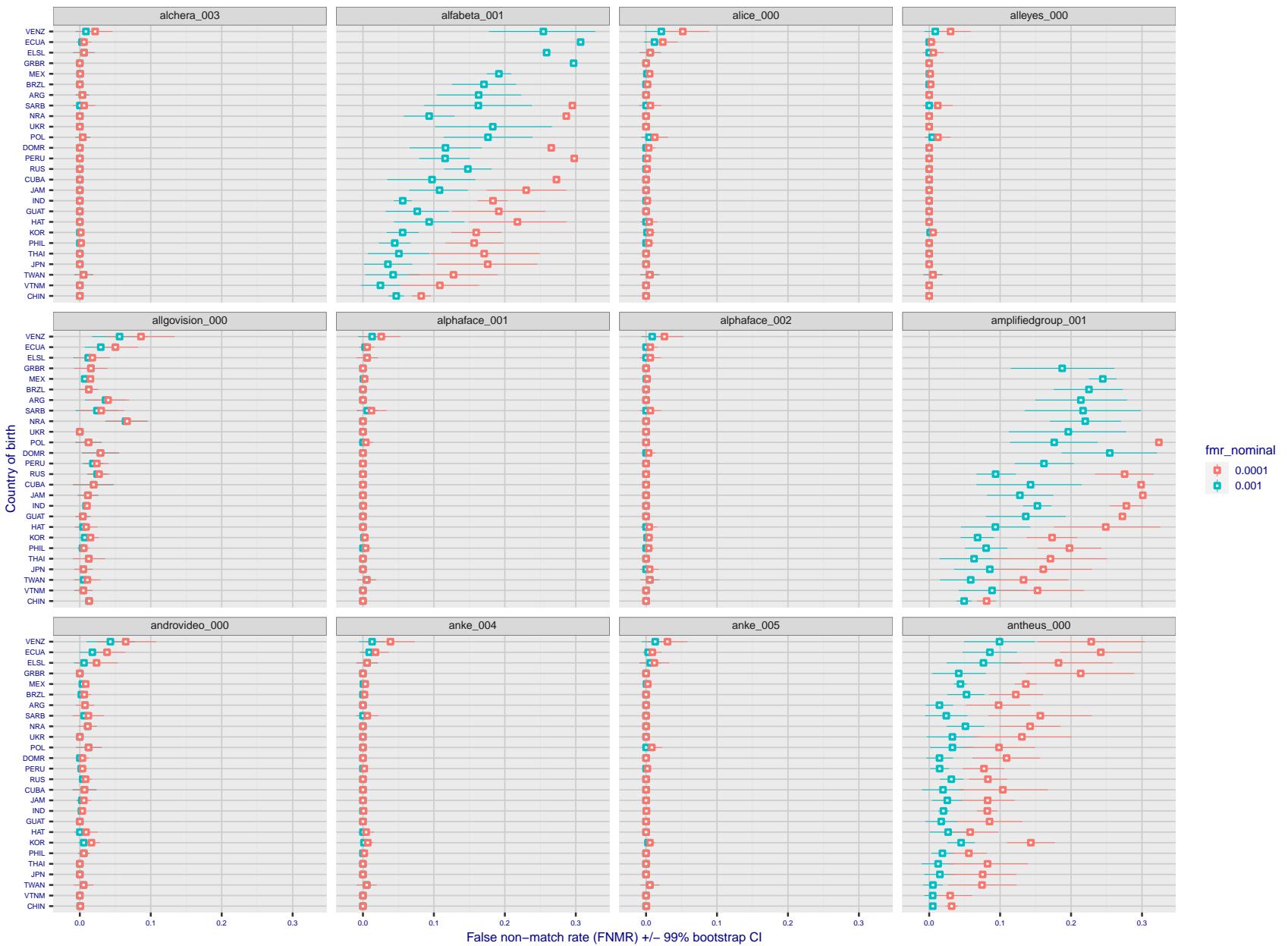


Figure 245: For the visa images, the dots show FNMR by country of birth for two globally set operating thresholds corresponding to  $FMR = \{0.001, 0.0001\}$  computed over all on the order of  $10^{10}$  impostor scores. The FMR in each bin will vary also - see subsequent impostor heatmaps in sec. 3.6.1. The figures shows an order of magnitude variation in FNMR across country of birth; these effects are likely due quality variations, then demographics like age and race. The error rates in some cases are zero, and in others the DET is flat so the error rates at the two thresholds are identical. The lines span 1% and 99% of bootstrap replicated FNMR estimates.

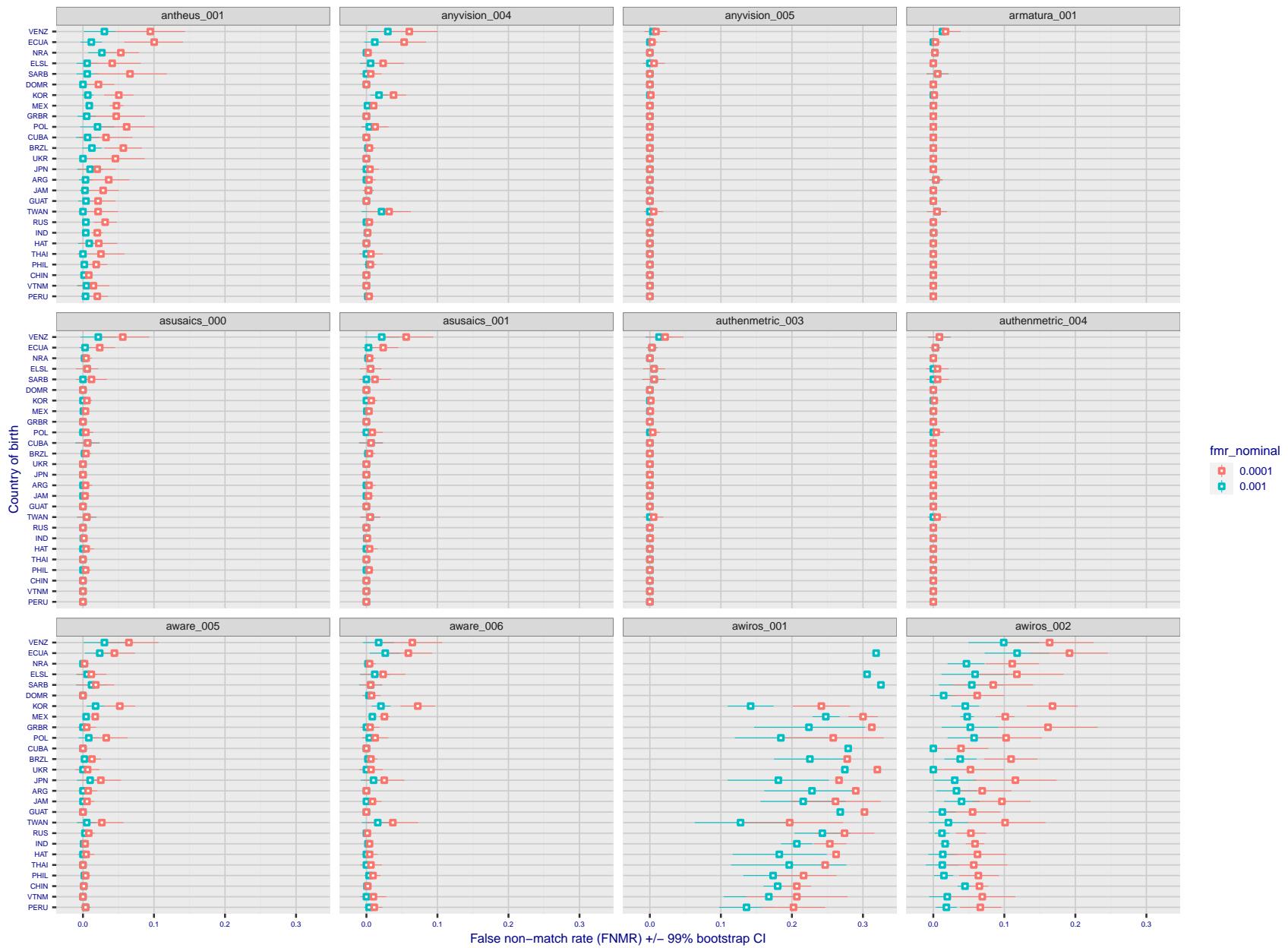


Figure 246: For the visa images, the dots show FNMR by country of birth for two globally set operating thresholds corresponding to  $FMR = \{0.001, 0.0001\}$  computed over all on the order of  $10^{10}$  impostor scores. The FMR in each bin will vary also - see subsequent impostor heatmaps in sec. 3.6.1. The figures shows an order of magnitude variation in FNMR across country of birth; these effects are likely due quality variations, then demographics like age and race. The error rates in some cases are zero, and in others the DET is flat so the error rates at the two thresholds are identical. The lines span 1% and 99% of bootstrap replicated FNMR estimates.

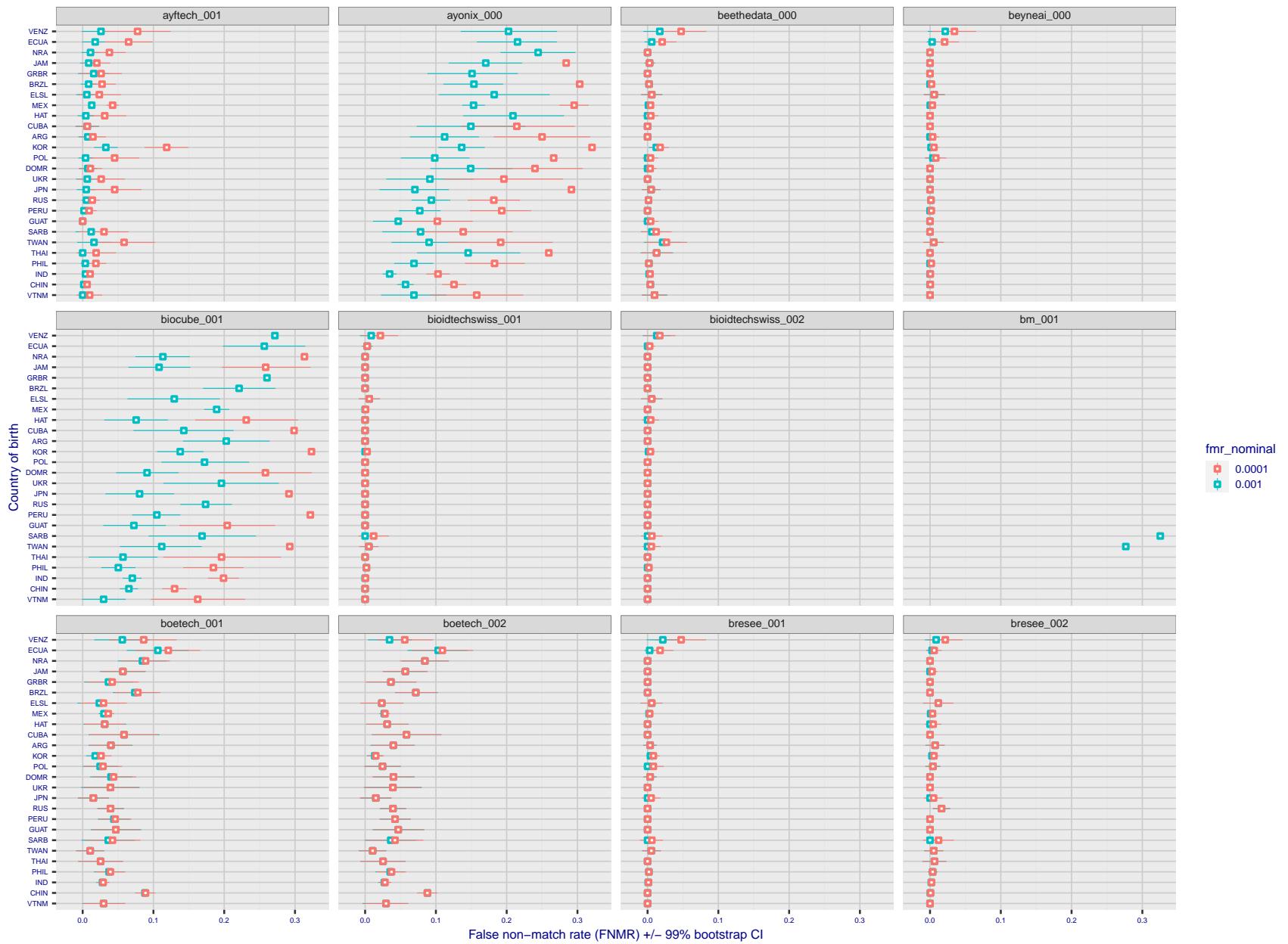


Figure 247: For the visa images, the dots show FNMR by country of birth for two globally set operating thresholds corresponding to  $FMR = \{0.001, 0.0001\}$  computed over all on the order of  $10^{10}$  impostor scores. The FMR in each bin will vary also - see subsequent impostor heatmaps in sec. 3.6.1. The figures shows an order of magnitude variation in FNMR across country of birth; these effects are likely due quality variations, then demographics like age and race. The error rates in some cases are zero, and in others the DET is flat so the error rates at the two thresholds are identical. The lines span 1% and 99% of bootstrap replicated FNMR estimates.

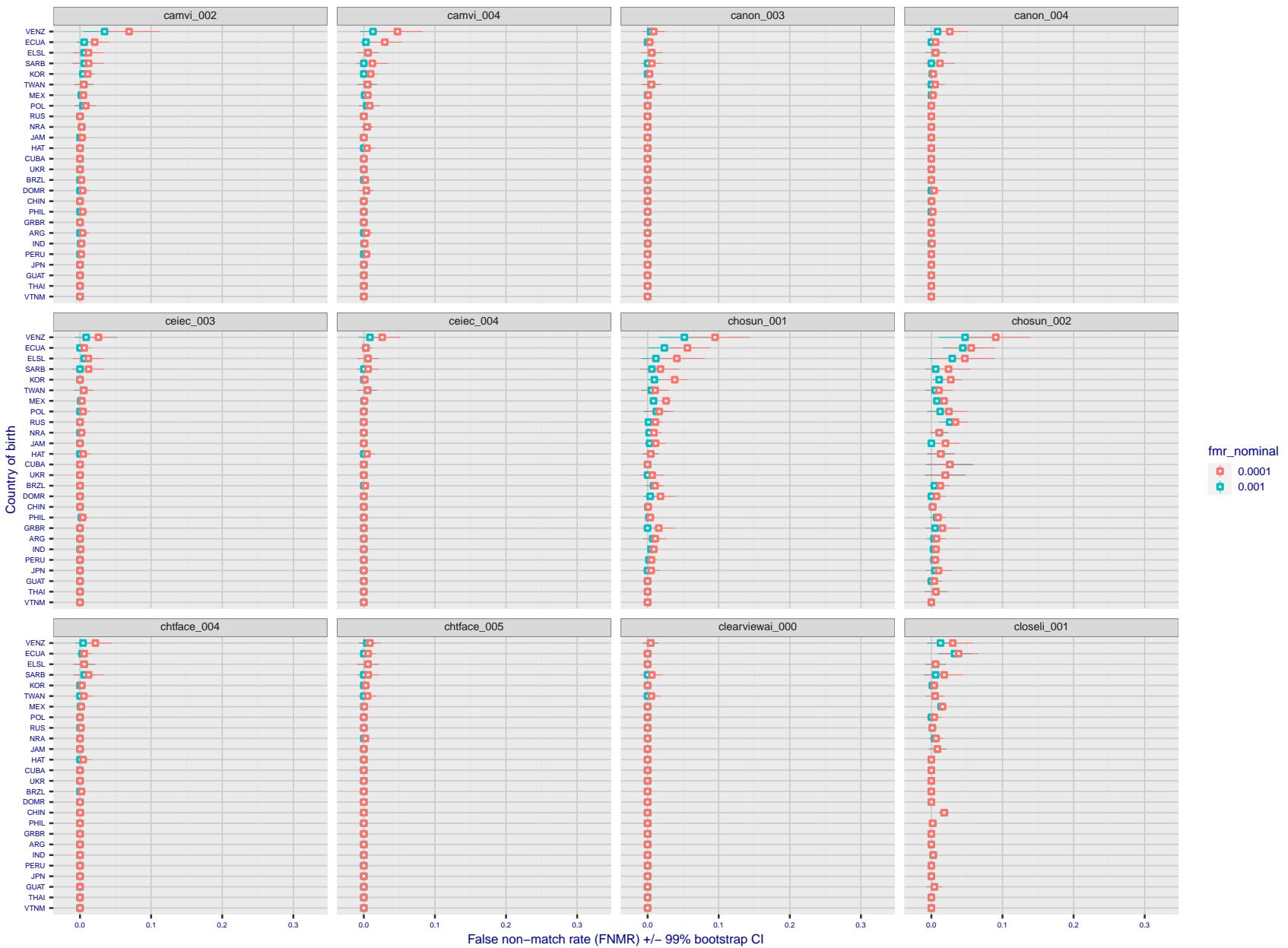


Figure 248: For the visa images, the dots show FNMR by country of birth for two globally set operating thresholds corresponding to  $FMR = \{0.001, 0.0001\}$  computed over all on the order of  $10^{10}$  impostor scores. The FMR in each bin will vary also - see subsequent impostor heatmaps in sec. 3.6.1. The figures shows an order of magnitude variation in FNMR across country of birth; these effects are likely due quality variations, then demographics like age and race. The error rates in some cases are zero, and in others the DET is flat so the error rates at the two thresholds are identical. The lines span 1% and 99% of bootstrap replicated FNMR estimates.

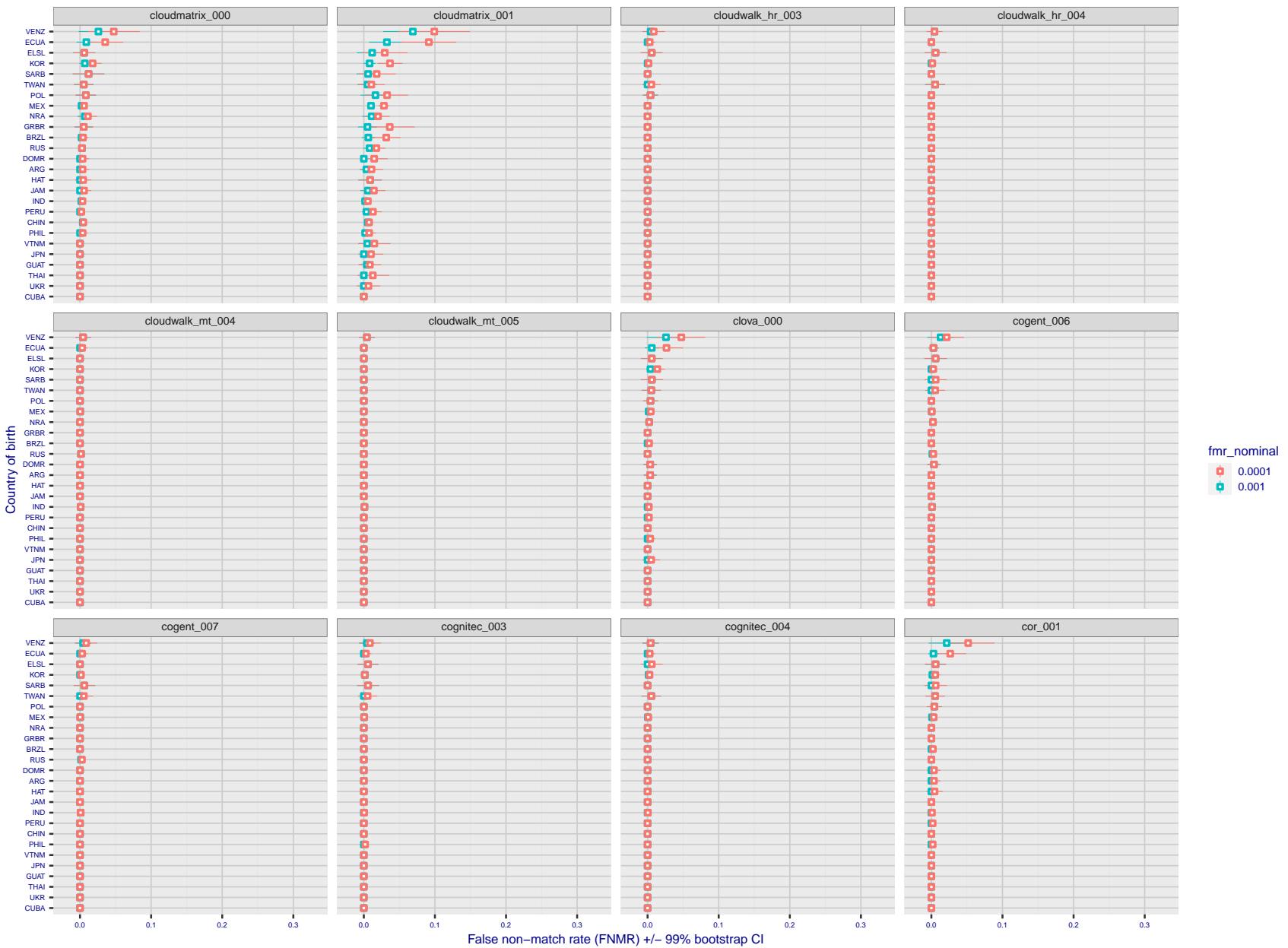


Figure 249: For the visa images, the dots show FNMR by country of birth for two globally set operating thresholds corresponding to  $FMR = \{0.001, 0.0001\}$  computed over all on the order of  $10^{10}$  impostor scores. The FMR in each bin will vary also - see subsequent impostor heatmaps in sec. 3.6.1. The figures shows an order of magnitude variation in FNMR across country of birth; these effects are likely due quality variations, then demographics like age and race. The error rates in some cases are zero, and in others the DET is flat so the error rates at the two thresholds are identical. The lines span 1% and 99% of bootstrap replicated FNMR estimates.

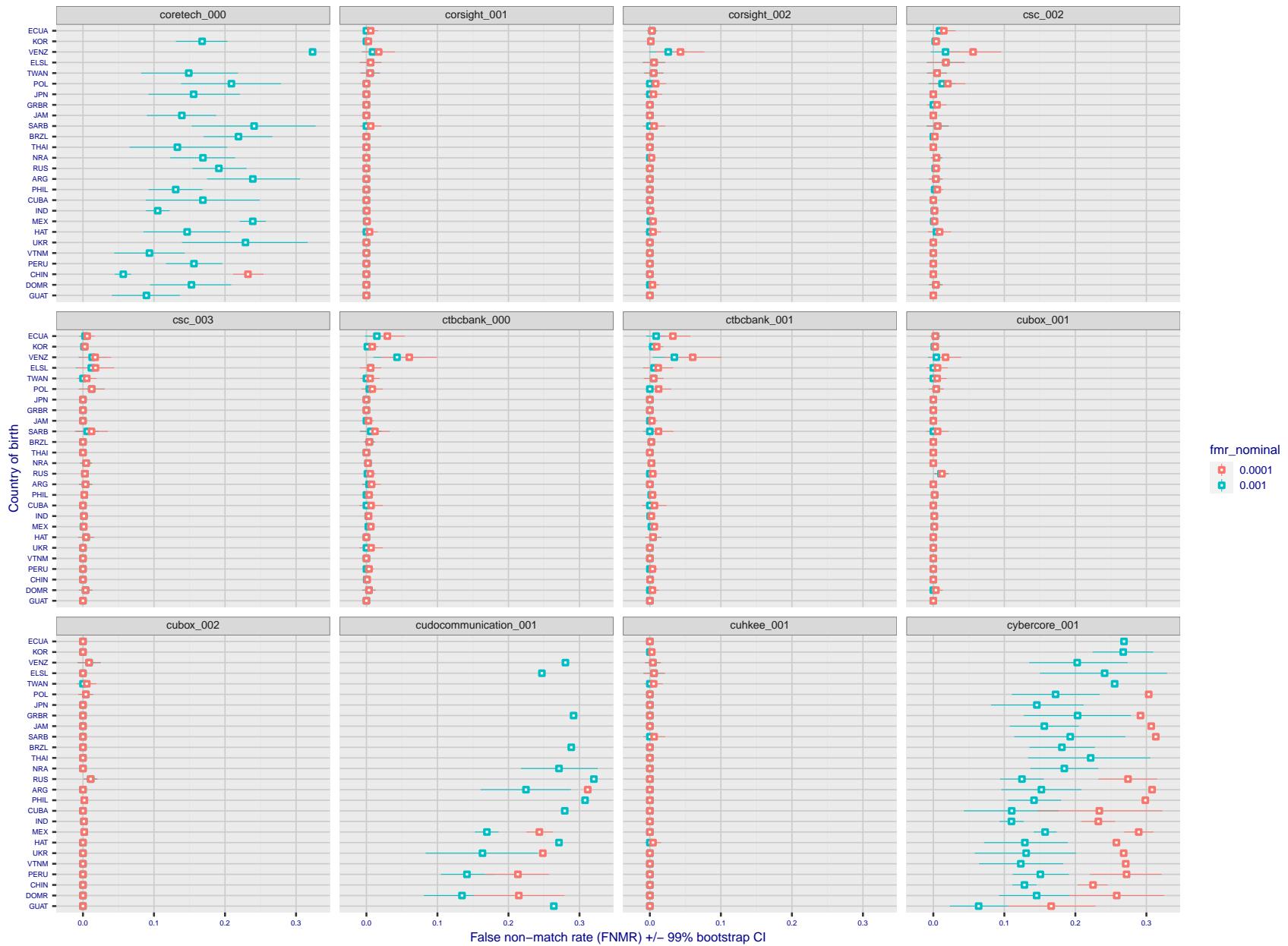


Figure 250: For the visa images, the dots show FNMR by country of birth for two globally set operating thresholds corresponding to  $FMR = \{0.001, 0.0001\}$  computed over all on the order of  $10^{10}$  impostor scores. The FMR in each bin will vary also - see subsequent impostor heatmaps in sec. 3.6.1. The figures shows an order of magnitude variation in FNMR across country of birth; these effects are likely due quality variations, then demographics like age and race. The error rates in some cases are zero, and in others the DET is flat so the error rates at the two thresholds are identical. The lines span 1% and 99% of bootstrap replicated FNMR estimates.

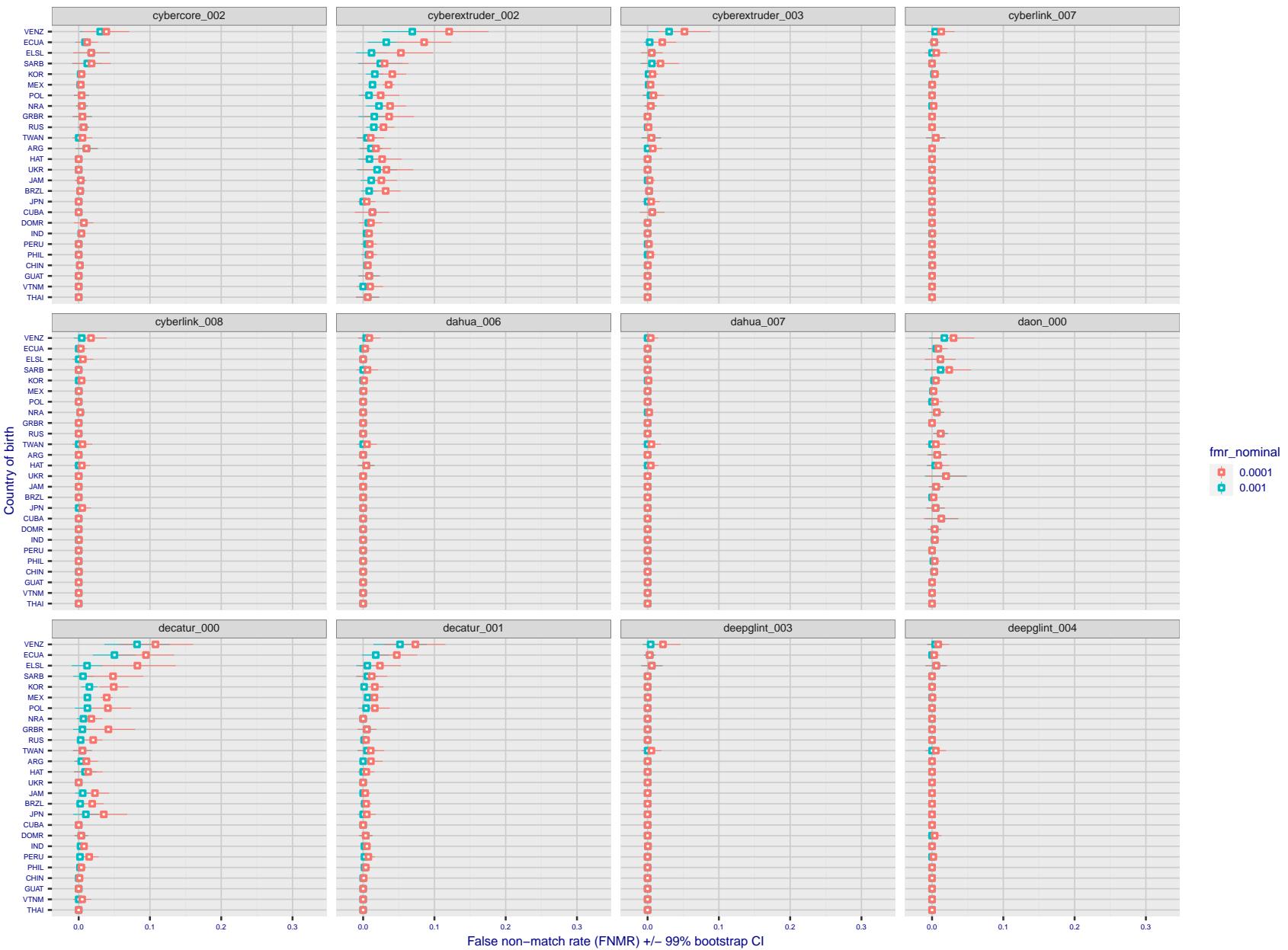


Figure 251: For the visa images, the dots show FNMR by country of birth for two globally set operating thresholds corresponding to  $FMR = \{0.001, 0.0001\}$  computed over all on the order of  $10^{10}$  impostor scores. The FMR in each bin will vary also - see subsequent impostor heatmaps in sec. 3.6.1. The figures shows an order of magnitude variation in FNMR across country of birth; these effects are likely due quality variations, then demographics like age and race. The error rates in some cases are zero, and in others the DET is flat so the error rates at the two thresholds are identical. The lines span 1% and 99% of bootstrap replicated FNMR estimates.

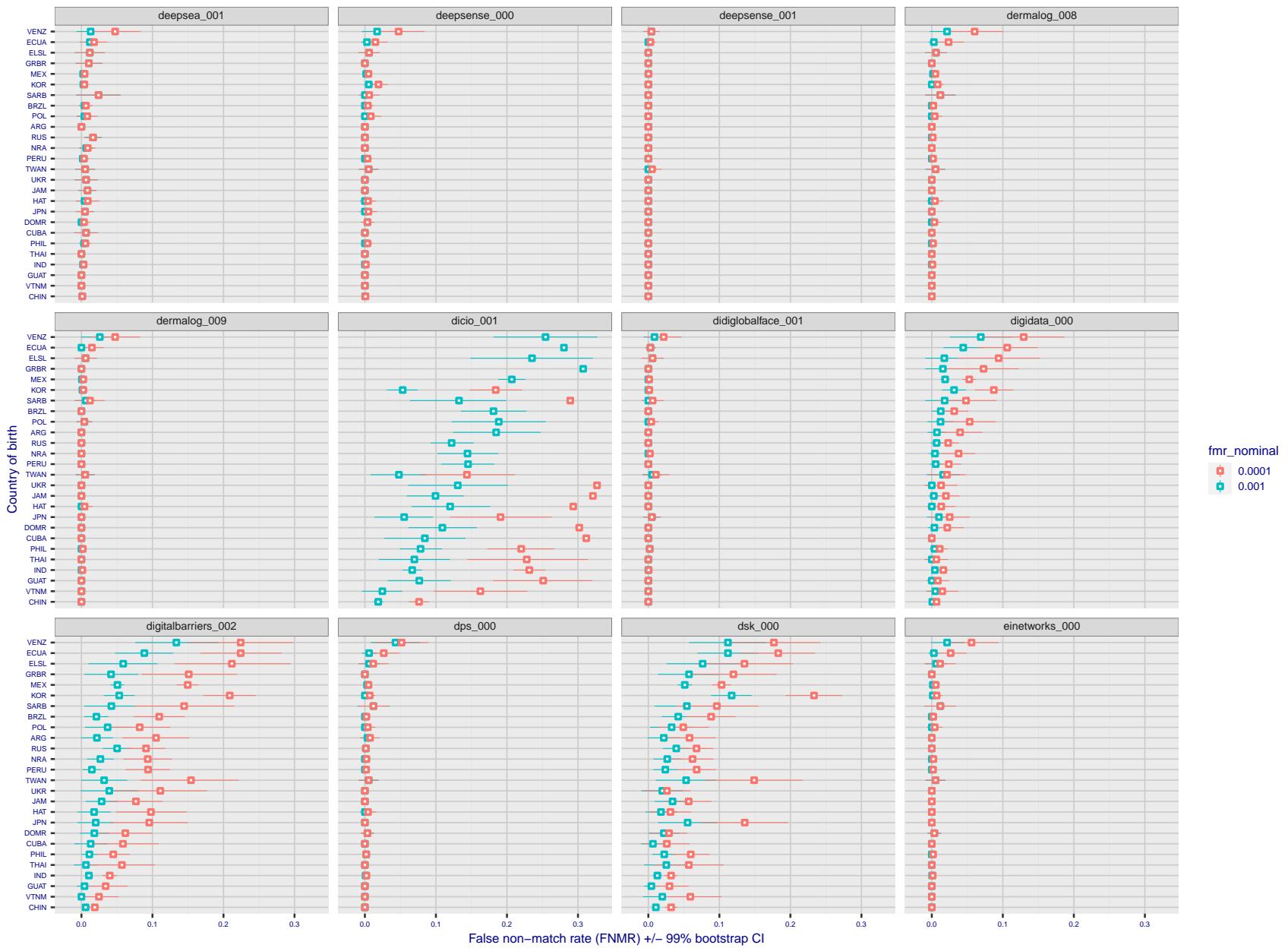


Figure 252: For the visa images, the dots show FNMR by country of birth for two globally set operating thresholds corresponding to  $FMR = \{0.001, 0.0001\}$  computed over all on the order of  $10^{10}$  impostor scores. The FMR in each bin will vary also - see subsequent impostor heatmaps in sec. 3.6.1. The figures shows an order of magnitude variation in FNMR across country of birth; these effects are likely due quality variations, then demographics like age and race. The error rates in some cases are zero, and in others the DET is flat so the error rates at the two thresholds are identical. The lines span 1% and 99% of bootstrap replicated FNMR estimates.

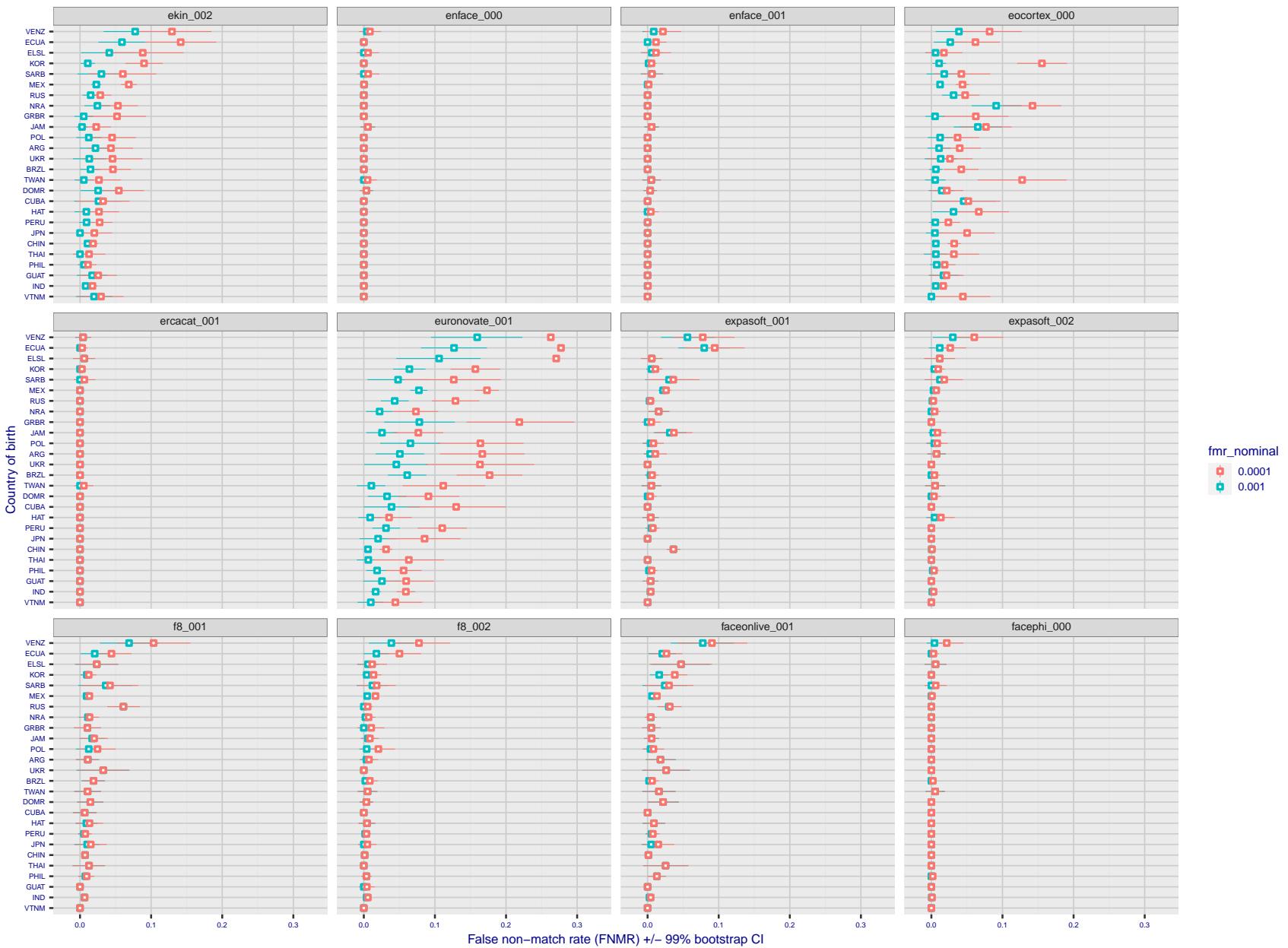


Figure 253: For the visa images, the dots show FNMR by country of birth for two globally set operating thresholds corresponding to  $FMR = \{0.001, 0.0001\}$  computed over all on the order of  $10^{10}$  impostor scores. The FMR in each bin will vary also - see subsequent impostor heatmaps in sec. 3.6.1. The figures shows an order of magnitude variation in FNMR across country of birth; these effects are likely due quality variations, then demographics like age and race. The error rates in some cases are zero, and in others the DET is flat so the error rates at the two thresholds are identical. The lines span 1% and 99% of bootstrap replicated FNMR estimates.

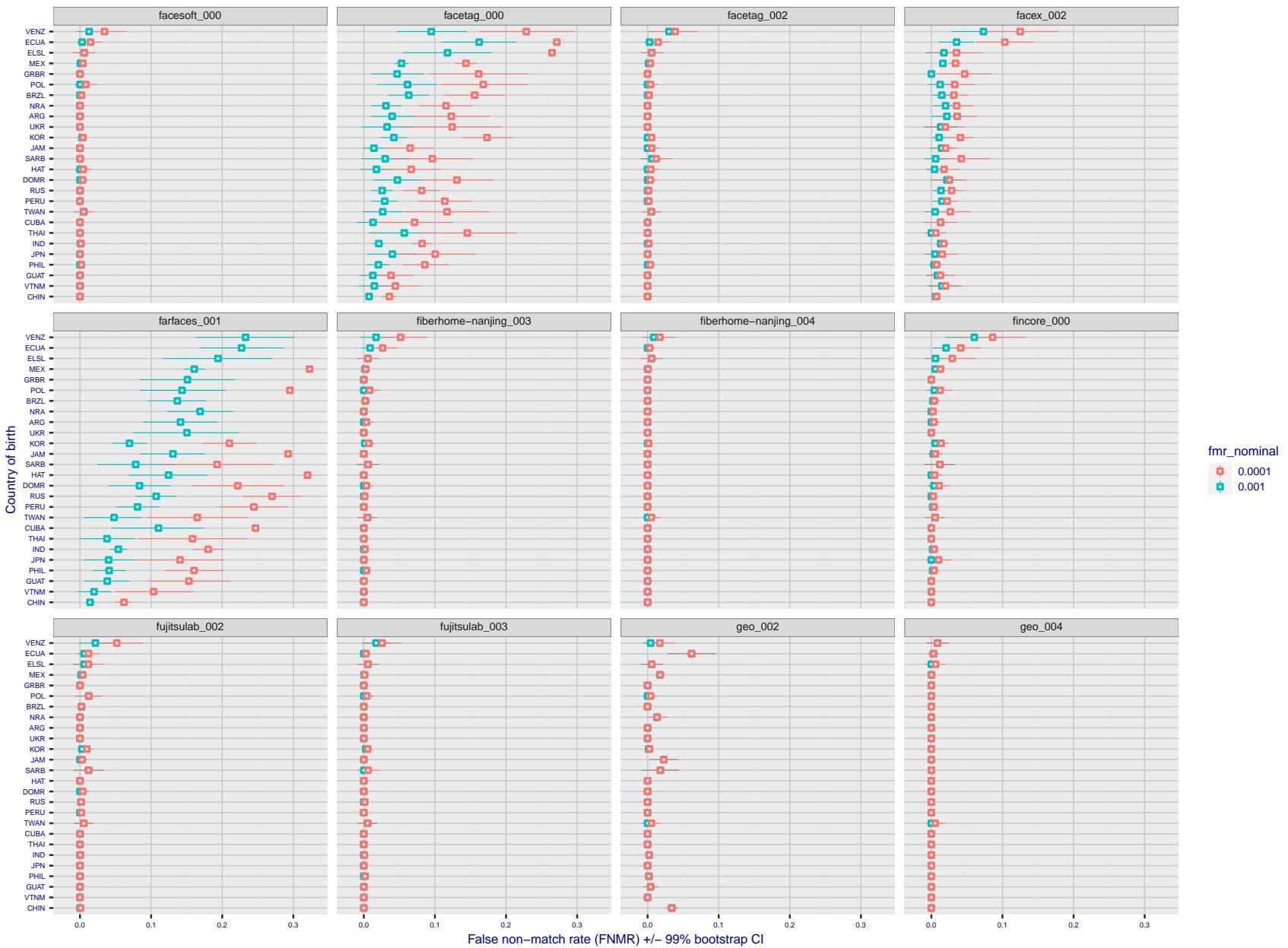


Figure 254: For the visa images, the dots show FNMR by country of birth for two globally set operating thresholds corresponding to  $FMR = \{0.001, 0.0001\}$  computed over all on the order of  $10^{10}$  impostor scores. The FMR in each bin will vary also - see subsequent impostor heatmaps in sec. 3.6.1. The figures shows an order of magnitude variation in FNMR across country of birth; these effects are likely due quality variations, then demographics like age and race. The error rates in some cases are zero, and in others the DET is flat so the error rates at the two thresholds are identical. The lines span 1% and 99% of bootstrap replicated FNMR estimates.

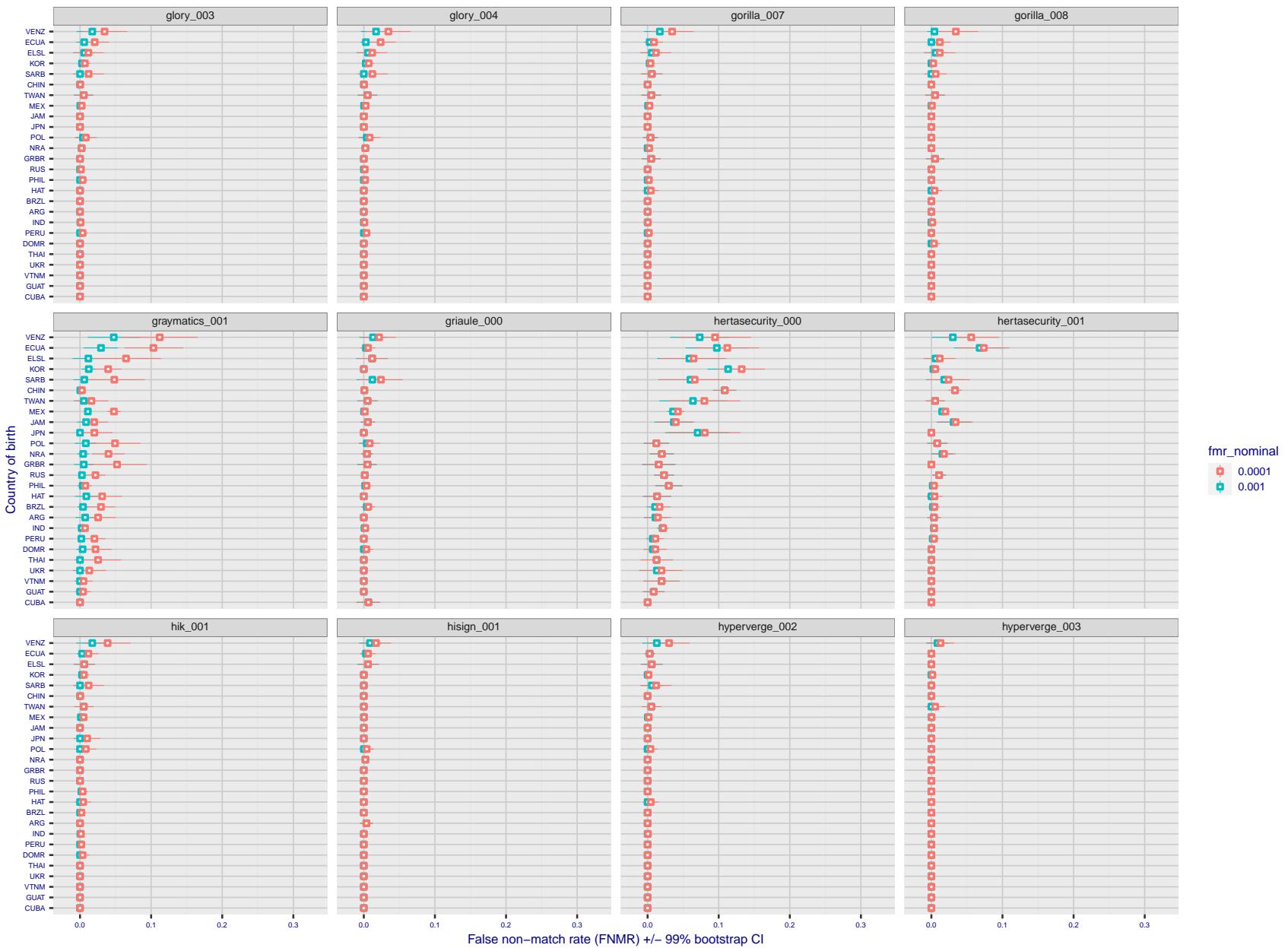


Figure 255: For the visa images, the dots show FNMR by country of birth for two globally set operating thresholds corresponding to  $FMR = \{0.001, 0.0001\}$  computed over all on the order of  $10^{10}$  impostor scores. The FMR in each bin will vary also - see subsequent impostor heatmaps in sec. 3.6.1. The figures shows an order of magnitude variation in FNMR across country of birth; these effects are likely due quality variations, then demographics like age and race. The error rates in some cases are zero, and in others the DET is flat so the error rates at the two thresholds are identical. The lines span 1% and 99% of bootstrap replicated FNMR estimates.

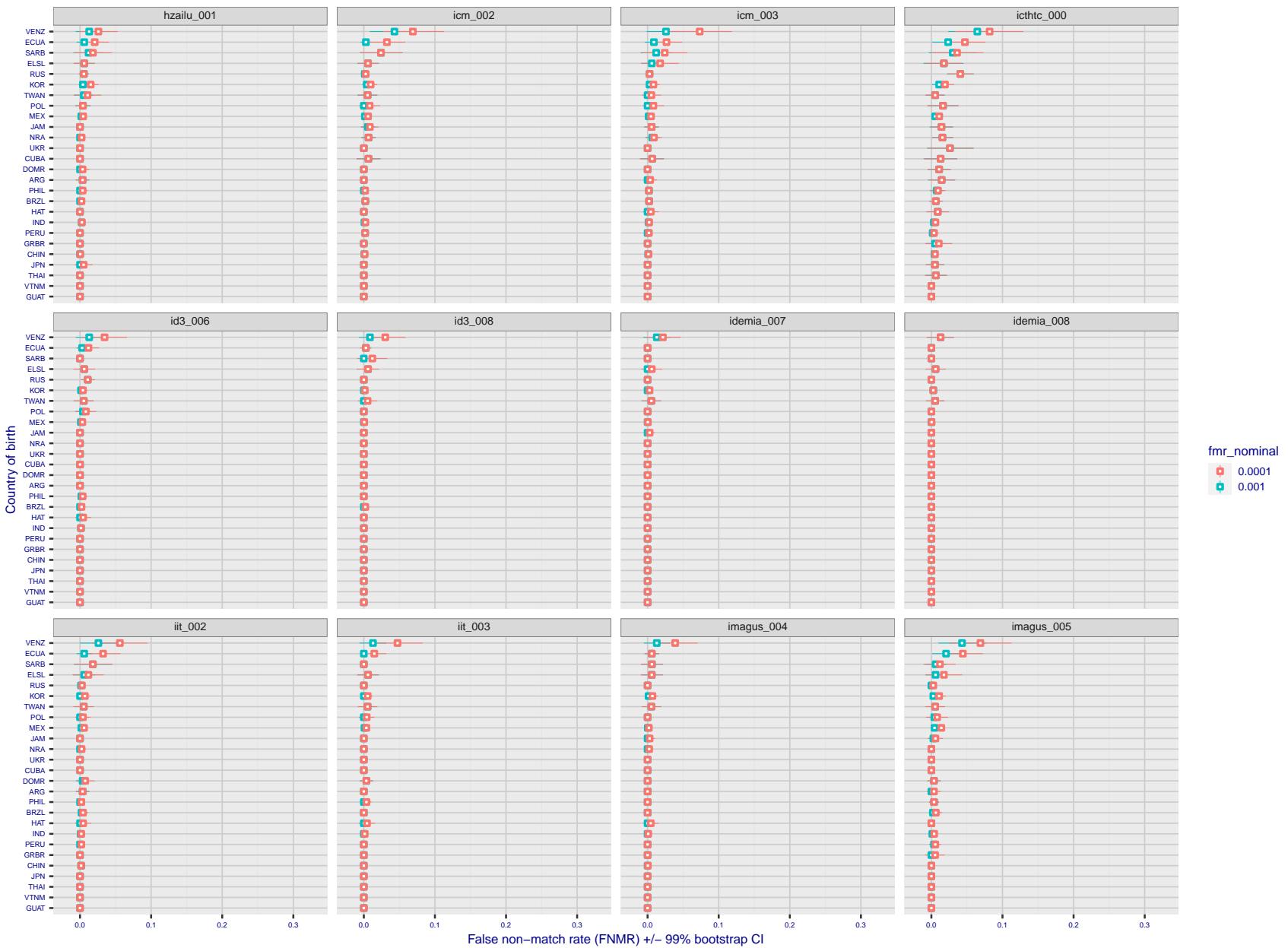


Figure 256: For the visa images, the dots show FNMR by country of birth for two globally set operating thresholds corresponding to  $FMR = \{0.001, 0.0001\}$  computed over all on the order of  $10^{10}$  impostor scores. The FMR in each bin will vary also - see subsequent impostor heatmaps in sec. 3.6.1. The figures shows an order of magnitude variation in FNMR across country of birth; these effects are likely due quality variations, then demographics like age and race. The error rates in some cases are zero, and in others the DET is flat so the error rates at the two thresholds are identical. The lines span 1% and 99% of bootstrap replicated FNMR estimates.

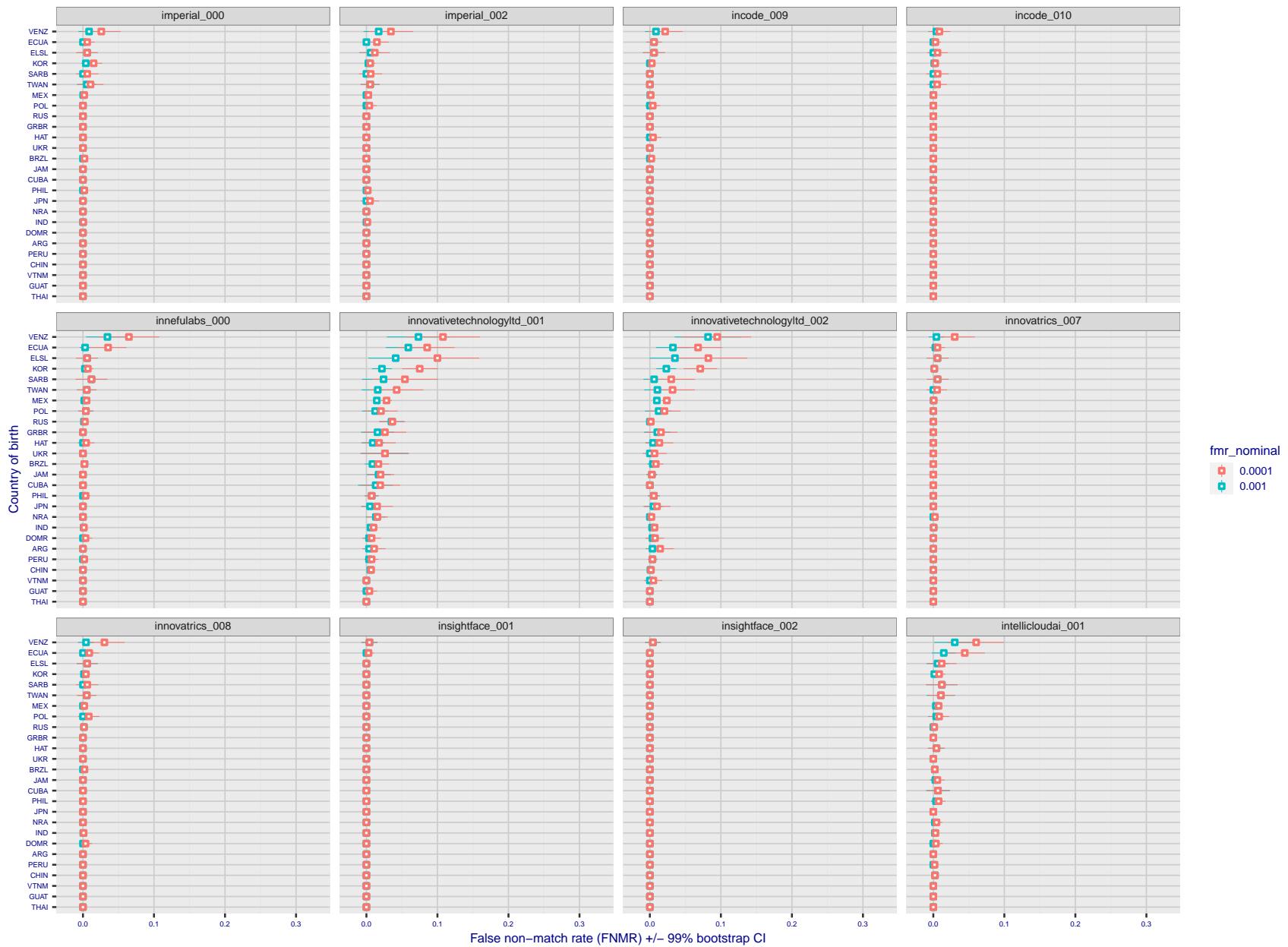


Figure 257: For the visa images, the dots show FNMR by country of birth for two globally set operating thresholds corresponding to  $FMR = \{0.001, 0.0001\}$  computed over all on the order of  $10^{10}$  impostor scores. The FMR in each bin will vary also - see subsequent impostor heatmaps in sec. 3.6.1. The figures shows an order of magnitude variation in FNMR across country of birth; these effects are likely due quality variations, then demographics like age and race. The error rates in some cases are zero, and in others the DET is flat so the error rates at the two thresholds are identical. The lines span 1% and 99% of bootstrap replicated FNMR estimates.

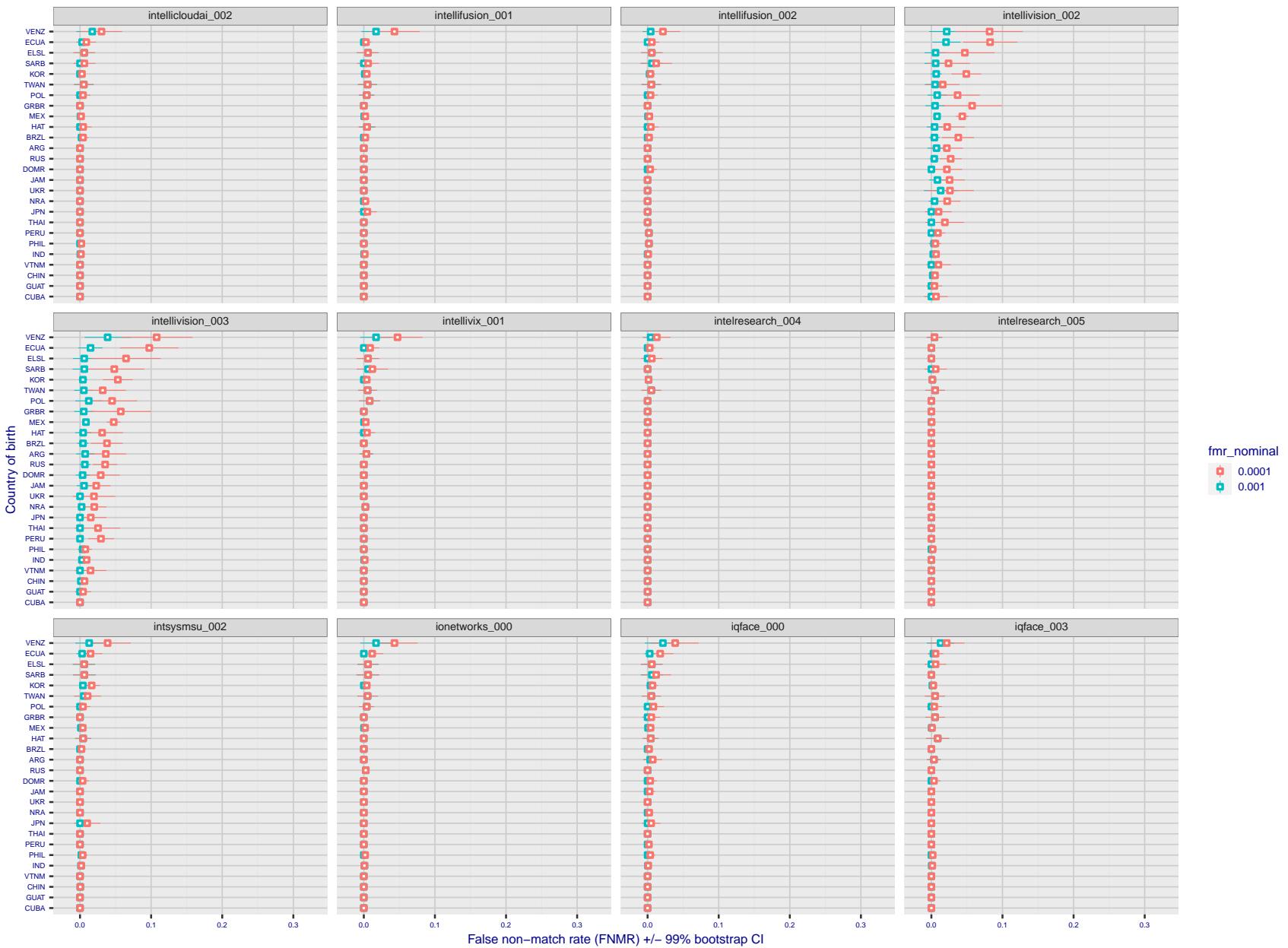


Figure 258: For the visa images, the dots show FNMR by country of birth for two globally set operating thresholds corresponding to  $FMR = \{0.001, 0.0001\}$  computed over all on the order of  $10^{10}$  impostor scores. The FMR in each bin will vary also - see subsequent impostor heatmaps in sec. 3.6.1. The figures shows an order of magnitude variation in FNMR across country of birth; these effects are likely due quality variations, then demographics like age and race. The error rates in some cases are zero, and in others the DET is flat so the error rates at the two thresholds are identical. The lines span 1% and 99% of bootstrap replicated FNMR estimates.

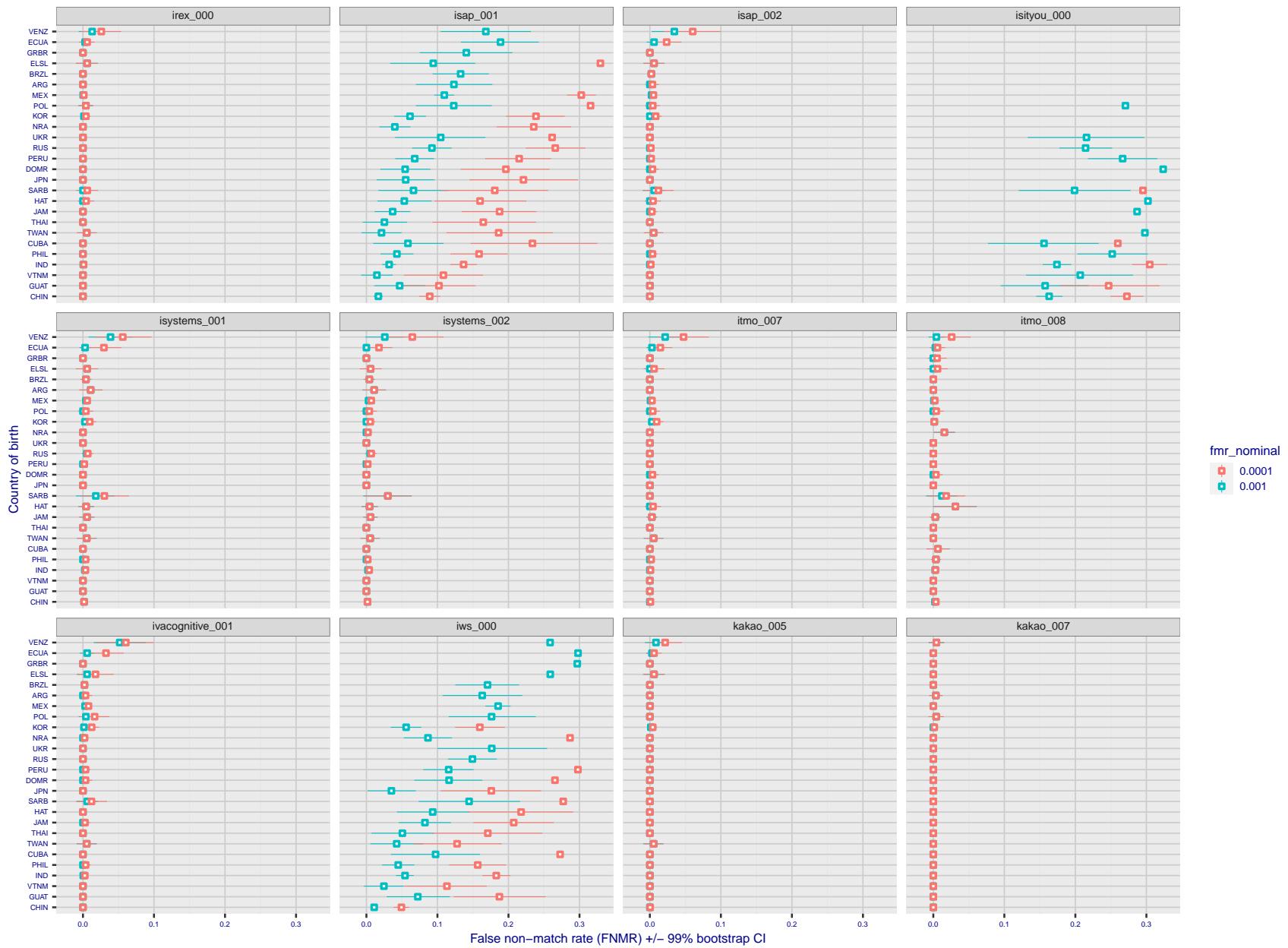


Figure 259: For the visa images, the dots show FNMR by country of birth for two globally set operating thresholds corresponding to  $FMR = \{0.001, 0.0001\}$  computed over all on the order of  $10^{10}$  impostor scores. The FMR in each bin will vary also - see subsequent impostor heatmaps in sec. 3.6.1. The figures shows an order of magnitude variation in FNMR across country of birth; these effects are likely due quality variations, then demographics like age and race. The error rates in some cases are zero, and in others the DET is flat so the error rates at the two thresholds are identical. The lines span 1% and 99% of bootstrap replicated FNMR estimates.

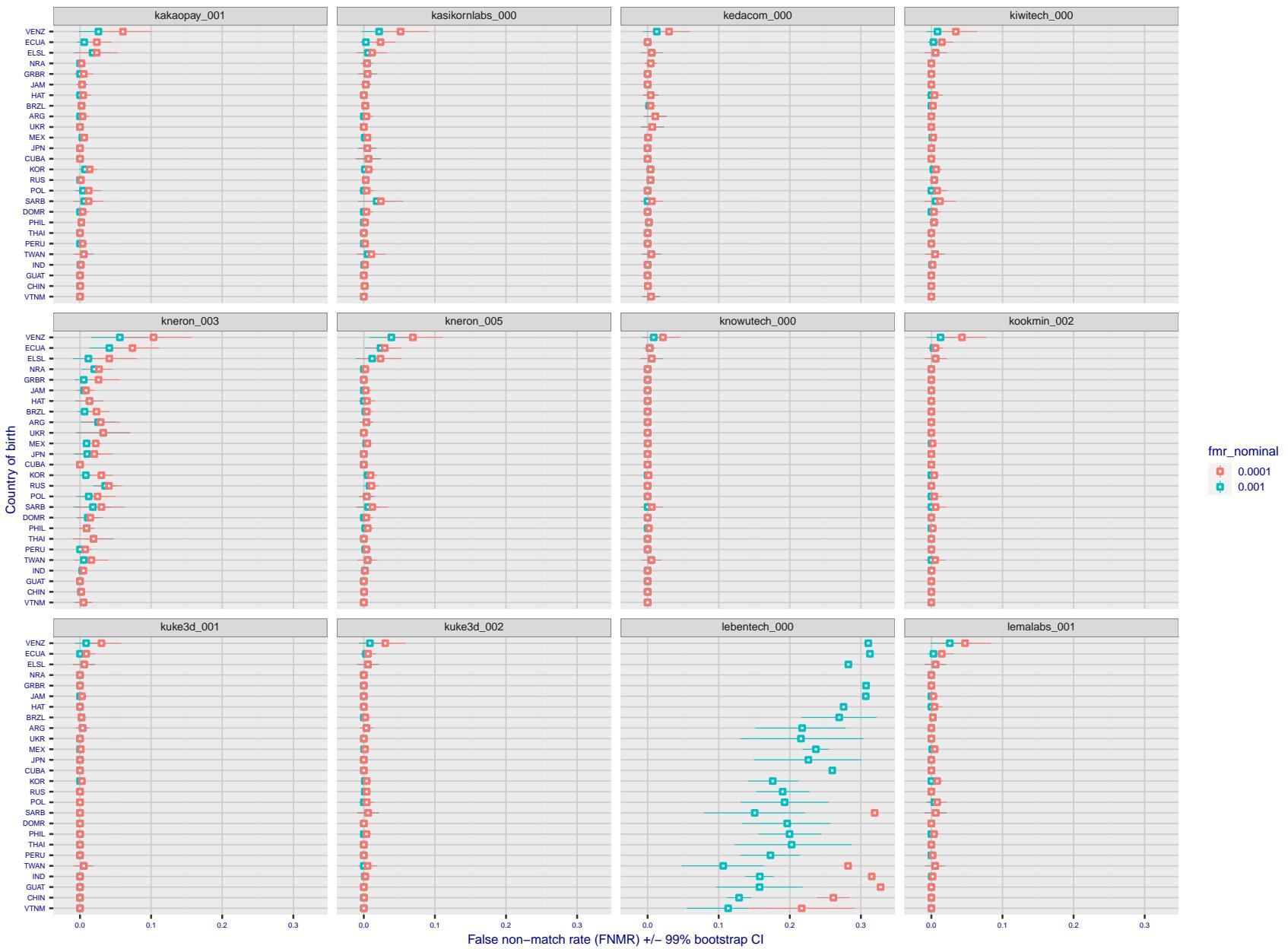


Figure 260: For the visa images, the dots show FNMR by country of birth for two globally set operating thresholds corresponding to  $FMR = \{0.001, 0.0001\}$  computed over all on the order of  $10^{10}$  impostor scores. The FMR in each bin will vary also - see subsequent impostor heatmaps in sec. 3.6.1. The figures shows an order of magnitude variation in FNMR across country of birth; these effects are likely due quality variations, then demographics like age and race. The error rates in some cases are zero, and in others the DET is flat so the error rates at the two thresholds are identical. The lines span 1% and 99% of bootstrap replicated FNMR estimates.

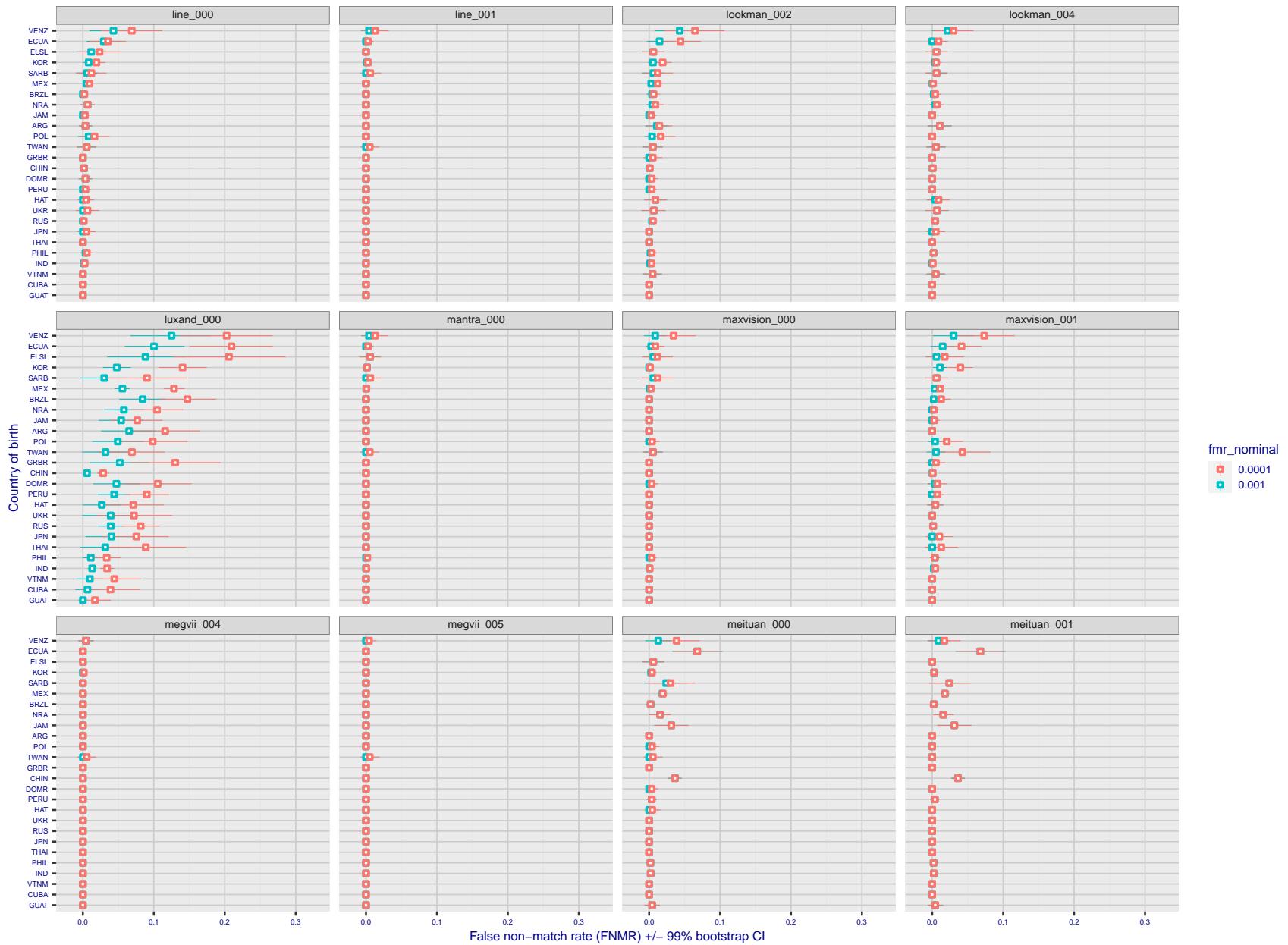


Figure 261: For the visa images, the dots show FNMR by country of birth for two globally set operating thresholds corresponding to  $FMR = \{0.001, 0.0001\}$  computed over all on the order of  $10^{10}$  impostor scores. The FMR in each bin will vary also - see subsequent impostor heatmaps in sec. 3.6.1. The figures shows an order of magnitude variation in FNMR across country of birth; these effects are likely due quality variations, then demographics like age and race. The error rates in some cases are zero, and in others the DET is flat so the error rates at the two thresholds are identical. The lines span 1% and 99% of bootstrap replicated FNMR estimates.

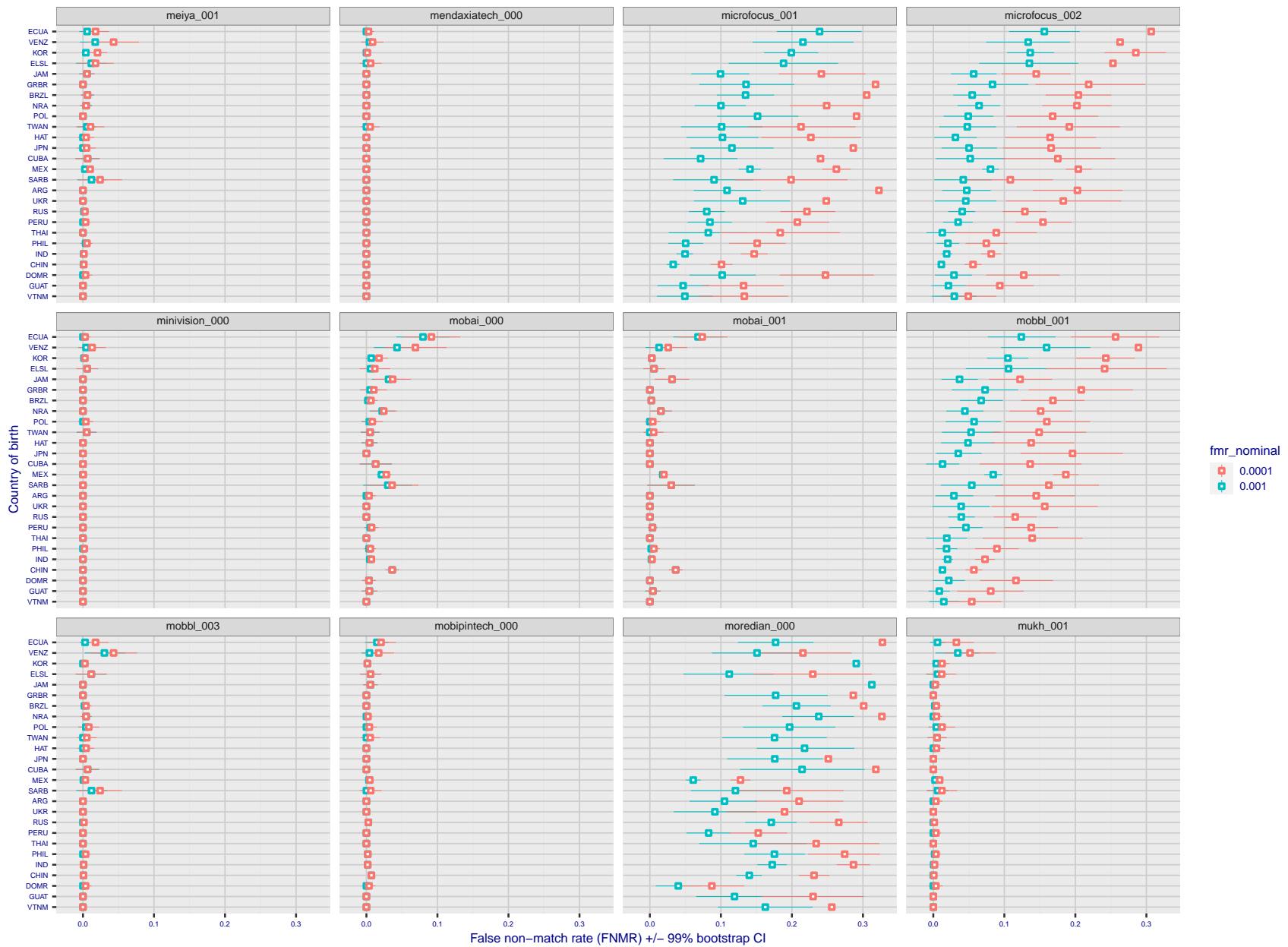


Figure 262: For the visa images, the dots show FNMR by country of birth for two globally set operating thresholds corresponding to  $FMR = \{0.001, 0.0001\}$  computed over all on the order of  $10^{10}$  impostor scores. The FMR in each bin will vary also - see subsequent impostor heatmaps in sec. 3.6.1. The figures shows an order of magnitude variation in FNMR across country of birth; these effects are likely due quality variations, then demographics like age and race. The error rates in some cases are zero, and in others the DET is flat so the error rates at the two thresholds are identical. The lines span 1% and 99% of bootstrap replicated FNMR estimates.

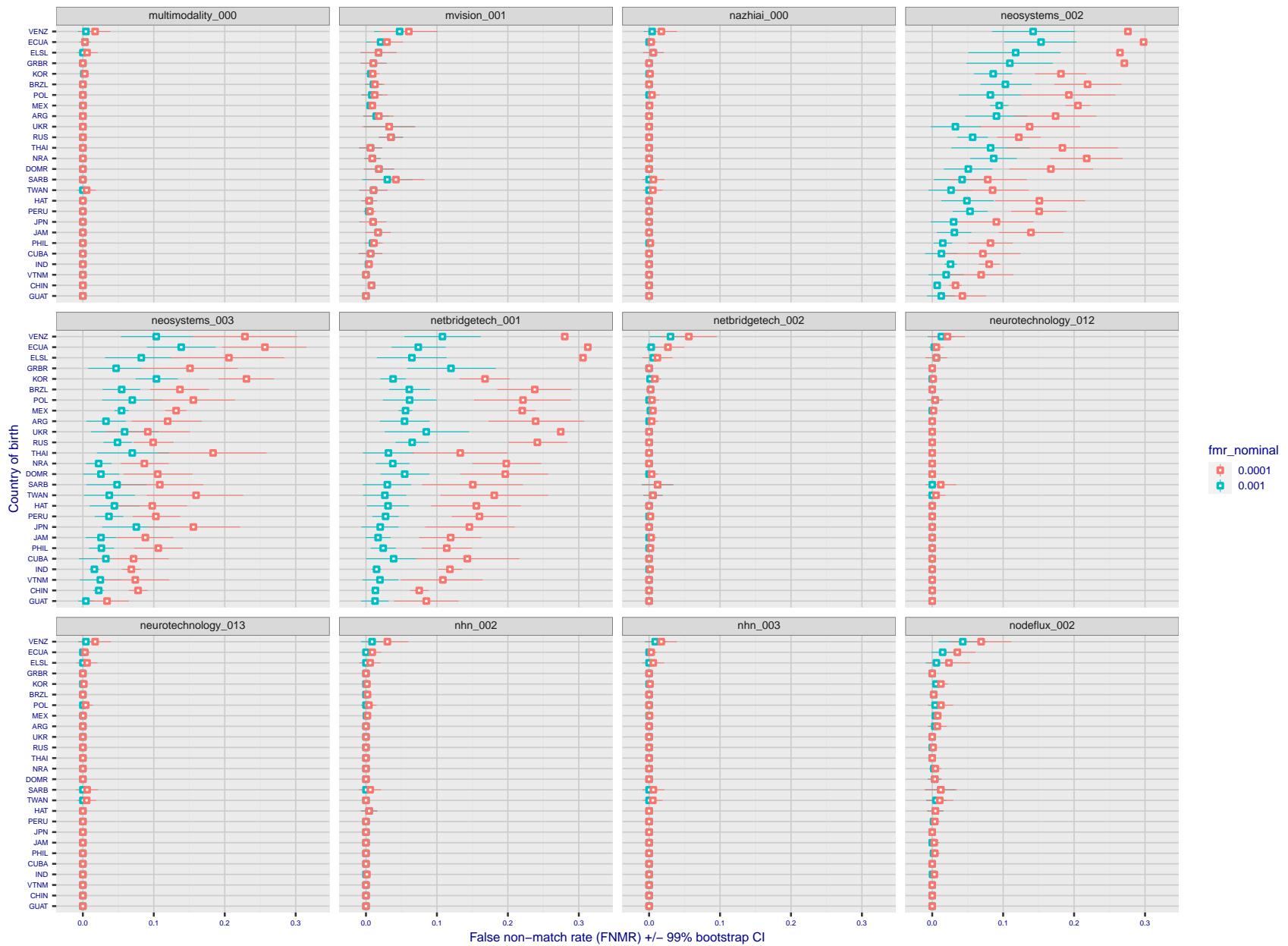


Figure 263: For the visa images, the dots show FNMR by country of birth for two globally set operating thresholds corresponding to  $FMR = \{0.001, 0.0001\}$  computed over all on the order of  $10^{10}$  impostor scores. The FMR in each bin will vary also - see subsequent impostor heatmaps in sec. 3.6.1. The figures shows an order of magnitude variation in FNMR across country of birth; these effects are likely due quality variations, then demographics like age and race. The error rates in some cases are zero, and in others the DET is flat so the error rates at the two thresholds are identical. The lines span 1% and 99% of bootstrap replicated FNMR estimates.

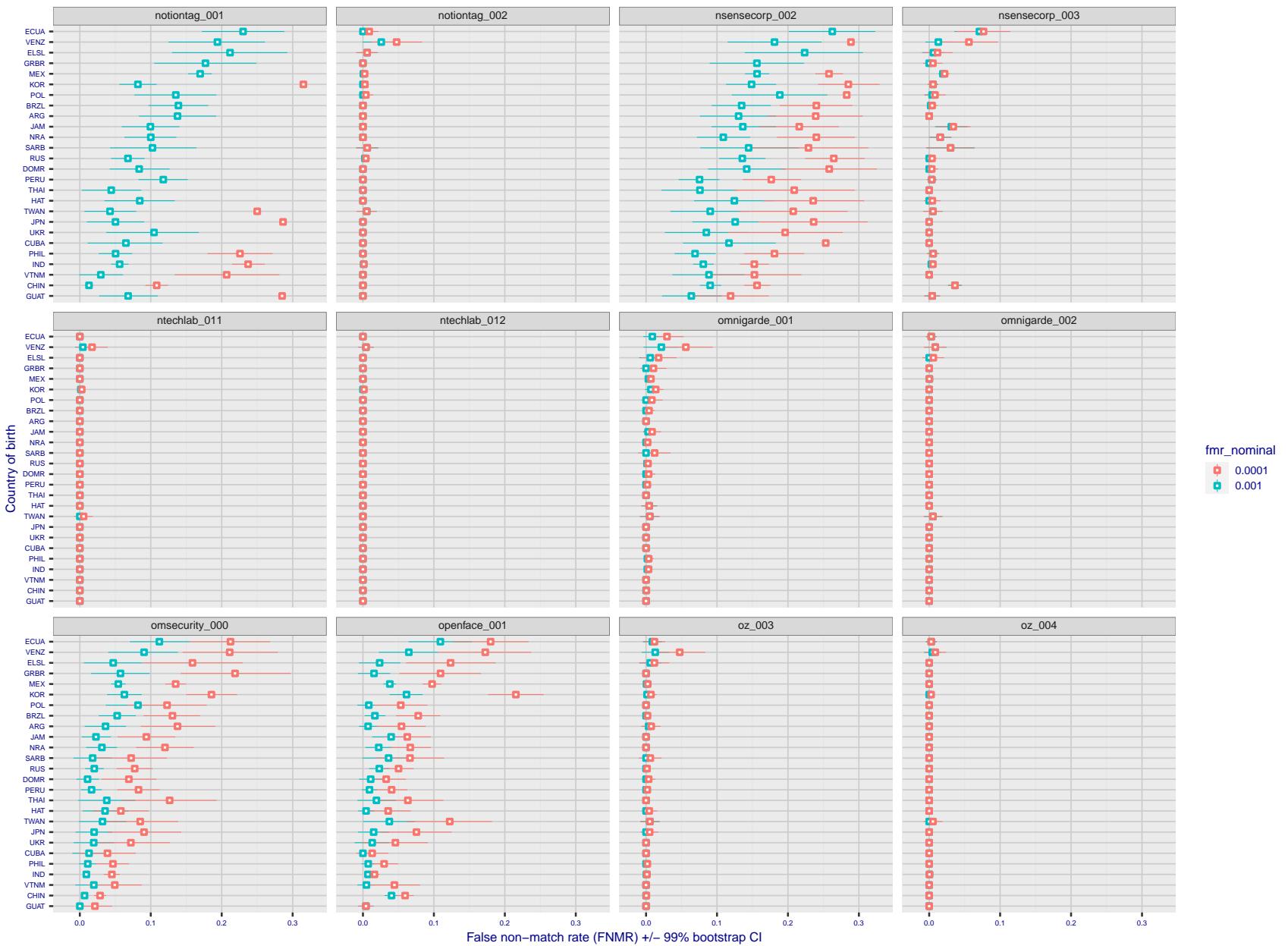


Figure 264: For the visa images, the dots show FNMR by country of birth for two globally set operating thresholds corresponding to  $FMR = \{0.001, 0.0001\}$  computed over all on the order of  $10^{10}$  impostor scores. The FMR in each bin will vary also - see subsequent impostor heatmaps in sec. 3.6.1. The figures shows an order of magnitude variation in FNMR across country of birth; these effects are likely due quality variations, then demographics like age and race. The error rates in some cases are zero, and in others the DET is flat so the error rates at the two thresholds are identical. The lines span 1% and 99% of bootstrap replicated FNMR estimates.

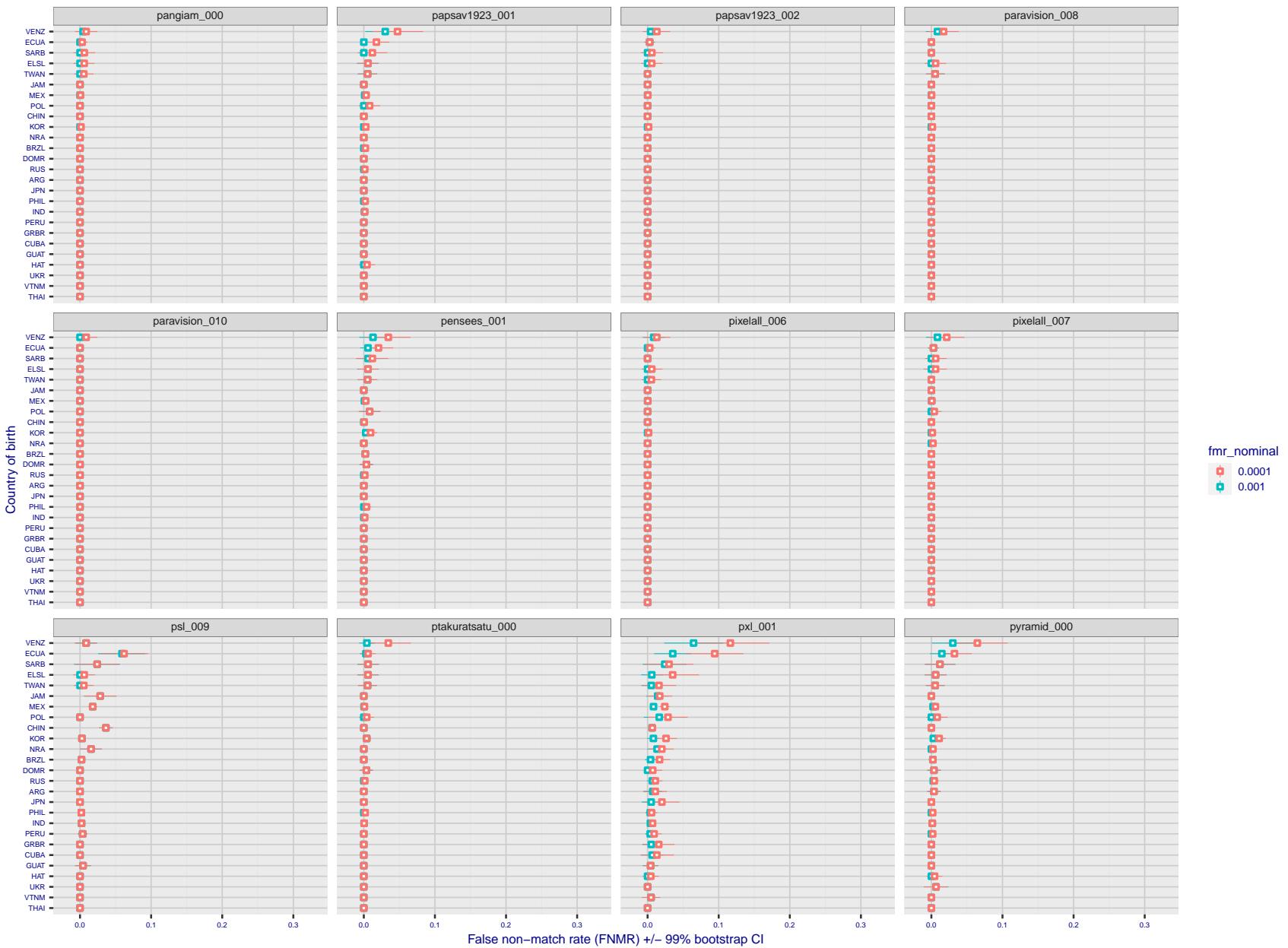


Figure 265: For the visa images, the dots show FNMR by country of birth for two globally set operating thresholds corresponding to  $FMR = \{0.001, 0.0001\}$  computed over all on the order of  $10^{10}$  impostor scores. The FMR in each bin will vary also - see subsequent impostor heatmaps in sec. 3.6.1. The figures shows an order of magnitude variation in FNMR across country of birth; these effects are likely due quality variations, then demographics like age and race. The error rates in some cases are zero, and in others the DET is flat so the error rates at the two thresholds are identical. The lines span 1% and 99% of bootstrap replicated FNMR estimates.

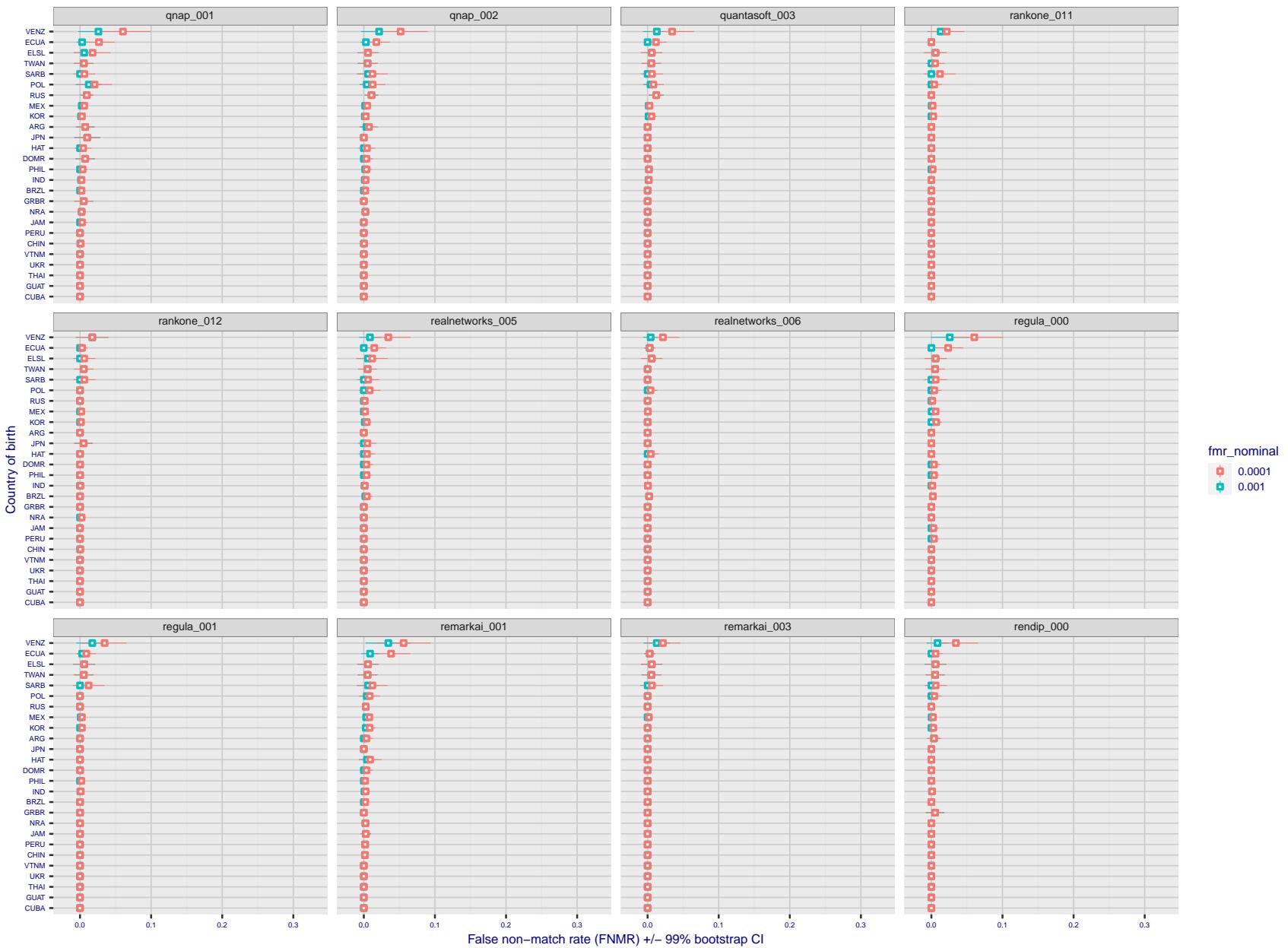


Figure 266: For the visa images, the dots show FNMR by country of birth for two globally set operating thresholds corresponding to  $FMR = \{0.001, 0.0001\}$  computed over all on the order of  $10^{10}$  impostor scores. The FMR in each bin will vary also - see subsequent impostor heatmaps in sec. 3.6.1. The figures shows an order of magnitude variation in FNMR across country of birth; these effects are likely due quality variations, then demographics like age and race. The error rates in some cases are zero, and in others the DET is flat so the error rates at the two thresholds are identical. The lines span 1% and 99% of bootstrap replicated FNMR estimates.

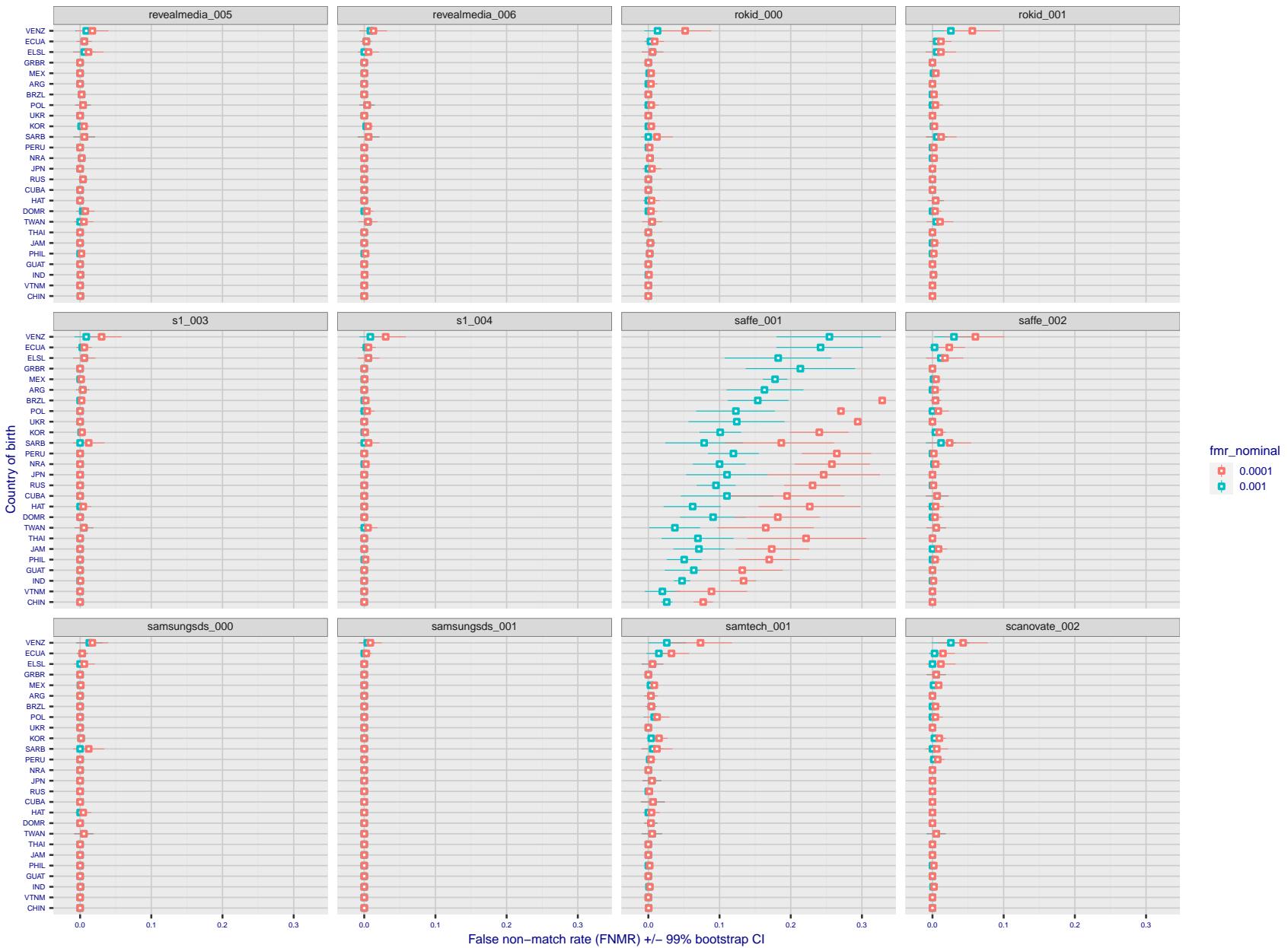


Figure 267: For the visa images, the dots show FNMR by country of birth for two globally set operating thresholds corresponding to  $FMR = \{0.001, 0.0001\}$  computed over all on the order of  $10^{10}$  impostor scores. The FMR in each bin will vary also - see subsequent impostor heatmaps in sec. 3.6.1. The figures shows an order of magnitude variation in FNMR across country of birth; these effects are likely due quality variations, then demographics like age and race. The error rates in some cases are zero, and in others the DET is flat so the error rates at the two thresholds are identical. The lines span 1% and 99% of bootstrap replicated FNMR estimates.

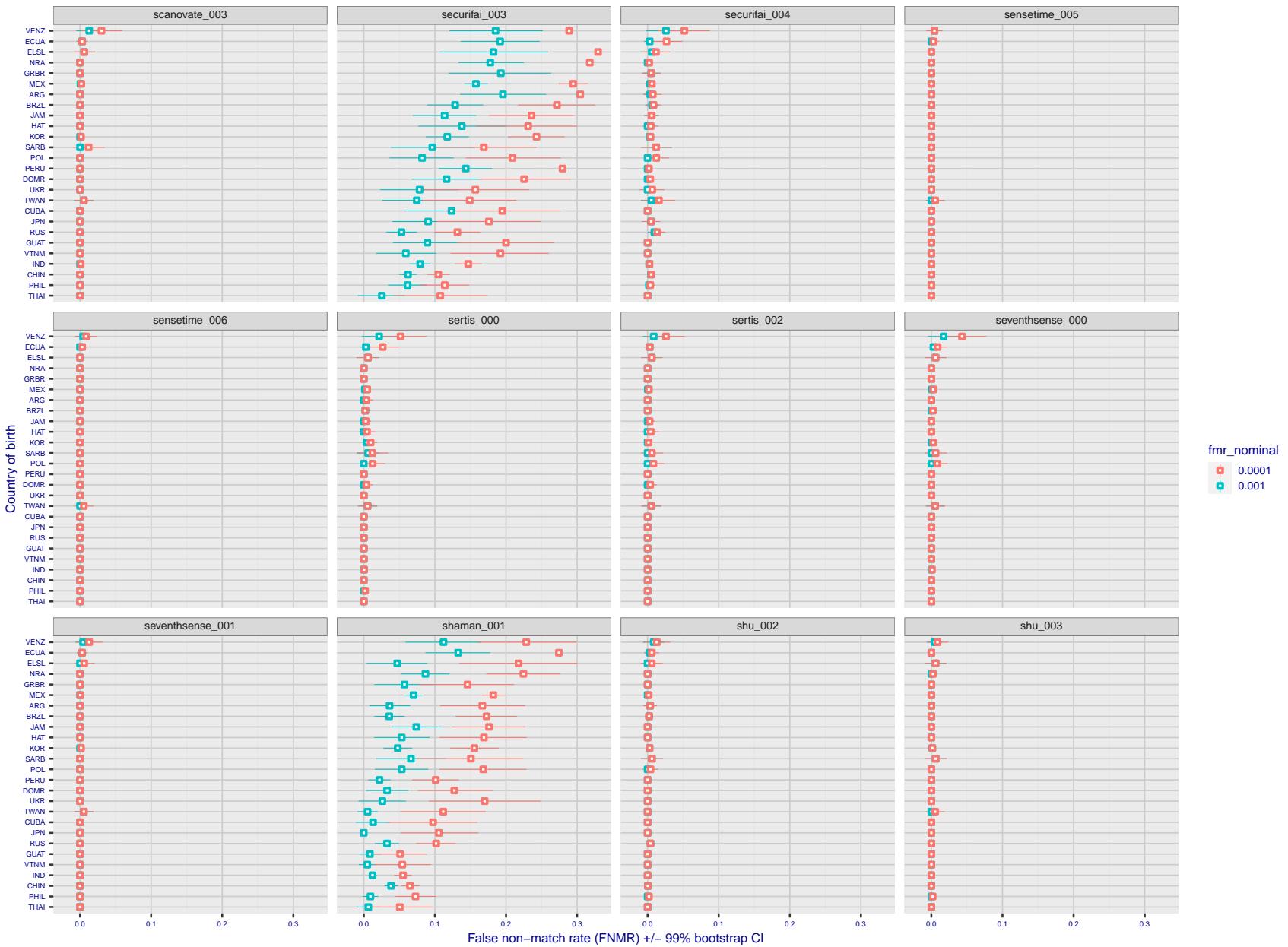


Figure 268: For the visa images, the dots show FNMR by country of birth for two globally set operating thresholds corresponding to  $FMR = \{0.001, 0.0001\}$  computed over all on the order of  $10^{10}$  impostor scores. The FMR in each bin will vary also - see subsequent impostor heatmaps in sec. 3.6.1. The figures shows an order of magnitude variation in FNMR across country of birth; these effects are likely due quality variations, then demographics like age and race. The error rates in some cases are zero, and in others the DET is flat so the error rates at the two thresholds are identical. The lines span 1% and 99% of bootstrap replicated FNMR estimates.

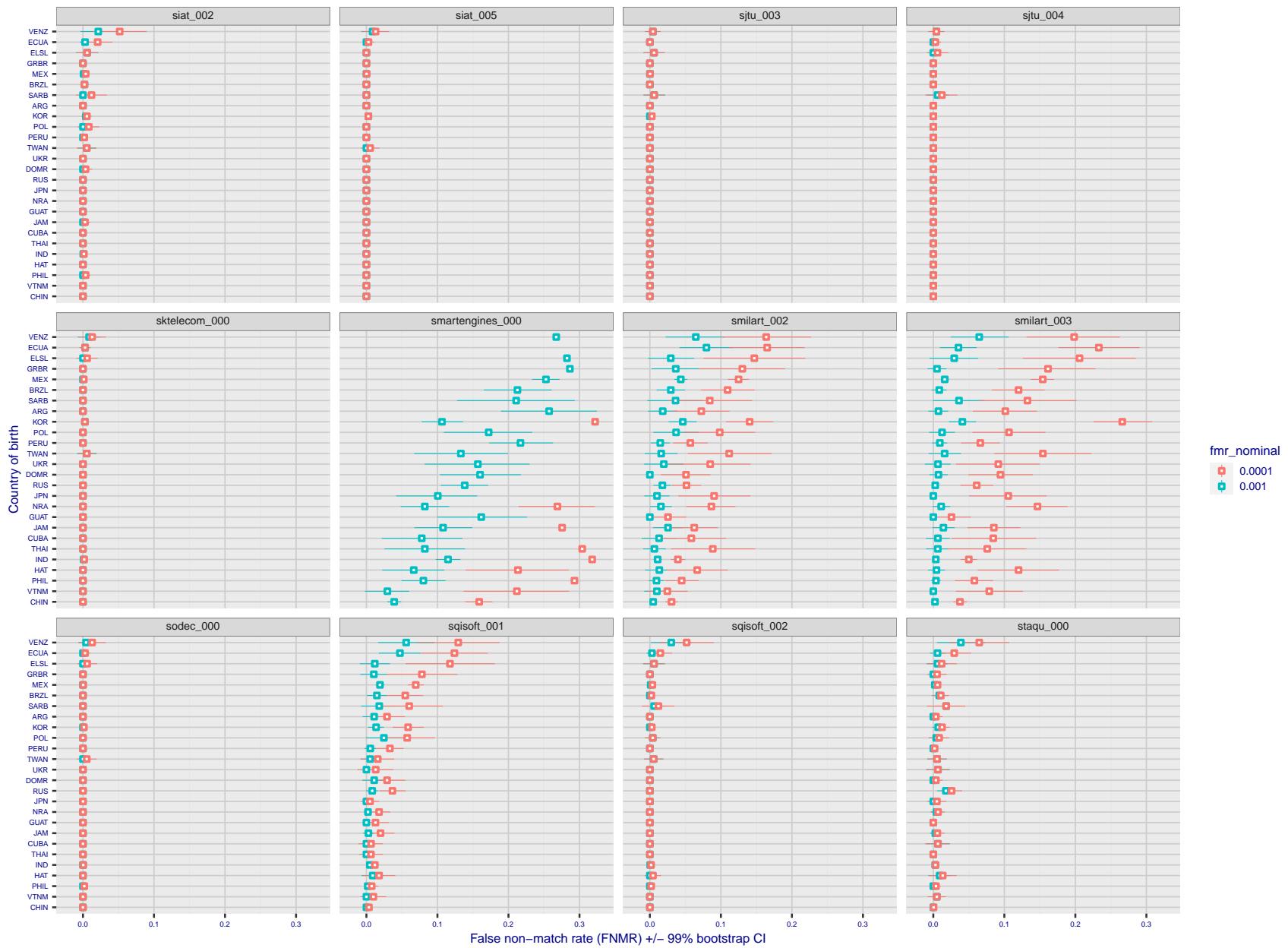


Figure 269: For the visa images, the dots show FNMR by country of birth for two globally set operating thresholds corresponding to  $FMR = \{0.001, 0.0001\}$  computed over all on the order of  $10^{10}$  impostor scores. The FMR in each bin will vary also - see subsequent impostor heatmaps in sec. 3.6.1. The figures shows an order of magnitude variation in FNMR across country of birth; these effects are likely due quality variations, then demographics like age and race. The error rates in some cases are zero, and in others the DET is flat so the error rates at the two thresholds are identical. The lines span 1% and 99% of bootstrap replicated FNMR estimates.

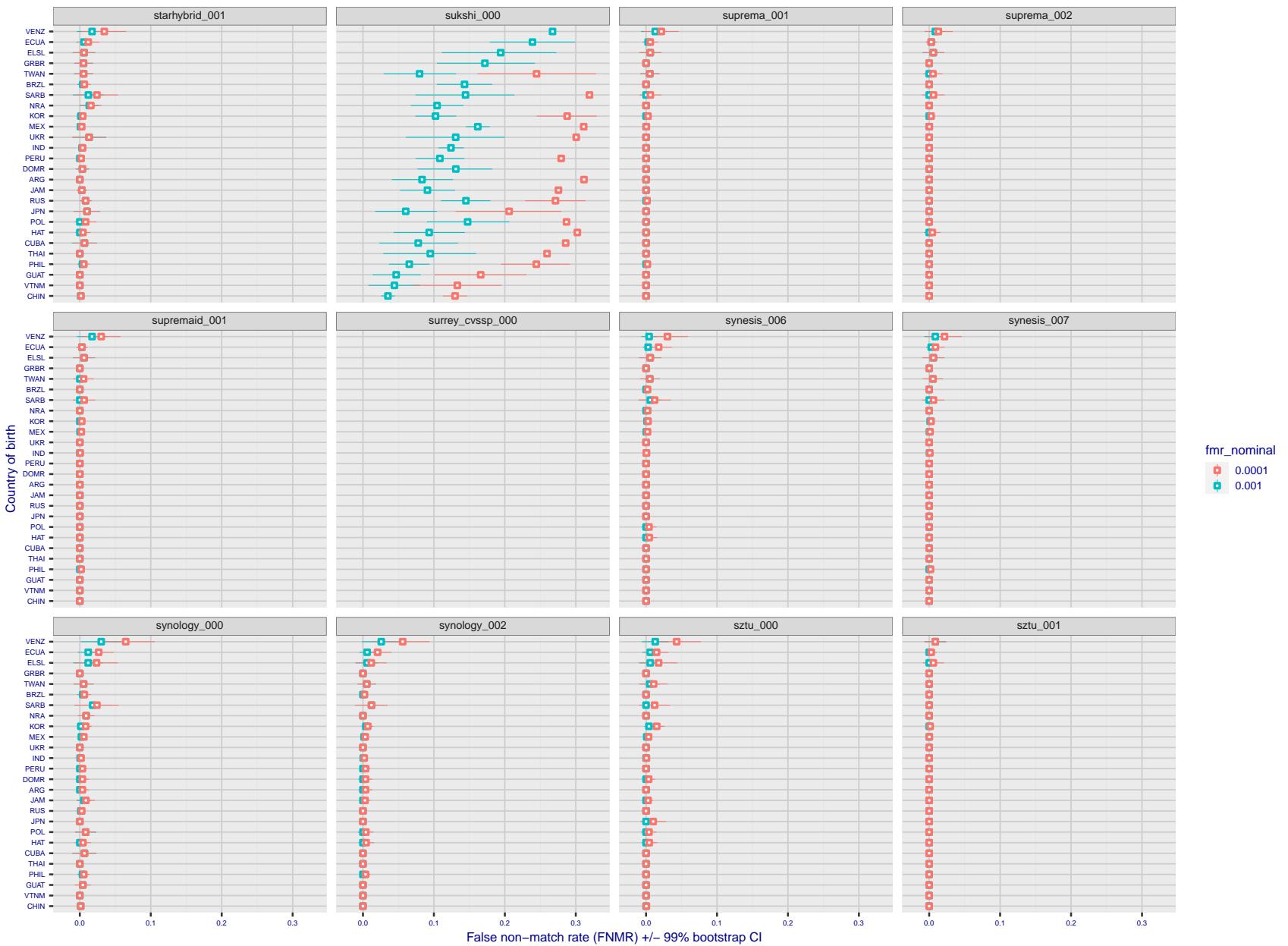


Figure 270: For the visa images, the dots show FNMR by country of birth for two globally set operating thresholds corresponding to  $FMR = \{0.001, 0.0001\}$  computed over all on the order of  $10^{10}$  impostor scores. The FMR in each bin will vary also - see subsequent impostor heatmaps in sec. 3.6.1. The figures shows an order of magnitude variation in FNMR across country of birth; these effects are likely due quality variations, then demographics like age and race. The error rates in some cases are zero, and in others the DET is flat so the error rates at the two thresholds are identical. The lines span 1% and 99% of bootstrap replicated FNMR estimates.

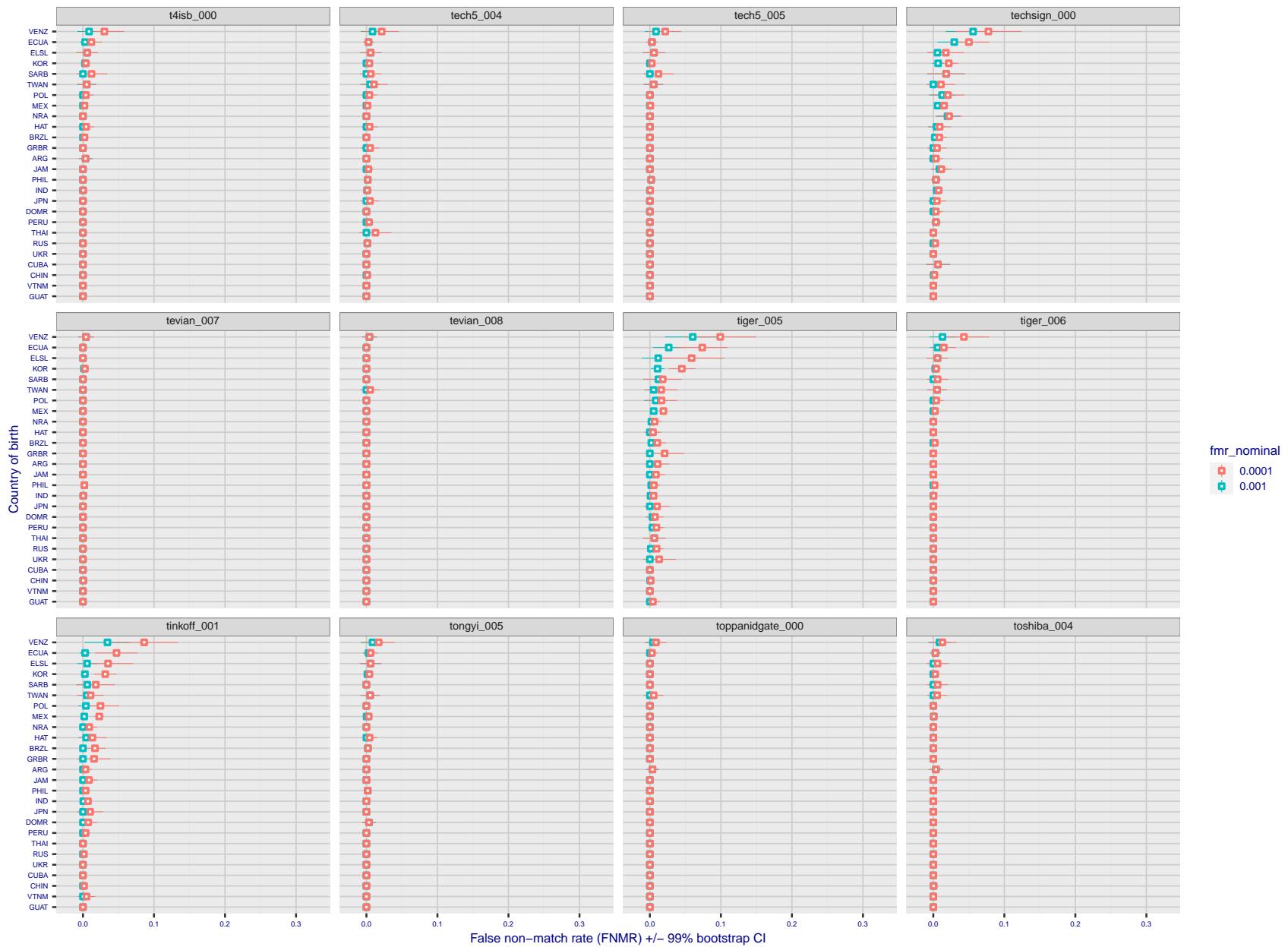


Figure 271: For the visa images, the dots show FNMR by country of birth for two globally set operating thresholds corresponding to  $FMR = \{0.001, 0.0001\}$  computed over all on the order of  $10^{10}$  impostor scores. The FMR in each bin will vary also - see subsequent impostor heatmaps in sec. 3.6.1. The figures shows an order of magnitude variation in FNMR across country of birth; these effects are likely due quality variations, then demographics like age and race. The error rates in some cases are zero, and in others the DET is flat so the error rates at the two thresholds are identical. The lines span 1% and 99% of bootstrap replicated FNMR estimates.

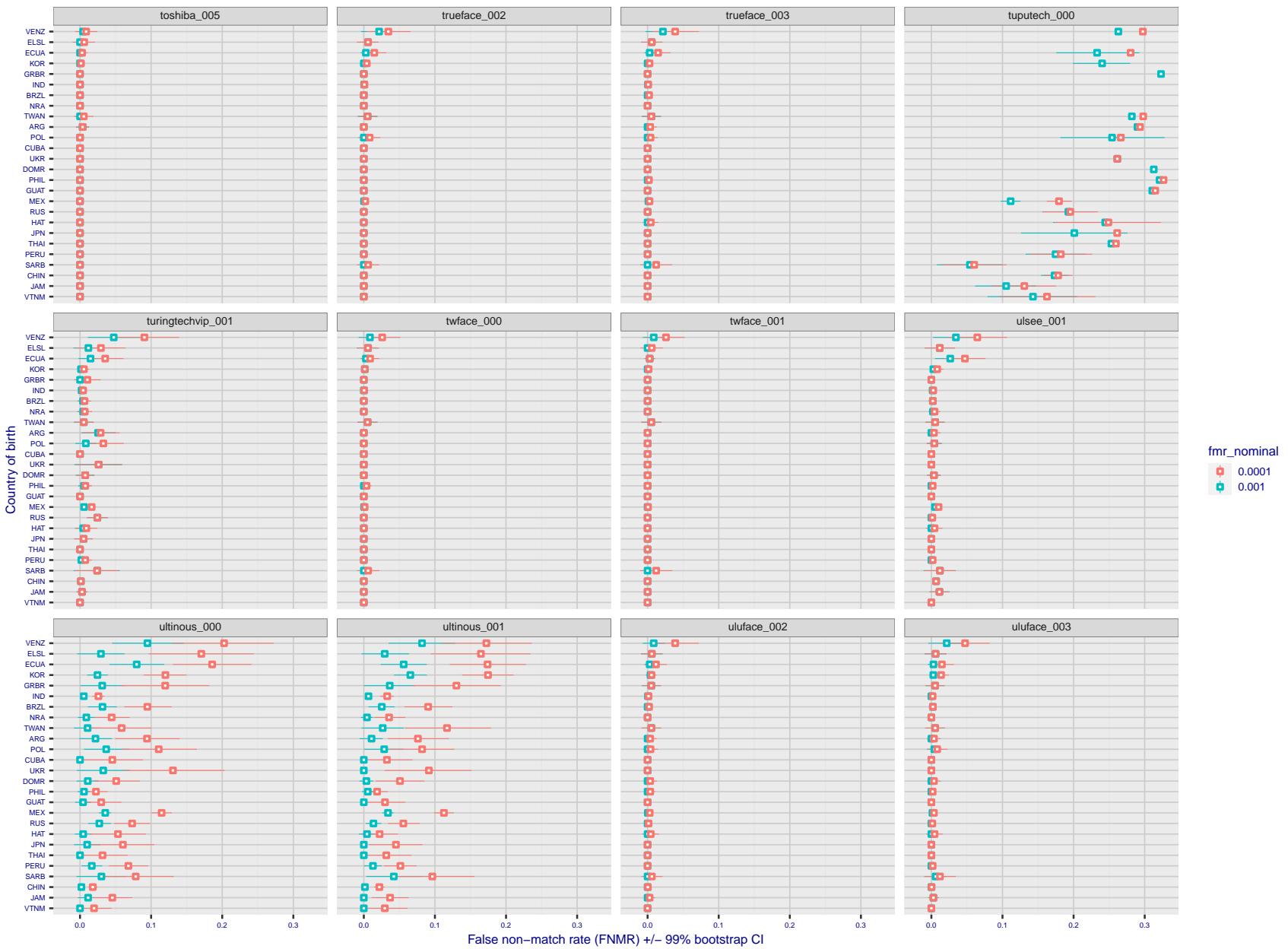


Figure 272: For the visa images, the dots show FNMR by country of birth for two globally set operating thresholds corresponding to  $FMR = \{0.001, 0.0001\}$  computed over all on the order of  $10^{10}$  impostor scores. The FMR in each bin will vary also - see subsequent impostor heatmaps in sec. 3.6.1. The figures shows an order of magnitude variation in FNMR across country of birth; these effects are likely due quality variations, then demographics like age and race. The error rates in some cases are zero, and in others the DET is flat so the error rates at the two thresholds are identical. The lines span 1% and 99% of bootstrap replicated FNMR estimates.

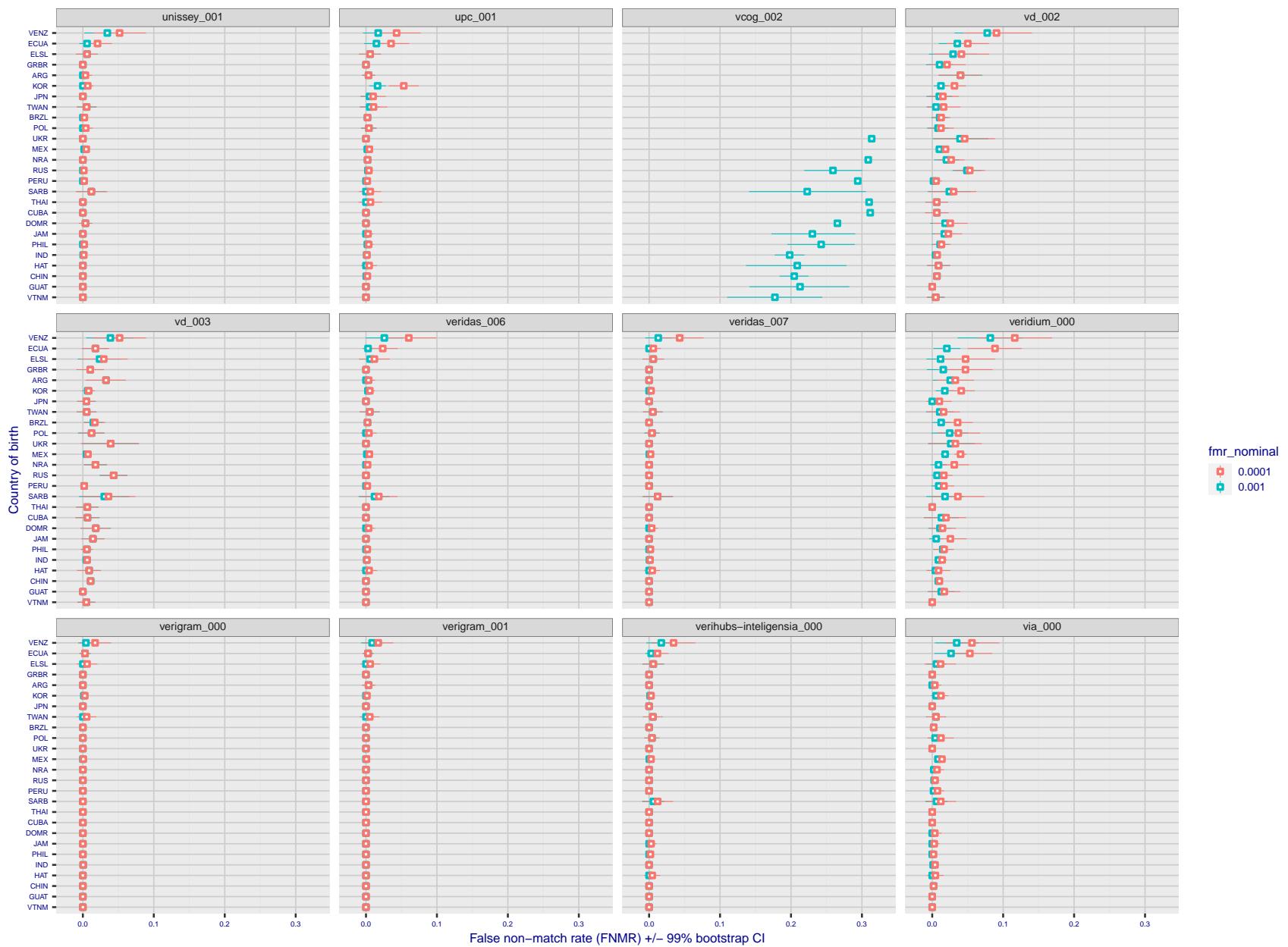


Figure 273: For the visa images, the dots show FNMR by country of birth for two globally set operating thresholds corresponding to  $FMR = \{0.001, 0.0001\}$  computed over all on the order of  $10^{10}$  impostor scores. The FMR in each bin will vary also - see subsequent impostor heatmaps in sec. 3.6.1. The figures shows an order of magnitude variation in FNMR across country of birth; these effects are likely due quality variations, then demographics like age and race. The error rates in some cases are zero, and in others the DET is flat so the error rates at the two thresholds are identical. The lines span 1% and 99% of bootstrap replicated FNMR estimates.

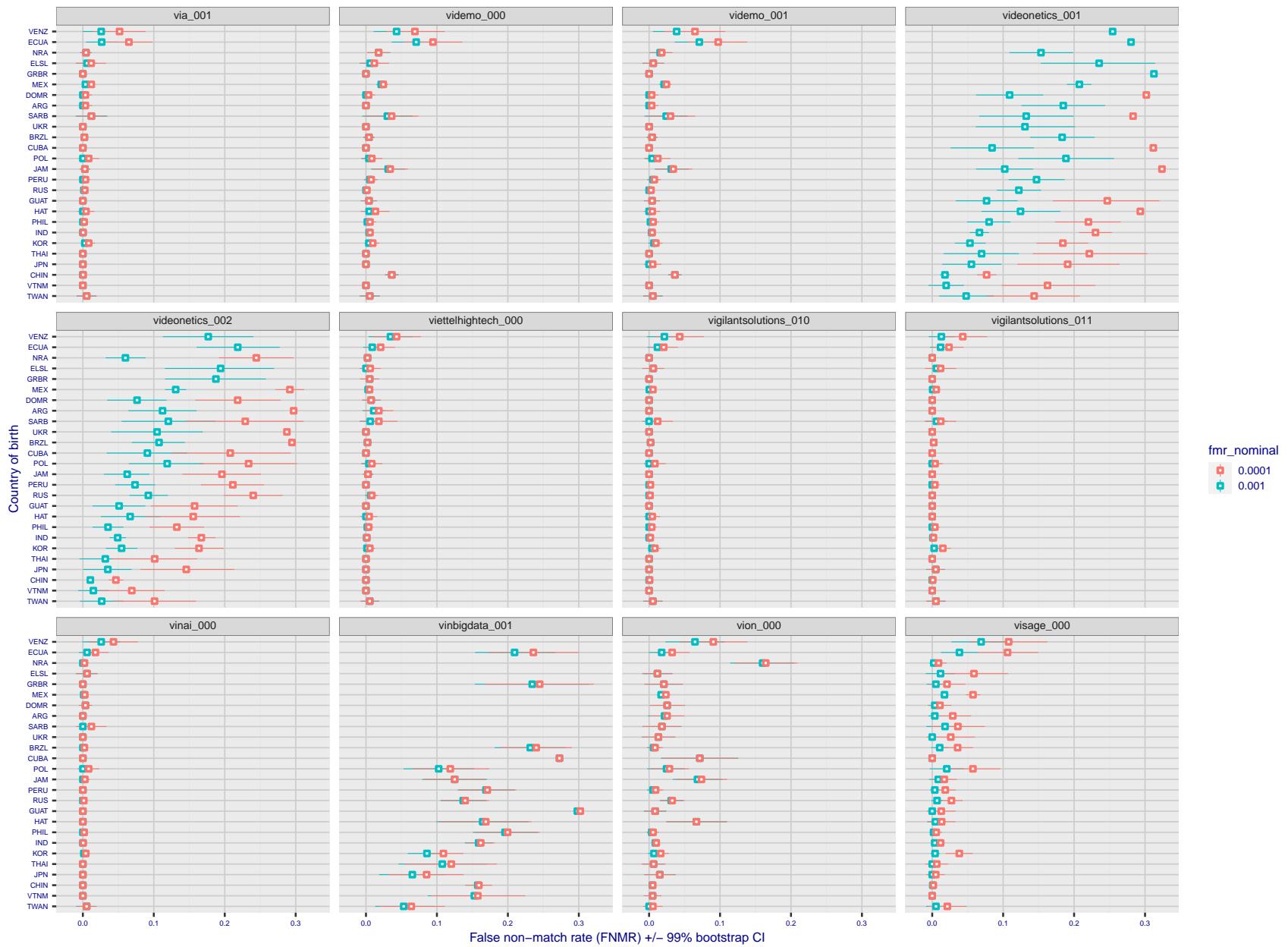


Figure 274: For the visa images, the dots show FNMR by country of birth for two globally set operating thresholds corresponding to  $FMR = \{0.001, 0.0001\}$  computed over all on the order of  $10^{10}$  impostor scores. The FMR in each bin will vary also - see subsequent impostor heatmaps in sec. 3.6.1. The figures shows an order of magnitude variation in FNMR across country of birth; these effects are likely due quality variations, then demographics like age and race. The error rates in some cases are zero, and in others the DET is flat so the error rates at the two thresholds are identical. The lines span 1% and 99% of bootstrap replicated FNMR estimates.

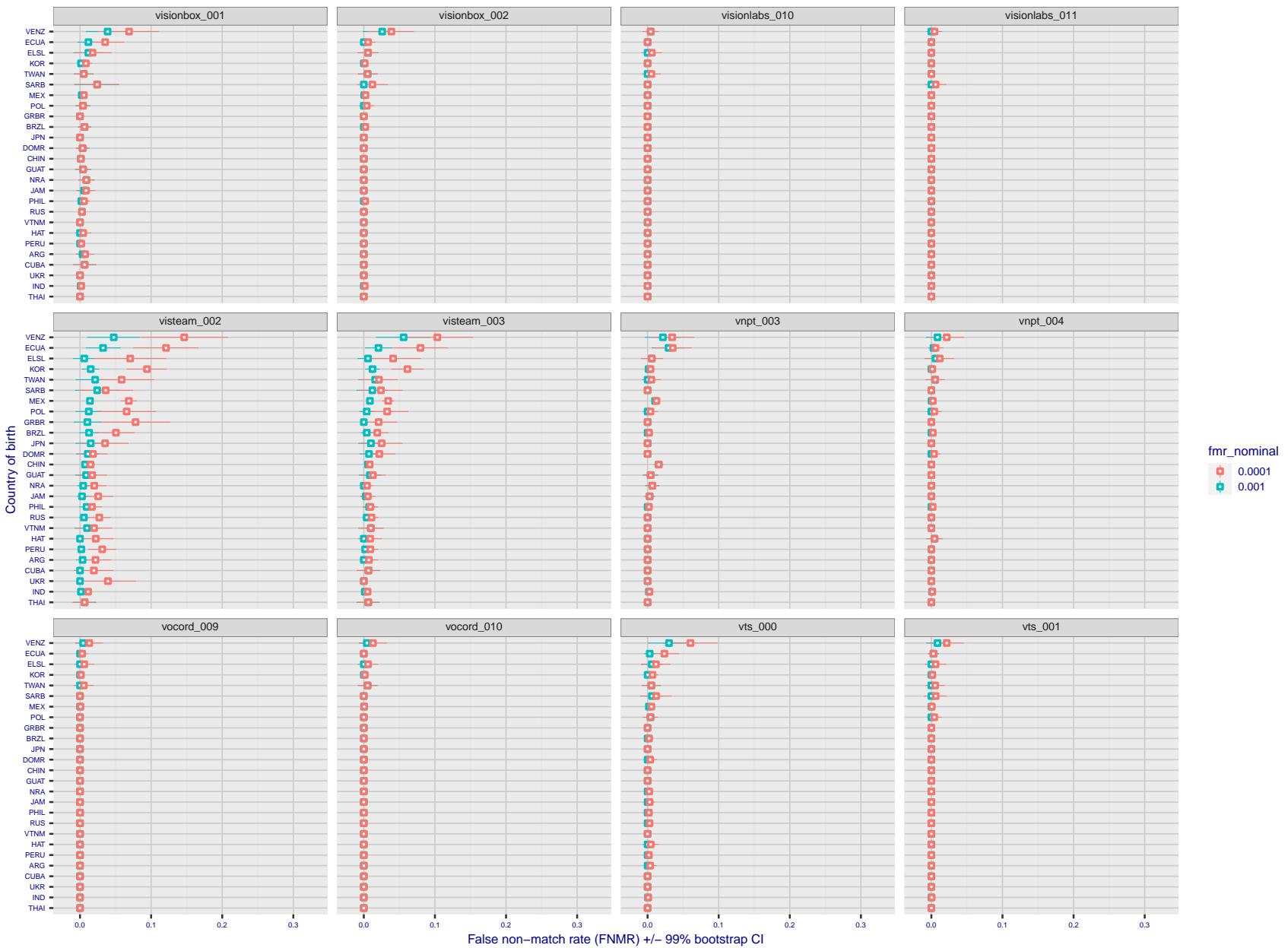


Figure 275: For the visa images, the dots show FNMR by country of birth for two globally set operating thresholds corresponding to  $FMR = \{0.001, 0.0001\}$  computed over all on the order of  $10^{10}$  impostor scores. The FMR in each bin will vary also - see subsequent impostor heatmaps in sec. 3.6.1. The figures shows an order of magnitude variation in FNMR across country of birth; these effects are likely due quality variations, then demographics like age and race. The error rates in some cases are zero, and in others the DET is flat so the error rates at the two thresholds are identical. The lines span 1% and 99% of bootstrap replicated FNMR estimates.

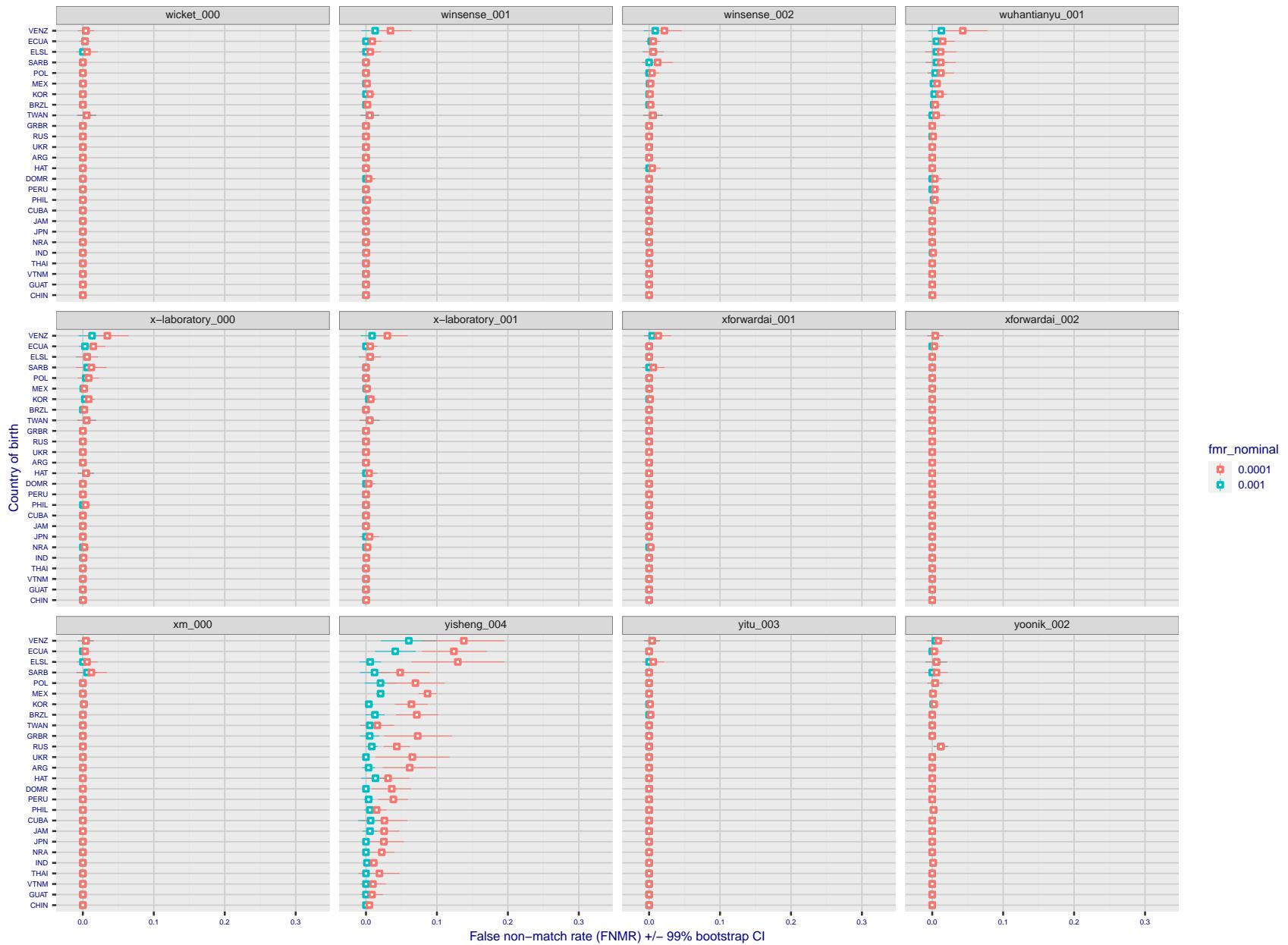


Figure 276: For the visa images, the dots show FNMR by country of birth for two globally set operating thresholds corresponding to  $FMR = \{0.001, 0.0001\}$  computed over all on the order of  $10^{10}$  impostor scores. The FMR in each bin will vary also - see subsequent impostor heatmaps in sec. 3.6.1. The figures shows an order of magnitude variation in FNMR across country of birth; these effects are likely due quality variations, then demographics like age and race. The error rates in some cases are zero, and in others the DET is flat so the error rates at the two thresholds are identical. The lines span 1% and 99% of bootstrap replicated FNMR estimates.



Figure 277: For the visa images, the dots show FNMR by country of birth for two globally set operating thresholds corresponding to  $FMR = \{0.001, 0.0001\}$  computed over all on the order of  $10^{10}$  impostor scores. The FMR in each bin will vary also - see subsequent impostor heatmaps in sec. 3.6.1. The figures shows an order of magnitude variation in FNMR across country of birth; these effects are likely due quality variations, then demographics like age and race. The error rates in some cases are zero, and in others the DET is flat so the error rates at the two thresholds are identical. The lines span 1% and 99% of bootstrap replicated FNMR estimates.

**Caveats:** The results may not relate to subject-specific properties. Instead they could reflect image-specific quality differences, which could occur due to collection protocol or software processing variations.

### 3.5.2 Effect of ageing

**Background:** Faces change appearance throughout life. This change gradually reduces similarity of a new image to an earlier image. Face recognition algorithms give reduced similarity scores and more frequent false rejections.

**Goal:** To quantify false non-match rates (FNMR) as a function of elapsed time in an adult population.

**Methods:** Using the mugshot images, a threshold is set to give FMR = 0.00001 over the entire impostor set. Then FNMR is measured over 1000 bootstrap replications of the genuine scores.

**Results:** For the visa images, Figure 303 shows how false non-match rates for genuine users, as a function of age group.

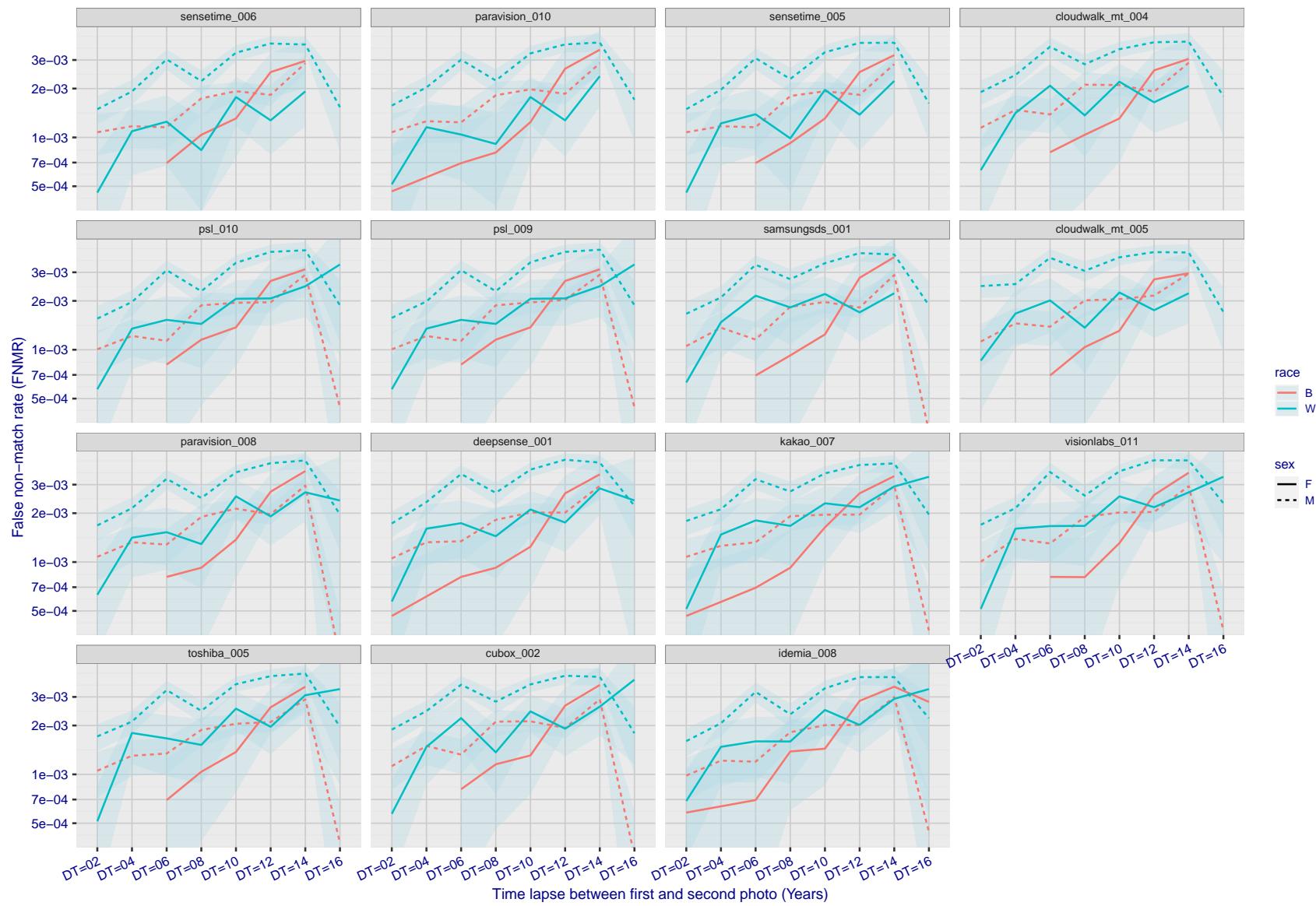


Figure 278: For the mugshot images, FNMR as a function of elapsed time between initial enrollment and second verification images. The panels appear most accurate first, and vertical scale changes on each page. The four traces correspond to images annotated with codes for black female, black male, white female, white male. The threshold is fixed for each algorithm to give  $FMR = 0.00001$  over all ( $10^8$ ) impostor comparisons. For short time-lapses, the most accurate algorithms give very few errors ( $FNMR < 0.001$ ) so that the uncertainty estimates are high.

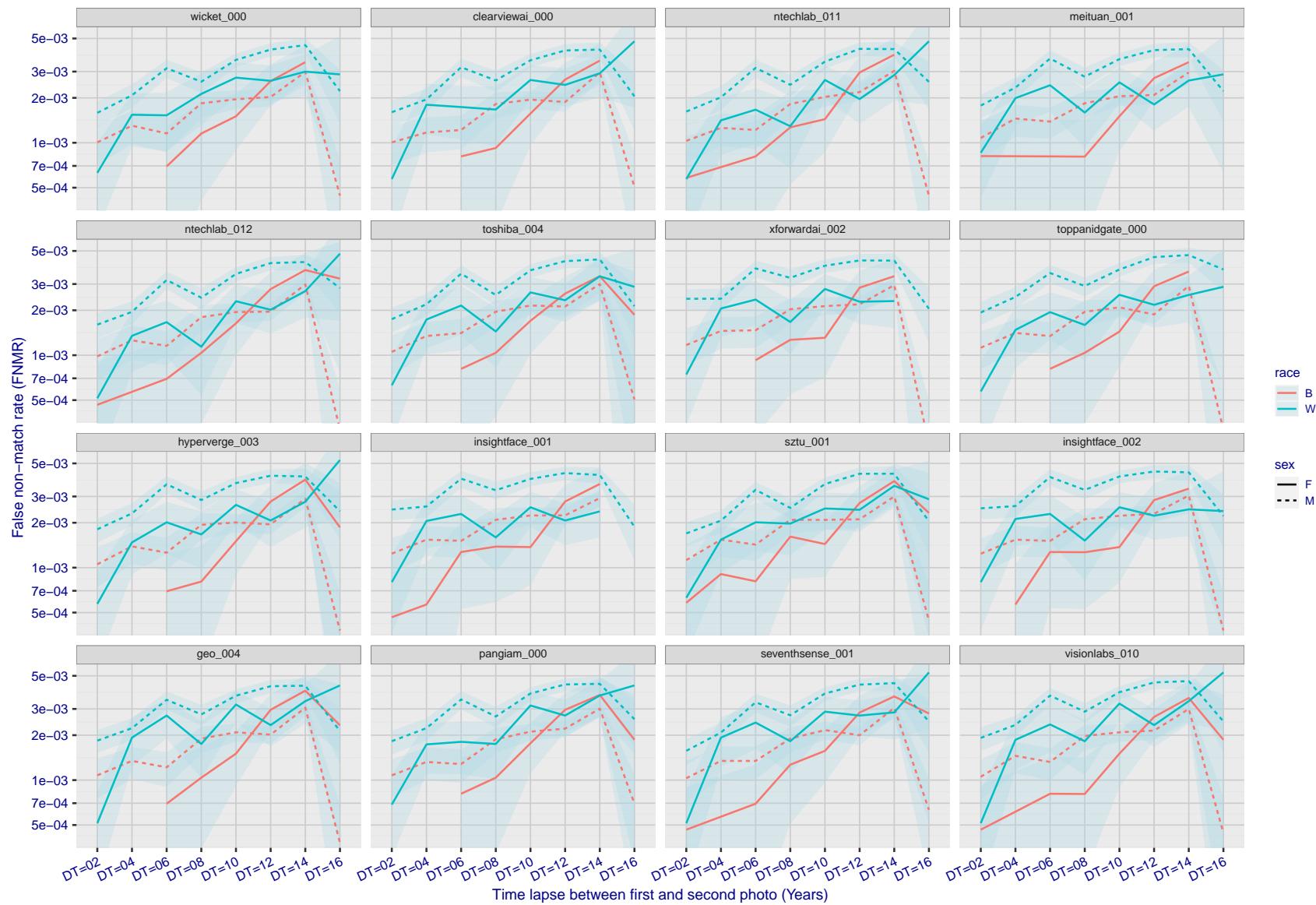


Figure 279: For the mugshot images, FNMR as a function of elapsed time between initial enrollment and second verification images. The panels appear most accurate first, and vertical scale changes on each page. The four traces correspond to images annotated with codes for black female, black male, white female, white male. The threshold is fixed for each algorithm to give FMR = 0.00001 over all ( $10^8$ ) impostor comparisons. For short time-lapses, the most accurate algorithms give very few errors (FNMR < 0.001) so that the uncertainty estimates are high.

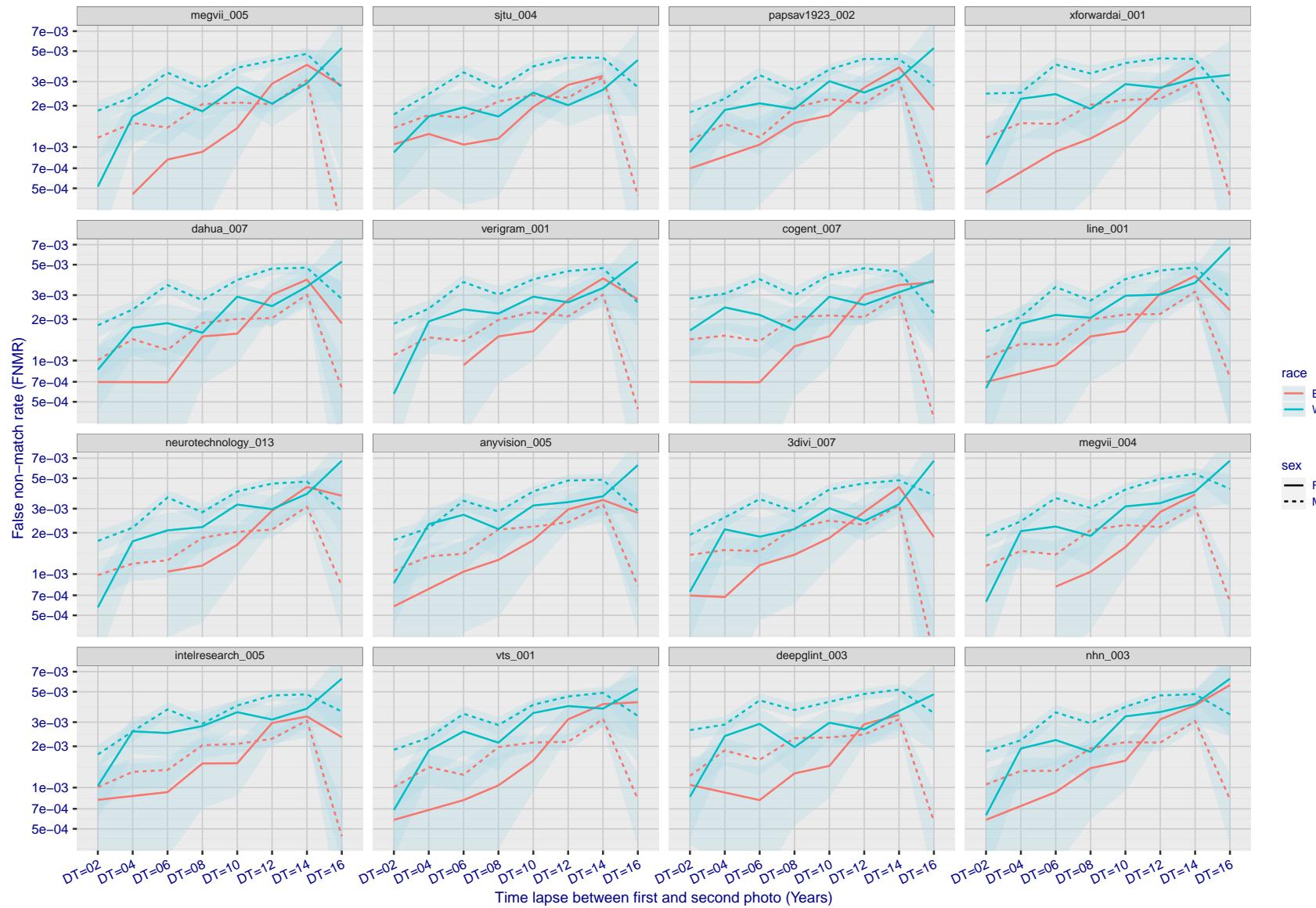


Figure 280: For the mugshot images, FNMR as a function of elapsed time between initial enrollment and second verification images. The panels appear most accurate first, and vertical scale changes on each page. The four traces correspond to images annotated with codes for black female, black male, white female, white male. The threshold is fixed for each algorithm to give FMR = 0.00001 over all ( $10^8$ ) impostor comparisons. For short time-lapses, the most accurate algorithms give very few errors (FNMR < 0.001) so that the uncertainty estimates are high.

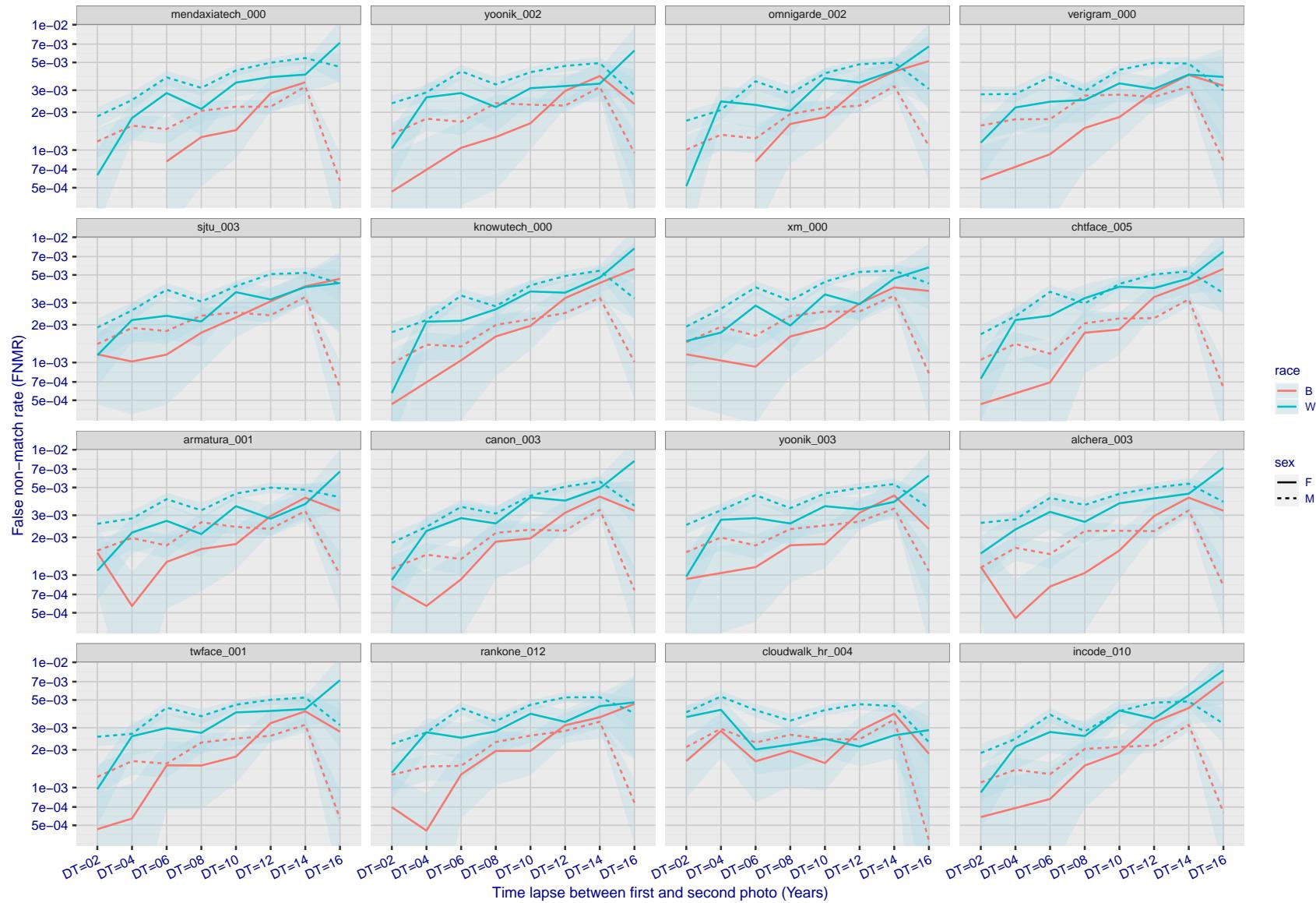


Figure 281: For the mugshot images, FNMR as a function of elapsed time between initial enrollment and second verification images. The panels appear most accurate first, and vertical scale changes on each page. The four traces correspond to images annotated with codes for black female, black male, white female, white male. The threshold is fixed for each algorithm to give  $FMR = 0.00001$  over all ( $10^8$ ) impostor comparisons. For short time-lapses, the most accurate algorithms give very few errors ( $FNMR < 0.001$ ) so that the uncertainty estimates are high.

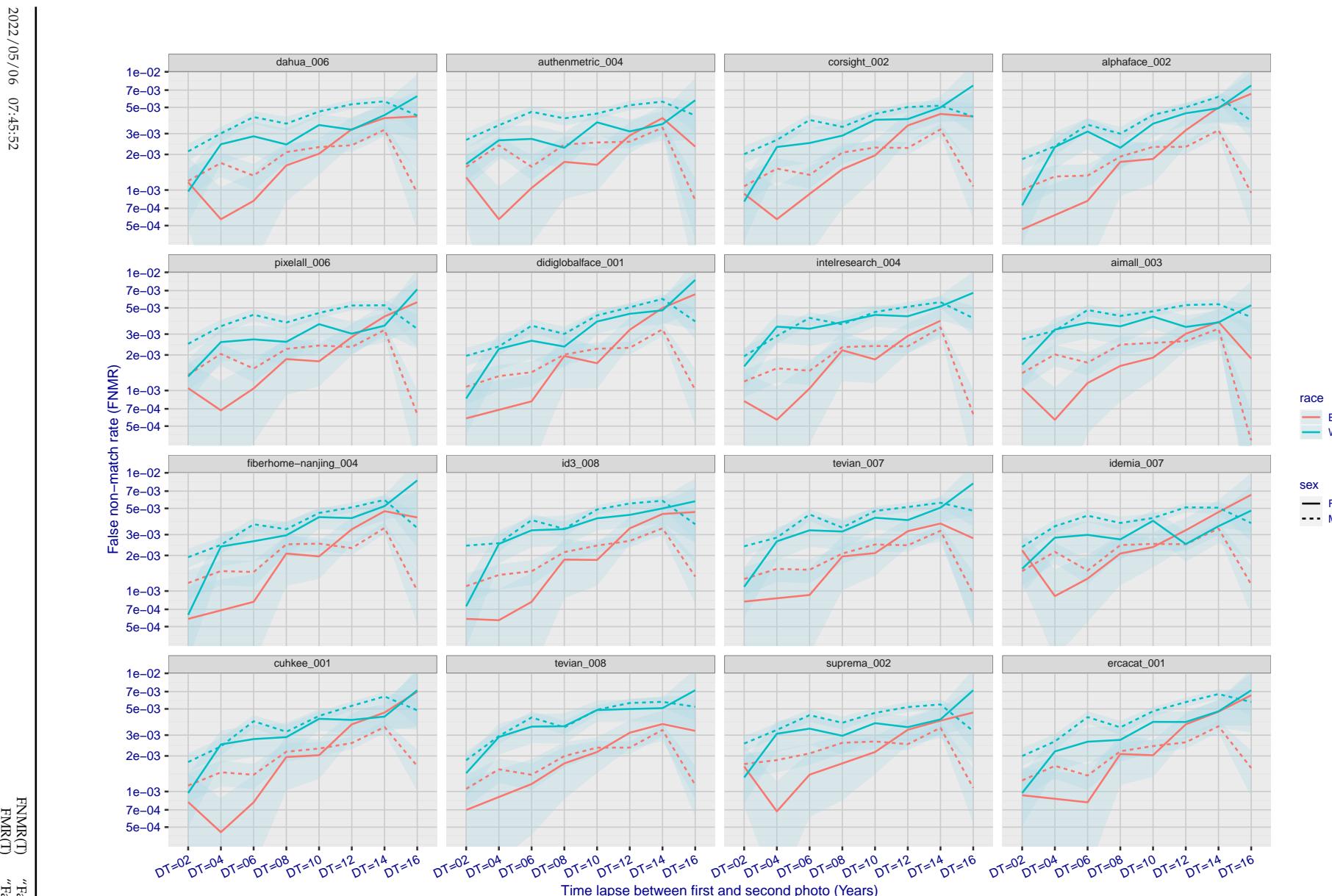


Figure 282: For the mugshot images, FNMR as a function of elapsed time between initial enrollment and second verification images. The panels appear most accurate first, and vertical scale changes on each page. The four traces correspond to images annotated with codes for black female, black male, white female, white male. The threshold is fixed for each algorithm to give  $FMR = 0.00001$  over all ( $10^8$ ) impostor comparisons. For short time-lapses, the most accurate algorithms give very few errors ( $FNMR < 0.001$ ) so that the uncertainty estimates are high.

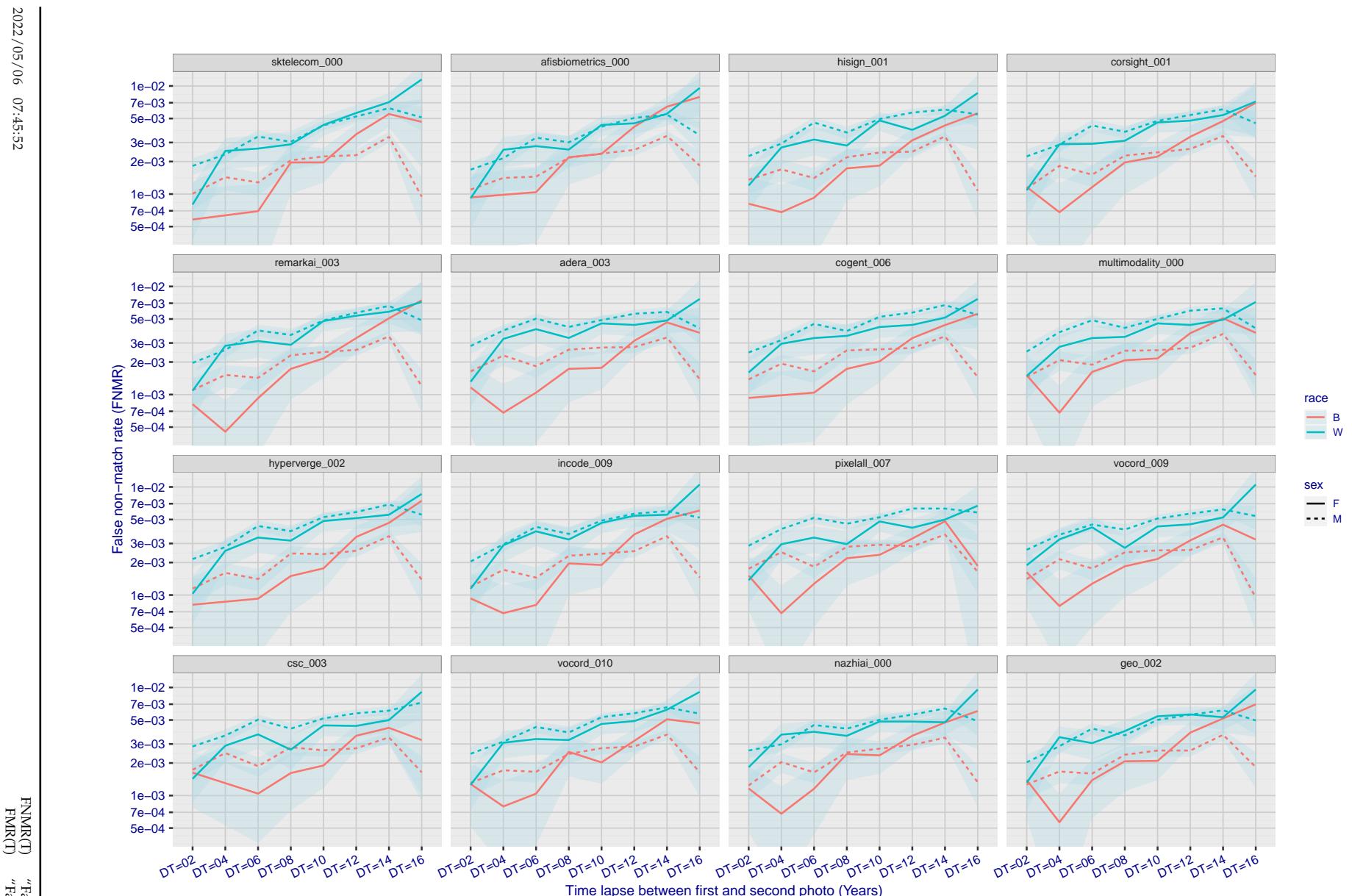


Figure 283: For the mugshot images, FNMR as a function of elapsed time between initial enrollment and second verification images. The panels appear most accurate first, and vertical scale changes on each page. The four traces correspond to images annotated with codes for black female, black male, white female, white male. The threshold is fixed for each algorithm to give FMR = 0.00001 over all ( $10^8$ ) impostor comparisons. For short time-lapses, the most accurate algorithms give very few errors (FNMR < 0.001) so that the uncertainty estimates are high.

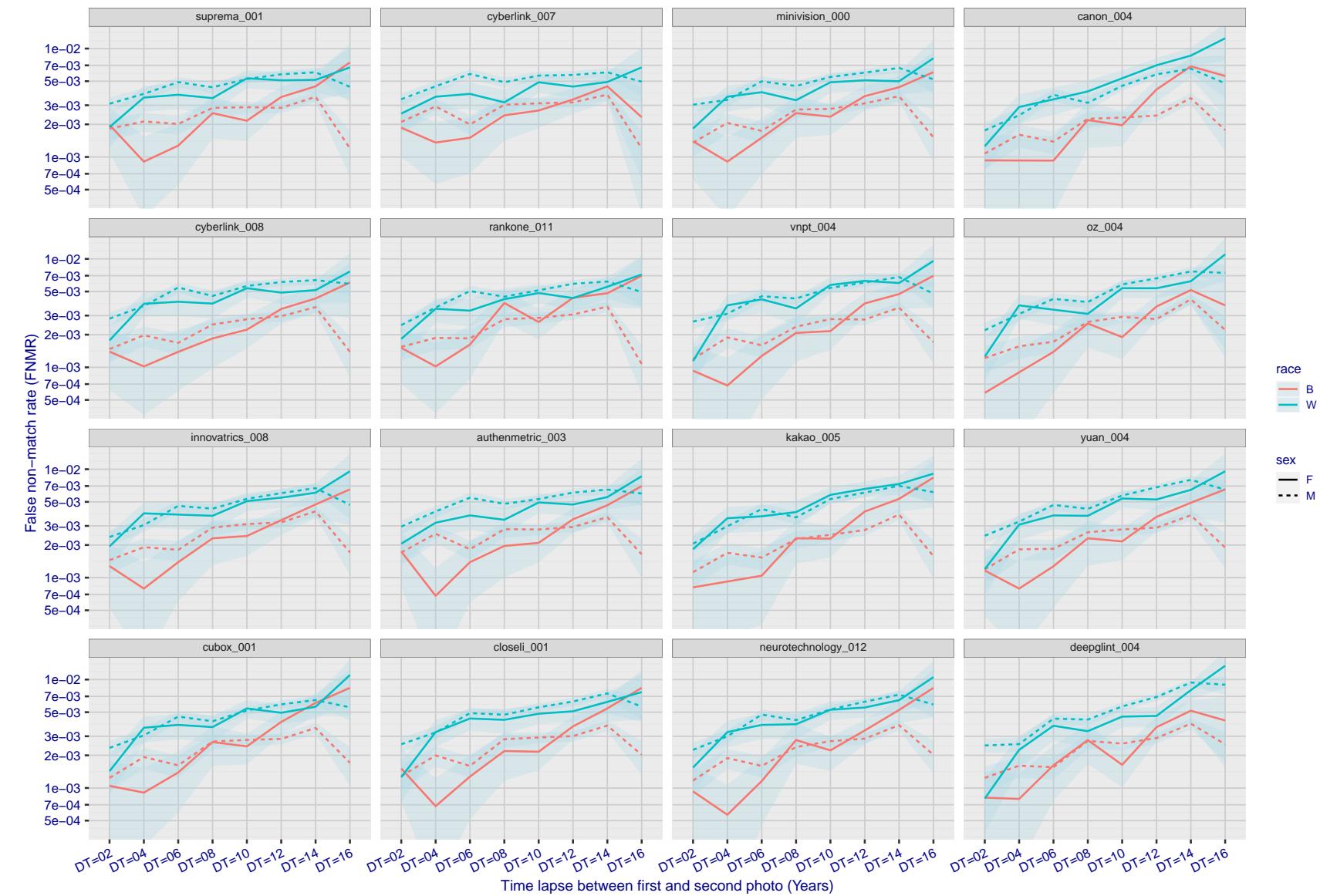


Figure 284: For the mugshot images, FNMR as a function of elapsed time between initial enrollment and second verification images. The panels appear most accurate first, and vertical scale changes on each page. The four traces correspond to images annotated with codes for black female, black male, white female, white male. The threshold is fixed for each algorithm to give FMR = 0.00001 over all ( $10^8$ ) impostor comparisons. For short time-lapses, the most accurate algorithms give very few errors (FNMR < 0.001) so that the uncertainty estimates are high.

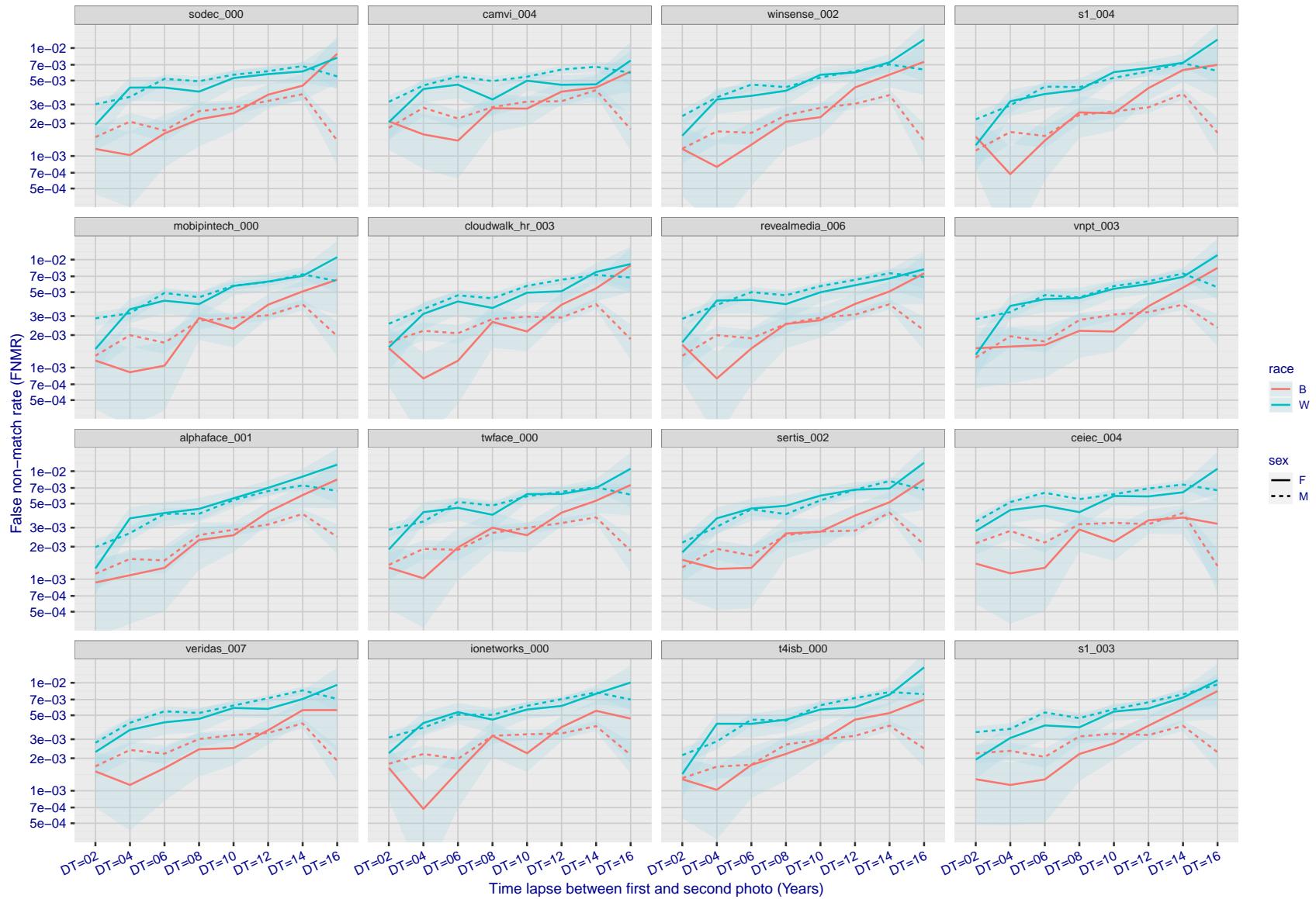


Figure 285: For the mugshot images, FNMR as a function of elapsed time between initial enrollment and second verification images. The panels appear most accurate first, and vertical scale changes on each page. The four traces correspond to images annotated with codes for black female, black male, white female, white male. The threshold is fixed for each algorithm to give  $FMR = 0.00001$  over all ( $10^8$ ) impostor comparisons. For short time-lapses, the most accurate algorithms give very few errors ( $FNMR < 0.001$ ) so that the uncertainty estimates are high.

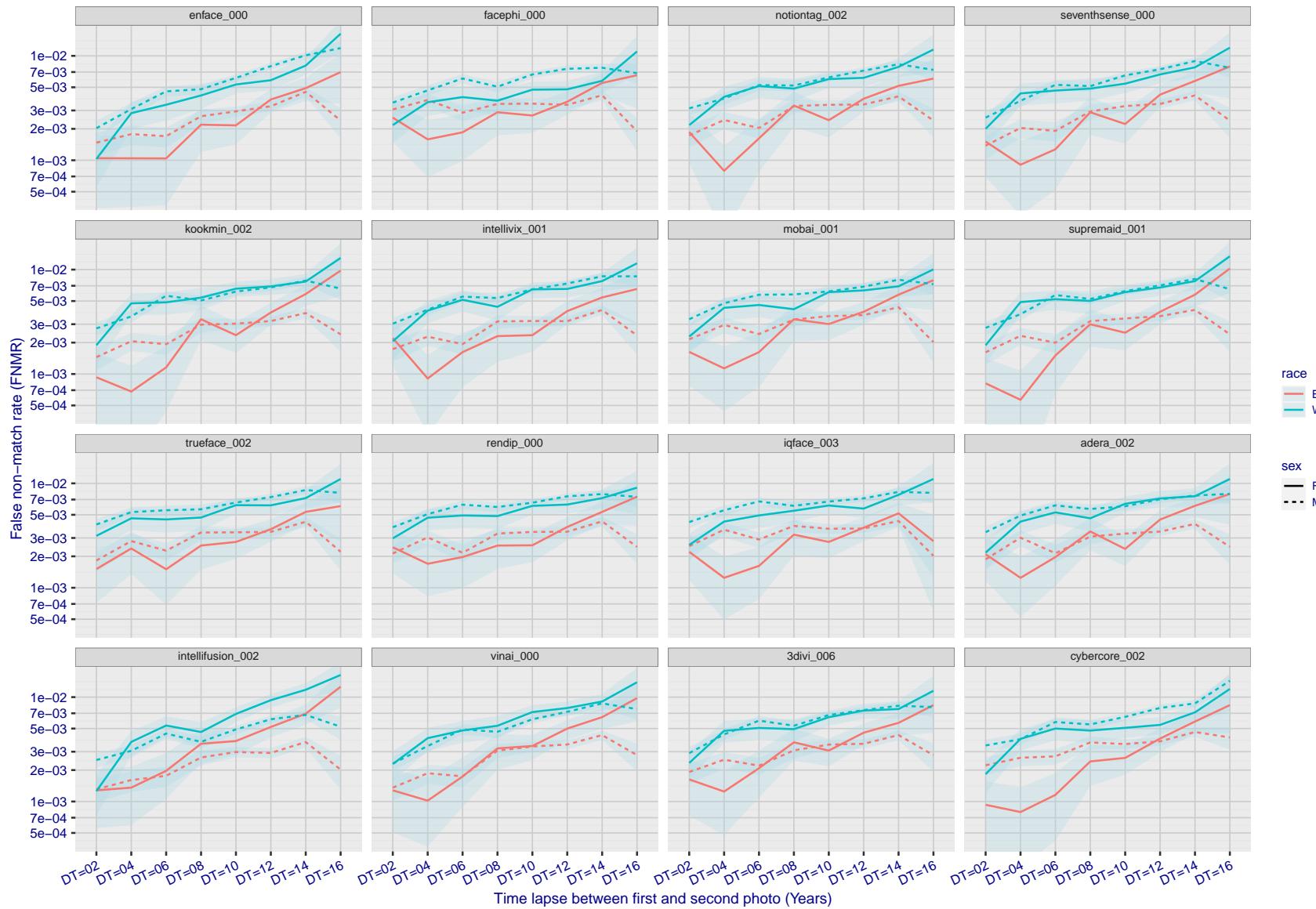


Figure 286: For the mugshot images, FNMR as a function of elapsed time between initial enrollment and second verification images. The panels appear most accurate first, and vertical scale changes on each page. The four traces correspond to images annotated with codes for black female, black male, white female, white male. The threshold is fixed for each algorithm to give  $FMR = 0.00001$  over all ( $10^8$ ) impostor comparisons. For short time-lapses, the most accurate algorithms give very few errors ( $FNMR < 0.001$ ) so that the uncertainty estimates are high.

2022/05/06 07:45:52

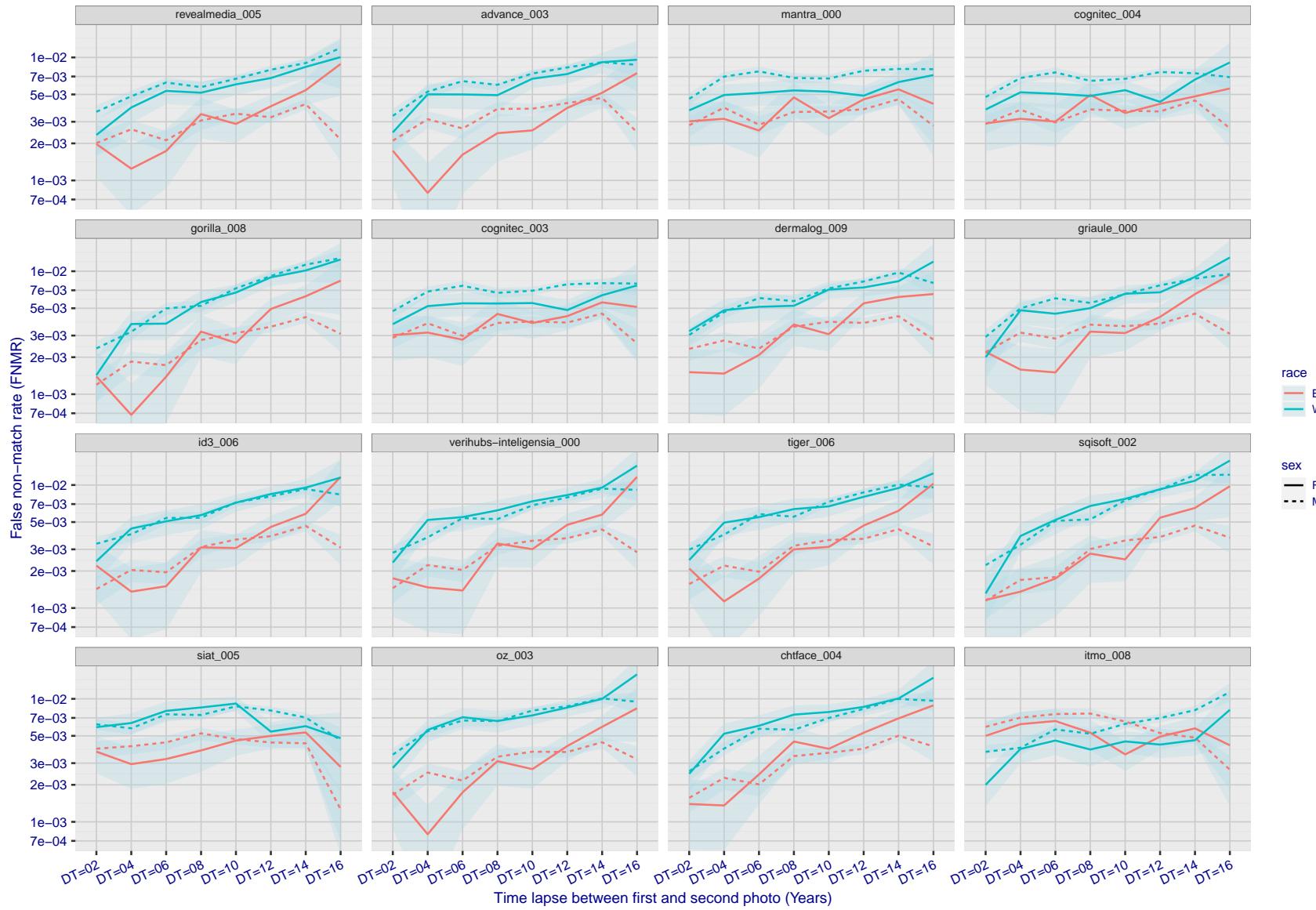


Figure 287: For the mugshot images, FNMR as a function of elapsed time between initial enrollment and second verification images. The panels appear most accurate first, and vertical scale changes on each page. The four traces correspond to images annotated with codes for black female, black male, white female, white male. The threshold is fixed for each algorithm to give FMR = 0.00001 over all ( $10^8$ ) impostor comparisons. For short time-lapses, the most accurate algorithms give very few errors (FNMR < 0.001) so that the uncertainty estimates are high.

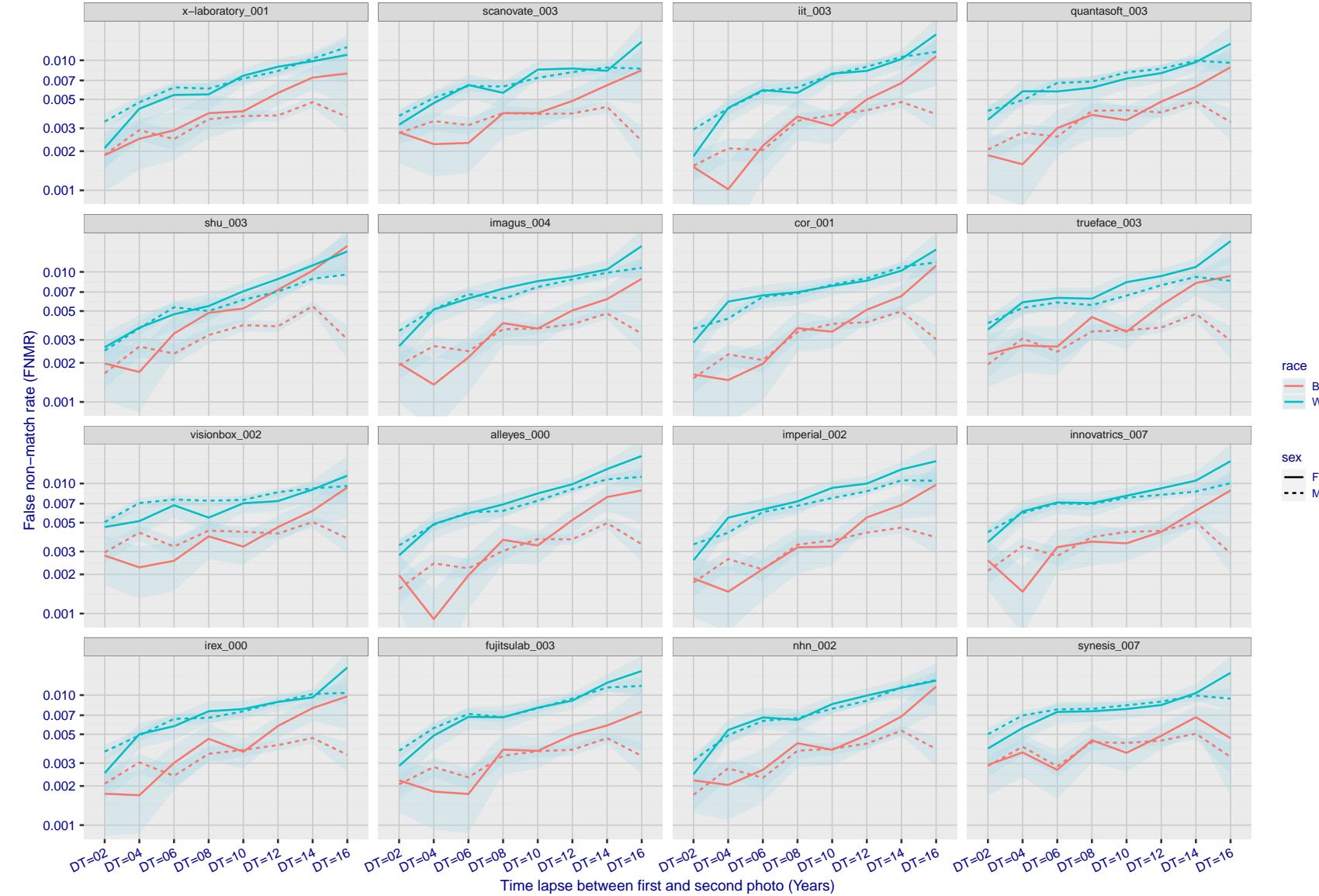


Figure 288: For the mugshot images, FNMR as a function of elapsed time between initial enrollment and second verification images. The panels appear most accurate first, and vertical scale changes on each page. The four traces correspond to images annotated with codes for black female, black male, white female, white male. The threshold is fixed for each algorithm to give FMR = 0.00001 over all ( $10^8$ ) impostor comparisons. For short time-lapses, the most accurate algorithms give very few errors (FNMR < 0.001) so that the uncertainty estimates are high.

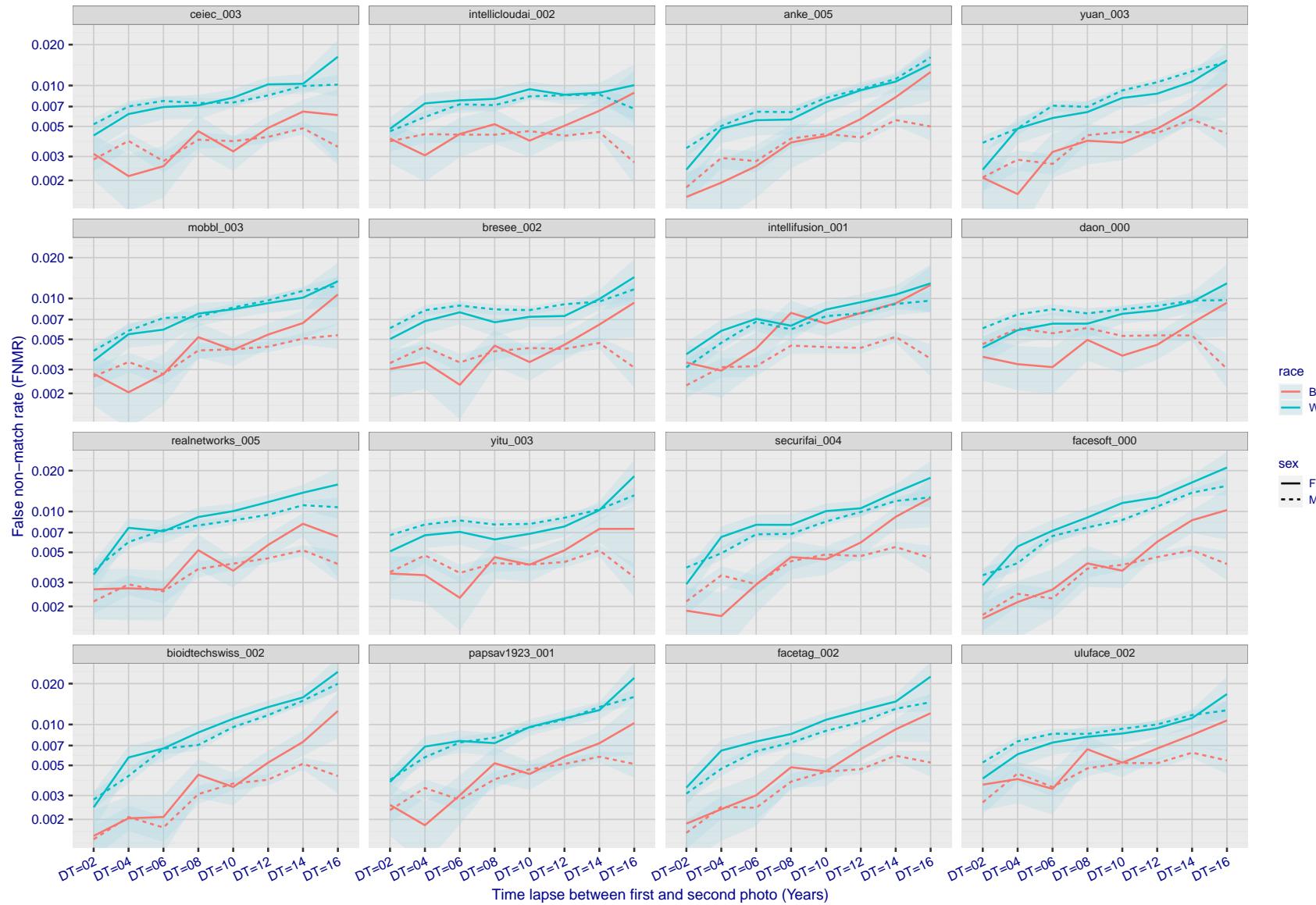


Figure 289: For the mugshot images, FNMR as a function of elapsed time between initial enrollment and second verification images. The panels appear most accurate first, and vertical scale changes on each page. The four traces correspond to images annotated with codes for black female, black male, white female, white male. The threshold is fixed for each algorithm to give FMR = 0.00001 over all ( $10^8$ ) impostor comparisons. For short time-lapses, the most accurate algorithms give very few errors (FNMR < 0.001) so that the uncertainty estimates are high.

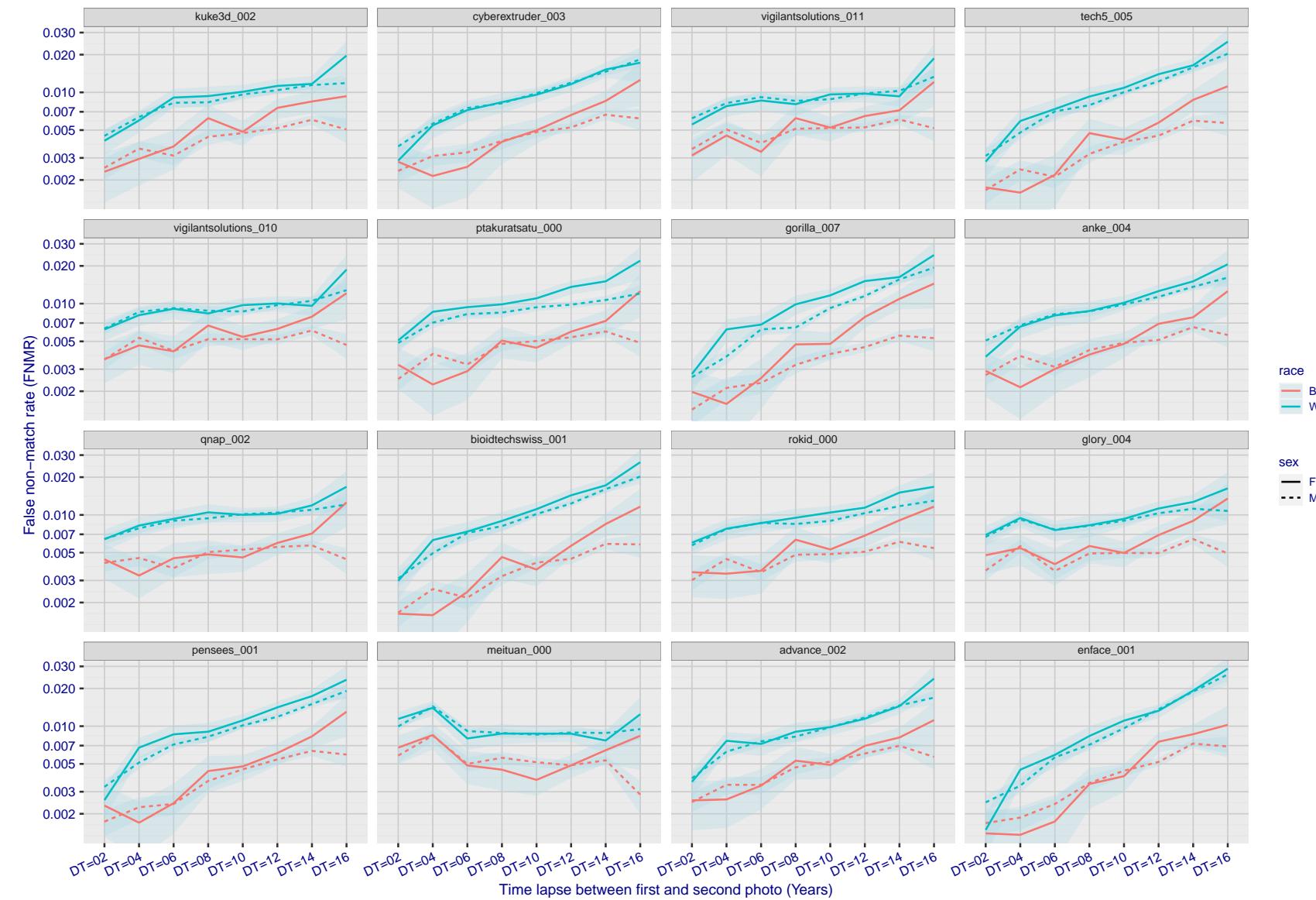


Figure 290: For the mugshot images, FNMR as a function of elapsed time between initial enrollment and second verification images. The panels appear most accurate first, and vertical scale changes on each page. The four traces correspond to images annotated with codes for black female, black male, white female, white male. The threshold is fixed for each algorithm to give  $FMR = 0.00001$  over all ( $10^8$ ) impostor comparisons. For short time-lapses, the most accurate algorithms give very few errors ( $FNMR < 0.001$ ) so that the uncertainty estimates are high.

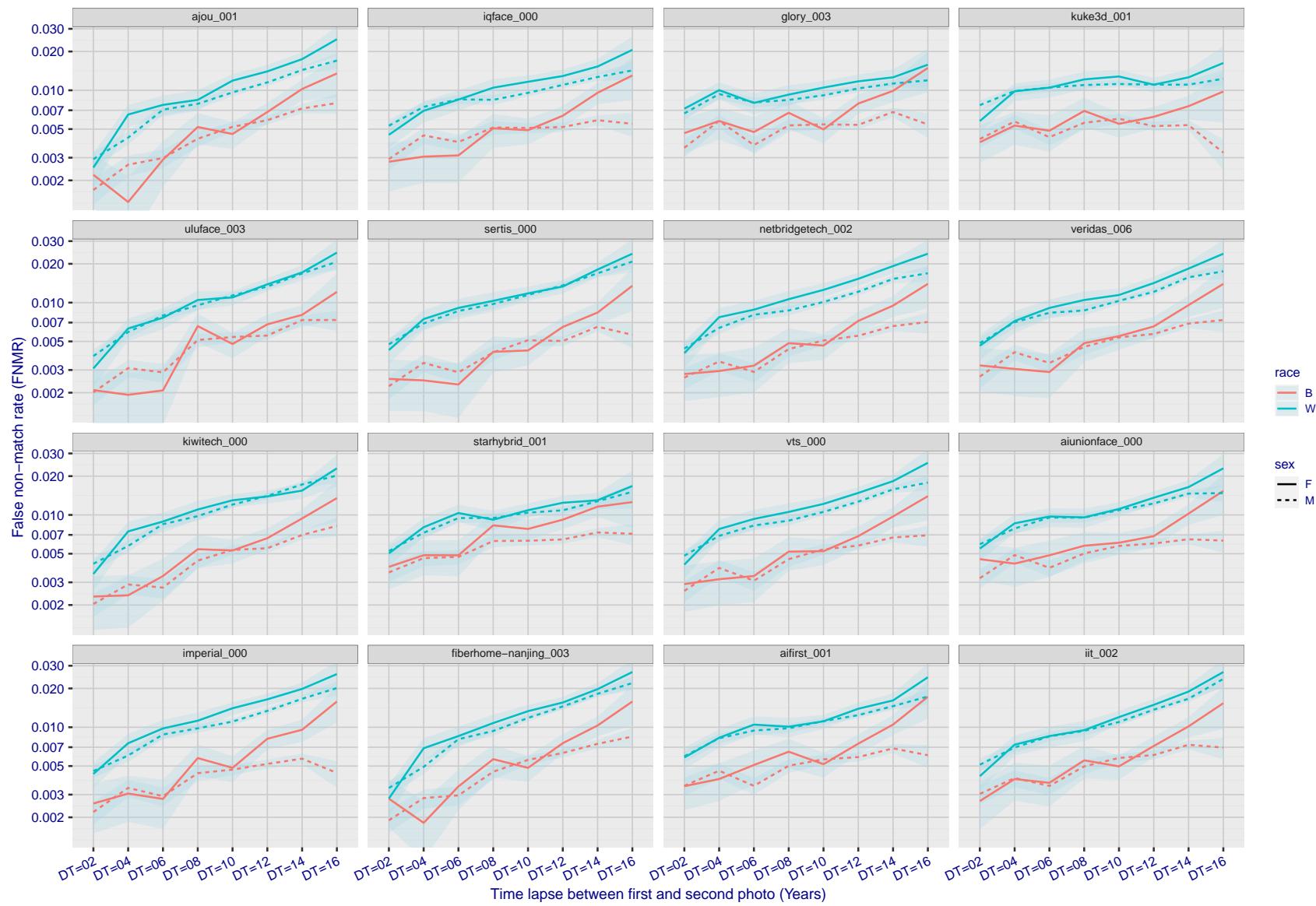


Figure 291: For the mugshot images, FNMR as a function of elapsed time between initial enrollment and second verification images. The panels appear most accurate first, and vertical scale changes on each page. The four traces correspond to images annotated with codes for black female, black male, white female, white male. The threshold is fixed for each algorithm to give FMR = 0.00001 over all ( $10^8$ ) impostor comparisons. For short time-lapses, the most accurate algorithms give very few errors (FNMR < 0.001) so that the uncertainty estimates are high.

2022/05/06 07:45:52

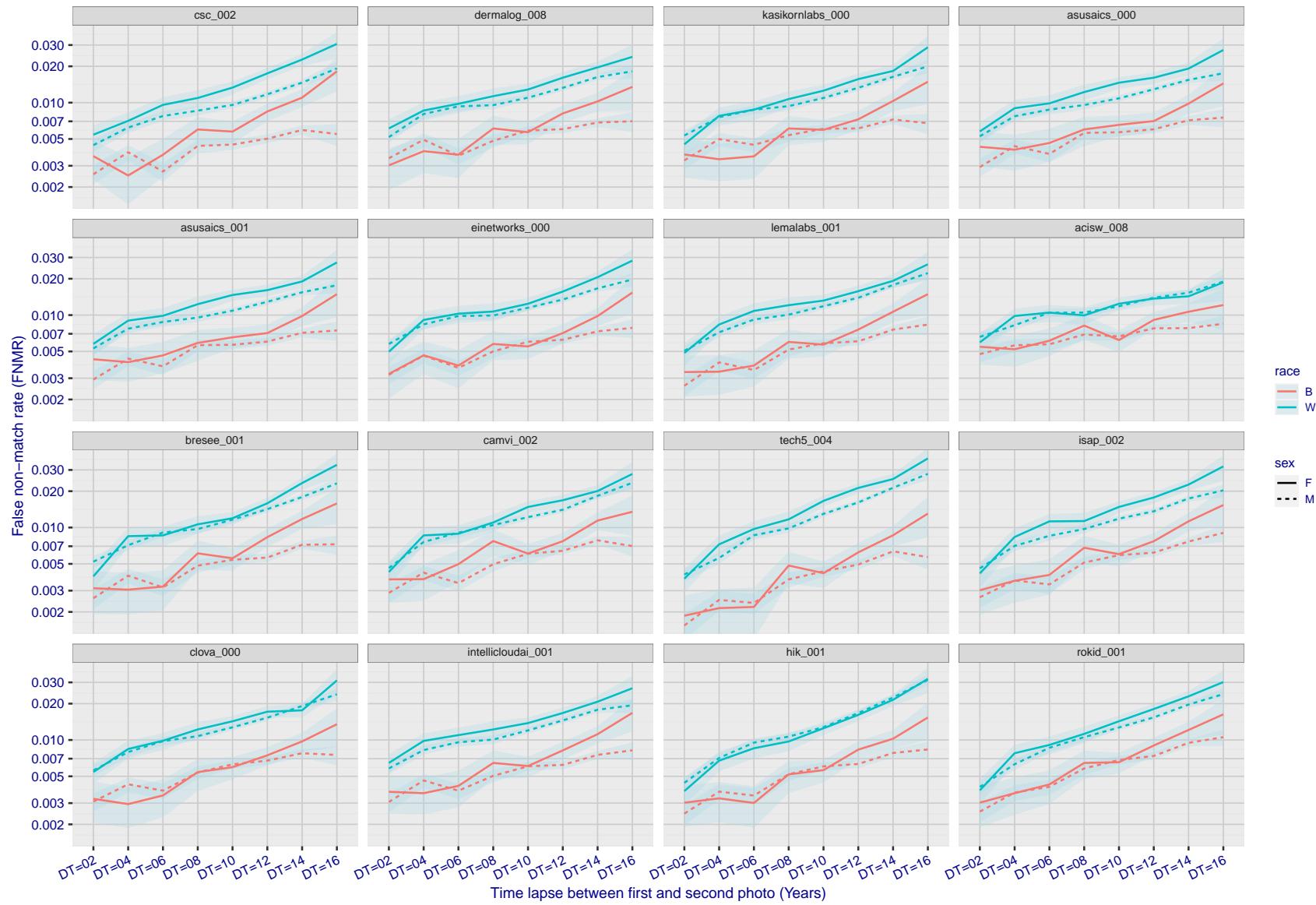


Figure 292: For the mugshot images, FNMR as a function of elapsed time between initial enrollment and second verification images. The panels appear most accurate first, and vertical scale changes on each page. The four traces correspond to images annotated with codes for black female, black male, white female, white male. The threshold is fixed for each algorithm to give FMR = 0.00001 over all ( $10^8$ ) impostor comparisons. For short time-lapses, the most accurate algorithms give very few errors (FNMR < 0.001) so that the uncertainty estimates are high.

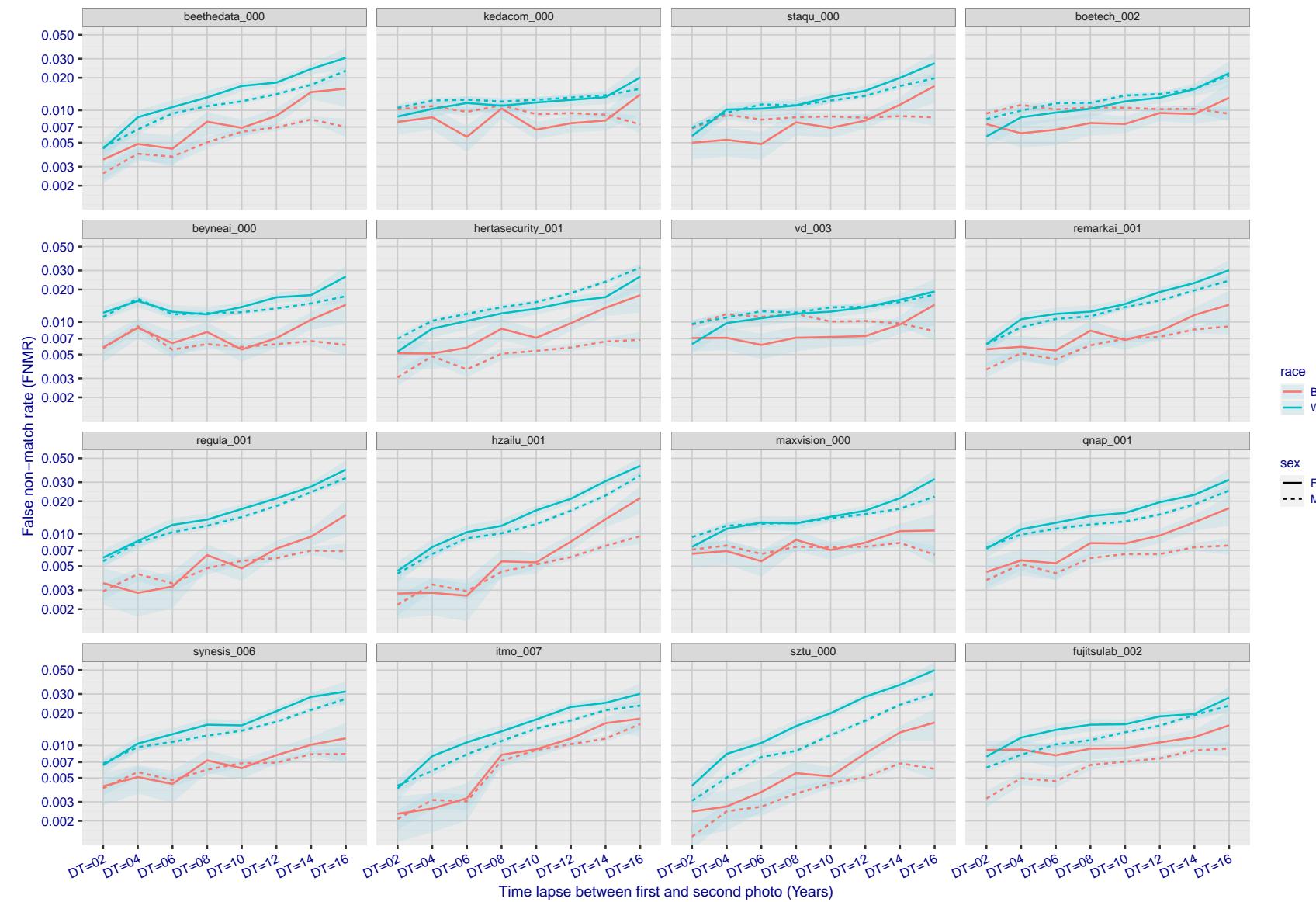


Figure 293: For the mugshot images, FNMR as a function of elapsed time between initial enrollment and second verification images. The panels appear most accurate first, and vertical scale changes on each page. The four traces correspond to images annotated with codes for black female, black male, white female, white male. The threshold is fixed for each algorithm to give  $FMR = 0.00001$  over all ( $10^8$ ) impostor comparisons. For short time-lapses, the most accurate algorithms give very few errors ( $FNMR < 0.001$ ) so that the uncertainty estimates are high.

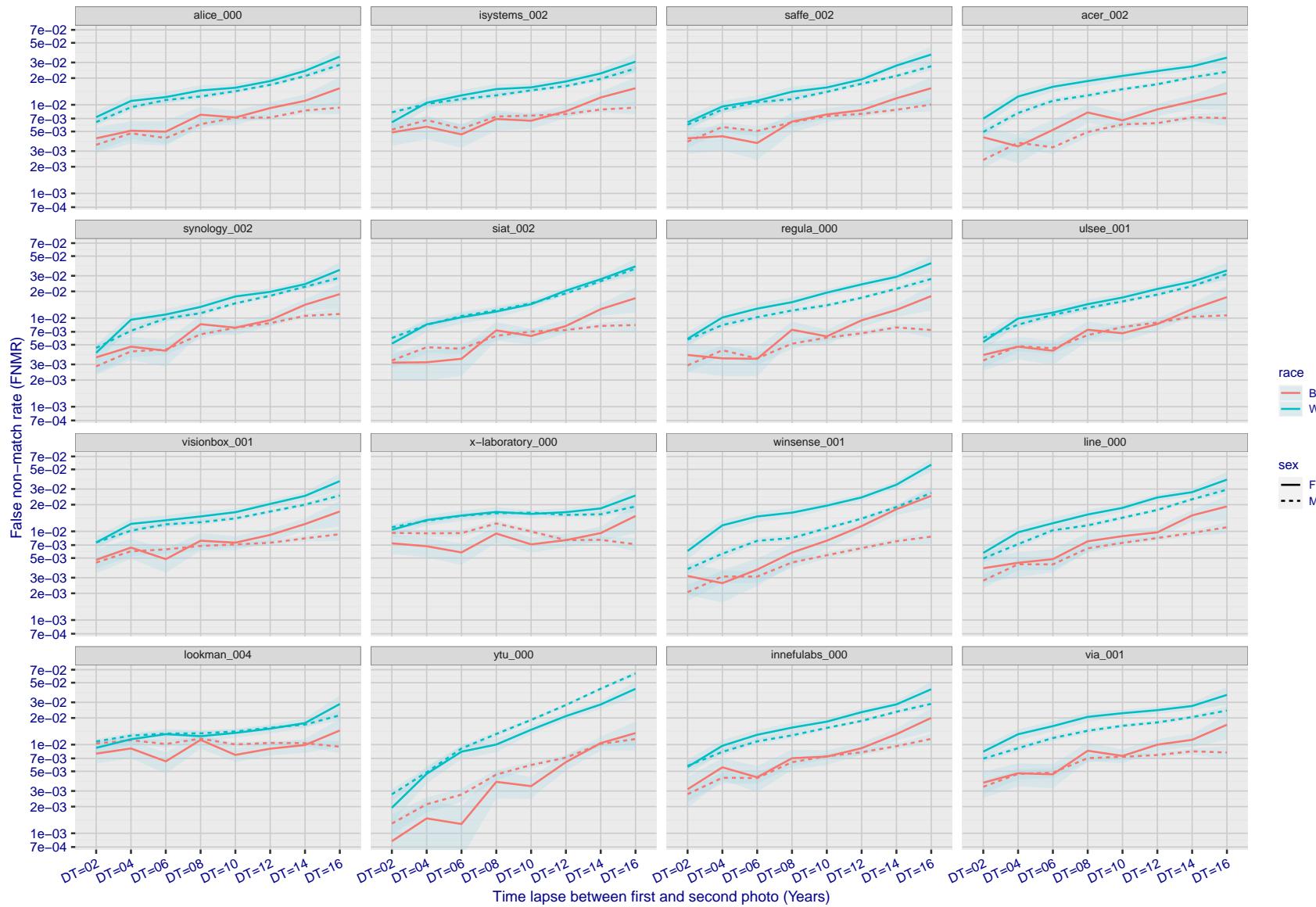


Figure 294: For the mugshot images, FNMR as a function of elapsed time between initial enrollment and second verification images. The panels appear most accurate first, and vertical scale changes on each page. The four traces correspond to images annotated with codes for black female, black male, white female, white male. The threshold is fixed for each algorithm to give  $FMR = 0.00001$  over all ( $10^8$ ) impostor comparisons. For short time-lapses, the most accurate algorithms give very few errors ( $FNMR < 0.001$ ) so that the uncertainty estimates are high.

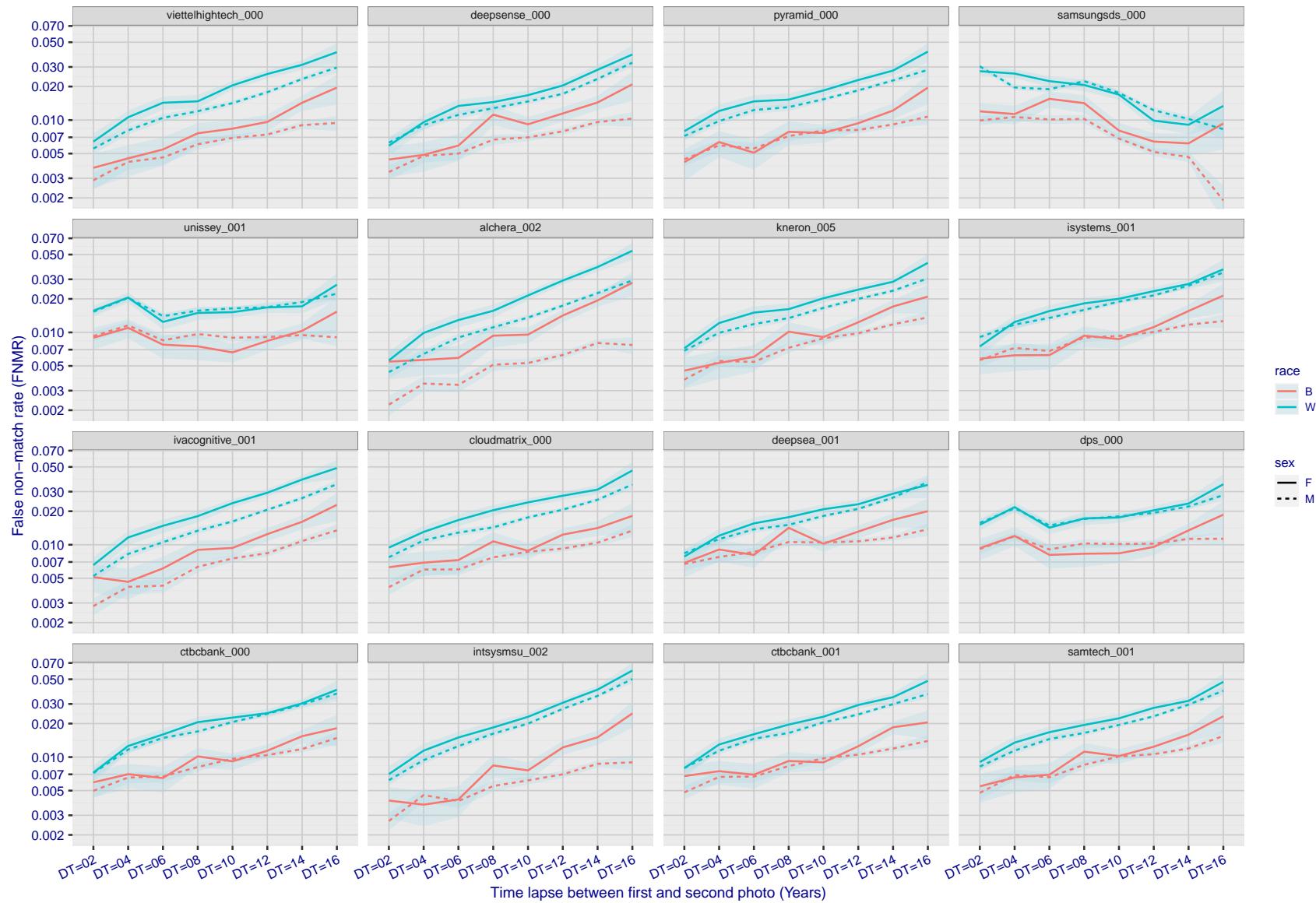


Figure 295: For the mugshot images, FNMR as a function of elapsed time between initial enrollment and second verification images. The panels appear most accurate first, and vertical scale changes on each page. The four traces correspond to images annotated with codes for black female, black male, white female, white male. The threshold is fixed for each algorithm to give  $FMR = 0.00001$  over all ( $10^8$ ) impostor comparisons. For short time-lapses, the most accurate algorithms give very few errors ( $FNMR < 0.001$ ) so that the uncertainty estimates are high.

2022/05/06 07:45:52

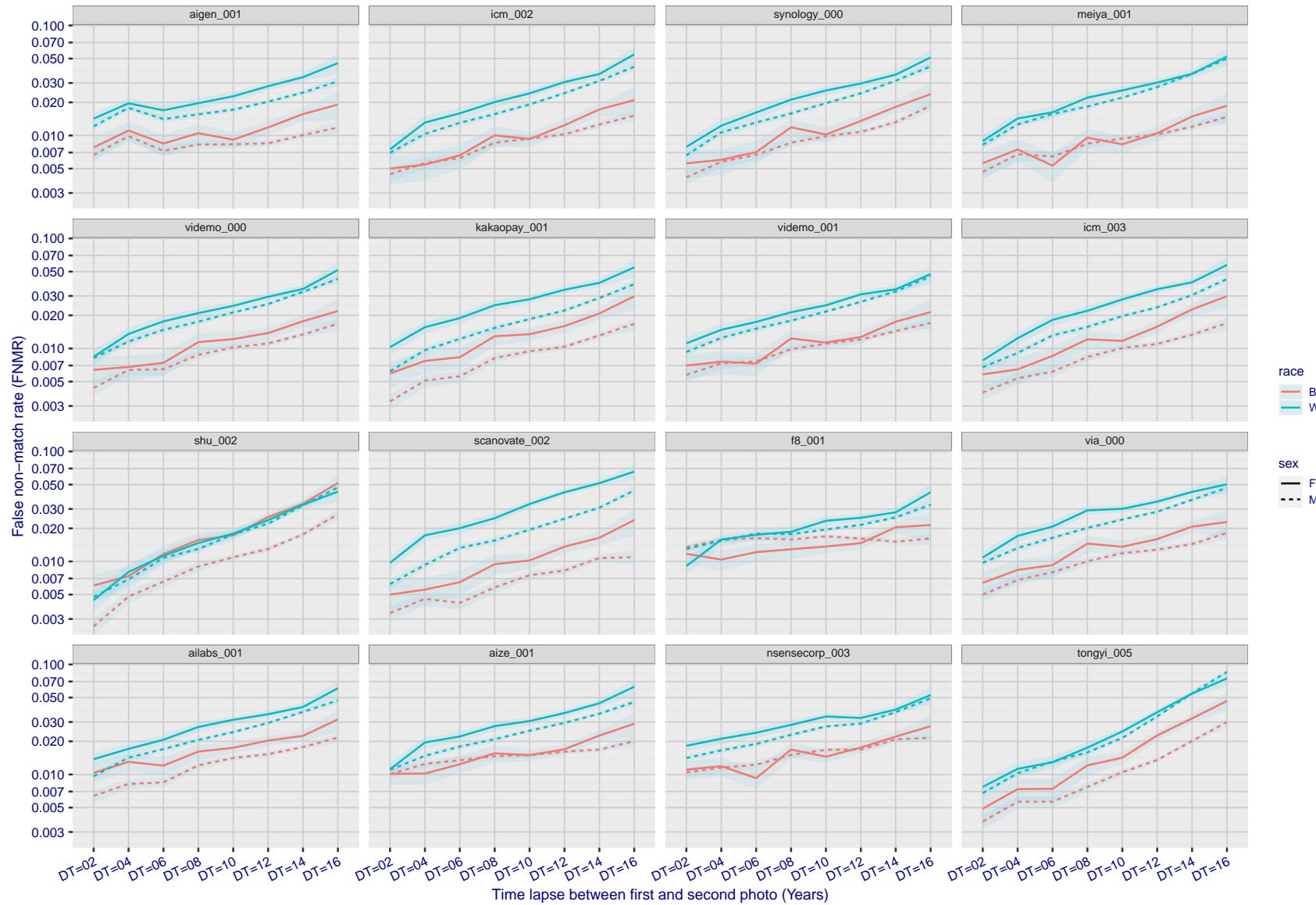


Figure 296: For the mugshot images, FNMR as a function of elapsed time between initial enrollment and second verification images. The panels appear most accurate first, and vertical scale changes on each page. The four traces correspond to images annotated with codes for black female, black male, white female, white male. The threshold is fixed for each algorithm to give FMR = 0.00001 over all ( $10^8$ ) impostor comparisons. For short time-lapses, the most accurate algorithms give very few errors (FNMR < 0.001) so that the uncertainty estimates are high.

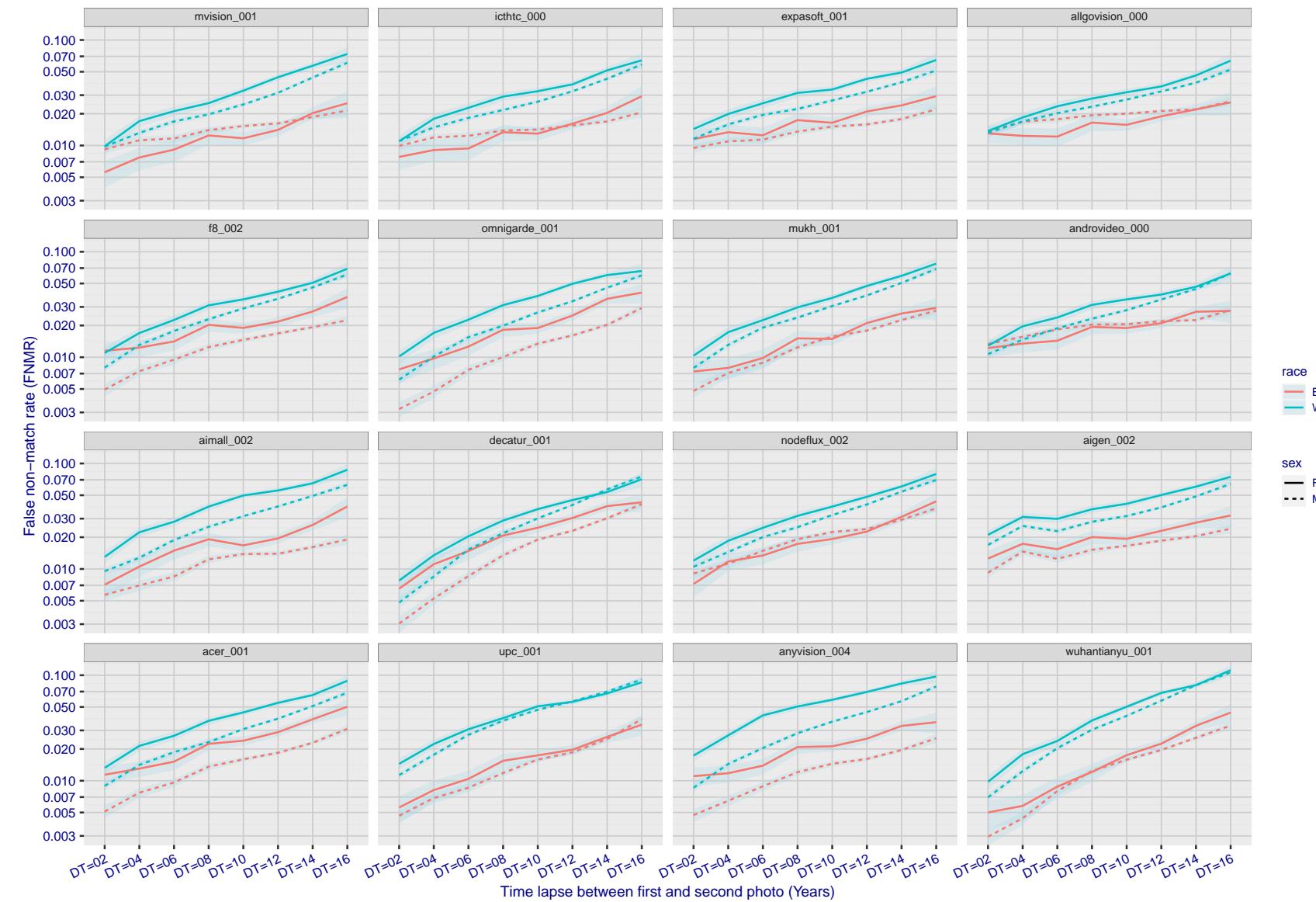


Figure 297: For the mugshot images, FNMR as a function of elapsed time between initial enrollment and second verification images. The panels appear most accurate first, and vertical scale changes on each page. The four traces correspond to images annotated with codes for black female, black male, white female, white male. The threshold is fixed for each algorithm to give  $FMR = 0.00001$  over all ( $10^8$ ) impostor comparisons. For short time-lapses, the most accurate algorithms give very few errors ( $FNMR < 0.001$ ) so that the uncertainty estimates are high.

2022/05/06 07:45:52

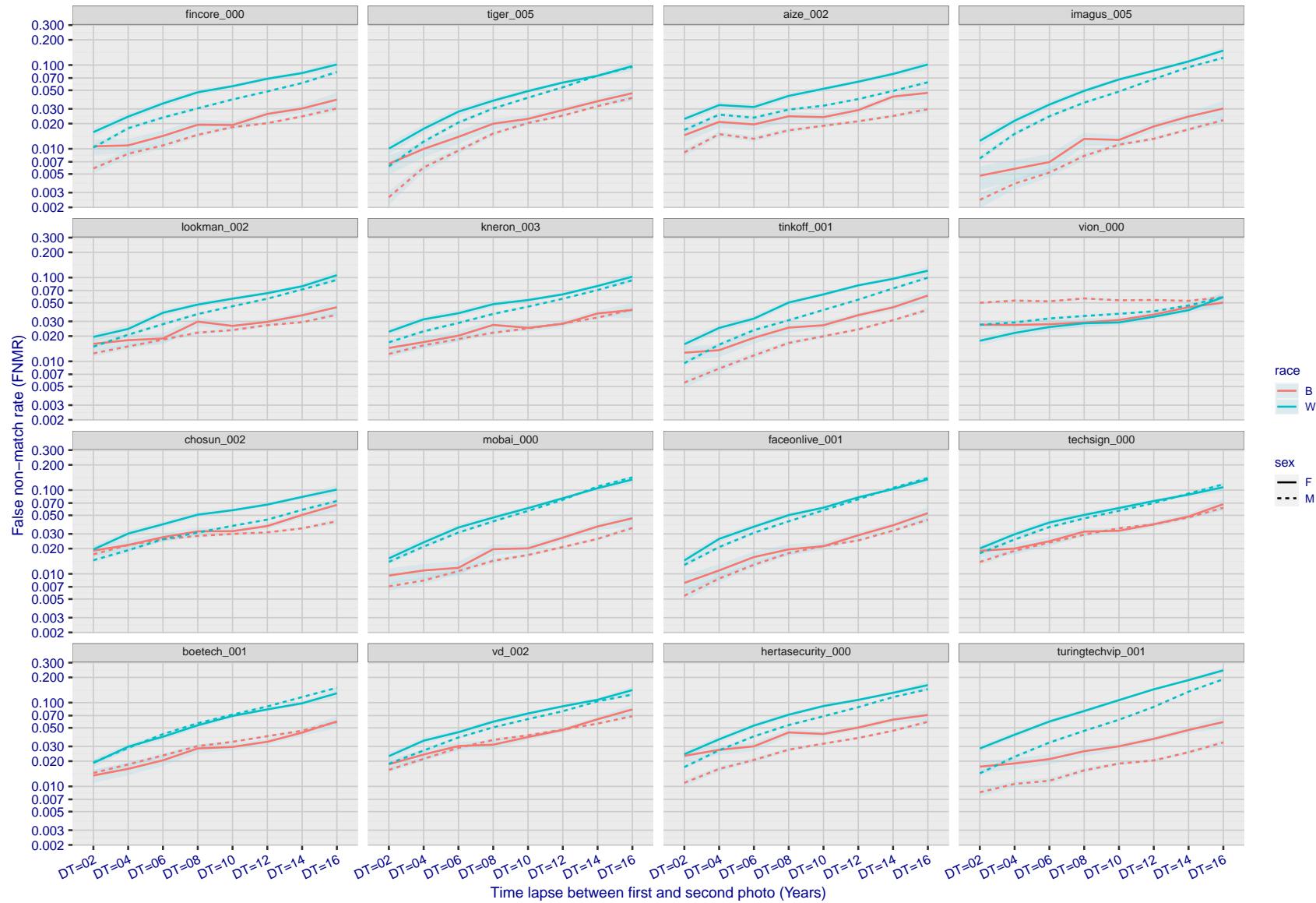


Figure 298: For the mugshot images, FNMR as a function of elapsed time between initial enrollment and second verification images. The panels appear most accurate first, and vertical scale changes on each page. The four traces correspond to images annotated with codes for black female, black male, white female, white male. The threshold is fixed for each algorithm to give FMR = 0.00001 over all ( $10^8$ ) impostor comparisons. For short time-lapses, the most accurate algorithms give very few errors (FNMR < 0.001) so that the uncertainty estimates are high.

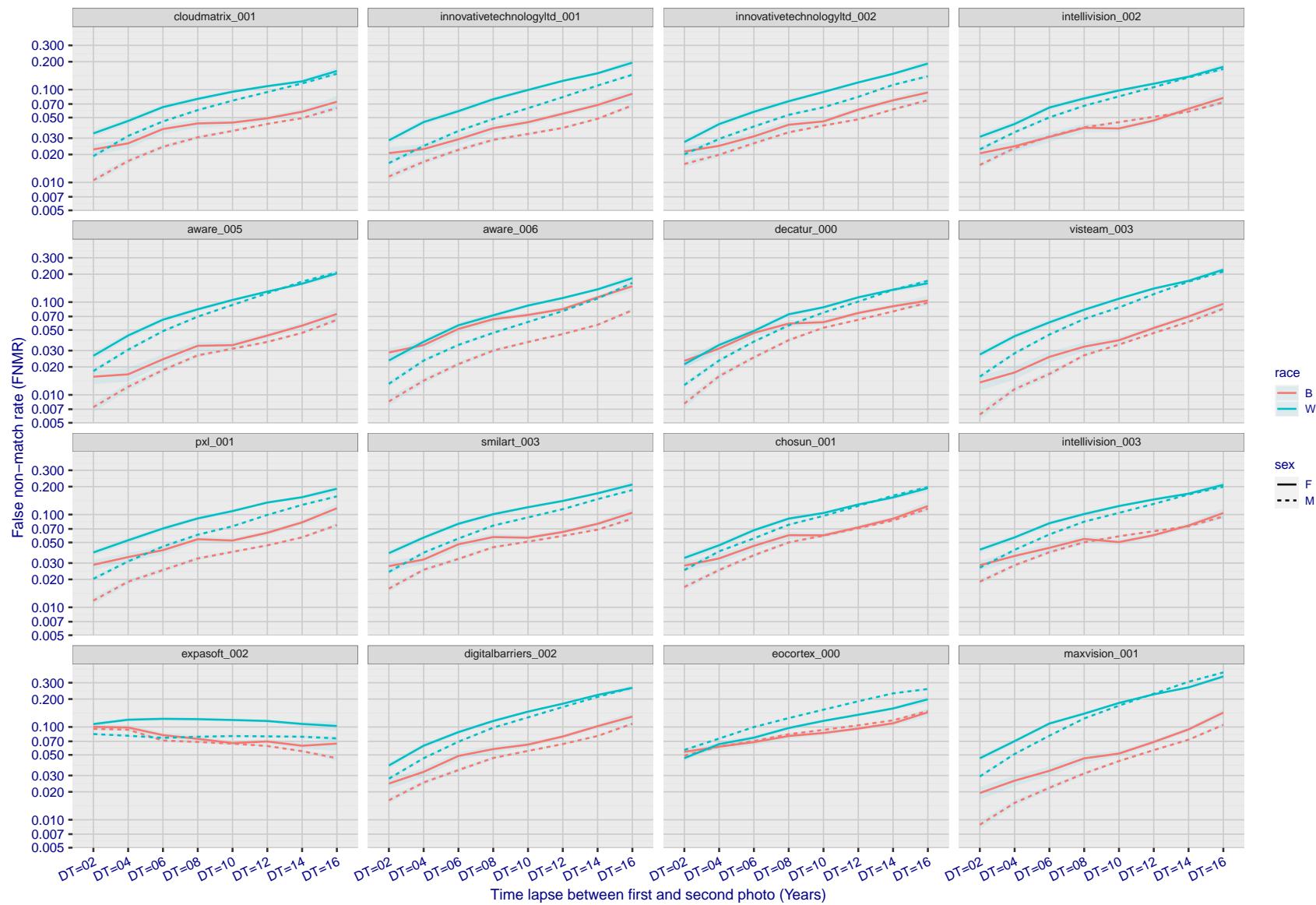


Figure 299: For the mugshot images, FNMR as a function of elapsed time between initial enrollment and second verification images. The panels appear most accurate first, and vertical scale changes on each page. The four traces correspond to images annotated with codes for black female, black male, white female, white male. The threshold is fixed for each algorithm to give FMR = 0.00001 over all ( $10^8$ ) impostor comparisons. For short time-lapses, the most accurate algorithms give very few errors (FNMR < 0.001) so that the uncertainty estimates are high.

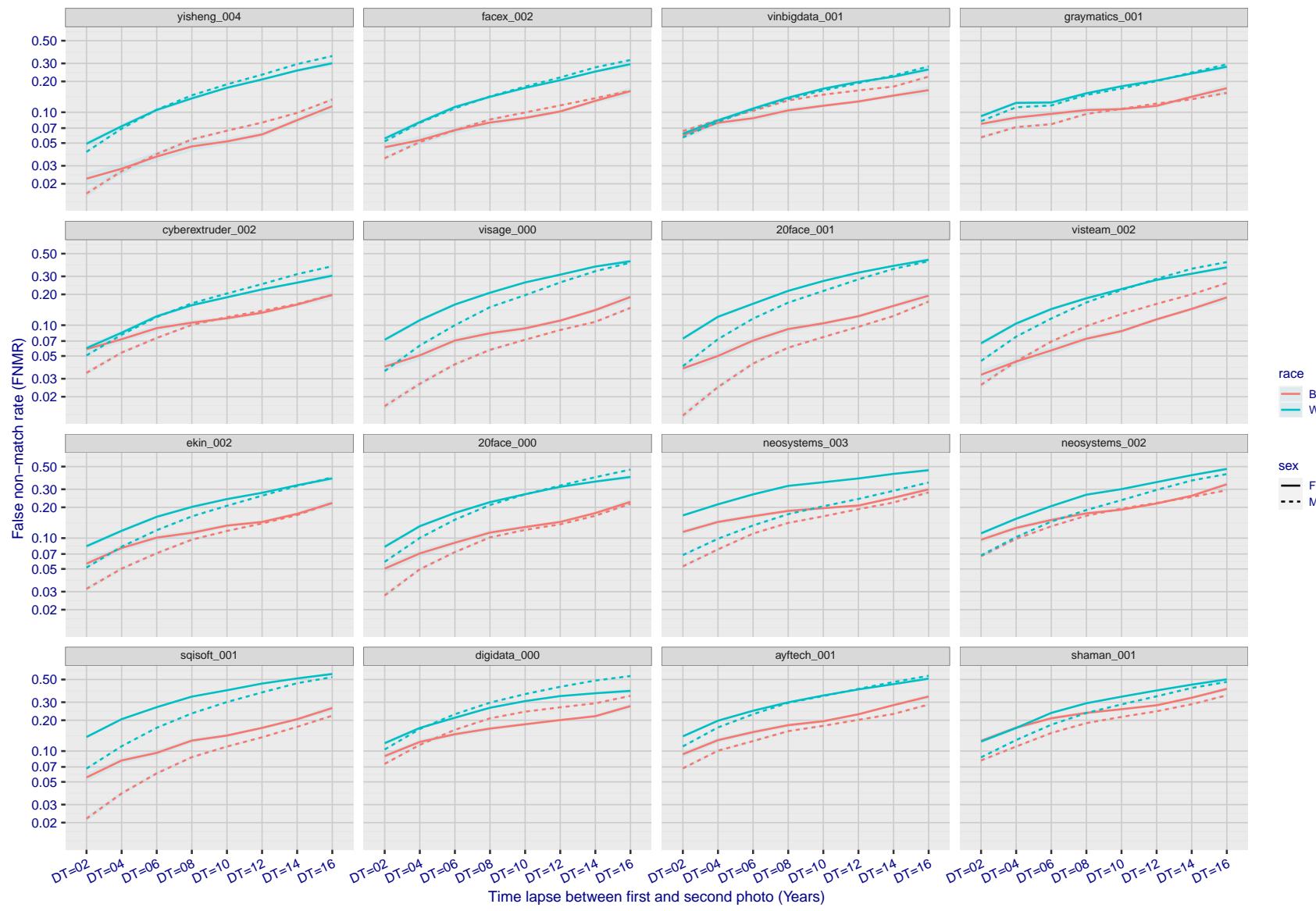


Figure 300: For the mugshot images, FNMR as a function of elapsed time between initial enrollment and second verification images. The panels appear most accurate first, and vertical scale changes on each page. The four traces correspond to images annotated with codes for black female, black male, white female, white male. The threshold is fixed for each algorithm to give FMR = 0.00001 over all ( $10^8$ ) impostor comparisons. For short time-lapses, the most accurate algorithms give very few errors (FNMR < 0.001) so that the uncertainty estimates are high.

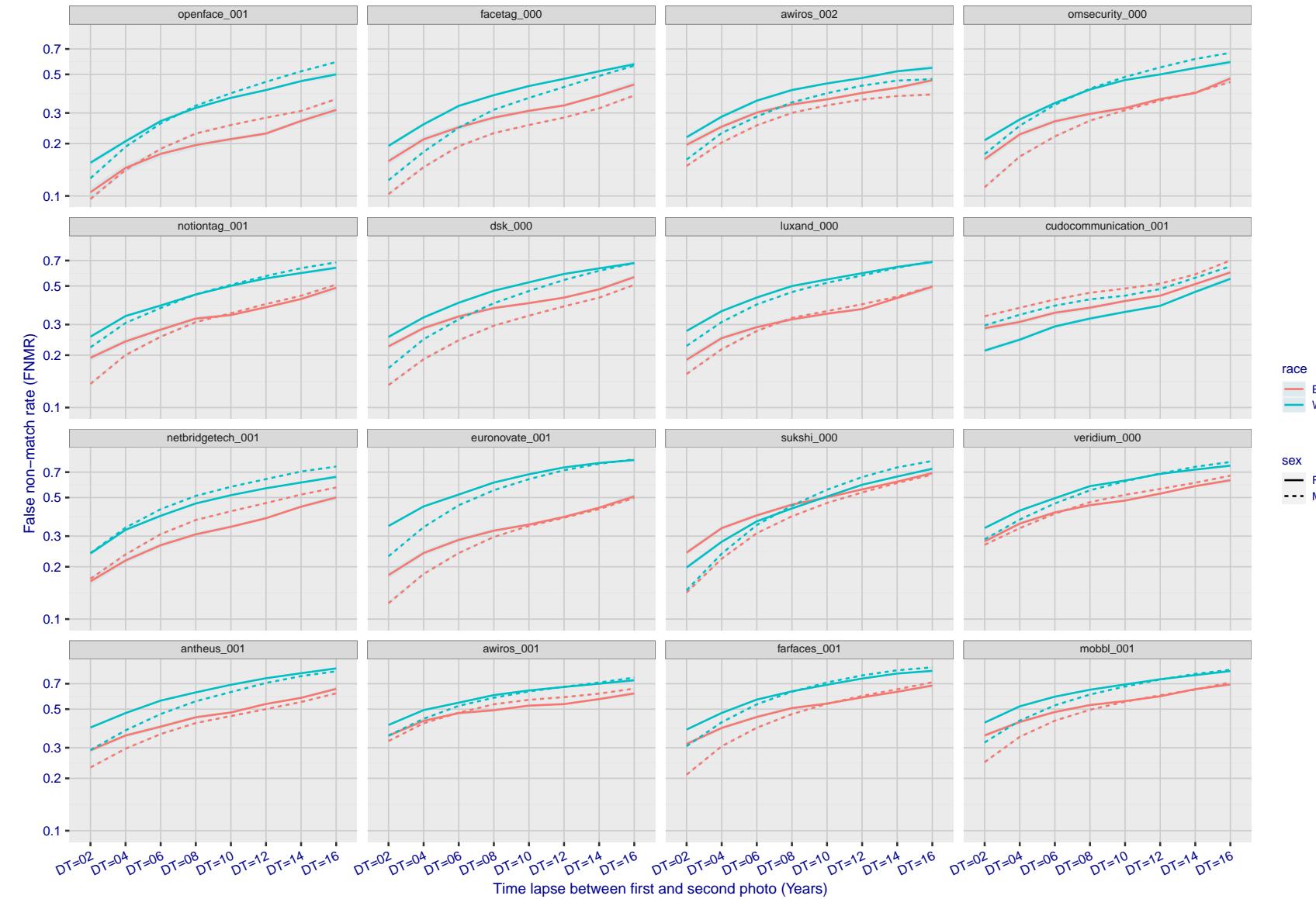


Figure 301: For the mugshot images, FNMR as a function of elapsed time between initial enrollment and second verification images. The panels appear most accurate first, and vertical scale changes on each page. The four traces correspond to images annotated with codes for black female, black male, white female, white male. The threshold is fixed for each algorithm to give  $FMR = 0.00001$  over all ( $10^8$ ) impostor comparisons. For short time-lapses, the most accurate algorithms give very few errors ( $FNMR < 0.001$ ) so that the uncertainty estimates are high.

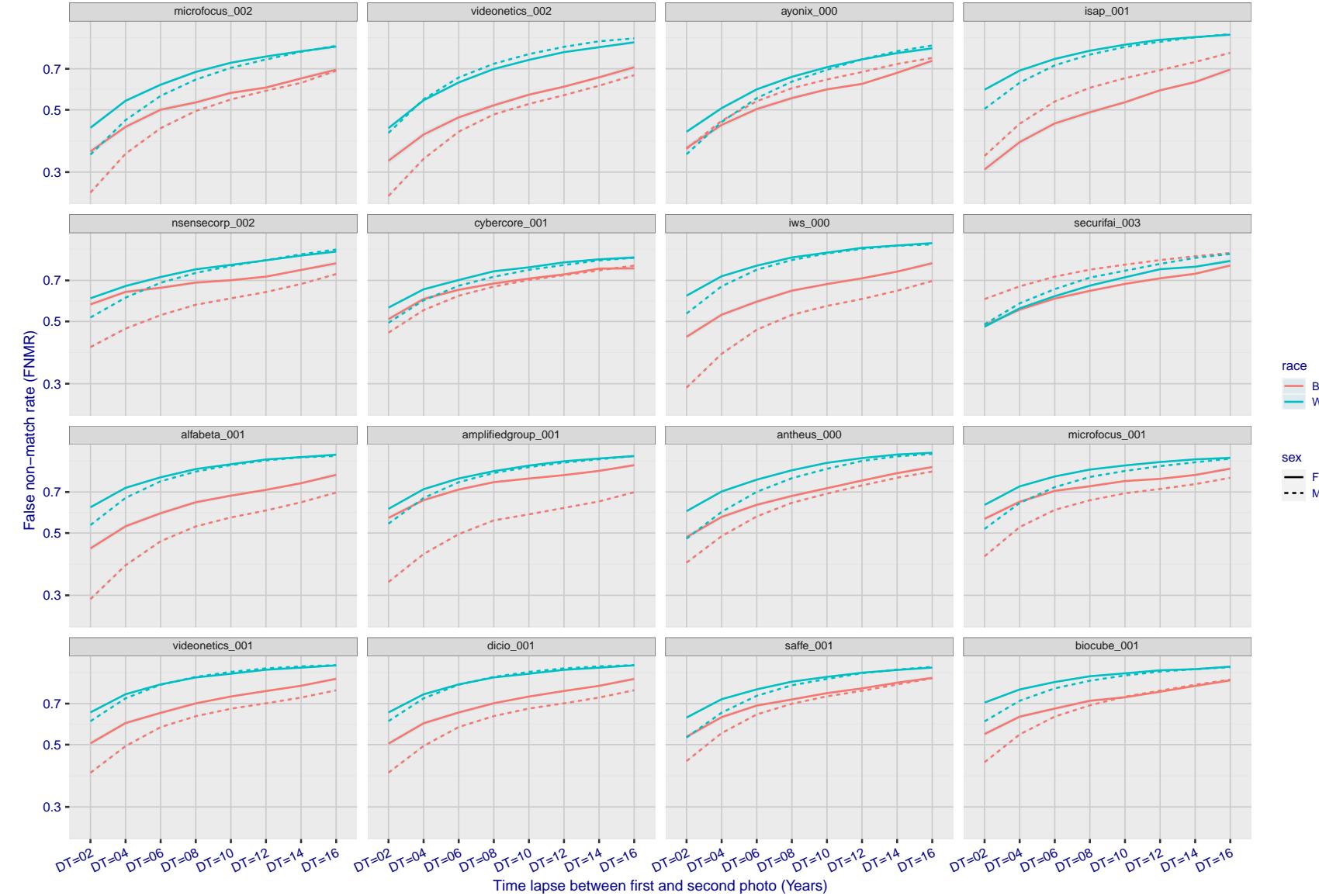


Figure 302: For the mugshot images, FNMR as a function of elapsed time between initial enrollment and second verification images. The panels appear most accurate first, and vertical scale changes on each page. The four traces correspond to images annotated with codes for black female, black male, white female, white male. The threshold is fixed for each algorithm to give FMR = 0.00001 over all ( $10^8$ ) impostor comparisons. For short time-lapses, the most accurate algorithms give very few errors (FNMR < 0.001) so that the uncertainty estimates are high.

2022/05/06 07:45:52

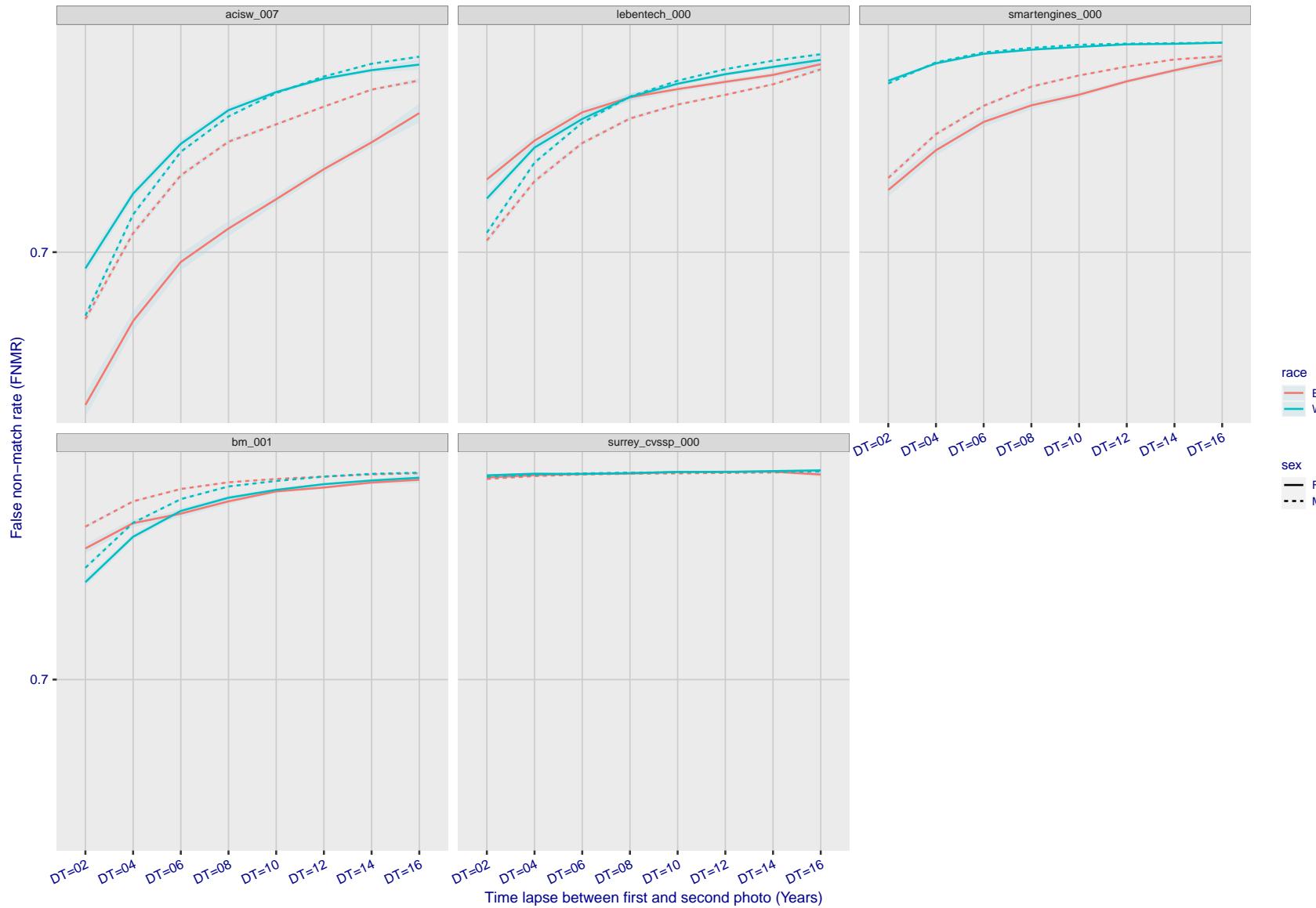


Figure 303: For the mugshot images, FNMR as a function of elapsed time between initial enrollment and second verification images. The panels appear most accurate first, and vertical scale changes on each page. The four traces correspond to images annotated with codes for black female, black male, white female, white male. The threshold is fixed for each algorithm to give  $FMR = 0.00001$  over all ( $10^8$ ) impostor comparisons. For short time-lapses, the most accurate algorithms give very few errors ( $FNMR < 0.001$ ) so that the uncertainty estimates are high.

### 3.5.3 Effect of age on genuine subjects

**Background:** Faces change appearance throughout life. Face recognition algorithms have previously been reported to give better accuracy on older individuals (See NIST IR 8009).

**Goal:** To quantify false non-match rates (FNMR) as a function of age, without an ageing component.

**Methods:** Using the visa images, which span fewer than five years, thresholds are determined that give FMR = 0.001 and 0.0001 over the entire impostor set. Then FNMR is measured over 1000 bootstrap replications of the genuine scores.

**Results:** For the visa images, Figure 338 shows how false non-match rates for genuine users, as a function of age group.

The notable aspects are:

- ▷ Younger subjects give considerably higher FNMR. This is likely due to rapid growth and change in facial appearance.
- ▷ FNMR trends down throughout life. The last bin, AGE > 72, contains fewer than 140 mated pairs, and may be affected by small sample size.

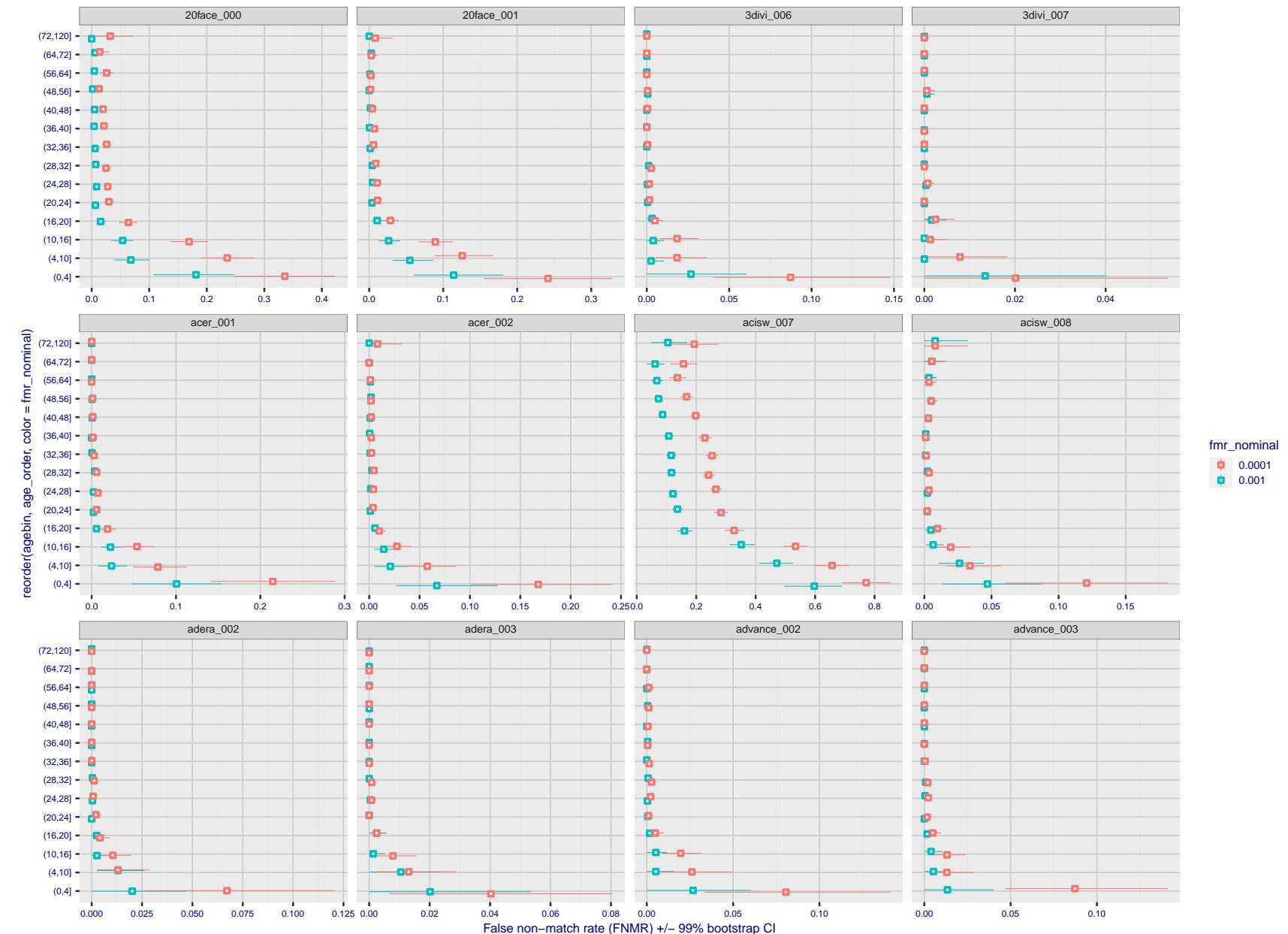


Figure 304: For the visa images, the dots show FNMR by age group for two operating thresholds corresponding to  $FMR = \{0.001, 0.0001\}$  computed over all on the order of  $10^{10}$  impostor scores. The FMR in each bin will vary also - see subsequent impostor heatmaps in sec. 3.6.2. Given a pair of face images taken at different times, we assign the comparison to the bin that is the arithmetic average of the subject's ages. This plot shows only the effect of age, not ageing. The number of comparisons in each bin is generally in the thousands, however the first and last bins are computed over 149 and 124 respectively. The error rates in some (adult) cases are zero, and in others the DET is flat so the error rates at the two thresholds are identical. The lines span 1% and 99% of bootstrap replicated FNMR estimates.



Figure 305: For the visa images, the dots show FNMR by age group for two operating thresholds corresponding to  $FMR = \{0.001, 0.0001\}$  computed over all on the order of  $10^{10}$  impostor scores. The FMR in each bin will vary also - see subsequent impostor heatmaps in sec. 3.6.2. Given a pair of face images taken at different times, we assign the comparison to the bin that is the arithmetic average of the subject's ages. This plot shows only the effect of age, not ageing. The number of comparisons in each bin is generally in the thousands, however the first and last bins are computed over 149 and 124 respectively. The error rates in some (adult) cases are zero, and in others the DET is flat so the error rates at the two thresholds are identical. The lines span 1% and 99% of bootstrap replicated FNMR estimates.

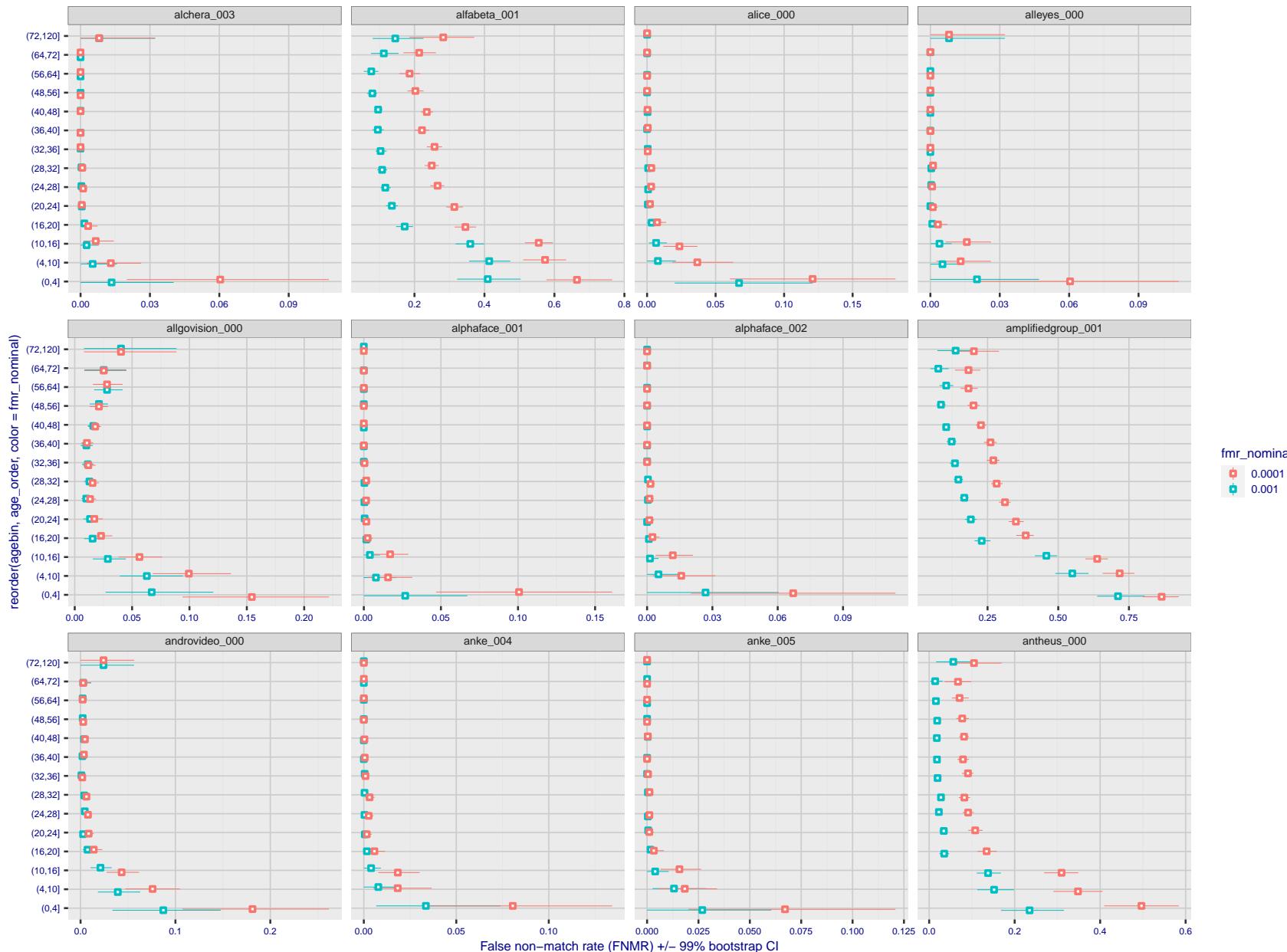


Figure 306: For the visa images, the dots show FNMR by age group for two operating thresholds corresponding to  $FMR = \{0.001, 0.0001\}$  computed over all on the order of  $10^{10}$  impostor scores. The FMR in each bin will vary also - see subsequent impostor heatmaps in sec. 3.6.2. Given a pair of face images taken at different times, we assign the comparison to the bin that is the arithmetic average of the subject's ages. This plot shows only the effect of age, not ageing. The number of comparisons in each bin is generally in the thousands, however the first and last bins are computed over 149 and 124 respectively. The error rates in some (adult) cases are zero, and in others the DET is flat so the error rates at the two thresholds are identical. The lines span 1% and 99% of bootstrap replicated FNMR estimates.

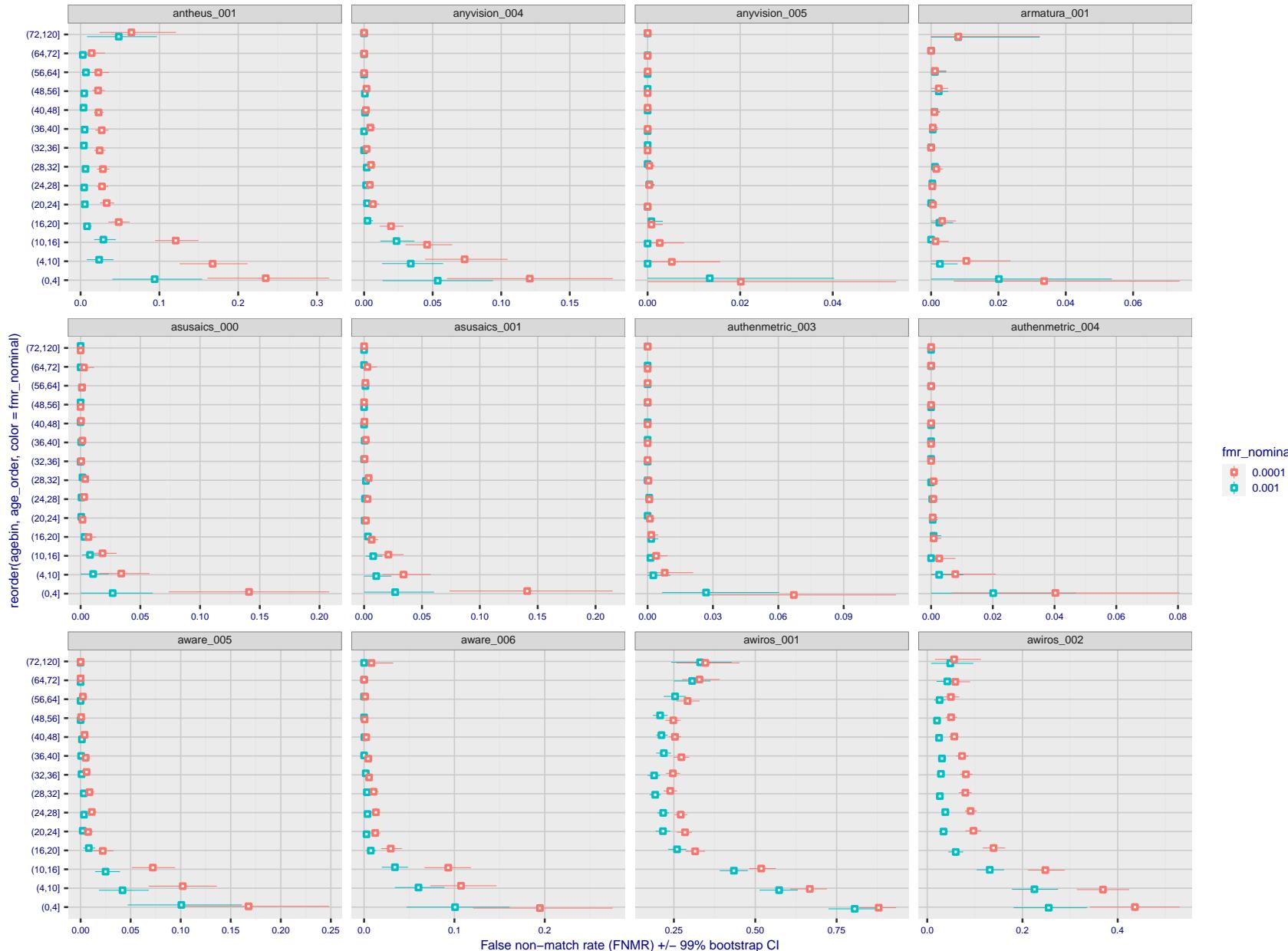


Figure 307: For the visa images, the dots show FNMR by age group for two operating thresholds corresponding to  $FMR = \{0.001, 0.0001\}$  computed over all on the order of  $10^{10}$  impostor scores. The FMR in each bin will vary also - see subsequent impostor heatmaps in sec. 3.6.2. Given a pair of face images taken at different times, we assign the comparison to the bin that is the arithmetic average of the subject's ages. This plot shows only the effect of age, not ageing. The number of comparisons in each bin is generally in the thousands, however the first and last bins are computed over 149 and 124 respectively. The error rates in some (adult) cases are zero, and in others the DET is flat so the error rates at the two thresholds are identical. The lines span 1% and 99% of bootstrap replicated FNMR estimates.

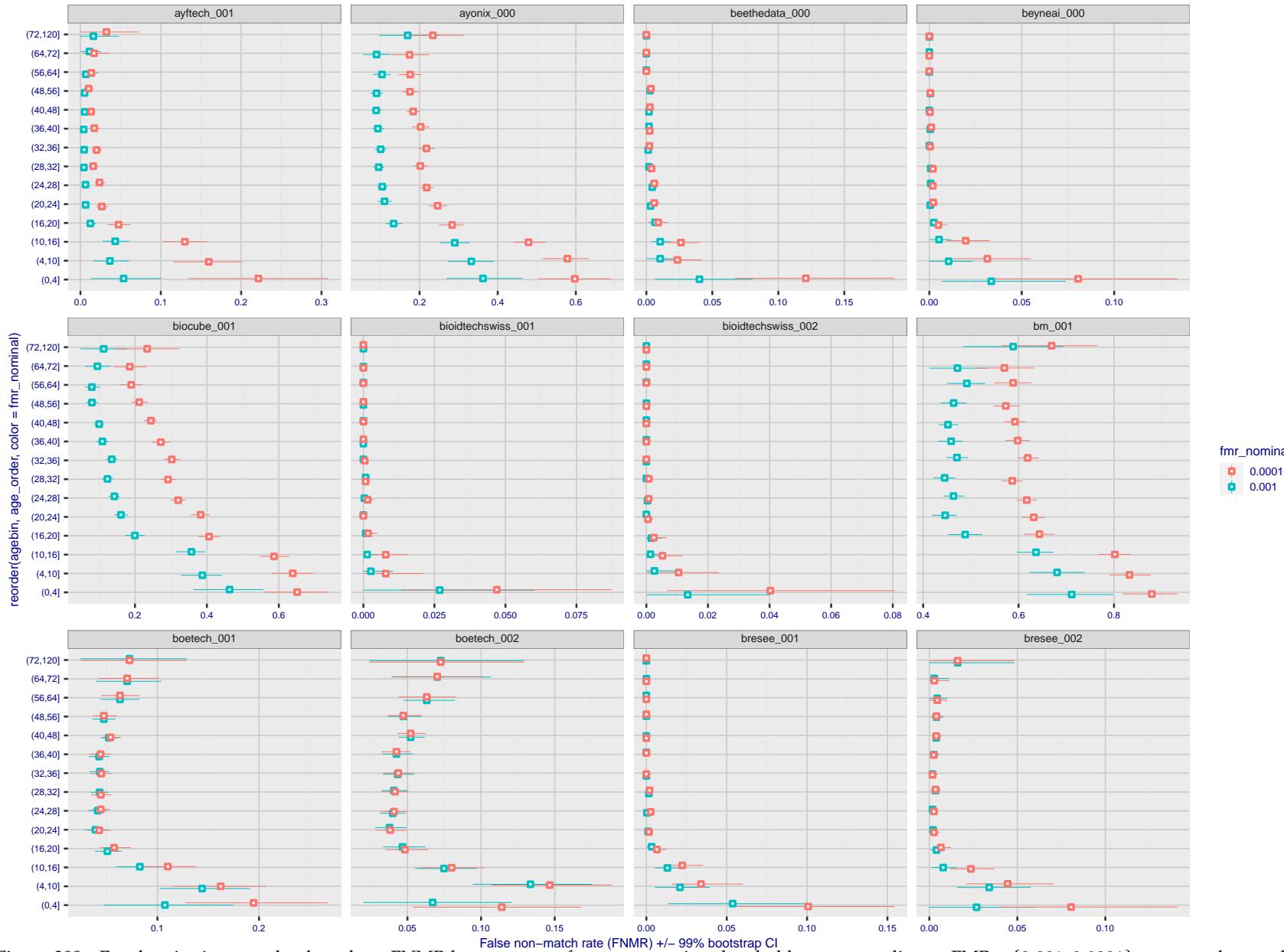


Figure 308: For the visa images, the dots show FNMR by age group for two operating thresholds corresponding to  $FMR = \{0.001, 0.0001\}$  computed over all on the order of  $10^{10}$  impostor scores. The FMR in each bin will vary also - see subsequent impostor heatmaps in sec. 3.6.2. Given a pair of face images taken at different times, we assign the comparison to the bin that is the arithmetic average of the subject's ages. This plot shows only the effect of age, not ageing. The number of comparisons in each bin is generally in the thousands, however the first and last bins are computed over 149 and 124 respectively. The error rates in some (adult) cases are zero, and in others the DET is flat so the error rates at the two thresholds are identical. The lines span 1% and 99% of bootstrap replicated FNMR estimates.



Figure 309: For the visa images, the dots show FNMR by age group for two operating thresholds corresponding to  $FMR = \{0.001, 0.0001\}$  computed over all on the order of  $10^{10}$  impostor scores. The FMR in each bin will vary also - see subsequent impostor heatmaps in sec. 3.6.2. Given a pair of face images taken at different times, we assign the comparison to the bin that is the arithmetic average of the subject's ages. This plot shows only the effect of age, not ageing. The number of comparisons in each bin is generally in the thousands, however the first and last bins are computed over 149 and 124 respectively. The error rates in some (adult) cases are zero, and in others the DET is flat so the error rates at the two thresholds are identical. The lines span 1% and 99% of bootstrap replicated FNMR estimates.



Figure 310: For the visa images, the dots show FNMR by age group for two operating thresholds corresponding to  $FMR = \{0.001, 0.0001\}$  computed over all on the order of  $10^{10}$  impostor scores. The FMR in each bin will vary also - see subsequent impostor heatmaps in sec. 3.6.2. Given a pair of face images taken at different times, we assign the comparison to the bin that is the arithmetic average of the subject's ages. This plot shows only the effect of age, not ageing. The number of comparisons in each bin is generally in the thousands, however the first and last bins are computed over 149 and 124 respectively. The error rates in some (adult) cases are zero, and in others the DET is flat so the error rates at the two thresholds are identical. The lines span 1% and 99% of bootstrap replicated FNMR estimates.



Figure 311: For the visa images, the dots show FNMR by age group for two operating thresholds corresponding to  $FMR = \{0.001, 0.0001\}$  computed over all on the order of  $10^{10}$  impostor scores. The FMR in each bin will vary also - see subsequent impostor heatmaps in sec. 3.6.2. Given a pair of face images taken at different times, we assign the comparison to the bin that is the arithmetic average of the subject's ages. This plot shows only the effect of age, not ageing. The number of comparisons in each bin is generally in the thousands, however the first and last bins are computed over 149 and 124 respectively. The error rates in some (adult) cases are zero, and in others the DET is flat so the error rates at the two thresholds are identical. The lines span 1% and 99% of bootstrap replicated FNMR estimates.



Figure 312: For the visa images, the dots show FNMR by age group for two operating thresholds corresponding to  $FMR = \{0.001, 0.0001\}$  computed over all on the order of  $10^{10}$  impostor scores. The FMR in each bin will vary also - see subsequent impostor heatmaps in sec. 3.6.2. Given a pair of face images taken at different times, we assign the comparison to the bin that is the arithmetic average of the subject's ages. This plot shows only the effect of age, not ageing. The number of comparisons in each bin is generally in the thousands, however the first and last bins are computed over 149 and 124 respectively. The error rates in some (adult) cases are zero, and in others the DET is flat so the error rates at the two thresholds are identical. The lines span 1% and 99% of bootstrap replicated FNMR estimates.



Figure 313: For the visa images, the dots show FNMR by age group for two operating thresholds corresponding to  $FMR = \{0.001, 0.0001\}$  computed over all on the order of  $10^{10}$  impostor scores. The FMR in each bin will vary also - see subsequent impostor heatmaps in sec. 3.6.2. Given a pair of face images taken at different times, we assign the comparison to the bin that is the arithmetic average of the subject's ages. This plot shows only the effect of age, not ageing. The number of comparisons in each bin is generally in the thousands, however the first and last bins are computed over 149 and 124 respectively. The error rates in some (adult) cases are zero, and in others the DET is flat so the error rates at the two thresholds are identical. The lines span 1% and 99% of bootstrap replicated FNMR estimates.

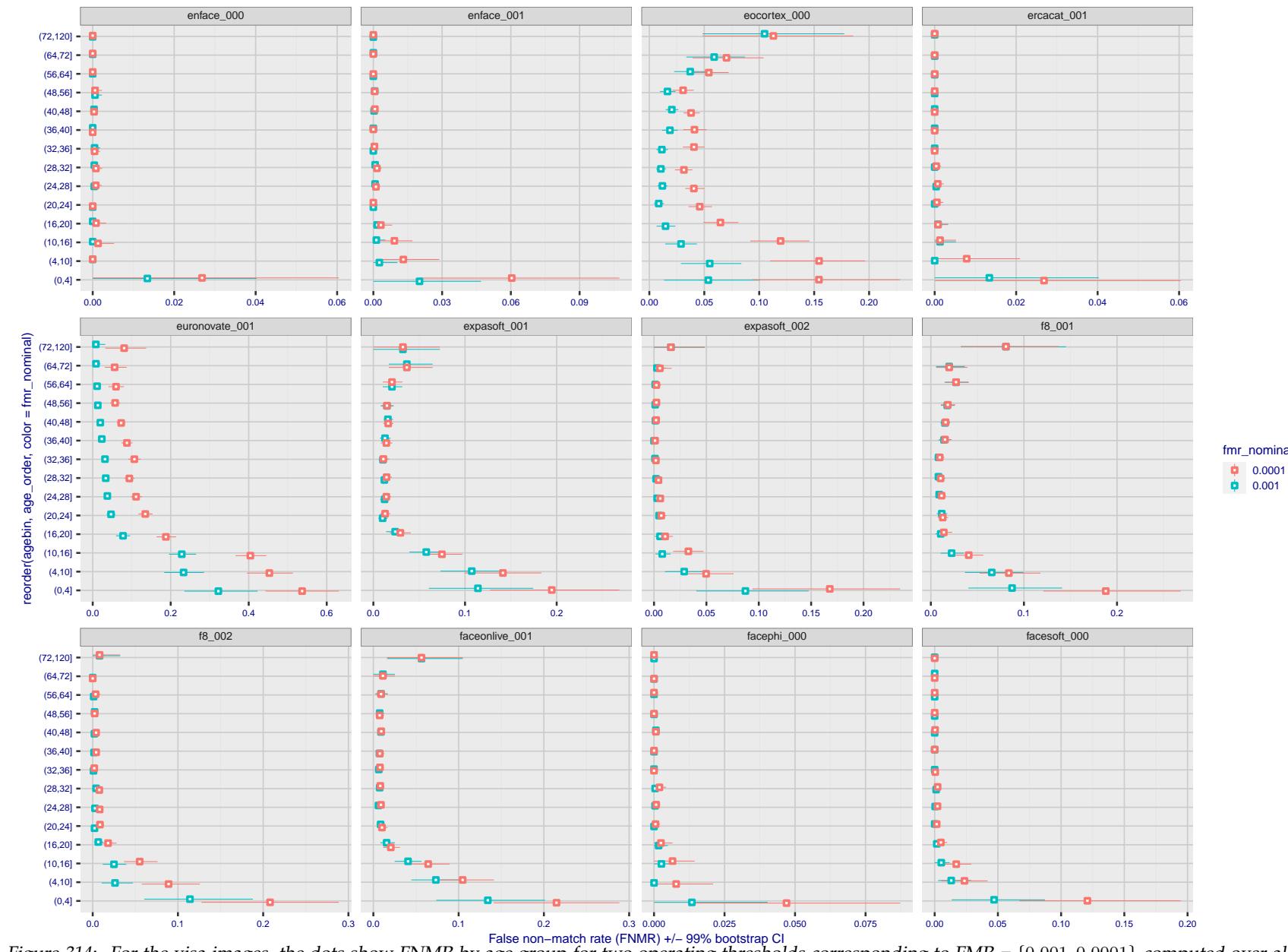


Figure 314: For the visa images, the dots show FNMR by age group for two operating thresholds corresponding to  $FMR = \{0.001, 0.0001\}$  computed over all on the order of  $10^{10}$  impostor scores. The FMR in each bin will vary also - see subsequent impostor heatmaps in sec. 3.6.2. Given a pair of face images taken at different times, we assign the comparison to the bin that is the arithmetic average of the subject's ages. This plot shows only the effect of age, not ageing. The number of comparisons in each bin is generally in the thousands, however the first and last bins are computed over 149 and 124 respectively. The error rates in some (adult) cases are zero, and in others the DET is flat so the error rates at the two thresholds are identical. The lines span 1% and 99% of bootstrap replicated FNMR estimates.

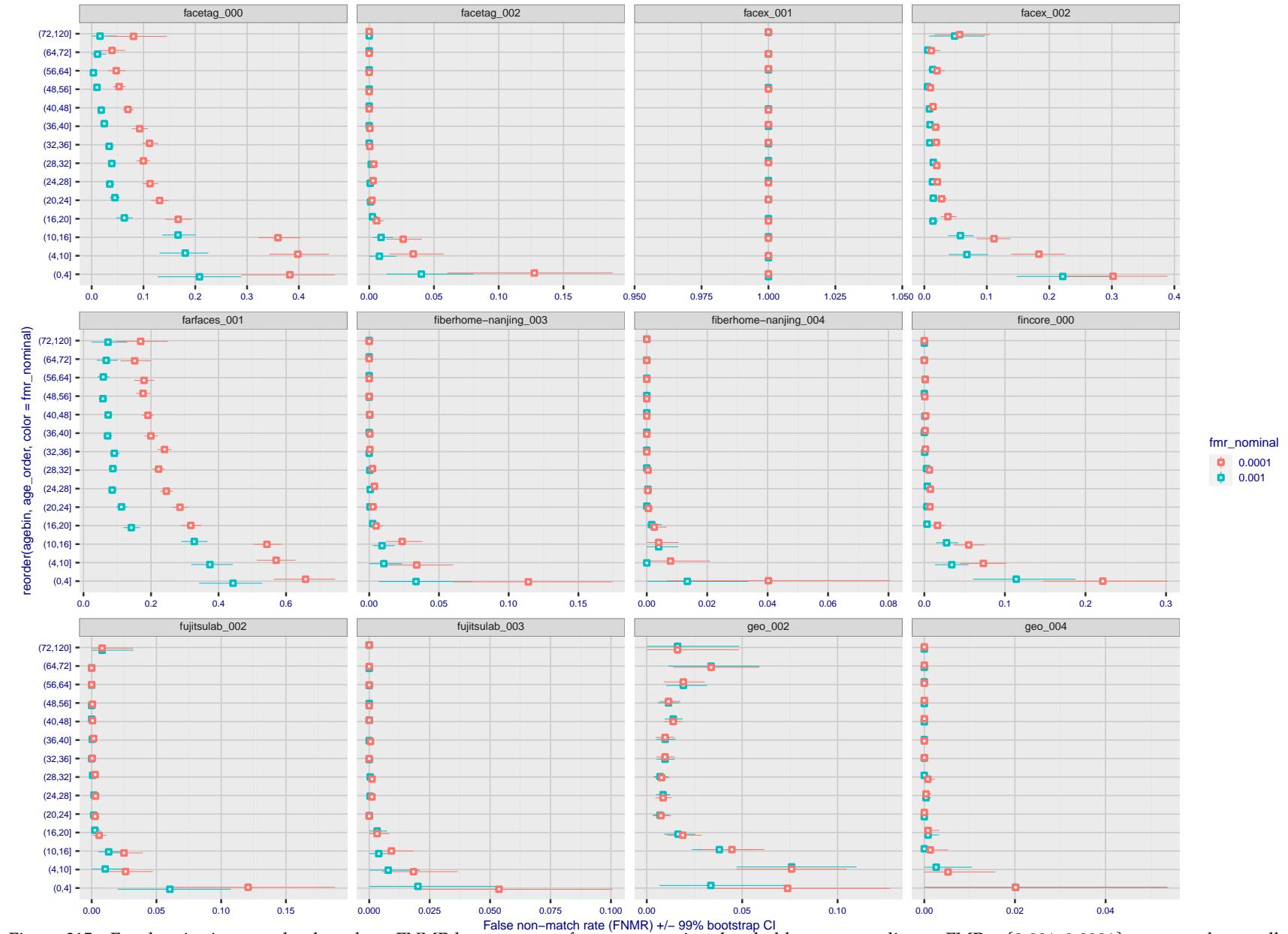


Figure 315: For the visa images, the dots show FNMR by age group for two operating thresholds corresponding to  $FMR = \{0.001, 0.0001\}$  computed over all on the order of  $10^{10}$  impostor scores. The FMR in each bin will vary also - see subsequent impostor heatmaps in sec. 3.6.2. Given a pair of face images taken at different times, we assign the comparison to the bin that is the arithmetic average of the subject's ages. This plot shows only the effect of age, not ageing. The number of comparisons in each bin is generally in the thousands, however the first and last bins are computed over 149 and 124 respectively. The error rates in some (adult) cases are zero, and in others the DET is flat so the error rates at the two thresholds are identical. The lines span 1% and 99% of bootstrap replicated FNMR estimates.

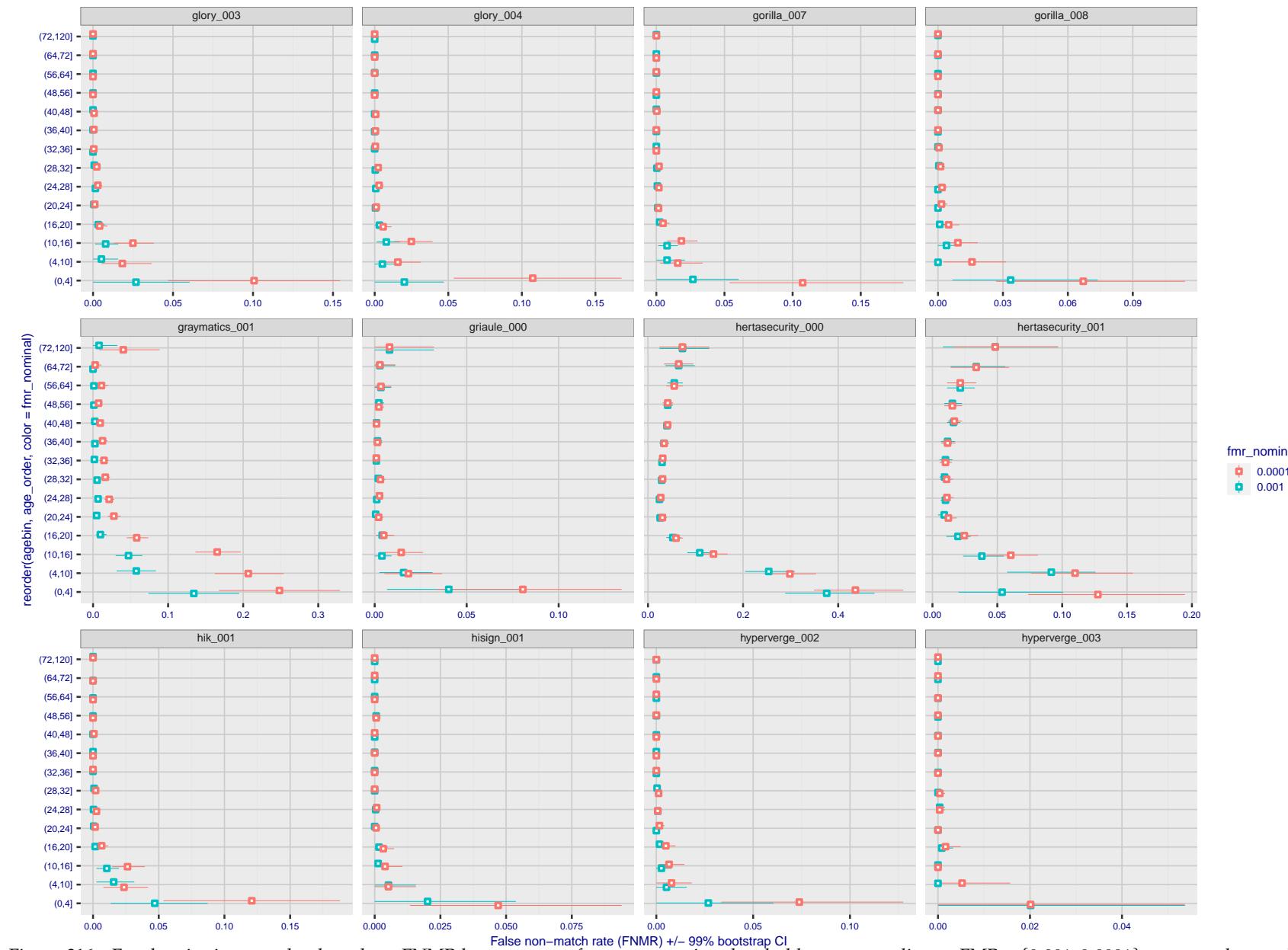


Figure 316: For the visa images, the dots show FNMR by age group for two operating thresholds corresponding to  $FMR = \{0.001, 0.0001\}$  computed over all on the order of  $10^{10}$  impostor scores. The FMR in each bin will vary also - see subsequent impostor heatmaps in sec. 3.6.2. Given a pair of face images taken at different times, we assign the comparison to the bin that is the arithmetic average of the subject's ages. This plot shows only the effect of age, not ageing. The number of comparisons in each bin is generally in the thousands, however the first and last bins are computed over 149 and 124 respectively. The error rates in some (adult) cases are zero, and in others the DET is flat so the error rates at the two thresholds are identical. The lines span 1% and 99% of bootstrap replicated FNMR estimates.



Figure 317: For the visa images, the dots show FNMR by age group for two operating thresholds corresponding to  $FMR = \{0.001, 0.0001\}$  computed over all on the order of  $10^{10}$  impostor scores. The FMR in each bin will vary also - see subsequent impostor heatmaps in sec. 3.6.2. Given a pair of face images taken at different times, we assign the comparison to the bin that is the arithmetic average of the subject's ages. This plot shows only the effect of age, not ageing. The number of comparisons in each bin is generally in the thousands, however the first and last bins are computed over 149 and 124 respectively. The error rates in some (adult) cases are zero, and in others the DET is flat so the error rates at the two thresholds are identical. The lines span 1% and 99% of bootstrap replicated FNMR estimates.



Figure 318: For the visa images, the dots show FNMR by age group for two operating thresholds corresponding to  $FMR = \{0.001, 0.0001\}$  computed over all on the order of  $10^{10}$  impostor scores. The FMR in each bin will vary also - see subsequent impostor heatmaps in sec. 3.6.2. Given a pair of face images taken at different times, we assign the comparison to the bin that is the arithmetic average of the subject's ages. This plot shows only the effect of age, not ageing. The number of comparisons in each bin is generally in the thousands, however the first and last bins are computed over 149 and 124 respectively. The error rates in some (adult) cases are zero, and in others the DET is flat so the error rates at the two thresholds are identical. The lines span 1% and 99% of bootstrap replicated FNMR estimates.



Figure 319: For the visa images, the dots show FNMR by age group for two operating thresholds corresponding to  $FMR = \{0.001, 0.0001\}$  computed over all on the order of  $10^{10}$  impostor scores. The FMR in each bin will vary also - see subsequent impostor heatmaps in sec. 3.6.2. Given a pair of face images taken at different times, we assign the comparison to the bin that is the arithmetic average of the subject's ages. This plot shows only the effect of age, not ageing. The number of comparisons in each bin is generally in the thousands, however the first and last bins are computed over 149 and 124 respectively. The error rates in some (adult) cases are zero, and in others the DET is flat so the error rates at the two thresholds are identical. The lines span 1% and 99% of bootstrap replicated FNMR estimates.

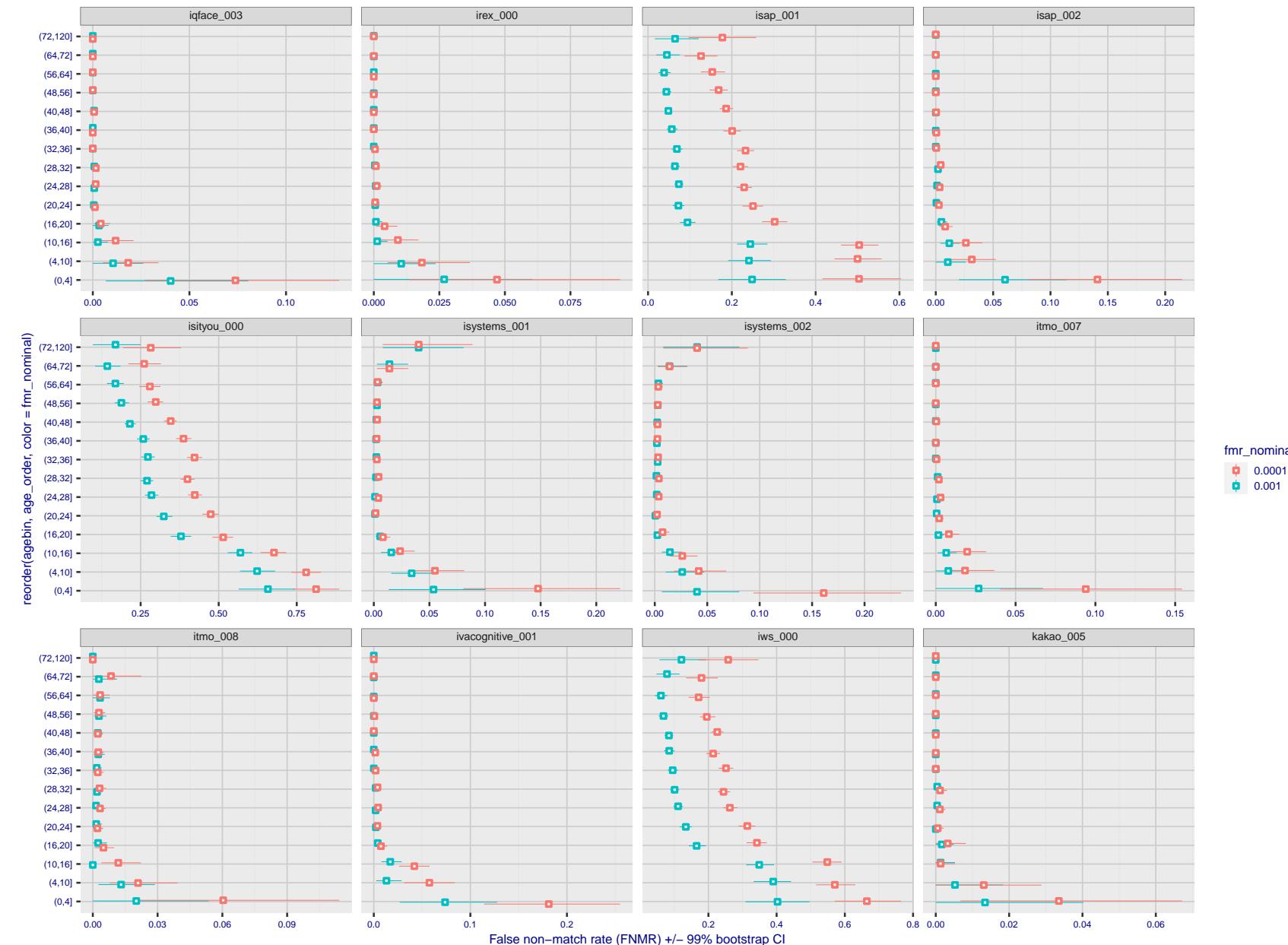


Figure 320: For the visa images, the dots show FNMR by age group for two operating thresholds corresponding to  $FMR = \{0.001, 0.0001\}$  computed over all on the order of  $10^{10}$  impostor scores. The FMR in each bin will vary also - see subsequent impostor heatmaps in sec. 3.6.2. Given a pair of face images taken at different times, we assign the comparison to the bin that is the arithmetic average of the subject's ages. This plot shows only the effect of age, not ageing. The number of comparisons in each bin is generally in the thousands, however the first and last bins are computed over 149 and 124 respectively. The error rates in some (adult) cases are zero, and in others the DET is flat so the error rates at the two thresholds are identical. The lines span 1% and 99% of bootstrap replicated FNMR estimates.

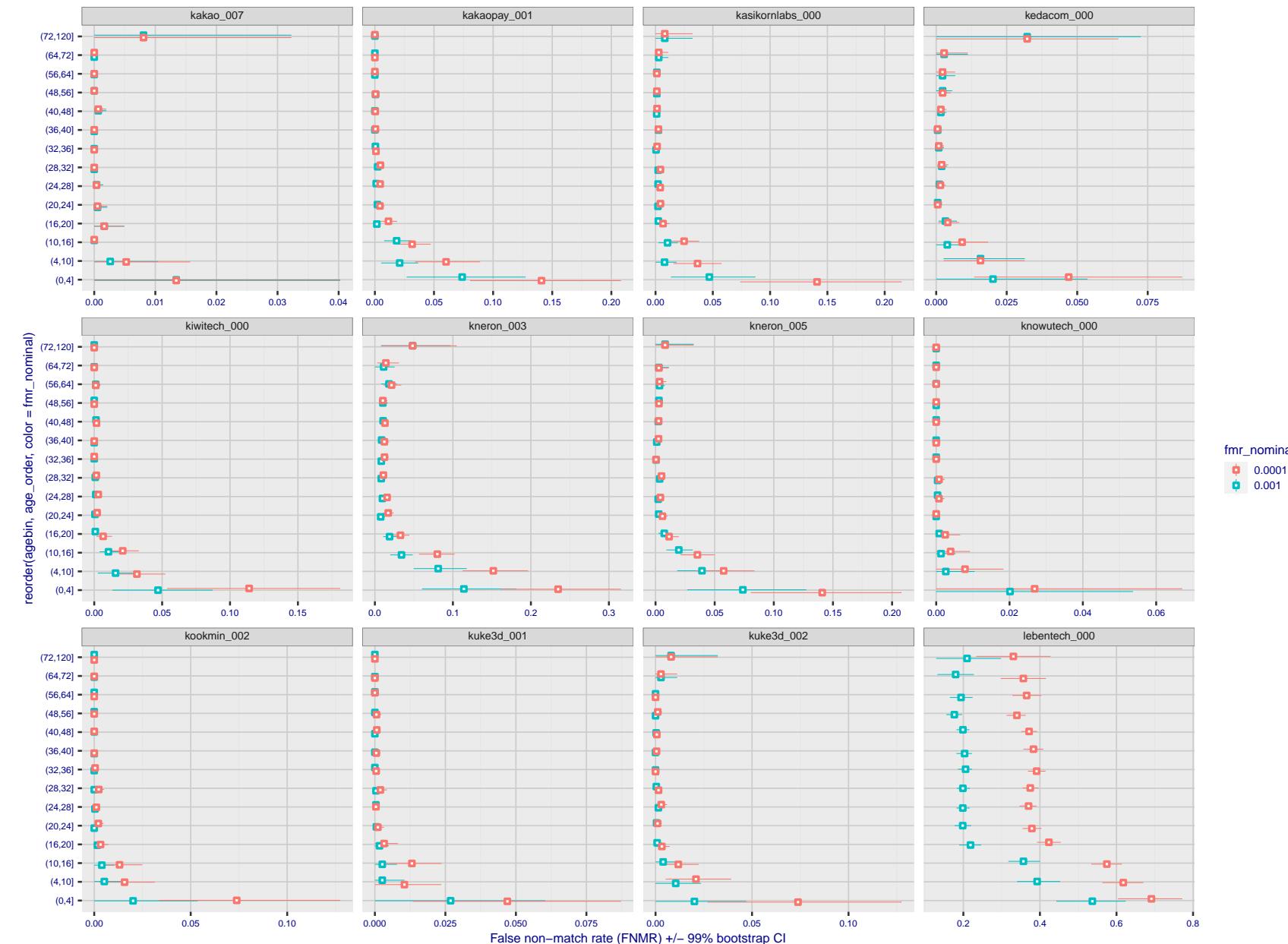


Figure 321: For the visa images, the dots show FNMR by age group for two operating thresholds corresponding to  $FMR = \{0.001, 0.0001\}$  computed over all on the order of  $10^{10}$  impostor scores. The FMR in each bin will vary also - see subsequent impostor heatmaps in sec. 3.6.2. Given a pair of face images taken at different times, we assign the comparison to the bin that is the arithmetic average of the subject's ages. This plot shows only the effect of age, not ageing. The number of comparisons in each bin is generally in the thousands, however the first and last bins are computed over 149 and 124 respectively. The error rates in some (adult) cases are zero, and in others the DET is flat so the error rates at the two thresholds are identical. The lines span 1% and 99% of bootstrap replicated FNMR estimates.



Figure 322: For the visa images, the dots show FNMR by age group for two operating thresholds corresponding to  $FMR = \{0.001, 0.0001\}$  computed over all on the order of  $10^{10}$  impostor scores. The FMR in each bin will vary also - see subsequent impostor heatmaps in sec. 3.6.2. Given a pair of face images taken at different times, we assign the comparison to the bin that is the arithmetic average of the subject's ages. This plot shows only the effect of age, not ageing. The number of comparisons in each bin is generally in the thousands, however the first and last bins are computed over 149 and 124 respectively. The error rates in some (adult) cases are zero, and in others the DET is flat so the error rates at the two thresholds are identical. The lines span 1% and 99% of bootstrap replicated FNMR estimates.

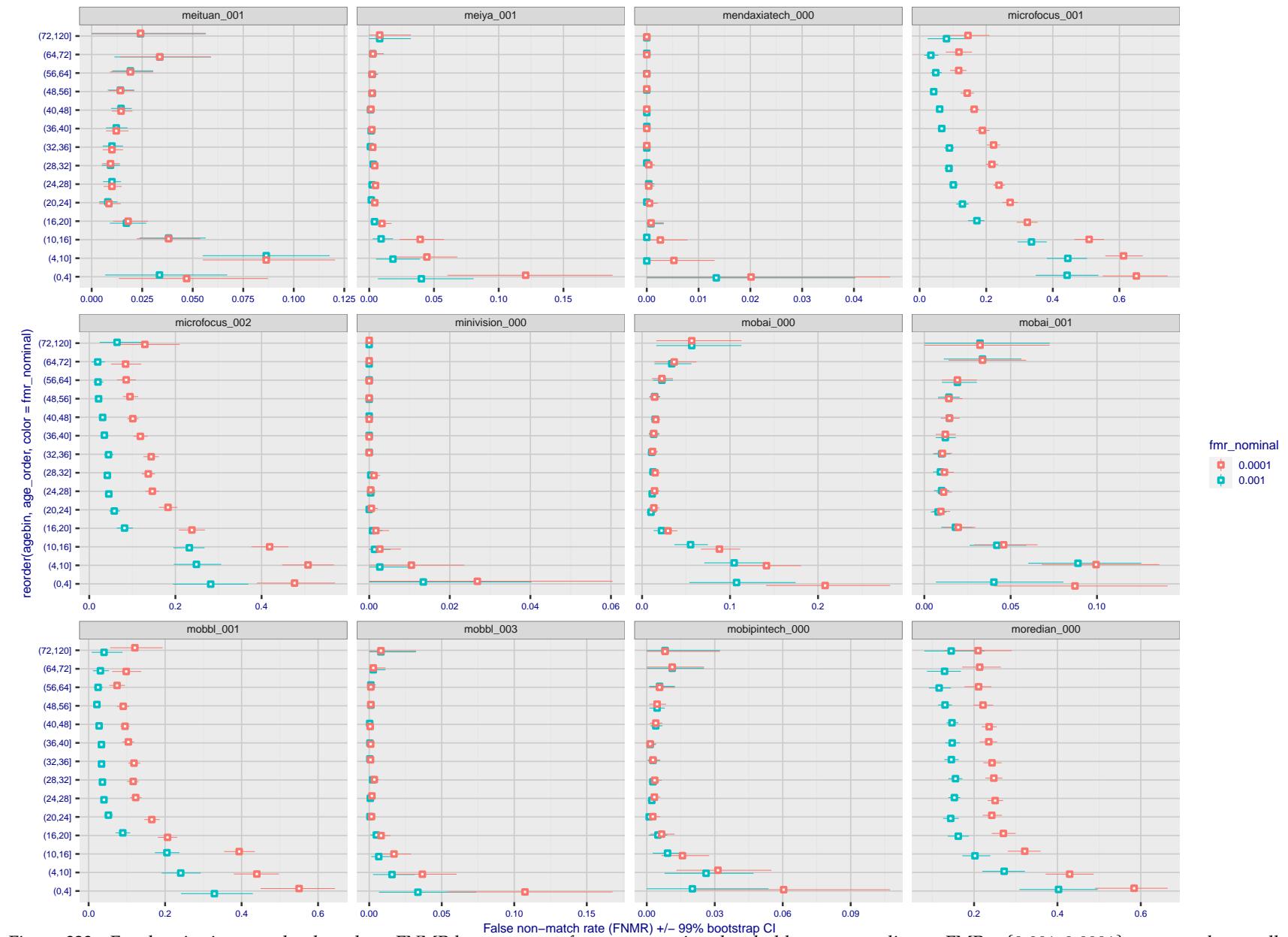


Figure 323: For the visa images, the dots show FNMR by age group for two operating thresholds corresponding to  $FMR = \{0.001, 0.0001\}$  computed over all on the order of  $10^{10}$  impostor scores. The FMR in each bin will vary also - see subsequent impostor heatmaps in sec. 3.6.2. Given a pair of face images taken at different times, we assign the comparison to the bin that is the arithmetic average of the subject's ages. This plot shows only the effect of age, not ageing. The number of comparisons in each bin is generally in the thousands, however the first and last bins are computed over 149 and 124 respectively. The error rates in some (adult) cases are zero, and in others the DET is flat so the error rates at the two thresholds are identical. The lines span 1% and 99% of bootstrap replicated FNMR estimates.

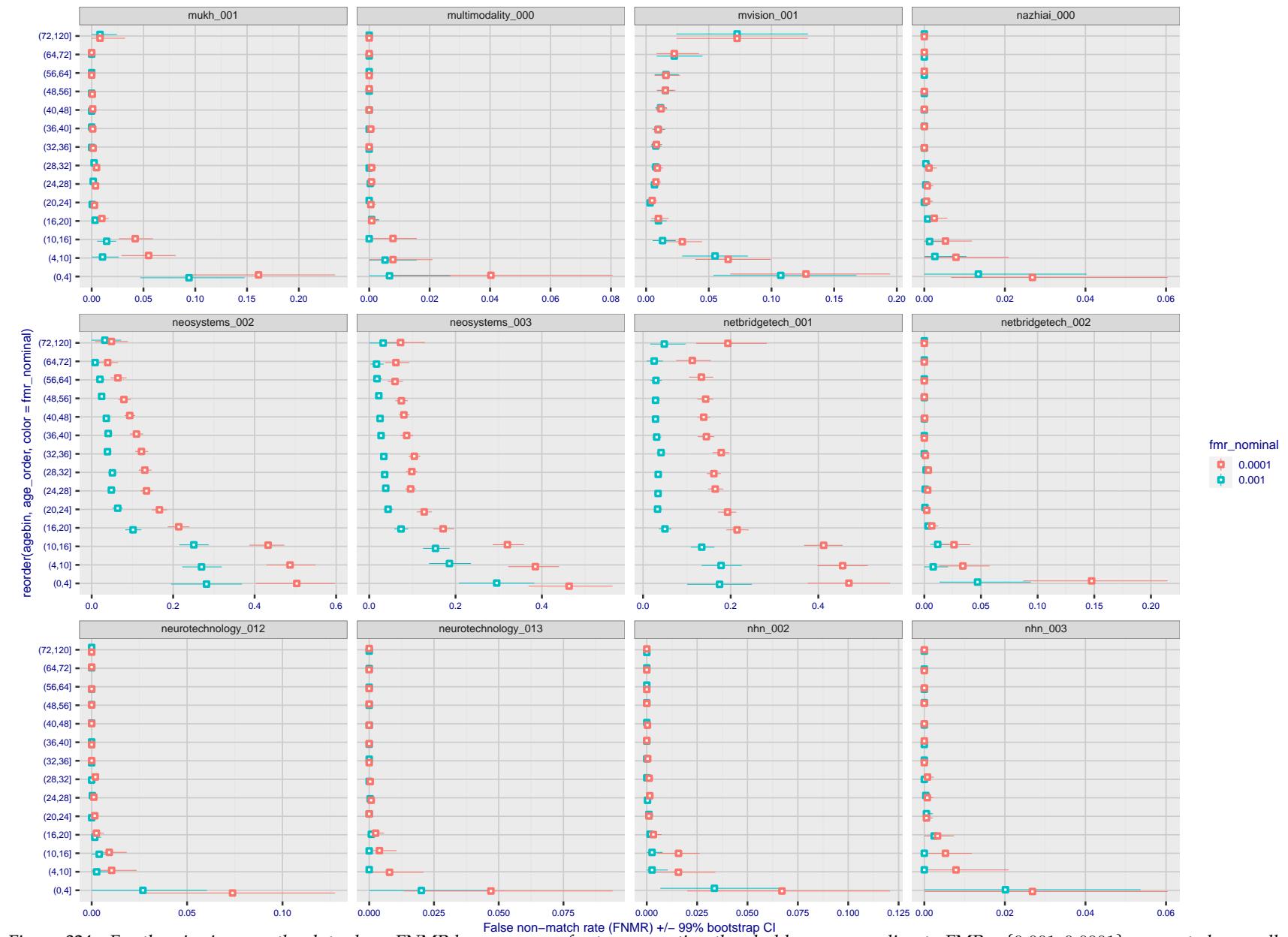


Figure 324: For the visa images, the dots show FNMR by age group for two operating thresholds corresponding to  $FMR = \{0.001, 0.0001\}$  computed over all on the order of  $10^{10}$  impostor scores. The FMR in each bin will vary also - see subsequent impostor heatmaps in sec. 3.6.2. Given a pair of face images taken at different times, we assign the comparison to the bin that is the arithmetic average of the subject's ages. This plot shows only the effect of age, not ageing. The number of comparisons in each bin is generally in the thousands, however the first and last bins are computed over 149 and 124 respectively. The error rates in some (adult) cases are zero, and in others the DET is flat so the error rates at the two thresholds are identical. The lines span 1% and 99% of bootstrap replicated FNMR estimates.

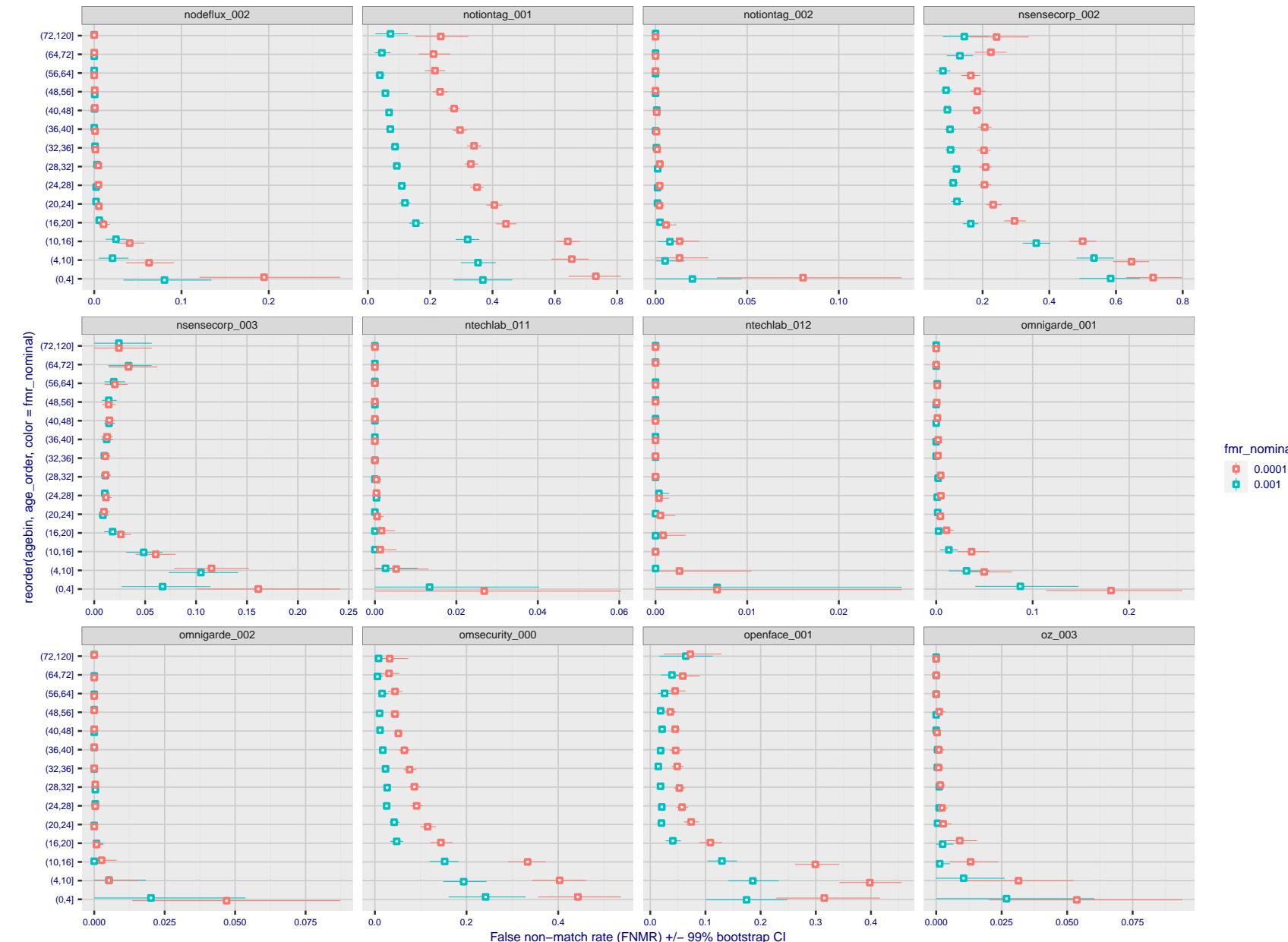


Figure 325: For the visa images, the dots show FNMR by age group for two operating thresholds corresponding to  $FMR = \{0.001, 0.0001\}$  computed over all on the order of  $10^{10}$  impostor scores. The FMR in each bin will vary also - see subsequent impostor heatmaps in sec. 3.6.2. Given a pair of face images taken at different times, we assign the comparison to the bin that is the arithmetic average of the subject's ages. This plot shows only the effect of age, not ageing. The number of comparisons in each bin is generally in the thousands, however the first and last bins are computed over 149 and 124 respectively. The error rates in some (adult) cases are zero, and in others the DET is flat so the error rates at the two thresholds are identical. The lines span 1% and 99% of bootstrap replicated FNMR estimates.



Figure 326: For the visa images, the dots show FNMR by age group for two operating thresholds corresponding to  $FMR = \{0.001, 0.0001\}$  computed over all on the order of  $10^{10}$  impostor scores. The FMR in each bin will vary also - see subsequent impostor heatmaps in sec. 3.6.2. Given a pair of face images taken at different times, we assign the comparison to the bin that is the arithmetic average of the subject's ages. This plot shows only the effect of age, not ageing. The number of comparisons in each bin is generally in the thousands, however the first and last bins are computed over 149 and 124 respectively. The error rates in some (adult) cases are zero, and in others the DET is flat so the error rates at the two thresholds are identical. The lines span 1% and 99% of bootstrap replicated FNMR estimates.



Figure 327: For the visa images, the dots show FNMR by age group for two operating thresholds corresponding to  $FMR = \{0.001, 0.0001\}$  computed over all on the order of  $10^{10}$  impostor scores. The FMR in each bin will vary also - see subsequent impostor heatmaps in sec. 3.6.2. Given a pair of face images taken at different times, we assign the comparison to the bin that is the arithmetic average of the subject's ages. This plot shows only the effect of age, not ageing. The number of comparisons in each bin is generally in the thousands, however the first and last bins are computed over 149 and 124 respectively. The error rates in some (adult) cases are zero, and in others the DET is flat so the error rates at the two thresholds are identical. The lines span 1% and 99% of bootstrap replicated FNMR estimates.

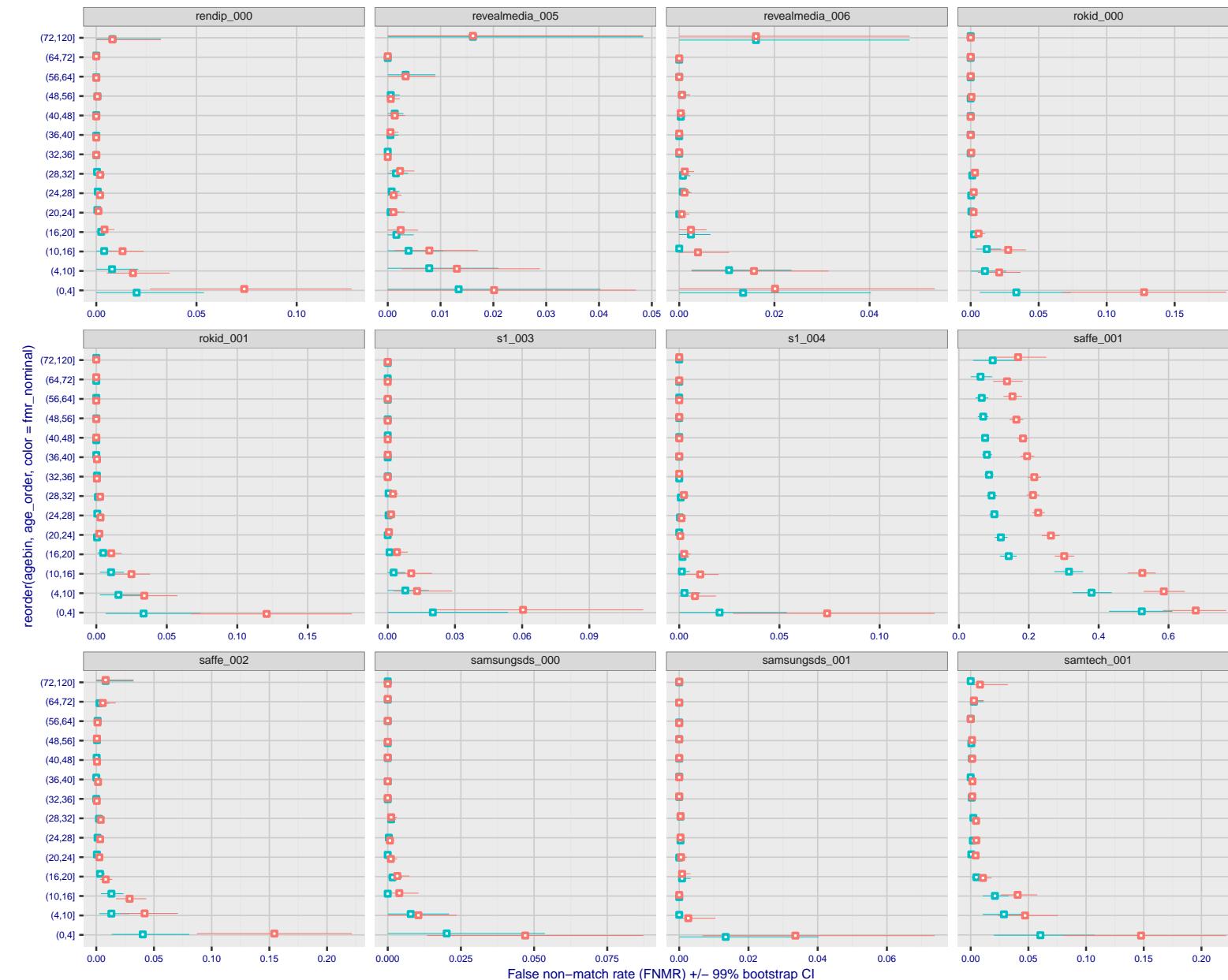


Figure 328: For the visa images, the dots show FNMR by age group for two operating thresholds corresponding to  $FMR = \{0.001, 0.0001\}$  computed over all on the order of  $10^{10}$  impostor scores. The FMR in each bin will vary also - see subsequent impostor heatmaps in sec. 3.6.2. Given a pair of face images taken at different times, we assign the comparison to the bin that is the arithmetic average of the subject's ages. This plot shows only the effect of age, not ageing. The number of comparisons in each bin is generally in the thousands, however the first and last bins are computed over 149 and 124 respectively. The error rates in some (adult) cases are zero, and in others the DET is flat so the error rates at the two thresholds are identical. The lines span 1% and 99% of bootstrap replicated FNMR estimates.

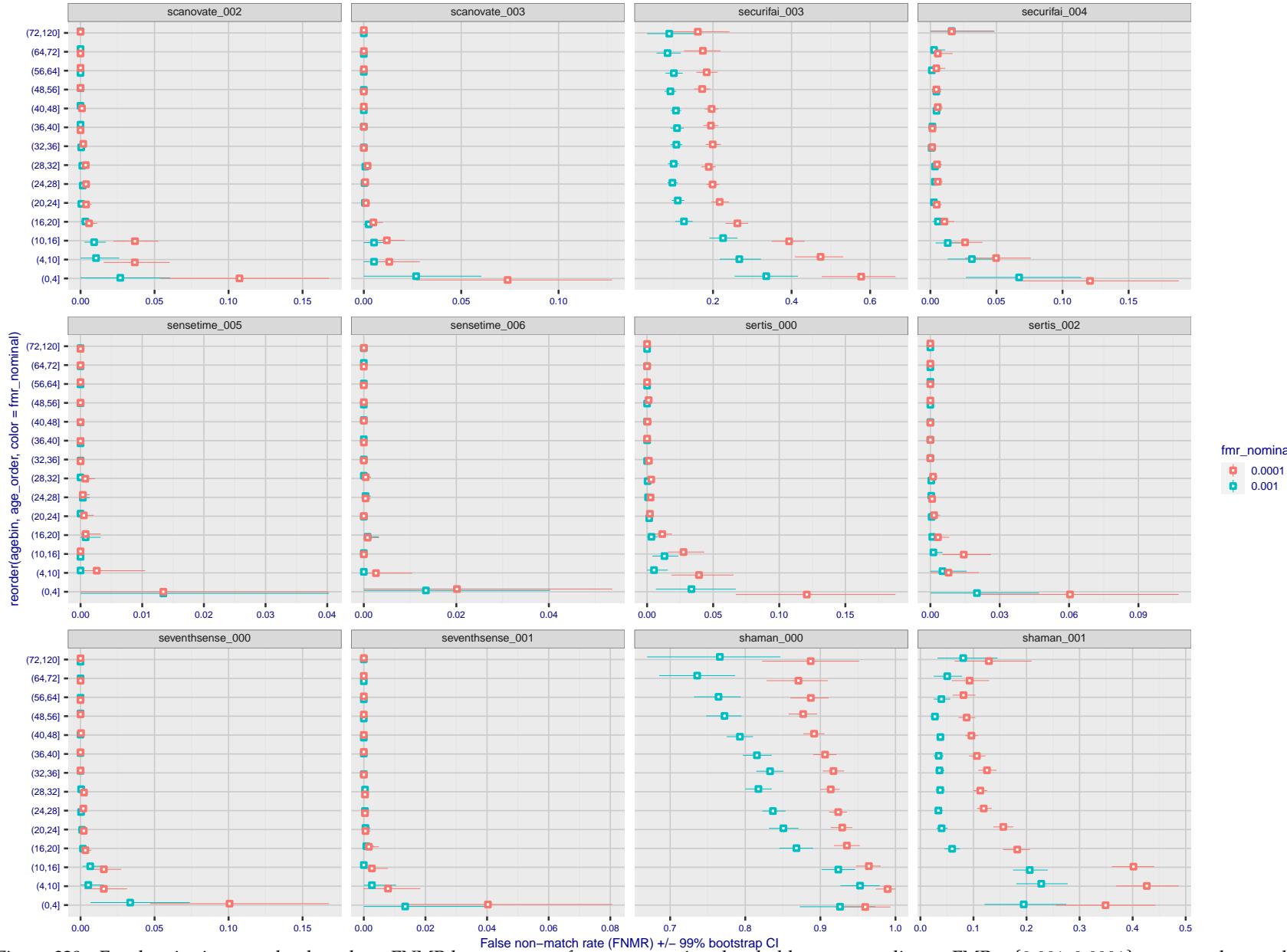


Figure 329: For the visa images, the dots show FNMR by age group for two operating thresholds corresponding to  $FMR = \{0.001, 0.0001\}$  computed over all on the order of  $10^{10}$  impostor scores. The FMR in each bin will vary also - see subsequent impostor heatmaps in sec. 3.6.2. Given a pair of face images taken at different times, we assign the comparison to the bin that is the arithmetic average of the subject's ages. This plot shows only the effect of age, not ageing. The number of comparisons in each bin is generally in the thousands, however the first and last bins are computed over 149 and 124 respectively. The error rates in some (adult) cases are zero, and in others the DET is flat so the error rates at the two thresholds are identical. The lines span 1% and 99% of bootstrap replicated FNMR estimates.

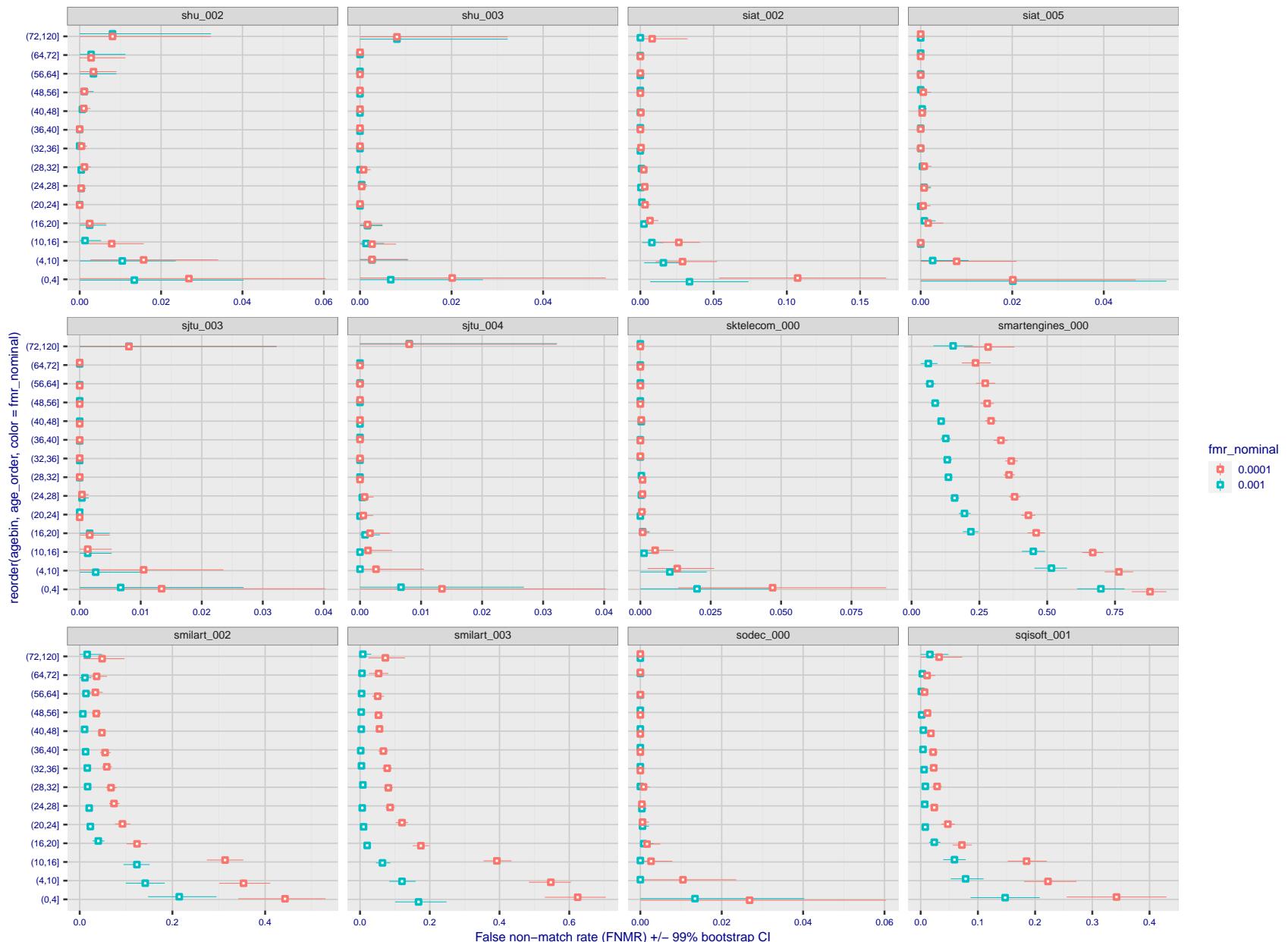


Figure 330: For the visa images, the dots show FNMR by age group for two operating thresholds corresponding to  $FMR = \{0.001, 0.0001\}$  computed over all on the order of  $10^{10}$  impostor scores. The FMR in each bin will vary also - see subsequent impostor heatmaps in sec. 3.6.2. Given a pair of face images taken at different times, we assign the comparison to the bin that is the arithmetic average of the subject's ages. This plot shows only the effect of age, not ageing. The number of comparisons in each bin is generally in the thousands, however the first and last bins are computed over 149 and 124 respectively. The error rates in some (adult) cases are zero, and in others the DET is flat so the error rates at the two thresholds are identical. The lines span 1% and 99% of bootstrap replicated FNMR estimates.

2022/05/06 07:45:52

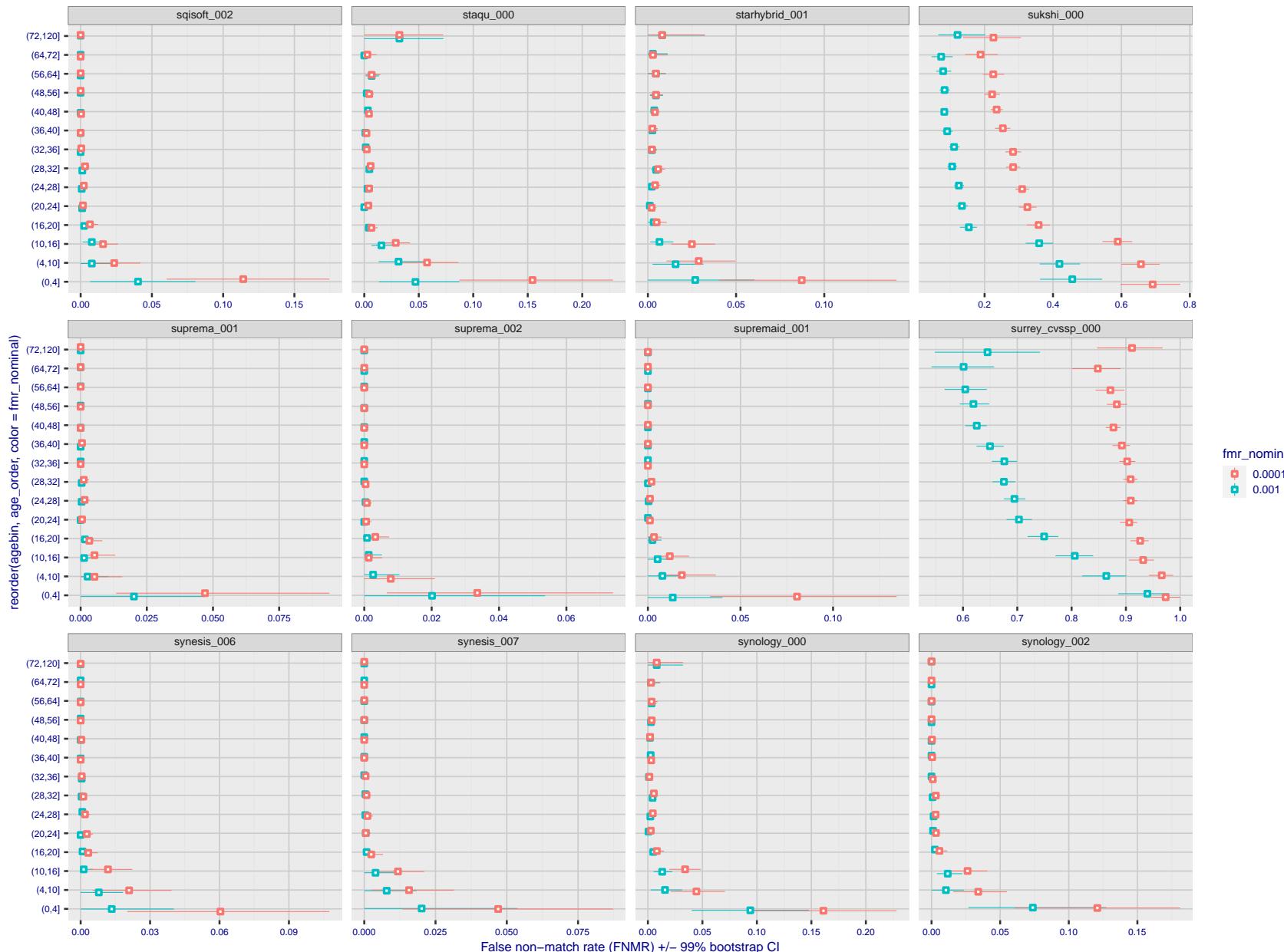


Figure 331: For the visa images, the dots show FNMR by age group for two operating thresholds corresponding to  $FMR = \{0.001, 0.0001\}$  computed over all on the order of  $10^{10}$  impostor scores. The FMR in each bin will vary also - see subsequent impostor heatmaps in sec. 3.6.2. Given a pair of face images taken at different times, we assign the comparison to the bin that is the arithmetic average of the subject's ages. This plot shows only the effect of age, not ageing. The number of comparisons in each bin is generally in the thousands, however the first and last bins are computed over 149 and 124 respectively. The error rates in some (adult) cases are zero, and in others the DET is flat so the error rates at the two thresholds are identical. The lines span 1% and 99% of bootstrap replicated FNMR estimates.

FNMR(T)  
FMR(T)  
"False non-match rate"  
"False match rate"



Figure 332: For the visa images, the dots show FNMR by age group for two operating thresholds corresponding to  $FMR = \{0.001, 0.0001\}$  computed over all on the order of  $10^{10}$  impostor scores. The FMR in each bin will vary also - see subsequent impostor heatmaps in sec. 3.6.2. Given a pair of face images taken at different times, we assign the comparison to the bin that is the arithmetic average of the subject's ages. This plot shows only the effect of age, not ageing. The number of comparisons in each bin is generally in the thousands, however the first and last bins are computed over 149 and 124 respectively. The error rates in some (adult) cases are zero, and in others the DET is flat so the error rates at the two thresholds are identical. The lines span 1% and 99% of bootstrap replicated FNMR estimates.



Figure 333: For the visa images, the dots show FNMR by age group for two operating thresholds corresponding to  $FMR = \{0.001, 0.0001\}$  computed over all on the order of  $10^{10}$  impostor scores. The FMR in each bin will vary also - see subsequent impostor heatmaps in sec. 3.6.2. Given a pair of face images taken at different times, we assign the comparison to the bin that is the arithmetic average of the subject's ages. This plot shows only the effect of age, not ageing. The number of comparisons in each bin is generally in the thousands, however the first and last bins are computed over 149 and 124 respectively. The error rates in some (adult) cases are zero, and in others the DET is flat so the error rates at the two thresholds are identical. The lines span 1% and 99% of bootstrap replicated FNMR estimates.

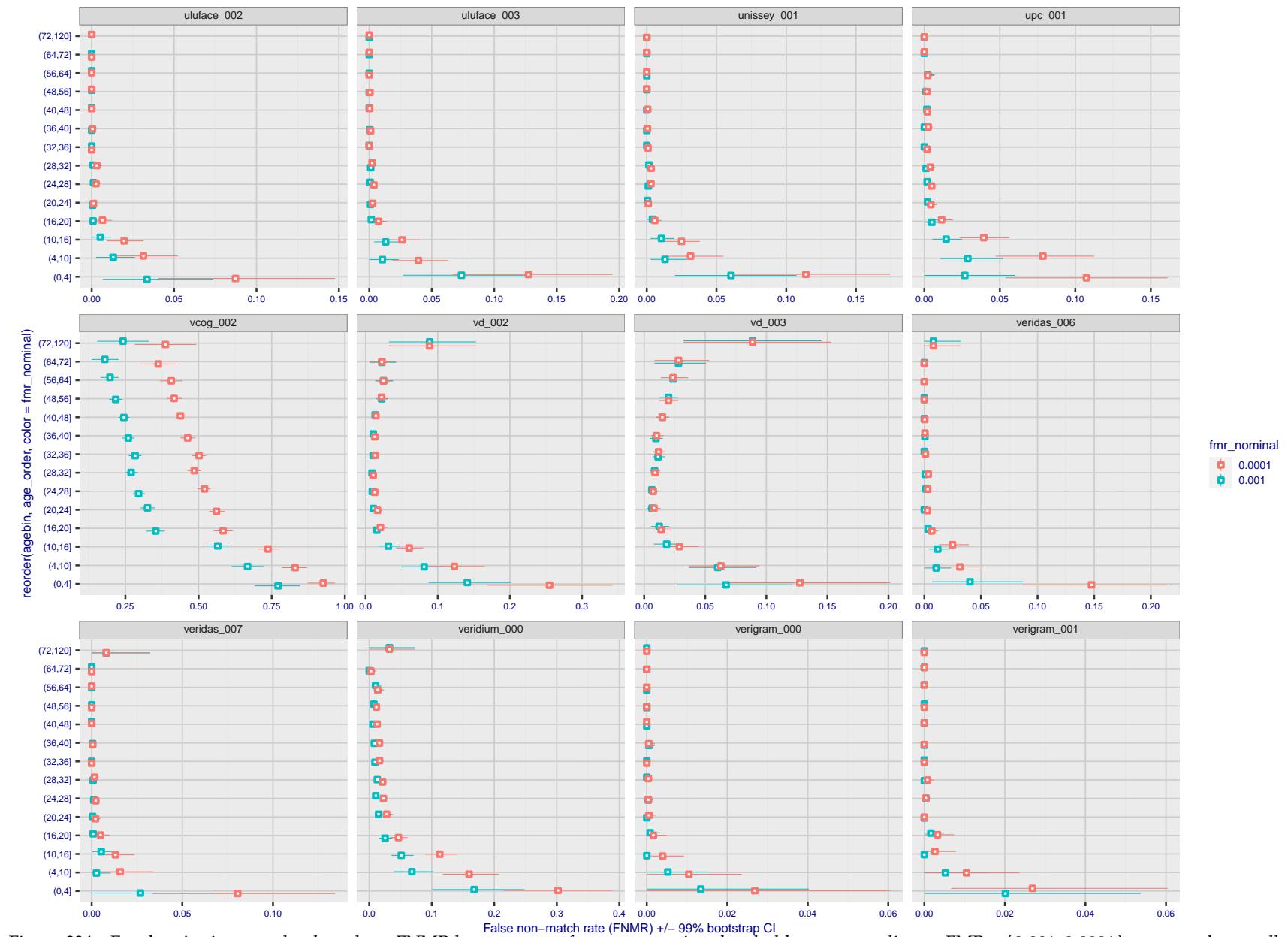


Figure 334: For the visa images, the dots show FNMR by age group for two operating thresholds corresponding to  $FMR = \{0.001, 0.0001\}$  computed over all on the order of  $10^{10}$  impostor scores. The FMR in each bin will vary also - see subsequent impostor heatmaps in sec. 3.6.2. Given a pair of face images taken at different times, we assign the comparison to the bin that is the arithmetic average of the subject's ages. This plot shows only the effect of age, not ageing. The number of comparisons in each bin is generally in the thousands, however the first and last bins are computed over 149 and 124 respectively. The error rates in some (adult) cases are zero, and in others the DET is flat so the error rates at the two thresholds are identical. The lines span 1% and 99% of bootstrap replicated FNMR estimates.

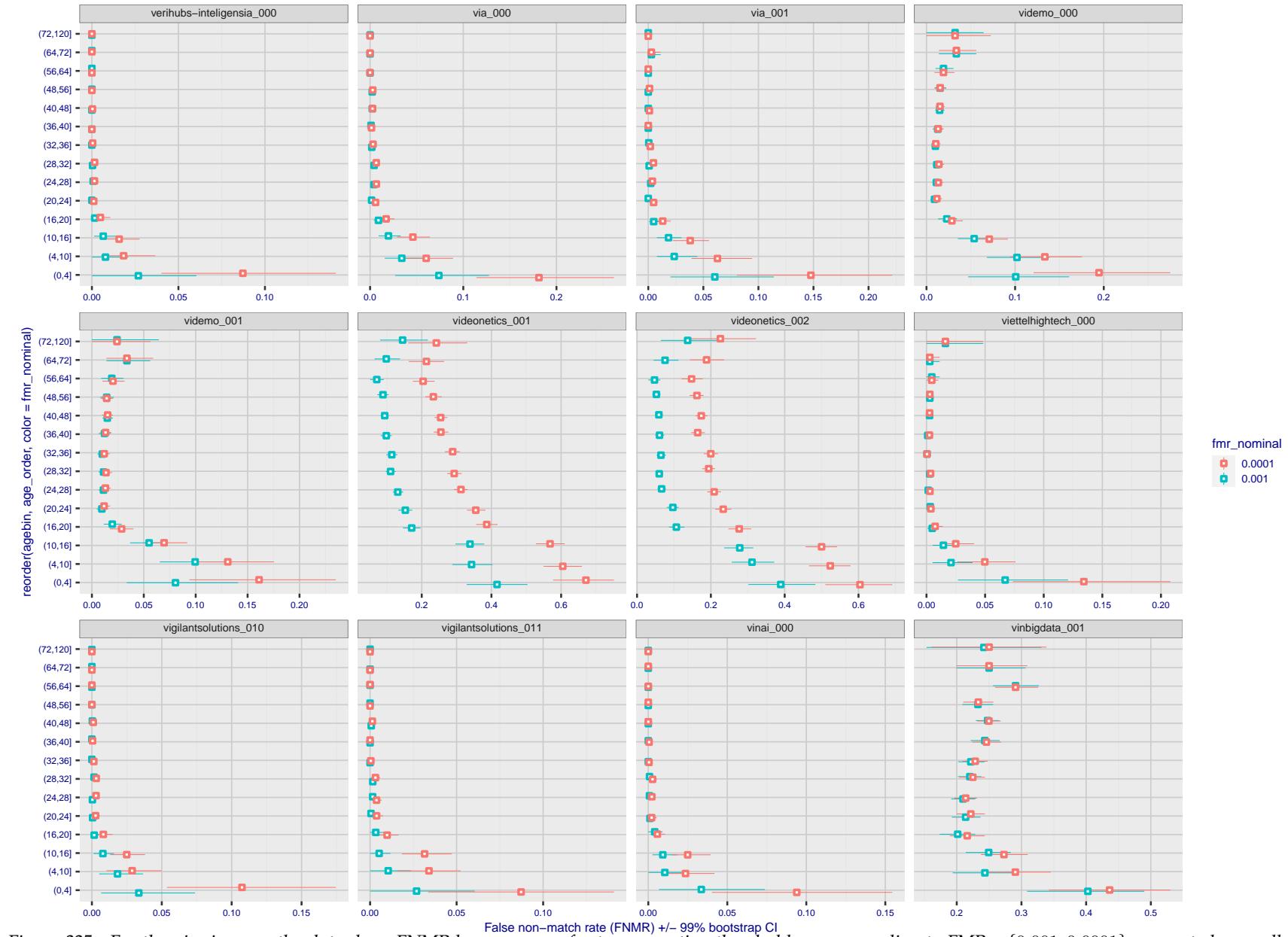


Figure 335: For the visa images, the dots show FNMR by age group for two operating thresholds corresponding to  $FMR = \{0.001, 0.0001\}$  computed over all on the order of  $10^{10}$  impostor scores. The FMR in each bin will vary also - see subsequent impostor heatmaps in sec. 3.6.2. Given a pair of face images taken at different times, we assign the comparison to the bin that is the arithmetic average of the subject's ages. This plot shows only the effect of age, not ageing. The number of comparisons in each bin is generally in the thousands, however the first and last bins are computed over 149 and 124 respectively. The error rates in some (adult) cases are zero, and in others the DET is flat so the error rates at the two thresholds are identical. The lines span 1% and 99% of bootstrap replicated FNMR estimates.



Figure 336: For the visa images, the dots show FNMR by age group for two operating thresholds corresponding to  $FMR = \{0.001, 0.0001\}$  computed over all on the order of  $10^{10}$  impostor scores. The FMR in each bin will vary also - see subsequent impostor heatmaps in sec. 3.6.2. Given a pair of face images taken at different times, we assign the comparison to the bin that is the arithmetic average of the subject's ages. This plot shows only the effect of age, not ageing. The number of comparisons in each bin is generally in the thousands, however the first and last bins are computed over 149 and 124 respectively. The error rates in some (adult) cases are zero, and in others the DET is flat so the error rates at the two thresholds are identical. The lines span 1% and 99% of bootstrap replicated FNMR estimates.

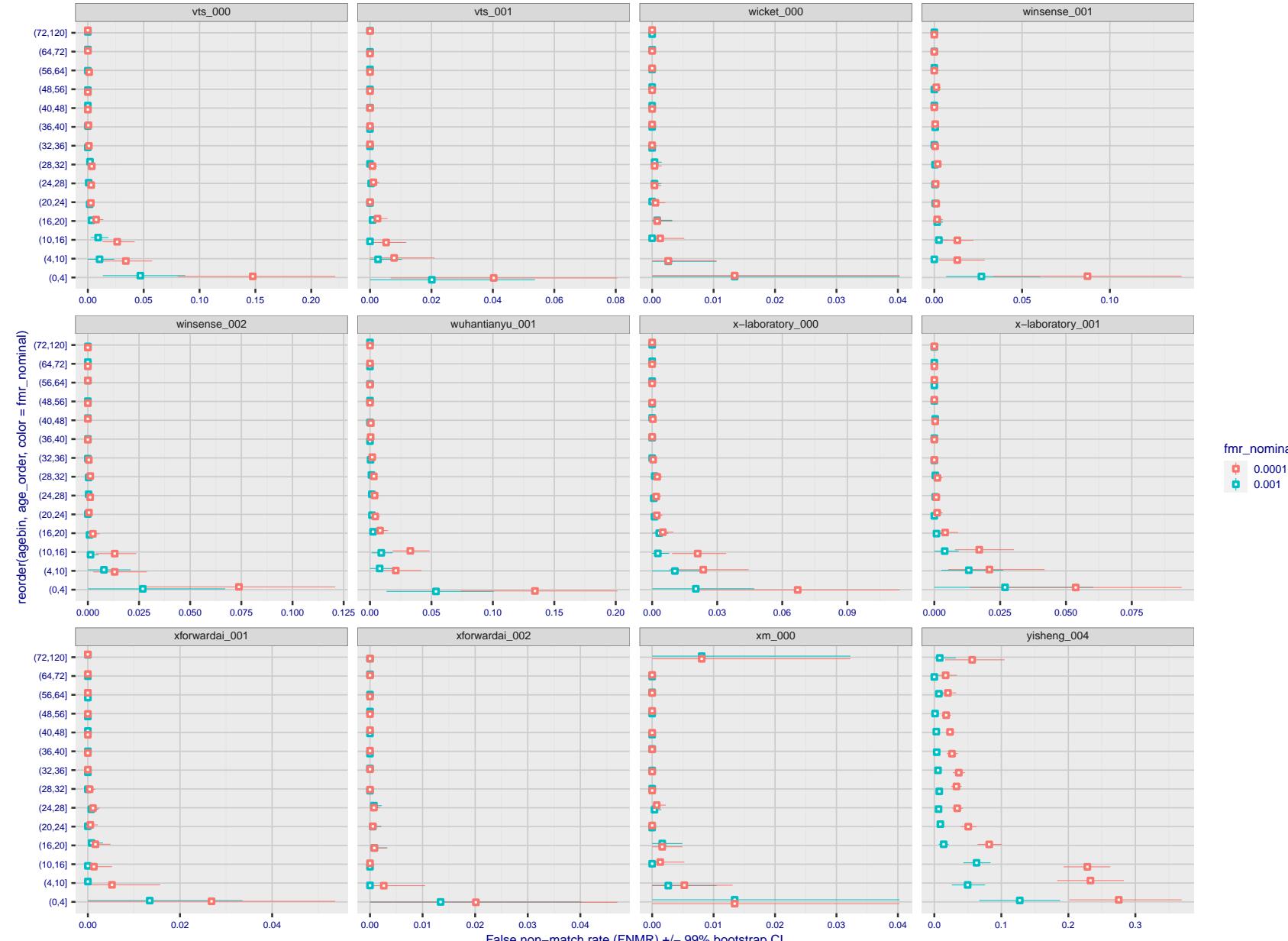


Figure 337: For the visa images, the dots show FNMR by age group for two operating thresholds corresponding to  $FMR = \{0.001, 0.0001\}$  computed over all on the order of  $10^{10}$  impostor scores. The FMR in each bin will vary also - see subsequent impostor heatmaps in sec. 3.6.2. Given a pair of face images taken at different times, we assign the comparison to the bin that is the arithmetic average of the subject's ages. This plot shows only the effect of age, not ageing. The number of comparisons in each bin is generally in the thousands, however the first and last bins are computed over 149 and 124 respectively. The error rates in some (adult) cases are zero, and in others the DET is flat so the error rates at the two thresholds are identical. The lines span 1% and 99% of bootstrap replicated FNMR estimates.

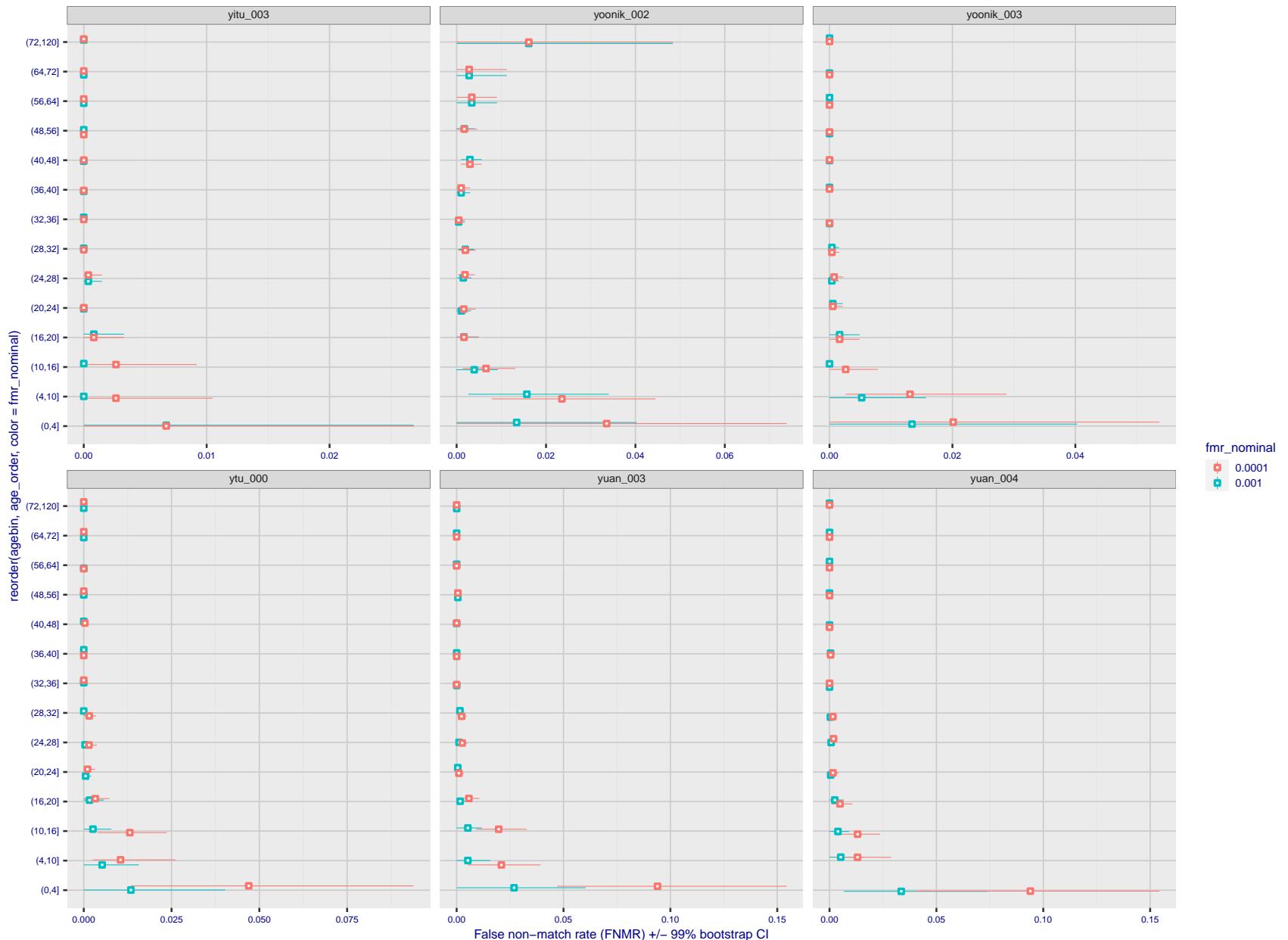


Figure 338: For the visa images, the dots show FNMR by age group for two operating thresholds corresponding to  $FMR = \{0.001, 0.0001\}$  computed over all on the order of  $10^{10}$  impostor scores. The FMR in each bin will vary also - see subsequent impostor heatmaps in sec. 3.6.2. Given a pair of face images taken at different times, we assign the comparison to the bin that is the arithmetic average of the subject's ages. This plot shows only the effect of age, not ageing. The number of comparisons in each bin is generally in the thousands, however the first and last bins are computed over 149 and 124 respectively. The error rates in some (adult) cases are zero, and in others the DET is flat so the error rates at the two thresholds are identical. The lines span 1% and 99% of bootstrap replicated FNMR estimates.

**Caveats:** None.

## 3.6 Impostor distribution stability

### 3.6.1 Effect of birth place on the impostor distribution

**Background:** Facial appearance varies geographically, both in terms of skin tone, cranio-facial structure and size. This section addresses whether false match rates vary intra- and inter-regionally.

**Goals:**

- ▷ To show the effect of birth region of the impostor and enrollee on false match rates.
- ▷ To determine whether some algorithms give better impostor distribution stability.

**Methods:**

- ▷ For the visa images, NIST defined 10 regions: Sub-Saharan Africa, South Asia, Polynesia, North Africa, Middle East, Europe, East Asia, Central and South America, Central Asia, and the Caribbean.
- ▷ For the visa images, NIST mapped each country of birth to a region. There is some arbitrariness to this. For example, Egypt could reasonably be assigned to the Middle East instead of North Africa. An alternative methodology could, for example, assign the Philippines to *both* Polynesia and East Asia.
- ▷ FMR is computed for cases where all face images of impostors born in region  $r_2$  are compared with enrolled face images of persons born in region  $r_1$ .

$$\text{FMR}(r_1, r_2, T) = \frac{\sum_{i=1}^{N_{r_1, r_2}} H(s_i - T)}{N_{r_1, r_2}} \quad (5)$$

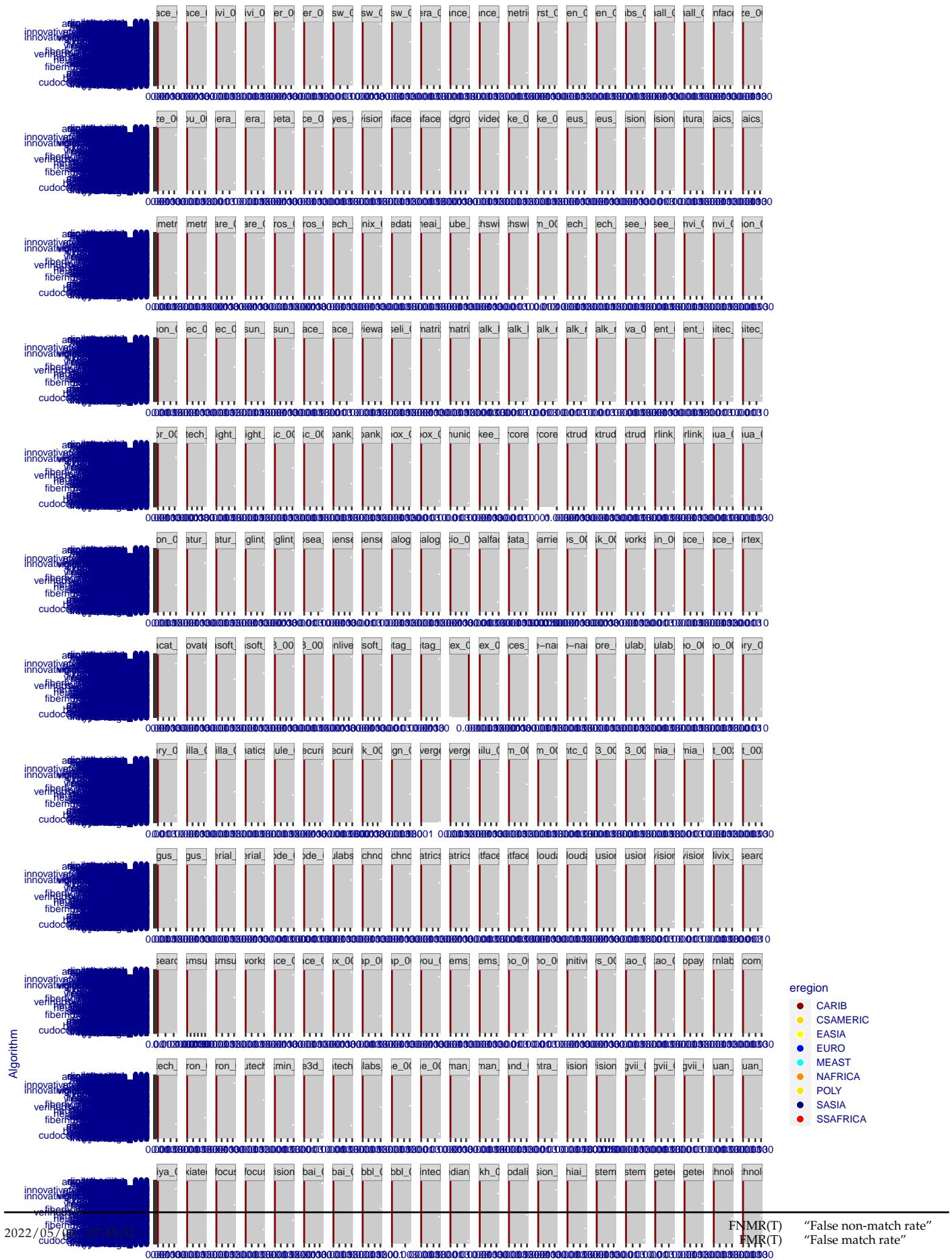
where the same threshold,  $T$ , is used in all cells, and  $H$  is the unit step function. The threshold is set to give  $\text{FMR}(T) = 0.001$  over the entire set of visa image impostor comparisons.

- ▷ This analysis is then repeated by country-pair, but only for those country pairs where both have at least 1000 images available. The countries<sup>1</sup> appear in the axes of graphs that follow.
- ▷ The mean number of impostor scores in any cross-region bin is 33 million. The smallest number of impostor scores in any bin is 135000, for Central Asia - North Africa. While these counts are large enough to support reasonable significance, the number of individual faces is much smaller, on the order of  $N^{0.5}$ .
- ▷ The numbers of impostor scores in any cross-country bin is shown in Figure ??.

**Results:** Subsequent figures show heatmaps that use color to represent the base-10 logarithm of the false match rate. Red colors indicate high (bad) false match rates. Dark colors indicate benign false match rates. There are two series of graphs corresponding to aggregated geographical regions, and to countries. The notable observations are:

- ▷ The on-diagonal elements correspond to within-region impostors. FMR is generally above the nominal value of  $\text{FMR} = 0.001$ . Particularly there is usually higher FMR in, Sub-Saharan Africa, South Asia, and the Caribbean. Europe and Central Asia, on the other hand, usually give FMR closer to the nominal value.
- ▷ The off-diagonal elements correspond to across-region impostors. The highest FMR is produced between the Caribbean and Sub-Saharan Africa.
- ▷ Algorithms vary.

<sup>1</sup>These are Argentina, Australia, Brazil, Chile, China, Costa Rica, Cuba, Czech Republic, Dominican Republic, Ecuador, Egypt, El Salvador, Germany, Ghana, Great Britain, Greece, Guatemala, Haiti, Hong Kong, Honduras, Indonesia, India, Israel, Jamaica, Japan, Kenya, Korea, Lebanon, Mexico, Malaysia, Nepal, Nigeria, Peru, Philippines, Pakistan, Poland, Romania, Russia, South Africa, Saudi Arabia, Thailand, Trinidad, Turkey, Taiwan, Ukraine, Venezuela, and Vietnam.



- ▷ We computed the same quantities for a global FMR = 0.0001. The effects are similar.

**Caveats:**

- ▷ The effects of variable impostor rates on one-to-many identification systems may well differ from what's implied by these one-to-one verification results. Two reasons for this are a) the enrollment galleries are usually imbalanced across countries of birth, age and sex; b) one-to-many identification algorithms often implement techniques aimed at stabilizing the impostor distribution. Further research is necessary.
- ▷ In principle, the effects seen in this subsection could be due to differences in the image capture process. We consider this unlikely since the effects are maintained across geography - e.g. Caribbean vs. Africa, or Japan vs. China.



Figure 340: For visa images, the heatmap shows how the mean of the impostor distribution for the country pair (a,b) is shifted relative to the mean of the global impostor distribution, expressed as a number of standard deviations of the global impostor distribution. This statistic is designed to show shifts in the entire impostor distribution, not just tail effects that manifest as the anomalously high (or low) false match rates that appear in the subsequent figures. The countries are chosen to show that skin tone alone does not explain impostor distribution shifts. The reduced shift in Asian populations with the Yitu and Tong YiTrans algorithms, is accompanied by positive shifts in the European populations. This reversal relative to most other algorithms, may derive from use of nationally weighted training sets. The figure is computed from same-sex and same-age impostor pairs.

### 3.6.2 Effect of age on impostors

**Background:** This section shows the effect of age on the impostor distribution. The ideal behaviour is that the age of the enrollee and the impostor would not affect impostor scores. This would support FMR stability over sub-populations.

**Goals:**

- ▷ To show the effect of relative ages of the impostor and enrollee on false match rates.
- ▷ To determine whether some algorithms have better impostor distribution stability.

**Methods:**

- ▷ Define 14 age group bins, spanning 0 to over 100 years old.
- ▷ Compute FMR over all impostor comparisons for which the subjects in the enrollee and impostor images have ages in two bins.
- ▷ Compute FMR over all impostor comparisons for which the subjects are additionally of the same sex, and born in the same geographic region.

**Results:**

The notable aspects are:

- ▷ Diagonal dominance: Impostors are more likely to be matched against their same age group.
- ▷ Same sex and same region impostors are more successful. On the diagonal, an impostor is more likely to succeed by posing as someone of the same sex. If  $\Delta \log_{10} \text{FMR} = 0.2$ , then same-sex same-region FMR exceeds the all-pairs FMR by factor of  $10^{0.2} = 1.6$ .
- ▷ Young children impostors give elevated FMR against young children. Older adult impostor give elevated FMR against older adults. These effects are quite large, for example if  $\Delta \log_{10} \text{FMR} = 1.0$  larger than a 32 year old, then these groups have higher FMR by a factor of  $10^1 = 10$ . This would imply an FMR above 0.01 for a nominal (global) FMR = 0.001.
- ▷ Algorithms vary.
- ▷ We computed the same quantities for a global FMR = 0.0001. The effects are similar.

Note the calculations in this section include impostors paired across all countries of birth.

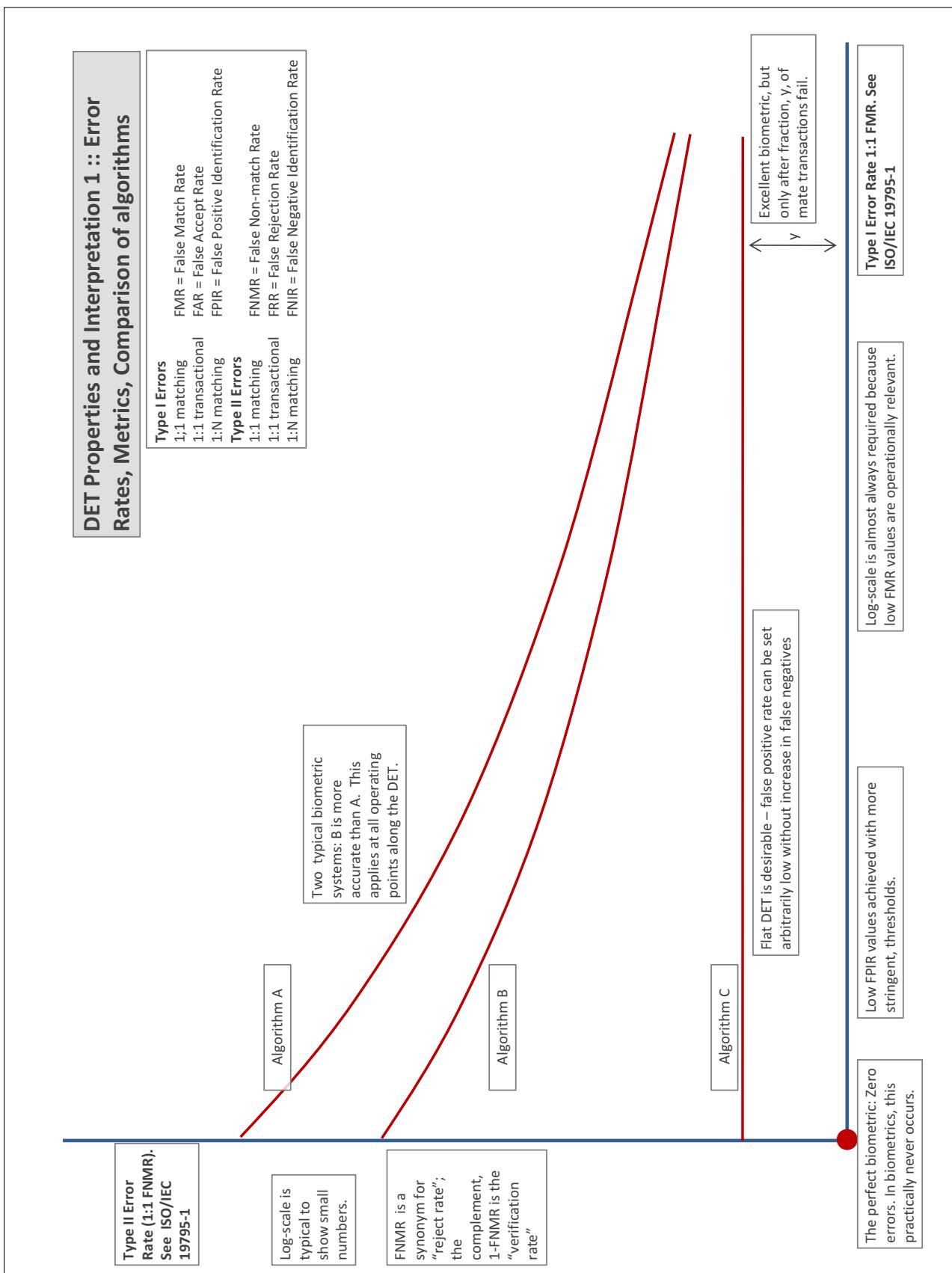
# Accuracy Terms + Definitions

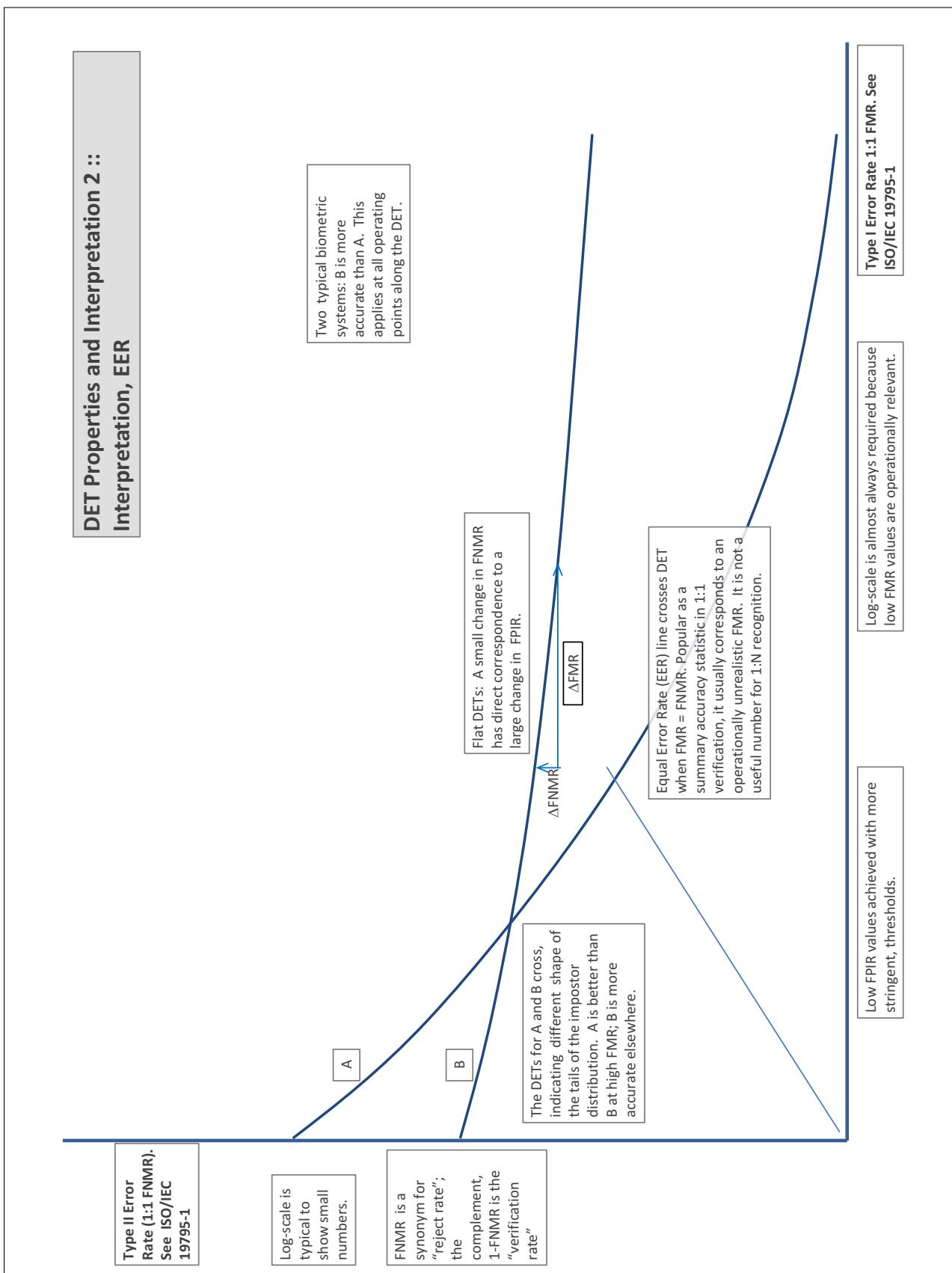
In biometrics, Type II errors occur when two samples of one person do not match – this is called a **false negative**. Correspondingly, Type I errors occur when samples from two persons do match – this is called a **false positive**. Matches are declared by a biometric system when the native comparison score from the recognition algorithm meets some **threshold**. Comparison scores can be either **similarity scores**, in which case higher values indicate that the samples are more likely to come from the same person, or **dissimilarity scores**, in which case higher values indicate different people. Similarity scores are traditionally computed by **fingerprint** and **face** recognition algorithms, while dissimilarities are used in **iris recognition**. In some cases, the dissimilarity score is a distance; this applies only when **metric** properties are obeyed. In any case, scores can be either **mate** scores, coming from a comparison of one person's samples, or **nonmate** scores, coming from comparison of different persons' samples. The words **genuine** or **authentic** are synonyms for mate, and the word **impostor** is used as a synonym for nonmatch. The words mate and nonmatch are traditionally used in identification applications (such as law enforcement search, or background checks) while genuine and impostor are used in verification applications (such as access control).

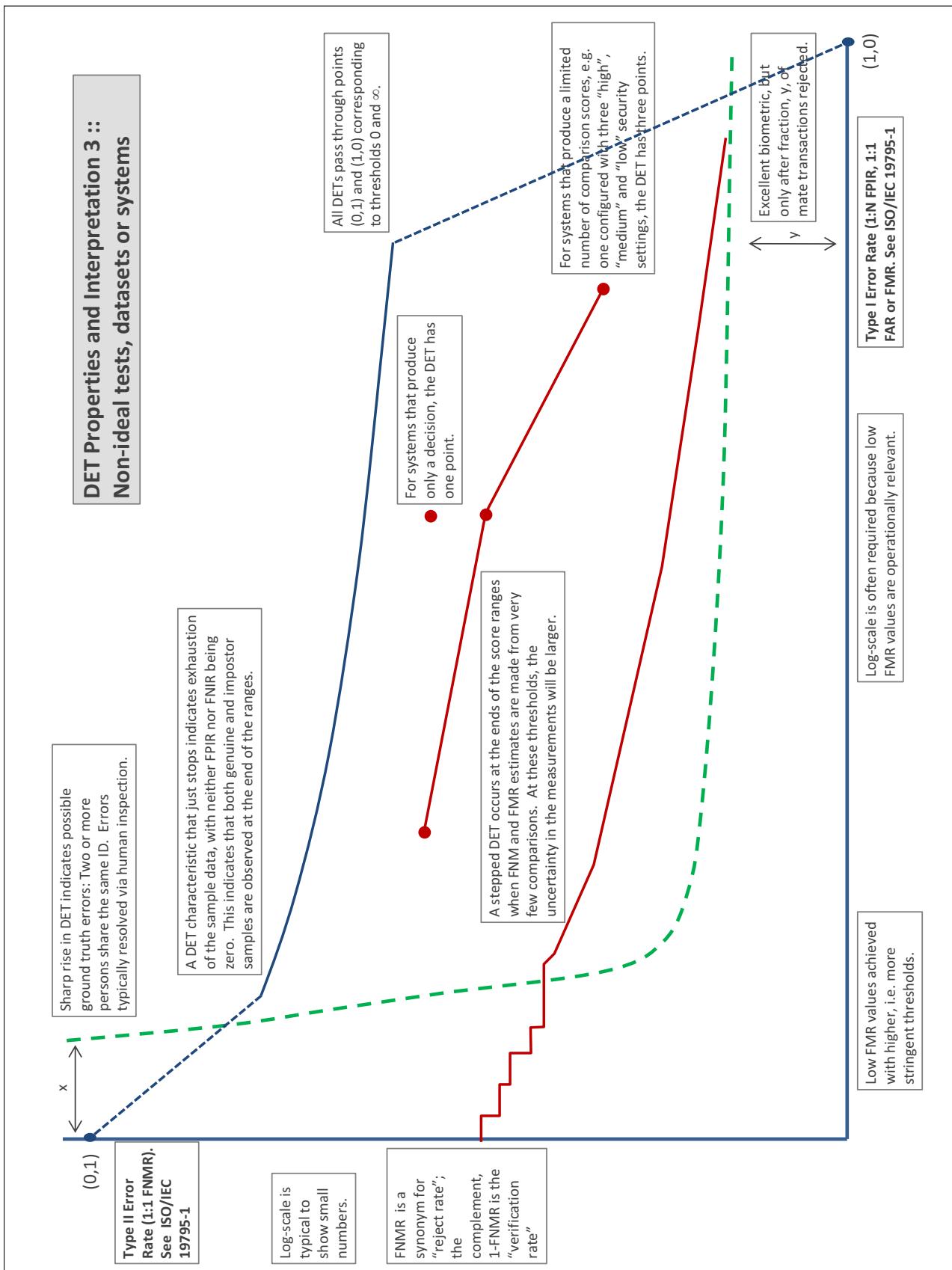
A **error tradeoff** characteristic represents the tradeoff between Type II and Type I classification errors. For verification this plots false non-match rate (FNMR) vs. false match rate (FMR) parametrically with T.

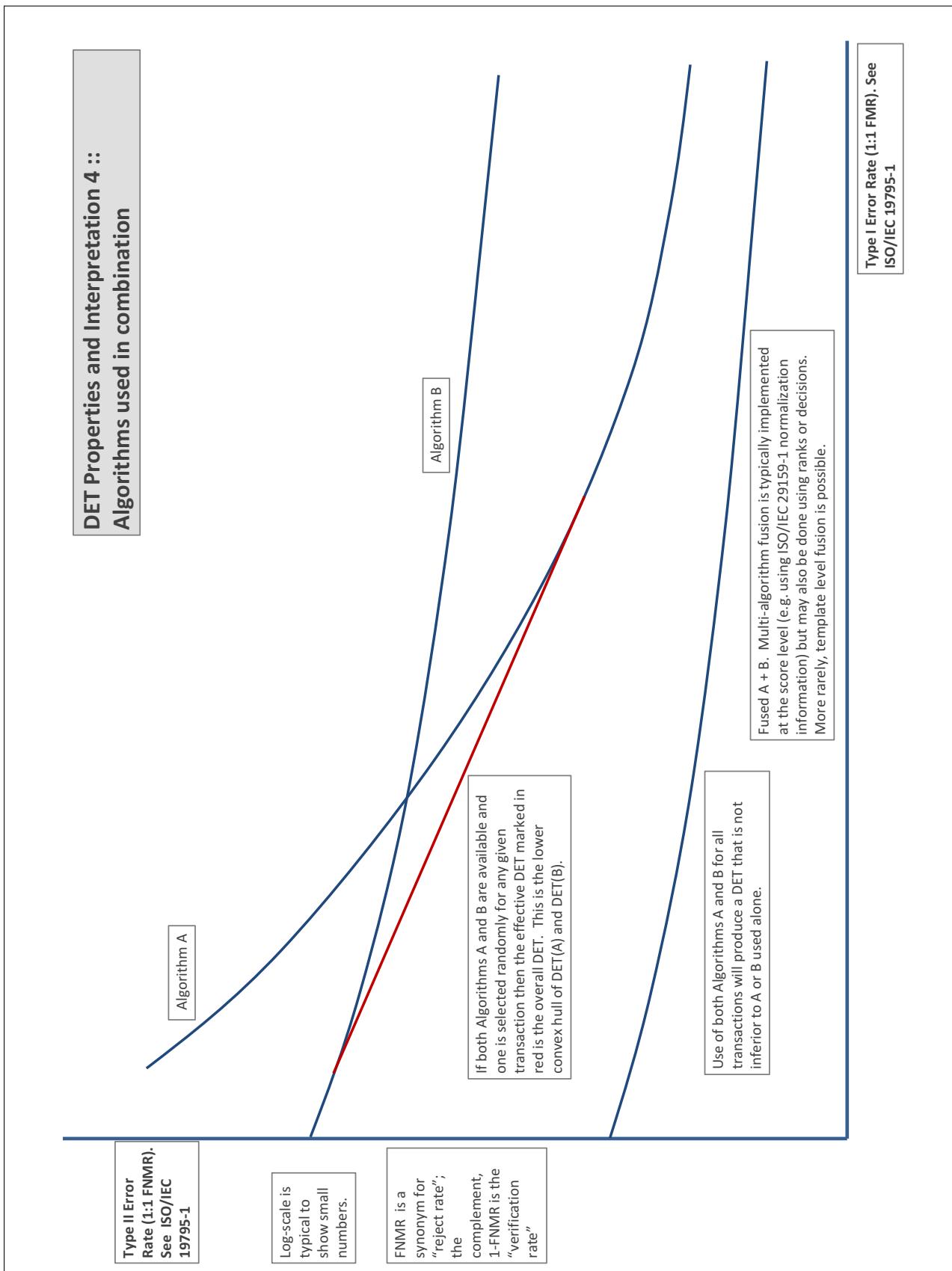
The error tradeoff plots are often called **detection error tradeoff (DET)** characteristics or **receiver operating characteristic (ROC)**. These serve the same function but differ, for example, in plotting the complement of an error rate (e.g.,  $TMR = 1 - FNMR$ ) and in transforming the axes most commonly using logarithms, to show multiple decades of FMR. More rarely, the function might be the inverse Gaussian function.

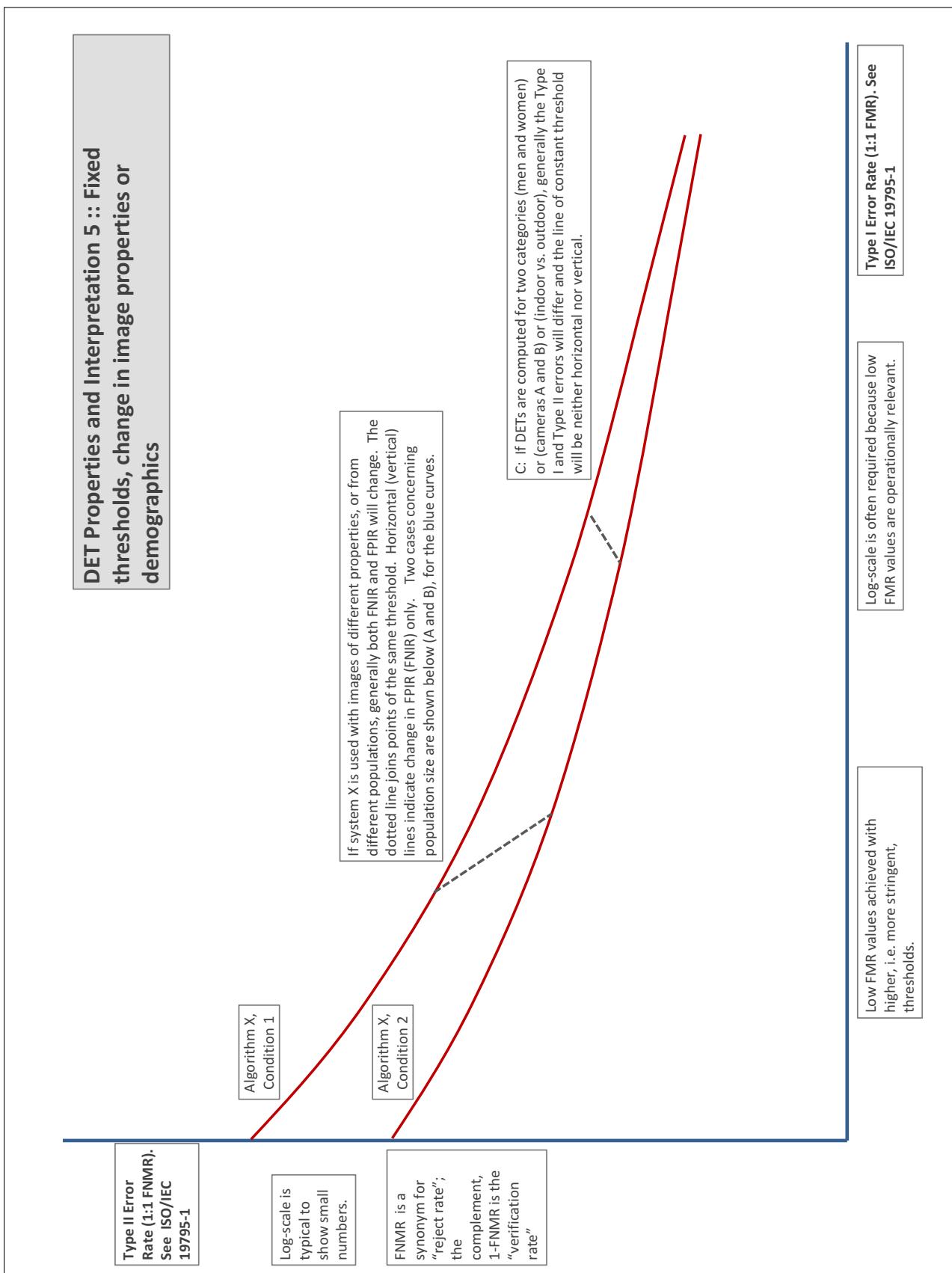
More detail and generality is provided in formal biometrics testing standards, see the various parts of [ISO/IEC 19795 Biometrics Testing and Reporting](#). More terms, including and beyond those to do with accuracy, see [ISO/IEC 2382-37 Information technology -- Vocabulary -- Part 37: Harmonized biometric vocabulary](#)











## References

- [1] P. Jonathon Phillips, Amy N. Yates, Ying Hu, Carina A. Hahn, Eilidh Noyes, Kelsey Jackson, Jacqueline G. Cavazos, Géraldine Jeckeln, Rajeev Ranjan, Swami Sankaranarayanan, Jun-Cheng Chen, Carlos D. Castillo, Rama Chellappa, David White, and Alice J. O'Toole. Face recognition accuracy of forensic examiners, superrecognizers, and face recognition algorithms. *Proceedings of the National Academy of Sciences*, 115(24):6171–6176, 2018.